FTD-MT-24-103-68

FOREIGN TECHNOLOGY DIVISION

HELICOPTERS: CALCULATION AND DESIGN. VIBRATIONS AND DYNAMIC STABILITY

by

M. L. Mil', A. V. Nekrasov, et al.

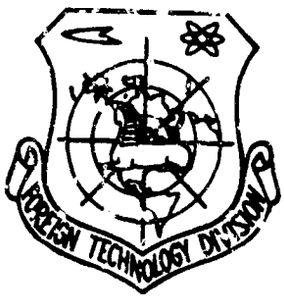

FTD-MT-24-103-68

EDITED MACHINE TRANSLATION

HELICOPTERS: CALCULATION AND DESIGN. VIBRATIONS AND DYNAMIC STABILITY

By: M. L. Mil', A. V. Nekrasov, et al.

English pages: 632

PREPARED BY:

TRANSLATION DIVISION
FOREIGN TECHNOLOGY DIVISION
WP-AFB, OHIO.

This document is a machine translation of Russian text which has been processed by the AN/GSQ-16(XW-2) Machine Translator, owned and operated by the United States Air Force. The machine output has been post-edited to correct for major ambiguities of meaning, words missing from the machine's dictionary, and words out of the context of meaning. The sentence word order has been partially rearranged for readability. The content of this translation does not indicate editorial accuracy, nor does it indicate USAF approval or disapproval of the material translated.

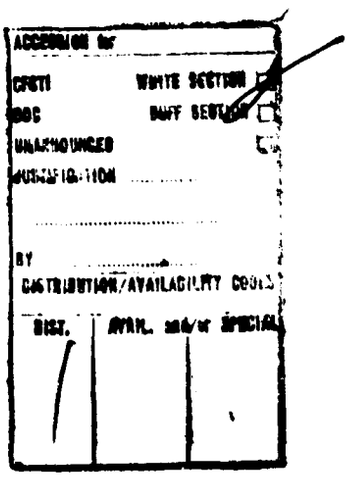

Posvyashchayetsya 50-y Godovshchine Velikoy
Oktyabr'skoy Sotsialisticheskoy
Revolyutsii

M. L. Mil', A. V. Nekrasov, A. S. Braverman,
L. N. Grodko, M. A. Leykand

VERTOLETY

Rachet i Proyektirovaniye

2

Kolebaniya i Dinamicheskaya Prochnost'

Pos Redaktsiyey D-ra Tekhn. Nauk M. L. Milya

Izdatel'stvo
"Mashinostroyeniye"
Moskva-1967
424 pages

DATA HANDLING PAGE

01-ACCESSION NO.	98-DOCUMENT LOC	30-TOPIC TAGS
TM8501473		aerodynamic load, aircraft stability, helicopter rotor, stress analysis, rotor blade, torsional vibration, vibration analysis, vibration theory

09-TITLE: HELICOPTERS: CALCULATION AND DESIGN. VIBRATIONS AND DYNAMIC STABILITY

47-SUBJECT AREA: 01, 20

42-AUTHOR/CO-AUTHORS	10-DATE OF INFO
MIL', M. L.; 16-NEKRASOV, A. V.; BRAVERMAN, A. S.; GRODKO, L. N.; 16- LEYKAND, M. A.	-----67
43-SOURCE: VERMOLEMY; RASCHEM I PROYEKMIROVANIYE. KOLEBANIYA I DINAMICHESKAYA PROCHNOSM. MOSCOW, IZD-VO MASHINOSTROYENIYE (RUSSIAN)	66-DOCUMENT NO. FTD-MT-24-103-68
	66-PROJECT NO. 72002-23

63-SECURITY AND DOWNGRADING INFORMATION	64-CONTROL MARKINGS	97-HEADER CLASN
UNCL, 0	NONE	UNCL

76-REEL/FRAME NO.	77-SUPERSEDES	78-CHANGES	40-GEOGRAPHICAL AREA	NO. OF PAGES
1886 0645			UR	632

CONTRACT NO.	X REF ACC. NO.	PUBLISHING DATE	TYPE PRODUCT	REVISION FREQ
	65-AM7019729	94-00	Translation	NONE

STEP NO.	ACCESSION NO.
02-UR/0000/67/002/000/0001/0424	

ABSTRACT (67) Additional Info - 9 unnumbered pp.

This book is volume two of Helicopters: Calculation and Design. In it ~~hthers~~ are discussed certain questions of the theory of vibrations and methods of calculating stresses appearing during these vibrations. Methods of calculating structural service life are given, as well as methods of calculating vibrations of the helicopter, which allow the determination of the amplitude of these vibrations and their comparison with comfort norms. The problem of combined vibrations of the rotor and fuselage is examined for the first time in Soviet literature. The theory of self-exited oscillations of a special type, called "ground resonance" is discussed in detail. Peculiarities of the appearance of such oscillations of the helicopter on land, during takeoff and landing and in flight. In a separate chapter there are examined special cases of the calculation of bearings operating in specific conditions of oscillatory motion. Here there is discussed the theory and method of the calculation of a new type of thrust bearing of increased load capacity and also bearings absorbing combined loads. The original book has many formulas, diagrams and tables.

TABLE OF CONTENTS [Abridged]

TM8501473

FTD-MT-24-103-68

TABLE OF CONTENTS

The work, Helicopters: (Calculation and Design) is published in the three following books.

Book One - Aerodynamics;

Book Two - Vibrations and dynamic stability;

Book Three - Design.

In this second book there are discussed certain questions of the theory of vibrations and methods of calculation of stresses appearing during these vibrations in the construction of a helicopter in flight and, in particular, in the blade of the main rotor.

Methods are given of the calculation of the structural service life and there are also methods of calculating vibrations of the helicopter, which allow the determination of the amplitude of these vibrations and the comparison of them with comfort norms. For the first time in Soviet literature there is examined the problem of combined vibrations of the rotor and fuselage.

The theory of self-excited oscillations of special type, bearing the name "ground resonance," is discussed in detail. Peculiarities of the appearance of such oscillations of the helicopter on land, during takeoff and landing and under flight conditions are examined.

In a separate chapter there are examined special cases (touched upon little in general literature) of the calculation of bearings operating in specific conditions of oscillatory motion. Here there is also discussed the theory and method of calculation of a new type of thrust bearing of increased load capacity and also bearings absorbing combined loads.

The book is intended for engineers of design offices, scientists, graduate students and instructors of higher educational institutions. It can also be useful to engineers of helicopter manufacturers and students who are engaged in thorough study of vibrations and dynamic stability of helicopters. Certain sections of the book will also be useful to the flying and technical personnel of helicopter flight units.

The book contains 35 tables, 246 illustrations, and 47 references.

PREFACE

The first book of the work, Helicopters, (Calculation and Design), published in 1966, was devoted to aerodynamics: theory and methods of calculation of aerodynamic properties of the main rotor and aerodynamic design of helicopters of different configurations on the whole.

In the first book there is included an account of the theory of flutter of the main rotor, which is usually attributed to aeroelasticity — the region bordering between aerodynamics and stability.

The second book is a logical continuation of the first and deals with vibrations and dynamic stability of helicopters.

Questions of static stability of helicopters in principle do not contain anything new as compared to that known in aircraft manufacturing. Regarding vibrations and dynamic stability, helicopters have a number of peculiarities which were designated from the first steps of helicopters as a new type of aircraft. These peculiarities acquired great acuity in the process, if it can be so expressed, of the "fight for existence" of these apparatuses in the general system of airportless aviation transport means.

An account of problems of vibrations and dynamic stability of the helicopter starts with a description of methods of calculation of elastic vibrations of the blade of its main rotor, which are close

in fundamental equations and methods of solution to that utilized in the theory of flutter but have different directivity, since in the final analysis it leads mainly to the solution of strictly a stability problem – to the determination of varying stresses effective in the blade, and then with the use of data on fatigue limit of concrete construction, to the determination of the service life, i.e., service life of the blade.

Problems of vibrations in dynamic stability are important not only from the point of view of reliability of the apparatuses; and the solution to these problems governs the service life of the machines, and this means their economy.

In the book, in particular, there are examined contemporary methods of calculation of elastic vibrations of the blade carried out on high-speed computers, which makes it possible to determine the varying stresses acting in the blade.

Investigations of vibrations of the "ground resonance" type, just as the study of construction vibrations strictly comprise the main subject of the theory of vibrations of the helicopter.

The elimination of vibrations of the "ground resonance" type, leading in the case of their appearance and development to the destruction of the apparatus on land and in multirotor configurations in air, was always one of the main problems confronting designers. The question of oscillations (vibrations) of parts of helicopter is very important, which is examined from the point of view of comfort for the crew and passengers. It is easy to estimate the acuteness of this problem if one were to imagine the power of the vibrations' constant source – a huge main rotor operating in a greatly alternating velocity field.

The last chapter of the book is devoted to the calculation of special bearings necessary in the designing of many units of the helicopter and thus is the transition to the third book – Design.

In the book Design there will be briefly examined basic questions of the layout of the helicopter selection of basic parameters of helicopters, including having wings, and also auxiliary propulsive systems – tractor propellers or additional jet engines. There will be also discussed considerations about the economy of aviation materiel, which must be considered in designing.

Examined in this book will also be questions of balancing, controllability and stability from the point of view of selection of parameters of the control system, and also questions of designing of separate units of the helicopter.

M. Mil'

The second book Vibrations and Dynamic Stability was written by the following: Introduction – M. L. Mil'; Chapter I – A. V. Nekrasov; Chapters II and III – L. N. Grodko; Chapter IV – M. A. Leykand. § 11 of Chapter I was written by A. V. Nekrasov jointly with engineer Z. Ye. Shnurov.

In preparation of the manuscript the authors received much help from engineers F. L. Zarzhevskaya, V. M. Kostromin and I. V. Kurov.

In the book there are results of calculations, carried out by engineers Yu. A. Myagkov, O. P. Bakhov, V. F. Khvostov, A. A. Golubtsov, V. M. Pchelkin, S. Ye. Sno, V. G. Pashkin, N. P. Shevnyakova, N. M. Kiseleva, L. V. Artamonova, V. F. Perina, N. A. Matskevich, V. I. Kiryushkinoy and A. G. Orlova.

Many valuable instructions were made by critic R. A. Mikheyev.

Final preparation of the manuscript for publication was made by engineer L. G. Rudnitskiy.

The authors express sincere gratitude to all these colleagues.

INTRODUCTION

As soon as there was created a sufficiently powerful and light aircraft engine and the helicopter flew for the first time, there appeared the first problems related to balancing, controllability and stability of this machine. These were basically aerodynamic problems. If one were to consider as the beginning of flights on rotorcraft the first flights of gyroplanes Cierva during 1925-26, then it is possible to say that the given problem was basically solved already in first decade (192[illegible]-1936) of their development. The type of aircraft was thus cured of "children's diseases."

However, as soon as there appeared the first series of machines and practical exploitation of them began, more serious deficiencies of helicopters, such as, for example, fatigue connected with insufficient dynamic stability of certain elements of the construction were discovered.

With wider practical application of autogiros and especially helicopters, which were reactivated at the end of the 1930's and beginning of the 1940's in a new improved technical basis, there appeared new dynamic problems. These include, in the first place, oscillations and vibrations of separate elements of construction or helicopter as a whole, which are dangerous in conditions of appearing stresses or impermissible from the point of view of the creation of necessary comfort for the crew and passengers, and also the problem of service life, which is the period of service of elements of construction, operating under high varying stresses. The

last of the problems – increase in service life – takes on even greater importance at present, since the depreciation and overhaul periods of service of the helicopter, determined by the service life of its units, influence the economics of its application as a means of transport. The service life in turn is determined mainly by the level of varying stresses effective in the structure, and therefore the accuracy with which they are calculated comprises one of the basic problems of investigation of dynamic stability of helicopters.

The tractor propeller of an aircraft operates practically in axial flow and just as the engine does not create in the elements of structure any noticeable varying stresses. Only takeoff, landing and flight under conditions of atmospheric turbulence (and on a combat aircraft, the maneuver) create in the structure of the aircraft considerable dynamic loads but with a relatively small (of the order of tens and hundreds of thousands of cycles) number of loading during the period of service of the aircraft. In this case it is possible to indicate recurring static loads.

There is quite another character of the load in a helicopter. Its basic force elements are loaded dynamically, and the number of loads frequently exceeds tens of millions of cycles during the service period. This is explained first of all by the asymmetric flow of the main rotor, which rotates and simultaneously moves forward. The blade undergoes variable aerodynamic loads due to the change in relative flow rate and angles of attack of its sections. All forces and moments having effect on the blade are transmitted to the hub and control system by the main rotor. The forces and moments arriving from various blades are balanced mutually with the exception of loads effective at frequencies whose ratio to the number of revolutions of the rotor is a multiple to the number of blades. These loads are transmitted to the fuselage and irrotational parts of the control system by the rotor and create in them also very noticeable varying stresses.

Thus the problem of vibrations and dynamic stability in helicopter construction is not only considerably more extensive than in aircraft

construction, but in a whole number of cases it does not have a direct analogy in aircraft construction.

Understanding of the importance of problems of dynamic stability was not achieved at once. Thus even causes of first accidents of autogiros in 1936-37 during which autogiros flipped in air for a long time were attempted to be explained by insufficient dynamic stability. In connection with this, in particular, there were undertaken investigations of the dynamics of the main rotor with hinged attachment of blades with curvilinear motion of the apparatus (see § 2 of Chapter II, Book One). This theory subsequently found wide application during the during the development of problems of dynamic stability and controllability of helicopters. However, it did not uncover the real cause of the mentioned accidents. As it became apparent later, the cause of them was insufficient dynamic stability of the main rotor blades.

These problems are perceived literally by groping. The first experimental autogiros and helicopters had small dimensions and, as a result, quite high rigidity of construction. However, the first increase in dimensions immediately encountered great difficulties. Thus on the autogiro A-4, having a diameter of a little larger than its predecessor, autogiro 2EA, serious difficulties because of insufficient blade torsional rigidity appeared. Angle of incidence of blades in the first flight was increased so much because of twisting st in that autorotation was impossible, and the flight nearly ended in an accident.

Investigation of this phenomenon was completed by publication of a work on the dynamic blade twisting of a rotor in flight (see [2]) in which for the first time recommendations of the necessity of combining the center of gravity and center of pressure were given and considerations of the influence of the blade profile on static stability and controllability of the apparatus were examined. This investigation led to the fact that in the practice of Soviet helicopter construction there were accepted curved profiles, which provide a greater reserve of autorotation. In the layout of the blade

a set of different profiles was used. The recommendations made in the mentioned work were so sufficient that the first Soviet helicopters, which had a diameter of the rotor of about 14 m, did not experience flutter.

Development of Soviet helicopter construction is characterized by greater strides than that of foreign (this permitted our designers, who started to construct helicopters later, to develop machines considerably exceeding those of contemporary foreign in load capacity and dimensions). Whereas after the first successful helicopter, Sikorsky S-51, with a rotor diameter of 14 m, built in 1947, the Americans in 1950-51 proceeded to work on a machine with a diameter of 15.5 m (S-55), after creation of the helicopter Mi-1 with a 14-meter rotor in 1952 we built the helicopters Mi-4 and Yak-24 with rotors 21 m in diameter. It is not surprising that with such a jump in dimensions there was revealed a new phenomenon not encountered earlier - on both machines with the first flight flutter of the rotor began. We coped with this problem practically very rapidly, but problems of the theory of flutter for a long time still awaited their solution.

For the first time we enccuntered this new phenomenon when in April 1952 the helicopter Mi-4 was ready for the first flight. After the beginning of acceleration the blade started arbitrarily to flap, sagging greater and greater and threatening to touch the structure. The testers knew that they were dealing with a new phenomenon which no one had observed before. This was the flutter of the rotor blades. No one knew then that this was the very rotor flutter in whose investigation many scientists in the USSR and abroad were engaged. According to all data existing at that time, flutter was not expected, since it could not appear at the number of rotor revolutions of 100-110 per minute, as occurred on the helicopter Mi-4 in reality, but approximately at 500 revolutions. Decisive for the appearance of flutter was in this case the fact that great forces developed on a rotor of such a diameter caused considerable deformation of the cyclic pitch control, which is equivalent to the lowering of twisting rigidity of the blades, and also the fact that

then for these machines a large value of the coefficient of flap control (close to unity) was selected; in early investigations of flutter this factor was not taken into consideration. As a result it was not a question on the helicopter flights, since flutter started considerably earlier than the working number of rotor revolutions were attained.

With observation of the pattern of flutter (flapping, bend and torsion of blades) it became clear that this phenomenon could be eliminated only by using torques from inertial forces appearing in the process of the moving blade sections with its flapping. Not associating rotor flutter with the flutter of wings, where, as has long since been known, the main importance is the mutual location of the center of gravity, axis of rigidity and center of pressure, but simply by establishing the counterweights at several points along the length of the blade, which during vibrations should have created inertial moments of opposite sign, we repeated starting of the rotor and understood that in our hands there is reliable means to stop the flutter.

Thus in a short time the given problem was solved practically, and in May of 1952 the first flights of the helicopter Mi-4 were accomplished.

At the same time flutter appeared on the helicopter Yak-24, which had the very same hub and cyclic pitch control mechanism as those on the helicopter Mi-4, but the blade was of quite different design (with greater flexural and twisting rigidity). However, due to the fact that with the appearance of flutter there is decisive importance in the rigidity of the cyclic pitch control and parameters of the flap control, on blades of the helicopter Yak-24 flutter appeared of the very same form and at the same revolutions as that on helicopter Mi-4.

Thus during several weeks there was found practical solution for elimination of flutter which was used up till now. However, the scientific theory which would permit obtaining an answer whether

flutter will appear or not, and even if it appears, then at what numbers of revolutions and what form, was created by us during the subsequent four years.

It is necessary to say that the most complex was included in the fact that, having finished with flutter observed on earth (with the help of displacement of centering of the blade forward it was possible to "drive" it outside the limits of the working numbers of revolutions and even above the maximum permissible number of engine revolutions on earth), nevertheless there was not excluded the possibility of its appearance in flight. This led to unpleasant consequences. In January of 1953 a helicopter Mi-4 had a flight accident whose causes for almost three years were not sufficiently and convincingly explained. During investigation traces of the impact of blades against the cockpit were revealed. This was not observed in any other cases. It is necessary to note that with normal flapping motion the blade cannot touch the cabin, since for this it is necessary that in air the lower limiters of overhang of it were brought down.

It is possible to imagine how energetically we had to continue to look for the cause of this event, if one were to remember that after it there were stopped neither the flights nor the serial production of these machines.

During 1954 many pilots observed in flight an unusual phenomenon, which received the name "Kalibernyy effect" (surname of the pilot who first noticed it). Kalibernyy determined that in conditions of motor reduction, approximately at an angle of setting of the blades of 6°-7°, the blades begin to flap away from the cone of rotation described by them. After a regrouping of the blades having a somewhat different transverse centering this phenomenon was ceased. But once, after two years during a checking in flight of a set of blades for the absence of the Kalibernyy effect, i.e., with fulfillment in flight of motor reduction with the pitch angle of 6-7°,[1] this phenomenon appeared in such a degree where the flapping of the blades were so strong that in the machine forced landing

was accomplished with difficulty. It is necessary to note that near land with transition to other conditions the flapping of the blades ceased, and the machine behaved normally. With inspection of the helicopter after the flight there were revealed broken fixings of the blades (they are thus called the movable connections on the slit trailing edge of the blade) which indicated bending of the blade in the plane of rotation. Everything remaining was in good working order. It was decided to investigate in detail this helicopter with the same set of blades. Flight tests were conducted in order to repeat this phenomenon and study it.

Measurements of the blades showed that their centering appeared to be approximately 1% of the chord more to the rear than it was when the blades were manufactured at the plant. And this is explicable, as the blades were covered with plywood. The center of gravity of the plywood is approximately on half of the chord. Therefore, with swelling and loading of it from moisture, the center of gravity of whole blade is displaced to its trailing edge. The case with this helicopter occurred during a thaw when the humidity of the air was high.

During these tests it was also finally established that the character of the flapping motion of blades and motion of the control stick in flight on conditions of "Kalibernyy effect" are absolutely analogous to the flapping motion and motion of the stick, which were recorded on land during tests when the blades were subjected to flutter by means of artificially created rear centering. This complex means permitted setting that phenomenon appearing in flight identical with that which was noted on land. Thus it was established that the "Kalibernyy effect" is nothing else but the beginning of flutter in flight. On the basis of this conclusion and it was conjectured that the unexplained earlier flight accident with blows of blades against the cockpit was also nothing else but the flutter of blades in flight appearing at revolutions of the rotor, at which on land it did not appear.

With flutter vibrations of a hinged sealed blade, in contrast to vibrations of a wing of an aircraft are similar to a flapping motion whose amplitude increases until the blade hits against the limiters of overhang and then knocking them against cabin.

The fact that this phenomenon was not discovered for a long time is explained by the erroneous assumption resulting from model testing that if flutter on land is eliminated then in air with forward motion it is not able tc appear. But practice and then a more strictly set experiment on the helicopter, and, finally, theory showed that there are conditions of flight at which flutter during rotor revolutions can occur in flight although it does not appear on land.

It is necessary to say that as was established in the course of investigations, the phenomenon of flutter appeared on helicopters earlier. Even in 1949 on the helicopter Mi-1 to increase the stall reserve there was designed and built a main rotor with wider blades. This rotor in flight caused shaking which was never possible to eliminate. When there was developed the theory of flutter and all peculiarities of this phenomenon were explained, it became possible not only to explain the cause of shaking on the Mi-1 helicopter with wide blades, induced by proximity of conditions to flutter, but also without a single difficulty to design and construct even in 1956 a 35-meter rotor for helicopters Mi-6 and Mi-10. Perfection of this rotor is confirmed by the fact that in a week after first flight the new heavy helicopter Mi-6 could accomplish flight for training for participation in an air show on an aviation holiday in Tushino. There was no longer any unpleasant phenomena connected with flutter on these machines neither then nor later. Such is the history of the problem of flutter.

No less important is the problem of the determination of varying stresses in blades, which is solved by means of consideration of their forced vibrations.

During the first decade of their development main rotors of helicopters were designed actually without preliminary calculation of varying stresses which appear in flight. At that time this calculation was laborious and inaccurate, and not infrequently it was finished only after the roll out of the machine onto the airfield. Only the development of methods of calculation of varying stresses allowing the use of high-speed digital computers permitted the designing of blades with a conscious selection of the distribution of their rigidities and masses in such a way so as to avoid dangerous resonances, to lower the level of stresses and to provide long service life and reliability of the blades.

It is necessary to note that a refinement of the method of design of the blade for stability caused further deepening and refinement of the aerodynamic theory. As was already shown in the first book, refinement of calculation of flying data did not create a great necessity in the development of a complex and laborious (for calculations) vortex theory of the main rotor. However, only the vortex theory permits determining the irregularity of the field of induced velocities causing variable loads on the blade with frequencies exciting flexural vibrations of the blades at the second, third and higher tones. Therefore, only the vortex theory can give in the calculation of stresses results close to those which are observed in reality.

Another no less important problem was vibrations. This problem was always one of the most difficult in the development of rotorcraft. Dozens of constructions in the USSR and abroad, interesting in design and flying-tactical data, did not appear because of the high level of vibrations.

On aircraft there are not such powerful sources of excitation of vibrations as there are on helicopters. Furthermore, the engines and propellers, which are on aircraft the basic exciters of vibrations, can be sufficiently well insolated from the structure with the help of special shock absorption. Resonances with high frequencies from

these exciters enough can be easily eliminated by means of comparatively small changes in design. On the helicopter, besides the fact that the actual disturbing forces from rotors are considerably greater than those on aircraft, their frequencies from the slowly revolving rotor are rather low and at coincidence with natural frequencies of vibrations of the fuselage, engine, wing or empennage there appear resonances, which lead to considerable vibrations with amplitude movements attaining on the steady-state operations of flight quantities of the order of 0.3-0.4 mm and on short-term conditions before landing of the helicopter, even 1-2 mm in the crew's cabin.

To build up resonances with fundamental tones of natural oscillations of the fuselage by the change in rigidity of design on the constructed machine frequently appears practically impossible, since this is equivalent to total alteration of the fuselage. Therefore, it is important to be able correctly to estimate the frequencies of natural oscillations of the fuselage and to calculate the amplitude of vibrations in the process of designing of the machine.

The basic attention in combatting vibrations is given to the lowering of values of variable forces arriving on the fuselage from the rotor. These forces are caused by vibrations of the blades. In turn vibrations of the blades can be larger or smaller depending upon the proximity of their natural frequencies of sources of external excitation.

In all cases the proximity to resonance causes an increase in stresses in the blades. But if these oscillations occur with a harmonic frequency of $z_л + 1$ or $z_л - 1$ for oscillations in the plane of rotation of the rotor or harmonic frequency $z_л$ for oscillations in the plane of the stroke (where $z_л$ is the number of blades), then the forces are added and transmitted through hinges to the hub and through it to the fuselage, thus causing its oscillations.

The most unpleasant vertical vibrations for a person to a considerable degree are caused by forces effective in the plane of rotation of the rotor, since these forces, being applied high above the center of gravity of the helicopter, create considerable moments exciting oscillations of the fuselage bend. It is natural that the greatest amplitudes of vibrations (antinode) are reached on the ends of fuselage and, consequently, also in the cockpit.

It appears that with determination of frequencies of natural oscillations of blades of the helicopter it is necessary to consider the fact that the rotor hub during vibrations does not remain fixed, since it is fastened on an elastic fuselage. Thus with determination of vibrations the helicopter should be examined as a single dynamic system with elastic blades hinged suspended to the hub, which is fastened to the elastic fuselage.

It is obvious that such a calculation scheme could appear and be feasible for consideration only recently. As far as we know, this book gives for the first time an account of the method of calculation of vibrations of a helicopter during its designing.

Further in the book self-excited oscillations of a helicopter, are examined, which usually bear the name "ground resonance."

For the first time designers encountered the phenomenon of ground resonance more than 30 years ago when on one of the first Soviet autogiros A-6 (design of V. A. Kuznetsov) there were used wheels with low-pressure tires appearing at that time. Struts having air-oil shock absorption were removed from the helicopter. With the first starting unexpected oscillations appeared. The helicopter rocked from wheel to wheel with ever increasing amplitudes until it started to jump, detaching the wheels from land. Takeoff was completed with a crash.

Owing to the fact that these tests were photographed by a movie camera it was possible to establish that the blades accomplished growing oscillations around the vertical hinges. These oscillations,

occurring in the field of centrifugal forces, caused the periodic displacement of the center of gravity of the whole lift system relative to the center of the hub and thus excited oscillations of the helicopter standing on land. It is clear that if the frequency of displacements of the center of gravity of the rotor coincides with the frequency of natural oscillations of the helicopter on pneumatic tires, then such oscillations can grow. Here one would think that the physical picture of the phenomenon is clear. The energy which supplied these growing oscillations was either the energy of the engine rotating the rotor or when the engine is included, the kinetic energy of the rotating rotor.

However, for development of the theory of ground resonance and study of its new manifestations, possibly in new fundamentally different plans and designs of helicopters, numerous investigations were required, which continue even now.

The first theoretical works clearing up the nature of natural oscillations of the "ground resonance" type were carried out in 1936 by I. P. Bratukhin and B. Ya. Zherebtsov. Results of investigations conducted by them permitted the elimination, in particular, of ground resonance on the largest autogiro ever built in the world. the A-15, with a rotor with a diameter of 18 m, created in 1936 by the design of V. A. Kuznetsov and M. L. Mil'. In the construction of the hub of this autogiro there were used springs built into the limiters of blade vibrations around the vertical hinge. The springs change the natural frequency of oscillations of the blades in the plane of rotation, and thus ground resonance was eliminated.

There are no doubts in the fact that the phenomenon of ground resonance was at that time well-known and somehow studied in the West, inasmuch as already the first successful autogiros of Cierva, for example, the S-19, had elastic couplings (shock absorbers) included in the blades through frictional dampers.

However, many designers during a certain time period continued to create autogiros without dampers in vertical hinges. A sample of

such a machine was the autogiro A-7, created in 1937 by N. I. Kamov. He successfully flew it without having dampers on the rotor hub. The secret of successful flights consisted in the fact that this was the first machine with a tricycle landing gear providing practically vertical location of the axis of the main rotor during acceleration of it before takeoff and with the stop after landing. This circumstance conditioned the small magnitudes of initial disturbance due to deviation of blades in the plane of rotation, inasmuch as the initial deviations of the blades are caused by the projection of gravity on the plane of rotation. On the other hand, frictional forces in the hinges were also important (at that time in the hinges there were bronze bushings), which with considerable centrifugal forces cannot be disregarded; they gave in this case sufficiently great damping. However, once pilot S. A. Korzinshchikov after one of the flights immediately after landing did not push the control stick forward and thereby did not move the machine from a three-point position (skid and basic landing gear) to a standing position (with support on the front leg), as with subsequent drop in revolutions of the rotor because of a great initial disturbance in deviations of blades in the plane of rotation (axis of rotation of the rotor was inclined to earth at an angle of 14°) there appeared ground resonance — the blades broke and damaged the helicopter.

So from one experienced example to another all new aspects of this problem appeared.

Inasmuch as accurate calculation of necessary oscillation damping of blades (and with oscillations of ground resonance there is equal importance in oscillation damping of the apparatus carried out by the shock absorber of the landing gear) at that time did not exist, designers tried to select the minimum value of the moment of friction of the damper on the hub. This was dictated by a tendency to decrease variable bending moments appearing in the presence of the damper with forced oscillations of blades in flight.

With friction dampers, as is known, there appear oscillations with excitation threshold. If the excitation is small — the exciting moment is less than the moment of friction — oscillations in general,

do not appear. Here on a safe helicopter with respect to ground resonance, which is already in operation, vibrations suddenly appear. This is explained by the fact that in the given special case the initial disturbances proved to be greater than usual. This case occurred on the Mi-1 helicopter when it overtaxied obliquely through deep tracks from a motor vehicle. A random disturbance of the bank greatly rocked the machine on the pneumatic tires, and it acquired so large amplitudes of oscillations that the available damping in bushing was insufficient and ground resonance appeared. Pilot G. A. Tinuakov then coped with it very simply; he took off and the vibrations ceased, since the elastic coupling connection with earth was disturbed.

This case suggested the necessity of the application of viscous friction, i.e., hydraulic oscillation dampers of blades in the hub for which the moment of friction does not remain constant but grows with the amplitude of oscillations.

However, subsequent practice constantly required the improvement and development of the theory in this region. It suffices to remember at least the appearance of ground resonance when the helicopter operates on a tie.

Several cases of ground resonance occurred also at a time when the helicopter, in taxiing during takeoff or landing, only weakly touched land with its wheels, when the tractive force of the rotor becomes close to the weight of the apparatus and shock-absorber struts with the usual preliminary tightening appeared completely released. The difference between weight and tractive force of the apparatus was absorbed only by the pnuematic tires of the wheels.

It is clear that not only are frequencies of oscillation of the machine changed, but also damping of the struts is absent. Here then ground resonance appeared which on the helicopter not attached or not taxiing with a very small load on the wheels never appeared.

In order to avoid such cases there began to be used the so-called dual chamber struts of the landing gear – shock-absorbing struts

having a second low-pressure chamber absorbing the energy of oscillations of the apparatus when it touched land only by slightly pressed pneumatic tires and the main struts did not operate.

There is special importance in questions of the theory of ground resonance on two-rotor configurations when the elastic system connecting both rotors, be it the fuselage with a longitudinal or the wing with a transverse configuration, has low frequencies of natural oscillations. With such oscillations there can appear considerable movements of the rotor hub, which create the possibility of energy exchange between oscillations of the blades and oscillations of the lifting structure. Oscillations of such type are possible not only on land but also in flight.

A similar problem appears with the designing of tail rotors with vertical hinges located on the elastic tail girder.

The creation of a harmonious and perfected machine is possible only in the case when the designer is quite competent not only in the general problems of designing but also in special problems connected with the theory and design of its separate elements.

On the contemporary helicopter there is a large number of responsible high-loaded mechanical units whose reliability and service life in many respects depend on the efficiency of their bearing units. Therefore, designers of helicopters should be familiar with the theory and design of anti-friction bearings. This especially pertains to cases of operation of anti-friction bearings in complex combinations of external loads and during oscillatory motion with small amplitudes.

Therefore, in this book there is included a chapter in which the answer to questions of theory and design of bearing subassemblies of bushings, cyclic pitch controls and other units can be found. One of the most interesting questions described in Chpater IV is the theory of special thrust roller bearings, in which owing to the location of the rollers at an angle to the radial direction the

separator during oscillatory motion not only oscillates together with the sliding ring but also continuously revolves in one direction. This prevents local wear of the rocking paths and increases the service life of the bearing.

It should be noted that the application of such bearings in axial hinges of main rotor hubs provided a considerable increase in their service life.

Helicopter construction requires a high general level of theoretical and scientific training of the design engineer, since dynamic problems for helicopters (aircrafts with revolving wings) are of considerably greater importance than those for aircraft (apparatuses having stationary wings, and even now and wings turning and deflect back). This is confirmed by the fact that those few designers who were able to give a considerable contribution to the development of helicopter construction, and, even more, those who had practical success, were at the same time the great scientific theoreticians. These were Academician B. N. Yur'yev, Professor A. M. Cheremukhin and Professor I. P. Bratukhin – creators of first Soviet helicopters of the 1930's from 1EA to 11EA; Professor Focke – designer of helicopters FW-61 and FA-223 in Germany, one of pioneers of aviation Lours Brequet and Professor Doran, who created the first French helicopters, and others.

It should be noted that at present the theoretical training of designers working in leading firms of the world in the field of helicopter construction, as far as can be judged from literature, is very high. Therefore, not only the design engineer but also the designer working in helicopter construction should not have any difficulties in mastering of the material discussed below.

The authors hope that this second book of the given work will be discovered by readers and will be useful.

* * *

On the inserts there are photographs of basic Soviet helicopters found in serial production. The first Soviet series of helicopters with reciprocating engines, the Mi-1 and Mi-4, were created in 1949 and 1952. Built in great quantities, these are now some of the most widespread types of helicopters.

Shown further is the helicopter Mi-6 with two turboprop engines, developed in 1957, and helicopter Mi-10 (1962), a flying crane with high landing gear adapted for transport of large-scale loads rigidly secured under the fuselage. In 1965 it established the world record for load capacity for helicopters when 25 tons were lifted to an altitude of 2830 m.

Helicopters Mi-2 and Mi-8 are also shown, which are the second generation of Soviet light and medium helicopters. The lifting systems from Mi-1 and Mi-4 were retained on them, but instead of having one piston engine there are two turboprop engines.

Footnote

[1]On the helicopter Mi-4 flutter always appears primarily in these conditions.

C H A P T E R I

ELASTIC OSCILLATIONS AND BLADE STRENGTH

The calculation of elastic oscillations is an obligatory element in the process of the creation of new blade designs. It enters as an inalienable part into the calculation of blade for strength.

To create blades of a helicopter it is necessary to solve much of the time very complex technological and design problems. With their solution one should consider the most diverse requirements and first of all the requirement of providing high fatigue strength to the structure.

The work involved in the creation of blades includes usually the following basic stages:

- Selection of materials for separate elements of the structure, determination of optimum parameters and designing of the blade.

- Selection of the best technological processes providing the highest fatigue strength of its basic force elements and manufacture of the blade.

- Flight tests with the measurement of effective stresses in flight.

- Dynamic tests and appraisal of the blade service life.

– Carrying out of a complex of finishing works, including works on the lowering of effective stresses and increase in fatigue strength of the structure.

– Completing tests and starting construction in serial production.

– Analysis of the work of serial blades in different conditions of mass and prolonged operation and the carrying out further improvement of commercial construction according to the results of this analysis.

Calculations of elastic blade oscillations must be fulfilled in many stages of this work but mostly in the most initial stage, which is finished by designing of the blade.

In the selection of parameters of the blade and materials for its manufacture, one of the basic criteria is the magnitude of effective varying stresses in flight and the relationship between these stresses and stresses characterizing fatigue strength of the structure. It is possible to learn the magnitude of these stresses and to give an appraisal of the structure with respect to its strength in this stage only with the help of calculation. To design a blade in the required, usually very short, periods the designer should have at his disposal perfected methods and means of fulfillment of the design, which allow giving a rapid answer to any of the appearing questions.

Of no lesser importance is the calculation during finishing works. As a rule, in newly created blades there appear too great varying stresses, and the designer has the problem of reducing them. For this it is first of all necessary to confirm by calculation the regularity of the appearance of stresses measured in flight and then to find the possibility by means of changing certain parameters of the blade to decrease their magnitude. To find the solution of this problem without calculation, as a rule, means to lose very much time in checking incorrect proposals and to expend a great deal of means in the manufacture of blades, which subsequently after a flying check will be rejected.

Reducing varying stresses is extremely important and permits not only increasing the reliability and service time of the blade but also improving the technical flying characteristics of the helicopter such as, for example, the speed of flight and load capacity, since for contemporary helicopters they are frequently limited in conditions of stability.

The solution to all these questions would not create considerable difficulties if the calculation gave results, quite accurately coinciding with the fact that it is observed in reality during measurement of stresses in flight. Unfortunately, this is not quite so; not in all cases does the calculation give satisfactory results for practice.

The most reliable are calculations by determination of frequencies of natural oscillations. Attained in them is an accuracy usually of the order of ±2%. Therefore, all calculations connected with the exclusion of resonances provide a very high reliability. Of noticeably lesser reliability are calculations of varying stresses at cruising and maximum speeds of flight. The stresses obtained with these calculations usually prove to be 15-25% less than stresses measured in flight. Therefore, the calculation of stresses in these conditions does not always satisfy the designer. But it is necessary to say that this error can to a certain degree be compensated, if into the calculation there is introduced a correction which considers the constantly observed divergence with the experiment.

Still a great error is possible during calculation of varying stresses at low flight speeds.

From what nas been said it is obvious that the method of calculation of varying stresses in the blade still requires further development. Nonetheless, practice shows that the selection of parameters and finishing of blades without the use of even such still not quite perfected methods of calculation proves to be very ineffective. Therefore, in this chapter there is given a sufficiently detailed account of different methods of calculation. This, as it

seems to us, enables giving to the reader a concept about all peculiarities of the load of the blade in flight, showing the possible means of approach to its calculation, revealing and estimating the advantages and deficiencies of different methods and, finally, giving to engineers studying this problem the basis for further deepening of investigations and improvement of methods of calculation.

Along with a description of different methods of calculation of elastic oscillations of the blade, to which the basic attention is given, in this chapter there are also discussed basic principles on which are based calculations of blade for strength and determination of its service life (§ 11).

Regarding concrete data on the selection of parameters of the blade, it is expedient for us to refer this question to the section "Designing of the blade," which will be included in the third book.

§ 1. Problems of Calculation, Basic Assumptions and Derivation of Differential Equations of Flexural Deformations of the Blade

1. Finite Goal of the Calculation of Elastic Oscillations of the Blade

The calculation of elastic oscillations of blade appears necessary for the solution of a number of problems appearing in the designing and finishing of a helicopter. The most important of them is the problem of the determination of variable flexural stresses in the blade. Determination of these stresses is the main part of calculation for strength. Therefore, the main task of this chapter is to determine elastic oscillations of the blade for calculation of its strength.

GRAPHIC NOT
REPRODUCIBLE

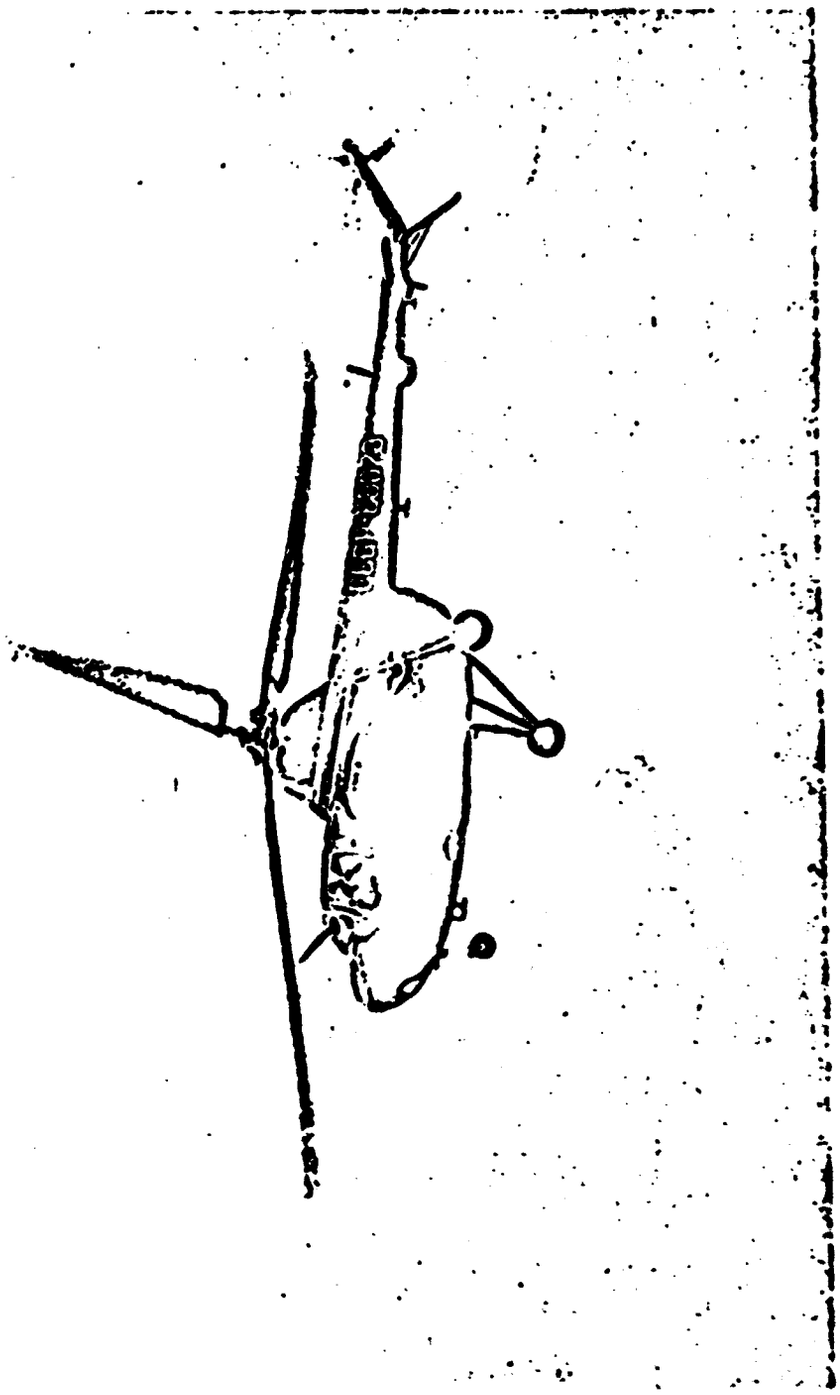

Hellcopter MI-1.

GRAPHIC NOT
REPRODUCIBLE

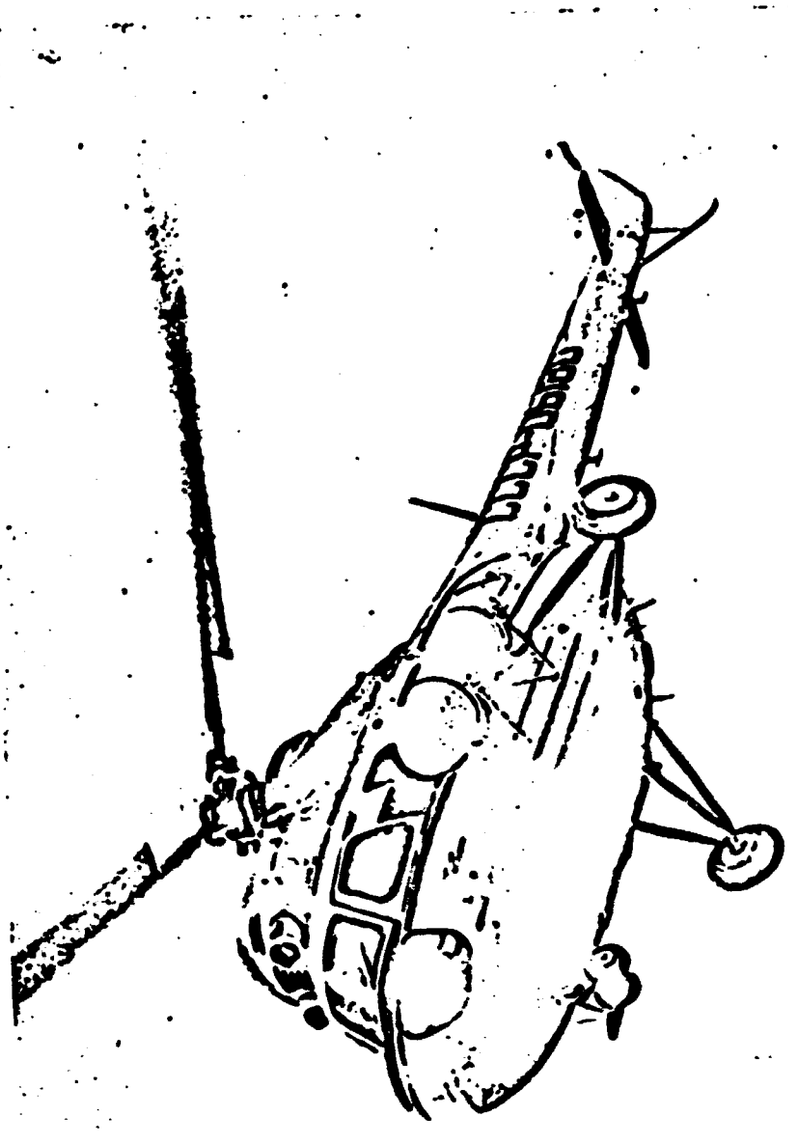

Helicopter Mi-2.

GRAPHIC NOT
REPRODUCIBLE

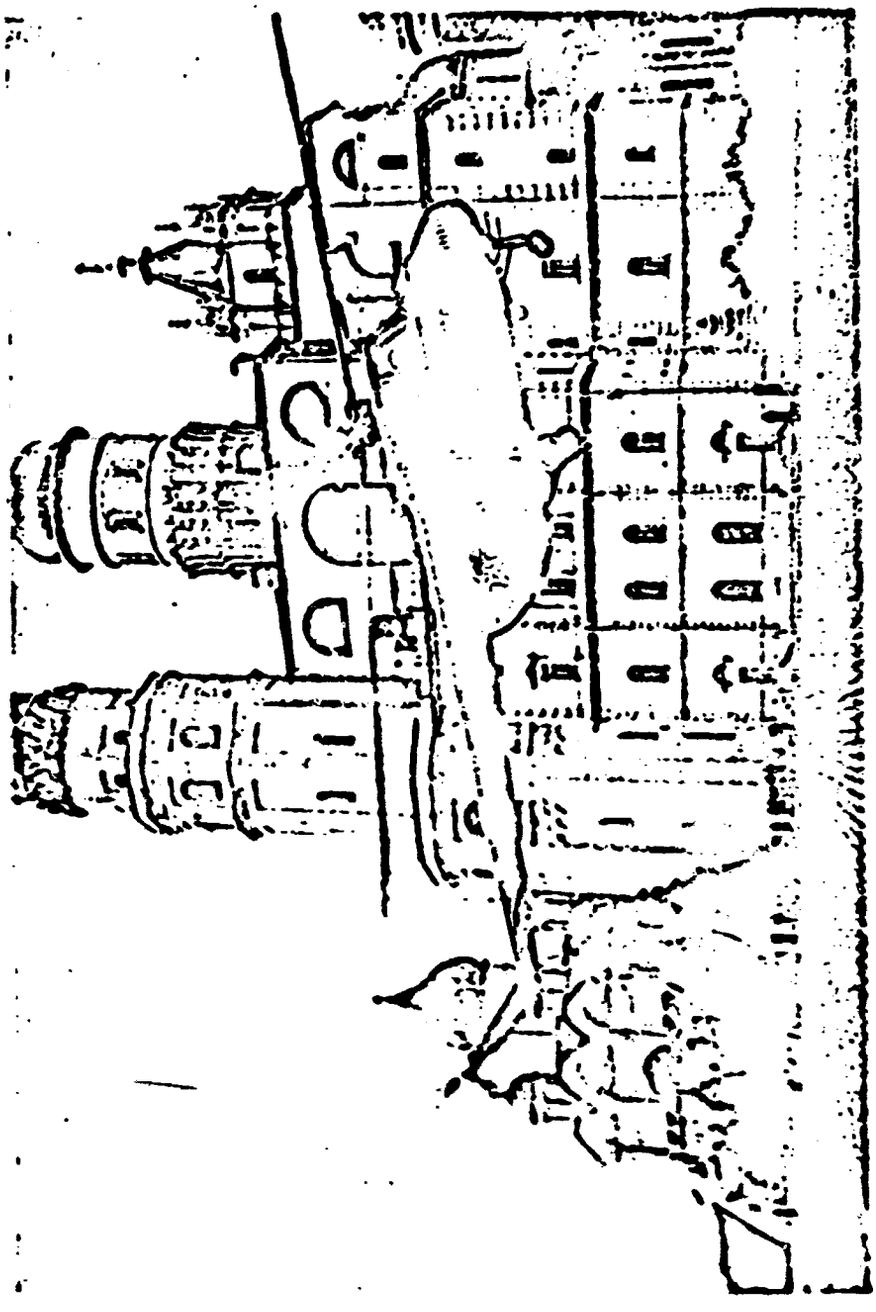

Helicopter MI-4.

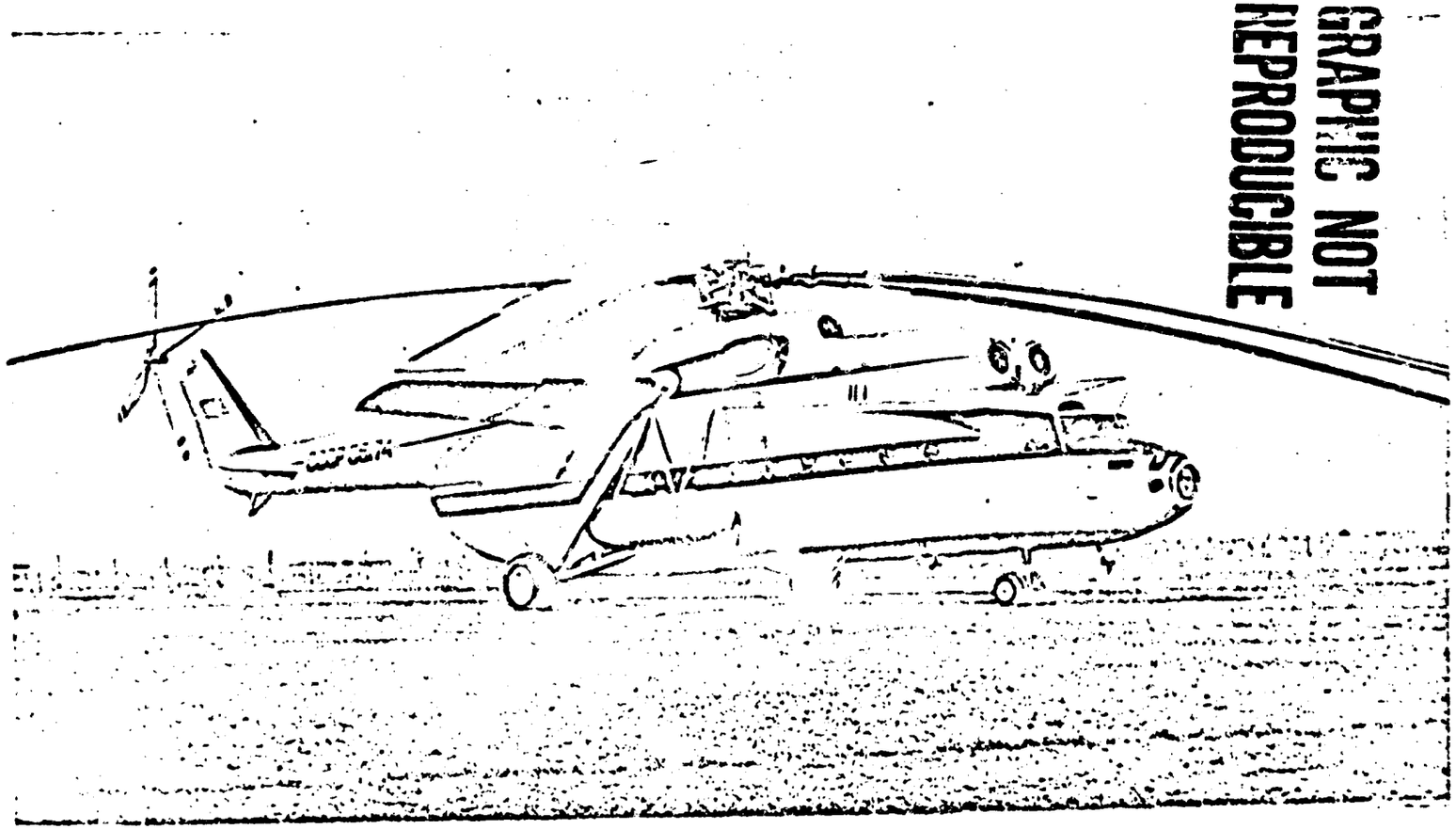

Helicopter Mi-6.

GRAPHIC NOT REPRODUCIBLE

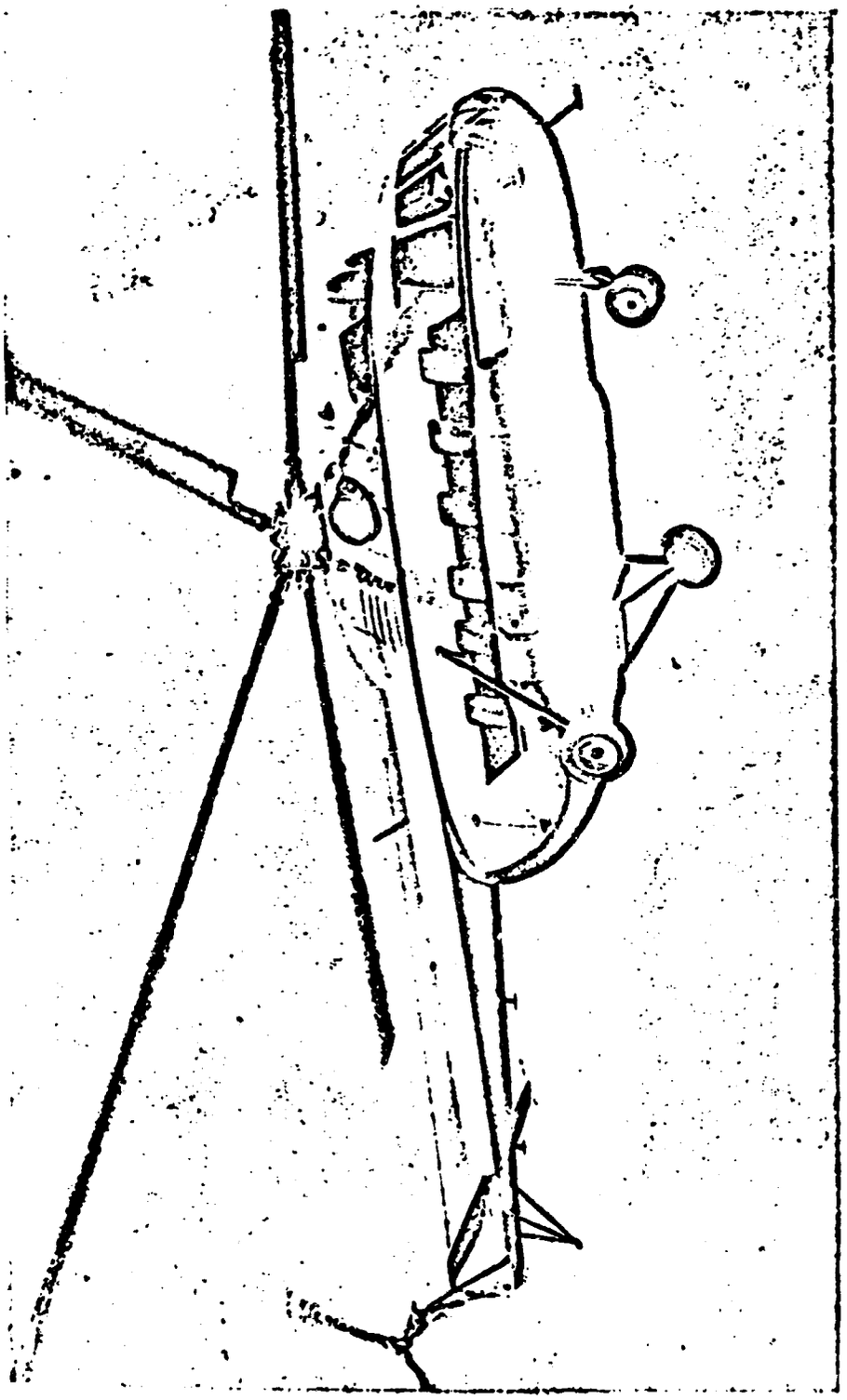

Helicopter MI-8.

Helicopter Mi-10.

Determination of oscillations of the blade appears necessary and for the solution of many other problems. Without the calculation of these oscillations it is impossible to find the loads, arriving on the helicopter, its hub, control system and on the drive transmission of the rotor. Determination of live loads arriving from the rotor blades to the helicopter to a considerable degree solves the problem of the determination of vibrations of a helicopter.

There is also interest in the question of the influence of oscillations of the blade on the flying characteristics of the helicopter. Limitations put on the flying characteristics by separation of flow from the rotor blades are determined previously always by the permissible amplitude of oscillations of the blade. With an increase in these amplitudes variable forces in the control system and vibration of the helicopter are increased. Therefore, the calculation of elastic oscillations of blades permits most accurately estimating the borders of conditions permissible in conditions of separation of flight of the helicopter.

To a certain degree the oscillations of the blade, and first of all its torsional vibrations, affect the aerodynamic properties of the rotor with removal from conditions with the separation of flow.

Let us discuss more specifically the first of the problems stated here.

2. Calculation of Blade Strength

Calculation of blade for strength includes determination of constant and varying stresses at all points of the blade structure in different load conditions. The most dangerous of them are separated as cases calculated for strength of the structure.

Usually with the creation of new blades, when the time assigned for fulfillment of the calculation and their analysis is very greatly limited, the number of calculation cases is desirably reduced

to a minimum. Experience shows that it is sufficient to examine one case of the loading of blades under conditions of helicopter operation on land and a number of flight cases on different flight conditions.

The first case provides for the necessity of design of a blade supported by a vertical hub limiter when the action of centrifugal forces was ceased or almost was ceased. This occurs when the rotor does not rotate or is in the initial stage of acceleration, or it stops after the flight. In the absence of centrifugal forces the forces of weight or inertial forces, appearing with a blow of the blade against the limiter, cause in it considerable flexural stresses. Especially difficult for the strength of the blade are compressive stresses. Experiments show that separate overloads of the blade, at which there appear considerable compressive stresses, can have an effect on the fatigue strength of the structure and, consequently, also on its service life. Usually static stresses from the bend of the blade, under the action of its intrinsic weight, are limited to magnitudes σ_G = 25-28 kG/mm^2 for a blade with a steel longeron and σ_G = 7.0-7.5 kG/mm^2 for a blade with a longeron made of Duralumin.

From the point of view of calculation this case presents no difficulties. Therefore, we will not discuss it in detail here.

Other cases pertain to different conditions of flight of the helicopter, when to the constantly effective stresses from centrifugal forces are added constant and varying stresses from bending of the blade. This combination of loads proves to be very difficult for fatigue strength of the blade construction.

3. Conditions of Flight Which are Dangerous for Fatigue Strength of the Construction

Measurements of stresses in flight show that blades of the helicopter experience considerable live loads dangerous for strength of construction in conditions of two different types.

The first type of conditions pertain to conditions of flight at low speeds when the speed of flight comprises 3-8% of the final velocity of the blade (μ = 0.03-0.08). In these conditions of flight there is observed a sharp increase in amplitudes of flexural vibrations of the blades, and varying stresses are increased respectively.

The indicated speeds of flight is used by the helicopter with acceleration, horizontal flight with stabilized low speed and in conditions of deceleration. Usually the greatest varying stresses appear in conditions of deceleration. Considerable stress can also appear in conditions of steep descent with low horizontal speed.

In conditions of design load flights at low speeds are, as a rule, short-term conditions of the flight, in any case for helicopters conducting transport work. However, because of great stresses frequently these conditions determine the service life of blade by conditions of durability.

Flights at high speeds belong to the second type of conditions dangerous for fatigue strength. These are, first of all, flights at cruising and maximum speeds. The flight at cruising speed is usually the most continuous mode of flight and therefore introduces into the design considerable fatigue damage.

The sharp increase in varying stresses at low speeds is explained first of all by the considerable irregularity of the field of inductive speeds appearing at these conditions in the flow flowing through the rotor. Moreover, in its absolute magnitude inductive speeds in these conditions reach the largest values as compared to all other conditions of flight. Therefore, their influence on the magnitude stresses at low speeds of flight considerably increases. The alternating field of inductive speeds leads to the appearance of variable aerodynamic loads on the blade. Under the impact of these loads the blade accomplishes flexural vibrations, and this is why in it there appear considerable varying stresses.

At high speeds of flight variable aerodynamic loads appear mainly due to the pulsation of relative flow rate and change in angles of attack of blade sections along the azimuth of the rotor. The alternating field of inductive speeds in these conditions weakly affects the values of the aerodynamic load.

With calculation for strength it sometimes is also necessary to examine the case of possible rotor acceleration in flight when centrifugal forces considerably increase. Here the constant part of effective stresses in the blade is increased.

4. Assumption of the Uniform Field of Induced Speeds

From what has been mentioned above, it is clear that the calculation of variable aerodynamic loads on low speeds is impossible without taking into account the alternating field of induced speeds.

With an increase in speed of the flight the absolute magnitude of induced speeds drops. The influence of their irregularity on magnitudes of aerodynamic loads decreases. Therefore, starting from average speeds of flight, when $\mu \geq 0.2$, with the calculation of varying stresses in the blade it is possible approximately to consider that the field of induced speeds is uniform, i.e., that the induced speeds are constant along the disk of the rotor. This assumption leads to very serious simplifications of all the computations and a sharp reduction of duration of the calculation. Therefore, it is widely used in practical calculations.

However, the accuracy of results obtained taking into account this assumption frequently does not satisfy the designer. Therefore, in many cases with the calculation of flight conditions with average and great speed this assumption must be renounced.

5. Assumptions Utilized During Calculation of Aerodynamic Loads on the Blade Profile

In all methods of calculation discussed in this chapter, it is assumed that the aerodynamic forces having an effect on the blade profile can be determined by using aerodynamic coefficients referrin-

to stationary flowing around of an infinitely long wing in plane-parallel flow. The nonstationaryity of the flowing around is considered only in values of angles of attack of the profile in which inductive downwash is introduced.

Consequently, to determine forces having an effect on the element of the profile, it is sufficient to determine its angle of attack α and relative speed of flowing around its flow U. Then, knowing α and Mach number $M = \frac{U}{a_\infty}$ (here a_∞ is the speed of sound), along the polar of the profile one can determine coefficients c_y and c_x and, consequently, also forces having an effect on the profile. When necessary there is determined also coefficient m_z.

If in examined flight conditions the angle of attack of the profile does not exceed $\alpha \approx 9°$, and the Mach number is not more than $M \approx 0.5$, then its influence can be disregarded, and we can assume that

$$c_y = c_y^\alpha \alpha, \qquad (1.1)$$

where c_y^α is the tangent of the angle of inclination of dependence $c_y = f(\alpha)$.

This assumption is used during calculation of loads in conditions sufficiently remote from separation in which, furthermore, it is possible to disregard phenomena connected with the compressibility of flow.

The possibility of application of certain assumptions with respect to the method of determination of aerodynamic forces has decisive importance in the selection of the method of calculation of stresses, which in the examined case should be used. Due to this in various conditions of flight the most expedient appears to be the application of different methods of calculation. Therefore, subsequently we will separate three types of conditions, which are distinguished by the fact that in each of them best results can be

obtained by different methods of calculation. These are conditions of low, average and high speeds.

In conditions of low speeds it is impossible not to consider the alternating field of inductive speeds, but with moderate loads on the blade it is possible to use linear aerodynamics. At average flight speeds calculation of the alternating field of inductive speeds appears necessary only with the solution of special problems connected with the necessity of separation of separate high harmonics of aerodynamic loads. Calculation of nonlinear dependences in the determination of aerodynamic coefficients at these speeds is almost always unnecessary. And, finally, in conditions of high speeds lying near the border of separation, calculation of these nonlinearities becomes obligatory, whereas the changeability of the field of inductive speeds in the greater part of cases cannot be considered.

The enumerated considerations lead to the fact that separate methods of calculation can be attached to definite conditions of flight.

6. The Connection Between Deformations with Bend in Two Mutually Perpendicular Directions and Assumptions in Calculations Taken in Connection with This

Usually the blade of a helicopter is designed in such a way that the main elastic moments of inertia of its sections are essentially different in magnitude. Therefore, the blade is a rod stretched by centrifugal forces whose every section possesses different rigidity in two mutually perpendicular directions. In order to characterize these directions through the axis of the rod in the direction of principal axes of the section there are conducted planes called planes of the greatest and least rigidity (Fig. 1.1).

Frequently for creation of aerodynamic blade twist not only frame forming its external surface twists, but also the blade longeron. In this case directions of the main elastic axes of the section are changed along the length of the blade, and geometrically

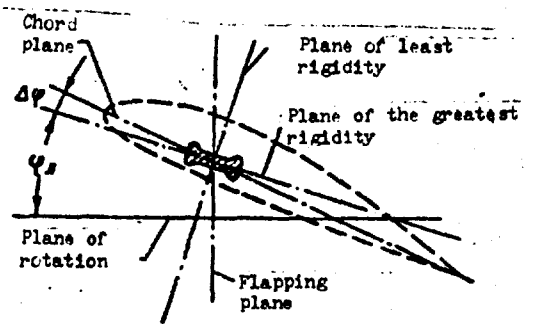

Fig. 1.1. Diagram of location of the longeron in the case when geometric twist is carried out with the help of turn of the frame with respect to the longeron ($\varphi_z = \text{const}$).

it becomes a twisted rod. In other cases aerodynamic twist is fulfilled only due to the turn of the blade frame with respect to the longeron.

In external forces in the most diverse directions act on the blade profile. This makes the problem of blade bending a very complex spatial problem.

At the same time the magnitude of geometric twist for blades of helicopters is not very great (of the order of 6-12°) and considerably less than that for aircraft propellers and blades of compressors and turbines. As different appraisals show, the influence of this twist on results of calculations is small. Therefore, in all the methods of calculation given here we will disregard twistness of elastic axes of the blade longeron and consider that the direction of the plane of greatest and least blade rigidity is constant along its length.

This assumption permits projecting all external forces on these planes and solving the two elastically unbound two-dimensional problems of blade bending in two mutually perpendicular directions. Upon completion of the calculation for determination of stresses at different points of the blade section, results of these two calculations can be added.

The profile of the blade section permits increasing dimensions of the longeron in the chord plane and limits them in a perpendicular direction. Therefore, the plane of the greatest rigidity is usually close to the plane passing through the blade chord. This circumstance

and also the fact that in the chord plane the magnitude of aerodynamic forces is usually less than that in the plane perpendicular to it leads to the fact that the magnitude of flexural stresses is usually larger with bending in the plane of least rigidity and less in the plane of greatest rigidity. If one were to examine contemporary designs of blades for which fatigue strength is approximately identical with bending in all directions, then it will appear that bending in the plane of least rigidity is considerably more dangerous. In practice usually all difficulties appear in connection with the necessity to provide strength with bending in this plane. Therefore, in this chapter methods of calculation of blade oscillations only in the plane of least rigidity will be examined. With calculation in this plane it is possible to apply the additional assumption about the fact that the plane of least rigidity coincides with the plane passing through the axis of the rotor. We will subsequently call this plane the flapping plane.

7. Calculation of Torsional Deformations of the Blade During Calculation of Flexural Oscillations

Twisting deformations change the angles of attack of the blade sections of blade and, consequently, also the aerodynamic forces having an effect on them. Therefore, they should be considered during calculation of aerodynamic loads and oscillations of the blade. However, calculation of torsional vibrations of the blade is considerably difficult and greatly complicates the calculation.

At the same time in a whole series of cases it does not lead to considerable refinement of the results. Therefore, calculation of torsional deformations should be produced only if there is an imperative necessity. For example, this is true in those cases when flexural flutter, although such a position indicates insufficient reserve prior to flutter and cannot be considered permissible.

To calculate torsional deformations it is necessary to solve a system of differential equations of flexural-torsional vibrations of the blade. The solution of this system is fulfilled with the calculation of flutter. Therefore, such a method of calculation,

called the general method of calculation of flutter and flexural stresses in the blade, is referred in the first book (see § 7 of Chapter IV).

In this chapter only methods of calculation of free torsional (§ 5) and flexural-torsional vibrations (§ 6).

8. Two Stages of Calculations in the Designing of the Blade: Calculation of Frequencies of Natural Oscillations and Calculation of Stresses

If a newly created blade of a helicopter does not very greatly differ in its geometric and mass characteristics from an already made and proved blade, then it is possible to affirm that on identical conditions of flight, the varying stresses acting in it will be approximately the same as in the blade which is its prototype. However, this position is disturbed in those cases, when due to a certain change in its parameters the blade appears in resonance with some harmonic of external forces.

The practice of blade designing shows that sufficiently reliable blades can be created only when none of the blade's natural frequencies coincides with frequencies of external forces and is at sufficient distance from them. This pertains to oscillations of the blade both in the plane of the least and in the plane of greatest rigidity. It follows, of course, to stipulate that not all harmonics of external forces are dangerous for strength but only those whose magnitude is sufficient for creation of stresses considerable in magnitude. In practice usually the absence of resonances should be provided with harmonics no higher than the eighth to revolution of the rotor. Higher harmonics of external forces are not substantial.

Thus, if a gross error in the selection of characteristics of the blade is not allowed, then for the limitation of varying stresses in permissible limits, it appears sufficient only to provide the absence of resonances. It is not necessary to produce calculation of values of amplitudes of varying stresses in this case. Therefore,

frequently an experienced designer can be limited only to the first stage of design of a blade: determination of its frequencies of natural oscillations and construction of a resonance diagram.

From what has been said it results that the calculation of frequencies and forms of natural oscillations of a blade is not only an auxiliary stage for the calculation of stresses, but it has an independent importance as a preliminary stage of calculation of blade for strength.

9. Idealized Blade Models Used in the Calculation

With fulfillment of the calculation it is necessary to present the blade in the form of a certain idealized mechanical model for which there would be correct all the accepted initial assumptions, so that subsequently in the process of calculations there would be no need to use approximate mathematical operations.

During calculation on digital computers the problem should be stated in such a way that its solution is possible with any accuracy assigned in advance and accessible for the machine.

As experience has shown, the application of methods of calculation using approximate mathematical operations very frequently leads to different misunderstandings. In a number of cases, only because of the inaccuracy with calculations, can it appear impossible to bring the calculation to an end. Thus, for example, during calculation of forms of natural oscillations by the method of successive approximations, it is necessary to calculate a whole series of integrals. Frequently this is done by the trapezoid method. With the limited quantity of intervals of integration this method gives so large an error that during calcualtion of forms of oscillations of higher tones, the ordinate of which are calculated in the form of small differences of large values, the method of successive approximations ceases to converge.

This circumstance requires special caution during the use of approximate methods of calculations. Therefore, it is more expedien

to introduce a simplified idealized model of a blade which would be convenient to calculate with an accuracy maximum permissible for the machine.

Three different types of mechanical models which are frequently used in calculations are well-known.

Beam model with continuously distributed parameters. In this model the blade is represented in the form of a beam with continuously distributed rigidities EI, linear mass m and parameters determining the magnitude of linear aerodynamic load.

Such a model is very convenient with the composition of initial differential equations and application to them of well-known methods of approximation of the solution, but it appears unsuitable for complete numerical calculation. Below we will frequently use such a model for the derivation of calculation formulas in order in the stage of numerical calculation to use formulas recorded by analogy and which pertain to the model with discrete parameters. In these formulas all the integrals of functions dependent on the radius of the blade are replaced by sums of discrete quantities referring to a series of fixed radii of the blade.

Beam model with concentrated loads. In this model the blade is represented in the form of a system of concentrated loads connected with each other. The connection between these loads is carried out by means of weightless beams possessing constant (in length) bend rigidity equal to the rigidity of corresponding sections of the blade.

With the determination of aerodynamic forces it is assumed that to every load is fastened a separate flap whose area is equal to the area of the corresponding blade section. Usually it is assumed that the area is

$$S_i = \frac{1}{2}(l_{i-1,i} + l_{i,i+1})\, b_i, \qquad (1.2)$$

where $\ell_{i-1,i}$ and $\ell_{i,i+1}$ are lengths of adjacent sections into which the blade is divided with calculation; b_i – chord of blade in the section between these sections.

This model most accurately reflects the properties of the real blade. Therefore, in almost all cases during practical calculation it will be used.

It is necessary, however, to note that the beam model possesses these positive properties only at the number of sections z equal to 25-30 and more. With a decrease in the number of sections the form of deformations of the beam model starts very greatly to differ from the form of deformations of the blade. This circumstance will be more specifically illustrated in § 10, No. 3. Furthermore, application of the beam model leads in a number of cases to a very complex system of formulas and sometimes even hampers fulfillment of the calculation. In these cases the simpler hinged model of the blade can be used.

Hinged blade model. In this model the blade is represented in the form of a multihinged link consisting of absolutely rigid weightless sections with masses concentrated in the hinges. The bending rigidity of the blade is simulated by elastic elements concentrated in the hinges. Under the impact of external forces the axis of such a chain will take the form of a broken line and not a smooth one as in the model of the beam type. This circumstance, just as the operation of the selection of rigidity of elastic elements, introduces a definite error with transition from the blade to a mechanical model.

At the same time the application of a hinged model creates so considerable simplifications in the calculation formulas that sometimes the application of improved methods of calculation which were practically unrealizable in the use of the beam model is possible. This compensates for deficiencies peculiar to this model.

It is still necessary to add that with a decrease in the number of sections into which the blade in the calculation is divided,

properties of models start very greatly to differ from properties of the real balde. But for the hinged model these errors increase not as rapid as those for the beam model. Due to this the hinged model can appear more profitable in the application of rough methods of calculation when the blade is divided into a small number of sections, let us say of the order of 10-12.

10. Derivation of the Differential Equation of Bend of the Blade in the Field of Centrifugal Forces with Oscillations in the Flapping Plane

Let us represent the blade in the form of a beam with continuously distributed parameters. Let us separate for consideration the element of the beam with length dr. The forces having an effect on this element are shown in Fig. 1.2.

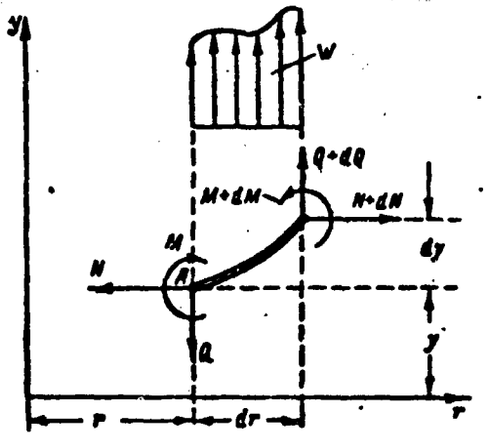

Fig. 1.2. Diagram of forces having an effect on the element of the blade.

Let us compose the equations of equilibrium of this element, being limited to quantities of only the first order of smallness. Then the sum of projections of forces on axis y can be recorded as

$$Wdr+dQ=0, \tag{1.3}$$

and the sum of moments of all forces with respect to point A

$$Qdr+dM-Ndy=0, \tag{1.4}$$

where W is the linear external load on the blade; Q – shear

force in the blade section; M – bending moment; N – centrifugal force in the blade section.

From equation (1.3) we will obtain

$$W=-Q'. \tag{1.5}$$

Here and below the prime denotes differentiation with respect to the radius of the blade.

Differentiating equation (1.4), we will obtain

$$Q'=-M''+[Ny']'. \tag{1.6}$$

If we assume M + Ely" and substitute expression (1.6) into equation (1.5), then we will obtain the well-known differential equation of flexural deformations of the blade in field of centrifugal forces:

$$[EIy'']''-[Ny']'=W. \tag{1.7}$$

Let us present the external load W, which consists of aerodynamic and innertial loads:

$$W=T-m\ddot{y}, \tag{1.8}$$

where T is the linear aerodynamic load; m – linear mass of the blade.

The two dots here denote differentiation with respect to time.

Substituting expression (1.8) into equation (1.7), we will obtain the differential equation of blade oscillations:

$$[EIy'']''-[Ny']'+m\ddot{y}=T. \tag{1.9}$$

In a vacuum, when the aerodynamic load T is equal to zero, equation (1.9) will describe free oscillations of the blade in the field of centrifugal forces:

$$[EJ_y y']' - [Ny']' + m\ddot{y} = 0. \qquad (1.10)$$

Solution to this equation has well-known difficulties. Therefore, in § 2 in the beginning its solution for the case N = 0 pertaining to an irrotational blade will be examined.

11. Differential Equation of Blade Bending in the Plane of Rotation of the Rotor

With bend of the blade of rotation, because of concentricity of the field of centrifugal forces on the element of the blade, there will act an additional force which did not enter into equations in the flapping plane. Taking into account this circumstance, equation (1.8) should be copied in the form

$$\bar{W} = Q + \omega^2 mx - m\ddot{x}, \qquad (1.11)$$

where Q is the aerodynamic force in the plane of rotation; x is the movement of blade elements in the plane of rotation.

Substituting (1.11) into the equation analogous (1.7) but recorded for the plane of rotation, we will obtain the differential equation of bend of the blade in this plane:

$$[EJ_x x']' - [Nx']' - \omega^2 mx + m\ddot{x} = Q. \qquad (1.12)$$

This equation differs from equation (1.9) only by the additional term $\omega^2 mx$.

§ 2. Free Oscillations of a Blade of an Irrotational Rotor

1. Method of Calculation Leading to the Solution of the Integral Equation of Blade Oscillations

The calculation of forms and frequencies of natural oscillations of a blade of an irrotational rotor is quite widely discussed in literature (see, for example, [1]). In this paragraph only certain

basic positions and somewhat refined formulas used during practical calculations will be briefly repeated.

Let us consider the differential equation of oscillations obtained for the blade model with continuously disturbed parameters. If in equation (1.10) we assume N = 0, then it will take the form

$$[EIy'']''+m\ddot{y}=0. \tag{2.1}$$

Having assumed

$$y=\bar{y}\sin pt \tag{2.2}$$

and substituting into (2.1), we will obtain

$$[EI\bar{y}'']''-p^2m\bar{y}=0. \tag{2.3}$$

With further calculations we will omit the dash above the y. Let us integrate equation (2.3), taking into account boundary conditions of the blade fastening. For simplicity we will examine the case of the blade rigidly sealed in the shank with these boundary conditions:

- for r = 0; y = 0; y' = 0;

- for r = R; M = 0; Q = 0.

As a result of the fourfold integration, equation (2.3) will be converted into an integral equation fo the form

$$y=p^2\int_0^r\int_0^r\int_0^r\int_0^r\frac{dr^4}{EI}\int_r^R\int_r^R\int_r^R\int_r^R my\,dr^4. \tag{2.4}$$

Equation (2.4) is solved usually by the method of successive approximations. Having assigned the arbitrary form of y, standardized by some manner, for example

$$y_n=1, \tag{2.5}$$

we will substitute it into the right-hand side of equation (2.4).

Fulfilling integration, we will obtain the function

$$u=\int_0^r\int_0^r\frac{dr^2}{EI}\int_r^R\int_r^R mydr^2, \tag{2.6}$$

such that $y = p^2u$.

Whence, using condition (2.5), we obtain

$$p^2=\frac{1}{u_R}, \tag{2.7}$$

where u_R is the value u for r = R.

Let us repeat the same operation, taking the new value

$$y=p^2u. \tag{2.8}$$

Fulfilling the above-described operation several times, one can be certain that the form of oscillations y and frequency p converges to defined values which are the solution of the integral equation (2.4).

The thus used method of successive approximations results in the fact that the determined form of y converges to the form of the lowest tone of natural oscillations of the blade.

To determine the subsequent tones it is necessary still to fulfill the condition of orthogonality of tones of natural oscillations. This condition will be examined in No. 3.

With practical application of the method of calculation expounded here it is very important to select a sufficiently accurate method for calculation of the integral expression (2.6). If parameters of the blade are assigned in the form of continuous functions, then the simplest method of calculation of integrals (2.6)

is the one usually used in such cases, the trapezium method. However, as was already noted above, with calculation of higher tones of oscillations the error inserted by this operation leads to so considerable errors that such a method cannot be used for practical purposes. This deficiency vanishes if for the calculation of integrals (2.6) we use the method resulting from examination of the mechanical model of the blade with discretely distributed parameters.

2. Calculation of Forms and Frequencies of Natural Oscillations of the Blade Model with Discretely Distributed Parameters

For the calculation let us use the model of the beam type with concentrated loads (see § 1, No. 9). For this we will divide the blade into z sections. Lengths of the separate sections can be different. The weight of the blade will be concentrated along the edges of these sections in the form of separate discrete loads with mass m_i. The flexural rigidity of the blade will be represented by a step curve in such a way that for the extent of each section it remains constant (Fig. 1.3).

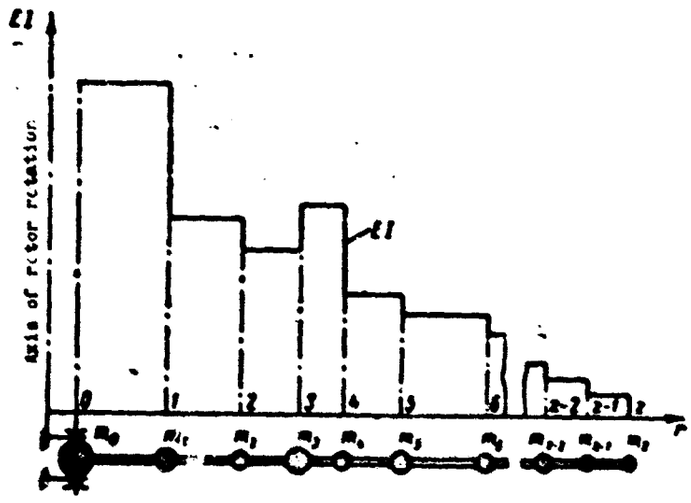

Fig. 1.3. Calculation model of the blade.

In the same way as in No. 1, we will examine in the beginning the case of the blade sealed in shank. The operation

determined by equation (2.6) in this case can be carried out absolutely accurately.

Actually, let us assign the arbitrary form of load movements of the model y_i. Here we call the form of movements the system of discrete values y_i ($i = 0, 1, 2, 3, \ldots, z$ – ordinal number of concentrated loads of the model). Thus, just as above (see condition 2.5), let us assume that $y_z = 1$. If movements y_i are known, one can determine the inertial forces of the loads iwth their oscillations at the frequency $p = 1$. They are determined by the expression

$$F_i = m_i y_i. \qquad (2.9)$$

Knowing the inertial forces, one can determine all the bending moments about the system of simple recurrence formulas of the form

$$M_i = l_{i,i+1}(F_{i+1} - a_{i+1}M_{i+1} - b_{i+1}M_{i+2}). \qquad (2.10)$$

where $l_{i,i+1}$ are the length of the blade section between the i-th and i + 1-th concentrated mass.

Coefficients a_i and b_i are determined by the formulas

$$b_i = -\frac{1}{l_{i,i+1}};$$
$$a_i = -b_{i-1} - b_i.$$

Calculation of bending moments by the formulas (2.10) should be started from the end of blade, assuming in the beginning that $i = z - 1$ and bending moments M_z and M_{z+1} are equal to zero.

After determination of the bending moments it is easy to determine deformations of the blade. Blade deformations with oscillations at frequency $p = 1$ will be, as above, designated by the letter u.

The magnitude of these deformations is determined by the recurrence formulas of the form:

$$u_i = l_{i-1,i}[D_{i-1} - b_{i-2}u_{i-2} - a_{i-1}u_{i-1}], \tag{2.11}$$

where

$$D_{i-1} = d_{i-1}M_{i-1} + c_iM_i + d_iM_{i+1}. \tag{2.12}$$

Here

$$\left.\begin{aligned} d_i &= \frac{l_{i,i+1}}{6EJ_{i,i+1}}; \\ c_i &= 2(d_{i-1} + d_i). \end{aligned}\right\} \tag{2.13}$$

Calculation deformation u_i should be started from the shank of the blade, assuming in accordance with boundary conditions accepted here that $u_0 = 0$. All quantities with negative indices should also be assumed equal to zero.

Thus fulfillment of operations (2.10) and (2.11) in reference to the beam model with discrete distribution of parameters leads to the calculation of accurate values of u_i.

Determining p^2 just as earlier [see (2.7)]

$$p^2 = \frac{1}{z_s} \tag{2.14}$$

and new values

$$y_i = p^2u_i, \tag{2.15}$$

we repeat all operations as many times as is necessary so that the method of successive approximations agrees. Usually the calculation is considered finished when the difference of values y_i in two successive approximations appears less than the assigned accuracy ε_y.

3. Condition of Orthogonality and the Calculation of Subsequent Tones of Natural Oscillations

The method of successive approximations stated above leads to the determination of lowest tone of natural oscillations. With determination of following tones it is necessary to still fulfill conditions of independence of oscillations according to different tones.

Let us imagine that free oscillations of the blade in a vacuum occur simultaneously by two forms $y_i^{(j)}$ and $y_i^{(m)}$. One can determine the energy of oscillations according to each of the forms separately by peak values of the kinetic energy:[1]

$$\left.\begin{aligned} K_j &= \sum_i m_i [p_j y_i^{(j)}]^2; \\ K_m &= \sum_i m_i [p_m y_i^{(m)}]^2. \end{aligned}\right\} \qquad (2.16)$$

On the other hand the total energy of the system, fluctuating simultaneously by two forms, can be determined by the peak value of the total kinetic energy:

$$K_s = \sum_i m_i [p_j y_i^{(j)} + p_m y_i^{(m)}]^2. \qquad (2.17)$$

The system possesses this kinetic energy at that moment of time when the blade passes during oscillations through the neutral position simultaneously by two forms $y_i^{(j)}$ and $y_i^{(m)}$. Because of the distinction in values of frequencies of natural oscillations such a position can appear relatively rarely, but can easily be created artificially by means of assignment of corresponding phases of oscillations at the initial instant.

If the amplitude with respect to each of the component forms of oscillations does not change with the course of time, then their energy, determined by formulas (2.16), remains constant.

The total energy of the oscillations should always be equal to the sum of energies of the ocmponent motions, i.e.,

$$K_s = K_j + K_m. \qquad (2.18)$$

As follows from expression (2.17), this is possible only under the condition if

$$\sum_i m_i y_i^{(j)} y_i^{(m)} = 0. \qquad (2.19)$$

This condition is called the condition of orthogonality of tones of natural oscillations. A more strict derivation of this condition will be given in § 2 of Chapter II.

With the calculation of any j-th tone, all preceding tones to which index m = 0, 1, 2, ..., j - 1 corresponds, whould already be calculated.

To fulfill the conditions of orthogonality with determination by the method of successive approximations of the form of the j-th tone, let us represent the unknown form $y_i^{(j)}$ as

$$y_i^{(j)} = p^2\left[a_i - \sum_{m=0}^{m=j-1} C_m y_i^{(m)}\right], \tag{2.20}$$

where $y_i^{(m)}$ are already defined forms of natural oscillations.

Constants C_m are determined from the condition of orthogonality (2.19) by formulas:

$$C_m = \frac{\sum_i a_i a_i y_i^{(m)}}{\sum_i a_i \left[y_i^{(m)}\right]^2}. \tag{2.21}$$

The value of the frequency of the j-th tone is calculated by the formula

$$p_j^2 = \frac{1}{a_s - \sum_{m=0}^{m=j-1} C_m}. \tag{2.22}$$

Knowing p^2, one can determine the form of oscillations by the expression (2.20).

4. Peculiarities of Calculation of Frequencies and Forms of Natural Oscillations of a Hinged Sealed Blade

All the above-mentioned calculations referring to the rigid sealed blade, can easily be widespread for a blade with hinged sealing in the shank.

For this case the integral equation (2.4) takes the following form:

$$y=p^2\left[\int_0^r\int_0^r\int_0^r\frac{dr^3}{EI}\int_r^R\int_r^R my\,dr^2+C_0r\right]. \qquad (2.23)$$

where the constant C_0 is determined from the condition of equality to zero of the sum of moments of all inertial forces with respect to the hinge. For the model with discrete distribution of parameters this condition can be thus recorded

$$\sum_i m_i y_i (r-r_0)=0. \qquad (2.24)$$

It is easy to note that this condition coincides with the condition of orthogonality to the form of oscillations which we will conditionally call the form of zero tone oscillations. If this form is standardized in accordance with condition (2.5), then it can be recorded as

$$y_1^{(0)}=\frac{r-r_0}{R-r_0}. \qquad (2.25)$$

Thus with calculation of the hinged sealed blade one should consider that the form of its zero tone is known beforehand and is assigned by formula (2.25), and with calculation of all subsequent tones, starting from the first, it follows to fulfill the condition of orthogonality to the zero tone (2.24). It is possible to determine function u_i by the same formulas which are given in No. 2.

5. Calculation of Forms and Frequencies of Natural Oscillations of the Blade as a Free Beam

In the whole series of cases it appears necessary to calculate the frequency of joint oscillations of the blade and fuselage of the helicopter. The rotor hub, which is the fastening point of the blade, can move itself together with the fuselage of the helicopter. Calculations of such oscillations are very easy to fulfill if one were to use the blade model constituting the free beam. Then in the determination of joint oscillations of the rotor and fuselage, it

is sufficient to calculate mass of fuselage m_0 reduced to the rotor (see Fig. 1.3) and to produce calculation of frequencies of natural oscillations of the blade.

Calculation of the blade as a free beam can be carried out by the formulas of No. 2, only all forms of the natural oscillations should be additionally orthogonalized to the form of the second zero tone:

$$y_1^{(0)} = 1 = \text{const}, \tag{2.26}$$

which is equivalent to the fulfillment of the condition of equality to zero of the sum of all inertial forces effective with the oscillations.

This method of calculation with small further improvements can be used during calculations of forms and frequencies of natural oscillations of the fuselage, which will be discussed in Chapter II.

§ 3. Approximate Method of Determination of Frequencies of Natural Oscillations of the Blade in the Field of Centrifugal Forces

1. Application of the Method of B. G. Galerkin for Determination of Frequencies of Natural Oscillations of the Blade

The method of B. G. Galerkin is very widely used to solve different problems about elastic blade oscillations.

The idea of the B. G. Galerkin method and its application to the solution of differential equations is discussed sufficiently in detail in literature (see for example, the reference book Mashinostroyeniye ("Machine Building," Vol. 1, Book One, Mashgiz, 1947).

Here we will not repeat the derivations which can be found in other sources, but will illustrate the application of this method in a number of simple examples.

In No. 10, § 1, of this chapter the differential equation of oscillations of the blade in the field of centrifugal forces was deduced. If one were to substitute into it y in the form of (2.2), then this equation will take the following form (the dash above y is rejected here):

$$[EIy'']''-[Ny']'-p^2my=0. \tag{3.1}$$

Let us assume that the forms of natural oscillations of the blade in the field of centrifugal forces do not differ from corresponding forms calculated for the case N = 0. Then, considering that the forms of oscillations $y^{(j)}$ are known, we will substitute any one form $y^{(j)}$ into equation (3.1), and, multiplying all terms of the equation by this form $y^{(j)}$, we will integrate the obtained expressions along the length of the blade.

After certain transformations the obtained equation can be represented in the form

$$\int_0^R EI[(y^j)'']^2 dr+\int_0^R N[(y^j)']^2 dr-p^2\int_0^R m(y^j)^2 dr=0. \tag{3.2}$$

The integrals entering into this equation

$$C_{EI}=\int_0^R EI[(y^j)'']^2 dr, \tag{3.3}$$

$$C_N=\int_0^R N[(y^j)']^2 dr \tag{3.4}$$

have fully defined physical meaning, namely:

C_{EI} is the elastic potential energy stored by the blade when in the process of flexural oscillations by the form of j-th tone it attains extreme deviations from the position of equilibrium;[2] C_N is the potential energy accumulated by the blade during its bend in the field of centrifugal forces. Here, just as in expression (3.3), different tones of natural oscillations can be examined.

The full potential energy accumulated by the blade during its bend in the field of centrifugal forces can by formula $y^{(j)}$ be recorded as

$$C_3 = C_{EJ} + C_N. \tag{3.5}$$

With flexural oscillations, when the blade passes through the position of equilibrium, the speed of movement of its poitns attain the largest values:

$$\dot{y}^{(j)} = p y^{(j)}. \tag{3.6}$$

The kinetic energy of the blade can be defined by the formula

$$K_j = p^2 \int_0^R m [y^{(j)}]^2 dr. \tag{3.7}$$

In the process of free oscillations the potential energy accumulated by the blade during its bend by form $y^{(j)}$ is turned into kinetic energy when the blade passes the position of equilibrium. The equality of peak values of potential and kinetic energy of the blade is expressed by equation (3.2).

From equation (3.2) one can determine the frequency of the j-th tone of natural oscillations of the blade in the field of centrifugal forces. This frequency is determined by the formula

$$p_j^2 = p_{0j}^2 + \kappa_j p^2, \tag{3.8}$$

where p_{0j} is the frequency of natural oscillations of the blade, neglecting of centrifugal forces; κ_j is the coefficient considering the influence of centrifugal forces.

Here

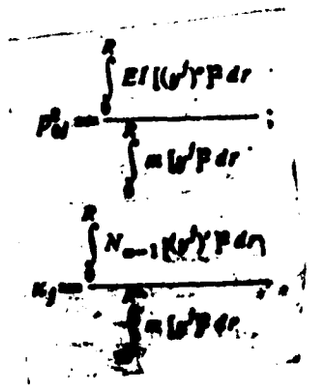

(3.9)

(3.10)

In expression (3.10) $N_{\omega=1}$ is the centrifugal force in the section of blade at $\omega = 1$.

Expression (3.9) for frequency of natural oscillations, neglecting the centrifugal forces, can be obtained if in this way one were to use the B. G. Galerkin method to equation (2.3).

The expressions obtained here for frequencies of natural oscillations of the blade in the field of centrifugal forces are approximate. However, calculations show that in the whole series of cases these expressions give fully satisfactory accuracy for practical purposes. A more detailed appraisal of the accuracy of results of these calculations will be given in § 4.

2. Resonance Diagram of Blade Oscillations

It was already noted above that in the process of designing a blade it is necessary to conduct calculations for the purpose of eliminating possible resonances of frequencies of natural oscillations of the blade with those harmonics of external forces which may cause varying stresses considerable in magnitude. As was already said, the harmonic components of aerodynamic forces having an effect on the blade in flight are of considerable importance to harmonics not higher than the eighth. Higher harmonics of aerodunamic forces are so small in magnitude that they cannot be taken into account.

Frequencies of forced oscillations, which one should fear with calculation of the blade, can be determined by the formula

(3.11)

where n = 1, 2, 3, ..., 8.

Equation (3.8) permits constructing the dependence of frequencies of natural oscillations of different tones from the angular velocity of the rotor rotation. Plotted jointly on one graph, the dependences (3.8) and (3.11) are usually called resonance diagram of the blade. Figures 1.4 and 1.5 give resonance diagrams plotted for blades with different parameters encountered in practice. These diagrams are plotted in relative values. The frequencies of natural oscillations p and numbers of turns of the rotor are referred to a defined working value of the number of turns $n_{раб}$.

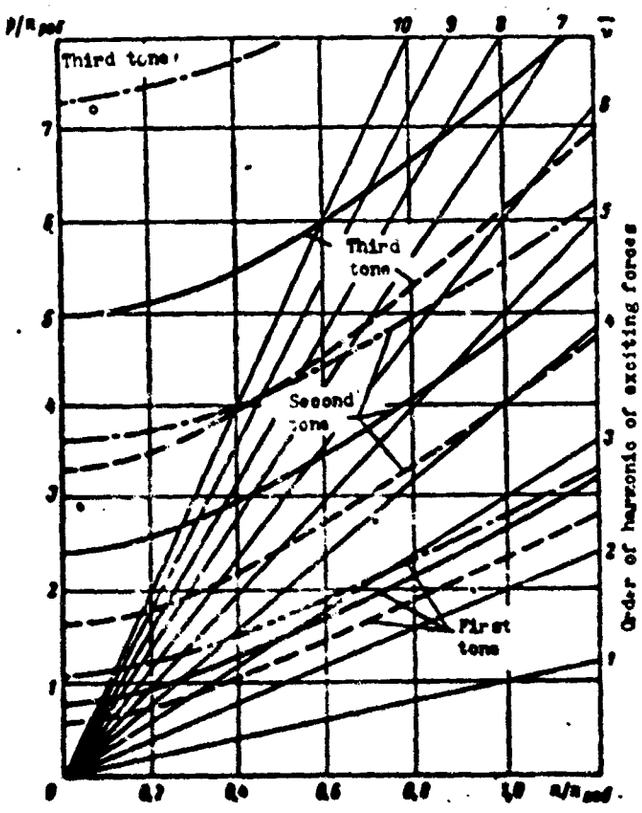

Fig. 1.4. Resonance diagrams of different types of blades in the flapping plane.

The resonance diagram permits in graphic form to trace in what direction one should change the blade parameters in order to exclude resonances in the whole range of working numbers of rotor revolutions.

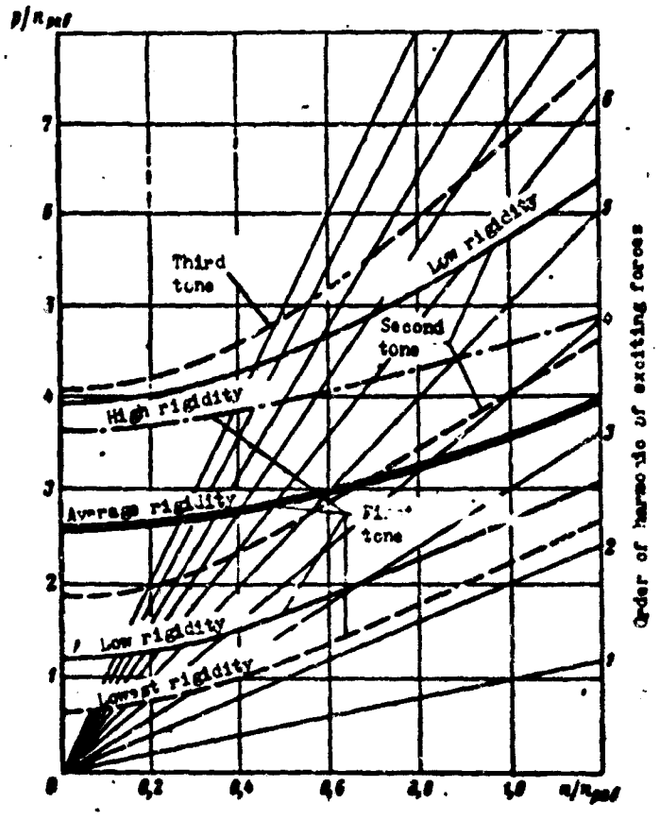

Fig. 1.5. Resonance diagrams of different types of blades in the plane of rotation.

3. Selection of Blade Parameters for Exclusion of Resonances with Oscillations in the Flapping Plane

If one were to examine the resonance diagrams, constructed for blades most diverse in design, then it turns out that they do not greatly differ from each other. This distinction is most frequently explained by the difference in rigidities of the blade to bending. Rarer, and to a lesser degree, it is caused by deviations in mass characteristics of the blade. This circumstance is explained very simply. The fact is that in designing the designer should follow by a set of different requirements limiting the possibilities of variation of blade parameters and leading in the end to the creation of blades which are very close in their characteristics.

A wide change in blade parameters is prevented, mainly, by the following conditions:

1. Spar depth is limited by the profile of the blade and cannot be considerably increased, since with an increase in relative thickness of the profile the lift-drag ratio of the rotor worsens. This circumstance limits the magnitude of rigidity of the blade to bending from above.

2. The sag of the blade under the impact of its weight should not be very great, since this causes difficulty in the layout of the helicopter. Flexural stresses in the longeron, appearing from intrinsic weight, also should not exceed the known values selected from conditions of strength, taking into account possible dynamic overloads. These considerations limit the possibilities of lowering the blade rigidity.

3. The weight of the blade appears concluded in even closer borders. A tendency to the increase of loading factor of the helicopter forces the designer to give a maximum weight reduction of the blade. But this leads to an increase in varying stresses from bending, which act in the blade in flight, and, consequently, to a lowering of service life. Therefore, usually the blade weight decreases as long as the longeron endures increasing varying stresses. As a result the blade weight is rigidly connected with dimensions of the rotor and strength characteristics of the material from which its longeron is prepared.

As a result, resonance diagrams of different blades are changed in practice within limits which are limited on the one hand by the possibility of creation of a very rigid blade, and on the other, by the possibility of providing satisfactory service life of blades having small rigidity.

At the assigned total weight of design the maximum rigid blade is obtained if the material of its longeron is disposed on the contour of the profile, i.e., to inscribe the longeron into the profile of the blade. With this a great percent of the blade weight can be inclosed in its force element - the longeron. Such blades

are usually the most profitable from the point of view of the value of effective stresses, but it is difficult to make them. Simpler in production were blades with a free form of sections of the longeron (for example, in the form of a pipe) not inscribed into profile of the blade. Such blades possess small bending strength and give the least successful resonance diagram during oscillations in the flapping plane.

According to dynamic characteristics in the plane of stroke, it is possible to distinguish the following types of blades:

Blades with low rigidity in the plane of stroke. Such blades are usually obtained in a construction based on a tubular steel longeron with a frame nonoperating during bending. On Fig. 1.4 the dotted line denotes the resonance diagram for a blade whose rigidity in the flapping plane is on the lower limit rigidities encountered in practice. With such parameters the blade falls into resonance of the second tone with the 4th harmonic and third tone with the 6th harmonic of exciting forces, which is why in it there appear considerable stresses with these frequencies (see also Fig. 1.66). These resonances appear especially sharply in conditions of low speeds, where for blades of this type the stresses appear even higher than at the maximum speed (Fig. 1.64). Therefore, their service life, as a rule, is limited by stay in conditions of low speeds.

Blades with low rigidity are usually a failure in strength and service life, but are often used, since their manufacture proves to be the simplest.

Blades with average rigidity in the flapping plane. With an increase in rigidity the frequencies of natural oscillations of the blade depart from these resonances. In this case it is possible to develop a fully successful blade. Figure 1.4 shows the resonance diagram of such a blade by a solid line. As follows from this diagram, the second tone of oscillations of such a blade still did not approach the 5th harmonic, and the third tone appeared somewhere between the 7th and 8th harmonics. Constructively these are usually blades with

a contour (or close to this form) longeron inscribed into the profile. The longeron can be both steel and Duralumin.

Without an increase in weight of the blade it is impossible to increase rigidity more. Moreover an insignificant increase of rigidity can lead to resonance of second tone with the 5th harmonic of external forces. Therefore the following in order of increase in rigidity can be only weighted blades with greatly increased rigidity.

Weighted blades with great rigidity in the flapping plane. If one were to increase the weight of the blade, putting this weight into the construction of the longeron, then it is possible to increase its rigidity so much that the frequency of the second tone will appear higher than the 5th harmonic. In this case the resonance diagram shown in Fig. 1.4 by a dot-dashed line is possible. In the blade longeron with such a resonance diagram even smaller varying stresses will occur, but the blades appear somewhat heavier as compared to blades of average rigidity. However, for small helicopters for which the relative weight of the rotor is small, such loading of blades is possible.

It is necessary to note that with an appraisal of the dynamic characteristics of different blades in the flapping plane there was absolutely not taken into account the location of the first tone of oscillations of the blade. Usually the first tone lies between the 2nd and 3rd harmonics and it is possible to change its location considerably only in designs distinguished by some peculiarities, for example, for jet rotors with engines on the ends of blades or for rotors with nonhinged fitting of the blades. The insignificant displacement of frequency of natural oscillations of the first tone, observed for standard rotors, as a rule, essentially does not have an effect on the magnitude of effective varying stresses.

4. Selection of Blade Parameters for Elimination of Resonances in the Plane of Rotation

In the designing of a blade it appears necessary to ensure the absence of resonances in the plane of the greatest rigidity of

the blade, which can approximately be considered as coinciding with the plane of rotor rotation. The plane of the greatest rigidity of the blade usually coincides with the plane of the chords. Therefore, rigidity characteristics of the blade in this plane can be changed in wider limits than in the flapping plane. Starting from the round pipe, the section of the longeron can be increased up to dimensions occupying practically the whole profile from the leading to trailing edge. However, there are definite limitations in this plane. Thus the increase in width of the longeron chordwise certainly leads to a shift in the centering of the blade to the trailing edge, which is usually impermissible from the point of view of requirements presented for elimination of flutter. Furthermore, the increase in width of the longeron can be accompanied by an increase in varying stresses in it. With the lowering of rigidity of the longeron by means of decreasing of its width the torsional rigidity of the blade simultaneously drops. This circumstance is one of factors preventing development of blades with very low rigidity in the plane of rotation.

With an estimate of resonance characteristics in the plane of rotation, one should examine, mainly, the first tone and in separate cases also the second tone of oscillations of the blade. The excitation of oscillations according to higher tones appears weak.

According to their dynamic characteristics in the plane of the greatest rigidity the blades can be divided into the following types:

Blades with lowest possible rigidity in the plane of rotation. This type of blade usually includes blades with a tubular longeron and a frame nonoperating during bending. Frequencies of natural oscillations of this type of blades in the plane of rotation appear to be approximately the same as those in the plane of thrust or even somewhat lower due to the fact that the value of coefficient $\varkappa_j$ [see formula (3.8)] in the examined plane is somewhat lower (this will still be discussed in § 4, No. 4). The first tone of oscillations in this case appears to be, as a rule, nevertheless somewhat higher

than the 2nd harmonic of external forces, and serious troubles from this resonance usually do not occur. It is a worse matter with the second tone. It can fall into the resonance with the 4th harmonic of external forces. This usually leads to considerable increase in stresses from this frequency in the plane of rotation. On Fig. 1.5 the dashed line shows the resonance diagram for a blade whose rigidity in the plane of rotation lies on the lower border of rigidities encountered in practice. This blade is close to the resonance of the second tone with the 4th harmonic of external forces.

Blades with low rigidity in the plane of rotation. If the rigidity of the blade in the plane of rotation is somewhat increased in such a way that its first tone remains between the 2nd and 3rd harmonics, and the second tone emerges from resonance with the 4th harmonic, then there will be obtained a blade fully satisfactory with respect to stresses in the plane of rotation. It is necessary to note that with an increase in rigidity one should fear resonance of the second tone with the 5th harmonic to the number of turns of the rotor. Practice shows that with this resonance stresses in the plane of rotation are rather greatly increased, which can even have an effect on their service life. The resonance diagram of blades with low rigidity in the plane of rotation, for which the second tone is located between the 5th and 6th harmonics, is shown on Fig. 1.5 by solid lines.

Blades with low rigidity in the plane of rotation are used widely in practice and, as a rule, cause no troubles connected with oscillations in this plane. However, frequently according to their rigidity characteristics in the flapping plane they approximate blades with low rigidity in the flapping plane which are distinguished by increased stresses at low speeds. With an increase in rigidity of the blade in the flapping plane rigidity in the plane of rotation is frequently simultaneously increased. This circumstance forces us to use the blade with even higher rigidity in the plane of rotation.

Blades with average and high rigidity in the plane of rotation. The blades with average rigidity in the plane of rotation usually include blades whose first tone lies between the 3rd and 4th harmonics of external forces, and the second tone emerges into the region of frequencies with so weak an excitation that it is of little interest to us. On Fig. 1.5 the frequency of the first tone of these blades is shown by a double line.

Blades with high rigidity in the plane of rotation include blades whose frequency of the first tone lies higher than the 4th harmonic of external forces (dot-dashed line on Fig. 1.5).

Blades with average and high rigidity in the plane of rotation can be carried out with fully moderate stresses. However, frequently with the use of such blades there are difficulties connected with the drop in frequencies of the blade due to the elasticity of the sealing of the rotor on the fuselage. This circumstance should certainly be considered in the designing of blades of this type.

§ 4. Calculation of Forms and Frequencies of Natural Oscillations of the Blade in the Field of Centrifugal Forces

1. Purposes and Problems of Calculation

Above in § 1, No. 8, it was already noted that the necessity in the determination of forms and frequencies of natural oscillations of the blade appears with the solution of two types of technical problems presenting different requirements to the method of calculation.

The first type includes problems in which the calculation of forms and frequencies is produced for selection of parameters of the blade, which exclude the possibility of the appearance of resonances. Calculation in this case is finished by construction of a resonance diagram, and forms of natural oscillations play the role of only intermediate results and subsequently are not used. Therefore, in widespread calculations of this type the form of natural oscillations of the blade in the field of centrifugal forces is considered coinciding with the form of an irrotational blade. The influence of centrifugal forces is considered only in values of frequencies which are calculated from power ratios determined by equation (3.8). Such a rather simple method of calculation fully satisfies purposes of problems of this type.

The second type pertains to problems in which forms and frequency of natural oscillations are used for calculation of forced oscillations with the determination of varying stresses effective in the blade design. To obtain results in this case there is much importance in calculation of those peculiarities which introduce tensile centrifugal forces into the form of oscillations.

In this paragraph it will be shown that centrifugal forces considerably change the form of natural oscillations of the blade. An especially great influence of centrifugal forces appears in the form of distribution of the curvature of the elastic line along the length of the blade and to a lesser degree in the form of movements

of the blade's elements. The change in form of distribution of the curvature naturally leads to the redistribution of flexural stresses along the blade. The influence of centrifugal forces on the distribution of stresses along the length of the blade has the greatest effect in places of a sharp drop in flexural rigidity and bracing of the concentrated load.

It is necessary to note that in the determination of forms of natural oscillations, taking into account centrifugal forces, definite difficulties are encountered which should be examined in greater detail.

2. Limits of Applicability of Methods of Calculation Reduced to the Solution of the Integral Equation Blade Vibrations

To calculate free oscillations of the blade in the field of centrifugal forces it would be very convenient to use the same method as is used for the blade of an irrotational rotor. However, it appears that the method of successive approximations (see § 2) occurring in the solution of integral equation (2.1) cannot be used in all cases for the solution of equation (3.1), which describes natural oscillations of the blade in the field of centrifugal forces.

In § 2, No. 1, it was shown that with fourfold integration of equation (2.1) the problem is reduced to the solution of integral equation (2.4). This integral equation can be recorded in somewhat different form:

$$y = p^2 \int_0^x \int_0^x \int_0^x \frac{M_{\omega=1}\, dx^3}{EJ}. \qquad (4.1)$$

where $M_{\omega=1} = \int_x^l \int_x^l m_1 dx^2$ is the bending moment from inertial forces appearing with oscillations of the blade with a frequency p = 1.

Analogously with integration of equation (3.1) the problem is reduced to the solution of an equation of the following form:

$$y = p^2 \int_0^x \int_0^x \int_0^x \frac{(M_{\omega=1} - \gamma M_{\omega=0})\, dx^3}{EJ}. \qquad (4.3)$$

where $M_{ц.с}$ is the bending moment of centrifugal forces at the angular velocity of rotor rotation $\omega = 1$.

$$M_{ц.с} = \int_r^R myrdr - y\int_r^R mrdr; \tag{4.4}$$

$$\gamma = \frac{\omega^2}{\beta^2}. \tag{4.5}$$

If the method of successive approximations applied to equation (4.1) gives good convergence in all cases pertaining to design of the rotors, then in the application to equation (4.3) it converges only in a certain region of values of the parameter γ.

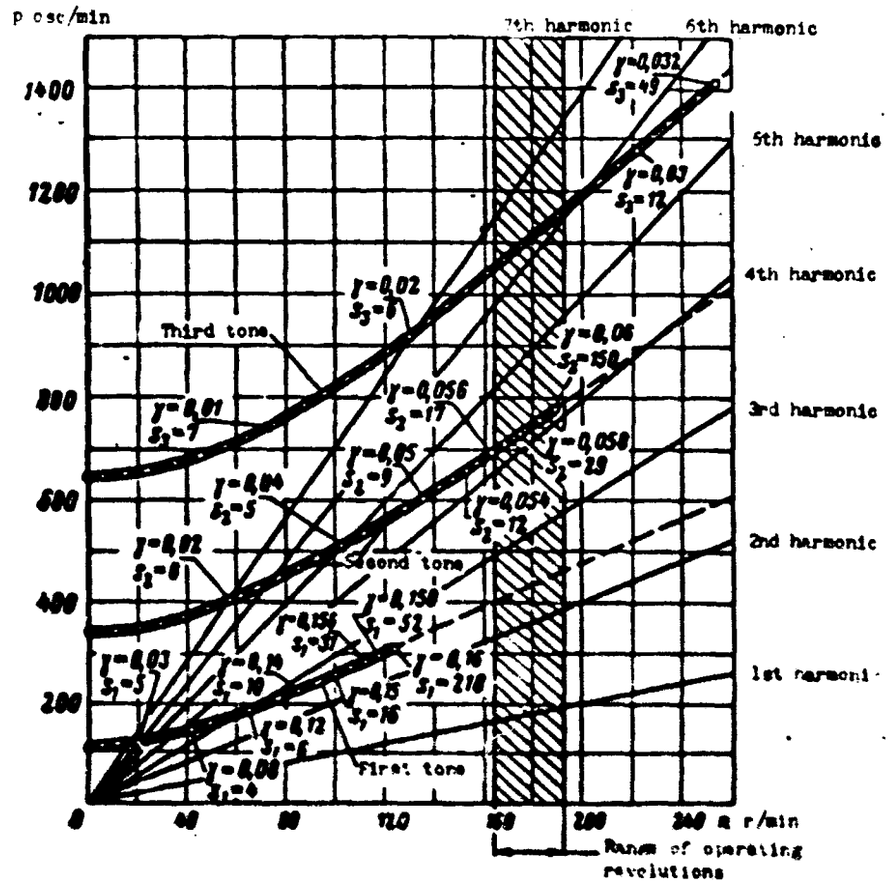

Fig. 1.6. Resonance diagram of helicopter blade in the thrust plane plotted by the method of successive approximations.

Figure 1.6 gives a resonance diagram for the standard blade of the helicopter with hinged fitting to the hub. Plotted along the axis of the abscissas on this graph are numbers of turns of the rotor and along the axis of the ordinates, the frequency of natural oscillations.

Values of frequencies of natural oscillations, obtained as a result of solution of equation (4.3) by the method of successive approximations, are noted on Fig. 1.6 by dots. Opposite every dot is the corresponding value of parameter γ and the quantity of approximations s necessary for achievement of the necessary accuracy equal to 0.001. From the graph it is clear that at certain γ the value s starts rapidly to be increased, and the method of successive approximations ceases to converge.

From Fig. 1.6 it follows that in the range of operating numbers of revolutions for blades of helicopters such a method permits determining the frequencies of natural oscillations of third and higher tones and only in the case when all tones of oscillations are determined for a constant value of parameter γ, which corresponds only approximately to conditions of the stated physical problem. If in the process of successive approximations parameter γ is refined under the assigned value of angular velocity ω, then the method will converge only in the range of numbers of revolutions considerably smaller than the operating ones.

This circumstance creates the need for the application of other methods which enable obtaining a reliable result in the whole range of numbers of rotor revolutions.

3. Possible Methods of the Calculation of Free Oscillations of the Blade in the Field of Centrifugal Forces

To calculate frequencies and forms of natural oscillations in the field of centrifugal forces different methods of calculation can be used. Of the works published concerning this question, it is possible to indicate works [4], [8], and [10]. Of foreign works

[33] and [34] are well-known. In works [33] and [34] an account is given of a very bulky method, which gives not very high accuracy in the final results, in spite of the fact that the calculation should be conducted with an accuracy of not less than 10-12 decimal places.

Here there will be discussed the method which from our point of view is the most convenient for calculation of frequencies of natural oscillations of the blade in the field of centrifugal forces. It is based on the use of the method of three moments, which was used by T. Morris and W. Tye [32] for calculation of flexural stresses in a blade stretched by centrifugal forces. The method of T. Morris and W. Tye is also discussed in work [12].

The method of three moments, used to calculate stretched centrifugal forces of the blade, has a number of considerable advantages. Among them the main one is the fact that it does not require high accuracy in the process of calculation. Calculations can be produced even on the standard slide rule.

The method of three moments for the calculation of natural frequencies has been used for a long time. It is programmed on the computers Strela and M-20. Calculation on the machine Strela of the first eight tones of natural blade vibrations only takes about three minutes. There is made a very large number of the most diverse calculations. Their results indicate the considerable conveniences and great reliability of this method.

It is necessary to note that with a program of such calculation there is no need to turn to any simplified methods of calculation as, for example, those which were discussed in § 3.

4. Method of Three Moments for the Calculation of Forms and Frequencies of Natural Blade Vibrations in the Field of Centrifugal Forces

To derive the calculation formulas we use the beam model of the blade with concentrated loads, which was already used in § 2.

No. 2. Just as earlier, the blade flexural rigidity will be represented in the form of a step curve in such a way that it remains constant for the extent of each section (see Fig. 1.3). The centrifugal force will be considered applied only to loads. Therefore, for the extent of each section its magnitude will not be changed. We will also consider that the centrifugal force is absorbed by a special bracing of zero load, which nonetheless can move freely along the vertical.

It is obvious that such an idealized calculation diagram can be reliably used if the number of sections z is sufficiently large. Usually the blade is divided into not less than 25-30 sections.

The method subsequently proposed consists in the determination of frequencies and forms of natural oscillations of such an idealized diagram without any additional assumptions.

Let us consider two adjacent sections of the blade deflected under the action of inertial forces from the plane of rotation of the rotor (Fig. 1.7). As usual, we will examine only small deflections.

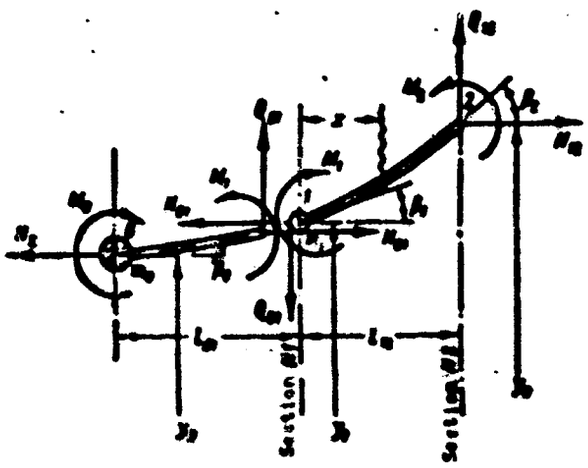

Fig. 1.7. Diagram of forces acting on two adjacent blade elements.

The equation of equilibrium of each of the sections under the action of forces external with respect to the given section can be recorded in the form of an equality to zero of the sum of moments

[illegible] these forces relative [illegible] point. In the sum of moments of these forces one should include both the shear force Q and bending moment M effective in the section.

Then the sum of moments of forces acting on the blade section 0-1 with reference to a point 0 can be recorded as

$$M_1 - M_0 - N_{01}(y_1 - y_0) + Q_{01} l_{01} = 0. \qquad (4.6)$$

The sum of moments of forces acting on sections 1-2 with reference to point 1 is:

$$M_2 - M_1 - N_{12}(y_2 - y_1) + Q_{12} l_{12} = 0. \qquad (4.7)$$

Here:

$$Q_{01} = -\sum_{1}^{0} m_i \bar{y}_i;$$

$$Q_{12} = -\sum_{2}^{0} m_i \bar{y}_i.$$

Dividing equations (4.6) and (4.7) respectively by $l_{01}N_{01}$ and $l_{12}N_{12}$ and adding them, we obtain the following equation of equilibrium:

$$b_0 y_0 + a_1 y_1 + b_1 y_2 = m_0 M_0 + a_1 M_1 + m_2 M_2 + \frac{Q_{12}}{N_{12}} - \frac{Q_{01}}{N_{01}}. \qquad (4.8)$$

Designations introduced here and also in equations (4.12), (4.13), (4.14), and (4.15), are copied below (see expressions 4.18-4.25).

Analogous to equation (4.8) equations of equilibrium and for all other sections of the blade can be written.

Examining as before only small movements of elements of the blade, let us determine the deformation of section 1-2. The equation of deformations of element 1-2 can be recorded as usual [see equation (3.1)]

$$(E I_{xx} \gamma')' - (N_{12} \gamma)' = 0.$$

The inertial term is absent here, inasmuch as inertial forces are applied only on borders of the section. Considering that on

the length of the section EI = const and N = const, and also that EIy" = M, we will obtain

$$\frac{d^2M}{dx^2} - p_1^2 M = 0, \tag{4.9}$$

where

$$p_1^2 = \frac{N_{12}}{EI_{12}}.$$

Solution of the equation (4.9) can be recorded in terms of hyperbolic functions in the following way:

$$M_x = A \operatorname{sh} \mu_1 x + B \operatorname{ch} \mu_1 x. \tag{4.10}$$

Coefficients A and B are found from the following boundary conditions:

- for $x = 0$, $M_x = M_1$;
- for $x = l_{12}$, $M_x = M_2$.

Whence

$$A = \frac{M_2}{\operatorname{sh} \alpha_1} - \frac{M_1}{\operatorname{th} \alpha_1};$$
$$B = M_1.$$

where $\alpha_1 = \mu_1 l_{12}$.

Substituting these values into equation (4.10), we get

$$M_x = EI_{12} y'' = \left[\frac{M_2}{\operatorname{sh} \alpha_1} - \frac{M_1}{\operatorname{th} \alpha_1}\right] \operatorname{sh} p_1 x + M_1 \operatorname{ch} p_1 x. \tag{4.11}$$

Integrating equation (4.11) twice, assuming that for $x = 0$ $y' = \theta_1$, $y = y_1$, and for $x = l_{12}$ $y' = \theta_2$, $y = y_2$, we obtain either

or

$$\left.\begin{aligned} b_1(y_2 - y_1) &= d_1 M_2 + e_1 M_1 + \beta_1, \\ b_1(y_2 - y_1) &= -e_1 M_2 - d_1 M_1 + \beta_2. \end{aligned}\right\} \tag{4.12}$$

The equation of deformations for the section 0-1 can be recorded by analogy with the second equation (4.12):

$$b_0(y_1 - y_0) = -e_0 M_1 - d_0 M_0 + \beta_0. \tag{4.13}$$

Changing in equation (4.[illegible] signs to the opposite and adding with the first equation of (4.12), we obtain:

$$[illegible] \qquad (4.14)$$

Substituting into the equation of equilibrium of elements (4.8) the left side expressed in terms of bending moments from equation (4.14), we will obtain the following equation:

$$[illegible] \qquad (4.15)$$

Repeating the made calculations for other sections of the blade, we will obtain system copied below of differential equations relative to unknown functions of time y_i and M_i.

This system, recorded in the form of tables, consists of two families of equations (4.16) and (4.17), each of which includes the z + 1 equation.

Any of the equations occupying one line in Table 1.1 constitutes a polynomial whose coefficients are copied in the squares of the table. All components of the polynomial are products of a certain coefficient determined by the formulas (4.18), (4.21), (4.23), and (4.24)-(4.27) on unknown functions M_i and y_i or on a second time derivative y_i.

In the squares of Table 1.1 there are written only coefficients at these functions, and the very function entering simultaneously into several equations are carried out vertically in a special line placed at the top of the tables.

Included in the described system of equations are also equations of type (4.12), which pertain only to the shank and end section of the blade and contain boundary values β_0 and β_z. These equations are necessary for calculation of boundary conditions of the problem.

The obtained system of equations has the following form:

Table 1.1.

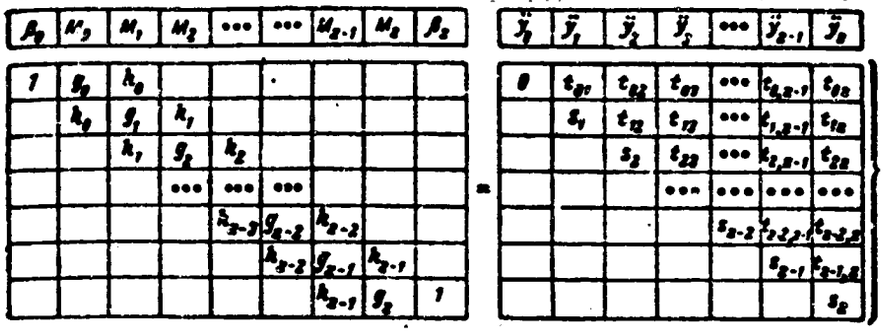

(4.16)

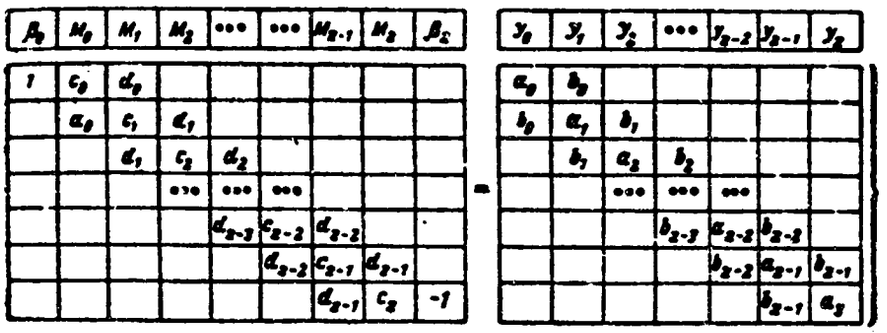

(4.17)

With the composition of the equations copied above the following designations are accepted:

$$\left.\begin{aligned} &b_0=\frac{1}{l_{01}};\quad a_0=-b_0;\\ &b_i=\frac{1}{l_{i,i+1}};\quad a_i=-b_{i-1}-b_i;\\ &b_s=0;\quad a_s=-b_{s-1}. \end{aligned}\right\} \tag{4.18}$$

$$\left.\begin{aligned} &m_0=\frac{1}{l_{01}N_{01}};\quad n_0=-m_0;\\ &m_i=\frac{1}{l_{i,i+1}N_{i,i+1}};\quad n_i=-m_{i-1}-m_i;\\ &m_s=0;\quad n_s=-m_{s-1}. \end{aligned}\right\} \tag{4.19}$$

$$\left.\begin{aligned} &\alpha_0=\sqrt{\frac{N_{01}l_{01}^2}{EI_{01}}};\\ &\alpha_i=\sqrt{\frac{N_{i,i+1}l_{i,i+1}^2}{EI_{i,i+1}}};\\ &\alpha_s=0. \end{aligned}\right\} \tag{4.20}$$

$$\left.\begin{aligned} &d_0=m_0\left(1-\frac{\alpha_0}{\operatorname{sh}\alpha_0}\right);\\ &d_i=m_i\left(1-\frac{\alpha_i}{\operatorname{sh}\alpha_i}\right);\\ &d_s=0. \end{aligned}\right\} \tag{4.21}$$

$$\left.\begin{aligned} e_0 &= m_0\left(\frac{\cdot}{\operatorname{th} a_0}-1\right);\\ e_i &= m_i\left(\frac{a_i}{\operatorname{th} a_i}-1\right);\\ e_s &= 0. \end{aligned}\right\} \tag{4.22}$$

$$\left.\begin{aligned} c_0 &= e_0;\\ c_i &= e_{i-1}+e_i;\\ c_s &= c_{s-1}. \end{aligned}\right\} \tag{4.23}$$

$$\left.\begin{aligned} h_0 &= d_0 - m_0;\\ h_i &= d_i - m_i;\\ h_s &= 0. \end{aligned}\right\} \tag{4.24}$$

$$\left.\begin{aligned} g_0 &= c_0 - n_0;\\ g_i &= c_i - n_i;\\ g_s &= c_s - n_s. \end{aligned}\right\} \tag{4.25}$$

In following expressions (4.26) and (4.27) m_i is the mass of the i-th load.

$$\left.\begin{aligned} s_0 &= 0;\\ s_i &= \frac{m_i}{N_{i-1,i}};\\ s_s &= \frac{m_s}{N_{s-1,s}}. \end{aligned}\right\} \tag{4.26}$$

$$\left.\begin{aligned} t_{01} &= m_1\left(-\frac{1}{N_{01}}\right);\\ t_{kk} &= m_i\left(\frac{1}{N_{i-1,k}}-\frac{1}{N_{k,k+1}}\right);\\ t_{s-1,s} &= m_s\left(\frac{1}{N_{s-2,s-1}}-\frac{1}{N_{s-1,s}}\right). \end{aligned}\right\} \tag{4.27}$$

Here the subscript k denotes the number of the line in Table 1.1.

To solve the system of equations recorded in Table 1.1, it is convenient to use the method of successive approximations. In reference to this system of equations it consists in the following. Let us present the time functions $y_i(t)$, $M_i(t)$, and $\beta_i(t)$ entering into the system (4.16) and (4.17) in the following form:

$$\begin{aligned} y_i(t) &= y_i \sin pt;\\ M_i(t) &= M_i \sin pt;\\ \beta_i(t) &= \beta_i \sin pt, \end{aligned}$$

where letters y_i, M_i, and β_i denote now only peak values of these functions.

Then, considering that $\ddot{y}_i(t) = -p^2 y_i \sin pt$, and cancelling by sin pt, we will obtain a system of algebraic equations analogous to the system of (4.16) and (4.17). Only in the right sides of the family of equations analogous (4.16) values p^2 will appear.

The method of successive approximations will be started from the fact that as the zero approximation we will assign a certain function y_{i_0}. The second subscript here denotes the number of the approximation. The function y_{i_0} taken as the zero approximation should be standardized in any form, for example,

$$y_{i_0} = 1. \tag{4.28}$$

If function y_i is known, then correct to a constant factor p^2 inertial forces entering into the right side of equations of (4.16) can be determined.

Let us assume temporarily that $p^2 = 1$. Then from equations (4.16) one can determine values of bending moments M_i and the angle of rotation of the blade in the butt β_0. After which according to already known values M_i and β_0 from equations (4.17) movements of the blade axis can be determined at deformations which for the case $p^2 = 1$ we will designate by u_i in such a way that

$$y_i = p^2 u_i. \tag{4.29}$$

After determination of movements u_i the frequency of natural oscillations can be determined. Its value is obtained on the basis of expressions (4.28) and (4.29) in the following way:

$$p^2 = \frac{y_{i_0}}{u_{i_0}} = \frac{1}{u_{i_0}}. \tag{4.30}$$

After which in accordance with expression (4.29) there is determined and refined after the first approximation the function

$$y_{i_1} = p^2 u_{i_1}. \tag{4.31}$$

Then the whole process is repeated until the required accuracy will be attained.

The method of successive approximations used permits that the determined form y_i converges to the form of lowest tone of natural oscillations of the blade.

In the determination of subsequent tones the condition of orthogonality should be observed. Operations resulting from observance of the condition of orthogonality remain the same as those for the blade of an irrotational rotor (see No. 3 of § 2).

The equations copied above in an equal degree apply for the calculation of frequencies of natural oscillations both in the flapping plane and in the plane of the rotor rotation. Only with calculation in the plane of rotation obtained should the values of frequencies obtained above be corrected by the formula

$$p^2_{\text{вр.прав}} = p^2_{\text{вр.взмах}} - \omega^2, \qquad (4.32)$$

where ω is the angular velocity of rotation of the rotor.

The method of calculation of forms of natural oscillations does not change from that in which plane the calculation is produced.

Let us consider more specifically certain operations in the fulfillment of one approximation.

5. Determination of Bending Moments According to Known Forces

Let us start from the determination of bending moments according to known inertial forces entering into the right side of equation (4.16), which we determine in each approximation by assigning in the beginning the value $p^2 = 1$.

Having assigned some form of oscillations y_i, we can determine coefficients of the right side of equations (4.16), which here we will designate by F_k.

Coefficients F_k can be defined by formulas

$$F_s = s_s y_s + \sum_{i=s+1}^{z} t_{si} y_i \qquad (4.33)$$

or better

$$F_s = \frac{Q_{s-1,s}}{N_{s-1,s}} + \frac{Q_{s,s+1}}{N_{s,s+1}}, \qquad (4.34)$$

where $Q_{s-1,s} = \sum_{s}^{z} m_i y_i$.

Then the system of equations (4.16) can be copied in the following form (Table 1.2):

Table 1.2.

β_0	M_0	M_1	M_2	...	...	M_{z-1}	M_z	β_z	
1	g_0	h_0							$p^2 F_0$
	h_0	g_1	h_1						$p^2 F_1$
		h_1	g_2	h_2					$p^2 F_2$
			...	...	...				...
				h_{z-3}	g_{z-2}	h_{z-2}			$p^2 F_{z-2}$
					h_{z-2}	g_{z-1}	h_{z-1}		$p^2 F_{z-1}$
						h_{z-1}	g_z	-1	$p^2 F_z$

(4.35)

For a solution to this system it is necessary to know two more additional equations considering the boundary conditions. These equations can be the following:

– with rigid sealing of shank of the blade

$$\beta_0 = 0;$$

– with rigid sealing of the blade tip

$$\beta_z = 0.$$

With hinged fastening of the blade tips or with completely free ends $M_0 = 0$ and $M_z = 0$.

Subsequently we will examine only the two most predominant cases, when the blade tip is free ($M_z = 0$), and in the shank there is either a hinged holder ($M_0 = 0$) or rigid sealing ($\beta_0 = 0$).

Let us consider in the beginning the first case when the blade is hinged fastened, i.e., $M_0 = 0$. In this case to determine the bending moments we use only those equations which in system (4.35) are outlined by a heavy line, after which from the first equation the value of the angle of rotation of the blade in the hinge β_0 can be determined. From the last equation of system (4.35) it would have been possible to determine the value β_z. However, we will not need this value for further solution. The equation itself is used only in a case rarely encountered in practice when $\beta_z = 0$.

With the solution of system (4.35) there can be selected the unsuccessful means leading to the appearance in the solution process of small differences of great magnitudes, which in certain cases can absolutely spoil the result even with the use of a machine provide an accuracy up to nine decimal places.

Here we propose repeatedly a proven means which permits producing calculation even on the common slide rule.

Let us divide the first equation of the system (4.35), written in reference to hinged bracing of the blade, by g_1 and the second equation by h_1:

$$M_1 + \frac{h_1}{g_1} M_2 = \frac{F_1}{g_1}; \tag{4.36}$$

$$M_1 + \frac{g_2}{h_1} M_2 + \frac{h_2}{h_1} M_3 = \frac{F_2}{h_1}. \tag{4.37}$$

Subtracting equation (4.36) from equation (4.37) and introducing the following designations

$$g_2' = \frac{g_2}{h_1} - \frac{h_1}{g_1};$$

$$h_2' = \frac{h_2}{h_1};$$

$$F_2' = \frac{F_2}{h_1} - \frac{F_1}{g_1}.$$

we will obtain an equation analogous to equation (4.36):

$$M_2 + \frac{h_2'}{g_2'} M_3 = \frac{F_2'}{g_2'}. \tag{4.38}$$

In combination with the following equation of system (4.39) this equation will form a system of two equations analogous to equations (4.36) and (4.37). Repeating the described operations a certain number of times, we will finally obtain one equation of the following form:

$$M_{z-1}=\frac{F^{\circ}_{z-1}}{\delta^{\circ}_{z-1}}. \qquad (4.39)$$

After determination of the moment M_{z-1} moment M_{z-2} is determined, etc., up to moment M_1. In other words, moment M_i is determined every time when moment M_{i+1} is already determined. The formula for determination of moment M_i can be recorded on the basis of equations (4.36) and (4.38) in the following way:

$$M_i=\frac{F^{\circ}_i}{\delta^{\circ}_i}-\frac{\Delta^{\circ}_i}{\delta^{\circ}_i}M_{i+1}. \qquad (4.40)$$

After determination of bending moments the angle of rotation of the blade in the butt hinge β_0 is determined by the formula

$$\beta_0=F_0-k_0M_1. \qquad (4.41)$$

The second stage of the method of successive approximations consists in the determination of deformations of the blade by the already known values of bending moments M_i and the angle of rotation of the blade in the hinge β_0.

6. Determination of Movements by the Known Bending Moments

Blade movements with its deformations, which here in accordance with that said above we designate u_i, can be determined from system (4.17). However, it is possible to show that equations of system (4.17) are insufficient for determination of all values of u_i.

Indeed, to determine the positions of the curve with a known distribution of curvature along the length, which is assigned by values M_i, and with a known value of the angle of rotation at one point β_0, one more additional condition superimposed on values of movements is necessary. The last equation of system (4.17), including the value of the angle of rotation in the other point β_z, is actually

identical to the first equation and is written by us especially by analogy with system (4.16).

Such an additional condition is either the condition

$$u_0 = 0, \tag{4.42}$$

if in the shank of the blade there is a holder, or the condition

$$\sum_{i=0}^{s} m_i u_i = 0, \tag{4.43}$$

if the blade is examined as free on two sides of the beam. Condition (4.43) coincides with the expression emanating from the condition of orthogonality with a zero tone of oscillations

$$y_i^{(0)} = 1 = \text{const}.$$

Having calculated the coefficients which include the already defined values M_i and β_0 and leaving only the first of the two identity equations, we will obtain the following system of equations, which in combination with equations (4.42) and (4.43) permits determining all values of u_i (see Table 1.3).

Table 1.3.

u_0	u_1	u_2	u_3	•••	u_{z-1}	u_z		
u_0	b_0						=	D_0
b_0	a_1	b_1					=	D_1
	b_1	a_2	b_2				=	D_2
		b_2	a_3	b_3			=	D_3
			•••	•••	•••		=	•••
				b_{z-2}	a_{z-1}	b_{z-1}	=	D_{z-1}
					b_{z-1}	a_z	=	D_z'

(4.44)

Here we introduced the following designations

$$D_i = d_{i-1}M_{i-1} + c_i M_i + d_i M_{i+1}, \tag{4.45}$$

where in this formula for i = -1 instead of the value M_{-1} one should put β_0, and the value d_{-1} should be considered equal to unity ($d_{-1} = 1$).

Under condition (4.42) solution to the system (4.44) is reduced to the determination of values u_i from simple recurrence formulas of the form

$$u_i = \frac{1}{b_{i-1}}[D_{i-1} - b_{i-2}u_{i-2} - a_{i-1}u_{i-1}]. \qquad (4.46)$$

In solving system (4.44) with condition (4.43) value u_i can be represented as

$$u_i = u_0 + \bar{u}_i \qquad (4.47)$$

where $\bar{u}_0 = 0$, and $\bar{u}_i$ can be determined by formulas (4.46), after which the value u_0 can be defined by formula

$$u_0 = -\frac{\sum_{i=0}^{i=s} a_i \bar{u}_i}{\sum_{i=0}^{i=s} a_i}. \qquad (4.48)$$

Further course of successive approximations has already been mentioned above.

In the examined case of hinged fitting of the blade in the butt, the method of successive approximations will lead in the beginning to the determination of the form of zero tone, which with coincidence of the blade hinge with the axis of rotation of the rotor will coincide with a straight line. It is natural that in this special case the calculation should be started directly from determination of the first tone, conducting in each approximation orthogonalization to the zero tone, considering it coinciding with a straight line.

Most frequently the shank hinge of the blade of a helicopter is ascribed from the axis of rotation of the rotor on a certain value r_0, which can comprise approximately 5-10% of the radius of the blade. The presence of this distance leads to the fact that the form of the zero tone of the hinged suspended blade can somewhat differ from a straight line, and the frequency of natural oscillations becomes noticeably different from the value equal to the number of revolutions of the rotor. Below (see Fig. 1.14) for

illustration of this effect we give a graph of the form of zero tone with very greatly increased distance from the axis of rotor rotation to the butt hinge.

7. Case of a Blade Rigidly Fastened in the Shank

Calculation of forms of natural oscillations for a blade rigidly sealed in the shank differs very little from the case of the hinged fitting examined above.

The first stage of calculation involving the determination of bending moments M_i is conducted in the manner as was described above, but here the system circled in (4.35) by a line is solved. This system includes one equation more, in which in virtue of boundary conditions it is assumed $\beta = 0$.

The same condition is used and in the solution of system (4.44), in which the coefficient D_0 is calculated by the formula

$$D_0 = c_0 M_0 + d_0 M_1.$$

8. Possible Simplifications in the Calculation of Coefficients

Let us still note that in those cases when the blade is divided into quite a large number of sections in such a way that the value of coefficients α_i in formulas (4.20) is less than 0.05-0.08, formulas (4.21) and (4.22) can be simplified by replacing the hyperbolic functions entering into them by first terms of their expansion in series.

Actually, let us assume in formulas (4.21) and (4.22) that

$$\operatorname{sh}\alpha = \alpha + \frac{\alpha^3}{3!} + \frac{\alpha^5}{5!} + \ldots \cong \alpha + \frac{\alpha^3}{6};$$
$$\operatorname{th}\alpha = \alpha - \frac{\alpha^3}{3} + \frac{2\alpha^5}{15} - \ldots \cong \alpha - \frac{\alpha^3}{3}$$

and let us disregard values α^2 as compared to unity. Then coefficients d_i and e_i can be calculated by the approximate formulas

$$d_i = \frac{l_{i,i+1}}{6Ef_{i,i+1}};$$

$$e_i = \frac{l_{i,i+1}}{3Ef_{i,i+1}} = 2d_i.$$

These simplifications somewhat decrease the laboriousness of calculation, which is inportant in its manual fulfillment.

9. Certain Results of the Calculation of Forms and Frequencies of Natural Oscillations of the Blade

Here we separate two questions, which represent from our point of view the greatest interest.

The first question will touch upon those more precise definitions which are introduced by calculation of frequencies and forms of natural oscillations of the blade in the field of centrifugal forces in final results as compared to the approximation of calculation expounded in § 3. Then we will discuss the consideration of cases of the appearance of sharp bends of the blade under the impact of local peculiarities in the distribution of rigidity and mass parameters along the length of the blade. The appearance of these bends is characteristic for beams stretched by centrifugal forces, and without extension centrifugal forces are not observed.

Let us start with the first question. In No. 1 of § 3 we already noted that the approximation method of calculation of frequencies of natural oscillations of blades in the field of centrifugal forces, as a basis of which there is assumed the assumption about the fact that the form of natural oscillations in the presence and absence of centrifugal forces are not distinguished, gives quite satisfactory results in values of frequencies.

For confirmation of this position let us give values of frequencies of natural oscillations of the first three tones of blades hinged suspended and rigidly sealed in the shank of one of the helicopters in the field of centrifugal forces. Values of frequencies calculated by the approximate power method (see § 3) are placed in the second column of Table 1.4. In the third column there are

Table 1.4.

Tone of oscillation	Frequency of natural oscillations	
	method of approxi-mation	exact method
Blade hinged suspended in the shank		
First.....	405.3	404.3
Second.....	708.5	705.9
Third.....	1069.7	1069.0
Blade rigidly sealed in the butt		
First.....	212.1	194.7
Second.....	463.7	461.9
Third.....	821.5	817.5

placed for comparison accurate values of frequencies calculated according to the method discussed in this paragraph.

A comparison of values of frequencies given in Table 1.4 shows that with a hinged suspension of the blade the distinction in their values is very insignificant. With rigid sealing it is somewhat more but also small. Therefore, as was already noted above, for calculations whose purpose is exclusion of the possibility of appearance of resonances, the method gives fully satisfactory results.

The influence of centrifugal forces has a greater effect on forms of natural oscillations and, especially, on the distribution of bending moments and curvature of elastic line along the length of the blade.

Figure 1.8 shows hinged forms of the first five tones (excluding the zero tone) for the same blade as in Table 1.4, and on Fig. 1.9 distribution of bending moments corresponding to these forms is given. Solid lines on Figs. 1.8 and 1.9 (just as on Figs. 1.10,

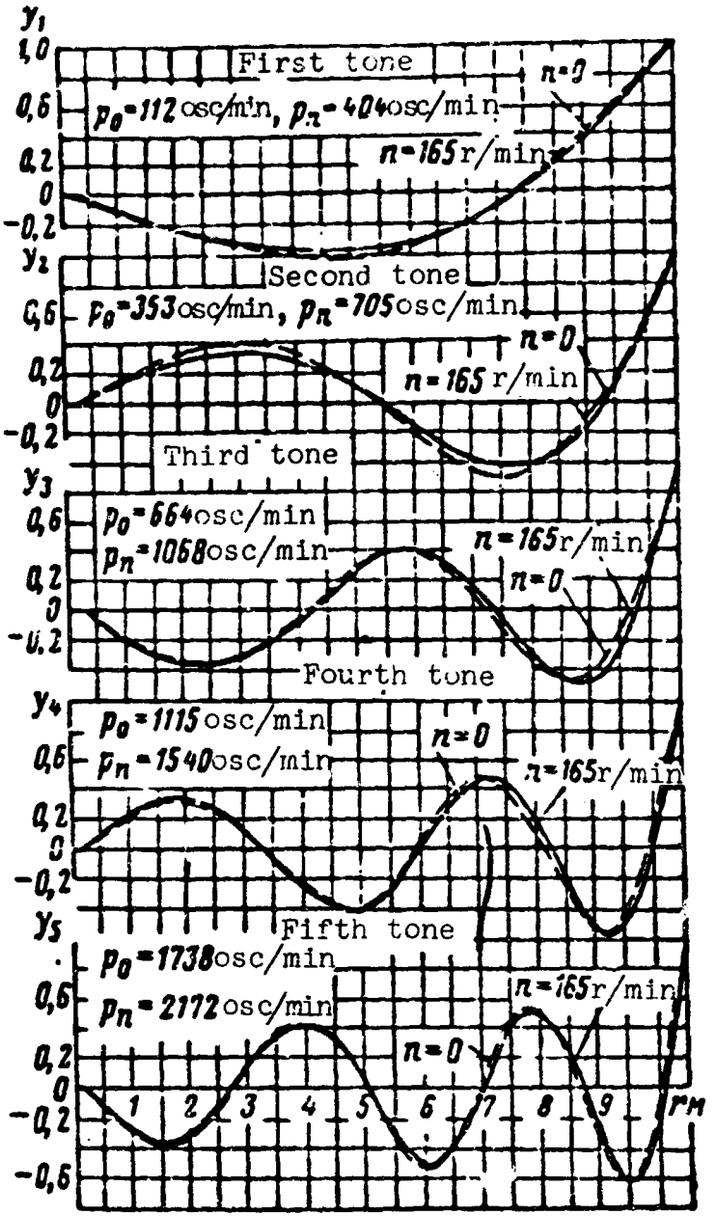

Fig. 1.8. Forms of first five tones of the blade in the field of centrifugal forces and at n = 0.

1.11, and 1.12) indicate the form of natural oscillations in the field of centrifugal forces and dashed lines, the same form for an irrotational blade.

Figure 1.10 gives the form of natural oscillations and bending moments corresponding to them for the first two tones of the blade sealed in the shank.

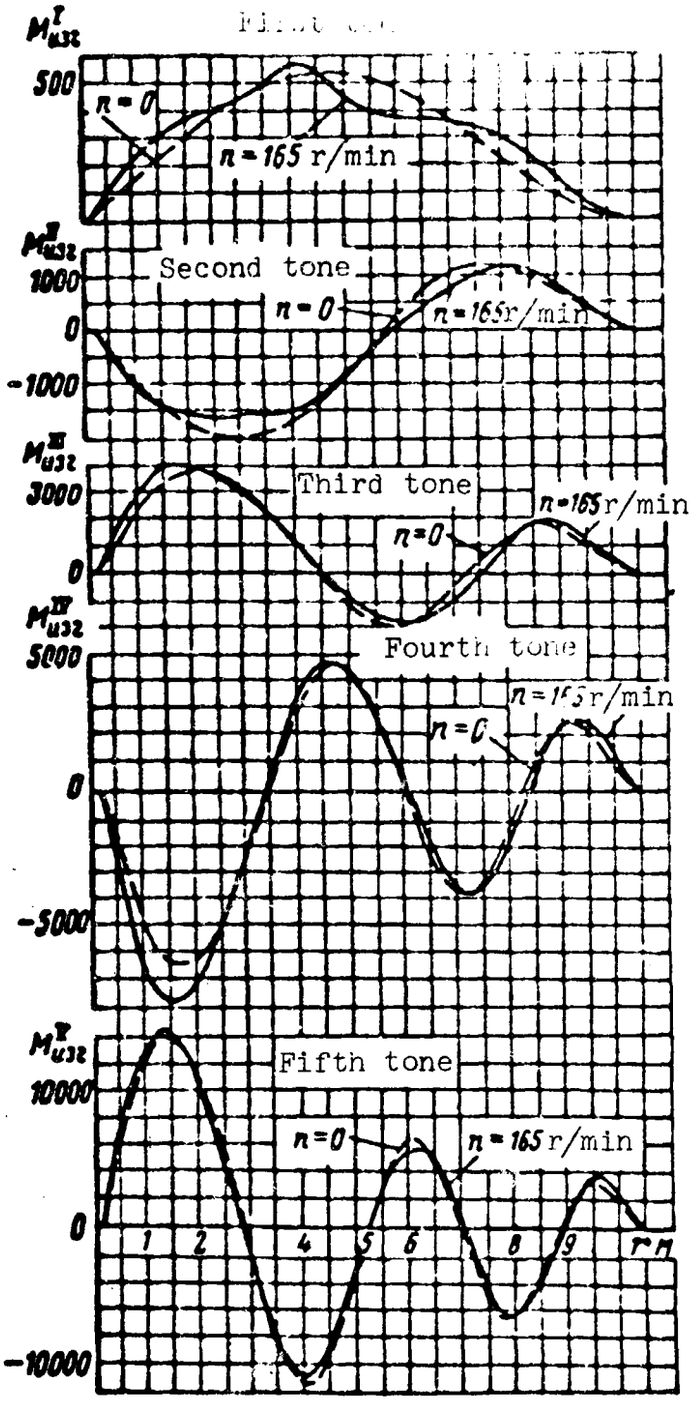

Fig. 1.9. Distribution of bending moments along the blade during oscillations in forms of the first five tones in the field of centrifugal forces and at n = 0.

As can be seen from all these graphs, calculation of centrifugal forces in certain sections of the blade has a very noticeable influence on the form of natural oscillations, which especially greatly appears in diagrams of bending moments and, consequently, also in the distribution of flexural stresses along the length of the blade. The greater the influence, the lower the tone of natural oscillations.

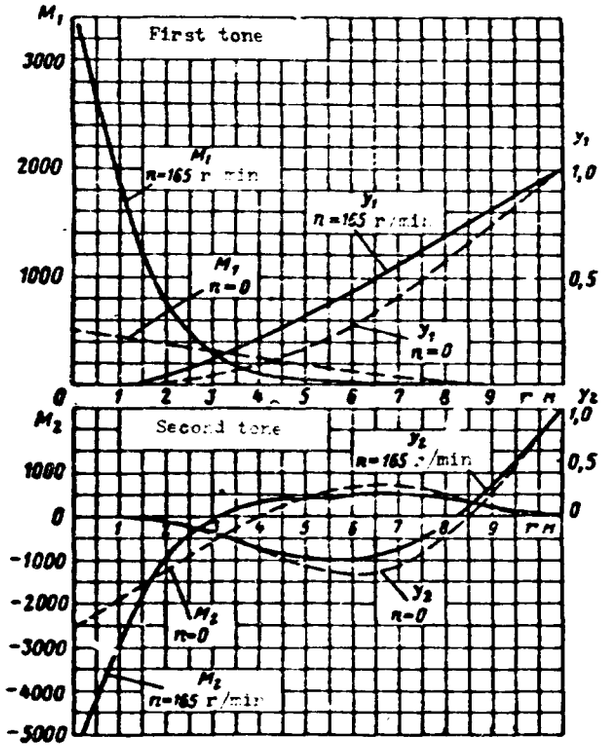

Fig. 1.10. Forms of the first and second tone of natural oscillations of a blade rigidly sealed in the shank.

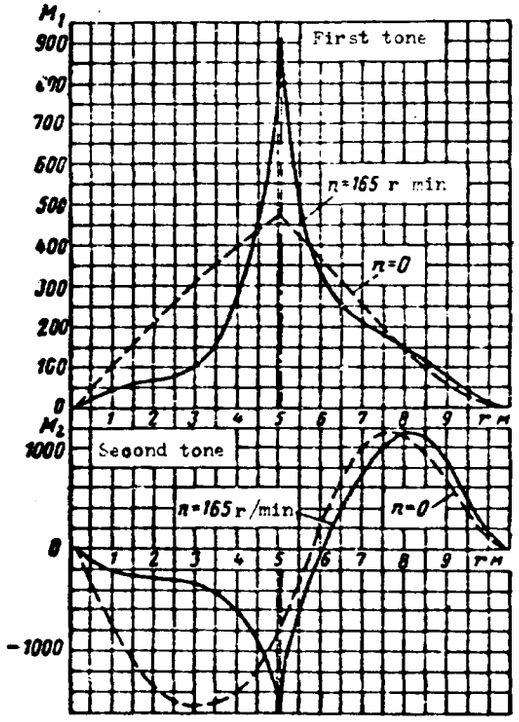

Fig. 1.11. Bending moment with oscillations in the first and second tone with load on the radius $\bar{r} = 0.48$ similar in weight to the weight of the blade.

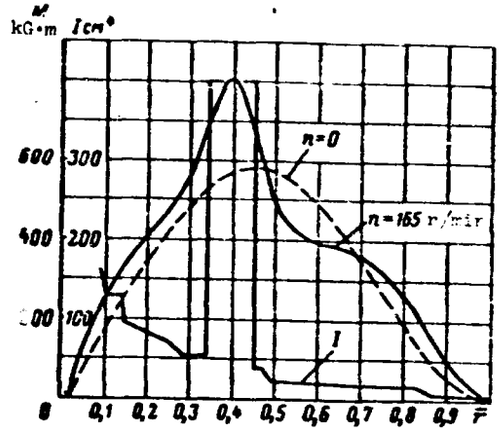

Fig. 1.12. Form of bending moment in the first tone for a blade with a section of increased rigidity.

Distribution of bending moments along the blade length with its oscillations in the field of centrifugal forces is characterized by an increase in bending moments on certain sections of the blade owing to their decrease in adjacent sections. Such a local increase in bending moments will be called the concentration of bending moments. The appearance of concentrations of bending moments is connected with the presence in the design of the blade of large concentrated loads and sharp drops in bend rigidity.

Concentrations of bending moments lead to the appearance on a series of sections of the blade of increased flexural stresses, which is caused by sharp bends in the blade on these sections.

This circumstance is of considerable interest for practice and therefore should be examined in more detail.

The character of blade oscillations in the field of centrifugal forces to a great degree is determined by the relationship between values of elastic and centrifugal forces. If the bending rigidity of the blade is sufficiently great (as this frequently happens, especially in the plane of rotation of the rotor), and the centrifugal forces are insignificant (small rotor revolutions), then the form of oscillations differs little from the form of oscillations of an irrotational blade.

If, however, conversely, the bending rigidity of the blade is small, and centrifugal forces are considerable, then the form of deformations of the blade is determined basically by inertial and centrifugal forces and depends little on elastic properties of the blade. In this case the form of deformations of the blade with oscillations differs very slightly from the form of deformations of an absolutely flexible heavy line stretched by centrifugal forces. Such a position, as a rule, is observed with oscillations in the thrust plane for blades of contemporary helicopters.

Quantitatively the relationship between elastic and centrifugal forces can be estimated with the help of coefficient α, which is

the ratio of the elastic potential energy to potential energy accumulated by the blade due to bending in the field of centrifugal forces:

$$a = \frac{C_{EI}}{C_N}.$$

Values C_{EI} and C_N are depicted in formulas (3.3) and (3.4).

For $\alpha > 1$ the influence of elastic properties of the blade is greater than the influences of centrifugal forces. For $\alpha < 1$ the opposite picture is observed.

Table 1.5.

Tone of oscillations	Coefficient α with	
	deformation in the flapping plane	deformation in the plane of rotation
First.....	0.083	2.2
Second....	0.332	3.7
Third.....	0.629	7.7
Fourth....	1.116	–

Table 1.5 gives values of coefficients α for a hinged suspended blade whose forms of oscillations are shown on Figs. 1.8 and 1.9. This blade can be examined as a typical helicopter blade.

Values of coefficients α given in Table 1.5 confirm the position that the helicopter blade by its characteristics in the flapping plane approaches an absolutely flexible heavy line stretched by centrifugal forces for which $\alpha = 0$.

The greater the properties of the blade and torsion fiber approach, the lower the tone of natural oscillations.

The basic peculiarity of an absolutely stretched torsion fiber is the fact that its axis undergoes fractures at points of application of concentrated transverse forces and in places of the connection of the line with rigid elements. Such a fracture, as a rule, appears at the place of sealing of the line. If into the torsion line there is inserted a rigid section, then along the edges of this section the same fractures will appear. Therefore, in those cases when properties of the blade and the stretched torsion fiber approach, these peculiarities appear with deformations of the blade. Of course, the elastic blade, no matter how low its flexural rigidity is, cannot undergo such fractures. Nevertheless, fractures peculiar to an absolutely torsion fiber are transmitted to the blade and appear in the form of sharp bends of its axis. These bends are accompanied by the appearance of concentrations of bending moments and the increase in flexural stresses at places of the bend.

Let us consider several examples confirming this position.

Figure 1.11 gives the distribution of bending moments along the length of the blade corresponding to forms of natural oscillations of the first and second tone with a load almost equal to the weight of the blade and placed on the relative radius $\bar{r} = 0.48$.

At the point of bracing of the load there is observed a sharp concentration of the bending moment, which leads to an increase in stresses almost twice as compared to an irrotational blade. Introduction into the blade of the section with increased rigidity leads to the appearance of the concentration of bending moment in the region of this section (Fig. 1.12). But inasmuch as the increase in flexural rigidity leads to an increase in the drag torque on the length of the rigid section, then the greatest stresses appear along the edges of the section, i.e., there where the absolutely torsion fiber would undergo fractures.

By the manifestation of the same properties of absolutely stretched torsion fiber there is explained the appearance of sharp

concentration in bending moment in the case of rigid blade sealing, since the torsion line would have at the sealing site the same fracture as that of a hinged-mounted blade.

The increase in bending moment corresponding to the first tone with rigid sealing of the blade in the shank occurs almost six times (see Fig. 1.10) as compared to the moment of an irrotational blade. Such a sharp concentration in bending moment has a noticeable influence even on values of frequencies of natural oscillations (see Table 1.4). This considerably lowers the possibilities of the method of approximation (see § 3) in the application to calculation of a blade with rigid sealing in the shank.

In a number of cases in practice it appears necessary to introduce into the rotor blade additional hinges or to displace the position of those hinges which are already in the construction of the hub. The need to create additional hinges can be connected with the necessity to lower the flexural stresses on some section of the blade or with the change in frequencies of its natural oscillations.

Let us see how the introduction into it of an additional hinge has an effect on flexural deformations of the blade. It was said earlier that the blade of a helicopter is similar in its characteristics to a stretched torsion fiber. The stretched chain with hinges continuously distributed along the length behaves just as the torsion fiber. Therefore, one can assume that the blade of a helicopter takes during deformations approximately the same form as a stretched multilinked chain. It is natural therefore that the introduction into the blade of an additional hinge cannot considerably affect the form of its deformations. This circumstance is illustrated in Fig. 1.13, where the form of the first tone of natural oscillations of the blade is shown with an additional hinge introduced into it and without it. From Fig. 1.13 also it is clear that the influence of an additional hinge noticeably has an effect on the form of bending moment only on the small section close to the hinge. On sections far from the hinge its influence is small.

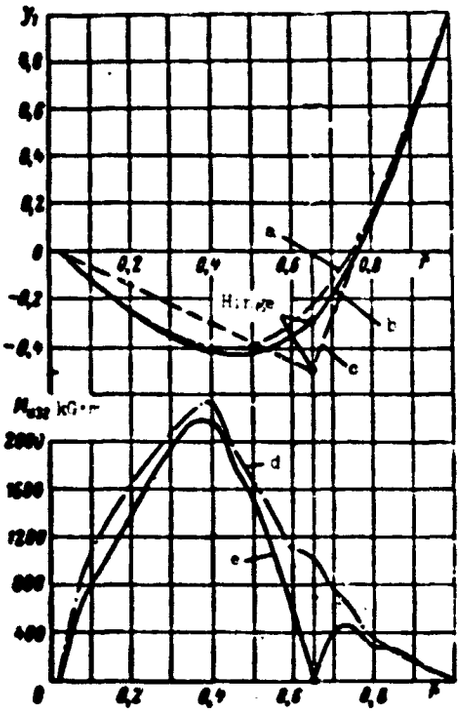

Fig. 1.13. Form of the first tone of natural oscillations of a blade with an additional hinge and without it: a and b) forms of first tone in the field of centrifugal forces without a hinge (a) and with a hinge (b); c) form of first tone of irrotational blades with a hinge; d and e) form of bending moment in first tone in the field of centrifugal forces without a hinge (d) and with a hinge (e).

It is necessary to note especially that in the examined case when the blade has two hinges, forms of its oscillations in the field of centrifugal forces very greatly differ from forms of oscillations of an irrotational blade. During oscillations in the first tone the irrotational blade is not at all deformed. Therefore, in the given special case the approximate power method of calculation of frequencies in such a form is expounded in § 3 will simply not be used.

It is also impossible to disregard the field of centrifugal forces in examining deformations of the blade in rotor of the Derschmidt type with a hinge greatly remote from the axis of rotation. The form of oscillations of the lowest tone of the blade of this rotor and the bending moment corresponding to it are shown on Fig. 1.14. Neglecting the centrifugal forces the form of blade would coincide with a straight line, and the magnitude of the bending moment shown on Fig. 1.14, which for this rotor is very great and actually determines the possibility of its application, would be impossible to find.

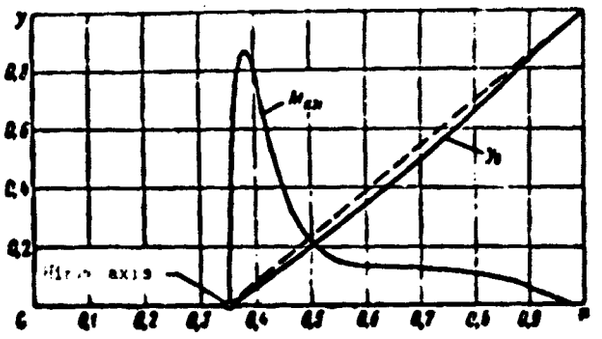

Fig. 1.14. Form of lowest tone of natural oscillations of a blade with a hinge ascribed from the axis of rotation and bending moment corresponding to this form (with oscillations in the flapping plane $p_0/n = 1.35$, with oscillations in plane of rotation $p_0/n = 0.91$).

The examples given show that in a whole series of cases the forms of natural oscillations in the field of centrifugal forces considerably differ from corresponding forms of an irrotational blade. This circumstance certainly should be considered in the designing of the blade. Therefore, in work in the design office, when all calculations are conducted on electronic computers and the degree of complexity of the method remains simply unnoticed, there is no sense in reverting to the methods of approximation.

§ 5. Torsional Blade Vibrations

1. Problems Solvable in the Calculation of Torsional Vibrations

Above in §§ 1 and 4 it was noted that the calculation of forms and frequencies of natural flexural oscillations of the blade has together with an auxiliary importance (for calculation of stresses) also an independent importance as a method for selecting parameters of the blade which exclude the possibility of flexural resonances. This problem does not exist for calculation of free torsional vibrations, since in practice oscillations considerable in amplitude which were caused by twisting resonance were never observed. As a rule, considerable torsional vibrations appear only with flutter or during forced oscillations under conditions of proximity of the flutter. Therefore, the magnitude of frequency of natural torsional vibrations itself is of no practical interest (if one were not to examine it as a parameter characterizing the torsional rigidity of the blade), and results of the calculation of forms and frequencies of natural oscillations have only an auxiliary assignment for calculation of flutter or of flexural stresses, which are calculated

taking into account torsional deformations of the blade. The other problem of calculation of free torsional vibrations of the blade is not raised.

There are basically two problems of the calculation of forced torsional vibrations. The first is the determination of elastic deformations of the blade the calculation of which is necessary for calculation of flexural stresses, and the second is the determination of values of hinged moments necessary for calculation of the rotor control system.

2. Differential Equation of Torsional Blade Vibrations

Let us represent the blade in the form of a cantilever rectilinear rod with torsional rigidity variable in length $GT_{кр}$. We will consider the mass moment of inertia of the rod sections relative to its axis I_m, just as the torsional rigidity, as a continuous function variable in length of the rod, the centers of gravity of all sections of the rod — as lying on the rod's axis, and sealing of the rod — elastic on torsion.

It is natural that reduction of the problem on oscillations of the blade to the calculation of such a model presupposes the application of a whole series of simplifying assumptions. We will consider that the axis of rigidity of the blade is rectilinear and coincides with the axis of axial hinge of the rotor hub. We will assume the flapping compensator $\varkappa$ equal to zero.

Calculation of the shift in centers of gravity and a determination of the influence of the flapping compensator on frequencies of natural oscillations will be examined in § 6.

Application of the enumerated assumptions permits solving the problem on torsional vibrations of the blade absolutely independently, not connecting them with its flexural vibrations.

Let us compose the differential equation of torsional vibrations of the blade. Torque in sections of the blade can be determined

from the differential equation:

$$[M_{кр}]' = -\mathfrak{M}, \tag{5.1}$$

where $\mathfrak{M}$ is the linear torque of external and inertial forces having an effect on the element of the blade.

Under the impact of torque every element of the blade twists at the angle:

$$d\varphi = \frac{M_{кр}}{GT_{кр}}\,dr, \tag{5.2}$$

where φ is the elastic angle of rotation of the blade section.

The value of torque, obtained from (5.2), will be substituted into (5.1). Then the differential equation of twisting deformations of the blade can be recorded in the form

$$[GT_{кр}\varphi']' + \mathfrak{M} = 0. \tag{5.3}$$

Let us examine the torsional vibrations of the rotor blade revolving in a vacuum. The linear torque in this case will be equal to:

$$\mathfrak{M} = -I_m\ddot{\varphi} - \omega^2(I_y - I_x)\varphi, \tag{5.4}$$

where I_y and I_x are mass moments of inertia of the blade section relative to its principal axes of inertia.

If the extent of the profile along the x axis is considerably larger than along the y axis, and this usually occurs, then it is possible approximately to assume that

$$I_y - I_x \cong I_m, \tag{5.5}$$

where I_m is the linear mass moment of inertia of the blade section with respect to the axis passing through the axis of rigidity.

Substituting expression (5.4), taking into account (5.5), into equation (5.3), we will obtain the differential equation of torsional vibrations of the rotor blade revolving in the field of centrifugal forces:

$$[GT_{кр}\varphi']' - I_m(\ddot{\varphi} + \omega^2\varphi) = 0. \tag{5.6}$$

The model of the blade examined here has the following boundary conditions:

for r = 0:

$$[GT_{кр}\varphi']_0 = c_{упр}\varphi_0;$$

for r = R:

$$[GT_{кр}\varphi']_R = 0, \tag{5.7}$$

where $c_{упр}$ is the rigidity of the rotor control system reduced to the axial hinge of the hub (rigidity of control determines the magnitude of rigidity of elastic sealing of the blade in the shank); φ_0 – rotation of blade in axial hinge due to deformations of rotor control system.

3. Determination of Forms and Frequencies of Natural Oscillations of the Torsional Blade

Here we will use the same method of solution which was discussed in No. 1 of § 2 for determination of forms and frequencies of flexural vibrations. Let us assume that

$$\varphi(t) = \varphi \sin \nu t. \tag{5.8}$$

Substituting expression (5.8) into equation (5.6), we will obtain

$$[GT_{кр}\varphi']' + (\nu^2 - \omega^2) I_m\varphi = 0. \tag{5.9}$$

From this equation it immediately follows that forms of natural torsional oscillations of a rotational and irrotational blade are identical, and the frequencies are connected by a simple relation of the form

$$\nu^2 = \nu_0^2 + \omega^2, \tag{5.10}$$

where ν is the frequency of natural oscillations in the field of centrifugal forces; ν_0 is the frequency of natural oscillations of the blade of an irrotational rotor.

Integrating equation (5.9), taking into account boundary conditions (5.7) for the case $\omega = 0$, we will obtain

$$\varphi = \nu^2\left[\int_0^r \frac{dr}{GT_{кр}}\int_r^R I_m\varphi dr + \frac{1}{c_{упр}}\int_0^R I_m\varphi dr\right]. \tag{5.11}$$

Here and below the index at ν, which denotes that the frequency of natural oscillations is determined for $\omega = 0$, will be omitted.

Equation (5.11) is solved by the method of successive approximations, just as this was carried out in the solution of equations (2.4) in § 2.

Let us assign the arbitrary form of oscillations φ. This form should be in some way standardized, for example

$$\varphi_R = 1, \tag{5.12}$$

where φ_R is the elastic angle of twist of the blade tip.

Then, fulfilling the operations assigned by expression (5.11), we will determine the function

$$\vartheta = \int_0^r \frac{dr}{GJ_{кр}} \int_r^R I_m \varphi dr + \frac{1}{c_{y\text{-}p}} \int_0^R I_m \varphi dr. \tag{5.13}$$

The frequency of natural torsional oscillations of the blade can be determined from the condition of standardization (5.12)

$$\nu^2 = \frac{1}{\vartheta_R}, \tag{5.14}$$

where ϑ_R is the value of function ϑ at r = R.

Assigning a new value of function

$$\varphi = \nu^2 \vartheta \tag{5.15}$$

and performing operations (5.13) and (5.14) still as many times as it is necessary to provide the necessary accuracy, we will obtain the final values ν and φ. As with the determination of forms and frequencies of natural flexural oscillations, such a method of successive approximations leads to the determination of the lowest tone of natural torsional oscillations. In the determination of subsequent tones it is necessary to fulfill the condition of orthogonality

$$\int_0^R I_m \varphi^{(1)} \varphi^{(n)} dr = 0. \tag{5.16}$$

Here the index j denotes the form of the sought tone of oscillations and index m the form of the already determined lowest tones. Assuming

$$\varphi^{(j)}=\nu^2\left[\vartheta-\sum_{m=1}^{m=j-1}c_m\varphi^{(m)}\right], \tag{5.17}$$

we will obtain from condition (5.16) expressions for constant coefficients c_m:

$$c_m=\frac{\int_0^R I_m\vartheta\varphi^{(m)}dr}{\int_0^R I_m(\varphi^{(m)})^2dr}. \tag{5.18}$$

Frequencies of natural oscillations of subsequent tones are determined with each approximation by the formula

$$\nu_j^2=\frac{1}{\vartheta_R-\sum_{m=1}^{m=j-1}c_m}. \tag{5.19}$$

Upon completion of the determination of all forms and frequencies of natural oscillations necessary for further calculations it is necessary to correct the frequencies by the formula (5.10), considering the influence of centrifugal forces.

Calculations of forms and frequencies of natural torsional oscillations of a blade for real helicopters show that of decisive importance in the determination of values of frequencies of the lowest tone of oscillations is the rigidity of the rotor control system. Almost always the torsional rigidity of the blade proves to be considerably higher than the rigidity of the control system. Figure 1.15 gives forms of the first tone of natural torsional vibrations of blades of different helicopters found in mass exploitation.

According to the relationship between twisting strains of the blade and rotor control system with oscillations in the first tone, it is possible to judge the magnitude of twisting rigidity of the blade as compared to rigidity of the control system. The relationship

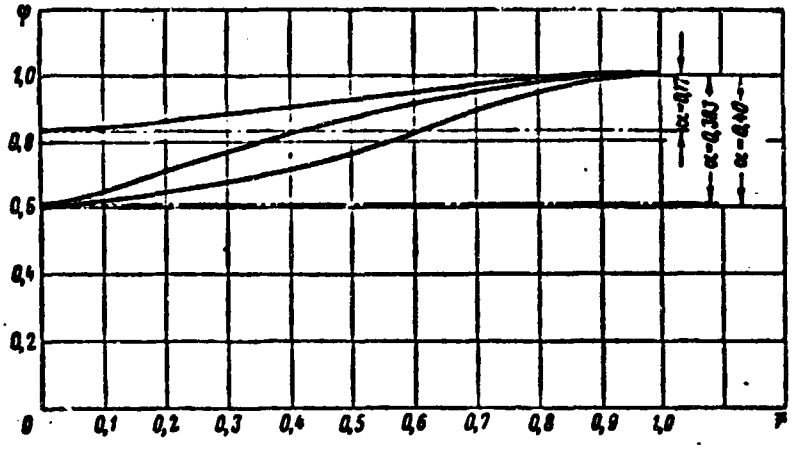

Fig. 1.15. Forms of natural torsional oscillations of the blade with different relationships of rigidity of the blade and control system.

between these rigidities is estimated by the coefficient α (see Fig. 1.15). This coefficient itself determines part of the total angle of rotation of the blade tip due to deformations of only the blade.

The described peculiarity in the relationship of rigidities of the blade and control permits in certain calculations using the assumption of the fact that twisting deformations of the blade are small as compared to deformations of control and introducing into the calculations only the twist of the blade due to the control deformation. This assumption is frequently used during calculation of flutter (see Chapter IV of Book One).

Results of the calculation by the expounded method permit judging the character of location of frequencies of natural torsional oscillations of blade with respect to harmonic components of aerodynamic forces. Figure 1.16 gives a resonance diagram of torsional vibrations of a blade, plotted for one of the existing helicopters, and Fig. 1.17 gives forms of the first three tones.

In No. 1 of this paragraph it was already noted that variable external forces twisting the blade are small, and therefore even with resonance of the amplitude of torsional vibrations they do not become dangerous for the blade strength. In view of this there is usually

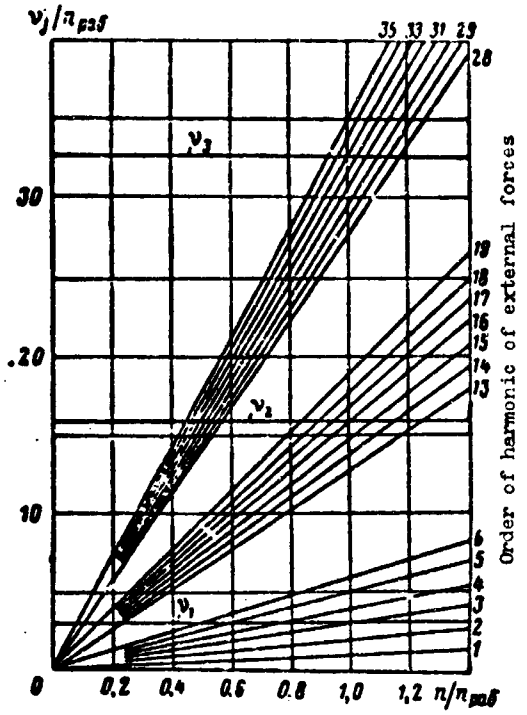

Fig. 1.16. Resonance diagram of torsional oscillations of the blade.

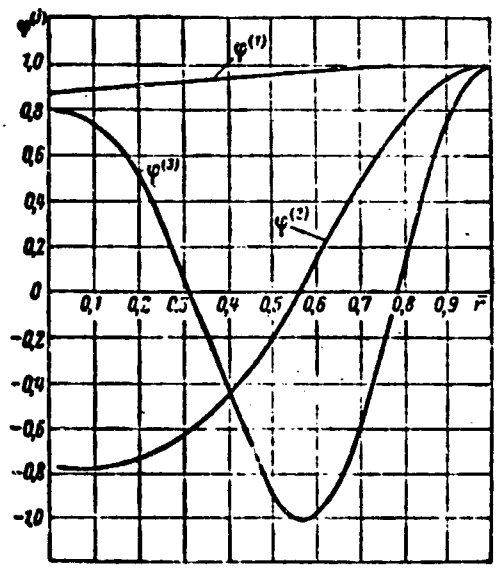

Fig. 1.17. Forms of first three tones of torsional vibrations of blade.

no attempt to avoid twisting resonances, and the resonance diagram shown in Fig. 1.16 is given only for an estimate of the absolute magnitude of frequencies of torsional vibrations.

From Fig. 1.16 it follows that even the second tone of torsional vibrations proves to be in operating revolutions $n_{раб}$ higher than the fifteenth harmonic to the number of revolutions of the rotor.

Frequencies of subsequent tones appear even above. Therefore, probably only the frequency of the first tone of natural torsional oscillations of the blade can be of practical interest.

All the above-mentioned considerations pertained to torsional vibrations of the rotor blade examined separately neglecting those connections which are superimposed on oscillations of construction of the blade fastening on the hub. It appears that the connection between torsional vibrations of separate blades of the rotor through the control system can considerably change the whole picture of oscillations.

4. Determination of Forms and Frequencies of Natural Oscillations of the Rotor as a Whole

Figure 1.18 gives a diagram of the control system of the angle of setting of blades used on the majority of contemporary helicopters.

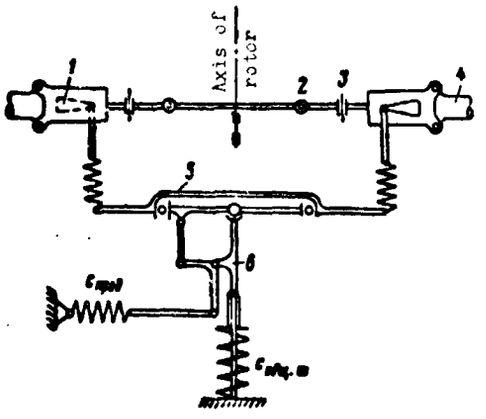

Fig. 1.18. Diagram of cyclic pitch control: 1 — lever of blade turn; 2 — horizontal hinge; 3 — vertical hinge; 4 — blade; 5 — disk of cyclic pitch control; 6 — slider.

Constructively this system is carried out in such a way that the loading of a certain control circuit depends on what combination of forces arrives on the disk of the cyclic pitch control from the blades. The form of this combination depends on the form of vibrations of the rotor, i.e., on the distribution of phases of vibrations by the blades. Thus, for example, in the case when all blades vibrate with an identical phase, only the control circuit is loaded by collective pitch. When oppositely located blades vibrate in a

reverse phase, circuits of transverse and longitudinal control are loaded. Finally, if the number of blades in the rotor is larger than three, then such forms of oscillations are possible when all forces arriving from the blades are locked on the disk of the cyclic pitch control.

The variable forces appearing during blade vibrations cause deformations of those control circuits which are loaded by these forces. With deformations of separate control circuits the disk of the cyclic pitch control oscillates, and vibrations of the disk tie fully defined phases to vibrations of the blades. Thus, for example, with vertical vibrations of the disk, appearing in the deformation of the control circuit by collective pitch, vibrations of the rotor of such form are excited at which phase of all blades are identical.

When the disk of the cyclic pitch control during vibrations is inclined, the oppositely located blades are excited in a reversed phase. Thus the disk of the cyclic pitch control connects vibrations of separate blades in the rotor. As a result it turns out that vibrations of blades can occur only with fully defined forms of vibrations of the entire rotor as a whole, and the number of such forms coincides with the number of blades in the rotor. With this each form of vibrations corresponds to its value of rigidity of control reduced to the axial hinge of the blade which depends on the rigidity of that control circuit which with this form is loaded. Accordingly, inherent to each form of vibrations of the rotor is its value of frequency of natural torsional oscillations of the blade.

Consequently, for a rotor with the number of blades $z_л$ there is $z_л$ different frequencies of natural oscillations, which correspond to each tone of torsional oscillations of the blade. Inherent to each frequency of natural oscillations is its definite form of distribution of angles of twist along the length of the blade, but qualitatively all forms corresponding to a definite tone of oscillations are not distinguished, and thus, for example, they have an identical number of nodes of oscillations.

As an example it is possible to cite values of frequencies of natural oscillations of the first tone for a four-bladed rotor of the helicopter Mi-4.

The lowest values of frequencies with loading of longitudinal and lateral controls attributed to working numbers of revolutions of the rotor are $\frac{\nu_1}{n_{раб}} = 3.4\text{-}3.5$. With loading of the circuit of the collective pitch this values takes the value $\frac{\nu_{1\,о\,м}}{n_{раб}} = 4.6$ and when all forces from the rotor are locked on the disk of the cyclic pitch control, $\frac{\nu_{1\,в\,п}}{n_{раб}} = 6.6$.

A very important circumstance is the fact that within frequencies of oscillations corresponding to harmonics to the number of revolutions of the rotor on which external forces have a noticeable magnitude lies only the first tone of natural torsional oscillations of blade. All subsequent tones of oscillations lie above and therefore are of no practical interest.

§ 6. Joint Flexural-Torsional Vibrations of the Blade

1. The Connection Between Flexural and Torsional Vibrations

Above free flexural and torsional vibrations of the blade as two independent problems not connected between themselves were examined. In a real blade torsional and flexural oscillations are always connected. How great this connection proves to be will be shown below. We will examine vibrations of the blade in a vacuum when the connection between torsional and flexural oscillations is carried out only owing to the shift in centers of gravity of sections with respect to the axis of rigidity of the blade and due to the nonholonomic constraint through the flapping balance. Let us use the method of calculation constructed on the basis of the method of three moments, described in § 4, in reference to calculation of flexural vibrations.

The possibility of fulfillment of the calculation of frequencies of natural flexural-torsional vibrations can be useful to the designer in the solution of a whole series of concrete practical problems.

Thus, for example, the necessity of fulfillment of such a calculation appears in those cases when to eliminate resonance it is proposed to install extension balancers on the blade. Here there are considered those relatively rare cases when arrangement of balancers is proposed not to eliminate flutter but to change the frequencies of natural oscillations.

The desire to consider the connection between flexural and torsional vibrations can appear for the designer also in the case when the calculation of frequencies of natural oscillations of the blade for some reason does not coincide with the experiment. Here in a number of cases it can appear that this distinction is explained by a disregard of this connection. It is possible to hope that results of calculations mentioned below will facilitate permission of those doubts.

It is necessary, however, to note that the calculation of frequencies of natural oscillations in a vacuum cannot give an answer to many questions appearing in practice in connection with the appearance in the blade of increased varying stresses with any frequency and estimated as resonances, since aerodynamic forces can introduce in many cases very substantial corrections into the pattern of the phenomenon.

2. Method of Calculation of Joint Vibrations

Fulfillment of the calculation of forms and frequencies of natural flexural-torsional vibrations is considerably simplified if one were to examine the blades of only the definite most widespread type, during the calculation of which the following assumptions can be used:

1. The axis of blade rigidity is a straight line coinciding with the axis of axial [illegible].

In principle the method of calculation will not be changed when these axes will not coincide. Only it will be necessary to introduce into the calculation formulas a number of additional terms consider-

the distance between these axes. For simplicity of computations let us assume that the axis of rigidity passes through the axis of rotation of the rotor.

2. The plane of least rigidity of the blade is considered coinciding with the flapping plane.

3. The blade accomplishes torsional vibrations due to twisting deformations of the actual blade, deformations of the control system by the blade angle and as a result of nonholonomic constraint through the flapping balance with vibrations of the blade in the flapping plane.

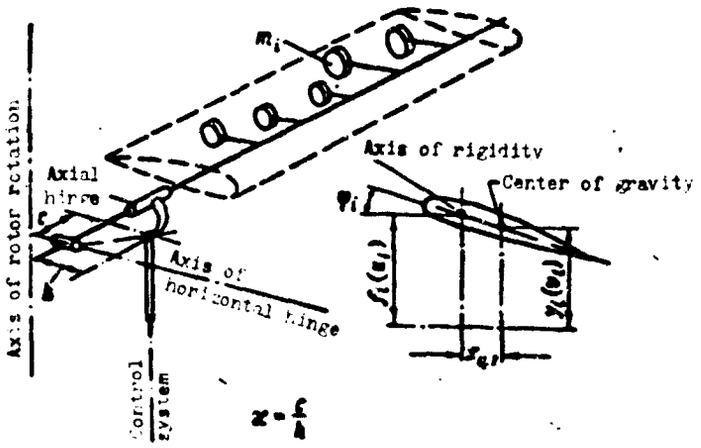

Fig. 1.19. Calculation model of the blade.

These assumptions permit representing the blade in the form of a weightless free beam divided into z sections, along the edges of which with a certain extension x_{a_i}, loads with mass m_i are located (Fig. 1.19). Every load except mass m_i, concentrated in the center of gravity of the corresponding element of the blade, possesses also a certain moment of inertia I_{a_i} with respect to the axis passing through the center of gravity of the load and parallel elastic axis of the blade.

Flexural and torsional rigidities will be presented in the form of step curves in such a way that they remain constant for the extent of each section.

The presence of a flapping balance leads to nonholonomic constraint between flexural and torsional vibrations, which can be expressed by formula

$$\varphi_0 = \frac{M_{кр_0}}{c_{упр}} - \varkappa\beta_0, \tag{6.1}$$

where φ_0 is the angle of rotation of the blade in the axial hinge; $M_{кр_0}$ – torque relative to the axial hinge; $c_{упр}$ – rigidity of blade angle control system reduced to the axial hinge; $\varkappa$ – flapping balance; β_0 – angle of rotation of the blade relative to the horizontal hinge.

Furthermore, boundary conditions in the shank of the hinge-mounted blade during its oscillations in the thrust plane somewhat change. In the presence of a flapping balance these conditions can be recorded as:

$$M_0 = \varkappa M_{кр_0}, \tag{6.2}$$

where M_0 is the bending moment and $M_{кр_0}$ the torque in the blade shank.

With the composition of differential equations of vibrations of the blade in the flapping plane we will use the method of three moments in that form which was discussed in § 4. The application of this method to the calculation case examined here leads to the following equations:

$$\left.\begin{aligned} &h_{i-1}M_{i-1} + g_i M_i + h_i M_{i+1} = \frac{Q_{i,i+1}}{N_{i,i+1}} - \frac{Q_{i-1,i}}{N_{i-1,i}}; \\ &d_{i-1}M_{i-1} + e_i M_i + d_i M_{i+1} = b_{i-1}f_{i-1} + a_i f_i + b_i f_{i+1}. \end{aligned}\right\} \tag{6.3}$$

Here

$$\left.\begin{aligned} Q_{i,i+1} &= -\sum_{i+1}^{s} m_i \bar{y}_i; \\ Q_{i-1,i} &= -\sum_{1}^{s} m_i \bar{y}_i \ (\text{где } i = 0, 1, 2, \ldots, s); \end{aligned}\right\} \tag{6.4}$$

f_i – vertical movements of points of elastic axis of the blade (see Fig. 1.19); y_i – vertical movements of centers of gravity of masses m_i.

Expressions for constant coefficients a_i, b_i, c_i, h_i, and g_i, are given in § 4, see formulas (4.18)-(4.25).

Movements in elastic axis f_i and centers of gravity of elements of the blade y_i are connected by the relationship

$$f_i = y_i + x_{\text{ц.т}_i}\varphi_i, \tag{6.5}$$

where φ_i are angles of rotation of elements of the blade around its elastic axis.

To determine the forms and frequencies of flexural-torsional vibrations of the blade one should add the equations of torsional vibrations to equations (6.3).

If the torque can be considered constant in magnitude for the extent of each section of the blade, it can be determined as

$$M_{\text{кр}_{i-1,i}} = -\sum_i^s I_{\text{ц.т}_i}\ddot{\varphi}_i - \omega^2\sum_i^s I_{\text{ц.т}_i}\varphi_i + \omega^2\sum_i^s m_i x_{\text{ц.т}_i} r_i f_i' + \sum_i^s m_i x_{\text{ц.т}_i}\ddot{y}_i. \tag{6.6}$$

In magnitude of torque torsional deformations of the blade can be determined thus

$$\varphi_i = \sum_0^i \frac{M_{\text{кр}_{i-1,i}} l_{i-1,i}}{GT_{\text{кр}_{i-1,i}}} - x\beta_0, \tag{6.7}$$

where $GT_{\text{кр}i-1,i}$ is the torsional rigidity of the section of the blade along a length equal to $l_{i-1,i}$, and φ_0 is determined by the formula (6.1).

In the use of the method of three moments boundary conditions of the problem are considered in coefficients of equations of the system. Thus, in the case examined here the boundary condition (6.2) leads to a change in coefficients of the first two equations of system (6.3). For a blade with hinged fitting in the shank these equations can be recorded in the following way:

– the first equation of system (6.3) from which the value β_0 is determined:

$$\beta_0 + \varkappa g_0 M_{\text{кр}_0} + h_0 M_1 = \frac{Q_{01}}{N_{01}}; \qquad (6.8)$$

– the second equation of system (6.3):

$$\varkappa h_0 M_{\text{кр}_0} + g_1 M_1 + h_1 M_2 = \frac{Q_{12}}{N_{12}} - \frac{Q_{01}}{N_{01}}. \qquad (6.9)$$

Thus the system of equations, including equations (6.3), (6.5), (6.6), and (6.7), constitutes a system of differential equations of flexural-torsional vibrations of the blade. The solution of this system permits determining the form and frequency of natural flexural-torsional vibrations of the blade, which enters into the problem of the calculation.

If one were to assume that the variables entering into differential equations (6.3), (6.5), (6.6), and (6.7) are changed according to the sinusoidal law of the form

$$y_i(t) = y_i \sin pt,$$

then these equations can be converted into a system of algebraic equations relative to unknowns, which are peak value of former variables. Only into certain coefficients of these equations will parameters p^2 and $\gamma = \frac{\omega^2}{p_3}$ enter by cofactors. If we assume $p^2 = 1$, then these equations can be copied in the form

$$\left.\begin{aligned} h_{i-1}\overline{M}_{i-1} + g_i\overline{M}_i + h_i\overline{M}_{i+1} &= \frac{\overline{Q}_{i,i+1}}{N_{i,i+1}} - \frac{\overline{Q}_{i-1,i}}{N_{i-1,i}}; \\ d_{i-1}\overline{M}_{i-1} + c_i\overline{M}_i + d_iM_{i+1} &= b_{i-1}u_{i-1} + a_iu_i + b_iu_{i+1}; \end{aligned}\right\} \qquad (6.10)$$

$$\overline{M}_{\text{кр}_{i-1,i}} = (1-\gamma)\sum_i^s I_{\text{м.т}_i}\vartheta_i + \gamma\sum_i^s m_i x_{\text{м.т}_i} r_i f_i' - \sum_i^s m_i x_{\text{м.т}_i}\eta_i; \qquad (6.11)$$

$$\vartheta_i = \sum_0^i \frac{\overline{M}_{\text{кр}_{i-1,i}} l_{i-1,i}}{GT_{\text{кр}_{i-1,i}}} - \varkappa\overline{\beta}_0; \qquad (6.12)$$

$$v_i = u_i - x_{\text{м.т}_i}\vartheta_i, \qquad (6.13)$$

where

$$\overline{Q}_{i,i+1} = \sum_{i+1}^s m_i\overline{y}_i;$$

$$\overline{Q}_{i-1,i} = \sum_i^s m_i\overline{y}_i.$$

The quantities entering into these equations are subordinated to the following relations:

$$\left.\begin{aligned} y_i &= p^2 v_i; \\ f_i &= p^2 u_i; \\ \varphi_i &= p^2 \theta_i; \\ M_i &= p^2 \overline{M}_i; \\ M_{\text{кр}\,i-1,i} &= p^2 \overline{M}_{\text{кр}\,i-1,i}; \\ \beta_0 &= p^2 \overline{\beta}_0. \end{aligned}\right\} \qquad (6.14)$$

It is convenient to solve the system of equations (6.10), (6.11), (6.12), and (6.13) by the method of successive approximations. In every approximation there should be fulfilled a more precise definition of parameter γ under the angular velocity of rotation of rotor ω assigned in the calculation.

Fulfillment of successive approximations is produced in the following order.

Let us assign a certain value of parameter γ and arbitrary form of zero approximation of functions y_{i_0} and φ_{i_0}.

The functions taken as the zero approximation should be standardized, for example,

$$y_z = 1.$$

After that by formula (6.5) there can be obtained function f_{i_0}. Then by equation (6.11) quantity $\overline{M}_{\text{кр}_0}$, which is necessary for solution of the system of equations (6.10) can be determined. Simultaneously $\overline{M}_{\text{кр}\,i-1,i}$ is determined.

After solving the system of equations (6.10) and determining u_i from the first equation of this system, $\overline{\beta}_0$ is determined:

$$\overline{\beta}_0 = \frac{\overline{\sigma}_m}{N_a} - h_0 \overline{M}_1 - x g_0 \overline{M}_{\text{кр}_0}. \qquad (6.15)$$

Then by equation (6.12) γ_i is determined, and by equation (6.13) values of v_i, which, furthermore, should satisfy the condition $\sum_0^s m_i v_i = 0$ are determined.

The frequency of natural oscillations is determined from the condition of standardization on the basis of the first relation of (6.14) thus:

$$p^2 = \frac{1}{v_s}. \tag{6.16}$$

After that from relations (6.14) functions y_i and φ_i can be determined, which are used for the following approximation fulfilled in the same order. Simultaneously there is refined parameter γ.

Such a method of successive approximations leads to the determination of the frequency and form of the lowest tone of natural oscillations. To determine the following tones there is used the condition of orthogonality, which for flexural-torsional vibrations has the following form:

$$\sum_0^s \left[m_i y_i^{(j)} y_i^{(m)} + I_{a.r_i} \varphi_i^{(j)} \varphi_i^{(m)} \right] = 0. \tag{6.17}$$

Here index j denotes the form of the sought tone and index m, the form of the already determined lowest tones.

Application of the expounded method of calculation gives results quite satisfactory for practice.

It is necessary to note that in those cases when the frequency of natural oscillations of two consecutive tones have sufficiently close values, this method of calculation does not give a convergent solution. Practically, however, this circumstance does not have great significance, since this can be only in the case when the connection between torsional and flexural vibrations is very weak, and corresponding forms of vibrations can be determined separately neglecting this connection.

3. Influence of the Connection Between Bending and Torsion on Frequency of Natural Oscillations

Here we will examine how much the frequencies of natural flexural-torsional vibrations of the blade can differ from corresponding partial frequencies, i.e., frequencies obtained neglecting the connection between bending and torsion.

Calculations show that the connection between bending and torsion has the greatest influence on frequencies of natural oscillations of the blade in those regions where partial frequencies of bending and torsion approach. Therefore, one should investigate only the given regions. Outside these regions partial frequencies of the blade and frequencies of the connected flexural-torsional vibrations practically coincide.

It is known that partial frequencies of natural oscillations of bending of a hinge-mounted blade for all contemporary helicopters lie in very narrow, fully defined, zones, the location of which with respect to harmonics of external excitation cannot be substantially modified. On Fig. 1.20 these zones are plotted on the resonance diagram of the blade. This diagram is constructed for a region of frequencies including only a number of first harmonics to the number of revolutions of the rotor, since external forces acting on the blade with higher harmonics are insignificant in magnitude and cannot cause any noticeable vibrations of blade. Falling into this region are only the first three tones of partial frequencies of the bending blade. Practically only these tones must be of interest during the designing of the blade. Frequencies of natural oscillations of bending can fall out of shown zones only for rotors with an unusual method of fastening of the blades on the hub, for example, for rotors with rigid fastening of blades or with a hub on a Cardan joint.

Partial frequencies of natural torsional oscillations of the blade can be changed in wider limits, basically due to the distinction in rigidities of the rotor control system whose construction can be

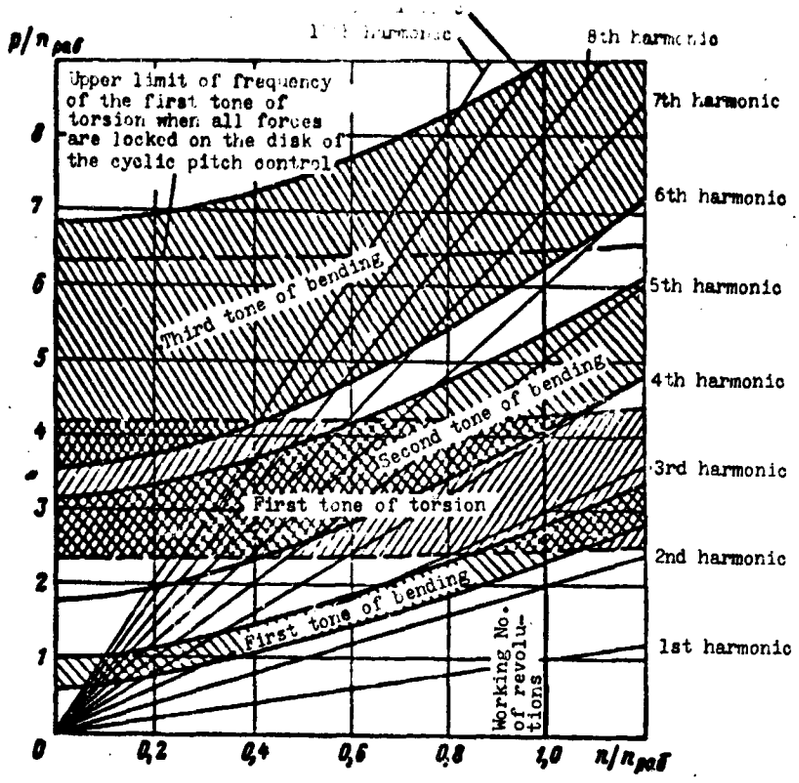

Fig. 1.20. Regions of location on a resonance diagram of frequencies of natural oscillations of the first, second and third tone of bending and first tone of torsion for blades of different helicopters.

very diverse. Nonetheless, with respect to values of partial frequencies of natural torsional oscillations of the blade there can be made a very important conclusion involving the following. Into the region of frequencies interesting to us there can fall only the first tone of torsional vibrations. The second tone of torsional vibrations appears, as a rule, in the region not lower than the 15th harmonic to the number of revolutions of the rotor (see Fig. 1.16), i.e., beyond the borders of the region interesting for the designer. Oscillations considerable in amplitude with such frequencies usually do not appear. Therefore, of practical interest from the point of view of the possibility of appearance of resonances is only the first tone of natural torsional oscillations of the blade.

Here it stands to remember that the rotor blade of the helicopter can have several first tones of torsional vibrations with different

frequencies depending upon the form of oscillations of the rotor on the whole and on what control circuit is loaded with this form of oscillations. The distinction in frequencies of natural oscillations of these forms will be determined solely by the difference in rigidity of loaded control circuits.

In flight every harmonic of external forces can exite only one fully defined form of oscillations. Therefore in the investigation the possibility of the appearance of resonance, one should certainly check whether the resonance is possible when the rigidity accepted in calculation corresponds to that form. In this paragraph only natural oscillations of the system are examined. Therefore, we will not dwell on this question in detail.

Figure 1.20 shows a region in which usually frequencies of the first tone of natural torsional oscillations of the blade lie for those forms of oscillations of the rotor when circuits of cyclical control and collective pitch control are loaded. For rotors with the number of blades of more than three a form of oscillations is possible at which all forces arriving from the blades are locked on the disk of the cyclic pitch control. The rigidity of control corresponding to this form appears usually very high. On Fig. 1.20 the upper limits of the region of the location of torsional vibrations in this case is noted by a dot-dashed line.

Let us consider the case most widespread in practice when partial frequencies of the first tone of bending and first tone of torsion coincide in magnitude in the zone of operating revolutions of the rotor. Let us investigate two variants of the distribution of centers of gravity of the blade along its length.

In both variants in accordance with the assumptions accepted above we will consider that the axis of rigidity of the blade is rectilinear and coincides with the axis of axial hinge of the hub. The distance to centers of gravity of the sections will be counted off from the axis of rigidity to the chord of the blade in percent. All investigations will be conducted in reference to the blade of

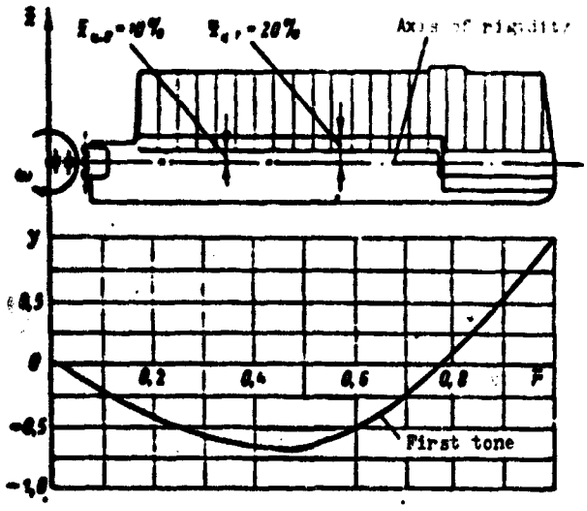

Fig. 1.21. Step centering of the blade with replacement of the sign in the node of the first tone of natural flexural oscillations.

the helicopter with a Duralumin pressed longeron with a chord constant along the length. Such a blade has approximately a constant linear weight along the length. Its chord consists of about one-twentieth of the radius of the rotor.

So that results of calculations are most obvious we will consider that with changes of the centering of the blade mass moments of inertia of its sections with respect to the axis passing through the centers of gravity are not changed, i.e., there is maintained the position

$$I_{a.t} = \text{const.}$$

In the beginning let us examine the case when the centering of sections of the blade are constant along its length, i.e.,

$$\bar{x}_{a.t} = \frac{x_{a.t}}{b} = \text{const,}$$

where b is the chord of the blade.

This variant of the distribution of centerings should be considered very widespread in practice. Furthermore, it permits in very clear form tracing the influence of centering and estimating its significance as factors of the connection between flexural and torsional vibrations.

Figure 1.22 gives a resonance diagram of the blade for this

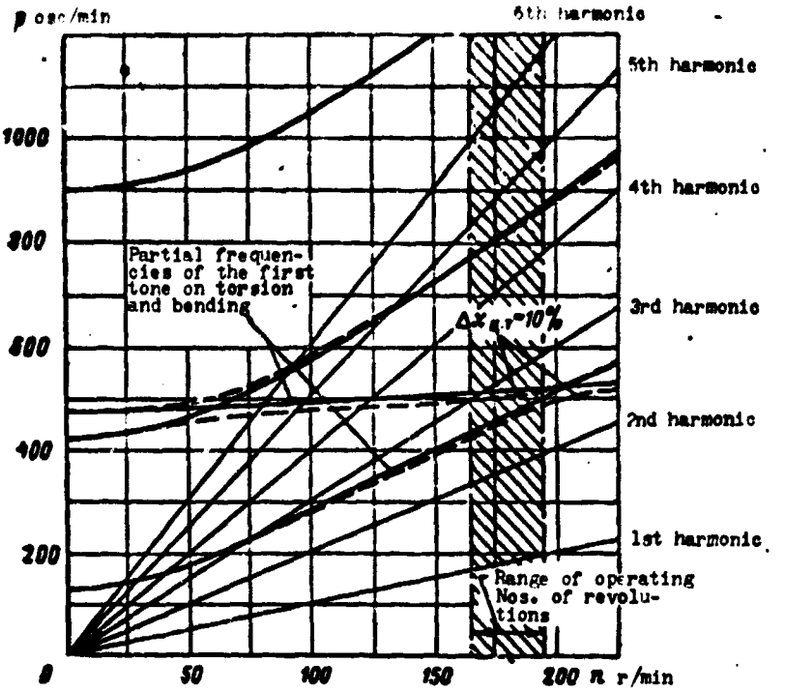

Fig. 1.22. Resonance diagram of the blade with shift (constant in length) in centering of 10% of the chord.

case. Solid lines show partial frequencies of bending and torsion of the blade, and dashed lines, the frequencies of joint flexural-torsional vibrations, which are calculated for a shift in centering with respect to the axis of rigidity equal to 10% of the chord of the blade. Calculations are carried out for the case when $\varkappa = 0$. Therefore, the sign of the shift in centering has no importance.

Here and later we intentionally examine the very wide range of the change in centerings so that in a clearer form we can trace its influence. In practice constructive possibilities and conditions superimposed by flutter permit changing the centering in very small limits. Usually for blades of rotors the centering changes from 20% to 25% of the chord of the blade (here there are given values counted off from the leading edge of the blade), i.e., the whole range of the change in centering consists of only about 5% of the chord of the blade. Therefore, from examining Fig. 1.22 the conclusion can be made that displacement of the centering, constant along the length of the blade, has a very slight effect on values of frequencies of natural oscillations.

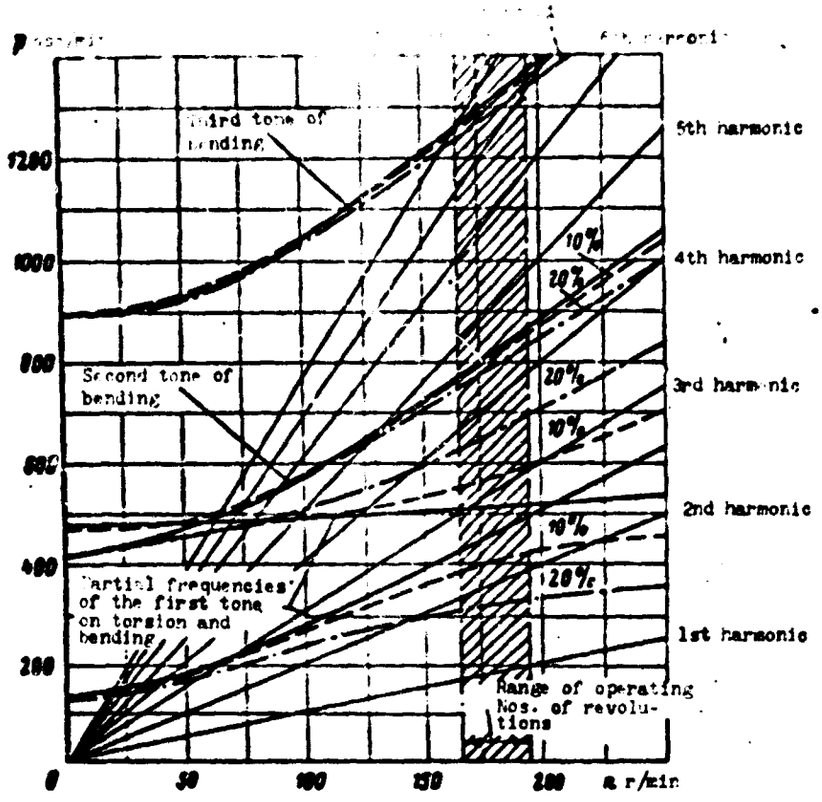

Fig. 1.23. Frequencies of natural flexural-torsional vibrations of the blade with the step law in the change of centering along the length of the blade with a shift of 10% and 20% chordwise from the axis of rigidity.

In the second case examined here the distribution of centering is selected in a way at which its influence appears the greatest during oscillations with a frequency close to the partial frequency of bending of the first tone. The centering is taken as constant along the length of the blade, but its sign is changed in the node of the first tone of partial flexural form.

Step centering can be created for the blade in those cases when an antiflutter balancer is introduced into the design not along the whole length but only on a small section on the blade tip. Results of the calculation for this variant of the distribution of centering are shown in Fig. 1.23. The influence of centering in this case is rather great. Therefore, with such distribution of it along the length the connection between bending and torsion should be considered during calculation of the blade.

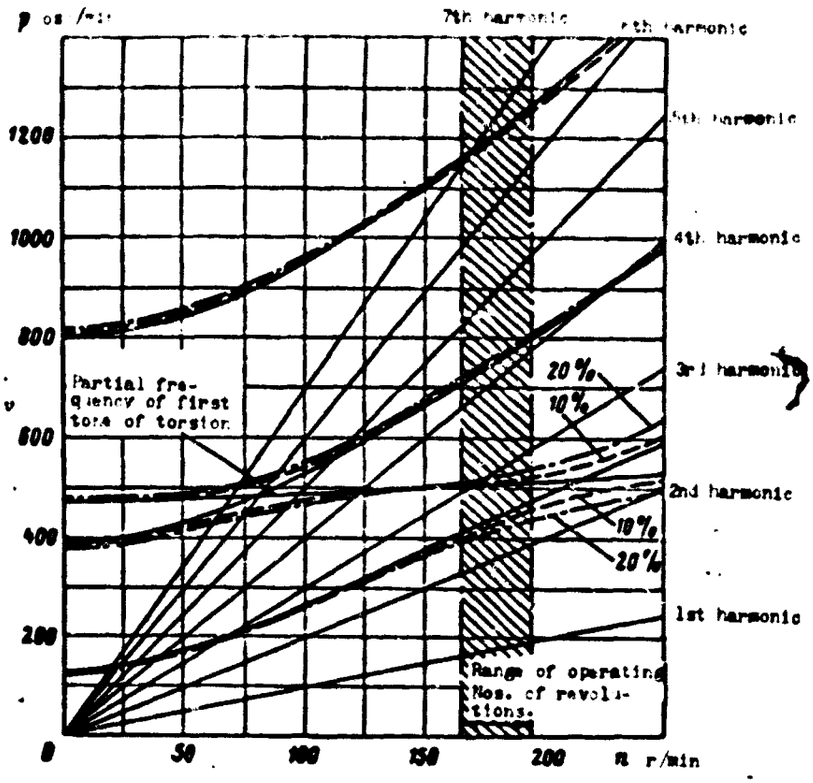

Fig. 1.24. Influence of shift chordwise by 10% and 20% of a load in 10 kg weight concentrated on the blade tip on magnitude of frequencies of natural flexural-torsional vibrations of the blade.

It is necessary to examine still the influence of the concentrated load transfered chordwise. We take the magnitude of load equal to 8% of the weight of the blade. This is probably that maximum magnitude of the load which can be practically secured on the blade. The most effective place of fixing such a load from the point of view of the creation of great factors of the connection of flexural and torsional vibrations is that point of the blade where movements in the thrust plane are maximum. Therefore, we will examine the case with fixing of the load on the blade tip.

Figure 1.24 shows results of the calculation for this case. The influence of the concentrated load on the frequency of natural oscillations with great limits of it can be considered substantial; however, it is doubtful whether the application of such means to

eliminate resonance can be recommended to the designer. Nonetheless, installation of the load can be examined as a temporary means of treatment of blades undergoing great varying stresses due to resonance.

The last parameter, which should be examined as a factor of the connection between bending and torsion, is the flapping balance. To estimate its influence on the magnitude of frequencies of natural flexural-torsional vibrations calculations with the flapping balance $\varkappa = 1.0$ were made. This is the largest value of the flapping balances ever used in practice. All the above-mentioned data were obtained with $\varkappa = 0$.

Of the calculations made it follows that the influence of the flapping balance is insignificant. However, calculation of the flapping balance can in some measure be justified, inasmuch as it introduces a certain refinement into the form of distribution of the bending moment in the blade shank.

§ 7. Forced Oscillations of the Blade

1. Application of the Method of B. G. Galerkin for Calculation Deformations of the Blade. Determination of Static Blade Deformations

The problem of determining blade deformations whose derivation is given in § 1 is reduced to the solution of the differential equation (1.9) already described above.

$$[EIy'']'' - [Ny']' + m\ddot{y} = T, \tag{7.1}$$

where T is the linear external load on the blade distributed along the radius and variable in time

Above in §§ 2, 3, and 4 we examined the solution of the homogeneous equation for T = 0, which describes natural oscillations of the blade. Here there will be examined forced oscillations of the blade when T is a certain periodic function variable with frequency ν.

In the special case when ν = 0 the problem is reduced to the determination of static deformations of the blade from a load T_0 constant in time.

The simplest method of solution of equation (7.1) is the method of B. G. Galerkin.

To illustrate the application of the method of B. G. Galerkin for determining deformations of the blade let us examine in the beginning the static problem when the external load is not changed with time. With this $\ddot{y}$ = 0, and equation (7.1) can be written as

$$[EIy'']'' - [Ny']' = T_0. \tag{7.2}$$

Let us represent deformations of the blade in the form

$$y = \sum_j \delta_j y^{(j)}, \tag{7.3}$$

where y^j is the form of natural oscillations of the blade with respect to the j-th tones; δ_j – certain coefficients which we will subsequently call coefficients of blade deformations. Coefficients of deformations

in all further calculations with the application of the method of B. G. Galerkin will play the role of generalized coordinates of the system.

We will substitute expression (7.3) into equation (7.2), multiply all terms of the equation successively by $y^{(0)}$, $y^{(1)}$, $y^{(2)}$, etc., and will integrate them along the radius of blade.

In virtue of the orthogonality of $y^{(j)}$ functions the operation made will convert the differential equation (7.2) to a series of independent equations of the form

$$C_j \delta_j = A_j, \tag{7.4}$$

where

$$\left.\begin{aligned} C_j &= \int_0^R EI\,[y'']_j^2\,dr + \int_0^R N\,[y']_j^2\,dr; \\ A_j &= \int_0^R T_0 y^{(j)}\,dr. \end{aligned}\right\} \tag{7.5}$$

The quantity C_j will be called the generalized rigidity of the blade with deformations with respect to the form of the j-th tone in the field of centrifugal forces. From consideration of formulas (7.5) it follows that the generalized rigidity of the blade C_j is equal to the doubled potential energy accumulated by the blade during its elastic deformations in the field of centrifugal forces with respect to the standardized form of the j-th tone. Quantity A_j will be called the generalized external force deforming the blade with respect to the form of the j-th tone. The quantity of generalized force A_j is equal to the doubled work of external bended forces T_0 on deformations of the blade with respect to the standardized form of the j-th tone of its natural oscillations.

From equation (7.4) coefficients of deformations of the blade δ_j can be determined

$$\delta_j = \frac{A_j}{C_j}, \tag{7.6}$$

after which the form of static deformations of the blade is determined from (7.3).

The more tones we take in the calculation of forms of natural oscillations, the more accurate the form of deformations is determined. However, for purposes of practice it appears sufficient to be limited to the first four tones of oscillations of the blade.

If coefficients of deformations δ_j are known, then it is easy to determine the bending moments and flexural stresses in the blade. They are determined by the formulas:

$$\left.\begin{aligned} M &= \sum_j \delta_j M^{(j)}; \\ \sigma &= \sum_j \delta_j \sigma^{(j)}. \end{aligned}\right\} \tag{7.7}$$

Here $M^{(j)}$ and $\sigma^{(j)}$ are forms of distribution of bending moments and flexural stresses with standardized deformations of the blade with respect to the j-th tone of its natural oscillations.

The quantities entering into formulas (7.7) obey these relationships:

$$\left.\begin{aligned} \sigma &= \frac{M}{W}; \\ \sigma^{(j)} &= \frac{M^{(j)}}{W}. \end{aligned}\right\} \tag{7.8}$$

where W is the drag torque of sections of the blade.

2. Determination of Deformations of the Blade with Periodic Application of the External Load

Let us examine the case when the external load is changed according to the law:

$$T = T_0 \sin \nu t. \tag{7.9}$$

To solve this problem we will also use the method of B. G. Galerkin. Representing the blade deformations in the form of (7.3), we will substitute expressions (7.3) and (7.9) into equation (7.1), multiply all terms of the obtained equation successively by $y^{(j)}$ and integrate along the length of the blade. In virtue of the orthogonality of functions $y^{(j)}$, we will obtain a series of independent differential equations of the form

$$m_j \ddot{\delta}_j + C_j \delta_j = A_j \sin \nu t. \tag{7.10}$$

where

$$\left.\begin{aligned} m_j &= \int_0^R m[y^{(j)}]^2 dr; \\ A_j &= \int_0^R T_\nu y^{(j)} dr. \end{aligned}\right\} \qquad (7.11)$$

Quanity m_j will be called the equivalent mass of the blade with its oscillations with respect to the form of the j-th tone. If forms of oscillations $y^{(j)}$ are standardized in such a way that $y_R^{(j)} = 1$, then m_j is the equivalent mass of the blade reduced to its end. From the first formula of (7.11) it also follows that the equivalent mass of the blade is equal to its doubled kinetic energy when elements of the blade move at speed $y^{(j)}$.

To determine the steady motion let us assume that

$$\delta_j = \delta_R^{(j)} \sin \nu t.$$

Substituting this expression into equation (7.10) and reducing all terms of the equation by the quantity sin νt, we will obtain the equation

$$-\nu^2 m_j \delta_R^{(j)} + C_j \delta_R^{(j)} = A_j, \qquad (7.12)$$

whence the value of the amplitude of deformations of the blade appears equal to

$$\delta_R^{(j)} = \frac{A_j}{C_j\left(1 - \frac{\nu^2}{C_j/m_j}\right)}. \qquad (7.13)$$

It is easy to note that the relation C_j/m_j is equal to the frequency of natural oscillations of the j-th tone of the blade. Actually, if one were to assume in equation (7.12) $A_j = 0$, then the value of ν in this case will determine the frequency of natural oscillations of the blade and can be obtained from equation (7.12):

$$\nu^2 = p_j^2 = C_j/m_j. \qquad (7.14)$$

In accordance with expression (7.6) the ratio A_j/C_j determines the magnitude of deformations in the case if the load T_ν would be applied statically.

It is convenient to represent expression (7.13) in form

$$\delta_{\lambda}^{(j)} = \lambda_{\lambda} \delta_{cr}^{(j)}, \tag{7.15}$$

where $\delta_{cr}^{(j)}$ is the coefficient determining the magnitude of deformation with a statically applied external force T_{ν}; subsequently this coefficient will be called the coefficient of quasi-static deformations of the blade; λ_{λ} – coefficient of dynamic increase in the amplitude of oscillations.

For the examined case

$$\lambda_{\lambda} = \frac{1}{1 - \frac{\nu^2}{p_j^2}}. \tag{7.16}$$

From expression (7.16) it follows that with resonance, when the frequency of forced oscillations ν is equal to the frequency of natural oscillations p_j, the coefficient of dynamic increase in amplitude turns into infinity. This result is regular for problems in which forced oscillations without damping are examined.

In reality the blade of the helicopter operating in an air medium undergoes with oscillations considerable aerodynamic damping. Aerodynamic damping limits the amplitude of oscillations of the blade during resonance and cannot fail to be considered, if problem of calculation includes the determination of oscillations of the blade under conditions of resonance.

With the determination of oscillations of the blade of the helicopter, when oscillations appear under the action of aerodynamic forces, it is very difficult strictly to separate forces of aerodynamic damping from aerodynamic forces causing oscillations of the blade. Such a separation can be carried out only conditionally. However, in a number of simplified methods of calculation such a separation is used. Therefore, here we will reproduce such an approach more specifically.

3. Simplified Approach to the Calculation of Forced Oscillations of the Blade

Let us assume that the external aerodynamic loads having an effect on the elastic blade in flight can be divided into two parts: into external loads having an effect on the blade and into forces of aerodynamic damping. We will approximately assume that external loads having an effect on an elastic blade coincide with loads having an effect on an absolutely bending rigid blade. Then for execution of the calculation it remains only to determine the forces of aerodynamic damping.

Usually forces of aerodynamic damping are determined for conditions with axial flowing around of the rotor, after which there is the assumption that in all other conditions of flight with oblique flowing around of the rotor the coefficients of aerodynamic damping are not changed.

In conditions with axial flowing around of the rotor the force of aerodynamic damping can be determined proceeding from the following.

During oscillations elements of the blade move with a speed of $\dot{y}$. Due to this angles of attack of all elements of the blade are changed by the magnitude

$$\Delta\alpha = -\frac{\dot{y}}{\omega r}.$$

With a change in angle of attack on elements of the blade, additional forces of aerodynamic damping act

$$T_{\text{доп}} = -\frac{1}{2} c_y^{\alpha} b \omega^2 r^2 \Delta\alpha = -\frac{1}{2} c_y^{\alpha} b \omega r \dot{y}. \qquad (7.17)$$

Let us assume that the aerodynamic load T can be represented as consisting of two components:

$$T = T_{\text{ж}} + T_{\text{доп}}, \qquad (7.18)$$

where $T_{\text{ж}}$ is the aerodynamic load acting on the rigid blade; and $T_{\text{доп}}$ is the additional load from aerodynamic damping appearing with elastic oscillations of the blade.

Then equation (7.1) can be rewritten in the following form:

$$[EIy'']'' - [Ny']' + m\ddot{y} + \frac{1}{2} c_x^* \rho b w r \dot{y} = T_x. \qquad (7.19)$$

Let us examine oscillations of the blade from the sinusoidal component of the aerodynamic load, which is variable according to the law

$$T_x = T_1 \sin \nu t.$$

If we represent deformations of the blade in the form of (7.3) and apply to equation (7.19) the method of B. G. Galerkin, then it is possible to arrive at a system of ordinary differential equations with respect to coefficients of deformations δ_j. Individual equations of this system will be connected with each other by terms into which there enters the integral:

$$D_{jm} = \int_0^R b r y^{(j)} y^{(m)} dr,$$

where $y^{(j)}$ and $y^{(m)}$ are forms of natural oscillations corresponding to different tones ($j \neq m$).

In simplified methods of calculation the integrals D_{jm} are usually assumed to be equal to zero, although such an assumption in many cases cannot be justified.

If, nevertheless, we take this assumption, then as a result using the method of B. G. Galerkin we will obtain a number of independent differential equations of form

$$m_j \ddot{\delta}_j + b_j \dot{\delta}_j + C_j \delta_j = A_j \sin \nu t, \qquad (7.20)$$

where the coefficient ξ_j determines the magnitude of aerodynamic damping:

$$b_j = \frac{1}{2} c_x^* \rho \omega \int_0^R b r [y^{(j)}]^2 dr. \qquad (7.21)$$

Dividing all terms of equation (7.20) by m_j, we obtain the equation of the form

$$\ddot{\delta}_j + 2n_j \dot{\delta}_j + p_j^2 \delta_j = p_j^2 \delta_{st}^{(j)} \sin \nu t. \qquad (7.22)$$

where

$$2n_j=\frac{\xi_j}{m_j};$$

$$a_{cr}^{(j)}=\frac{\lambda_j}{C_j}.$$

Usually for the characteristic of the magnitude of damping there is used the coefficient

$$\bar{n}_j=\frac{n_j}{p_j}.$$

Its magnitude in reference to aerodynamic damping of the blade is calculated by the formula

$$\bar{n}_j=\frac{1}{4}c_y\frac{\omega}{p_j}\cdot\frac{1}{m_j}\int_0^R br\,|y^{(j)}|^2\,dr. \qquad (7.23)$$

Solution of the equation (7.22) carried out in this way, as was done above in the solution of equation (7.10), leads to the formula

$$a_a^{(j)}=\lambda_a a_{cr}^{(j)},$$

where the coefficient of dynamic increase in the amplitude of oscillations

$$\lambda_a=\frac{1}{\left[1-\left(\frac{\omega}{p_j}\right)^2\right]^2+4\bar{n}_j^2\left(\frac{\omega}{p_j}\right)^2}. \qquad (7.24)$$

Thus, the solution of the problem examined here is composed of the determination of quasi-static coefficients of deformations $a_{cr}^{(j)}$ and their subsequent multiplication by the magnitude of coefficient of dynamic increase in amplitude λ_a.

Such an approach has certain discrepancies in virtue of the artificial separation of aerodynamic forces into two components by formula (7.18), the insufficiently founded assumption of the fact that $D_{jm} = 0$ and the approximate determination of coefficients of aerodynamic damping for conditions with axial flowing around of the rotor. Therefore, in §§ 8 and 9 there will be discussed methods of calculation in which the simplifications given here are not used.

However, such simplified approach describes very well the qualitative pattern of phenomena observed during oscillations of the blade.

4. Amplitude Diagram of Blade Oscillations

Above in § 3, it was already indicated that for an estimate of the character of blade oscillations a resonance diagram of the blade is widely used. A resonance diagram permits estimating how much the frequency of natural oscillations of the blade differ from frequencies of excitation and there is no danger in the appearance of resonance oscillations. However, in those cases when the frequency of natural oscillations and frequencies of excitation do not differ greatly, it is interesting to estimate to what amplitudes of oscillations of the blade this can lead. Such an estimate can be made by using the amplitude diagram of blade oscillations. This diagram, constructed for a blade with standard mass and rigidity characteristics, is shown in Fig. 1.25.

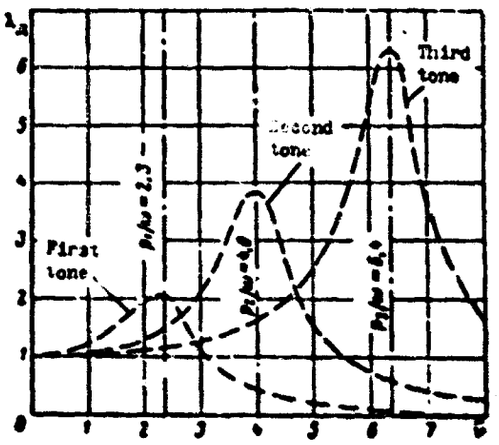

Fig. 1.25. Amplitude diagram of blade oscillations.

Plotted along the axis of abscissas on this diagram is the frequency of excitation referred to the angular velocity of rotation of the rotor,

$$\bar{\nu} = \frac{\nu}{\omega}. \qquad (7.25)$$

Plotted along the axis of ordinates are coefficients of dynamic increase in amplitude of oscillations. The diagram is constructed

only for the first three tones of elastic oscillations of the blade with the use of damping factors calculated by the formula (7.23).

5. Calculation of Oscillations in the Case when the Phase of Application of External Load is Variable Along the Length of the Blade

In No. 3 of this section there were given formulas for the case when the external load is represented in the form

$$T_z = T_z \sin \nu t.$$

Such a form of recording of the load is possible only in the case when the phase of its application along the length of blade is constant. As a rule, such a pattern during oscillations of the blade of the helicopter does not appear. The phase of the external load changes along the length of the blade, and therefore the load should be represented in form

$$T_z = \overline{T}_z \cos \nu t + \overline{\overline{T}}_z \sin \nu t, \tag{7.26}$$

where components of external load $\overline{T}_z$ and $\overline{\overline{T}}_z$ are changed along the length of the blade according to various laws.

Substituting the expression (7.26) into equation (7.19) and using the method of B. G. Galerkin, assuming that $D_{jm} = 0$, we will obtain

$$m_j \ddot{q}_j + b_j \dot{q}_j + C_j q_j = \overline{\lambda}_j \cos \nu t + \overline{\overline{\lambda}}_j \sin \nu t, \tag{7.27}$$

where

$$\overline{\lambda}_j = \int_0^R \overline{T}_z y_j^{(j)} dr,$$

$$\overline{\overline{\lambda}}_j = \int_0^R \overline{\overline{T}}_z y_j^{(j)} dr.$$

Let us assume that

$$q_j = \overline{q}_0^{(j)} \cos \nu t + \overline{\overline{q}}_0^{(j)} \sin \nu t. \tag{7.28}$$

Then

$$\left.\begin{aligned}\xi_{\alpha}^{(0)}&=\frac{\left[1-\frac{\omega^2}{p_j^2}\right]\xi_{\alpha\alpha}^{(0)}-2\bar{n}_j\frac{\omega}{p_j}\cdot\xi_{\alpha\alpha}^{(0)}}{\left[1-\frac{\omega^2}{p_j^2}\right]^2+4\bar{n}_j^2\frac{\omega^2}{p_j^2}};\\ \xi_{\alpha}^{(0)}&=\frac{\left[1-\frac{\omega^2}{p_j^2}\right]\xi_{\alpha\alpha}^{(0)}+2\bar{n}_j\frac{\omega}{p_j}\xi_{\alpha\alpha}^{(0)}}{\left[1-\frac{\omega^2}{p_j^2}\right]^2+4\bar{n}_j^2\frac{\omega^2}{p_j^2}}.\end{aligned}\right\} \qquad (7.29)$$

where

$$\left.\begin{aligned}\xi_{\alpha\alpha}^{(0)}&=\frac{\bar{\lambda}_j}{c_j}=\frac{\bar{\lambda}_j}{p_j^2 m_j};\\ \xi_{\alpha\alpha}^{(0)}&=\frac{\bar{\lambda}_j}{c_j}=\frac{\bar{\lambda}_j}{p_j^2 m_j}\end{aligned}\right\} \qquad (7.30)$$

are coefficients of quasi-static deformations of the blade.

Formulas (7.29) permit determing dynamic coefficients of deformations of the blade if quasi-static coefficients of deformations obtained with respect to aerodynamic loads $\bar{T}_\alpha$ and $\bar{T}_\beta$ are known.

6. Aerodynamic Load on a Rigid Blade

In flight variable loads with frequencies multiple to revolutions of the rotor act on the blade of the helicopter. As already was said, the greatest varying stresses in the blade cause the first to eight harmonics of aerodynamic load to revolutions of the rotor. Higher harmonics appear usually so small that they do not cause any noticeable stresses in the blade even with resonances.

The calculation of variable aerodynamic loads on the blade presents well-known difficulties. These difficulties are connected first of all with the necessity to determine the alternating field of induced speeds and to calculate the nonlinearity in the dependence of aerodynamic coefficients on the angle of attack of the profile, M number and connection of loads with torsional vibrations of the blade. An account of these peculiarities is examined in the appropriate paragraphs. Here we will compose formulas for determining variable

aerodynamic loads on a bending and torsional rigid blade with the following assumptions.

a) We will consider that the inflow angle to the profile of the blade Φ (Fig. 1.26) is small, and therefore it is possible approximately to assume that

$$\Phi = \operatorname{arctg}\frac{U_y}{U_x} \approx \frac{U_y}{U_x}, \tag{7.31}$$

where Φ is the inflow angle; U_x and U_y are mutually perpendicular components of the relative flow rate lying in a plane normal to the axis of the blade (see Fig. 1.26). Here the speed U_x is parallel to the plane of rotation of the rotor.

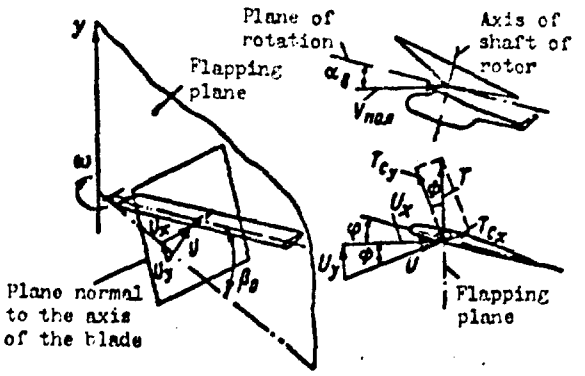

Fig. 1.26. Diagram of flowing around of a bending and torsional rigid blade.

Assuming also that $\cos\Phi \approx 1$, we will consider that the sought load T, effective in the flapping plane, does not differ from load T_{cy} perpendicular to flow flowing to the blade profile (Fig. 1.26).

b) We will assume that the quantity of relative flow rate U flowing around the profile differs little from quantity U_x:

$$U \approx U_x. \tag{7.32}$$

c) We will consider that with the determination of loads in the flapping plane the drag of the profile can be disregarded, and we can assume that $c_x = 0$.

The coefficient of lift of the profile c_y will be considered

linearly dependent on the angle of attack of the profile α:

$$c_y = c_y^{\alpha} \cdot \alpha. \tag{7.33}$$

d) The induced flow rate v flowing through the rotor will be considered constant along the entire area outlined by the rotor:

$$v = \text{const}. \tag{7.34}$$

With these assumptions only the constant part and first two harmonics of aerodynamic forces appear considerable and then only at average and high speeds of flight of the helicopter. Higher harmonics appear small, and their calculation with enumerated assumptions is of no interest.

Using these assumptions, the linear aerodynamic load on blade can be determined by the formula

$$T = \frac{1}{2} c_y^{\alpha} \cdot \alpha \rho b U_x^2. \tag{7.35}$$

Let us assume further that the angle of attack of the profile

$$\alpha = \varphi_r + \frac{U_y}{U_x}, \tag{7.36}$$

where φ_r is the angle of setting of the blade profile in the section at a distance r from the axis of rotation.

Then formula (7.35) can be converted to the form

$$T = \frac{1}{2} \cdot c_y^{\alpha} \rho b \left[\varphi_r U_x^2 + U_x U_y\right]. \tag{7.37}$$

For an absolutely bending rigid blade suspended to the hub with the help of a flapping hinge, speeds entering into formula (7.37) can be determined by the following formulas:

$$\left.\begin{aligned} U_x &= \omega R(\bar{r} + \mu \sin\psi); \\ U_y &= \omega R\left(\lambda_0 - \mu\cos\psi\beta_0 - \frac{\bar{r}}{\omega}\dot{\beta}_0\right). \end{aligned}\right\} \tag{7.38}$$

Here β_0 – the flapping angle of the blade relative to the flapping hinge; $\dot{\beta}_0 = \frac{d\beta_0}{dt}$ – derivative of angle β_0 with respect to time; λ_0 – relative flow rate through the rotor;

$$\lambda_0 = \mu \operatorname{tg} \alpha_0 + \bar{v}_0.$$

where α_s is the angle of attack of the rotor in axes of the shaft; $\bar{v}_0$ – induced flow rate constant along the disk of the rotor attributed to ωR.

The blade angle can be recorded as

$$\varphi_r = \theta_0 + \Delta\varphi - \theta_1 \sin\psi - \theta_2 \cos\psi - x\beta_0, \tag{7.39}$$

where θ_0 is the blade angle on the relative radius $\bar{r}=0,7$ or other radius accepted for reading of θ_0 when $\beta_0=0$; $\Delta\varphi$ – geometric twist of the blade; θ_1 and θ_2 are angles of cyclic control of the blade assigned by the cyclic pitch control.

If one were to represent flapping motion of the blade in the form of series

$$\beta_0 = a_0 - \sum_n (a_n \cos n\psi + b_n \sin n\psi) \tag{7.40}$$

and retain in it only the first two harmonic components, inasmuch as subsequent components under the accepted assumptions are small, then the expression (7.37) can be converted to the form

$$T = \frac{1}{2} c_y^{\alpha} \rho b_{0,7} \omega^2 R^2 \left[\bar{P}_0 + \sum_n (\bar{P}_n \cos n\psi + \bar{\bar{P}}_n \sin n\psi) \right], \tag{7.41}$$

where

$$\left.\begin{aligned}
\bar{P}_0 &= \bar{b}\left[\bar{r}\lambda_0^{\circ} + \left(\bar{r}^2 + \frac{1}{2}\mu^2\right)\varphi_r - \frac{1}{4}\mu^2 x a_2 + \frac{1}{4}\mu^2 b_2\right];\\
\bar{P}_1 &= \bar{b}\left[-\mu\bar{r}a_0 + \left(\bar{r}^2 + \frac{1}{4}\mu^2\right)b_1^{\circ} - \frac{1}{2}\mu\bar{r}a_2 + \mu\bar{r}xb_2\right];\\
\bar{\bar{P}}_1 &= \bar{b}\left[\mu\lambda_0^{\circ} + 2\mu\bar{r}\varphi_r + \left(-\bar{r}^2 + \frac{1}{4}\mu^2\right)a_1^{\circ} - \mu\bar{r}xa_2 - \frac{1}{2}\mu\bar{r}b_2\right];\\
\bar{P}_2 &= \bar{b}\left[-\frac{1}{2}\mu^2\varphi_r + \mu\bar{r}a_1^{\circ} + x\left(\bar{r}^2 + \frac{1}{2}\mu^2\right)a_2 + 2\bar{r}^2 b_2\right];\\
\bar{\bar{P}}_2 &= \bar{b}\left[-\frac{1}{2}\mu^2 a_0 + \mu\bar{r}b_1^{\circ} - 2\bar{r}^2 a_2 + x\left(\bar{r}^2 + \frac{1}{2}\mu^2\right)b_2\right].
\end{aligned}\right\} \tag{7.42}$$

In the process of fulfillment of these transformations, substitution allowing the carrying out of transition to the so-called equivalent rotor was used.

An equivalent rotor is called a rotor whose shaft we will mentally

turn relative to the real rotor at such an angle at which the same angles of attack of sections of the blade are attained without cyclic control of the blade angle. All formulas written for the equivalent rotor can be used without changes for the real rotor not having a cyclic pitch control. The equivalent rotor is usually also given properties of the rotor not having a flapping balance. In this case the equivalence of formulas is observed only with correct to the first harmonics of the flapping.

Transformation of formulas for aerodynamic loads in reference to the equivalent rotor was performed with the application of the following of substitutions:

$$\left.\begin{aligned}
&\varphi_r=\varphi_{\text{ист}}+\Delta\varphi=\theta_0-\varkappa a_0+\Delta\varphi;\\
&a_1^\circ=a_1-\varkappa b_1+\theta_1;\\
&b_1^\circ=b_1+\varkappa a_1-\theta_2;\\
&\lambda_0^\circ=\lambda_0+\mu(\varkappa b_1-\theta_1).
\end{aligned}\right\} \qquad (7.43)$$

where $\varphi_{\text{ист}}$ is the true blade angle taking into account the action of the flapping balance on that radius of which is accepted for reading of this angle; a_1°, b_1°, and λ_0° – coefficients of flapping and the relative rate for the equivalent rotor.

Higher harmonics of aerodynamic load will not be examined here.

Figure 1.27 shows the constant part and cosinusoidal and sinusoidal components of the first two harmonics of aerodynamic load for the typical blade of a helicopter obtained by formulas (7.42) for conditions of horizontal flight of the helicopter when $\mu=0.28$.

On Figs. 1.28 and 1.29 these loads are added, and there is shown the relative aerodynamic load P having an effect on the blade in the longitudinal plane of the rotor when $\psi=0°$ and $\psi=180°$ (Fig. 1.28) and in the transverse plane when $\psi=90°$ and $\psi=270°$ (Fig. 1.29).

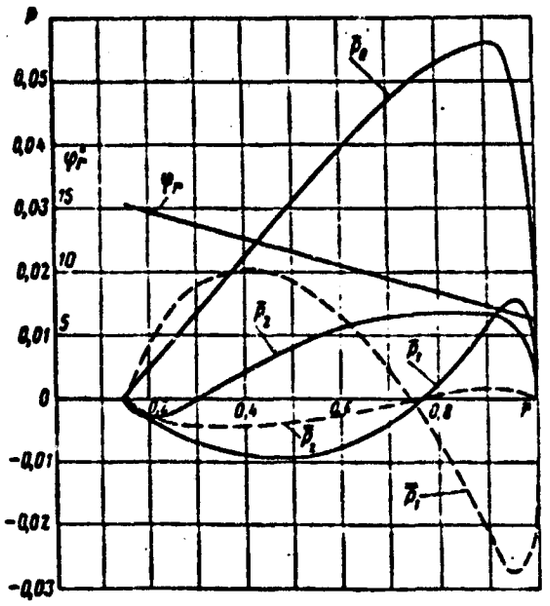

Fig. 1.27. Distribution of harmonic components of aerodynamic load along the radius of the blade for $\mu=0.28$.

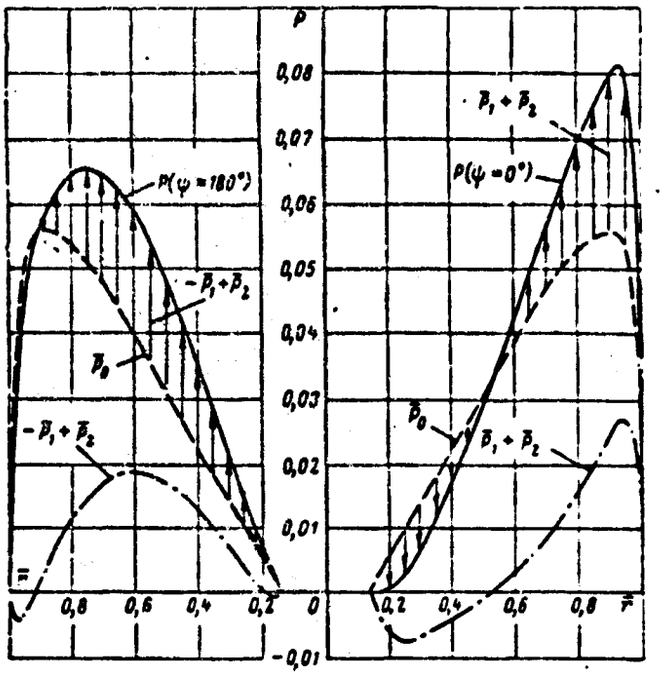

Fig. 1.28. Relative aerodynamic load having an effect on the blade in the longitudinal plane of the rotor.

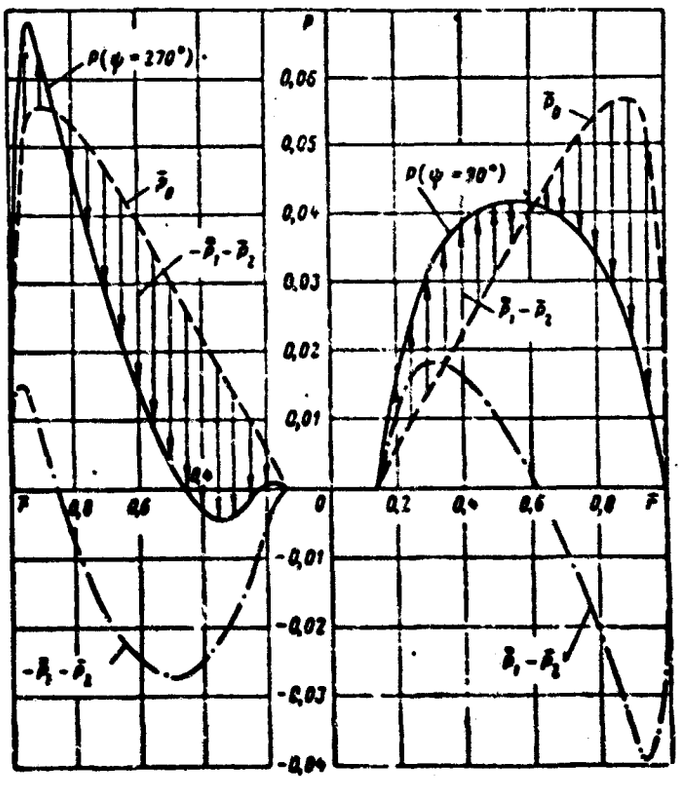

Fig. 1.29. Relative aerodynamic load acting on the blade in the transverse plane of the rotor.

7. Determining Coefficients of Flapping of the Blade

To determine aerodynamic loads by formulas (7.42) it is necessary to know the coefficients of flapping of the bending rigid blade.

Coefficients of flapping can be determined from the differential equation (7.1) if one were to represent the solution of the equation in the form

$$y=\beta_0 y^{(0)}, \tag{7.44}$$

where $y^{(0)}$ is the form of oscillations of the blade with respect to the zero tone.

For the rigid blade this form of oscillations coincides with a straight line.

$$y^{(0)}=\frac{r-l_{r.m}}{1-l_{r.m}/R}.$$

If the distance from the axis of rotation to the flapping hinge is equal to zero ($l_{r.m}=0$), then

$$y^{(0)}=r, \tag{7.45}$$

which is correct both for a rigid and for an elastic blade (see § 4).

Assuming $l_{r.m}=0$, we will substitute expression (7.45) into the differential equation (7.1) and apply to it the method of B. G. Galerkin. This operation leads to the differential equation of flapping oscillations of the blade

$$I(\ddot{\beta}_0+\omega^2\beta_0)=\int_0^R T dr, \tag{7.46}$$

where I is the moment of inertia of the blade relative to the flapping hinge.

Equation (7.46) can also be obtained from the condition of equality to the zero of the moment of all forces relative to the flapping hinge.

Substituting expressions (7.40) and (7.41) into equation (7.46)

and equating coefficients with similar harmonic functions of the azimuth, we will obtain the system of equations from which all coefficients of flapping can be determined. This system of equations will be written in the form of a table (see Table 1.6).

Table 1.6.

a_0	a_1^*	b_1^*	a_2	b_2	Φ
$1/\gamma$			$\frac{1}{4}\mu^2\varkappa C$	$-\frac{1}{4}\mu^2 C$	$= \lambda_0^* B + A\nabla + \frac{1}{2}\mu^2 C\nabla$
μB		$-A-\frac{1}{4}\mu^2 C$	$\frac{1}{2}\mu B$	$-\mu\varkappa B$	
	$A-\frac{1}{4}\mu^2 C$		μB	$\frac{1}{4}\mu B$	$= \mu\lambda_0^* C + 2\mu B\nabla$
	$-\mu B$		$\frac{3}{\gamma_0}-\varkappa(A+\frac{1}{2}\mu^2 C)$	$-2A$	$= -\frac{1}{2}\mu^2 C\nabla$
$\frac{1}{2}\mu^2 C$		$-\mu B$	$2A$	$\frac{3}{\gamma_0}-\varkappa(A+\frac{1}{2}\mu^2 C)$	

Every equation of the obtained system constitutes a sum of products of certain coefficients recorded in the squares of Table 1.6 on the unknown coefficients of flapping of the blade, which enter simultaneously into several equations and are carried out vertically in a special line placed above the table. Well-known coefficients of every equation occupy one line in Table 1.6. In the right side of the table in a special column there are given the coefficients of Φ, which form the right side of equations. Unfilled squares of the table correspond to coefficients equal to zero.

In the composition of the table the following designations are used:

$$\left.\begin{aligned} A &= \int_0^1 \bar{b}\bar{r}^2 d\bar{r}; \\ B &= \int_0^1 \bar{b}\bar{r}^3 d\bar{r}; \\ C &= \int_0^1 \bar{b}\bar{r} d\bar{r}. \end{aligned}\right\} \qquad (7.47)$$

$$\left.\begin{aligned} A^{\nu} &= \int_0^1 \bar{b}\bar{r}^3\bar{\gamma}_1 d\bar{r}; \\ B^{\nu} &= \int_0^1 \bar{b}\bar{r}^2\bar{\gamma}_1 d\bar{r}; \\ C^{\nu} &= \int_0^1 \bar{b}\bar{r}\bar{\gamma}_1 d\bar{r}. \end{aligned}\right\} \tag{7.48}$$

The mass characteristic of the rigid blade γ is determined by the following expression:

$$\gamma = \frac{c_y^{\alpha} \rho b a_1 R^4}{2I}. \tag{7.49}$$

With the solution of this system of equations it appears that coefficients a_2 and b_2 are considerably less than coefficients a_0, a_1^*, and b_1^*. Therefore, they can be disregarded in the determination of coefficients a_0, b_1^*, and a_1^*. This assumption leads to simple formulas for determining the coefficients of flapping of the blade

$$\left.\begin{aligned} a_0 &= \gamma\left[\lambda_0^{\circ} B + A^{\nu} + \frac{1}{2}\mu^2 C^{\nu}\right]; \\ a_1^{\circ} &= \frac{\mu\left[\lambda_0^{\circ} C + 2B^{\nu}\right]}{A - \frac{1}{4}\mu^2 C}; \\ b_1^{\circ} &= \frac{\mu B a_0}{A + \frac{1}{4}\mu^2 C}; \\ a_2 &= \frac{\gamma_*^2}{18 + 8A^2\gamma_*^2}\left[\mu\left(4ABb_1^{\circ} + \frac{6B}{\gamma_*}a_1^{\circ}\right) - \mu^2\left(2ACa_0 + \frac{3C^{\nu}}{\gamma_*}\right)\right]; \\ b_2 &= \frac{\gamma_*^2}{18 + 8A^2\gamma_*^2}\left[\mu\left(-4ABa_1^{\circ} + \frac{6B}{\gamma_*}\cdot b_1^{\circ}\right) + \mu^2\left(2AC^{\nu} - \frac{3C}{\gamma_*}\cdot a_0\right)\right], \end{aligned}\right\} \tag{7.50}$$

where

$$\gamma_* = \frac{\gamma}{1 - \frac{1}{3}\mu\gamma\left(A + \frac{1}{3}\mu^2 C\right)}.$$

8. Simplified Calculation of Elastic Oscillations of the Blade

On the basis of simplifying assumptions accepted in this paragraph there can be constructed a calculation of elastic oscillations and flexural stresses in the blade in conditions of horizontal flight of the helicopter. Such a calculation naturally cannot give positive results in the application to low flight speeds

when the basic role is played by variable loads connected with a nonuniform field of induced speeds, and high speeds when it is impossible not to consider the nonlinearity of aerodynamic coefficients depending on the angle of attack and phenomena induced by the compressibility of flow.

In accordance with the above-mentioned formulas it is convenient to produce calculation in axes of the equivalent rotor.

Calculation of elastic oscillations of the blade is fulfilled in the following order:

1. First of all there are determined parameters of conditions of the flight in which calculation of stresses should be performed. These are the following parameters:

a) angle of attack of the rotor $\alpha_{вн}$;

b) angular velocity of rotation of the rotor ω;

c) height and speed of flight, which are represented in the calculation by coefficients ρ and μ.

2. There is calculated the relative rate of flow through the rotor according to the formula

$$\lambda_0^\circ = \mu \operatorname{tg} \alpha_{вн} + \frac{C_T}{2\sqrt{\mu^2 + (\lambda_0^\circ)^2}}. \qquad (7.51)$$

where C_T is the thrust coefficient of the rotor.

3. The blade angle in the control section relative to which is assigned the geometric twist of the blade is calculated.

Neglecting forces connected with the second harmonic of the flapping motion this angle can be determined by formula

$$\vartheta_{пред} = \frac{\vartheta_0 - B^{(1)} + \frac{1}{2}\mu^2 D^{(1)} + \lambda_0^\circ C}{B + \frac{1}{2}\mu D}. \qquad (7.52)$$

Here

$$\left.\begin{aligned} B^{\mu\nu} &= \int_0^1 \bar{b}\bar{r}^{\mu}\Delta\varphi^{\nu}d\bar{r}; \\ D &= \int_0^1 \bar{b}d\bar{r}; \\ D^{\mu\nu} &= \int_0^1 \bar{b}\Delta\varphi^{\mu}d\bar{r}, \end{aligned}\right\} \qquad (7.53)$$

t – thrust coefficient;

σ – rotor solidity.

4. By formulas (7.50) there are calculated coefficients of flapping of the blade and by the formulas (7.41) and (7.42), external loads on the blade.

5. To determine flexural stresses it is necessary to calculate the forms and frequencies of natural oscillations of the blade.

6. If such a calculation is performed, then according to formulas (7.30) there can be determined quasi-static coefficients of deformations with respect to different tones of oscillations of the blade from the constant part of the first and second harmonics of the aerodynamic load.

Substituting expression (7.41) into formula (7.30), we will obtain values of quasi-static coefficients of deformations with respect to the j-th tone of oscillations of the blade.

$$\left.\begin{aligned} \xi_j^{(0)} &= \frac{\sigma}{\gamma_j}\cdot\nu_j\left[\lambda_0^0 B_j + A_j^0 + \frac{1}{2}\mu^2 C_j^0\right]; \\ \xi_j^{(1)} &= \frac{\sigma}{\gamma_j}\cdot\nu_j\left[-\mu B_j a_0 + \left(A_j + \frac{1}{4}\mu^2 C_j\right)b_1^0\right]; \\ \xi_j^{(2)} &= \frac{\sigma}{\gamma_j}\nu_j\left[\mu\lambda_0^0 C_j + 2\mu B_j^0 - \left(A_j - \frac{1}{4}\mu^2 C_j\right)a_1^0\right]; \\ \xi_j^{(3)} &= \frac{\sigma}{\gamma_j}\cdot\nu_j\left[-\frac{1}{2}\mu^2 C_j^0 + \mu B_j a_1^0 + \mu\left(A_j + \frac{1}{2}\mu^2 C_j\right)a_0 + 2A_j b_1^0\right]; \\ \xi_j^{(4)} &= \frac{\sigma}{\gamma_j}\cdot\nu_j\left[-\frac{1}{2}\mu^2 C_j a_0 + \mu B_j b_1^0 - 2A_j a_0 + \mu\left(A_j + \frac{1}{2}\mu^2 C_j\right)b_1\right]. \end{aligned}\right\} \qquad (7.54)$$

Here the subscript at coefficients of quasi-static deformations of the blade corresponds to the order of harmonic of aerodynamic forces. The index j denotes coefficients referring to the j-th tone of oscillations of the blade; γ_j is the mass characteristic of the blade with deformations with respect to the j-th tone:

$$\gamma_j = \frac{1/2 c_1^{\circ}(\quad R^2}{\quad} . \tag{7.55}$$

For integrals entering into formulas (7.54) there are accepted the following designations:

$$\left.\begin{aligned} A_j &= \int_0^1 \bar{b}\bar{r}^2 \bar{y}^{(j)}\, d\bar{r}; \\ B_j &= \int_0^1 \bar{b}\bar{r} \bar{y}^{(j)}\, d\bar{r}; \\ C_j &= \int_0^1 \bar{b} \bar{y}^{(j)}\, d\bar{r}; \\ A_j^{\circ} &= \int_0^1 \bar{b}\bar{r}^2 \bar{\gamma}_j \bar{y}^{(j)}\, d\bar{r}; \\ B_j^{\circ} &= \int_0^1 \bar{b}\bar{r} \bar{\gamma}_j \bar{y}^{(j)}\, d\bar{r}; \\ C_j^{\circ} &= \int_0^1 \bar{b} \bar{\gamma}_j \bar{y}^{(j)}\, d\bar{r}, \end{aligned}\right\} \tag{7.56}$$

where $y^{(j)}$ is the form of oscillations of the blade with respect to the j-th tone, standardized in such a way that for $\bar{r}=1$ $\bar{y}^{(j)}=1$.

7. Let us record deformations of the blade in the following form:

$$\begin{aligned} y = {} & [c_0 - c_1 \cos\psi - d_1 \sin\psi - c_2 \cos 2\psi - d_2 \sin 2\psi]\, y^{(1)} + \\ & + [e_0 - e_1 \cos\psi - f_1 \sin\psi - e_2 \cos 2\psi - f_2 \sin 2\psi]\, y^{(2)} + \\ & + [g_0 - g_1 \cos\psi - h_1 \sin\psi - g_2 \cos 2\psi - h_2 \sin 2\psi]\, y^{(3)} + \ldots \end{aligned} \tag{7.57}$$

Here to determine deformations of the blade, besides the form of the zero tone, which in the case $r_0 = 0$ coincides with a straight line, there are used first three tones of natural oscillations of the blade $y^{(1)}$, $y^{(2)}$, and $y^{(3)}$, standardized in such a way that for $r=R$ $y^{(1)}=R$. Then coefficients of deformations of the blade entering into formula (7.57) can be determined in terms of quasi-static coefficients of deformations in accordance with (7.29).

As an example let us write the formulas for determination of coefficients of deformations with respect to the first tone.

$$c_0 = \bar{\delta}_0;$$

$$\left.\begin{aligned} c_1 &= \frac{-\left[1-\frac{\omega^2}{p_1^2}\right]\bar{\delta}_1^{(1)} + 2\bar{n}_1\frac{\omega}{p_1}\cdot\bar{\delta}_2^{(1)}}{\left[1-\frac{\omega^2}{p_1^2}\right]^2 + 4\bar{n}_1^2\frac{\omega^2}{p_1^2}}; \qquad d_1 = \frac{-\left[1-\frac{\omega^2}{p_1^2}\right]\bar{\delta}_2^{(1)} + 2\bar{n}_1\frac{\omega}{p_1}\cdot\bar{\delta}_1^{(1)}}{\left[1-\frac{\omega^2}{p_1^2}\right]^2 + 4\bar{n}_1^2\frac{\omega^2}{p_1^2}}; \\ c_2 &= \frac{-\left[1-\frac{4\omega^2}{p_1^2}\right]\bar{\delta}_1^{(1)} + 2\bar{n}_1\frac{2\omega}{p_1}\bar{\delta}_2^{(1)}}{\left[1-\frac{4\omega^2}{p_1^2}\right] + 4\bar{n}_1^2\cdot\frac{4\omega^2}{p_1^2}}; \qquad d_2 = \frac{-\left[1-\frac{4\omega^2}{p_1^2}\right]\bar{\delta}_2^{(1)} - 2\bar{n}_1\cdot\frac{2\omega}{p_1}\bar{\delta}_1^{(1)}}{\left[1-\frac{4\omega^2}{p_1^2}\right]^2 + 4\bar{n}_1^2\frac{4\omega^2}{p_1^2}}. \end{aligned}\right\} \quad (7.58)$$

If dynamic coefficients of deformations are known, then there can easily be determined any components of stresses effective in the blade. This will be discussed in more detail in No. 17 of § 8 and in No. 8 of § 9.

In the simplified method of calculation discussed here, besides the initial assumptions concerning physical properties of the model of the blade, accepted with derivation of equation (7.1) and with calculation of the right side of this equation reduced to formula (7.35), there is used a multitude of additional assumptions of a calculating character used on almost all stages of the calculation. Although all these simplifications make the method of calculation fully useful for execution manually, they introduce a multitude of inaccuracies which yield badly to quantitative appraisal. Nevertheless, in spite of this deficiency, the described simplified method of calculation possesses a very important advantage – great clarity. In fact, all results of calculations obtained by other improved methods are estimated and analyzed on the basis of dependences represented here in simplified form.

However, even with the application of all these simplifications calculation by this method manually requires the work of one calculator for not less than a month. Contemporary rates of designing of the blade cannot be provided when calculating with such duration. Therefore, the calculation of elastic oscillations of the blade, utilized for selection of it in the process of designing, can be carried out only on high-speed electronic computers. It is natural

that in this case there is no need to use assumptions facilitating the process of the calculations.

Therefore, in § 8 there will be discussed the method of calculation founded on the same initial assumptions if one were not to consider the calculation of variable induced speeds but that fulfilled without any assumptions of a calculating character.

§ 8. Calculation of Flexural Stresses in the Blade at Low and Average Speeds of Flight

1. Peculiarities Distinguishing Conditions of Flight at Low and Average Speeds

Low and average speeds of a helicopter are examined here as conditions sufficiently remote from stall in which, furthermore, there cannot be taken into account phenomena connected with the compressibility of flow. Proceeding from this, during calculation of aerodynamic loads it is approximately assumed that

$$c_y = c_y^{\alpha} \cdot \alpha. \tag{8.1}$$

This assumption considerably simplifies computations necessary in the composition of calculation formulas.

On the other hand conditions of flight at low speed can be defined as conditions especially dangerous for fatigue strength in which the greatest variable flexural stresses in the blade frequently appear.

These considerations justify the application of the method of calculation useful only for low and average speeds of flight and not useful for high speeds and those conditions in which phenomena connected with the nonlinear character of the dependence $c_y = f(\alpha)$ and with the compressibility of flow become decisive.

It is necessary to note that assumption (8.1) does not always appear correct for conditions of flight at low speeds. In those cases when on the blade of the rotor there occurs an excessively great load, calculation should be produced taking into account the

nonlinear dependence of aerodynamic coefficients on the angle of attack of the profile. The method of such a calculation will be examined in § 9.

The overload of blades can be judged according to the magnitude of thrust coefficient of the rotor t. Calculations show that assumption (8.1) can be used in conditions of low speeds without the introduction of considerable errors into the results while $t < 0.18$.

In conditions with vertical overloads of such as, for example, conditions of braking of the helicopter before landing, disturbance of this inequality is possible for those rotors for which in a steady state of flight it is observed. All these considerations should be considered in the selection of the method for calculation.

2. The Method of Calculation of Stresses

Discussed in this paragraph is the most widespread method of calculation of varying stresses, which is based on the application of the method B. G. Galerkin with the expansion of coefficients of deformations in Fourier series with respect to harmonics.

In connection with the possibility of the application of this method for the calculation of conditions of low speeds, into all calculation formulas there are introduced harmonic components of the induced field, and the problem of deformations of the blade is solved jointly with the problem of the determination of inductive speeds.

However, such an approach is not an obligatory belonging of the proposed method here. With the calculation of stresses at average speeds of flight, when variable induced speeds introduce not very considerable refinements into the results, they cannot be considered. In this case the method of calculation will be very greatly simplified.

If one were to take the assumption (8.1), then the aerodynamic load will appear to be the linear function of movements of elements of the blade, and the problem of calculation of flexural deformations will lead to the solution of the linear differential equation (1.9).

To solve this equation the method of B. G. Galerkin is used. Deformations of the blade are in the form of a series with respect to eigenfunctions, and temporal coefficients of this series are expanded in a Fourier series. Application of the B. G. Galerkin method converts the differential equation of oscillations of the blade to a system of algebraic equations relative to unknown coefficients of Fourier series, and the determination of flexural deformations of the blade is reduced to the calculation of these unknown coefficients. Such a method of calculation will be discussed here.

3. Assumptions in Determining Induced Speeds

In calculating flexural stresses at low flight speeds when their magnitude is mainly determined by the degree of irregularity of induced speeds, it is very important to know on the basis of what assumptions this field is determined.

In Book One (Chapter II, § 5) it was already stated that induced speeds can be represented in the form of the sum of external and natural induced speeds. This division is somewhat conditional but appears very useful, since it permits giving an appraisal of the influence of separate components of induced speeds by analogy with the fact that it is already known for the wing of an aircraft and thereby justifies the acceptance of certain assumptions important for the following presentation.

The flow past a blade of a helicopter in the flow with a nonuniform field of induced speeds is analogous to the flowing around of a wing of an aircraft during flight in erratic air, when the wing continuously encounters air currents with different speed and direction. With rotation of the rotor the blade also encounters on its path a nonuniform field of speeds, but this field is caused not by atmospheric turbulence but by the induced influence of the whole vortex system of the rotor. This field, by analogy with a wing, is usually called the external field of induced speeds in contrast to the field of speeds induced in the region of the blade by its natural vortices flowing from it in connection with a change in circulation with respect to time and radius of the blade. These vortices create

considerable induced speeds at the blade only because they are at a very close distance to it. With departure at a distance of 20-30° in azimuth of the rotor, their influence on aerodynamic load on the blade vanishes.

Just as with calculation of a wing, in determining aerodynamic loads on the blade it is possible to use the "hypothesis of stationarity." By this hypothesis it is assumed that with nonstationary flowing around of the profile the same loads act on it as if the streamline flow appearing at the examined instant would remain constant in time. In accordance from this hypothesis, with calculation of aerodynamic loads on the wing there is considered a change in angle of attack only from the external velocity field, and the influence of natural induced speeds will be disregarded.

Let us use a similar approach to the blade. In the determination of aerodynamic loads we will consider only the external field of induced speeds.

During the calculation of this field certain additional assumptions connected with peculiarities of the vortex system in conditions of low speeds can be accepted.

Figure 1.30 shows the form in the plan on the system of free vortices flowing from blade tips of a five-blade rotor in conditions of flight with a speed corresponding to $\mu = 0.05$. At this speed the varying stresses in blades of the rotor reach maximum values.

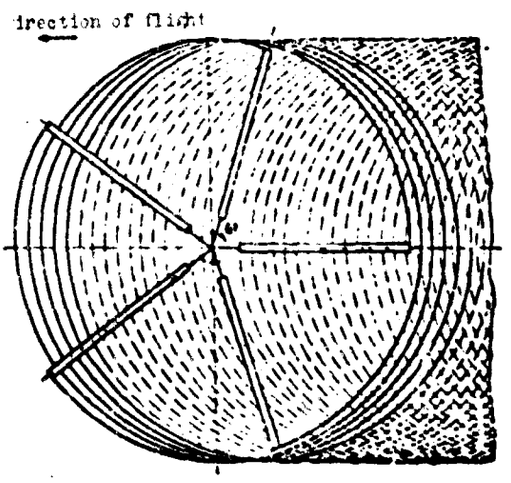

Fig. 1.30. Form in the plan on a system of vortices flowing from blade tips in conditions $\mu = 0.05$.

The picture shown in this figure is incomplete, since shown on it are only free vortices descending from blade tips and not vortices descending from all other radii of the blade. Radial (transverse) vortices are also not shown. However, even from this picture it is possible to form an idea as to how close vortices in conditions of low speeds are located. This peculiarity of the vortex system permits that induced influences of separate vortexes merge and appear in the form of a general irregularity of the total velocity field. Sharp peaks of induced speeds, which are characteristic for a vortex system with rarely located vortices, do not appear. Therefore, at low speeds of flight, especially for rotors with a large number of blades, induced speeds can be determined from the theory which examines the configuration of the rotor with an infinite number of blades.

With an increase in the speed of flight the system of free vortices starts to be extended and becomes more rare. In the same direction the vortex system is changed with a decrease in the number of blades in the rotor. Calculation with respect to a configuration with an infinite number of blades becomes less accurate.

With transition from the rotor to a configuration with an infinite number of blades, the local effect of vortices directly adjoining to the blade is so greatly weakened that we can approximately assume that this configuration does not consider the influence of adjoining vortices, and, consequently, the velocity field determined by it practically coincides with the field of external induced speeds.

The above-stated considerations lead to the conclusion that for the calculation of elastic oscillations of the blade at low speeds of flight there can be used the vortex theory founded on the configuration with an infinite number of blades.

In flight at low speeds there is usually measured varying stresses in which a large part consists of high harmonics to the number of revolutions of the rotor lying usually in the range of the 4th to the 6th. Therefore, the method of determination of induced speeds must include one more very important requirement. This method should determine the field of induced speeds at least correct to the 6th

harmonic, which is possible only in the case when the values of circulation are determined with correct to the same harmonic. Consequently, all methods not satisfying this requirement drop out and cannot be used in the calculation of elastic oscillations.

It was already stated above that here there will be discussed the method of calculation of stresses, in which all variables are expanded in Fourier series with respect to the harmonics. Therefore, it appears convenient to use the method of determination of the field of induced speeds in which these speeds are determined also in the form of expansion with respect to the harmonics.

These requirements are satisfied in the very best manner by the V. E. Baskin theory [3] (see also § 5, Chapter II, Book One). Therefore, this theory will be used in this paragraph during the calculation of stresses.

4. Calculation Formulas for Determining the Field of Induced Speeds

Let us consider the system of formulas proposed by V. E. Baskin for calculation of the field of induced speeds in the plane of rotation of the rotor.

Let us represent the field of these speeds in the form of the sum of its harmonic components. Here both the total flow rates and harmonic components of this speed are attributed to the peripheral speed of rotation of blade tips of the rotor ωR.

$$\lambda = \mu \operatorname{tg} \alpha_0 + \bar{\lambda}_0 + \sum_n (\bar{\lambda}_n^c \cos n\psi + \bar{\lambda}_n^s \sin n\psi). \qquad (8.2)$$

Here λ is the total flow rate through the rotor referred to ωR; $\bar{\lambda}_0$ – constant part of induced speed also referred to ωR. $\bar{\lambda}_n^c$ and $\bar{\lambda}_n^s$ – harmonic components of induced speed; ψ – azimuthal angle of the blade counted off from the axis coinciding in direction with the tail beam of a single-rotor helicopter;

$$\mu = \frac{V \cos \alpha_0}{\omega R},$$

where V is the speed of flight of the helicopter; α_0 – angle of attack of the rotor in axes of the shaft.

The linear aerodynamic load which affects the blade will be presented in the form

$$T=\frac{1}{2}c_y^{\alpha}\rho b_{0.7}\omega^2R^2P, \tag{8.3}$$

where c_y^{α} is the angle of inclination of the dependence $c_y=f(\alpha)$, which here is taken linear in the form of (8.1); ρ – air density; $b_{0.7}$ – value of chord of the blade on the relative radius $\bar{r}=0.7$.

The value P entering into this expression will subsequently be called the relative aerodynamic load.

Let us represent value P in the form:

$$P=\bar{P}_0+\sum_m(\bar{P}_m\cos m\psi+\bar{\bar{P}}_m\sin m\psi). \tag{8.4}$$

The harmonic components of speed λ_n are in the form of the sum of the so-called partial induced speeds, each of which is induced only by one harmonic of the aerodynamic load:

$$\left.\begin{aligned}\lambda_n&=\sum_m\lambda_{nm};\\ \bar{\lambda}_n&=\sum_m\bar{\lambda}_{nm}.\end{aligned}\right| \tag{8.5}$$

In these expressions the complete total components of induced speeds have one subscript n and the partial – two indices n and m.

Values of partial harmonic components of induced speeds are determined according to the following expressions:

$$\left.\begin{aligned}&\text{– for } n=0:\\ &\qquad\lambda_{0m}=-\frac{1}{8}c_y^{\alpha}\sigma A_0(-1)^m\tau^m J(\bar{P}_m);\\ &\text{– for } n\neq 0:\\ &\qquad\lambda_{nm}=-\frac{1}{8}c_y^{\alpha}\sigma A_0[\tau^{n-m}+(-1)^m\tau^{n+m}]J(\bar{P}_m);\\ &\qquad\bar{\lambda}_{nm}=-\frac{1}{8}c_y^{\alpha}\sigma A_0[\tau^{n-m}-(-1)^m\tau^{n+m}]J(\bar{P}_m).\end{aligned}\right| \tag{8.6}$$

If power in which τ is raised is negative $(n-m<0)$, then in formulas (8.6) one should assume that $\tau^{n-m}=(-\tau)^{m-n}$.

Coefficients entering into formulas (8.6) have the following values:

$$\left.\begin{aligned} A_0 &= \frac{1}{\sqrt{\mu^2+\lambda_{cp}^2}};\\ \tau &= \frac{\sqrt{\mu^2+\lambda_{cp}^2}-|\lambda_{cp}|}{\mu};\\ \sigma &= \frac{z_n b_{cp}}{\pi R}, \end{aligned}\right\} \qquad (8.7)$$

where σ is the rotor solidity and z_n is the number of blades in the rotor.

The value of flow rate λ_{cp} average along the radius of the blade is determined from the formula

$$\lambda_{cp} = \mu \operatorname{tg} a_0 + 2\int_0^1 \lambda_i \bar{r}\, d\bar{r}. \qquad (8.8)$$

To determine the functions $J(\bar{P}_m)$ and $J(\bar{P}_m)$ entering into equations (8.6) from the theory of V. E. Baskin there follows the following formulas:

$$\left.\begin{aligned} J(\bar{P}_m) &= \int_0^1 J_n(z\bar{r}) z \left[\int_0^1 \bar{P}_m(\bar{q}) J_m(z\bar{q})\, d\bar{q}\right] dz;\\ J(\bar{P}_m) &= \int_0^1 J_n(z\bar{r}) z \left[\int_0^1 \bar{P}_m(\bar{q}) J_m(z\bar{q})\, d\bar{q}\right] dz, \end{aligned}\right\} \qquad (8.9)$$

where $J_n(z\bar{r})$ and $J_m(z\bar{r})$ are Bessel functions of the first kind with the order n and m, respectively; z – parameter of integration.

Here in order to define more accurately according to what parameter integration is produced, a new designation for the relative radius of the blade $\bar{\rho}$ is introduced. This designation will be used only in the calculation of integrals (8.9).

3. Transformations of Calculation Formulas into Particular Cases

In particular cases expressions (8.6) are considerably simplified. So in the case when n = m = 0

$$\lambda_{ind} = -\frac{1}{8} c_y \sigma A_0 \frac{\bar{P}_0}{\mu}. \qquad (8.10)$$

For subsequent computations the result obtained for the case when n = m is especially important. It appears that the coinciding harmonics of the aerodynamic load and induced speed are uniquely connected by expressions:

$$\left.\begin{aligned}\bar{\lambda}_m &= \bar{a}_0 \frac{\bar{P}_0}{r};\\ \bar{\bar{\lambda}}_m &= \bar{\bar{a}}_0 \frac{\bar{\bar{P}}_0}{r}.\end{aligned}\right\} \qquad (8.11)$$

where

$$\left.\begin{aligned}\bar{a}_0 &= -\frac{1}{8} c_y^2 A_0 [1+(-1)^m \bar{\mu}^{2m}];\\ \bar{\bar{a}}_0 &= -\frac{1}{8} c_y^2 A_0 [1-(-1)^m \bar{\mu}^{2m}].\end{aligned}\right\} \qquad (8.12)$$

Such a form of expressions makes separation of the components of induced speeds into two types expedient. These include basic components of induced speed induced by the same harmonic of aerodynamic load as the harmonic of induced speed and side components, induced by all remaining harmonics of the aerodynamic load.

This separation permits recording expressions (8.5) in the form

$$\left.\begin{aligned}\bar{\lambda}_m &= \bar{a}_0 \frac{\bar{P}_0}{r} + \bar{\lambda}_m;\\ \bar{\bar{\lambda}}_m &= \bar{\bar{a}}_0 \frac{\bar{\bar{P}}_0}{r} + \bar{\bar{\lambda}}_m.\end{aligned}\right\} \qquad (8.13)$$

where basic components of the induced speed are defined by expressions (8.11), and the sum of all side components the induced speeds are introduced into equations with the help of new designations $\bar{\lambda}_m$ and $\bar{\bar{\lambda}}_m$:

$$\left.\begin{aligned}\bar{\lambda}_m &= \sum_{n=0}^{n=k-1} \bar{\lambda}_{mn} + \sum_{n=k+1}^{n=z} \bar{\lambda}_{mn};\\ \bar{\bar{\lambda}}_m &= \sum_{n=0}^{n=k-1} \bar{\bar{\lambda}}_{mn} + \sum_{n=k+1}^{n=z} \bar{\bar{\lambda}}_{mn}.\end{aligned}\right\} \qquad (8.14)$$

Here z is the number of harmonic components of induced speeds considered in the calculation.

At n = 0 the first terms of these expressions should be assumed

equal to zero, and at $n=z_n$ the same should be done with the second terms. In the formulation of equations for calculation of stresses the induced speeds will be represented in the form of (8.13).

6. Numerical Determination of Values of Integrals $J(\bar{P}_m)$ and $J(\bar{\bar{P}}_m)$

When $m \neq n$, calculation of integrals (8.9) is associated with well-known difficulties. To determine values of these integrals V. E. Baskin proposed a method in which components of the aerodynamic load are approximated with the help of trigonometric polynomials. For this it is necessary to determine values of P_m on radii of the blade assigned beforehand not coinciding with those which are used in the whole calculation. In reference to the method expounded here this is not very convenient. Therefore, here there will be used another method more suitable for the given case in which calculation of integrals $J(\bar{P}_m)$ and $J(\bar{\bar{P}}_m)$ is produced approximately according to the same form in which integrals during calculation of stresses in the blade are calculated. For this the blade is divided into separate sections within limits of which the aerodynamic load is represented in the form useful for integration. It is natural to divide the blade into the same sections in all cases both with calculation of stresses and with calculation of integrals (8.9). Let us present the load $P_m(\bar{\rho})$ in such a way that on each section of integration it changes according to the law

$$P_m(\bar{\rho}) = \frac{P_m(\bar{\rho}_k)}{\bar{\rho}_k^{m+1}} \bar{\rho}^{m+1}. \qquad (8.15)$$

Here $\bar{\rho}$ is the current value of the relative radius of the blade; after fulfillment of integration and substitution of limits the value $\bar{\rho}$ will not be encountered in the formulas without an index. $\bar{\rho}_k$ – the same value of relative radius but with index k denotes that the examined radius coincides with the radius for which the relative aerodynamic load $P_m(\bar{\rho}_k)$ is calculated.

Subsequently, as was already stated, we will distinguish the relative radii $\bar{\rho}_k$ on which there is taken the value of the aerodynamic load from relative radii $\bar{r}_i$ for which the induced speed is calculated.

This permits avoiding possible confusion.

We will consider that the relative aerodynamic load is changed according to the law (8.15) for the extent of each section limited by relative radii

$$\bar{r}=\frac{1}{2}(\bar{r}_{n-1}+\bar{r}_n) \text{ and } \bar{r}=\frac{1}{2}(\bar{r}_n+\bar{r}_{n+1}).$$

On Fig. 1.31 the solid step line shows the form of distribution of relative aerodynamic load along the length of the blade in which it is represented for calculation of induced speeds by expression (8.15) in the case m = 0. Such a form of presentation of aerodynamic load can, of course, introduce certain errors into values of induced speeds.

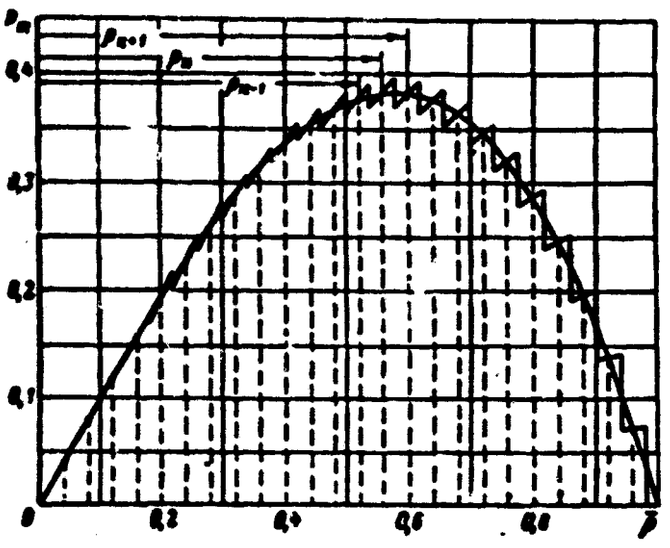

Fig. 1.31. Form of relative aerodynamic load accepted for calculation of induced speeds.

However, calculations made for estimating the magnitude of this error showed that it is small and cannot introduce considerable changes into results of the calculation.

If we substitute the value of relative aerodynamic load expressed in form (8.15) into the expression of the integrand of equation (8.9), then the internal integral in the right-hand side of this equation can be represented in the form of a certain sum of definite integrals:

$$\int_0^1 P_m(\bar{Q}) J_m(z\bar{Q})\, d\bar{Q} = \sum_k \frac{P_m(\bar{Q}_k)}{\bar{Q}_k^{m+1}} \int_{1/2(\bar{Q}_{k-1}+\bar{Q}_k)}^{1/2(\bar{Q}_k+\bar{Q}_{k+1})} \bar{Q}^{m+1} J_m(z\bar{Q})\, d\bar{Q}. \tag{8.16}$$

The definite integrals entering in this expression can be calculated analytically [see 11]. Substituting into the obtained expressions limits of integration, it is possible to write

$$\int_0^1 P_m(\bar{Q}) J_m(z\bar{Q})\, d\bar{Q} = \sum_k A_k \frac{1}{z} J_{m+1}\left(z \cdot \frac{\bar{Q}_k + \bar{Q}_{k+1}}{2}\right), \tag{8.17}$$

where

$$A_k = \frac{\bar{Q}_k + \bar{Q}_{k+1}}{2}\left[\frac{P_m(\bar{Q}_k)}{\bar{Q}_k^{m+1}} - \frac{P_m(\bar{Q}_{k+1})}{\bar{Q}_{k+1}^{m+1}}\right].$$

Substituting the thus expressed value of the internal integral into equations (8.9), we will obtain

$$\begin{aligned} J(\bar{P}_m) &= \int_0^\infty J_n(z\bar{r}) z \left[\int_0^1 P_m(\bar{Q}) J_m(z\bar{Q})\, d\bar{Q}\right] dz = \\ &= \sum_k A_k \int_0^\infty J_n(z\bar{r}_i) \cdot J_{m+1}\left(z \cdot \frac{\bar{Q}_k + \bar{Q}_{k+1}}{2}\right) dz. \end{aligned} \tag{8.18}$$

Or if we were to record in simpler form

$$J(\bar{P}_m) = \sum_k A_k s_k(\bar{r}_i), \tag{8.19}$$

where

$$s_k(\bar{r}_i) = \int_0^\infty J_n(z\bar{r}_i) J_{m+1}\left(z \cdot \frac{\bar{Q}_k + \bar{Q}_{k+1}}{2}\right) dz. \tag{8.20}$$

Integral (8.20) is breaking integral bearing the name of the integral Weber and Shafkheytlin [11]. Its analytic expression depending upon the relationship between $\bar{r}_i$ and $1/2(\bar{Q}_k + \bar{Q}_{k+1})$ has the following form:

If $\frac{1}{2}(\bar{Q}_k + \bar{Q}_{k-1}) < \bar{r}_i$, then

$$s_k(\bar{r}_i) = \int_0^\infty J_n(z\bar{r}_i) J_{m+1}\left(z \frac{\bar{Q}_k + \bar{Q}_{k+1}}{2}\right) dz = \frac{\left(\frac{\bar{Q}_k + \bar{Q}_{k+1}}{2}\right)^{m+1} \cdot \Gamma\left(\frac{m+2+n}{2}\right)}{\bar{r}_i^{m+2}\, \Gamma(m+2) \cdot \Gamma\left(\frac{n-m}{2}\right)} \times$$

$$\times F\left[\frac{m+2+n}{2};\ \frac{m+2-n}{2};\ m+2;\ \left(\frac{\bar{Q}_k + \bar{Q}_{k+1}}{2\bar{r}_i}\right)^2\right]. \tag{8.21}$$

If $\frac{1}{2}(\bar{Q}_k + \bar{Q}_{k+1}) > \bar{r}_i$, then

$$c_n(\bar{r}_i) = \int_0^{\bar{r}_i} J_n(z\bar{r}_i) J_{m+1}\left(z\frac{\bar{Q}_k + \bar{Q}_{k+1}}{2}\right) dz =$$

$$= \frac{\bar{r}_i^n \Gamma\left(\frac{m+2+n}{2}\right)}{\left(\frac{\bar{Q}_k + \bar{Q}_{k+1}}{2}\right)^{n+1} \Gamma(n+1)\Gamma\left(\frac{m+2-n}{2}\right)} \times$$

$$\times F\left[\frac{m+2+n}{2};\ \frac{n-m}{2};\ n+1;\ \left(\frac{2\bar{r}_i}{\bar{Q}_k + \bar{Q}_{k+1}}\right)^2\right]. \qquad (8.22)$$

Here Γ is the gamma function with different arguments, and F is the hypergeometric function of arguments α, β, γ, and z.

These arguments, as can be seen from expressions (8.21) and (8.22), can have various values depending on the relationship between $\bar{r}_i$ and $\frac{1}{2}(\bar{Q}_k + \bar{Q}_{k+1})$. Thus, for example, in expression (8.21)

$$\alpha = \frac{m+2+n}{2};$$

$$\beta = \frac{m+2-n}{2};$$

$$\gamma = m+2;$$

$$z = \left(\frac{\bar{Q}_k + \bar{Q}_{k+1}}{2\bar{r}_i}\right).$$

With calculation on electronic digital computers these functions are easily programmed. Therefore, their calculation presents no difficulties.

7. Assumptions Accepted in the Determination of Aerodynamic Forces

In the determination of aerodynamic loads, besides the assumptions (8.1) there are used the same assumptions which were used in the determination of loads on a rigid blade (§ 7, No. 6) with the exception of assumption (7.34).

1. We will consider that the inflow angle to blade profile Φ is small, and that therefore it is possible approximately to assume:

$$\Phi = \operatorname{arc\,tg}\frac{U_y}{U_x} \approx \frac{U_y}{U_x}, \qquad (8.23)$$

where Φ is the inflow angle; U_x and U_y are mutually perpendicular components of relative flow rate lying in the plane normal to the elastic axis of the blade (Fig. 1.32); here the speed U_x is parallel to the plane of rotation of the rotor.

2. We will consider that the quantity of relative flow rate U flowing past the profile differs little from quantity U_x. Therefore we will assume that $U \approx U_x$.

3. We will consider that with the determination of loads in the flapping plane (the plane passing through the axis of rotation of the rotor) the profile drag can be disregarded, and we can assume that $c_x = 0$.

4. Assuming that cos Φ = 1 we will consider that the load in the flapping plane does not differ from the load perpendicular to the flow flowing to the profile of the blade (see Fig. 1.32).

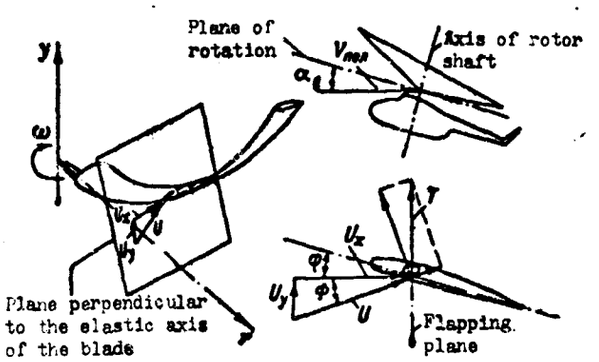

Fig. 1.32. Diagram of flowing around of the blade accepted in the calculation of stresses at low flight speeds.

8. Calculation Formulas

With the use of assumptions shown in No. 7 the value of relative aerodynamic load P entering in equation (8.3) can be determined by the formula:

$$P = \bar{b}_r [c_y \bar{U}_x^2 + \bar{U}_x \bar{U}_y], \qquad (8.24)$$

where $\bar{b}_r$ is the quantity of the chord of the blade on the examined radius referred to the chord on radius $\bar{r}$ = 0.7; $\bar{U}_x$ and $\bar{U}_y$ – the same components of relative flow rate which are in expression (8.23) but referred to the peripheral velocity of the blade tips ωR:

$$\left.\begin{aligned} \overline{U}_x &= \bar{r} + \mu \sin\psi; \\ \overline{U}_y &= \lambda - \mu\cos\psi \qquad \beta - \frac{1}{\omega R}\cdot \dot{y}. \end{aligned}\right\} \tag{8.25}$$

Here λ is the relative flow rate through the rotor; this speed is determined by expression (8.2); y – movements of elastic axis of the blade in the plane perpendicular to the plane of rotation from which these movements are reckoned; $\beta = y'$ – angle of inclination of elastic axis of the blade.

The prime here denotes differentiation with respect to the radius of the blade and the dot, with respect to time.

The blade angle can be recorded in the form

$$\varphi = \theta_0 + \Delta\varphi - \theta_1 \sin\psi - \theta_2 \cos\psi - \varkappa_0\beta_0. \tag{8.26}$$

Here θ_0 is the blade angle on the relative radius $\overline{r}$ = 0.7 or other radius accepted for the reading of θ_0 when the angle of rotation of the blade in the flapping hinge β_0 is equal to zero; $\Delta\varphi$ – geometric twist of the blade; θ_1 and θ_2 – angles cyclic control assigned by the cyclic pitch control; $\varkappa$ – flapping balance; β_0 – angle of rotation of the blade in the flapping hinge.

Let us represent deformations of the blade in the form

$$y = \sum_j \delta_j y^{(j)}, \tag{8.27}$$

where δ_j are coefficients of deformation of the blade corresponding to the j-th tone of its natural oscillations; these coefficients are functions of time and therefore are also called temporal factors; $y^{(j)}$ – forms of natural oscillations of the blade in a vacuum, which are standardized in such a way that $y_R^{(j)} = R$.

Let us expand the time factors δ_j in Fourier series with respect to the harmonics. Then it will be possible to represent deformations of the blade in the form:

$$\left.\begin{aligned}\overline{P}_n &= \overline{B}_n\left[\overline{f} + \overline{r}\overline{\lambda}_n^n - \frac{1}{2}\mu\left(\overline{\lambda}_{n-1} - \overline{\lambda}_{n+1}\right)\right];\\ \overline{\overline{P}}_n &= \overline{\overline{B}}_n\left[\overline{\overline{f}} + \overline{r}\overline{\overline{\lambda}}_n^n + \frac{1}{2}\mu\left(\overline{\overline{\lambda}}_{n-1} - \overline{\overline{\lambda}}_{n+1}\right)\right],\end{aligned}\right\} \qquad (8.30)$$

where

$$\left.\begin{aligned}\overline{B}_n &= \frac{\overline{b}_r}{1 + \frac{1}{8}c_y^{\alpha}\sigma A_0\left[1 + (-1)^n\tau^{2n}\right]\overline{b}_r};\\ \overline{\overline{B}}_n &= \frac{\overline{b}_r}{1 + \frac{1}{8}c_y^{\alpha}\sigma A_0\left[1 - (-1)^n\tau^{2n}\right]\overline{b}_r}.\end{aligned}\right\} \qquad (8.31)$$

We will subsequently call values B_n and $\overline{B}_n$ equivalent chords of the blade, since in the calculation they play the same role as real chords and are in formulas (8.30) at the same places where in formulas (8.29) values $\overline{b}_r$ are.

Thus the harmonic components of aerodynamic loads, taking into account variable induced speeds, should be determined by introducing into the formulas only side components of induced speeds and instead of real chords – equivalent chords of the blade. Values of equivalent chords of the blade can be different depending upon flight conditions and the order of the determined harmonic of aerodynamic loads. However, they appear to be less than the real chords. Consequently, all the harmonic components of aerodynamic loads appear less than those values which they would have if the basic components of induced speeds would be equal to zero and as many times as the equivalent chords are less than the real chords. The introduction of equivalent chords leads to a decrease in all components of aerodynamic load of both exciting and damping oscillations of the blade. Therefore, the values of relative coefficients of aerodynamic damping, which determine the amplitudes of oscillations with resonances are decreased. This leads to the fact that far from resonance variable deformations of the blade decrease and with resonance they remain approximately the same as with the calculation neglecting this effect.

Expressions of the type (8.30), copied for all harmonic components of the aerodynamic load, appear interconnected through components of

induced speeds. Consequently, they are a certain complex system of equations of relatively unknown loads, which can be solved only in the case when values f_n and $\bar{f}_n$ are known. These values depend on the value of coefficients of deformations of the blade. Therefore, to solve this system of equations it is necessary to formulate an equation for determination of coefficients of deformations. This will be carried out below.

If one were to depict in detail values f_n and $\bar{f}_n$ entering into equation (8.30), then expressions for harmonic components of the aerodynamic load can be represented in the form of Table 1.7.

The expression for each harmonic component of the load P_n and $\bar{P}_n$ occupies one line in the table and constitutes a sum of products of coefficients recorded in several expressions and carried out vertically in a special line placed at the top of the table. These factors, as was already stated above, will be called coefficients of deformations of the blade. In the right side of the table there is copied a number of terms f_n^0, f_n^1, f_n^2, and f_n^3, not connected with unknown coefficients of the deformations.

In order to determine the values P_n and $\bar{P}_n$ the sum of products of terms of each line by unknown coefficients of deformations formed with terms not dependent on coefficients of deformations must still be multiplied by values B_n and $\bar{B}_n$. For memory these quantities are copied in the left part of the table.

The number of terms entering into expressions for P_n and $\bar{P}_n$ depends on the number of harmonics and tones of natural oscillations considered in the calculation. In Table 1.7 there are copied expressions for the case when in the calculation only two tones and four harmonics of variable forces are considered.

In programs which are used during calculations on electronic digital computers there is usually considered four tones of natural oscillations and six to eight harmonics of variable forces.

Table 1.7.

					$s=0$										
				$\bar{z}_0$	a_0	a_1	b_1	a_2	b_2	a_3	b_3	a_4	b_4	...
$t=0$		$\bar{z}_0$	=	$\bar{z}_0$			$\mu^2 x_0$	$-\frac{1}{6}\mu^2 x_0$	$\frac{1}{6}\mu^2$					
$t=1$														
$t=2$	$\cos\varphi$	$\bar{z}_1$	=	$\bar{z}_1$	$-\mu^2$	$x_0(1+\frac{1}{6}\mu^2)$	$1+\frac{1}{6}\mu^2$	$-\frac{1}{2}\mu^2$	$\mu^2 x_0$	$-\frac{1}{2}\mu^2 x_0$	$\frac{1}{6}\mu^2$			
$t=3$	$\sin\varphi$	$\bar{z}_1$	=	$\bar{z}_1$		$-1+\frac{1}{6}\mu^2$	$x_0(1+\frac{1}{6}\mu^2)$	$-\mu^2 x_0$	$-\frac{1}{2}\mu^2$	$-\frac{1}{6}\mu^2$	$-\frac{1}{6}\mu^2 x_0$			
$t=4$	$\cos 2\varphi$	$\bar{z}_2$	=	$\bar{z}_2$		μ^2	$-\mu^2 x_0$	$x_0(1+\frac{1}{6}\mu^2)$	$2\mu^2$	$-\mu^2$	$\mu^2 x_0$	$-\frac{1}{6}\mu^2 x_0$	$\frac{1}{6}\mu^2$	
$t=5$	$\sin 2\varphi$	$\bar{z}_2$	=	$\bar{z}_2$	$-\frac{1}{2}\mu^2$	$\mu^2 x_0$	μ^2	$-2\mu^2$	$x_0(1+\frac{1}{6})\mu^2$	$-\mu^2 x_0$	$-\mu^2$	$-\frac{1}{6}\mu^2$	$-\frac{1}{6}\mu^2 x_0$	
$t=6$	$\cos 3\varphi$	$\bar{z}_3$	=	$\bar{z}_3$		$-\frac{1}{6}\mu^2 x_0$	$-\frac{1}{6}\mu^2$	$\frac{2}{3}\mu^2$	$-\mu^2 x_0$	$x_0(1+\frac{1}{6}\mu^2)$	$3\mu^2$	$-\frac{1}{6}\mu^2$	$\mu^2 x_0$	...
$t=7$	$\sin 3\varphi$	$\bar{z}_3$	=	$\bar{z}_3$		$\frac{1}{6}\mu^2$	$-\frac{1}{6}\mu^2 x_0$	$\mu^2 x_0$	$\frac{2}{3}\mu^2$	$-3\mu^2$	$x_0(1+\frac{1}{6}\mu^2)$	$-\mu^2 x_0$	$-\frac{2}{3}\mu^2$	...
$t=8$	$\cos 4\varphi$	$\bar{z}_4$	=	$\bar{z}_4$				$-\frac{1}{6}\mu^2 x_0$	$-\frac{1}{6}\mu^2$	$2\mu^2$	$-\mu^2 x_0$	$x_0(1+\frac{1}{6}\mu^2)$	$0\mu^2$	...
$t=9$	$\sin 4\varphi$	$\bar{z}_4$	=	$\bar{z}_4$				$\frac{1}{6}\mu^2$	$-\frac{1}{6}\mu^2 x_0$	$\mu^2 x_0$	$2\mu^2$	$-0\mu^2$	$x_0(1+\frac{1}{6}\mu^2)$	...
										...	...	...	...	...

Table 1.7. (Continued)

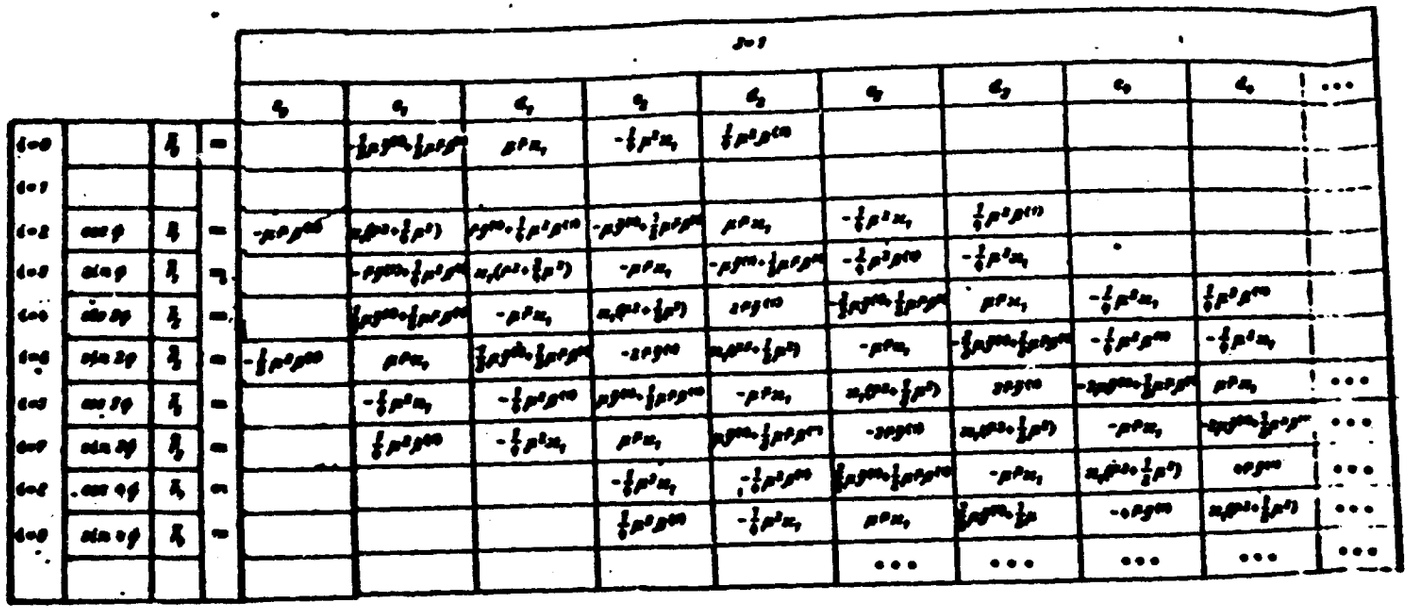

Table 1.7. (Continued)

				Terms not dependent on coefficients of deformations			
				f_n^0	f_n^m	f_n^7	f_n^1
i=0		$\bar{\lambda}_0$	=	$-\mu^2 e_1$	$\mu r \operatorname{tg}\alpha_2$	$(\varkappa^2+\frac{1}{3}\mu^2)\varphi_r$	$\varkappa\lambda_0^0+\frac{1}{2}\mu\bar{\lambda}_1$
i=1							
i=2	$\cos\phi$	$\bar{\lambda}_1$	=	$-(\varkappa^2+\frac{1}{3}\mu^2)e_2$			$\varkappa\bar{\lambda}_1^0+\frac{1}{2}\mu\bar{\lambda}_0$
i=3	$\sin\phi$	$\bar{\lambda}_1$	=	$-(\varkappa^2+\frac{1}{3}\mu^2)e_2$	$\mu^2\operatorname{tg}\alpha_2$	$2\mu^2\varphi_r$	$\varkappa\bar{\lambda}_1^0+\mu\bar{\lambda}_0-\frac{1}{2}\mu\bar{\lambda}_2$
i=4	$\cos 2\phi$	$\bar{\lambda}_2$	=	$\mu^2 e_1$		$-\frac{1}{2}\mu^2\varphi_r$	$\varkappa\bar{\lambda}_2^0-\frac{1}{2}\mu(\bar{\lambda}_1-\bar{\lambda}_3)$
i=5	$\sin 2\phi$	$\bar{\lambda}_2$	=	$-\mu^2 e_2$			$\varkappa\bar{\lambda}_2^0+\frac{1}{2}\mu(\bar{\lambda}_1-\bar{\lambda}_3)$
i=6	$\cos 3\phi$	$\bar{\lambda}_3$	=	$\frac{1}{6}\mu^2 e_2$			$\varkappa\bar{\lambda}_3^0-\frac{1}{2}\mu(\bar{\lambda}_2-\bar{\lambda}_4)$
i=7	$\sin 3\phi$	$\bar{\lambda}_3$	=	$\frac{1}{6}\mu^2 e_1$			$\varkappa\bar{\lambda}_3^0+\frac{1}{2}\mu(\bar{\lambda}_2-\bar{\lambda}_4)$
i=8	$\cos 4\phi$	$\bar{\lambda}_4$	=				$\varkappa\bar{\lambda}_4^0-\frac{1}{2}\mu(\bar{\lambda}_3-\bar{\lambda}_5)$
i=9	$\sin 4\phi$	$\bar{\lambda}_4$	=				$\varkappa\bar{\lambda}_4^0+\frac{1}{2}\mu(\bar{\lambda}_3-\bar{\lambda}_5)$
							...

9. Transition to the Equivalent Rotor

In orde. to show the possibility of transition to the equivalent rotor in the compilation of Table 1.7 there is used the equality

$$\bar{\rho}^{(m)}=\bar{r},$$

which is correct only in the case when the distance from the axis of rotation to the flapping hinge $l_{r.m}$ is equal to zero.

If one were now to use well-known formulas for coefficients of flapping motion and angle of attack of the equivalent rotor

$$a_1^*=a_1-mb_1+\theta_1;$$
$$b_1^*=b_1+ma_1-\theta_2;$$
$$\operatorname{tg}\alpha_{r.m}=\operatorname{tg}\alpha_0+mb_1-\theta_1,$$

then it will be possible somewhat to simplify expressions for P_n and $\bar{P}_n$ by introducing in the first line values a_1^* and b_1^* instead of a_1 and b_1. Here coefficients f_n^* will appear equal to zero, and values of angles θ_1 and θ_2, in general, will not enter into the equations. In other words, the well-known position about the fact that the loads on the blade do not depend on the deflection of the disk of the cyclic pitch control, when $l_{r.m}=0$ is completely observed in expressions of Table 1.7.

However, simplifications appearing with transition to the equivalent rotor are so immaterial that they do not justify assumptions about the fact that $l_{r.m}=0$. Therefore, we will subsequently examine oscillations of the blade only in axes of the shaft, and the idea of the equivalent rotor will not be used.

10. Basic Assumptions Utilized in the Calculation of Flexural Stresses

In the calculation of flexural stresses in the blade let us use all those assumptions which were accepted in the derivation of the differential equation of oscillations of the blade in the thrust plane (1.9). Let us represent the blade in the form of an elastic beam stretched by centrifugal forces N. Parameters of this beam – its linear mass m and flexural rigidity EI – will be considered continuously distributed along the length of the blade.

Furthermore, we will take the following assumptions:

1. We will consider that the plane of least rigidity of the blade coincides with the flapping plane, and therefore when bent in the flapping plane the blade will be only under the impact of forces acting in this plane.

2. In the determination of loads in the flapping plane we will not consider twisting deformations of the blade (for an account of twisting deformations see § 7, Chapter IV, Book One).

3. We will examine the standard type of rotor with articulated blades, and the distance from the axis of rotation to the flapping hinge will not be disregarded, i.e., we will assume $l_{ш} \neq 0$. We will not consider also the frictional force in the suspension hinges of the blade.

11. Differential Equation of Oscillations of the Blade and Its Solution

With the use of these assumptions calculation of flexural stresses will lead to the solution of the differential equation whose derivation is given in § 1 of this chapter:

$$[EJy'']'' - [Ny']' + m\ddot{y} = T. \tag{8.32}$$

With the examined fastening of the blade boundary conditions can be thus recorded so:

$$\left.\begin{array}{ll} y_0 = 0; & [EJy'']_0 = 0; \\ [EJy'']_b = 0; & [EJy'']'_b = 0. \end{array}\right\} \tag{8.33}$$

Entering into the right-hand side of equation (8.32), the value of linear aerodynamic load is determined by formulas (8.3) and (8.4) and according to Table 1.7.

Substituting into this equation the solution in the form of (8.28) and applying to it the method of B. G. Galerkin, we will obtain the system of algebraic equations relative to unknown coefficients of deformations. This system of equations will be presented in the form of Table 1.8.

Table 1.8. (Continued)

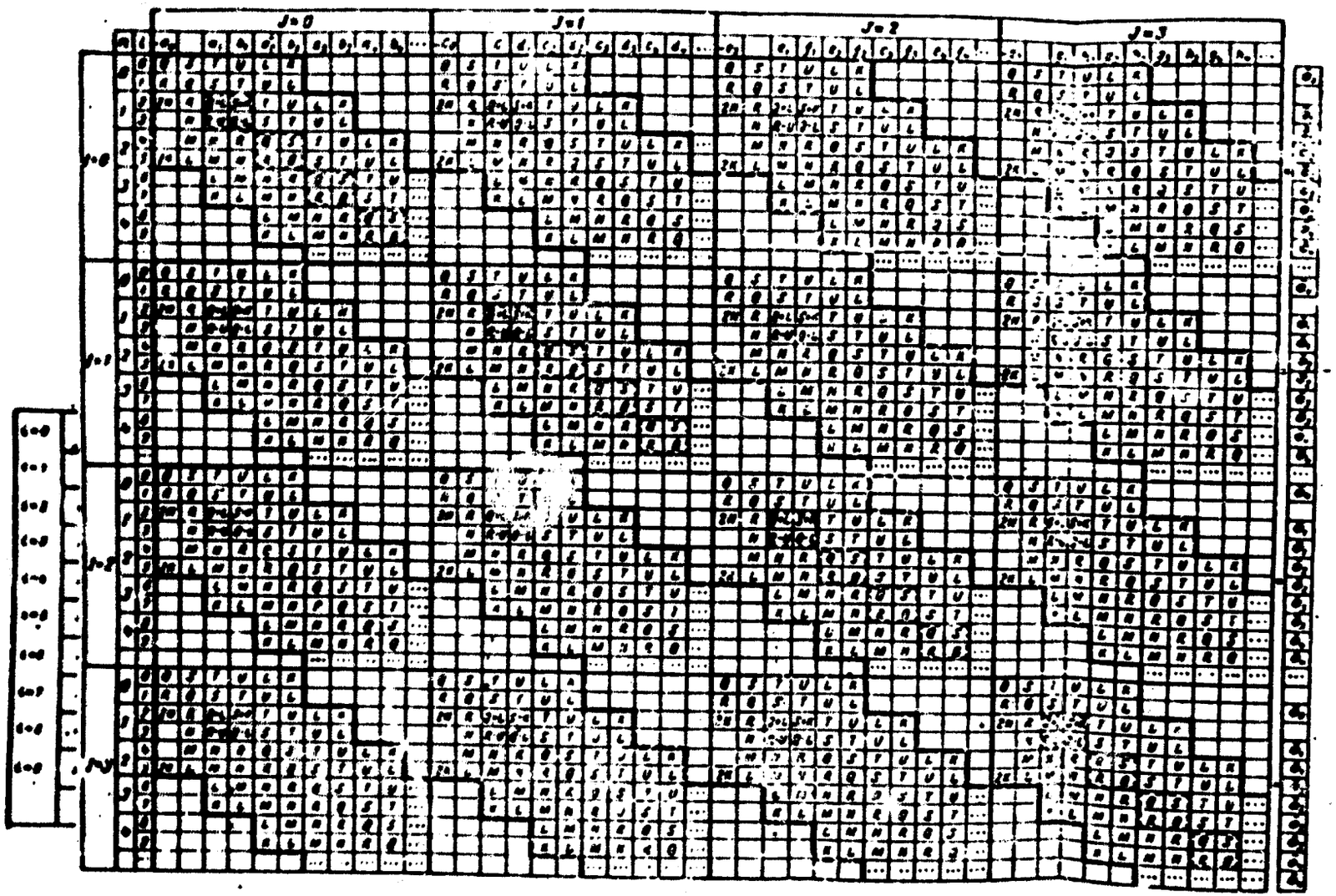

Each equation of the obtained system constitutes a sum of products of certain coefficients, recorded in squares of the table, by unknown coefficients of deformations entering simultaneously into several equations and carried out vertically in a special line placed at the top of the table. The known coefficients of each equation occupy one line in the table. On the right of the table in a special column there are copied coefficients $\bar{\Phi}_n$ and $\bar{\bar{\Phi}}_n$, which constitute the right-hand side of the equations.

In Table 1.8, just as in Tables 1.7 and 1.9, there are unfilled squares. This means that coefficients of equations for which these squares are intended are equal to zero.

12. Determination of Coefficients of the Left Side of Equations of Table 1.8

To determine coefficients of the left-hand side of equations in the program of calculation there should be created a special operator. This operator should give values of all coefficients of any equation of the system. In order to make this operator as simple as possible we will divide the whole table of coefficients into a series of zones according to the number of tones of natural oscillations utilized in the calculation. We will unite by these zones into separate groups those coefficients which have a similar means of formation in the application of the B. G. Galerkin method and can be calculated by the same formulas.

Transformation of differential equation (8.32) with the help of the B. G. Galerkin method to a system of algebraic equations of Table 1.8 consists of the following operations:

1. Substituted into the differential equation (8.32) is a solution in the form of (8.28) into which different forms of natural oscillations enter. If forms entering into the solution (8.28) are marked by index J, then all terms of the equation obtained as a result of this operation can be divided into several groups, each of which is characterized by the defined index J.

2. Then all terms of the equations are multiplied successively

Table 1.9.

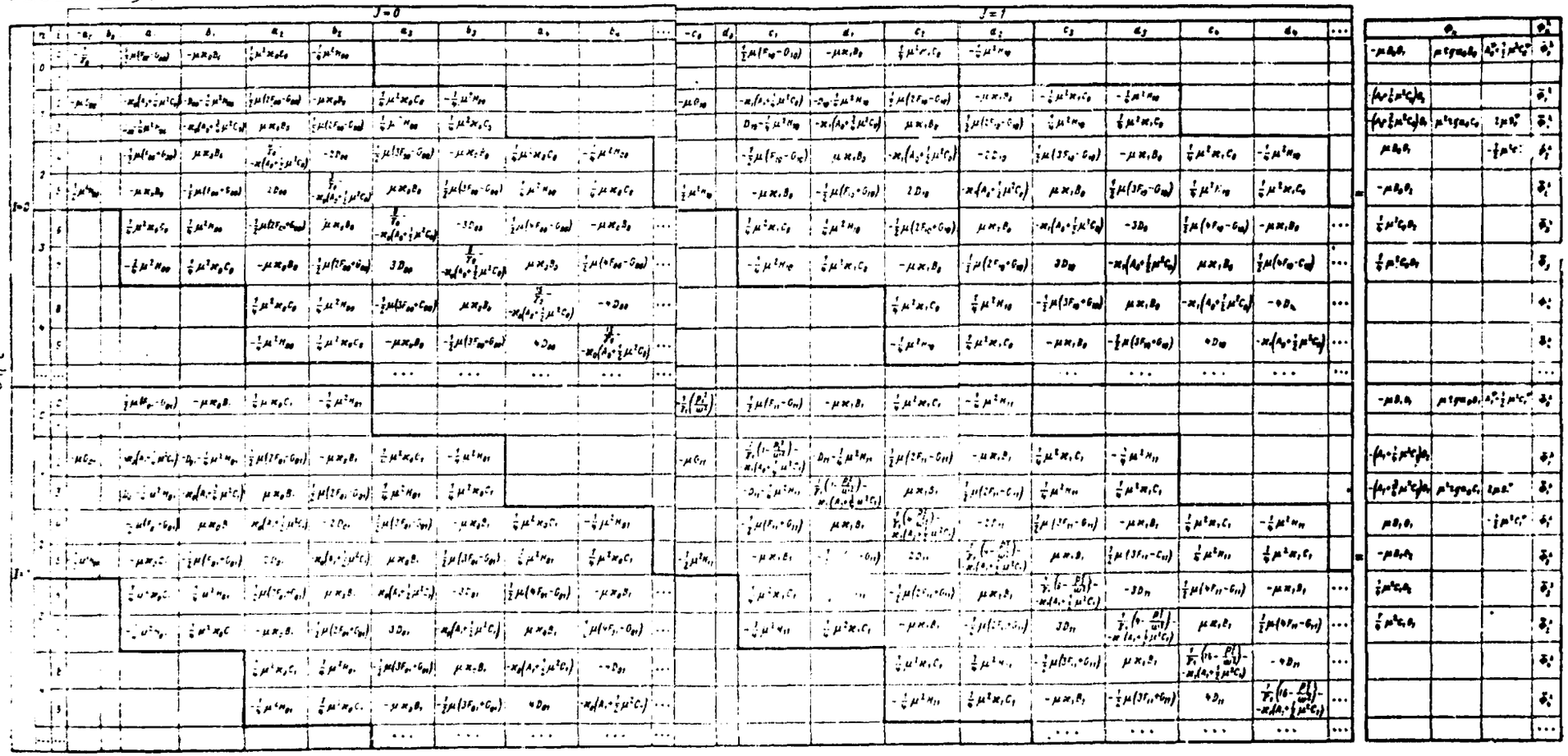

by the same forms of natural oscillations $y^{(I)}$. As a result of this operation there will be formed a system of equations where every equation of this system differs from others by the form of the tone of natural oscillations $y^{(I)}$ by which all terms of the equation were multiplied. Therefore, the thus obtained equations are numbered by us by values of the index I.

3. The following action of the B. G. Galerkin method is the integration of all functions obtained as a result of preceding operations along the length of the blade. As a result of this operation all terms of equations, which were earlier functions of the radius of the blade, become constant coefficients.

4. After that each thus obtained equation can be divided into a whole series of simpler equations, if one were to equate between themselves all coefficients standing at similar values $\cos n\psi$ and $\sin n\psi$. As a result of this operation each equation with the number I will be turned into a whole family of equations. Separate equations entering in this family in Table 1.8 are coordinated by index i. Furthermore, every pair of equations referring to similar harmonics is noted by the index n, which is equal to an order of the appropriate harmonic.

Analyzing the thus obtained system of algebraic equations, it is possible to note that all analogous coefficients of equations were placed in Table 1.8 along the diagonals. Such location is repeated in all zones corresponding to different indices of J and I. Here one should stipulate that this rule has individual exceptions, which can easily be noted in examining Table 1.8.

Using indices i, n, J, and I introduced above, it appears possible to form general formulas for all coefficients entering into the left-hand side of equations of Table 1.8. In the forming of these formulas we will also use special functions $f_1(a)$ and $f_2(a)$, which takes the following values depending upon parity and value of their argument:

$$f_1(a)=\begin{cases}1 \text{ at a even;}\\ 0 \text{ at a odd;}\end{cases}$$

$$f_2(a)=\begin{cases}1 \text{ at } a=0;\\ 0 \text{ at } a\neq 0.\end{cases}$$

These formulas have the following form:

$$\begin{aligned}
Q&=\frac{f_2(l-j)}{\nu_j}\left[n^2-\frac{p_j^2}{\omega^2}\right]-x_j\left[A_l+\frac{1}{2}\mu^2 C_l\right][1-f_2(l)];\\
R&=nf_1(l+1)D_{jl}+\mu x_j f_1(l)B_l;\\
S&=-nf_1(l)D_{jl}+\mu x_j f_1(l+1)B_l;\\
N&=\frac{1}{2}\mu[(1-n)F_{jl}-G_{jl}];\\
T&=\frac{1}{2}\mu[(1+n)F_{jl}-G_{jl}];\\
M&=\frac{1}{4}\mu^2 f_1(l)H_{jl}-\mu x_j f_1(l+1)B_l;\\
U&=\frac{1}{4}\mu^2 f_1(l+1)H_{jl}-\mu x_j f_1(l)B_l;\\
L&=\frac{1}{4}\mu^2 x_j C_l;\\
K&=-\frac{1}{4}\mu^2 H_{jl}.
\end{aligned}\qquad (3.34)$$

Here $x_j=x_0\beta_0^{(j)}$, where $\beta_0^{(j)}$ is the angle of rotation in the flapping hinge with oscillations according to the standardized form in accordance with (3.27) of the j-th tone of natural oscillations; ν_l – mass characteristic of the blade with oscillations with respect to the i-th tone:

$$\nu_l=\frac{c_{y0}\rho b_{0.7}R^2}{2m_l^{экв}};\qquad (3.35)$$

$m_l^{экв}$ – equivalent mass of the blade with its oscillations with respect to the form of the I-th tone:

$$m_l^{экв}=\int_0^R m\left[\bar{y}^{(l)}\right]^2 dr;$$

in the special case when I = 0 and it is possible to assume $\bar{y}^{(0)}=\bar{r}$, and the expression for ν_0 coincides with the conventional expression (7.49) for mass characteristic of the rigid blade (7.49); p_j – frequency of natural oscillations of the blade with respect to the form of the

J-th tone; in the process of the fulfillment of computations the value of the frequency is ascribed by expression

$$p_j^2=\frac{\int_0^R EI[(y^I)'']^2dr+\int_0^R N[(y^I)']^2dr}{\int_0^R m[y^I]^2dr}; \qquad (8.36)$$

ω – angular velocity (or number of turns of the rotor depending upon in what units p_j is determined); the ratio p_j/ω should be a dimensionless value.

Other quantities entering into formulas (8.34) have the following values:

$$\begin{aligned}
A_I&=\int_0^1 B^{(i)}\bar{r}^2\bar{y}^I d\bar{r};\\
B_I&=\int_0^1 B^{(i)}\bar{r}\bar{y}^I d\bar{r};\\
C_I&=\int_0^1 B^{(i)}\bar{y}d\bar{r};\\
D_{JI}&=\int_0^1 B^{(i)}\bar{r}\bar{y}^J\bar{y}^I d\bar{r};\\
F_{JI}&=\int_0^1 B^{(i)}\bar{y}^J\bar{y}^I d\bar{r};\\
G_{JI}&=\int_0^1 B^{(i)}\bar{r}^2\bar{y}^J\bar{y}^I d\bar{r};\\
H_{JI}&=\int_0^1 B^{(i)}\bar{r}^J\bar{y}^I d\bar{r}.
\end{aligned} \qquad (8.37)$$

Here $B^{(i)}$ is the equivalent chord of the blade determined by formulas (8.31) and having, consequently, different values depending upon the number of the equation:

$B^{(i)}=\bar{B}_a$ at i even;
$B^{(i)}=\bar{B}_a$ at i odd;

$\bar{y}^J$ and $\bar{y}^I$ – forms of natural oscillations of the blade whose tone is determined by value of indices J and I.

Literal designations of these forms are noted above by a bar. This means that they are standardized in such a way that $\bar{y}_R=1$. At the same time values of the first derivative of these forms in differentiation with respect to the radius of the blade β^J are not noted by a bar. This means that these derivatives are taken from forms of oscillations y^J, which are standardized in such a way that $y'_R=R$.

Formulas (8.34) permit determining the line of coefficients K, L, M, N, R, Q, S, T, U, L, K for any zone of Table 1.8, if coordinates of this zone J and I and the number of equation in zone i are prescribed. Thus assigning consecutively different values of J, I, and i and turning to the operator, which includes actions provided for by formulas (8.34), one can determine all coefficients of the left side of equations of Table 1.8.

13. Determination of Coefficients of the Right Side of the Equation of Table 1.8

To determine coefficients of the right side $\bar{\Phi}_n$ and $\bar{\bar{\Phi}}_n$ in the program of calculation there should be formed a special operator in which these coefficients are determined according to the following formulas:

$$\left.\begin{aligned}
&\bar{\Phi}_0=-\mu B_I\theta_1+\mu\operatorname{tg}\alpha_0 B_I+A_I^\circ+\frac{1}{2}\mu^2C_I^\circ+\bar{\Phi}_0^\lambda;\\
&\bar{\Phi}_1=-\left[A_I+\frac{3}{4}\mu^2C_I\right]\theta_2+\bar{\Phi}_1^\lambda;\\
&\bar{\bar{\Phi}}_1=-\left(A_I+\frac{3}{4}\mu^2C_I\right)\theta_1+\mu^2\operatorname{tg}\alpha_0C_I+2\mu B_I^\circ+\bar{\bar{\Phi}}_1^\lambda;\\
&\bar{\Phi}_2=\mu B_I\theta_1-\frac{1}{2}\mu^2C_I^\circ+\bar{\bar{\Phi}}_2^\lambda;\\
&\bar{\bar{\Phi}}_2=-\mu B_I\theta_2+\bar{\Phi}_2^\lambda;\\
&\bar{\Phi}_3=\frac{1}{4}\mu^2C_I\theta_2+\bar{\Phi}_3^\lambda;\\
&\bar{\bar{\Phi}}_3=\frac{1}{4}\mu^2C_I\theta_1+\bar{\Phi}_3^\lambda.
\end{aligned}\right\}\qquad(8.38)$$

For harmonics higher than the third (when $n>3$)

$$\bar{\Phi}_n=\bar{\Phi}_n^\lambda;\quad\bar{\bar{\Phi}}_n=\bar{\bar{\Phi}}_n^\lambda.$$

In formulas (8.38) new designations for a series of integrals are used:

$$\left.\begin{aligned} A_j^{\lambda} &= \int_0^1 B^{(1)} \varphi_r \bar{r}^{\lambda} \bar{y}^j d\bar{r}; \\ B_j^{\lambda} &= \int_0^1 B^{(1)} \varphi_r \bar{r}^{\lambda} \bar{y}^j d\bar{r}; \\ C_j^{\lambda} &= \int_0^1 B^{(1)} \varphi_r \bar{y}^j d\bar{r}; \\ \Phi_n^{\lambda} &= \int_0^1 B^{(1)} f_n^{\lambda} \bar{y}^j d\bar{r}. \end{aligned}\right\} \qquad (8.39)$$

Here

$$\varphi_r = \varphi_{\text{кон}\,r} + \Delta\varphi,$$

where

$$\varphi_{\text{кон}\,r} = \theta_0 - x_0\alpha_0 - x_1 c_0 - x_2 e_0 - x_3 g_0;$$

φ_r is the constant part of the blade angle counted off from the plane of rotation of the rotor; over the radius of the blade this quantity changes only owing to its geometric twist $\Delta\varphi$.

Values f_n^{λ} are copied in the far right column of Table 1.7.

Thus, formulas (8.38) permit determining all coefficients of the right side of equations if value I is assigned.

14. System of Equations After Substitution of Formulas (8.34) and (8.38)

If values of coefficients determined by formulas (8.34) and (8.38) are substituted into equations of Table 1.8, then the same system of equations can be represented in the form of Table 1.9.

Here for simplicity we were limited to the case when calculation is conducted correct to two tones of oscillations and four harmonics with respect to revolutions of the rotor. However, the above-mentioned calculation formulas (8.34) and (8.38) are written in general form and permit performing calculation with any accuracy.

By estimating the real needs of practice, it is possible in the composition of the program to be limited to calculation of only four

tones of natural oscillations and six to eight harmonics to revolutions the rotor.

15. General Scheme of Calculation

The system of algebraic equations copied in Table 1.8 constitutes a certain complex system of equations which allows determining all unknown quantities convergent in it. Determination of these unknown quantities and, first of all, coefficients of deformations of the blade, is the purpose of the method of calculation expounded here.

Above, in § 7, during calculation of bending stresses with the use of the B. G. Galerkin method, there were used different simplifications both in the derivations of equations given here and in their solution. The application of digital computers permits without special difficulty to solve this system of equations not introducing into it any simplifications, which permits considerably increasing the reliability of the obtained results. In any case errors of the calculation can be connected only with the initial assumptions. Fulfillment of all the required mathematical operations does not introduce any errors and is produced with any accuracy assigned in advance.

How do we solve this very complex system of equations? The simplest method here, without any doubt, appears to be the method of successive approximations in the form in which here it will be discussed below. This method was used in the forming of programs and checked by a large quantity of calculations. The method very rapidly coincides, and to obtain an accuracy necessary for practice three to four approximations appears sufficient.

In the use of method of successive approximations unknown coefficients of deformations are determined successively in order of increase in the index determining their belonging to the appropriate harmonic. Therefore, before turning to a description of the order of all operations in using the method of successive approximations, it is necessary to discuss the determination of coefficients of deformations.

16. Determination of Coefficients of Deformations

In the determination of coefficients of deformations, in all cases there is used the same principle involving the following. Coefficients of deformations are determined pairwise from two equations of the system of Table 1.8, which pertain to cosinusoidal and sinusoidal components of any harmonic. These equations are, first of all, formed in the following way. The sum of products $\Delta\bar{\Phi}_n$ and $\Delta\bar{\bar{\Phi}}_n$ of coefficients in Table 1.8 is determined by coefficients of deformations already determined at the moment of fulfillment of this operation, with the exception of those products into which enter coefficients enclosed in Table 1.8 by a dashed line. These sums of products are transferred to the right side of equations. After that coefficients of deformations referring to analogous harmonics (true, only in the case when $n > 1$) and forms of deformations are determined from two algebraic equations of the following form:

$$\left.\begin{aligned} \bar{Q}a_n + Sb_n &= \bar{\Phi}_n^1; \\ Ra_n + \bar{\bar{Q}}b_n &= \bar{\bar{\Phi}}_n^1. \end{aligned}\right\} \tag{8.40}$$

where

$$\bar{\Phi}_n^1 = \bar{\Phi}_n - \Delta\bar{\Phi}_n; \quad \bar{\bar{\Phi}}_n^1 = \bar{\bar{\Phi}}_n - \Delta\bar{\bar{\Phi}}_n.$$

Coefficients a_n and b_n here have a generalized character in the sense that such an entry of equations is possible with coefficients c_n and d_n, e_n and f_n, and g_n and h_n.

Coefficients $\bar{Q}$, S, R, and $\bar{\bar{Q}}$ entering into equations (8.40) are determined by formulas (8.34) for the case when $J = I$. The value 1 for the first equation is an even quantity and for the second equation, an odd quantity. Consequently, these coefficients in this special case can be written in accordance with (8.34) in such a form:

$$\left.\begin{aligned} \bar{Q} = \bar{\bar{Q}} &= \frac{1}{\nu_J}\left[n^2 - \frac{p_J^2}{\omega^2}\right] - \varkappa_J\left[A_J + \frac{1}{2}\mu^2 C_J\right]; \\ S &= -nD_J; \\ R &= nD_J. \end{aligned}\right\} \tag{8.41}$$

In this case, when $J = I$,

$$D_J = \int_0^1 B^{(1)}\bar{r}\,[\bar{y}^J]^2\,d\bar{r}.$$

If in the first formula of (8.41) we disregard the second term and approximately assume $B_n = \bar{\bar{B}}_n = b_n$, then equation (8.40) can be converted to the form utilized in the simplified methods of calculation (see § 7).

Indeed, by producing these simplifications, we will multiply all terms of (8.40) by $\gamma_j \frac{\omega^2}{p_j^2}$.

Let us introduce new designations. Quantity $\bar{n}_j$, determined by expression

$$\bar{n}_j = \frac{1}{2} \frac{\omega}{p_j} \nu_j D_j, \tag{8.42}$$

will be called the relative coefficient of aerodynamic damping.

Quantity $\nu_n = n\omega$ will be called the forced frequency of excitation of oscillations.

Then equation (8.40) can be rewritten in the form utilized in § 7:

$$\left.\begin{aligned} \left[\left(\frac{\nu_n}{p_j}\right)^2 - 1\right] a_n - 2\bar{n}_j \frac{\nu_n}{p_j} \cdot b_n &= \frac{\omega^2}{p_j^2} \gamma_j \bar{\Phi}_n^2; \\ 2\bar{n}_j \frac{\nu_n}{p_j} a_n + \left[\left(\frac{\nu_n}{p_j}\right)^2 - 1\right] b_n &= \frac{\omega^2}{p_j^2} \gamma_j \bar{\bar{\Phi}}_n^2. \end{aligned}\right\} \tag{8.43}$$

From these equations the peak value of coefficients of deformations, which corresponds to the J-th tone of natural oscillations, can be determined as

$$\delta_{\max}^{(j)} = \lambda_д \delta_{ст}^{(j)},$$

where $\lambda_д$ is the coefficient of dynamic increase in amplitude; $\delta_{ст}^{(j)}$ — sag of the blade with respect to the form of the J-th tone with static application of external forces.

$$\left.\begin{aligned} \delta_{ст}^{(j)} &= \frac{\omega^2}{p_j^2} \gamma_j \sqrt{(\bar{\Phi}_n^2)^2 + (\bar{\bar{\Phi}}_n^2)^2}; \\ \lambda_д &= \frac{1}{\sqrt{\left[\left(\frac{\nu_n}{p_j}\right)^2 - 1\right]^2 + 4\bar{n}_j^2 \left(\frac{\nu_n}{p_j}\right)^2}}. \end{aligned}\right\} \tag{8.44}$$

Thus the accepted form of determining coefficients of deformations in principle coincides with the form which is used in problems of mechanics in the determination of the amplitude of oscillations of a system with damping and is described above in § 7.

It is necessary to note that in determining coefficients of deformations equations of the system (see Table 1.8) will be converted to the form of (8.40) only in the case when $n > 1$. In the determination of coefficients referring to the first harmonic, into the left side of equations (8.40) even certain additional coefficients K, L, and U will enter, which, however, do not change the essence of the matter.

The determination of coefficients a_0, c_0, e_0, and g_0, determining the constant part of deformations, appear somewhat different. They can be determined from one equation with the number $i = 0$. However, in order not to disturb the community of approach, it is convenient to determine them in the program also from two equations with numbers $i = 0$ and $i = 1$, the coefficients of which are determined by the same formulas (8.34). Here one should assume $\bar{\Phi}_0^s = 0$. Such an approach permits somewhat simplifying the program of calculation.

17. Program of Calculation

In the composition of the program of calculation there is set about the following sequence of fulfillment of necessary operations:

1. According to the separate program which is absolutely necessary in the designing of blades and therefore should certainly be formed, forms and frequencies of natural oscillations of the blade in the thrust plane are determined. In the process of this calculation there should be obtained the following quantities: y', β', σ', ρ_j, and $m_j^{\sigma^{(j)}}$. Here $\sigma^{(j)}$ is the distribution of flexural stresses over the radius of the blade with its oscillations with respect to the standardized form of the J-th tone.

2. Parameters characterizing conditions of flight of the helicopter are prescribed: $\mu, Q, \omega, a_s, \varphi_{\text{ист}}, \theta_1$, and θ_2. Values a_s and $\varphi_{\text{ист}}$ can be determined from the calculation if the necessary propulsive

force and thrust of the rotor are assigned. Angles of cyclical control θ_1 and θ_2 can be determined if from balancing conditions of the helicopter there are determined the necessary moments M_x and M_z having an effect on its hub on the side of the rotor blades. These operations are usually included in the program of calculation.

3. In order to proceed to solving the system of equations, copied in Table 1.7 and 1.8, it is necessary still to determine coefficients γ_j and n_j. This system of equations is solved by the method of successive approximations, and in each approximation all unknown values are determined in sequence, which is copied in Table 1.10. First there are determined coefficients recorded in the first line, then those in the second, and so on.

4. After determination of all values copied in Table 1.10, it is possible to refine parameters of conditions of flight $\varphi_{\text{пст}}$, a_0, θ_1, and θ_2 and to calculate all coefficients in the following to approximation in the same order.

5. The sequence of operations copied in Table 1.10 is repeated until the difference of analogous coefficients of deformations in two successive approximations appears less than the assigned accuracy of calculation $\varepsilon\delta$. Value $\varepsilon\delta$ can be taken equal to 1/1000 or a somewhat smaller value.

6. Quantities of bending stresses in the blade on each azimuth can be determined by the formula

$$a_\psi = \sum_j \delta_j \rho^j,$$

where values δ_j are determined by coefficients of deformations $a_0\ a_n\ b_n\ c_0\ c_n\ b_n$, etc., in accordance with formulas (8.27) and (8.28).

This sequence of operations form the content of the method of calculation discussed here. Fulfillment of calculation permits obtaining the following:

– flexural stresses and form of deformations of the blade on

Table 1.10.

	Coefficients of deformations				Harmonic components of load	Partial induced speed	Total induced speed	
	Determined by equations (8.40)				Determined by Table 1.7	Determined by the formulas (8.6)	Determined by the formulas (8.5)	Determined by the formulas of Table 1.
Constant part	a_0	c_0	e_0	g_0	$\bar{P}_0$	$\bar{\lambda}_{0n}$	$\bar{\lambda}_n$ u $\bar{\bar{\lambda}}_n$	$\bar{f}_1^{\lambda}$ u $\bar{\bar{f}}_1^{\lambda}$
First harmonic	a_1, b_1	c_1, d_1	e_1, f_1	g_1, h_1	$\bar{P}_1$ u $\bar{\bar{P}}_1$	$\bar{\lambda}_{1n}$ u $\bar{\bar{\lambda}}_{1n}$	$\bar{\lambda}_n$ u $\bar{\bar{\lambda}}_n$	$\bar{f}_2^{\lambda}$ u $\bar{\bar{f}}_2^{\lambda}$
Second harmonic	a_2, b_2	c_2, d_2	e_2, f_2	g_2, h_2	$\bar{P}_2$ u $\bar{\bar{P}}_2$	$\bar{\lambda}_{2n}$ u $\bar{\bar{\lambda}}_{2n}$	$\bar{\lambda}_n$ u $\bar{\bar{\lambda}}_n$	$\bar{f}_3$ u $\bar{\bar{f}}_3^{\lambda}$
Third harmonic	a_3, b_3	c_3, d_3	e_3, f_3	g_3, h_3	$\bar{P}_3$ u $\bar{\bar{P}}_3$	$\bar{\lambda}_{3n}$ u $\bar{\bar{\lambda}}_{3n}$	$\bar{\lambda}_n$ u $\bar{\bar{\lambda}}_n$	$\bar{f}_4$ u $\bar{\bar{f}}_4^{\lambda}$
Fourth harmonic	a_4, b_4	c_4, d_4	e_4, f_4	g_4, h_4	$\bar{P}_4$ u $\bar{\bar{P}}_4$	$\bar{\lambda}_{4n}$ u $\bar{\bar{\lambda}}_{4n}$	$\bar{\lambda}_n$ u $\bar{\bar{\lambda}}_n$	$\bar{f}_5$ u $\bar{\bar{f}}_5^{\lambda}$
Fifth harmonic	a_5, b_5	c_5, d_5	e_5, f_5	g_5, h_5	$\bar{P}_5$ u $\bar{\bar{P}}_5$	$\bar{\lambda}_{5n}$ u $\bar{\bar{\lambda}}_{5n}$	$\bar{\lambda}_n$ u $\bar{\bar{\lambda}}_n$	$\bar{f}_6^{\lambda}$ u $\bar{\bar{f}}_6^{\lambda}$
Sixth harmonic	a_6, b_6	c_6, d_6	e_6, f_7	g_6, h_6	$\bar{P}_6$ u $\bar{\bar{P}}_6$	$\bar{\lambda}_{6n}$ u $\bar{\bar{\lambda}}_{6n}$	$\bar{\lambda}_n$ u $\bar{\bar{\lambda}}_n$	$\bar{f}_0^{\lambda}$

each azimuth of the rotor; all harmonic components of these quantities are determined simultaneously;

– field of axial induced speeds in the plane of the rotor and all harmonic components of this field;

– angle of attack and angle of setting of blades of the rotor in flight conditions with assigned values of propulsive force and thrust;

– angles of deflection of the disk of the cyclic pitch control, necessary for creation of moments M_x and M_z necessary for balancing of the helicopter.

18. Comparison of the Calculation with the Experiment at Low Flight Speed

In flights at low speed the magnitude of varying stresses measured in the blade usually has a very unstable character.

During the period of one flight condition assigned to pilot, the amplitude of stresses can be changed in magnitude two-three times. This is explained by the fact that the angle of attack of the rotor and speed of flight in these conditions are very difficult to maintain constant. Conditions of flight change continuously. However, the designer is basically interested in values of maximum amplitudes of varying stresses, since they, as a rule, introduce the greatest fatigue damage into the construction.

Usually the maximum varying stresses in the blade appear in conditions of flight with the largest angles of attack of the rotor. These conditions include conditions of deceleration of the helicopter and conditions steep descent at great vertical velocity.

For comparison of results of the calculation and experiment let us proceed in the following way. Let us consider all conditions of flight with sudden deceleration of the helicopter before landing in which there was taken measurement of stresses in the blade. From each flight we will select the value of maximum amplitude of stresses over

the radius of the blade appearing during the period of the entire landing conditions. The field of values of these stresses is shaded on Fig. 1.33.

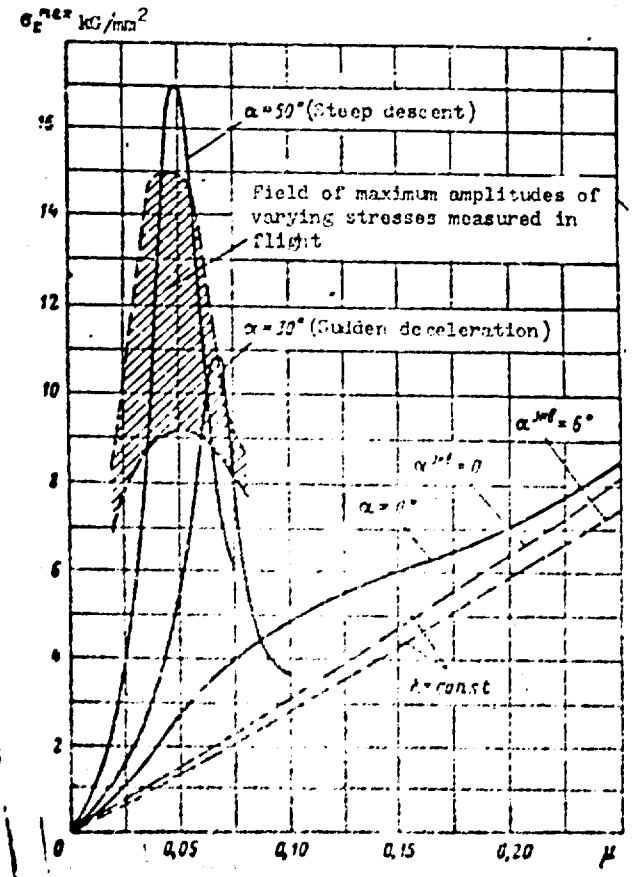

Fig. 1.33. Results of calculation of varying stresses taking into account the nonuniform field of induced speeds and a comparison of them with the experiment.

Calculation of stresses will be made for conditions with various speeds of flight and with an identical angle of attack of the rotor. The speed flight in the conditions will be characterized by quantity μ. Results of these calculation are shown in Fig. 1.33. The solid lines denote the dependences of maximum varying stresses in the blade obtained from the calculation on the speed of flight. With this there are examined conditions with the angle of attack $\alpha = 0$ and $\alpha = 30^\circ$, which can be reached in conditions of sudden deceleration and with an angle of attack of $\alpha = 50^\circ$, which is possible during steep descent

with great vertical velocity. The dashed line shows the same dependence for $\alpha = 0$ and $\alpha = -6^{\circ}$ but neglecting of the variable field of induced speeds. In the fulfillment of these calculations there were investigated conditions of flight without overload, when the thrust of the rotor is equal to the weight.

From the calculations made it follows that the greatest increase in variable stresses at low speeds is observed in those conditions of flight at which the sheet of free vortices flowing from the blades becomes flat. With departure of the sheet from the rotor plane the varying stresses sharply decrease and approximate stresses calculated, neglecting the alternating field of induced speeds.

With a comparison of conditions with identical angles of attack a sharp increase in varying stresses is observed in a very narrow speed range of the flight.

Results of the calculation to some degree reflect the pattern of the phenomenon observed in flight. Thus, just as in flight, the computed values of varying stresses increase at low speeds and are increased with an increase in the angle of attack of the rotor. However, considerable divergence is observed between calculation and experiment.

1. In identical flight conditions the amplitudes of varying stresses obtained in the calculation, appear less than tests measured during flight.

2. Amplitudes of varying stresses, obtained in the calculation and during the experiment, appear similar in a quantitative respect if one were to compare the conditions with different angles of attack, taking in the calculation an angle of attack of the rotor somewhat larger than occurs in flight.

3. If one were to compare conditions of flight at which values of stresses obtained in the calculation and during the experiment coincide, then a considerable distinction in their harmonic composition is observed. In stresses measured in flight the content

of high harmonics is higher that that in the calculation. Thus in stresses measured in conditions of sudden deceleration and shown in Fig. 1.33 harmonics in the range of the fourth to the sixth predominate. At the same time in the composition of varying stresses obtained by calculation stresses with the first, third, and fifth harmonics predominate. Here they are named in decreasing order of their amplitude. As an example Fig. 1.34 shows the distribution of stresses over the radius of the blade and their harmonic composition in conditions of flight with $\alpha = 50^{\circ}$ and $\mu = 0.048$.

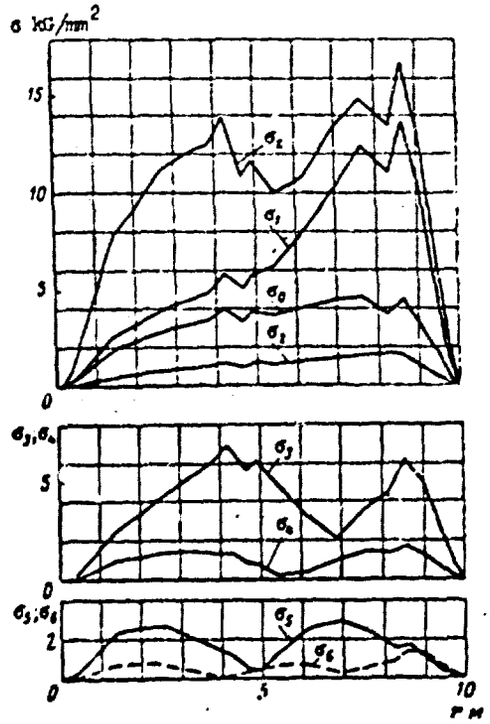

Fig. 1.34. Distribution of stresses over the radius of the blade and their harmonic composition in flight conditions ($\mu = 0.048$ and $\alpha = 50^{\circ}$).

It is necessary to note that in the calculation there was investigated a blade with characteristics providing the absence of resonances in working revolutions. Its resonance diagram is shown in Fig. 1.35. The working revolutions accepted in the calculation, are noted on the resonance diagram by a vertical line.

The data given show that the application of the method of calculation, taking into account mean induced speeds with those assumptions which were described in No. 3, approaches the results of the calculation and experiment at low speeds of flight. However, to

obtain results acceptable for practical purposes further refinements are necessary.

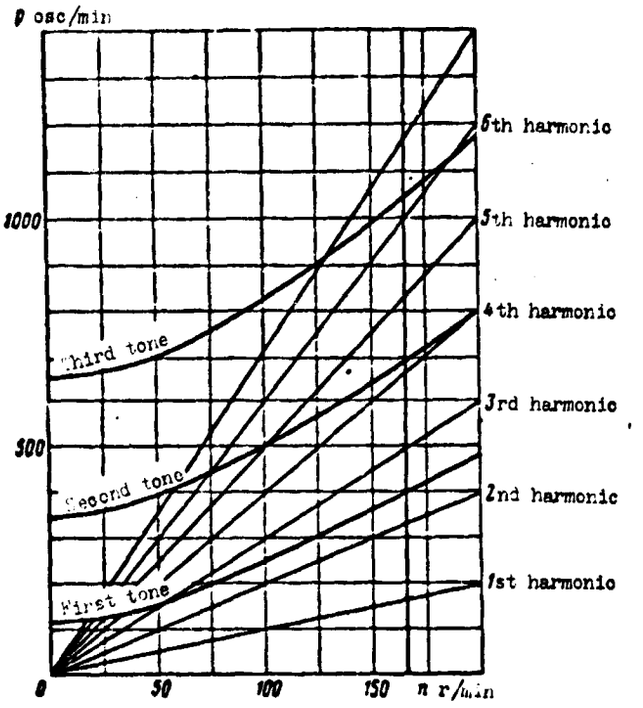

Fig. 1.35. Resonance diagram of the blade.

19. Comparison of the Calculation with the Experiment at Average Speeds of Flight

By average speeds of flight we here refer all speeds at which there still is not affected nonlinearity in the dependence $c_y = f(\alpha)$ and phenomena connected with the compressibility of flow. In many cases, therefore, average speeds of flight can be the cruising speed of a helicopter, which is especially interesting from the point of view of fatigue strength, since at this speed the helicopter spends the greatest percentage of time in operation.

Figure 1.36 gives a comparison of amplitudes of varying stresses and their first and second harmonics to the number of revolutions obtained by calculation with stresses measured in the blade at cruising speed when $\mu = 0.25$. Stresses obtained in the flight are shown by dots. The dashed line shows stresses calculated taking into

account the assumption of the fact that $\lambda = \lambda_{ocp} = const$ and solid lines, taking into account that which $\lambda = var$.

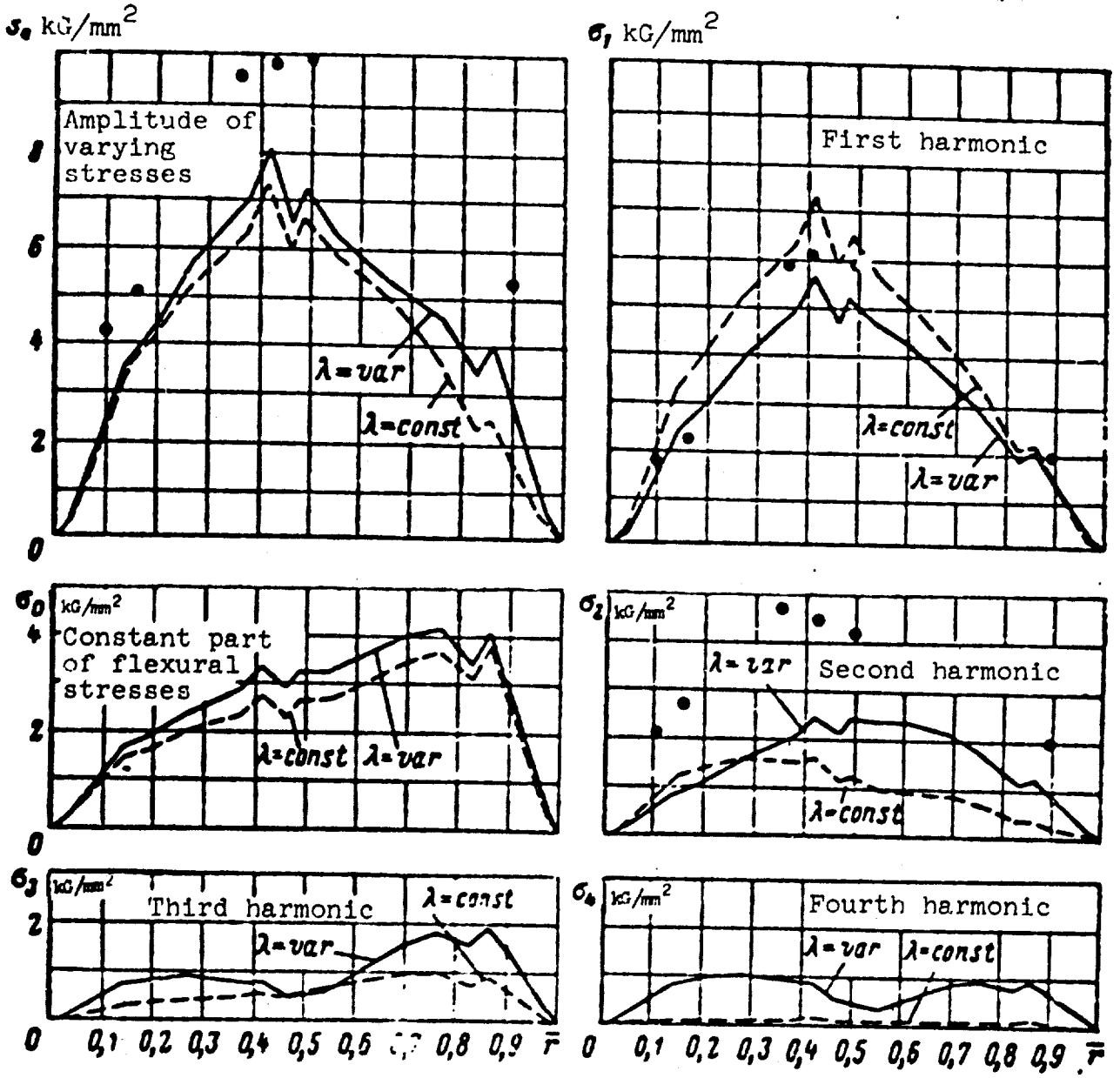

Fig. 1.36. Comparison of values of varying stresses calculated taking into account the variable field of induced speeds, with stresses measured in flight.

From this figure it follows that results of the calculation and experiment at cruising speed are distinguished rather considerably. The total amplitude of calculation stresses comprises not more than 80% of the values measured in flight. This divergence occurs basically

due to the distinction in values of the second harmonic of stresses to the number of revolutions of the rotor. Coincidence in the first harmonic of stresses is quite good. Higher harmonics of stresses in these conditions of flight are minute and do not have substantial influence on the amplitude of the stresses.

Results shown in Fig. 1.36 are typical for conditions of flight with $\mu = 0.25$ and are repeated almost on all helicopters.

From Fig. 1.36 it is also clear that the calculation of variable induced speeds does not give in these conditions noticeable refinements in values of varying stresses. However, if one were to discuss only any one harmonic, for example, the fourth, then it is clear that its value considerably increases with calculation of the alternating field of induced speeds. Therefore, if this harmonic is flow-passage and determines the magnitude of forces arriving at the fuselage and causing its vibrations, then this refinement appears very important.

Above nothing was said about the constant part of flexural stresses. Usually their magnitude, obtained on the basis of calculation, appears so accurate that its measurement in flight, as a rule, is not even taken. Calculation in this case gives more reliable results.

20. Possible Means of Further Refinement of Results of Calculation

As follows from the above-stated, calculation of varying stresses in the blade still does not give results which would satisfy the designer. If at average speeds of flight results of the calculation more or less will satisfactorily agree with the experiment (although further refinements of values of the second harmonic are extremely desirable), then at low speeds of flight very remote coincidence is observed.

In connection with this the direction in which searches are conducted with respect to further refinement of results is very important. It is possible to propose the following means.

In the calculation of varying stresses at low speeds of flight the most important refinements must be considered:

– calculation of the influence of natural induced speeds (rejection of the "hypothesis of stationarity");

– application of the vortex theory, considering deformations of the system of free vortices (rejection of the assumption that vortices depart from rotor at a constant speed equal to the average rate of flow λ_{orp}).

In the calculation of varying stresses at average speeds of flight, where the basic divergence is observed in values of the second harmonic of stresses, the most useful refinement would be the application of the vortex theory with a finite number of blades and introduction into calculation of the influence of both external and natural induced speeds.

In those cases when the blade has low torsional rigidity or when external forces excite the form of vibrations of the rotor coinciding with a form of flutter, and their frequency is close to the frequency of the flutter, noticeable refinements can be given by the calculation of torsional deformations of the blade. A method of similar calculation was given in § 7 of Chapter IV in Book One.

In many cases with calculation of varying stresses at cruising speed at the flight (just as at maximum speed) noticeable refinements can be given by the calculation of nonlinear dependences $c_y = f(\alpha)$ and compressibilities of flow, which will be discussed in the following paragraph.

§ 9. Calculation of Flexural Stresses in the Blade Taking Into Account the Nonlinear Dependence of Aerodynamic Coefficients on the Angle of Attack of the Profile and M Number

1. Examined Flight Conditions

Calculation of the nonlinear dependence of aerodynamic coefficients on the angle of attack of the profile is necessary in those conditions of flight when these angles reach so considerable magnitudes that it is no longer allowed to use the linear dependence (8.1). To such conditions pertain flights at speeds close to maximum, and those conditions of flight at low speeds when due to a great load on the blade and very great irregularity of the field of induced speeds on separate sections of the area marked by the rotor the angles of attack emerge into a nonlinear region of dependence $c_y = f(\alpha)$. In a number of cases calculation of these nonlinearities appears necessary in other conditions, including conditions of flight at cruising speed.

Calculation of phenomena connected with the compressibility of flow is necessary, as a rule, at high speeds of flight for helicopters having rotors with high peripheral velocities.

2. Determining Aerodynamic Loads

Above, in § 8, it was assumed that the in flow angle to the profile of the blade Φ is a small magnitude, and therefore the approximate formula (8.23) for determination of this angle was used. Here let us assume that the angle Φ can be changed within 360°, and its magnitude will be calculated by the formula

$$\Phi = \operatorname{arctg}\frac{U_x}{U_y}, \tag{9.1}$$

where values U_x and U_y are determined by the formulas

$$\left.\begin{aligned} U_x &= -\omega R(\bar{V} + p\sin\psi), \\ U_y &= -\omega R\left(\lambda - p\cos\psi - \frac{1}{\omega R}\dot{\beta}\right). \end{aligned}\right\} \tag{9.2}$$

Formulas (9.2) coincide with formulas used in § 8. This means that with their composition it was assumed that movements of the blade are small, and therefore it is possible to assume that:

$$\left.\begin{aligned}\sin\beta &\cong \beta;\\ \cos\beta &\cong 1.\end{aligned}\right\} \tag{9.3}$$

The value of angle Φ, determined by formula (9.1), with calculations on a digital computer is given usually only in the range of $\mp 90°$. This should be considered in the calculation of the angle of attack by the formula

$$\alpha = \varphi + \Phi. \tag{9.4}$$

Therefore, formula (9.1) can be used only when $U_x > 0$. If $U_x < 0$, then, as follows from Fig. 1.37,

$$\Phi = \pi + \operatorname{arctg}\frac{U_y}{U_z}. \tag{9.5}$$

The inflow angle, determined by formulas (9.1) and (9.5), is changed in the range of $-90° < \phi < 270°$.

If one were to assume that the angle of setting can be changed from $\phi = -15°$ to $\phi = +45°$, then the aerodynamic coefficients should be assigned within limits of the change in angle of attack from -105° to +315°.

The M number necessary for determination of the aerodynamic coefficients is calculated by the formula

$$M = \frac{U}{a_{зв}}. \tag{9.6}$$

Here $a_{зв}$ is the speed of sound:

$$a_{зв} = \sqrt{\frac{kp}{\varrho}}, \tag{9.7}$$

where k is the specific heat ratio; p – atmospheric pressure.

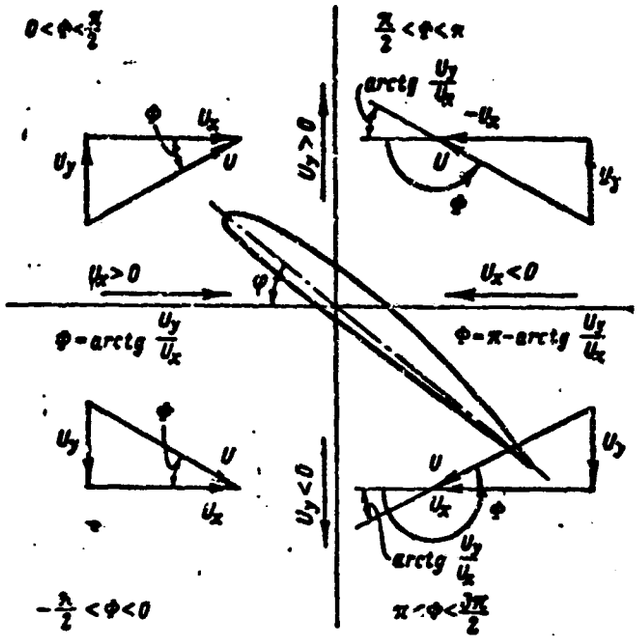

Fig. 1.37. Diagram of the flowing around of a profile for the determination of the inflow angle Φ.

The aerodynamic coefficients necessary for calculation are determined as a result of circular blowing of the profile in a wind tunnel. In calculations on a machine for determination of aerodynamic coefficients it is convenient to use the program formed by Engineer M. N. Tishchenko. In this program the influence of the M number on aerodynamic coefficients is considered only in the angular region of attack of the profile from $\alpha = -2°$ to $\alpha = +15°$. In the other range of the change in angles of attack aerodynamic coefficients are considered not dependent on the M number.

Figure 1.38, as an example, shows the dependence of the coefficient of lift c_y accepted in one of variants of this program on the angle of attack α for the profile NACA-230.

If coefficients of lift c_y and drag c_x are known, then aerodynamic forces effective in the flapping plane T and in the plane of rotation Q can be determined by formulas

$$\left.\begin{aligned} T&=\frac{1}{2}(c_yU_a+c_xU_\beta)\rho bU;\\ Q&=\frac{1}{2}(c_xU_a-c_yU_\beta)\rho bU. \end{aligned}\right\} \qquad (9.8)$$

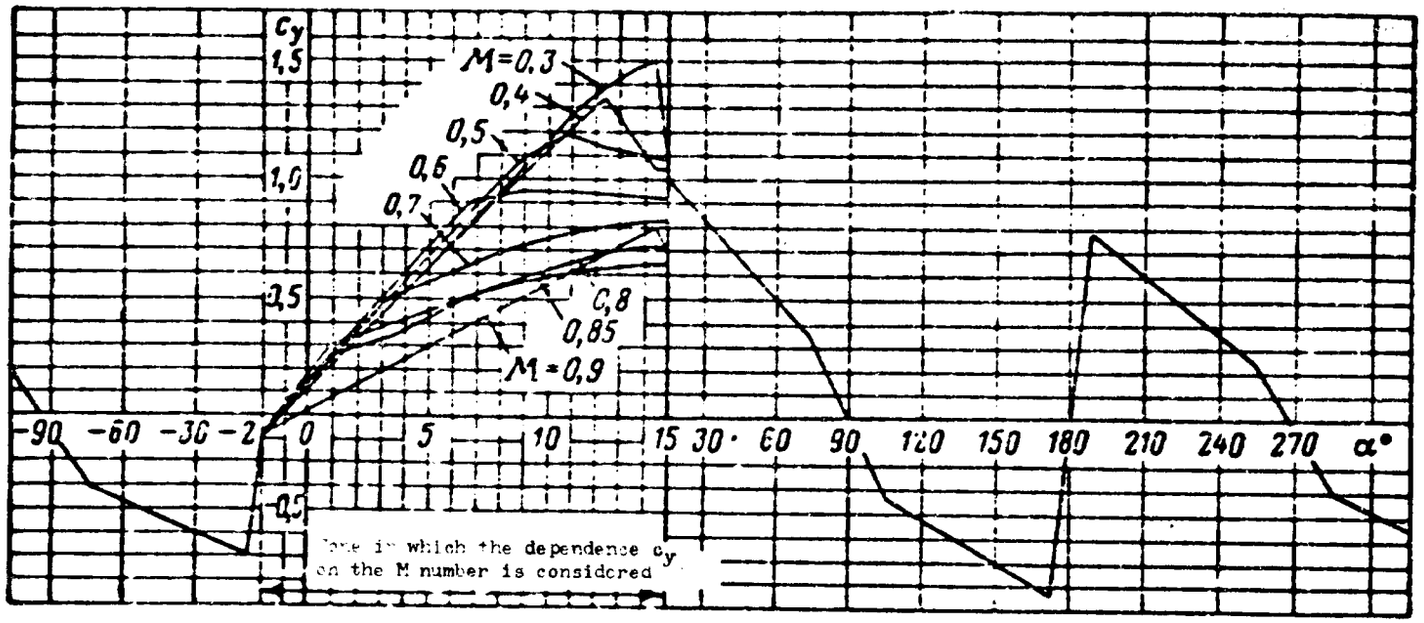

Fig. 1.38. Dependence $c_y = f(\alpha, M)$ accepted in the program.

3. Method of Calculation of the Blade as a System Whose Motion is Connected with Forms of Oscillations Prescribed Beforehand

As above, in § 8, the calculation of elastic oscillations of the blade is reduced to the solution of the differential equation

$$[EJy'']'' - [Ny']' + m\ddot{y} = T, \tag{9.9}$$

where under the accepted assumptions the aerodynamic force T is a nonlinear function of movements of elements of the blade y.

In this case to solve equation (9.9) it is convenient to use method in which motion of the blade with respect to time is found by numerical integration of ordinary differential equations obtained from equation (9.9) with the help of the B. G. Galerkin method. With such an approach to the problem these equations appear to be connected only through aerodynamic forces. Therefore, if at any arbitrary instant the aerodynamic forces are possible to calculate, the deformations of the blade with respect to each assigned form of oscillations are determined independently if these forms are orthogonal.

Let us represent the form of oscillations of the blade in the form of a sum of a certain number of tones of natural oscillations of the blade:

$$y = \sum_j \delta_j y^{(j)}, \tag{9.10}$$

where $j = 0, 1, 2, \ldots, j_B$ (j_B is the number of the highest tone of natural oscillations of the blade considered in the solution); $y^{(j)}$ – form of the j-th tone of natural oscillations of the blade standardized in such a way that for $\bar{r} = R\, y_R^{(j)} = R$; δ_j – certain coefficients determining the magnitude of deformations of the blade with respect to the j-th tone.

Coefficients δ_j, as above, will be called coefficients of deformations of the blade. Values δ_j are time functions.

Coefficients of deformation of the blade δ_j; in the present method calculation are accepted as the generalized coordinates of

the system. Determination of the law of their change with respect to time comprises the contents of the calculation.

Differentiating expression (9.10) twice with respect to time, we obtain

$$\left.\begin{aligned}\dot{y}&=\sum_j \dot{\delta}_j y^{(j)};\\ \ddot{y}&=\sum_j \ddot{\delta}_j y^{(j)}.\end{aligned}\right\} \tag{9.11}$$

If expression (9.10) and (9.11) are substituted into equation (9.9), and all terms of equation (9.9) are successively multiplied by $y^{(j)}$ (where $j = 0, 1, 2, \ldots, j_B$) and integrated over the radius of the blade, then in virtue of the orthogonality of forms of natural oscillations equation (9.9) decomposes into $j_B + 1$ independent equations of the form:

$$m_j\ddot{\delta}_j + C_j\delta_j = A_j. \tag{9.12}$$

Here

$$\left.\begin{aligned}C_j&=\int_0^R EI\,[(y^j)'']^2\,dr+\int_0^R N\,[(y^j)']^2\,dr;\\ m_j&=\int_0^R m\,(y^j)^2\,dr;\\ A_j&=\int_0^R T y^{(j)}\,dr.\end{aligned}\right\} \tag{9.13}$$

Above in Nos. 1 and 2 of § 7 it already was noted that quantities entering into equation (9.12) have a fully defined physical meaning. Quantity C_j, called the generalized rigidity of the blade with deformations in form of the j-th tone, is also the doubled potential energy accumulated by the blade with bending in the field of centrifugal forces with respect to the form of the same tone. Quantity m_j is the equivalent mass of the blade reduced to its end. It is equal also to the doubled kinetic energy of oscillations of the blade with respect to the form of the j-th tone with frequency $p = 1$. Integral A_j, standing in the right-hand side of equation (9.12), is the generalized force and is equal to the doubled work of aerodynamic forces on movements induced by deformations of the blade with respect

to the j-th tone.

It is known that the frequency of the j-th tone of natural oscillations of the blade can be determined by the formula

$$p_j = \sqrt{\frac{c_j}{m_j}}.$$

Therefore, it is convenient to transform equation (9.12) referring all terms to values m_j. Then they can be written as

$$\ddot{\delta}_j + p_j^2 \delta_j = \frac{A_j}{m_j} \tag{9.14}$$

or

$$\ddot{\delta}_j + p_j^2 \delta = \frac{\delta_{CT}^{(j)}}{p_j^2}, \tag{9.15}$$

where $\delta_{CT}^{(j)}$ is the coefficient of quasi-static deformations of the blade with respect to the form of the j-th tone from aerodynamic forces T (see § 7, No. 7).

As follows from formulas (9.8) and (9.2), the magnitude of aerodynamic force changes along the azimuth of the blade and depends on deformations of the blade or more accurately on values $\dot{y}$ and β, which determine the quantities of relative speed U_y. Therefore, to calculate aerodynamic forces it is necessary preliminarily to determine values $\dot{y}$ and β by formulas:

$$\left.\begin{aligned} \dot{y} &= \sum_j \dot{\delta}_j y^{(j)}; \\ \beta &= \sum_j \delta_j \beta^{(j)}, \end{aligned}\right\} \tag{9.16}$$

where $\beta^{(j)}$ is the angle of rotation of the elastic axis of the blade with respect to the plane of rotation corresponding to the standardized form of natural oscillations of the i-th tone.

If the coefficients of deformations δ_j and their first derivatives $\dot{\delta}_j$, pertaining to any azimuthal position of the blade or any instant t are known, then the calculation can be carried out in the following

order.

In the beginning values $\dot{\gamma}$ and β are determined by formulas (9.16). After that by formulas (9.2) components of relative flow rate U_y and U_x and speed U can be determined:

$$U=\sqrt{U_y^2+U_x^2}. \tag{9.17}$$

It is true that for determination of speed U_y it is still necessary to know the relative flow rate λ, which in general is a variable which changes over the radius and azimuth of the blade. The determination of quantity λ will be discussed in No. 5 of this paragraph.

If speeds U_y and U_x are known, then by formulas (9.1) and (9.5) the inflow angle Φ can be determined and by formula (9.4), the angle of attack of the profile α. The M number is determined by formula (9.6). These data are sufficient to determine aerodynamic coefficients by circular blowing of the profile, and, consequently, aerodynamic forces T.

Thus in the examined azimuth there appear the well-known deformations of the blade, speeds of these deformations and aerodynamic forces T acting on the blade. Consequently, by using formula (9.14), one can determine the coefficients $\ddot{\delta}_j$ determining the accelerations of elements of the blade:

$$\ddot{\delta}_j=\frac{A_j}{m_j}-p^2\delta_j. \tag{9.18}$$

After this by means of numerical integration of equations (9.14) with respect to time, one can determine new values of coefficients of deformations of the blade δ_j and their first derivatives $\dot{\delta}_j$ on the following azimuth of the blade after a certain time Δt determined by the integration step. Transition from instant t, on which coefficients of deformations δ_j and their first $\dot{\delta}_j$ and second $\ddot{\delta}_j$ derivatives are known, to the following instant $t+\Delta t$ can be performed with the help of a number of well-known methods of numerical integration of equations.

Here, only as an example, let us copy the formulas of such a transition referring to the method called the Euler method:

$$\left.\begin{aligned} \delta_{i+\Delta i} &= \delta_i + \Delta i \dot{\delta}_i; \\ \dot{\delta}_{i+\Delta i} &= \dot{\delta}_i + \Delta i \ddot{\delta}_i. \end{aligned}\right\} \tag{9.19}$$

Below the peculiarities of different methods of numerical integration will be examined in more detail. In particular, it will be shown that the Euler method, represented by formulas (9.19), is not useful for calculation of elastic oscillations of the blade.

Application of numerical integration of equations (9.14) with respect to time permits determining coefficients of deformations and their first derivatives on a new azimuth of the blade. Then, by determining at this azimuth new values of aerodynamic forces, one can determine and the new coefficients of $\ddot{\delta}_j$. This process can be continued until values of coefficients of deformations are determined on all azimuths of the blade during the period of one revolution of the rotor.

If the initial value of coefficients δ_j and $\dot{\delta}_j$ is prescribed arbitrarily, then after integration of equations during the period of one revolution of the rotor values δ_j and $\dot{\delta}_j$, obtained on the same azimuth as a result of integration, will already appear different, which are distinguished from values taken arbitrarily at the initial instant. However, if motion of the blades is stable, then numerical integration can be continued. Then after several revolutions of the rotor the motion will be steady and repeated in each following revolution of the rotor. This steady motion is the sought solution of equation (9.9).

Thus the method of calculation proposed here constitutes a resolution of the Cauchy problem with integration of equations of motion of the blade with respect to time under prescribed initial conditions.

4. Calculation Formulas for a Model of the Blade with Discrete Parameters

Usually in practical calculations the blade of the rotor is examined in the form of a weightless beam with concentrated loads simulating its mass fixed to it. It is also convenient to represent aerodynamic forces acting on the blade in the form of a series of concentrated forces. We will consider that aerodynamic forces are applied at attachment, points of concentrated loads, as if to every load there is fastened a separate flap with a certain area S_i (see § 1, No. 9). Then the aerodynamic forces can be determined by formulas analogous formulas (9.8):

$$T_i = \frac{1}{2}(c_y U_{x_i} + c_x U_{y_i}) \rho S_i U_i; \tag{9.20}$$

$$Q_i = \frac{1}{2}(c_x U_{x_i} - c_y U_{y_i}) \rho S_i U_i. \tag{9.21}$$

where index i denotes all values referring to the section of the blade with number i (see Fig. 1.51). The magnitude of area of concentrated flaps S_i is determined by formula (1.2).

For the blade of the rotor represented not in the form of a beam with distributed parameters and in the form of a model with a finite number of concentrated masses elastically connected with each other, equations analogous to equations (9.14) can be obtained. Only quantities m_j and A_j entering in equations will be determined not as integrals but as the sum of the form:

$$\left.\begin{aligned} m_j &= \sum_i m_i (y_i^{(j)})^2; \\ A_j &= \sum_i T_i y_i^{(j)}. \end{aligned}\right\} \tag{9.22}$$

where m_i is the value of concentrated masses of the system; $y_i^{(j)}$ – values determing the form of natural oscillations of the j-th tone; the form of natural oscillations should in this case be represented by a series of discrete values of ordinates y_i, which determine movements of the i-th masses of the blade; T_i – discrete values of aerodynamic forces determined by formula (9.20).

In everything else calculation of the model of the blade with discrete parameters does not differ from calculation of the model with parameters continuously distributed along the length of the blade. However, with calculation on digital computers it is incomparably more convenient to examine the model with discrete parameters.

5. Calculation of the Alternating Field of Induced Speeds

Application of the method of calculation expounded here does not exclude the possibility of calculation of the alternating field of induced speeds represented by the relative coefficient of flow in formula (9.2). For this in the determination of aerodynamic forces acting on the blade at the examined instant t, there should be solved the intero-differential equation of vortex theory of the rotor (see formula (5.29) of § 5, Chapter II, Book One).

Reduction of the problem on elastic oscillations of the blade to the Cauchy problem with determination of motion of the blade, starting from any initial instant, leads to considerable simplifications in the solution of the integro-differential equation of vortex theory.

With turning of the rotor one pitch along the azimuth from the blade vortices connected with changes in circulation flow only during the period of this last pitch. All vortices descending from the blade at preceding instants only move in space, and their circulation no longer changes. Therefore, in the solution of the integro-differential equation, which refers to some definite instant, it is necessary to find the connection only between circulation of adjacent vortices and vortices descending from the blade during the time of its movement only with the last step of integration. Quantities of circulations of all remaining free vortices already appear to be known and defined by the whole history of the process of motion.

To simplify the problem at the initial instant there can be accepted any schematic model of the vortex system consisting, for example, of only rotor vortices descending from the end of the blade with constant circulation along the length. It is impossible to assume that toward the moment of the beginning of calculation no

free vortices exist, since the mean induced speed through the rotor will appear equal to zero.

The method examined here permits attaining the highest possible accuracy, which can only provide calculation of induced speeds according to a rotor configuration with a finite number of blades. Application of this configuration in other methods of calculation of elastic oscillations of the blade leads to very serious complications.

The use of methods of calculation of induced speeds, founded on the rotor configuration with an infinite number of blades, in reference to the method of calculation examined in this paragraph is associated with many difficulties. Thus the method of successive approximations usually seems to be the simplest. However, if one were to use the method by which induced speeds are calculated upon completion of calculation of motion of the blade for the period of each revolution of the rotor (when values of aerodynamic forces T are known on all azimuths and radii of the blade and, consequently, values of circulation at the same points can be determined) and introduced these speeds into the calculation of aerodynamic forces on the next revolution of the rotor, then it appears that such a solution process does not converge. Therefore, it is necessary to use different procedures to bypass these difficulties, which, as a rule, leads to considerable complications which in the end can appear unjustified.

6. Peculiarities of Numerical Integration of Differential Equations of Elastic Oscillations of the Blade

To successfully perform the calculation of elastic oscillations of the blade it is very important to select the most advantageous method of numerical integration possessing good accuracy with a minimum number of operations connected with the solution of the differential equation of motion. This operation consists of the main part of the machine time during the calculation, and the greatest part of it is expended to determine external forces. Therefore, the calculation period is determened mainly by the number of transformations to the motion equation. This number is determined by the selected method and integration step. The smaller the step, the more prolonged the calculation.

An analysis shows that with the detecting of the periodic resolution of the problem of elastic oscillations the necessary integration step changes in very wide limits depending upon what method of numerical integration is used. Very poor results are given by many widespread methods of numerical integration, such as the already mentioned Euler method [see formula (9.19)]. Unsuitable also for the examined problem appeared to be the widely known method of solution by means of the Taylor series. This method leads to the following formulas of transition from instant t to the instant t + Δt:

$$\left.\begin{aligned}\delta_{t+\Delta t}&=\delta_t+\Delta t\dot{\delta}_t+\frac{1}{2}\Delta t^2\ddot{\delta}_t;\\ \dot{\delta}_{t+\Delta t}&=\dot{\delta}_t+\Delta t\ddot{\delta}_t.\end{aligned}\right\} \tag{9.23}$$

Value $\ddot{\delta}_{t+\Delta t}=f(\delta_{t+\Delta t}, \dot{\delta}_{t+\Delta t})$ is determined from the differential equation. Here Δt is the integration step.

More suitable to the given case but still insufficiently convenient are also the widely known methods of numerical integration of Runge-Kutta and Adams.

The best method of checking the applicability of the method of numerical integration for resolution of the problem on oscillations of the blade is the numerical solution of the equation

$$\ddot{\delta}+2\bar{n}\dot{\delta}+\delta=\sin\nu t, \tag{9.24}$$

which describes oscillations of a certain mechanical model constituting a mass on a spring with a damper (see Fig. 1.39).

The rotor blade can be examined as the totality of a certain number of such models possessing various frequencies of natural oscillations and various coefficients of damping corresponding to frequencies and damping factors of different tones of oscillations of the blade.

With relatively small steps of Δt the application of the Taylor series for integration of equation (9.24) leads to the solution

constituting the oscillatory process whose amplitude approaches a certain definite value different from the accurate analytic value by a value of error of the calculation. With an increase in the integration step, at certain definite values of Δt, the solution disagrees. If the solution does not disagree, the greatest error appears with resonance, i.e., when $\nu = 1$. Therefore, we subsequently will estimate the error by this most difficult case.

Figure 1.39 shows the change in peak values of the oscillatory process, which is obtained as a result of numerical solution of equation (9.24) with the help of the Taylor series. As initial values accurate analytic values δ_0 and $\dot{\delta}_0$ are taken. These are examined cases with relative coefficients of damping equal to $2\bar{n} = 0.1$ and $2\bar{n} = 0.2$ and different integration steps.

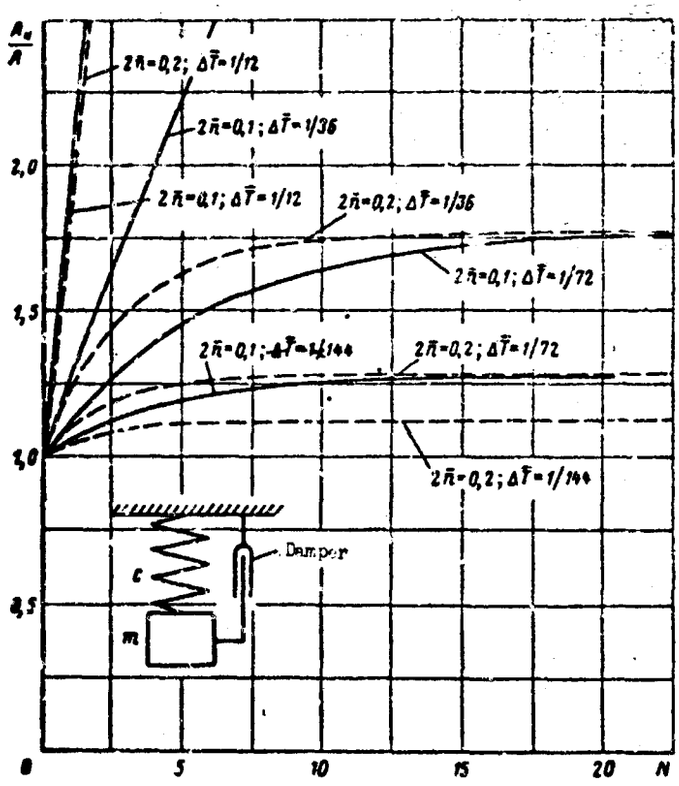

Fig. 139. Influence of relative integration step in the accuracy of the solution.

Maximum values of δ, obtained in the extent of the period of integration with the ordinal number N, are accepted as the amplitude of oscillations A_N in this period and are referred to the analytic value of the amplitude

$$A=\frac{1}{2\bar{n}}. \tag{9.25}$$

From Fig. 1.39 it follows that in the process of numerical integration the solution departs from the accurate analytic curve. The steady oscillatory process has an amplitude always greater than that of the accurate value. The greater the relative integration step $\Delta\bar{T}$, the greater the error. The relative integration step here is the quantity

$$\Delta\bar{t}=\frac{\Delta t}{T}, \tag{9.26}$$

where Δt is the integration time step; T – period of oscillations of the model.

The quantity of relative damping factor $\bar{n}$ also noticeably affects the accuracy of the solution. From calculations it follows that to obtain satisfactory accuracy the relative integration step should be of the order of 1/200 of the period of oscillations or even less.

In the numerical integration of equations describing elastic oscillations, it is important not only to provide the required accuracy but to use such an integration step at which there would not be a divergent solution.

Determination of the maximum integration step at which the solution will still be stable can be carried out in the following way.

Equations (9.23) and (9.24) can be examined as a certain system of difference equations. To determine the stability of the solution let us examine the uniform system of difference equations [without the right-hand side in equation (9.24)].

Let us write equations (9.23) in a somewhat more general form introducing a certain constant coefficient κ:

$$\left.\begin{aligned}\delta_{t+\Delta t}&=\delta_t+\Delta t\dot{\delta}_t+\kappa\Delta t^2\ddot{\delta}_t;\\ \dot{\delta}_{t+\Delta t}&=\dot{\delta}_t+\Delta t\ddot{\delta}_t.\end{aligned}\right\} \tag{9.27}$$

When $\kappa = 0$ these formulas coincide with Euler formulas (9.19) and when $\kappa = 1/2$, with Taylor formulas (9.23).

From equation (9.24) for the case when $\sin \nu t = 0$, let us determine value $\ddot{\delta}_t$, and, substituting it into equations (9.27), we will obtain the following system of difference equations:

$$\left.\begin{aligned} \delta_{t+\Delta t} &= (1-\varkappa\Delta t^2)\,\delta_t + (\Delta t - 2\bar{n}\varkappa\Delta t^2)\,\dot{\delta}_t; \\ \dot{\delta}_{t+\Delta t} &= -\Delta t\delta_t + (1-2\bar{n}\Delta t)\,\dot{\delta}_t. \end{aligned}\right\} \tag{9.28}$$

We will seek the solution of this system in the form:

$$\left.\begin{aligned} \delta_t &= A\alpha^n; \quad \delta_{t+\Delta t} = A\alpha^{(n+1)}; \\ \dot{\delta}_t &= B\alpha^n; \quad \dot{\delta}_{t+\Delta t} = B\alpha^{(n+1)}. \end{aligned}\right\} \tag{9.29}$$

Substituting (9.29) into the system of uniform difference equations (9.28), we will obtain the characteristic equation relative to α. From this equation we will find α.

$$\alpha = 1 - \Delta t\left(\bar{n} + \frac{1}{2}\varkappa\Delta t\right) \mp \Delta t\sqrt{\left(\bar{n} + \frac{1}{2}\varkappa\Delta t\right)^2 - 1}. \tag{9.30}$$

In order that value δ_t does not tend to infinity, for $n \to \infty$ there is necessary the condition:

$$|\alpha| < 1.$$

At relatively small Δt and $\bar{n}$ the value α, as follows from equation (9.30), is the complex quantity.

Determining modulus α, we will obtain the condition of the nondivergent solution:

$$\left|\sqrt{1 + \Delta t^2 - 2\Delta t\left(\bar{n} + \frac{1}{2}\varkappa\Delta t\right)}\right| < 1 \tag{9.31}$$

or

$$\Delta t - 2\left(\bar{n} + \frac{1}{2}\varkappa\Delta t\right) < 0. \tag{9.32}$$

Whence

$$\Delta t \leqslant \frac{2\bar{n}}{1-\varkappa}. \qquad (9.33)$$

If the integration step is referred to the period of oscillations of system T equal for the examined simplified model 2π, then we will obtain the condition of the nondivergent solution

$$\overline{\Delta T} \leqslant \frac{\bar{n}}{\pi(1-\varkappa)}. \qquad (9.34)$$

Then for the Euler method at $\kappa = 0$, we will obtain that the solution is possible when

$$\overline{\Delta T} \leqslant \frac{\bar{n}}{\pi}, \qquad (9.35)$$

and for the Taylor method at $\kappa = \frac{1}{2}$

$$\overline{\Delta T} \leqslant \frac{2\bar{n}}{\pi}. \qquad (9.36)$$

Thus in order not to obtain a divergent solution, in the use of the Euler method there is required a twice smaller step than that in Taylor method. Both methods give a divergent solution no matter how small is taken an integration step, if the relative damping factor $\bar{n}$ is equal to zero.

With an increase in $\bar{n}$ and Δt value α becomes a real number. Value α can never be larger than unity but can appear as a negative value larger than unity in absolute value.

The condition that $\alpha < 1$ is observed if

$$(2\varkappa - 1)\Delta t^2 + 4\bar{n}\Delta t - 4 > 0. \qquad (9.37)$$

Whence the instability of the solution for the Euler method at $\kappa = 0$ approaches when $\overline{\Delta T} > \frac{\bar{n} - \sqrt{\bar{n}^2 - 1}}{\pi}$ and only if $\bar{n} > 1$, and for the Taylor method ($\kappa = \frac{1}{2}$) in the case when $\overline{\Delta T} > \frac{1}{2\pi\bar{n}}$. However, these conditions are usually overlapped by a more rigid condition (9.36).

If these results are transferred to a system which represents the blade of the rotor, then the magnitude of relative step must be selected proceeding from the period of the highest tone of oscillations possible in the system, since this will lead to the least value of necessary step at which numerical integration is possible.

Figure 1.40 shows the typical character of the change in the period of natural oscillations of the blade T_ψ and relative coefficient of aerodynamic damping $\bar{n}$ with respect to the number of the tone of oscillations j. The value of the period of oscillations is calculated in degrees along the azimuth of the blade. Given on the same graph is the dependence $\sqrt{p_j}$ on the number of the tone; p_j is the frequency of the j-th tone of natural oscillations of the blade calculated in oscillations per minute. In the region of lowest tones quantity p_j considerably changes with a change in the number of revolutions of the rotor from n = 0 to working numbers of revolutions $n = n_{раб}$.

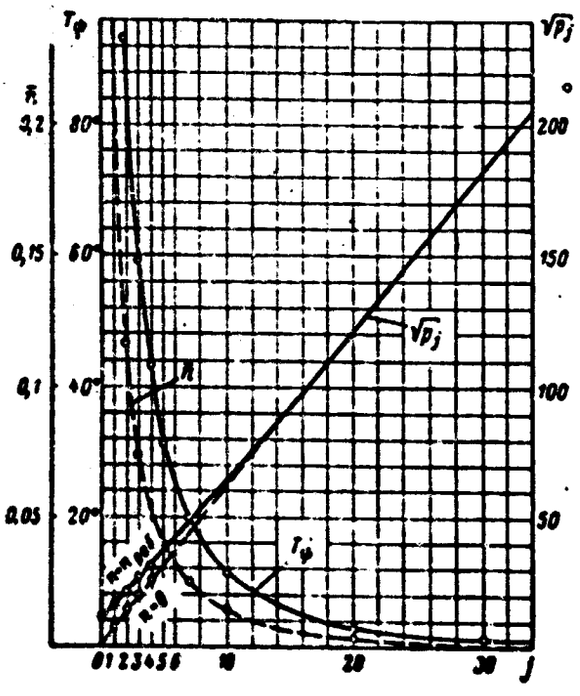

Fig. 1.40. Dependence of the period of oscillations T_ψ of the relative coefficient of aerodynamic damping $\bar{n}$ on the number of the tone of natural oscillations j.

If during calculation we are limited to the calculation of only the first four tones of natural oscillations including the zero, which is usually sufficient for obtaining necessary accuracy in practice, then the integration step will have to be selected proceeding from the

period and coefficient of relative damping of the highest (for this system) third tone of natural oscillations.

If one were to consider that the period of oscillations with respect to the third tone cannot be less than 45° in azimuth of the rotor, and the relative coefficient of aerodynamic damping is not less than n = 0.07, then for obtaining only a nondivergent solution the integration step in accordance with expression (9.36), should be less than 2° and in accordance with expression (9.35), less than 1° in azimuth. To obtain a satisfactory accuracy (see Fig. 1.39) it would be necessary to decrease the step even more.

This example shows that the application of shown methods of integration to calculation of the blade leads to very unsatisfactory results. Methods of Runge-Kutta and Adams permit for the same example to use an integration step of the order of 3°, but they prove to be not very convenient because of the fact that storage in the memory of the machine is required of too large variables calculated for preceding instants.

Good results are achieved by the method of integration mentioned in Book One (Chapter IV, § 7) with expansion of the solution in Taylor series and with repeated scaling of each integration step. This method is recognized as being fully suitable in application to the examined problem and is used at present in many programs of calculation.

Transition from instant t to instant t + Δt is produced by this method of numerical integration in such a sequence:

First miscalculation:

$$\delta^{I}_{i+1} = \delta_i + \Delta t \dot{\delta}_i + \frac{1}{2}\Delta t^2 \ddot{\delta}_i;$$

$$\dot{\delta}^{I}_{i+1} = \dot{\delta}_i + \Delta t \ddot{\delta}_i;$$

$\ddot{\delta}^{I}_{i+1} = f(\delta^{I}_{i+1}, \dot{\delta}^{I}_{i+1})$ is determined from the differential equation. Then $\ddot{\delta}_{cp}$ is determined by formula

$$\ddot{\delta}_{cp} = \frac{1}{2}(\ddot{\delta}_t + \ddot{\delta}'_{t+\Delta t}). \qquad (9.38)$$

Repeated scaling:

$$\delta''_{t+\Delta t} = \delta_t + \Delta t \dot{\delta}_t + \frac{1}{2}\Delta t^2 \ddot{\delta}_{cp};$$
$$\dot{\delta}''_{t+\Delta t} = \dot{\delta}_t + \Delta t \ddot{\delta}_{cp};$$

$\ddot{\delta}''_{t+\Delta t} = f(\delta''_{t+\Delta t}, \dot{\delta}''_{t+\Delta t})$ is determined from the differential equation.

Values $\delta''_{t+\Delta t}$, $\dot{\delta}''_{t+\Delta t}$ and $\ddot{\delta}''_{t+\Delta t}$ are considered final for the instant $t + \Delta t$.

The change in variable δ and its first and second time derivative, determined, in accordance with formulas (9.38), is shown on Fig. 1.41.

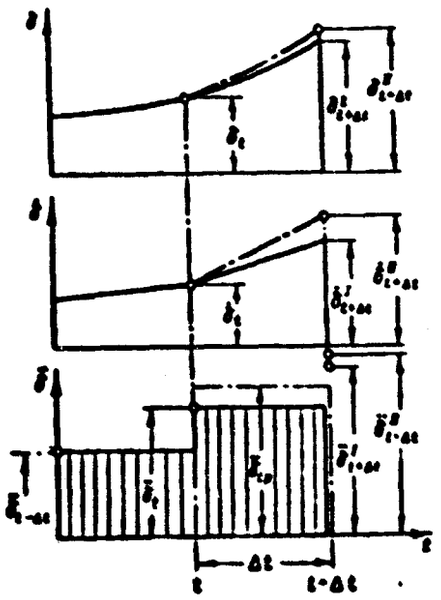

Fig. 1.41. Dependence of variable δ and its first and second time derivative.

Figure 1.42 gives the stabilized solution of equation (9.24), obtained as a result of numerical integration by this method. The solution is given with various values of the integration step. The heavy line shows the accurate analytic solution.

At the relative step 1/72 and less, numerical integration gives a solution almost accurately coinciding with the analytic. At a

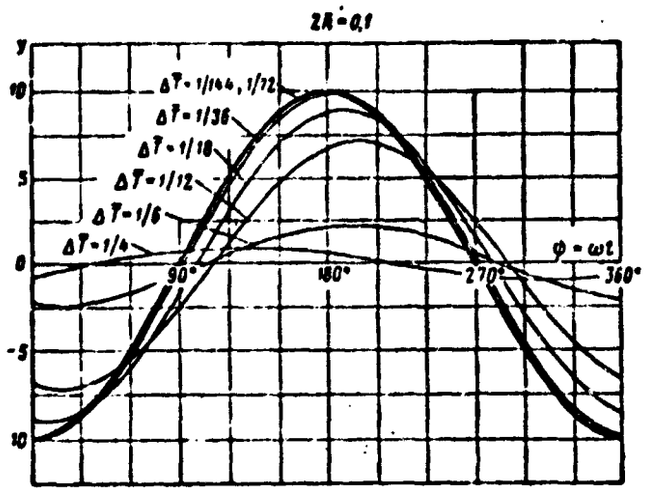

Fig. 1.42. Results of numerical solution of equation (9.26) depending upon the relative integration step.

larger relative step there appears considerable distinction between the accurate and numerical solution, which can be seen in Fig. 1.42.

At the relative step

$$\Delta\bar{t} > \frac{1}{s} \tag{9.39}$$

the solution diverges.

To exclude the possiblity of the appearance in the system of divergent solutions the integration step should not be larger than approximately one-third of the period of the highest tone of oscillations of the system having the smallest period. A very important advantage of this method is the fact that the maximum integration step practically does not depend on the value of the relative damping factor.

For the blade with parameters shown on Fig. 1.40, Fig. 1.43 gives a comparison of maximum steps $\Delta\psi_{\text{пред}}$ for the examined methods of integration depending upon the number of highest tone $j_в$ of natural oscillations of the system.

If one were to be limited to calculation of only the first four tones of natural oscillations, then in accordance with expression (9.39) to obtain a nondivergent solution it is sufficient to have an

integration step of about 15° in azimuth of the blade, i.e., approximately 7 times larger than in the same without repeated scaling.

Results of the solution of equation (9.24) permit tentatively determining the error in values of amplitudes corresponding to different tones of oscillations of the blade depending upon the integration step used. By error we mean here the difference between the exact analytic value of the amplitude of oscillations and the value obtained as a result of numerical integration. With integration by means of Taylor series with repeated scaling, this difference is always positive. This means that the numerical solution always leads to an understating of the amplitude of oscillations.

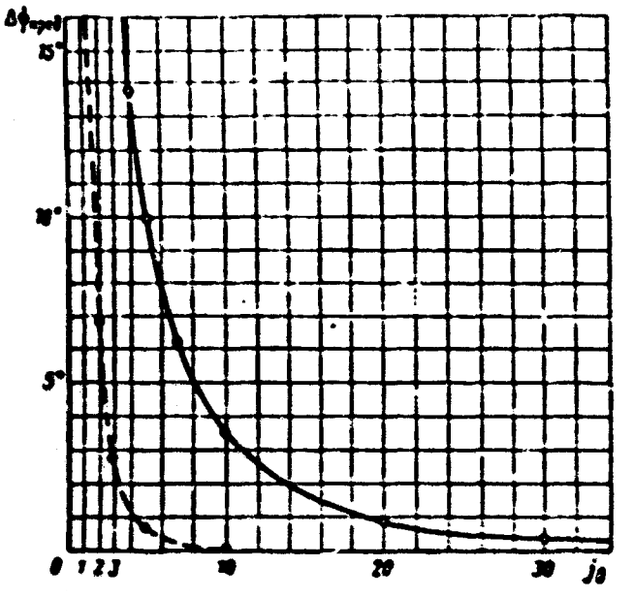

Number of tone

Fig. 1.43. Comparison of maximum steps for two methods of numerical integration: ---- maximum step during integration with expansion of the solution in Taylor series, —— maximum step during integration with repeated scaling by formulas (9.38).

Errors of calculation in percent of the exact value of the amplitude for various tones of oscillations of the blade, with the usual parameters depending upon the step during integration by means of Taylor series with repeated scaling, are given in Table 1.11.

The given data show that the value of the necessary integration step and, consequently, the duration of calculation are determined mainly by parameters of that system which represents the blade of the rotor. The greater the system has degrees of freedom, the greater it has tones of natural oscillations, the less the period of oscillations,

Table 1.11.

Number of tone	Error of calculation in % of the exact value of the amplitude with integration step in degrees					
	0,3	1,0	2,5	5	10	20
zero	<0,1%	<0,1%	<0,1%	0,3%	5%	25%
1 st	<0,1%	<0,1%	0,4%	6%	12%	50%
2 nd	<0,1%	0,3%	5%	25%	45%	80%
3 rd	<0,1%	0,4%	15%	30%	75%	
5 th	<0,1%	2%	20%	70%		
10 th	1%	30%	90%			
20 th	40%	Divergent solution				
30 th	90%					

of the highest tone and the less should be the integration step. Therefore, the duration of calculation is considerably reduced if one were to decrease the number of degrees of freedom of the system. All these considerations appear expecially important in the application of direct methods of calculation not using limitations superimposed on forms of oscillations of the blade. These methods will be examined in § 10 this chapter.

7. Method of Numerical Integration Proposed by L. N. Grodko and O. P. Bakhov

In the numerical integration of differential equations of elastic oscillations of the blade by the method proposed by L. N. Grodko and O. P. Bakhov, in formulas (9.27) the value of coefficient κ is taken to be equal to unity,

The condition of stability (9.31) is simplified and takes the form

$$|\sqrt{1-2\Delta t\sigma}|<1. \tag{9.40}$$

Consequently, at $\kappa = 1$ a divergent solution with the complex value σ is not possible. From the condition that σ is the complex number, condition (9.40) is correct only for values $\Delta t \leq 2 - 2\bar{n}$.

From condition (9.37) we will obtain that the solution will not be divergent while

$$\Delta\psi < 2\sqrt{\frac{1}{2\varkappa-1}+\frac{\bar{n}^2}{(2\varkappa-1)^2}}-\frac{2\bar{n}}{2\varkappa-1}. \qquad (9.41)$$

Whence at $\varkappa = 1$ we will obtain that

$$\Delta\psi < \frac{\sqrt{1+\bar{n}^2}-\bar{n}}{n}. \qquad (9.42)$$

Just as with integration by means of the Taylor series with double scaling, this method does not give a divergent solution when $\bar{n} = 0$ and has approximately the same value of the maximum step.

In reference to resolution of problems of elastic oscillations, its accuracy is no worse than that of the preceding method. The volume of computing operations decreases almost twice. Therefore the given method of numerical integration can be recommended for practical application.

9. Sequence of Operations in the Fulfillment of the Calculation and a Practical Evaluation of Different Integration Steps

On the whole the calculation of elastic oscillations of the blade is conducted in such a sequence:

1. Arbitrary initial values δ_j and $\dot{\delta}_j$ on the azimuth $\psi = 0$ are prescribed.

2. By formula (9.20) there are determined values of aerodynamic forces T_1, for the determination of which preliminarily such parameters should be calculated as γ_{∞}, β_{∞}, U_{∞}, $U_{p\infty}$, Φ, a_{∞}, M_{∞}, $c_{y\infty}$ and $c_{x\infty}$.

3. From equations (9.18) values $\ddot{\delta}_j$ are determined. Values a_{ij} and p_j^2 entering in this equation are calculated beforehand, after determination of forms of natural oscillations of the blade, and are not changed in process of calculation.

4. Transition to the following azimuth is carried out in

accordance with the selected method of numerical integration, for example, by formulas (9.38)

$$\left.\begin{aligned}
\delta^{I}_{i+\Delta t} &= \delta_i + \Delta t\dot{\delta}_i + \frac{1}{2}\Delta t^2\ddot{\delta}_i;\\
\dot{\delta}^{I}_{i+\Delta t} &= \dot{\delta}_i + \Delta t\ddot{\delta}_i;\\
\ddot{\delta}^{I}_{i+\Delta t} &= \frac{A_j}{m_j} - p_j^2\delta^{I}_{i+\Delta t};\\
\ddot{\delta}_{cp} &= \frac{\ddot{\delta}_i + \ddot{\delta}^{I}_{i+\Delta t}}{2};\\
\delta^{II}_{i+\Delta t} &= \delta_i + \Delta t\dot{\delta}_i + \frac{1}{2}\Delta t^2\ddot{\delta}_{cp};\\
\dot{\delta}^{II}_{i+\Delta t} &= \dot{\delta}_i + \Delta t\ddot{\delta}_{cp};\\
\ddot{\delta}^{II}_{i+\Delta t} &= \frac{A_j}{m_j} - p_j^2\delta^{II}_{i+\Delta t}.
\end{aligned}\right\} \qquad (9.43)$$

Values $\delta^{II}_{i+\Delta t}$, $\dot{\delta}^{II}_{i+\Delta t}$ and $\ddot{\delta}^{II}_{i+\Delta t}$ for the instant t + Δt are considered by final. For transition to the following azimuth the whole cycle is again repeated.

This method of integration can be recommended as being highly accurate and quite fully proved in practice in the calculation of elastic oscillations of the blade.

Numerical integration is fulfilled during the period of several revolutions of the rotor, until all values δ_j in two consecutive revolutions will be distinguished by less than the prescribed accuracy of the calculation. The performed calculations show that any prescribed accuracy can be attained.

Practically, however, it is assumed that the calculation is completed when the accuracy in the determination of coefficients of deformations becomes equal to R/1000 (R - radius of the rotor). When necessary there can be assigned and high accuracy.

Values of flexural stresses on each azimuth can be determined by formula

$$\sigma = \sum_j k_j\delta_j. \qquad (9.44)$$

where σ^j are standardized values of flexural stresses, i.e., bending stresses of the blade according to the standardized form of natural oscillations of the j-th tone.

The duration of the period of the transition process to steady motion very greatly depends on assigned initial values of coefficients of deformations. At the correctly assigned initial values δ_j and $\dot{\delta}_j$ the calculation is finished after miscalculation of two revolutions of the rotor. With unsuccessfully determined initial vlaues of δ_j the calculation can involve 8-10 revolutions.

In the program of calculation there should also be provided for the possibility of the refinement parameters of conditions of flight θ_0, α_B, μ and λ_{ocp} after miscalculation of each revolution. These parameters are refined in such a way that the rotor provides values of thrust and propulsive force prescribed in initial data. It is natural, therefore, that the duration of calculation is determined also by the correctness of assignment of parameters of flight conditions.

For a more precise definition of parameters of flight conditions and also for the solution of other problems in the process of calculation different integral characteristics of the rotor, such as thrust T_{HB}, longitudinal force H, torque M_K, etc., should be determined.

Proceeding from practical needs, oscillations of the blade can quite fully be represented with the help of four tones of natural oscillations. In this case, even proceeding from Table 1.11, where the greatest errors appearing with resonance are given, good accuracy can be obtained with the integration step $\Delta\psi = 2.5°$.

However, practically in those cases when clearly expressed resonances are absent, or in the system there are quite large damping forces which provide a damping factor larger than $2\bar{n} = 0.1$, used in the composition of Table 1.11, the accuracy of the calculation actually does not drop at the step $\Delta\psi = 5°$ and sometimes even at the step $\Delta\psi = 10°$. This circumstance is of great importance for saving time during calculation on computers with an average counting rate. Thus

with calculation on the computer "Strela" to determine the motion of the blade during the period of one revolution of the rotor about 6 minutes is required at the step of 10°. With a decrease in the step the counting time is increased accordingly, and at the step of 2.5° the duration increases so much that fulfillment of calculation on this computer becomes difficult. In the calculation on a more high-speed computer M-20 these considerations lose their value.

Figure 1.44 gives as an example values of coefficients of deformations calculated for one of the helicopters in flight conditions at a speed corresponding to $\mu = 0.3$. These conditions for the examined helicopter are far from stall, and therefore, the calculation is performed in the linear setting under assumptions described in No. 3 of § 8. Under these assumptions the calculation was made with the step of integration of 2.5°, 5° and 10°. Results of these calculations shown on Fig. 1.44 by a solid line, practically completely coincide. On the basis of these data the conclusion can be made that in conditions of flight quite remote from stall, when there is used a linear approach to resolution of the problem and in the solution low tomes of oscillations prevail, and acting on the blade are considerable forces of aerodynamic damping, without essential losses the calculation can be accurately fulfilled with the integration step of $\Delta\psi = 10°$.

The pattern changes in examining conditons in which the beginning of stall is noted. The stall leads to an increase in oscillations with respect to higher tones and to a sharp decrease in coefficients of aerodynamic damping. Due to this it is necessary to decrease the integration step.

Figure 1.45 shows results of calculation of coefficients of deformation with the use of the step $\Delta\psi = 5°$ and $\Delta\psi = 10°$ for the same rotor which was examined above but in conditions with $\mu = 0.4$ with the stall which was begun. Calculation was performed taking into account the nonlinear dependence of aerodynamic coefficients on the angle of attack of the profile α and the M number. The appearance of stall leads to a sharp increase in amplitudes of oscillations with respect to forms of highest tones, which, as is known, without

stall have less values than do coefficients of aerodynamic damping. Therefore, the lowering of aerodynamic damping with stall, first of all, has an effect on amplitudes of oscillations with respect to these forms. All of this led to the fact that the calculation with step $\Delta\psi = 10°$ introduced considerable errors into the calculation of coefficients of deformations δ_2 and δ_3. In Fig. 1.45 this can be seen from a comparison with the calculation where $\Delta\psi = 5°$. Therefore, to reduce the error during calculation of deformations in conditions with a stall which has begun, the integration step must be decreased down to values of the order of $\Delta\psi = (2.5\text{-}5)°$.

9. Comparison of Results of the Calculation According to the Method of Numerical Integration with the Method of Calculation with Respect to Harmonics

Discussed above was the method of calculation of stresses with respect to harmonics in a linear setting with assumptions enumerated

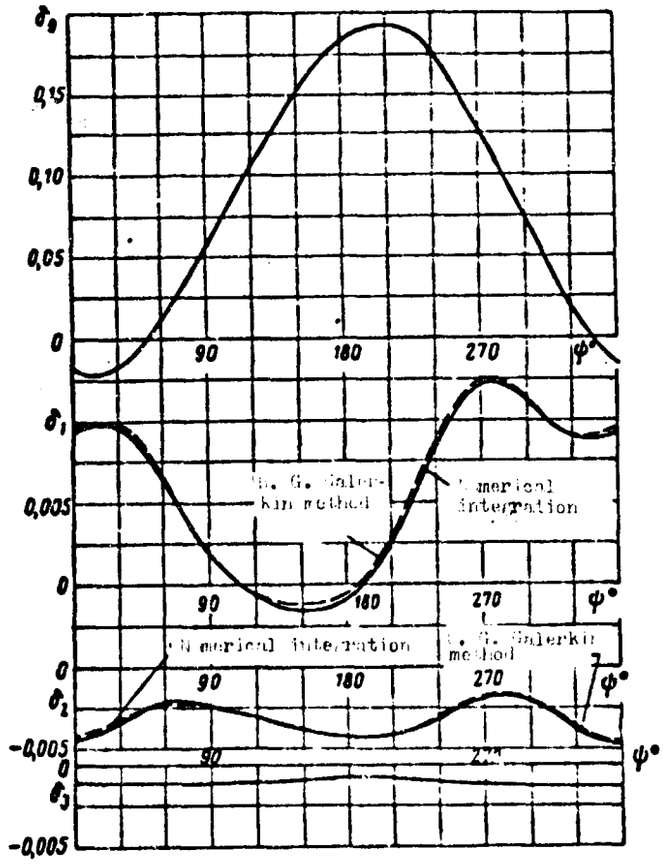

Fig. 1.44. Comparison of coefficients of deformations obtained as a result of solution of equations according to the method of B. G. Galerkin and numerical integration when $c_y = c_y^{\alpha}\alpha$ and $\mu = 0.3$.

in No. 3 of § 8. Such a method can be used with success for conditions of flight quite remote from stall. It has a great number of advantages, first of all, being a relatively small duration of calculations.

Figure 1.44, by a dashed line for a comparison, gives coefficients of deformations calculated by the method of calculation with resepct to harmonics discussed in § 8 for the same conditions of flight at $\mu = 0.3$ with the linear dependence $c_y = c_y^{\alpha}\alpha$. The comparison of methods of calculation indicates the good coincidence of results. The small distinction can be explained by a certain difference in initial parameters of conditions of flight.

10. Certain Results of Calculations

Let us give individual results characterizing those new possibilities for theoretical researches which reveal the method of numerical integration, taking into account the nonlinear dependence of aerodynamic coefficients with respect to the angle of attack α and M number as compared to linear methods of calculation.

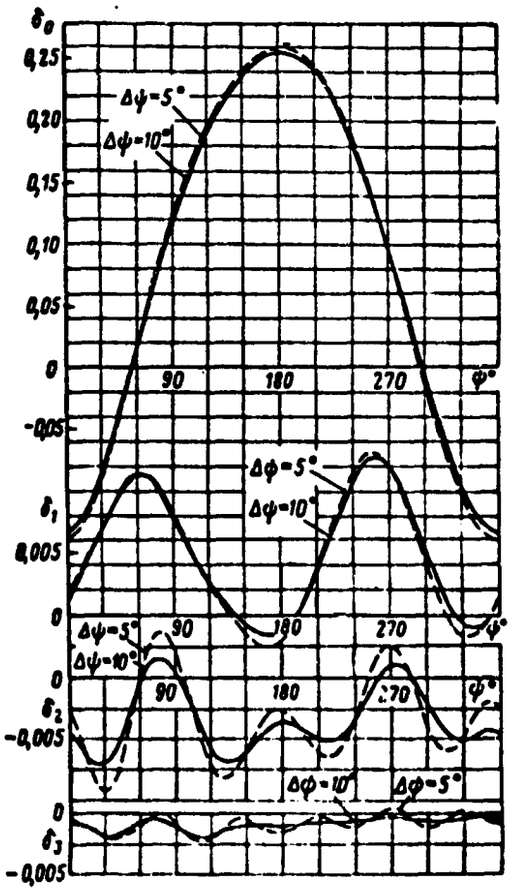

Fig. 1.45. Coefficients of deformations at the beginning of stall at $\mu = 0.4$.

One of the important advantages of the method of numerical integration is the possibility to perform calculations of stresses under conditions similar to stall conditions of flight.

Calculations show that with an approach to stall there is a sharp decrease in aerodynamic oscillation damping of the blade and an increase in amplitudes of oscillations with those harmonics which are found in resonance or near resonance with frequencies of natural oscillations of the blade. From the examination of deformation ratios given in Fig. 1.45, it is clear that oscillations with respect to the first tone occur basically with the second harmonic, oscillations with respect to the second tone – with the fourth harmonic, and oscillations with respect to the third tone – with the sixth harmonic to revolutions of the rotor, i.e., only frequencies close to frequencies of natural oscillations of the examined blade. An especially sharp increase in the amplitude of oscillations occurs with respect to forms of relatively higher tones of oscillations, which on Fig. 1.45 can be observed in the example of coefficients δ_2 and δ_3.

The appearance of stall is characterized by a sharp increase in amplitudes of varying stresses in the blade. Figure 1.46 gives values of maximum amplitudes of varying stresses over the radius of the blade according to the speed of flight calculated taking into account the linear and nonlinear dependence $c_y = f(\alpha, M)$. The sharp increase in stresses is a very convenient criterion in the determination of the

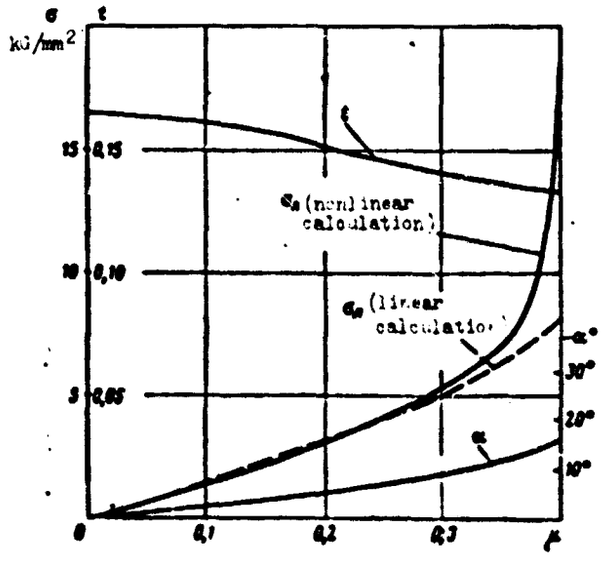

Fig. 1.46. Dependence of maximum amplitude of varying stresses over the blade on the speed of flight.

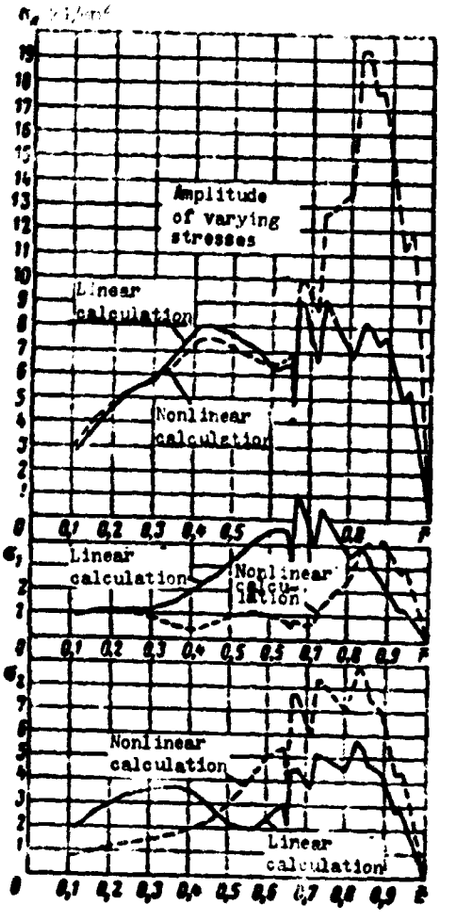

Fig. 1.47. Distribution of the amplitude of varying stresses and first two harmonic components of stresses over the radius of blade at $\mu = 0.4$.

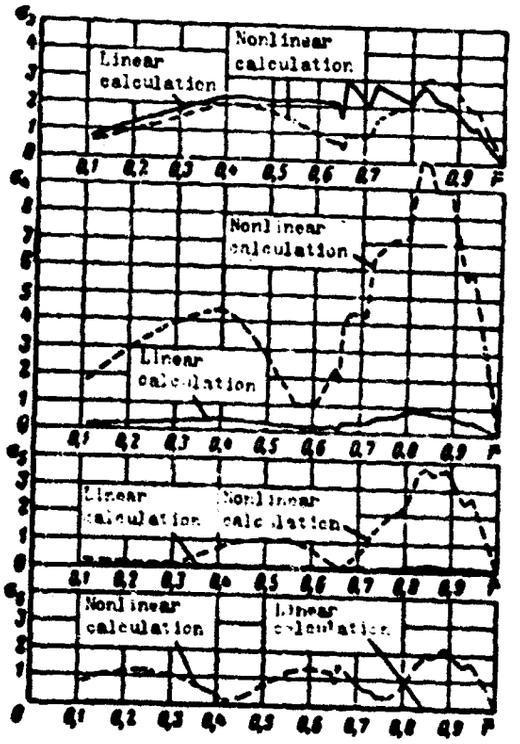

Fig. 1.48. Distribution of amplitudes of the third, fourth, fifth and sixth harmonic components of stresses over the radius of the blade at $\mu = 0.4$.

beginning of stall in the calculation of aerodynamic properties of the rotor.

The harmonic composition of varying stresses acting with stall and their distribution over the radius of the blade are shown in Figs. 1.47 and 1.48.

It is necessary to pay attention also to the fact that a substanital difference in results of linear and nonlinear calculation is observed in conditions sufficiently remote from stall.

Figure 1.49 shows coefficients of deformations calculated for the same helicopter at $\mu = 0.3$ with a linear and nonlinear dependence $c_y = f(\alpha, M)$, and Fig. 1.50 shows harmonic components of stresses corresponding to them and their amplitudes σ_A, constructed over the radius of the blade. As can be seen from this figure, the results are distinguished quite substantially.

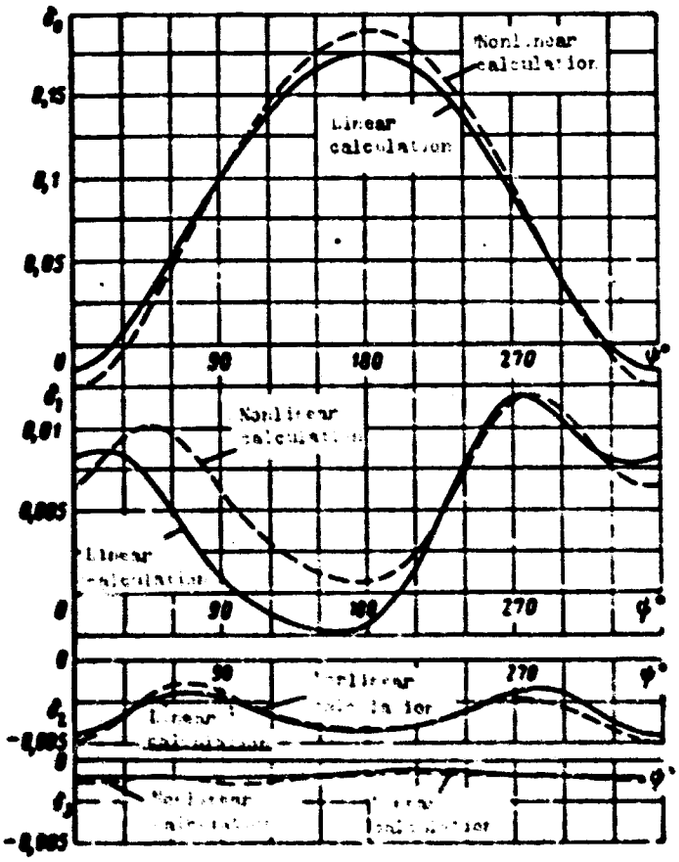

Fig. 1.49. Comparison of coefficients of deformations calculated by calculation of the linear and nonlinear dependence $c_y = f(\alpha, M)$ for conditions $\mu = 0.3$ far from stall.

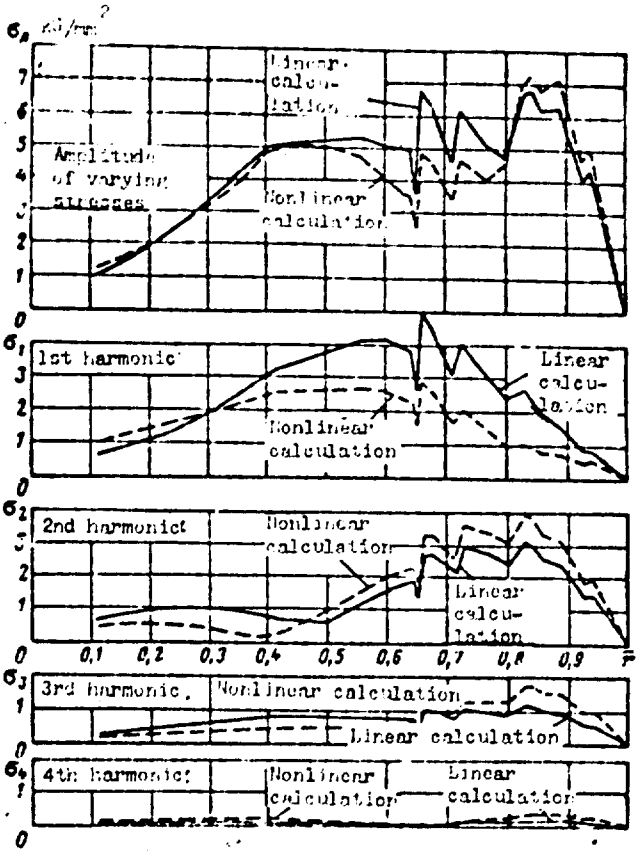

Fig. 1.50. Distribution of the amplitude of varying stresses and first four harmonic components over the radius of the blade at $\mu = 0.3$.

Thus even from those data which are given here by us, it is clear that calculation of varying stresses in the blade taking into account the nonlinear dependence $c_y = f(\alpha, M)$ permits revealing a whole series of interesting peculiarities having considerable influence on the strength of the rotor.

§ 10. Calculation of Flexural Oscillations with a Direct Determination of Trajectories of the Motion of Points of the Blade

1. Essence of the Method of Calculation

In paragraphs of § 7, 8, and 9 there were discussed methods of calculation of flexural oscillations of the blade where the form of its deformations was determined with the help of the B. G. Galerkin method. For this deformations of the blade were expanded in series with respect to known functions assigned beforehand. As these functions it was proposed to use forms of natural flexural oscillations of the blade in a vacuum. It was affirmed that for practical purposes

it sufficiently to be limited only to the first four tones of natural oscillations.

Here methods will be examined which allow rejecting this assumption and finding deformations of the blade by means of direct determination of trajectories of the motion of a certain number of points of the blade without decomposition of the form of oscillations with respect to function[3] assigned beforehand.

To determine the motion of separate points of the blade it is convenient to use a model of the blade with discretely distributed parameters. In this case the mass of the blade is simulated with the help of a number of concentrated loads distributed along its length.

For such a mechanical model there can be written a system of differential equations of the form:

$$m_i\ddot{y}_i=C_i+T_i, \tag{10.1}$$

where $i = 0, 1, 2, \ldots, z$; $\ddot{y}_i$ – second time derivative of movements y_i of the i-th concentrated load with mass m_i; values y_i are counted off from the plane of rotation of the rotor; C_i – elastic force affecting the i-th mass of m_i from the side of adjacent sections of the mechanical model of the blade; T_i – external aerodynamic force affecting the i-th point of the blade where one of the concentrated loads is located.

The system of equations (10.1) describes the motion of all masses of the mechanical model of the blade. Therefore, it consists of such a number of equations with variables y_i, which is equal to the number of masses of the examined mechanical model.

However, not all variables y_i entering into system (10.1) are independent, since the motion should satisfy the condition of equilibrium of the whole system:

$$\sum_0^z (m_i\ddot{y}_i-T_i)=0. \tag{10.2}$$

It is most convenient of all to consider that the independent variables are movements of all the masses besides the shank mass m_0. Then motion of the shank mass, if we assume $T_0 = 0$, can be determined in accordance with (10.1) as

$$m_0\ddot{y}_0 = C_0,$$

where

$$C_0 = \sum_1^s (T_i - m_i\ddot{y}_i). \tag{10.3}$$

This condition of equilibrium of forces is automatically fulfilled with the use of formulas mentioned below.

Thus the examined system can be described by independent variables y_i whose number per unit is less than the number of concentrated masses of the mechanical model of the blade. Consequently, the number of degrees of freedom which this system has is equal to the number of sections of the calculation diagram and is less per unit than the number of concentrated masses.

Solution of the system of equations (10.1) can be obtained with the help of numerical integration with respect to time. For this at each instant it is necessary to determine forces C_i and T_i. Determination of forces T_i can be carried out by formulas (9.20) whose derivation of which is given in § 9. Determination of elastic forces C_i has many peculiarities which should be discussed here.

2. Determination of Elastic Forces Applied to the Examined Point of the Blade from the Side of Adjacent Sections

Let us examine more specifically the mechanical model of the blade accepted for calculation. In the beginning we will examine the model of the beam type. Let us represent the blade in the form of a weightless free beam, subordinated to certain boundary conditions on the ends and divided into z sections, along the edges of which concentrated loads are located (Fig. 1.51). Lengths of the sections can be different.

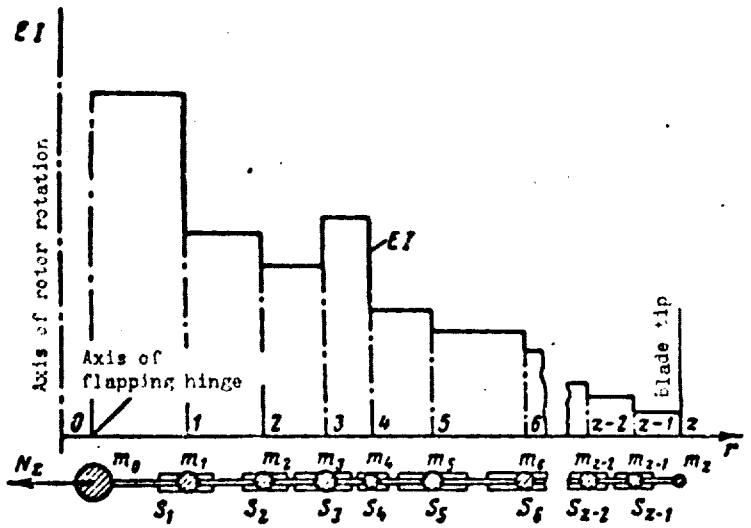

Fig. 1.51. Model of the blade examined in the calculation.

The flexural rigidity of the blade, as earlier, will be represented in the form of a step curve in such a way that it remains constant in the extent of each section. We will consider the centrifugal force as being applied only to the loads. Therefore, in the extent of each section the magnitude of it will not be changed. We will also consider that aerodynamic forces are applied only at attachment points of loads as if to each load a separate flap with an area S_i is attached.

To create conditions of sealing of the blade in the shank we will consider that the centrifugal force is received by special attaching of the shank mass m_0, which can freely move vertically. With solution of the present problem the creation of the freedom of motion of the shank mass vertically is not obligatory. However, in other problems connected with the determination of joint forms of oscillations of the blade and fuselage, this condition appears necessary. When oscillations of the fuselage are not considered and the blade is considered fastened to the hub as on a rigid base, conditions of shank sealing in the calculation are created by means of assignment of a necessary, usually quite large mass m_0.

It is natural that the nearer such an idealized diagram will describe the true picture of oscillations of the blade, the larger the number of sections the blade will have. Practically quite accurate the blade can be represented by a configuration in the form of a

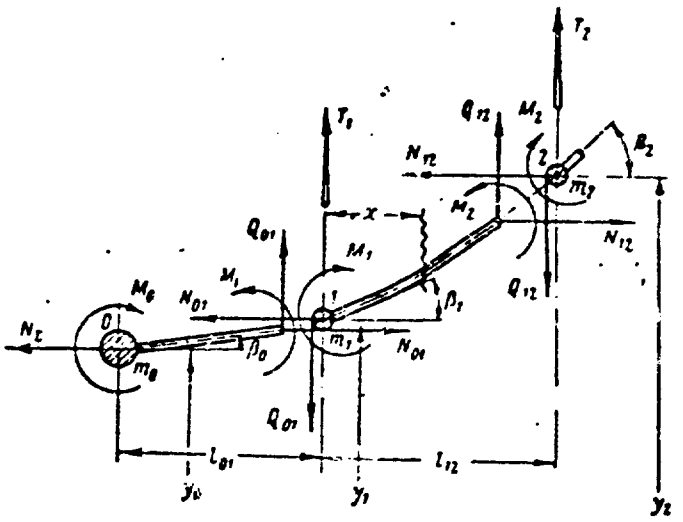

Fig. 1.52. Diagram of forces affecting adjacent elements of the blade.

beam consisting of 25-30 sections and of such number of concentrated masses.

To determine elastic forces C_i we will formulate equations of deformations of the blade. Figure 1.52 shows forces affecting two adjacent seconds of the deformed blade. Let us write out equations of deformations of these sections.

Inasmuch as the inertial and aerodynamic forces for the examined mechanical model of the blade are applied only along edges of the seconds, deformations of each section can be determined by the equation

$$[EIy']' - [Ny']' = 0. \tag{10.4}$$

The magnitude of flexural rigidity EI and centrifugal force N does not change in the extent of each section. Therefore, they can be carried out beyond the sign of differentiation. Then equation (10.4) can be copied in the form

$$M'' - \mu^2 M = 0, \tag{10.5}$$

where $M = EIy''$ is the bending moment in the section of the blade, and $\mu^2 = \frac{N}{EI}$.

The solution of equation (10.5) can be recorded as

$$M_x = A \operatorname{sh} \mu x + B \operatorname{ch} \mu x, \tag{10.6}$$

where coefficients A and B can be obtained from boundary conditions. Thus for the section 1-2 at $x = 0$ $M_x = M_1$, and $x = \ell_{12}$ $M_x = M_2$. Substituting these conditons into (10.6), we will obtain:

$$\left.\begin{aligned} A &= \frac{M_2}{\operatorname{sh} \alpha_1} - \frac{M_1}{\operatorname{th} \alpha_1}; \\ B &= M_1. \end{aligned}\right\} \tag{10.7}$$

Here $\alpha_1 = \mu_1 l_{12}$, a $\mu_1 = \sqrt{\frac{N_{12}}{EI_{12}}}$.

Taking into account (10.7) and the fact that $M_x = EI_{12}y''$, equation (10.6) can be recorded in the form:

$$EIy'' = \left[\frac{M_2}{\operatorname{sh} \alpha_1} - \frac{M_1}{\operatorname{th} \alpha_1}\right] \operatorname{sh} \mu x + M_1 \operatorname{ch} \mu_1 x. \tag{10.8}$$

Integrating equation (10.8) twice and considering that at $x = 0$ $y' = \beta_1$; $y = y_1$, and at $x = \ell_{12}$ $y' = \beta_2$; $y = y_2$, we will obtain:

$$b_1(y_2 - y_1) = d_1 M_2 + e_1 M_1 + \beta_1 \tag{10.9}$$

or

$$b_1(y_2 - y_1) = -e_1 M_2 - d_1 M_1 + \beta_2. \tag{10.10}$$

Here:

$$b_1 = \frac{1}{l_{12}};$$
$$d_1 = \frac{1}{l_{12} N_{12}} \left(1 - \frac{\alpha_1}{\operatorname{sh} \alpha_1}\right);$$
$$e_1 = \frac{1}{l_{12} N_{12}} \left(\frac{\alpha_1}{\operatorname{th} \alpha_1} - 1\right).$$

The equation of deformations for section 0-1 can be recorded by analogy with equation (10.10):

$$b_0(y_1 - y_0) = -e_0 M_1 - d_0 M_0 + \beta_1. \tag{10.11}$$

Changing in equation (10.11) all signs to the opposite and adding with equation (10.9), we will obtain:

$$d_0M_0+c_1M_1+d_1M_2=A_1, \qquad (10.12)$$

where

$$c_1=c_0-e_1;$$
$$A_1=b_0y_0+(b_0+b_1)y_1+b_1y_2.$$

Performing the same operation for other adjacent sections, we will obtain the system z of equations of the following form:

Table 1.12.

β_0	M_0	M_1	M_2	...	...	M_{z-2}	M_{z-1}		
1	c_0	d_0						=	A_0
	d_0	c_1	d_1					=	A_1
		d_1	c_2	d_2				=	A_2
			...	...	...			=	...
				...	...	...		=	...
					d_{z-1}	c_{z-2}	d_{z-2}	=	A_{z-2}
						d_{z-2}	c_{z-1}	=	A_{z-1}

This system of equations is recorded here by us in form of a table. Any of the equations of the system constitutes a sum of products of coefficients occupying in the rectangular Table 1.12 one line by unknown functions M_i, which enter simultaneously into several equations and carried out vertically in a special line placed from at the top of the Table 1.12. In this line there is recorded the unknown function β_0 entering only in first equation. Right sides of equations A_i are placed in a special column.

The system of equations of Table 1.12 is solved by the elimination of unknowns. This method was already described in No. 5 of § 4.

Thus the system of equations written above permits determining values of the angle of rotation of the blade in the shank β_0 and all

values of bending moments M_i if the form of deformations of the blade as a totality of values y_i is known.

To determine the elastic force C_i it is necessary to fulfill a number of consecutive operations, the first of which consists in the solution of the system represented by Table 1.12. In this sequence of operations it is expedient to include the determination of aerodynamic forces of angles of turn by the elastic axis of the blade β_i subsequently necessary for calculation:

$$\beta_i = b_i(y_i - y_{i-1}) - e_{i-1}M_i + d_{i-1}M_{i-1}. \qquad (10.13)$$

According to known values M_i from the condition of equilibrium of elements, one can determine the shear force $Q_{i,i+1}$, constant in the extent of each section of the blade. Actually, equating to zero of the sum of moments of all forces acting on the section i, i + 1, we will obtain the equation

$$Q_{i,i+1}l_{i,i+1} = N_{i,i+1}(y_{i+1} - y_i) + M_i - M_{i+1}. \qquad (10.14)$$

from which the value $Q_{i,i+1}$.

Knowing the values of shear forces along the length of the blade, one can determine the elastic force C_i applies to the mass m_i from the side of the adjacent sections:

$$C_i = Q_{i,i+1} - Q_{i-1,i}. \qquad (10.15)$$

The given calculations permit determining all values of elastic forces C_i acting from the side of adjacent sections on the given mass m_i the form of deformation y_i is known.

3. Peculiarities of Numerical Integration of Equations (10.1)

Above in § 9, there were already described the basic peculiarities of the application of numerical integration to the solution of differential equations of elastic oscillations of the blade. It was

shown that the success of numerical integration to a considerable degree is determined by the magnitude of maximum step, which is directly connected with the least period of oscillations of the mechanical model examined as an analog of the blade. The maximum step of integration should not be too small, since the calculation in this case will be excessively extended in time.

A peculiarity of the model examined here is the fact that it has as many tones of natural oscillations as there are sections along the length of the blade. As was noted above, to decrease the errors with transition from the blade to the analog of the mechanical model it is necessary to represent the blade by means of not less than 25-30 sections with the same quantity of concentrated masses. Therefore, in the determination of the maximum step of integration in this case it is necessary to proceed from the period of the highest – thirtieth tone of natural oscillations of the model.

Figure 1.40 shows the dependence of the frequency and period of natural oscillations of the standard blade of a helicopter with respect to the number of the tone. From this figure it follows that the period of thirtieth tone of natural oscillations consists of about one degree in azimuth of the rotor. Above it was already stated that in the use of the most profitable method of numerical integration for obtaining a nondivergent solution the step of integration should be less than one-third of the period of the highest tone. Consequently, for the method of calculation examined here the step of integration should be less than 0.3° in azimuth of the rotor. In this case the solution will be stable, and the considerable error appearing in the determination of amplitudes corresponding to high tones of oscillations cannot be taken into account, since their values are usually small and stresses in the blade are determined basically by several first tones of natural oscillations. The amplitude of oscillations with respect to these tones will be determined with good accuracy.

From the given considerations it becomes clear that for the use of the method of calculation with a direct determination of trajectories of motion of points of the blade it is profitable to use a model with the minimum number of concentrated loads. It is desirable to be

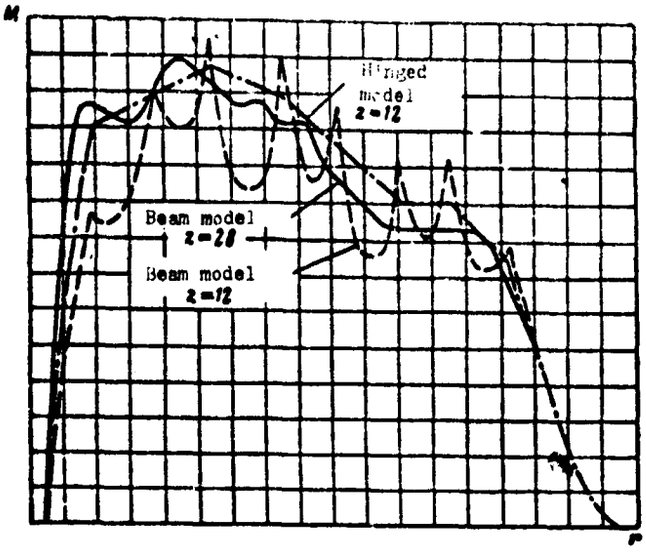

Fig. 1.53. Bending moments with respect to the first tone of natural oscillations calculated with a different number of masses.

limited to models with a number of loads of the order of not more than 12-15. It is necessary to note that at such a small number of sections the beam model of the blade examined above begins to introduce into the calculation errors connected with peculiarities of this model. For an illustration of these peculiarities Fig. 1.53 gives the form of the bending moment, which corresponds to the first tone of natural oscillations of the blade calculated for z = 28 (solid line) and z = 12 (dashed line). From Fig. 1.53 it follows that with a small number of sections the bending moment in the beam model begins to reveal peculiarities characteristic for very flexible beams loaded by shearing forces in the field of centrifugal forces, i.e., at location places of the masses concentrations of the bending moment appear. This peculiarity was already discussed in § 4, No. 9. The appearance of these concentrations considerably reduces the accuracy of the calculation. Therefore, application of beam models with a number of sections less than 25 (z = 25) is not recommended. At a small number of masses errors of such kind do not appear in the use of a multihinged segmented model, although forms of oscillations of higher tones will be quite greatly distorted. On Fig. 1.53 the bending moment, calculated for the multihinged model with the number sections z = 12, is shown by a dot-dashed line.

On the basis of these considerations, let us examine more specifically the method expounded here in reference to the multihinged model. Furthermore, in No. 6 of this paragraph it will be shown that

the multihinged model allows application of the method of calculation of elastic oscillations with the use of the method of numerical integration with the reverse order of determination of variables, which is excluded practically in the beam model.

4. Equations of Motion in Examining a Multihinged Articulated Model of the Blade

Let us present the blade in the form of a chain consisting of absolutely rigid weightless sections united with each other with the help of hinges. The weight of the blade will be concentrated in hinges of this chain in the form of separate loads with mass m_i. The bending rigidity of the blade will also be concentrated in the hinges, presenting that in each hinge as if it is built-in spring with rigidity c_i, preventing fracture of the blade in this hinge (Fig. 1.54).

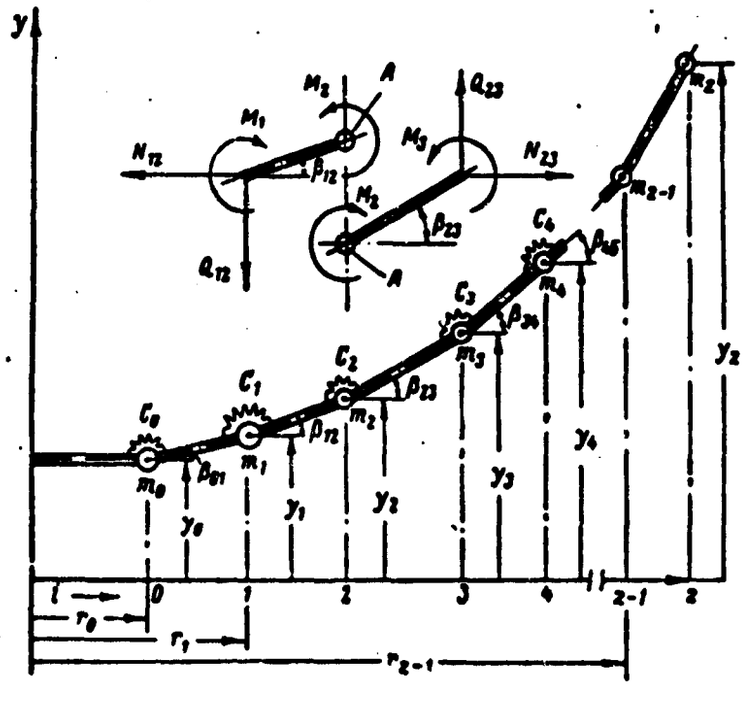

Fig. 1.54. Diagram of a multihinged articulated model of blade.

Let us write the system of differential equations of oscillations referring to this model of the blade, starting from the equation describing the equilibrium of the load with the ordinal number i = 2. Then by analogy let us formulate all remaining equations of the system.

The equation of equilibrium of the load with mass m_2 can be written in form:

$$m_2\ddot{y}_2=C_2+T_2. \tag{10.16}$$

Elastic force C_2, acting on mass m_2 from the side of the adjacent sections of the model, is determined by the formula:

$$C_2=Q_{23}-Q_{12}, \tag{10.17}$$

where Q_{12} and Q_{23} are shear forces on sections of the blade model adjacent with the load.

To determine magnitudes of shear forces Q_{12} and Q_{23} we will write equations of the equality to zero of the sum of moments of all forces with respect to the point of location of the load with mass m_2 (point A) for both sections of the model adjacent with this load. These equations have the following form:

$$\left.\begin{aligned} Q_{12}l_{12}-N_{12}(y_2-y_1)+M_2-M_1=0;\\ Q_{23}l_{23}-N_{23}(y_3-y_2)+M_3-M_2=0. \end{aligned}\right\} \tag{10.18}$$

Determining hence Q_{12} and Q_{23} and substituting them into formula (10.17), we will obtain:

$$\begin{aligned} C_2&=Q_{23}-Q_{12}=\\ &=\frac{1}{l_{12}}M_1+\left(\frac{1}{l_{12}}+\frac{1}{l_{23}}\right)M_2-\frac{1}{l_{23}}M_3+\\ &+\frac{N_{12}}{l_{12}}y_1-\left(\frac{N_{12}}{l_{12}}+\frac{N_{23}}{l_{23}}\right)y_2+\frac{N_{23}}{l_{23}}y_3. \end{aligned} \tag{10.19}$$

The bending moments entering into this equation can be expressed in terms of movements of elements of the blade by the formulas:

$$\left.\begin{aligned} M_1&=c_1(\beta_{12}-\beta_{01})=\frac{c_1}{l_{01}}y_0-c_1\left(\frac{1}{l_{01}}+\frac{1}{l_{12}}\right)y_1+\frac{c_1}{l_{12}}y_2;\\ M_2&=c_2(\beta_{23}-\beta_{12})=\frac{c_2}{l_{12}}y_1-c_2\left(\frac{1}{l_{12}}+\frac{1}{l_{23}}\right)y_2+\frac{c_2}{l_{23}}y_3;\\ M_3&=c_3(\beta_{34}-\beta_{23})=\frac{c_3}{l_{23}}y_2-c_3\left(\frac{1}{l_{23}}+\frac{1}{l_{34}}\right)y_3+\frac{c_3}{l_{34}}y_4. \end{aligned}\right\} \tag{10.20}$$

$$C_2 = d_1 y_0 + e_1 y_1 + f_2 y_2 + e_2 y_3 + d_2 y_4. \qquad (10.21)$$

where

$$\left.\begin{aligned}
d_1 &= -\frac{c_1}{l_{01} l_{12}};\\
d_2 &= -\frac{c_2}{l_{23} l_{34}};\\
e_1 &= \frac{c_1}{l_{12}}\left(\frac{1}{l_{01}}+\frac{1}{l_{12}}\right)+\frac{N_{12}}{l_{12}}+\frac{c_2}{l_{12}}\left(\frac{1}{l_{12}}+\frac{1}{l_{23}}\right);\\
e_2 &= \frac{c_2}{l_{23}}\left(\frac{1}{l_{12}}+\frac{1}{l_{23}}\right)+\frac{N_{23}}{l_{23}}+\frac{c_2}{l_{23}}\left(\frac{1}{l_{23}}+\frac{1}{l_{34}}\right);\\
f_2 &= -\frac{N_{12}}{l_{12}}-\frac{c_1}{l_{12}^2}-c_2\left(\frac{1}{l_{12}}+\frac{1}{l_{23}}\right)^2-\frac{c_2}{l_{23}^2}-\frac{N_{23}}{l_{23}}.
\end{aligned}\right\} \qquad (10.22)$$

If analogously we depict all the remaining values C_i and to set them in (10.16), then the system of differential equations of oscillations of the blade can be represented in the form of Table 1.13.

Table 1.13.

y_0	y_1	y_2	y_3	y_4	y_5	...	y_{n-1}	y_n		
f_0	e_0	d_1	·						=	$m_0\ddot{y}_0$
e_0	f_1	e_1	d_2						=	$m_1\ddot{y}_1 - T_1$
d_1	e_1	f_2	e_2	d_3					=	$m_2\ddot{y}_2 - T_2$
	d_2	e_2	f_3	e_3	d_4				=	$m_3\ddot{y}_3 - T_3$
		...	...	...	...	...			=	...
			...	...	...	...	...		=	...
				...	...	...	...	...	=	...
					d_{n-2}	e_{n-2}	f_{n-1}	e_{n-1}	=	$m_{n-1}\ddot{y}_{n-1} - T_{n-1}$
						d_{n-1}	e_{n-1}	f_n	=	$m_n\ddot{y}_n - T_n$

Each equation of the obtained system occupying one line in 1.13 constitutes the sum of products of known coefficients d_i, e_i, and f_i by variables y_i, which enter simultaneously into several equations.

Variables y_i are carried out vertically in a special line placed in the upper part of Table 1.13. The right side of equations, which is the sum of inertial and aerodynamic forces, is placed in a special column in the right part of Table 1.13.

This system of equations connects deformations of the blade with forces acting on it directly without an intermediate connection through the bending moments, as this took place in analogous equations referring to the beam model described above in No. 3 this paragraph and in equations used earlier for calculation of free oscillations of the blade in § 4.

Such a form of differential equations considerably simplifies calculations in the determination of elastic deformations of the blade, but it has definite deficiencies. The first of them, as was already noted, should be considered the fact that the elastic axis of the blade is in the form of not a smooth but a broken line. Also represented in the form of a broken line is the form of distribution of the bending moment along the length of the blade. The second deficiency should be recognized as the well-known arbitrariness in the selection of hinged rigidities c_i.

Let us give one of the methods of determination of these rigidities. For this we will examine two adjacent sections of the blade. The value of the hinged rigidity c_i will be determined from the condition that angles of rotation of ends of the adjacent sections β_0 and β_2 of the equivalent beam configuration coincide with angles β_{01} and β_{12} for the hinged diagram (Fig. 1.55)

$$(\beta_2 - \beta_0)_{\text{балка}} = (\beta_{12} - \beta_{01})_{\text{шарн.}} \qquad (10.23)$$

If in the comparison of these angles we disregard the influence of centrifugal forces and consider that the bending moment in the extent of these two sections is constant ($M_0 = M_1 = M_2 = \text{const}$), then from condition (10.23) for determining the hinged rigidity there can be obtained the formula:

$$\frac{1}{c_1} = \frac{l_{01}}{EI_{01}} + \frac{l_{12}}{EI_{12}}. \qquad (10.24)$$

In practice these assumptions can be observed only approximately. This creates known errors in the application of such a calculation diagram.

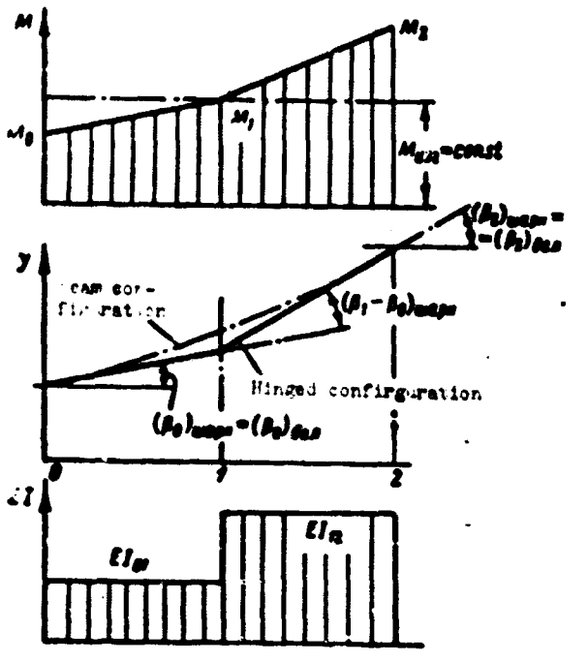

Fig. 1.55. Determination of hinged rigidity.

5. Sequence of Operation During the Calculation of Elastic Oscillations by the Method of Numerical Integration

On the whole calculation of the blade by the method discussed is produced in the following sequence. At the initial instant, which is usually connected with azimuth $\psi = 0$, there is prescribed an arbitrary form of deformations of the blade y_i and velocity distribution of movements of masses $\dot{y}_i$. If all values of y_i are known, then by the formulas discussed in Nos. 2 and 4 of this paragraph, elastic forces P_i can be determined. Simultaneously angles of rotation of the elastic axis of the blade β_i should be calculated. For the beam model they are determined by the formula (10.13). For the articulated model they can be determined in the form of a half-sum of angles of turn of two point of sections of the model adjacent with the examined point:

$$\beta_i = \frac{\beta_{i-1,l} + \beta_{i,l+1}}{2}.$$

If values β_i and y_i are known, then by the formulas (9.20) aerodynamic forces T_i can be obtained. These data are sufficient so that by the formulas (10.1) values $\ddot{y}_i$ are determined.

Further transition to the following azimuth of the blade is fulfilled by formulas analogous to (9.43):

$$\left.\begin{aligned}
y^{I}_{t+\Delta t} &= y_t + \Delta t \dot{y}_t + \frac{1}{2}\Delta t^2 \ddot{y}_t;\\
\dot{y}^{I}_{t+\Delta t} &= \dot{y}_t + \Delta t \ddot{y}_t;\\
\ddot{y}^{I}_{t+\Delta t} &= \frac{1}{m}(C^{I}_{t+\Delta t} + T^{I}_{t+\Delta t});\\
\ddot{y}_{cp} &= \frac{\ddot{y}_t + \ddot{y}^{I}_{t+\Delta t}}{2};\\
y^{II}_{t+\Delta t} &= y_t + \Delta t \dot{y}_t + \frac{1}{2}\Delta t^2 \ddot{y}_{cp};\\
\dot{y}^{II}_{t+\Delta t} &= \dot{y}_t + \Delta t \ddot{y}_{cp};\\
\ddot{y}^{II}_{t+\Delta t} &= \frac{1}{m}(C^{II}_{t+\Delta t} + T^{II}_{t+\Delta t}).
\end{aligned}\right\} \qquad (10.25)$$

Value $y^{II}_{t+\Delta t}$, $\dot{y}^{II}_{t+\Delta t}$ and $\ddot{y}^{II}_{t+\Delta t}$ for the instant t + Δt are considered final. Index i, pertaining to the number of the concentrated load, is omitted in formulas (10.25) in order not to excessively complicate the expressions.

For a transition to a new azimuth all operations are again repeated. This process continues for several revolutions of the rotor until the motion of the blade becomes steady. Calculation is finished on that turn when the solution converges to a steady one with the assigned accuracy. The accuracy of the solution is determined by the difference in the ordinates of movement of masses during calculation of motion in two consecutive turns of the rotor.

Evaluation of results of the calculation can be carried out in any form depending upon the purpose of calculation. To solve problems determining the strength of the blade we usually engage in deriving in auxiliary storage values of bending moments M_i through 10° in azimuth of the rotor. Upon completion of the calculation with

respect to values M_i and drag torques of sections of the blade, values of stresses and their amplitude are determined

$$\sigma_i^A = \frac{\sigma_{\max i} - \sigma_{\min i}}{2} \tag{10.26}$$

and decomposition of stresses with respect to harmonics is produced.

Calculation of elastic oscillations by the method discussed constitutes a continuous repetition of the same operations which are reduced to the determination of forces C_i and T_i and the solution of equation (10.1). Therefore, the duration of the calculation, first of all, will depend on the number of these repetitions. This number is determined only by two factors. The first is the duration of the period of transition to a steady process, which depends only on the correspondence of initial conditions to steady motion and on physical properties of the rotor and does not depend on the method of calculation. The second fact, which was already discussed above, is the necessary step of integration.

6. Method of Calculation with a Reverse Order of Determination of Variables During Numerical Integration

Above, in § 9 and in this paragraph, direct methods of numerical integration of differential equations were examined. When in the transition to a new instant in the begining variable y and its first derivative $\dot{y}$ are determined, and then form the differential equation the second derivative $\ddot{y}$ is determined. Here we will examine the method of calculation proposed by V. E. Baskin when these values are determined in reverse order.

Let us consider successively three instants: the instant at which it is necessary to determine deformations of the blade t_n and two instants $t_{n-1} = t_n - \Delta t$ and $t_{n-2} = t_n - 2\Delta t$ preceding it.

If one were to assume that the second derivative $\ddot{y}$ is preserved constant in the extent of each section of integration, as is shown in Fig. 1.56c, then value $\ddot{y}_{n-1}$ can be expressed in terms of $\dot{y}_{n-2}$ and $\dot{y}_{n-1}$:

$$\ddot{y}_{n-1}=\frac{\dot{y}_{n-1}-\dot{y}_{n-2}}{\Delta t}. \qquad (10.27)$$

If one were to assume now that the first derivative $\dot{y}$ is also maintained constant in the extent of the section of integration, as

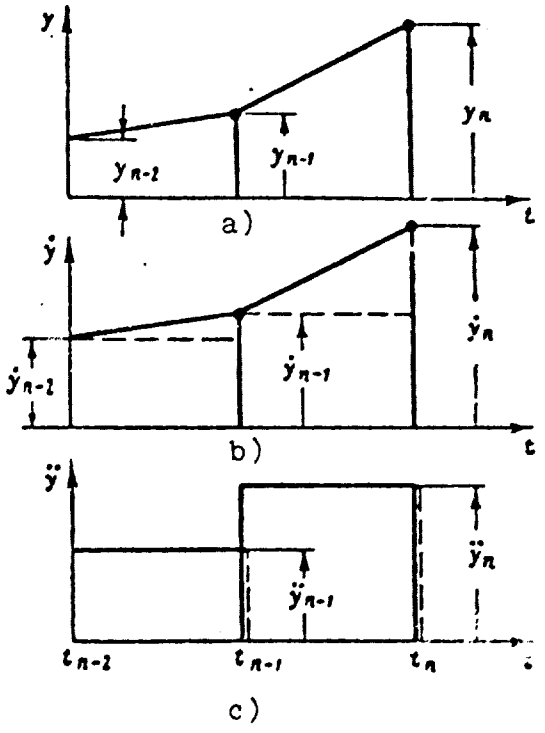

Fig. 1.56. Change of variable y and its time derivatives during numerical integration.

is shown on Fig. 1.56b by a dashed line, then values $\dot{y}_{n-1}$ and $\dot{y}_{n-2}$ can be determined by the formulas:

$$\left.\begin{aligned}\dot{y}_{n-1}&=\frac{y_n-y_{n-1}}{\Delta t};\\ \dot{y}_{n-2}&=\frac{y_{n-1}-y_{n-2}}{\Delta t}.\end{aligned}\right\} \qquad (10.28)$$

Substituting (10.28) into (10.27), we will obtain the expression for $\ddot{y}_{n-1}$:

$$\ddot{y}_{n-1}=\frac{1}{\Delta t^2}(y_n-2y_{n-1}+y_{n-2}). \qquad (10.29)$$

If the integration step is taken quite small, then it is possible approximately to assume that

$$\ddot{y}_n = \ddot{y}_{n-1} \qquad (10.30)$$

and to write expression (10.29) in the form

$$\ddot{y}_n = \frac{1}{\Delta t^2}(y_n - 2y_{n-1} + y_{n-2}). \qquad (10.31)$$

Substituting values $\ddot{y}_n$ into the system of differential equations represented by Table 1.13, we will obtain a system of algebraic equations relative to unknowns y_n. As above, this system will be written in the form of Table 1.14.

For variables y entering into Table 1.14, the index determining the instant is written above, and below, as earlier, there is placed the index referring to the number of the concentrated load of the model.

In the composition of Table 1.14 there is accepted also the assumption of the fact that aerodynamic forces calculated for instant t_{n-1} can be approximately assumed equal to these forces for the moment t_n.

Table 1.14.

y_0^n	y_1^n	y_2^n	y_3^n	y_4^n	y_5^n	...	y_{z-1}^n	y_z^n	
$f_0 - \frac{m_0}{\Delta t^2}$	e_0	d_1							$= \frac{m_0}{\Delta t^2}\left[y_0^{(n-2)} - 2y_0^{(n-1)}\right]$
e_0	$f_1 - \frac{m_1}{\Delta t^2}$	e_1	d_2						$= \frac{m_1}{\Delta t^2}\left[y_1^{(n-2)} - 2y_1^{(n-1)}\right] - T_1^{(n-1)}$
d_1	e_1	$f_2 - \frac{m_2}{\Delta t^2}$	e_2	d_3					$= \frac{m_2}{\Delta t^2}\left[y_2^{(n-2)} - 2y_2^{(n-1)}\right] - T_2^{(n-1)}$
	d_2	e_2	$f_3 - \frac{m_3}{\Delta t^2}$	e_3	d_4				$= \frac{m_3}{\Delta t^2}\left[y_3^{(n-2)} - 2y_3^{(n-1)}\right] - T_3^{(n-1)}$
		...	...	...	...	...			= ...
			...	...	...	...	...		= ...
				...	...	...	...	...	= ...
					d_{z-2}	e_{z-2}	$f_{z-1} - \frac{m_{z-1}}{\Delta t^2}$	e_{z-1}	$= \frac{m_{z-1}}{\Delta t^2}\left[y_{z-1}^{(n-2)} - 2y_{z-1}^{(n-1)}\right] - T_{z-1}^{(n-1)}$
						d_{z-1}	e_{z-1}	$f_z - \frac{m_z}{\Delta t^2}$	$= \frac{m_z}{\Delta t^2}\left[y_z^{(n-2)} - 2y_z^{(n-1)}\right] - T_z^{(n-1)}$

Assumption (10.30) permits expressing the acceleration $\ddot{y}_n$ at the instant t_n in terms of deformations y_{n-2}, y_{n-1} and y_n. By determining the inertial forces as a product of masses m_i by the corresponding

accelerations and adding them with aerodynamic forces, the total external forces acting on the blade can be obtained. Then deformations y_n are determined as in an ordinary static problem. This is done as a result of solution of the system of equations recorded in Table 1.14. The only peculiarity of these equations is the fact that components of inertial forces, expressed in terms of not yet calculated values y_n, are transferred to the left part and are determined simultaneously with solution of the system of equations.

Thus determination of different parameters of motion of the blade is produced by this method in an unusual order. In the beginning it is as if accelerations are determined and then deformations. Therefore, this method of solution is called by us here the reverse method of numerical integration. Frequently it is also called the implicit method.

The method of calculation with the application of the reverse method of numerical integration does not lead to a divergent solution even with a quite large integration step. Therefore, the magnitude of the necessary step of integration should be determined only on the basis of the magnitude of errors which appear in the application of this method. The magnitude of error can be estimated if one were to use the reverse method of numerical integration to solve the equation (9.24). Results of such a calculation are shown in Fig. 1.57.

From these calculations it follows that for the achievement of satisfactory accuracy in values of deformations corresponding to frequencies equal to the number of revolutions of the rotor the integration step should be less than 1° in azimuth of the rotor ($\Delta\bar{T} = 1/360$).

In the process of calculation with the application of the method with reverse order of the determination of variables, the solution of the system of equations recorded in Table 1.14 is fulfilled successively on each azimuth with the use of values y_i^{n-2} and y_i^{n-1} already earlier defined. At the initial instant these values can be taken arbitrarily.

The method of calculation discussed is distinguished by greater laboriousness as compared to methods using the decomposition of the solution according to forms of oscillations assigned beforehand, and it requires, therefore, during calculations on digital computers a very great expenditure of time. However, such a method has serious advantages in those cases when it is necessary to estimate the influence of different concentrated effects on the blade, for example, with the evaluation of effects on the side of dampers in hinges, and in all those cases when the solution cannot be sufficiently accurately represented with the help of a limited number of form oscillations assigned beforehand.

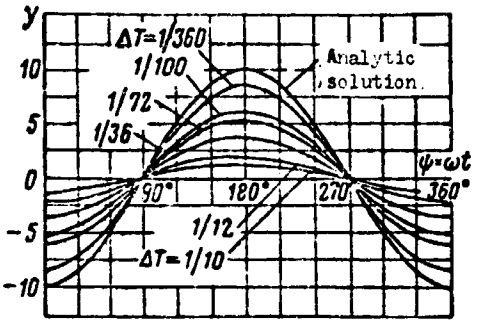

Fig. 1.57. Results of numerical solution of equation (9.26) by the "reverse method of integration" depending upon the relative integration step.

7. Comparative Evaluation of Different Methods of Calculation of Flexural Oscillations of the Blade

Discussed in this chapter was a great number of different methods of calculation of flexural oscillations of the blade and, naturally, the question can arise what sort of method should be selected for practical use, and on the basis of what criteria should this selection be realized. The answer to this question is very simple. For practical purposes the best will always be that method which most fully and accurately considers all peculiarities of operation of the rotor, including the variable field of induced speeds and the nonlinear character of the dependence of aerodynamic coefficients on the angle of attack and Mach number. But it appears impossible to reject the available limitations consisting in the fact that the fuller and more accurate the method calculation, the greater the time of calculations it requires in calculation on digital computers. Therefore, in the selection of the best method of calculation the main criterion appears

to be the possibilities of the machine which limit the application of the most improved methods of calculation.

In order to select the most suitable method of calculation, let us cite the Table 1.15 with an indication of the necessary speed of calculations in the application of different methods of calculation. This table gives the basic characteristics of different methods of calculation.

Here we give tentative values of the necessary speed of operations in one second $V_{потр}$ for execution of the calculation in 5-10 minutes. The necessary speed is given for all methods of calculation in four variants of the assumptions used. In Table 1.15 there is not estimated the necessary volume of memory of the machine, since for contemporary machines it usually does not hamper the calculator.

From the examination of data of Table 1.15 it follows that for a machine with a low counting rate (of the order of 5000 operations per second) only one method, called the method of calculation with respect to the harmonics, can be widely used. In this method the solution is decomposed with respect to eigenfunctions. Temporary factors with these functions are represented in the form of Fourier series with respect to harmonics. Coefficients this series are determined from the system of algebraic equations obtained from the differential equation with help of the B. G. Galerkin method. This method is discussed in § 8.

On machines with a low counting rate this method can be used only with the assumption of equal distribution of induced speeds λ = const. For calculation of the nonlinear dependence of aerodynamic coefficients on the angle of attack of the profile and Mach number this method is not useful practically. Calculation of these dependences with such a method can be carried out only with very serious assumptions. But even with such an approach the laboriousness of computations necessary for formulation of calculation formulas is so great that practically it is simply unrealizable.

Table 1.15.

			Method of finite-difference with decomposition of the unknown functions and with the determination of temporary factors by the method of numerical integration of converted equation	Method of calculation with direct determination of trajectories of motion of separate points of the blade
Differential equations		$[EIy'']'' - [N_y \cdot]' + m\ddot{y} = f$		$m_i \ddot{y}_i = C_i T_i$
Form of writing the solution of a stationary type		$y = (a_0 - a_1 \cos\psi - b_1 \sin\psi - a_2 \cos 2\psi - b_2 \sin 2\psi \ldots) \cdot y^{(0)} + (c_0 - c_1 \cos\psi - d_1 \sin\psi - c_2 \cos 2\psi - d_2 \sin 2\psi \ldots) \cdot y^{(1)} + (e_0 - e_1 \cos\psi - f_1 \sin\psi - e_2 \cos 2\psi - f_2 \sin 2\psi \ldots) \cdot y^{(2)} + (g_0 - g_1 \cos\psi - h_1 \sin\psi - g_2 \cos 2\psi - h_2 \sin 2\psi \ldots) \cdot y^{(3)}$	$y = \sum_j \delta_j y^{(j)}$	$y_i = f(t)$
Method of solving the equations		B. G. Galerkin method		Equations are not transformed
Method of determining the unknown factors		Coefficients of decomposition of temporary factors are determined from the system of algebraic equations	Direct method of numerical integration	Runge-Kutt method of numerical integration
Characteristics of the aerodynamic factors	$\lambda = const$ $c_y = c_y^\alpha \alpha$ $c_x = 0$	$V_{ЭВМ} = 5000$ operations/s	$\Delta\psi_{ЭВМ} = 2.5 - 5°$ $V_{ЭВМ} = 20000$ operations/s	$\Delta\psi_{ЭВМ} = 0.5 - 1{,}0°$ $V_{ЭВМ} = 100000$ operations/s
	$\lambda = var$ $c_y = c_y^\alpha \alpha$ $c_x = 0$	Method is convenient for calculation of a non-uniform field of induced speeds decomposed with respect to harmonic components $V_{ЭВМ} = 50000$ operations/s	Methods are convenient for calculation of induced speed determined by the rotor configuration with a finite number of blades (with the number of points over the radius c_y $z_p \leq 12$) $V_{ЭВМ} = 100000$ operations/s	$V_{ЭВМ} = 500000$ operations/s
	$\lambda = const$ $c_y = f(\alpha, M)$ $c_x = f(\alpha, M)$	For calculation of the aerodynamic $C_y = f(\alpha, M)$ and $C_x = f(\alpha, M)$ the method is practically unsuitable	Methods are convenient for calculation of nonlinear dependences $C_y = f(\alpha, M)$ etc $C_x = f(\alpha, M)$ $V_{ЭВМ} = 50000$ operations/s	$V_{ЭВМ} = 200000$ operations/s
	$\lambda = var$ $c_y = f(\alpha, M)$ $c_x = f(\alpha, M)$		при $z_p = 12$ $V_{ЭВМ} = 250000$ operations/s	$V_{ЭВМ} > 1000000$ operations/s

For machines with an average counting rate (of the order of 20,000-50,000 operations per second) the most convenient is the method of calculation with decomposition of the solution with respect to eigenfunctions and by the determination of temporal factors with these functions by means of numerical integration. This method is discussed in § 9. It is very convenient for calculation of nonlinear dependence of aerodynamic coefficients on the angle of attack of the profile and Mach number.

With the necessity of calculation of the alternating field of induced speeds, application of this method is possible only on machines at a high counting rate. If in the determination of induced speeds we are limited by the number of calculation points along the radius and azimuth of the rotor, then calculation can be carried out on machines with an average counting rate.

The method of calculation with direct determination of trajectories of motion of separate points of the blade (§ 10) can be used only on machines with a counting rate of greater than V > 100,000 operations per second. Calculation of the alternating field of induced speeds and nonlinear dependences of aerodynamic coefficients on the angle of attack of the profile and Mach number increases even more the necessary counting rate with this method. In the last column of Table 1.15 only the method with reverse method of numerical integration of equations is examined. In the case of application of the direct method of numerical integration, the necessary counting rate for the method with direct determination of trajectories of motion of separate points of the blade can increase even greater.

The necessary counting rates given in Table 1.15 are obtained for the case when calculation continues for 5-10 minutes. With such a duration it is possible to carry out different investigations required in the process of designing of the blade with a variation in parameters of the rotor and flight conditions.

If one were to be limited to calculation for only one variant of the parameters, then it is possible to use a long counting duration. In this case the necessary counting rates given in Table 1.15 can be

§ 11. Fatigue Strength and Service Life of the Blade

1. Tests of the Construction for Determination of Its Service Life

The service life of the construction is established usually on the basis of results of its dynamic tests.

Depending upon the degree of responsibility of the construction for flight safety tests of one or several specimens of this construction are conducted. Frequently tests are conducted only on separate parts of the construction, the strength of which is decisive for the entire unit checked as a whole.

In the determination of the blade service life there are usually conducted tests of samples of separate sections of the spar with parts of frame creating concentrations of stresses in the spar. Samples of not less than three different sections of the spar are tested. This, as a rule, is the section including the shank joint and two sections along the length of the spar. Sometimes it is necessary to subject to tests additional samples for checking design features of the spar (for example, transition places of sections of the spar).

Tests of samples of the blade are almost always conducted on resonance stands with excitation from mechanical vibrators. The length of the sample is selected in such a way that its frequency of natural bending oscillations fits into the working range of the vibrator. Usually the tests are conducted at a frequency of 1500 to 2500 oscillations per minute. The lengths of the samples are on the order of 3-4 m. Besides varying bending stresses the sample is necessarily stretched by longitudinal forces, which create a constant static loading close to that which the blade undergoes in flight from the action of centrifugal forces. Figure 1.58 shows a test stand for testing samples of the blade of a helicopter with a centrifugal force of the order of 100 tf.

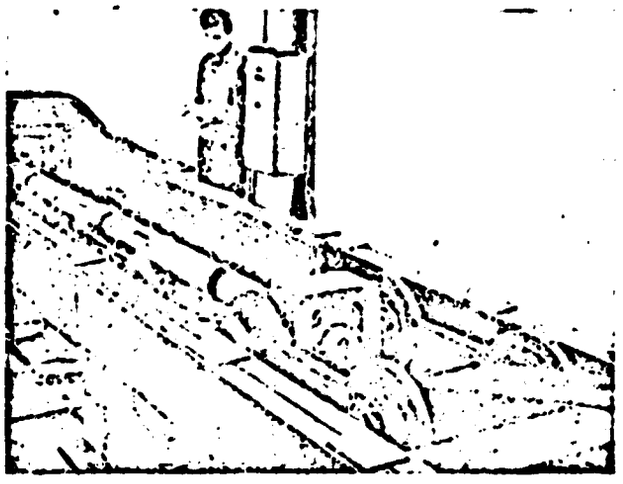

Fig. 1.58. Test stand for tests of blade samples.

Tests of the blade as a whole, and not of separate short samples, as a rule, are not conducted in view of the too great complexity of test stands, which are required for this, and the considerable duration of the tests, since the frequency of oscillations in this cage cannot be more than a 300-400 oscillations per minute.

2. Scattering of Strength Characteristics During Fatigue Tests

In carrying out fatigue tests of a certain number of samples made under identical conditions, considerable scattering of results of tests is revealed. Destruction of the samples, tested under the same level of stresses, occurs with a different number cycles N. Frequently the ratio of the greatest number cycles to the least reaches 20-40.

The scattering of characteristics of fatigue strength is explained by heterogeneity of the structure of the material, distinction in conditions of manufacture and treatment of samples. Destruction of samples of a construction always starts from small defects in the material and on the surface of the sample. In an overwhelming majority of the cases destruction starts from a defect located on the surface. Here the characteristics of strength of samples are determined by the character and magnitude of these defects.

The scattering of service life during tests of samples is characterized usually by the distribution function of numbers of cycles N prior to the destruction of the samples. Analysis of results of tests shows that the distribution of logarithms of numbers of cycles lg N prior to destruction quite well obeys the normal law of distribution almost with all mean values of probability of destruction, starting approximately from the probability equal to 0.01-0.02.

Figure 1.59 shows the probability distribution of destruction P and probability density ϕ, which correspond to real characteristics of service life of the construction (solid curves) and determined by the normal law of distribution (dashed curves):

$$\varphi(\lg N)=\frac{1}{S_{\lg N}\sqrt{2\pi}}\cdot e^{-\frac{(\lg N-m_{\lg N})^2}{2S^2_{\lg N}}}; \qquad (11.1)$$

$$P(\lg N)=\int_{-\infty}^{\xi}\varphi(t)\,dt. \qquad (11.2)$$

Here $\varphi(\lg N)$ – density of probability distribution of destruction of the construction; $P(\lg N)$ – probability of destruction of construction with the number of loads smaller than N; $\xi=\lg N$ – value of logarithm of number cycles prior to destruction of the construction; $S_{\lg N}$ – root-mean-square deviation of the distribution of logarithms of numbers of cycles prior to destruction of the construction; $m_{\lg N}$ – mathematical expectation of the distribution logarithms of numbers of cycles.

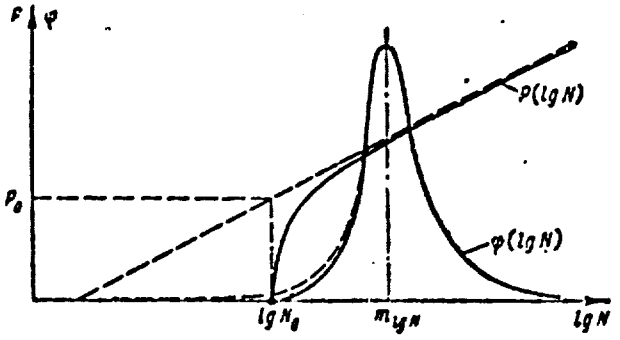

Fig. 1.59. Distribution curves of service life during tests and corresponding to the normal law.

In the region of small probabilities of destruction the distribution function usually deviates from the normal law (Fig. 1.59). This is connected with the very important peculiarity of characteristics of service life. The fact is that fatigue breakdown can occur only after some cycles of loading N_0 and never occurs earlier. This peculiarity of characteristics of service life leads to the concept of dead zone with respect to N, in which the probability of destruction of the construction is equal to zero ($P = 0$). Hence, in particular, there follows the very important conclusion concerning the possibility of assignment of service life of operating the construction with respect to conditions of endurance with the probability of destruction equal to zero even at quite high varying stresses.

Unfortunately, determination of the threshold of sensitivity N_0 with any satisfactory accuracy appears practically impossible. Therefore, in the determination of the service life of construction the law of distribution of service life is taken usually to be normal, and the requirement $P = 0$ is replaced by the requirement of a very small probability of destruction.

Deviation of values of logarithms of numbers of cycles from the normal law should be observed also in the region of great probabilities of destruction. With the relatively low level of varying stresses this is connected with the fact that almost always there is some number of samples which are not destroyed even at a very large number cycles of loading.

3. Basic Characteristics of Fatigue Strength of a Construction

Fatigue strength of construction is usually characterized by the number cycles N, which maintains prior to destruction at the assigned amplitude of varying stresses σ. The larger the amplitude of varying stresses σ, the smaller the number cycles of loading the construction maintains.

The curve characterizing the number cycles N prior to destruction, depending on the amplitude of varying stresses σ, is called the Wöhler curve.

The Wöhler curve can be described approximately by the equation:

$$\left.\begin{array}{l}\sigma^m N = \text{const} \text{ for } \sigma > \sigma_w \text{ and } N < N_w; \\ \sigma = \sigma_w = \text{const} \text{ for } N > N_w.\end{array}\right\} \qquad (11.3)$$

Here σ_w is the largest amplitude of stresses at which the construction can sustain any large number cycles of load N without destruction; this amplitude is usually called fatigue limit; N_w – minimum number cycles of loading corresponding to the fatigue limit; m – certain exponent value of which is determined according to the results of tests.

The Wöhler curve can be plotted for different values of the probability of destruction. For this it is necessary to divide the batch of samples into several groups and test them at different amplitudes of varying stresses.

Constructing the distribution functions of service life at various levels of varying stresses (Fig. 1.60) and connecting the points with identical probability of destruction, Wöhler curves corresponding to a different probability of destruction can be obtained. Usually it appears that the less the scattering of characteristics of service life, the higher the level of varying stresses, and the threshold of sensitivity N_0 is more clearly marked at smaller stresses. At small stresses the threshold of sensitivity is observed at relatively great probabilities P, and at great stresses it moves at so small probabilities that it usually cannot be noted

Results of tests almost always confirm the presence of fatigue limit σ_w. At the assigned stress σ some number of samples is usually not destroyed even at a very large number of cycles of loading. The existence of fatigue limit also undergoes operational experience of different machines and mechanisms. There is known a multitude set of different components, a very large number of which constantly operates under considerable varying stresses and is not destroyed at the number cycles of loading of 10^8 and more. There are individual exceptions to this general rule. It is noted that for certain structural elements of aluminum alloys the fatigue curve continues to

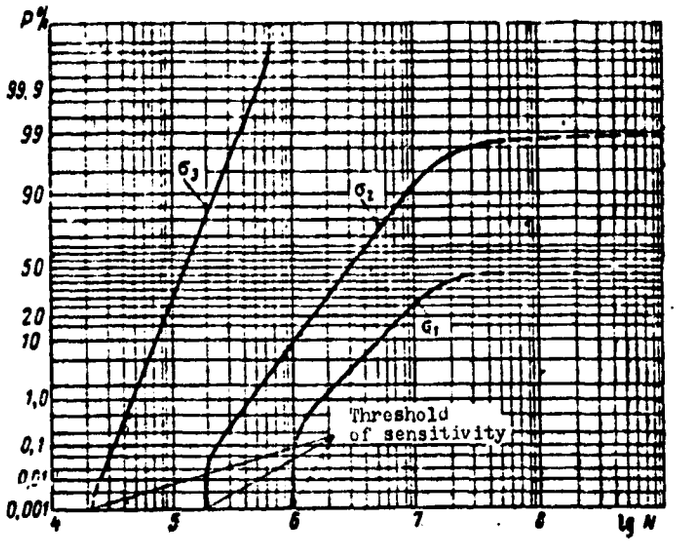

Fig. 1.60. Distribution of service life at a different level of varying stresses.

decend at service lives of the order of 10^8-10^{10} cycles. However, this lowering is so insignificant that in this case the Wöhler curve can be approximately represented in the form of (11.3). In any case in reference to the basic units of the helicopter, calculation of this lowering does not lead to any considerable refinements.

In values of fatigue limits definite scattering is also observed. For their distribution the presence of the threshold of sensitivity with respect to the amplitude of stresses is characteristical. This threshold of sensitivity will subsequently be called the minimum fatigue limit $\sigma_{w_{min}}$. At stresses smaller than $\sigma_{w_{min}}$ not one sample is destroyed even at a very large number of cycles of loading. In accordance with the enumerated peculiarities of characteristics of fatigue, Wöhler curves should have the form depicted on Fig. 1.61.

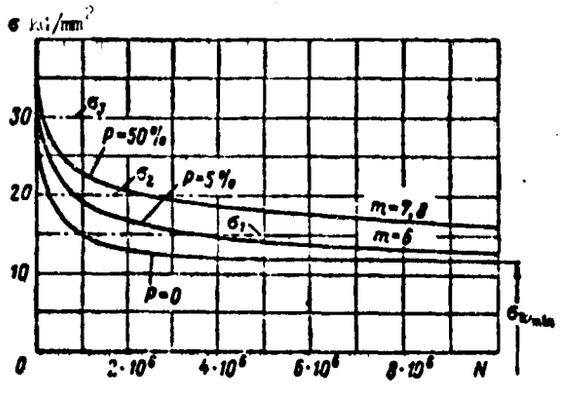

Fig. 1.61. Wöhler curves corresponding to various probability of destruction.

If curves corresponding to various probability of destruction are replaced by the approximate analytic dependence (1...3), then in logarithmic scale the Wöhler curves will have the form depicted on Fig. 1.62. The dead zone corresponding to zero probability of

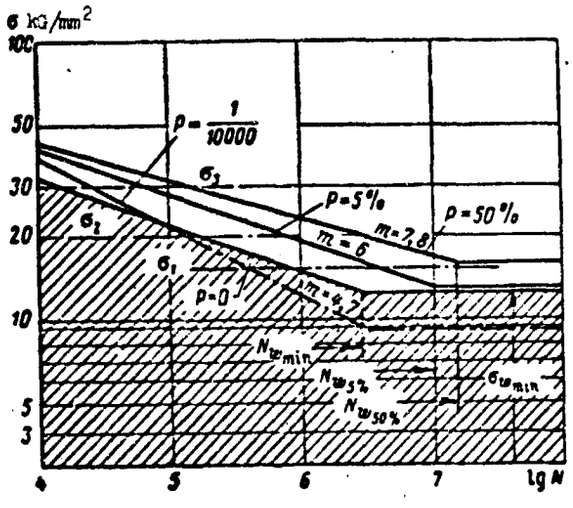

Fig. 1.62. Wöhler curves corresponding to various probability of destruction in logarithmic scale.

destruction is shaded on this chart. With such an image of the Wöhler curves the number cycles N_w corresponding to the fatigue limit and exponents m appear different for curves corresponding to various probabilities of destruction.

It should be noted that the plotting of Wöhler curves in the form as they are depicted on Figs. 1.61 and 1.62 is practically possible only with tests of small laboratory samples, since for this it appears necessary to have a very large number of them.

In the evaluation of strength of onstruction the plotting of such curves is practically impossible, since it is necessary to be limited to a test of a very small number of samples. Frequently this number does not exceed n = 3-5 (where n is the number tests of the samples). Here to evaluate strength the tests give only n values of the numbers of cycles prior to destruction at the given magnitude of loads. According to such a limited number of results it is possible to formulate a concept on the fatigue characteristics of the construction only on the basis of definite assumptions with respect t... curv...

The value of the amplitude of varying stresses at which the construction maintains the assigned number cycles of load N prior to destruction depends also on the value of the constant part of stresses of the cycle σ_m (static loading). The greater the static loading, the less the amplitude of stresses at which the construction maintains the assigned number of cycles. This dependence is usually characterized by the Hay diagram. As an example Fig. 1.63 shows the approximate form of such a diagram.

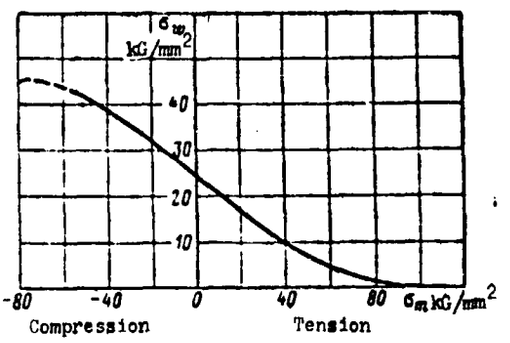

Fig. 1.63. Hay Diagram for samples of spar ducts of the blade.

For steel spar ducts at σ_m = 20-30 kG/mm^2 the increase in static loading by the quantity $\Delta\sigma_m$ leads to a lowering of the fatigue limit by the value $\Delta\sigma_w \approx 0{,}4\Delta\sigma_m$. For Duralumin spars at σ_m = 6-8 kG/mm^2 the quantity $\Delta\sigma_w \approx 0{,}3\,\Delta\sigma_m$.

It is necessary to pay attention to the fact that in the region of constant compressive stresses fatigue limits increase considerably. This circumstance is used in the hardening of structural parts by cold hardening (see Nos. 16 and 17).

4. Stresses, Effective in the Construction of a Blade in Flight

In § 1 of this chapter (No. 3) it was already said that in flight under the action of aerodynamic forces blades of a helicopter undergo considerable live loads in conditions of two different types, which are called by us conditions of low and high speeds.

Figure 1.64 shows the approximate character of the change in amplitudes of varying stresses with respect to the speed of flight for two blade designs: steel and Duralumin spars. As can be seen

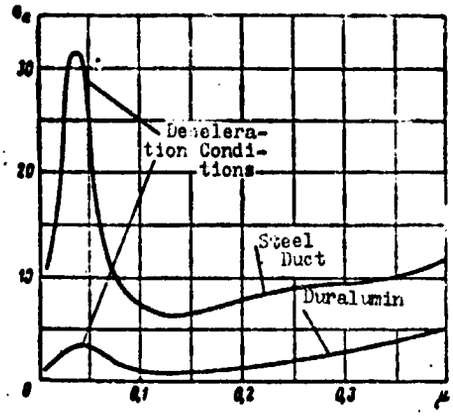

Fig. 1.64. Character of the change in amplitudes of varying stresses with respect to the flight speed in blades with small (steel duct) and average (Duralumin spar) rigidity in the flapping plane.

from this figure, the maximum varying stresses can appear at low speeds (conditions of deceleration) and at a maximum flight speed. As was already shown, the blades accomplish flexural oscillations so that at each point of the spar stresses are changed according to the periodic law, being repeated for each revolution of rotor. Figure 1.65 gives as an example the recording of stresses, obtained in sections of the blade on relative radii $\bar{r}=0{,}73$ and $\bar{r}=0{,}8$ in conditions of level flight at a relatively high speed. The same figure gives the harmonic composition of stresses acting in these sections of the blade.

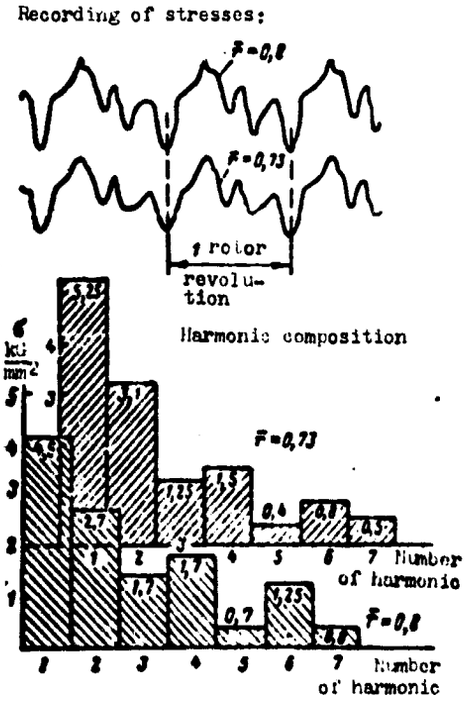

Fig. 1.65. Recording of stresses in two sections of the blade of a helicopter in conditions of level speed ($\mu = 0.3$) and their harmonic composition.

Usually in level flight at $\mu = 0.2-0.4$ the greatest values are reached by the first harmonic component of the stresses. The second harmonic is less in amplitude and comprises usually 30-70% of the first harmonic. The first and second harmonic in sum, as a rule, determine 70-90% of the value of total varying stresses in these conditions in the blade, since higher harmonics usually appear small. Their value almost always decreases with an increase in the order of the harmonic. Such a character of change in value of the harmonics is connected with a decrease in the value of harmonic components of aerodynamic forces with transition to higher harmonics.

There are recurrent (for all blades) exceptions to this general rule which are connected with the appearance of resonances or proximity to them.

In conditions of low speeds the harmonic composition of effective stresses appears different. Here the predominate become higher harmonics where in the first place there are distinguished harmonics close in frequencies to the frequency of natural oscillations of the second and third tones. An especially great increase in varying stresses in these conditions of flight (see Fig. 1.64) occurs for blades with low rigidity in the flapping plane (see § 3, No. 3). For such blades the greatest of all appear to be stresses with fourth and sixth harmonics (Fig. 1.66). Conditions of low speeds give for such blades the basic defectibility of design (see Table 1.21).

For blades with average rigidity in the flapping plane the increase in varying stresses at low speeds proves to be considerably less (see Fig. 1.64), and the predominance of higher harmonics is not observed so sharply (Fig. 1.67). For such blades (just as for blades with great rigidity) the basic defectibility is given by conditions of flight at high speed.

Along with varying stresses from flexural oscillations, the spar of the blade will stretch and bend by constant (in magnitude)

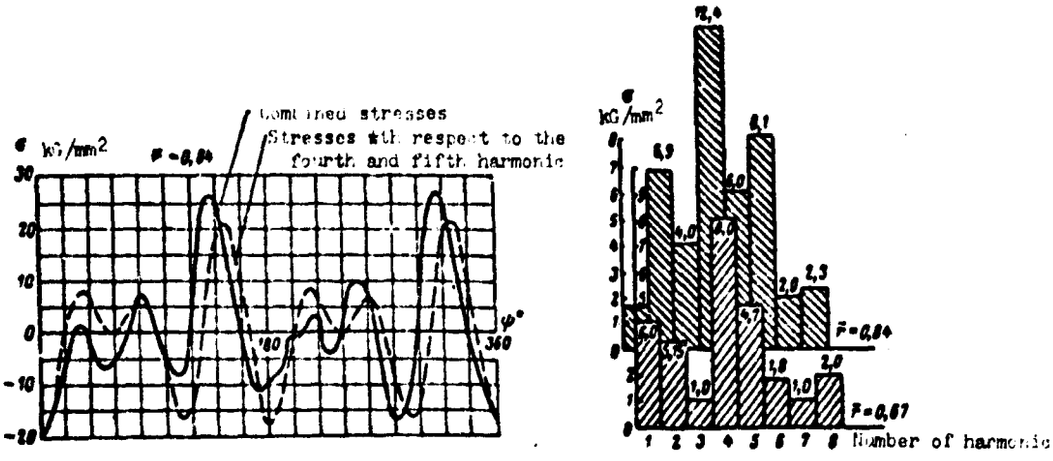

Fig. 1.66. Oscillogram of the recording of varying stresses in a blade with a steel tublar spar, having low rigidity in the flapping plane in the process of deceleration, and their harmonic composition.

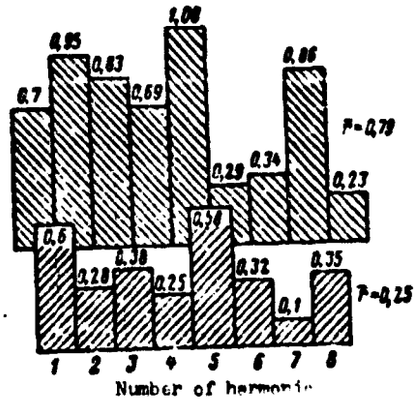

Fig. 1.67. Harmonic composition of varying stresses in a blade of average rigidity with a pressed Duralumin spar in conditions of deceleration.

centrifugal forces and constant part of aerodynamic forces. Therefore, the material of the spar works at varying stresses with great static loading. Static loading greatly reduces the fatigue strength of the spar.

5. Hypothesis of Linear Summation of Defectibilities and Average Equivalent Amplitude of Varying Stresses

In different flight conditions the most diverse varying stresses act in the construction. The duration of individual flight conditions can be considerably diverse. Thus the most continuous operation of flight is usually a flight at cruising speed. For

helicopters utilized for carrying transport, these conditions occupy 60-70% of the service life. The maximum speed of flight of transport helicopters used in the national economy is almost never used. Of very short duration for these helicopters are also conditions of flight at low speeds, which are usually only passage in acceleration and deceleration.

However, helicopters can be used in the most diverse forms of operations where the duration of individual flight conditions appears different. As an example Table 1.21 gives values of the relative duration of different conditions α_i, accepted for one of the military transport helicopters.

The service life of the construction should be determined taking into account the temporal composition of the stay of the helicopter in conditions with a diverse level of varying stresses, and therefore introducing into the construction a different portion of fatigue defectibility. For an account of this circumstance it is convenient to use the hypothesis of the linear summation of defectibilities. This hypothesis assumes the possibility of summation of separate portions of defectibility introduced by different levels of stresses and says that destruction of construction approaches when

$$\left.\begin{aligned} \Delta V_\Sigma &= 1, \\ \text{where} \qquad \Delta V_\Sigma &= \sum_i \frac{\Delta N_i}{N_i}. \end{aligned}\right\} \qquad (11.4)$$

where N_i is the number cycles prior to destruction with continuous maintaining of the level of loading with the amplitude σ_i; ΔN_i – number cycles of loading with amplitude σ_i, tested by the construction in the i-th conditions of flight.

The relation $\Delta V_i = \frac{\Delta N_i}{N_i}$ is usually called the defectibility of construction in conditions with the amplitude of stresses σ_i, and ΔV_Σ – is the total defectibility.

In certain works it is proved that with definite alternating of conditions of loading, destruction of the construction can

approach, when

$$\Delta\bar{N}_i < 1.$$

However, the cases examined in these works basically do not correspond to conditions of loading of units of a helicopter. Therefore, almost always during the calculations it is possible to use formula (11.4).

Due to the scattering of characteristics of service life, the defectibility of separate copies of the construction even at identical (in duration) composition of levels of loading proves to be different. The greatest defectibility is in constructions with the least values of service life. Therefore, it is possible to indicate the defectibility corresponding to a definite probability of the destruction.

If in formula (11.4) we assign values N_i corresponding to the assigned probability of destruction $P_{зад}$, then $\Delta\bar{N}_i = 1$ the probability of destruction will also be equal to $P_{зад}$. Hence there can be obtained the formula for calculation of the safe number cycles of loads $N_{без}$ with the assigned probability of destruction $P_{зад}$ determining the service life of constructions according to conditions of endurance:

$$N_{без} = \frac{1}{\sum_i \frac{a_i}{N_i}}. \qquad (11.5)$$

Here $a_i = \frac{\Delta N_i}{N_{рас}}$ is the relative duration of conditions with the stress σ_i; $N_{рас}$ is the number cycles of loading for service life of construction in the determination of relative duration of separate conditions of flight a_i (in general, any arbitrary interval of time of operation of the helicopter taken with the number cycles N is not necessarily equal to the number cycles of loading for the established service life of construction $N_{рас}$); N_i is the number cycles of loading with the amplitude σ_i at which the probability of destruction is equal to assigned ($P_{зад}$).

If effective stresses are lower than the minimum fatigue limit, then defectibility is not introduced into the construction. In this case the number cycles N_1 in formula (11.5) must be assumed equal to infinity.

It is possible to introduce the concept about the relative duration of conditions ε introducing defectibility into the construction:

$$\varepsilon = \frac{N_{повр}}{N_{рас}},$$

where $N_{повр}$ is the number of cycles of loading for the service life of construction introducing defectibility.

Thus during the time of service life R the construction is damaged only during the time equal to εR.

Frequently for giving to calculations greater clarity it appears convenient to introduce the concept of the average equivalent amplitude of varying stresses.

The average equivalent amplitude of stresses consists of such an amplitude constant in time and effective during the part of service life equal to εR, which introduces into the construction a defectibility equal to the defectibility introduced by amplitudes of varying stresses different in magnitude in all conditions of flight encountered during operation of the helicopter.

With the introduction of this concept it is assumed that at stresses greater than the limit the durability of the construction can be determined as

$$N_1 = N_0 \left(\frac{\sigma_a}{\sigma_1}\right)^m. \qquad (11.6)$$

Then, substituting (11.6) into (11.4), we will obtain

$$\frac{\sum_i \Delta N_i \sigma_i^m}{N_0 \sigma_0^m} = 1. \qquad (11.7)$$

where summation is produced only with respect to those conditions which introduce defectibility into the construction.

If one were to introduce one equivalent level of stresses with the amplitude $\sigma_{ЭКВ}$ and the number cycles determined from the condition that stresses act $\sigma_{ЭКВ}$ act continuously during part of the service life εR, i.e., that $N_{экв} = \varepsilon N_{рес}$, then it is possible to write

$$\sum_i \Delta N_i \sigma_i^m = \varepsilon N_{рес} \sigma_{экв}^m. \qquad (11.8)$$

Consequently:

$$\sigma_{экв} = \sqrt[m]{\frac{1}{\varepsilon} \sum_i \alpha_i \sigma_i^m}. \qquad (11.9)$$

As an example later at point 12, see also Table 1.21, there is given the calculation of equivalent stresses for the blade of one of the helicopters in the most stressed section on the relative radius $\bar{r} = 0.74$. The spar of this blade is a steel tube pressed in an ellipse along the whole length, starting from the radius $\bar{r} = 0.3$. The minimum fatigue limit of the tube of the blade in this section, according to results of dynamic tests, can be accepted as equal to $\sigma_{w_{min}} = 13$ kG/mm^2.

Measurement of stresses in the blade with a spar of steel tube is usually produced in two planes: in the plane of least (σ_y) and in the plane of the greatest rigidity (σ_x). With this it can appear that at some point of the perimeter of the spar section the amplitude of varying stresses attains the magnitude $\sigma_a = \sqrt{\sigma_x^2 + \sigma_y^2}$, greater than that of the amplitude σ_y.

However, usually because of the distinction in phases of effective stresses in these two planes such a magnitude of varying stresses is almost never attained. Therefore, with calculation of service life of the blade it is possible to use the approximate formula:

$$\sigma_a = \sigma_y + \xi \left(\sqrt{\sigma_x^2 + \sigma_y^2} - \sigma_y \right).$$

Coefficient ξ can be calculated if there is simultaneous recording of stresses σ_x and σ_y. If there are no data for the determination of ξ, then practically quite reliable results can be obtained if we assume $\xi = 0.5$.

6. Scattering of Amplitudes of Varying Stresses in Assigned Flight Conditions

With the measurement of varying stresses in flight it is revealed that in the assigned conditions of flight values of stresses appear different during the period of conditions of the flight and in various flights. Therefore, it is necessary to introduce its average-equivalent amplitude of varying stresses in all conditions of the flight.

To determine this amplitude it is possible to use special decoders of oscillograms, which allow determining the number of amplitudes of stresses n_k lying in the range

$$\Delta\sigma_k = \sigma_k - \sigma_{k-1},$$

where σ_k and σ_{k-1} - levels of amplitudes of varying stresses selected for the calculation.

Then the average-equivalent amplitude of varying stresses in the examined conditions can be determined by the formula analogous to (11.9),

$$\sigma_i = \sqrt[m]{\frac{1}{\varepsilon_i}\sum_k \bar{n}_k \sigma_k^m}. \qquad (11.10)$$

Here $\bar{n}_k$ is the relative number cycles with amplitude σ_k.

$$\bar{n}_k = \frac{n_k}{n_\Sigma},$$

where n_k is the number cycles with amplitude σ_k, and n_Σ is the total number of cycles recorded by the decoder; ε_i is the relative number cycles with stresses greater than the minimum fatigue limit in i-th flight conditions.

Summing with respect to k is produced only for those intervals of time in i-th conditions where the amplitude of stresses σ_k is larger than the minimum fatigue limit $\sigma_{w_{min}}$.

In the determination of the average-equivalent amplitude for the whole service life of the helicopter by formula (11.9) the amplitude in each flight condition should be calculated by the formula (11.10) and the relative duration of conditions introducing defectibility into the construction, by the formula:

$$\varepsilon = \sum_i \varepsilon_i a_i.$$

In practice for simplification of deciphering we often determine in each condition not the average-equivalent amplitude but the maximum one that enters into the safety margin, but this leads to a decrease in the service life of the construction.

7. Method of Calculation of Service Life with the Use of Safety Factors

The problem of determining service life of the construction is reduced to the finding of such a safe number of cycles of loading with operation of $N_{без}$ at which the probability of destruction of the construction is very small and equal to the assigned. If it were possible to test a sufficiently large number of samples, then, by determining the characteristic of distribution of their service life (Fig. 1.68), it would be easy to find $N_{без}$. Based on such approach are many methods of calculation of service life (see, for example, [43]). However, usually the service life of the construction must be determined on the basis of results of dynamic tests of some small number of samples of the construction n, when the law of distribution of service life is impossible to determine with the necessary accuracy. Therefore, in practice there is wide spread use in the method of calculation of service life of the construction founded on the introduction of definite safety margins by the number of cycles of n_N and amplitude of varying stresses n_σ.

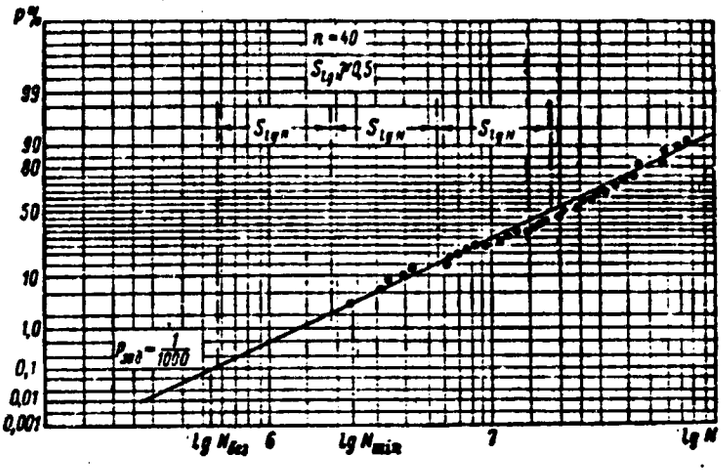

Fig. 1.68. Determination of the safe number cycles by the distribution curve of service life.

To calculate the service life by this method it is necessary to take the measurement of stresses in the construction on different conditions of flight, determine the equivalent value of stresses and conduct dynamic tests of one or several specimens of the construction during stresses

$$\sigma_{экв} = \eta_\sigma \sigma_{экв}. \qquad (11.11)$$

The reserve η_σ here is introduced for calculation of the possible distinction in values of varying stresses in analogous units of different helicopters.

By conducting tests of samples and obtaining the minimum value of the number cycles prior to destruction N_{min} we determine the safe number cycles of loading in the operation by formula:

$$N_{без} = \frac{N_{min}}{\eta_N}. \qquad (11.12)$$

The safety margin η_N is introduced for the calculation of scattering of characteristics of service life.

Then the service life of the construction in hours can be determined by the formula

$$R=\frac{N_{\text{без}}}{60f},$$

where f is the frequency of loading of the blade in operation (oscillations per minute).

In certain cases the service life of the construction appears dependent on the frequency of the load. Therefore, if dynamic tests are conducted at a frequency of greater than the frequency of loading in flight, then it is necessary to introduce still an additional reserve on the frequency of loading η_f. This reserve is introduced basically for components made of Duralumin and when tests are conducted at a frequency 5-10 times greater than the frequency of loading in flight. In this case it is taken equal to $\eta_f = 1.5\text{-}2.0$. In the calculation of these reserves the formula for determining service life can be written in the form:

$$R=\frac{N_{\text{min}}}{60f\eta_N\eta_f}. \qquad (11.13)$$

If one were to assume that the distribution of characteristics of service life obeys the normal law and that parameters of this law are well-known, then, as was already stated, values of necessary safety margins with respect to the number cycles η_N and amplitude of varying stresses η_σ would have been possible to determine by calculation means having assigned the determined quite small probability of destruction of the construction in the operation. However, such calculations cannot claim to be of high accuracy. Therefore, by the same right the method of assignment of values of these coefficients can be used on the basis of operational experience of helicopters.

Proceeding from this experiment, the safety factor with respect to the amplitude of varying stresses η_σ can be accepted as equal to 1.2 and the reserve with respect to the number cycles of loading η_N as different depending upon the number of tested samples and degree of responsibility of the unit for flight safety.

With respect to the degree of responsibility for flight safety all units and components of the helicopter can be divided into

four groups:

Group I – units whose destruction leads to immediate and full disturbance of the efficiency and safety with the difficultly revealed beginning of the appearance of a fatigue crack. This group can include blades whose spar is covered by the housing and does not permit inspecting it after a flight, a series of components closed for inspection of the hub and control system of the main and tail rotor, shaft of the rotor, etc.

Group II – units whose destruction could lead to immediate and full disturbance of the efficiency of construction and flight safety, but there is a possibility of early detection of the appearance of a fatigue crack. This group can include blades with a reliably operating system of signalling of the appearance of cracks and all remaining units attributed to group I, if the appearance of fatigue crack in them can be revealed in preflight inspection.

Group III – units whose destruction leads to a partial loss in efficiency, threatens the flight safety, but permits accomplishing a forced landing without a crash of the helicopter. This group can include many elements of the fuselage, even the reduction gear frame if it is carried out in a statically indeterminate configuration.

Group IV – units whose destruction creates partial loss of efficiency, permits continuing the flight, does not involve rapid destruction of other units and permits revealing destruction during ground inspection. This can include many elements of the fuselage, stabilizer of the helicopter and a series of analogous elements of the construction.

The more important the unit, the larger the value of margin with respect to the number of cycles should be taken. The following values of these reserves can be proposed (Table 1.16).

Table 1.16. Safety margins with respect to the number cycles.[1]

Number of tested samples	Safety factor η_N			
	I Group	II Group	III Group	IV Group
1	12	6.0	6	2.5
2	8	4.0	4	2.0
3	6	3.0	3	1.5
6	4	2.5	2	1.0

[1]Margins η_N given for group I of units are twice larger than well-known values, since included in them are also margins η_Σ, introduced frequently into the inaccuracy of hypothesis of linear summation of defectibilities.

To realize margins with respect to the number cycles required for groups I and II of units of the helicopter in practice proves to be possible only at very low frequency of the change in loads in the flight. In the establishment of the service life with such great margins for all basic units of the helicopter, it would be necessary to conduct tests up to a very large number cycles considerably larger than 10^7 cycles. It would be necessary to spend very much time on this. Therefore, even greater widespread use is achieved in the accelerated method of dynamic tests with a margin with respect to the number cycles $\eta_N = 1$ or even smaller than unity. In this case safeguard of the required reliability is attained by means of introducing only a margin with respect to stresses. For conversion of margins η_N into margin with respect to η_σ we usually use formula (11.3) with the exponent $m = 6$. With such approach the necessary margin with respect to amplitude of varying stresses appears different depending upon the number of tested samples and large for Duralumin, for which it appears necessary to introduce an additional margin into the difference in frequency during tests and in flight.

Taking into account everything that has been said, for group I of units of the helicopter it is possible to take margins with respect to the amplitude of varying stresses, shown in Table 1.17.

Table 1.17.

Number of tested samples n	η_σ ($r_\sigma=-1$)	
	steel	Dura-lumin
1	1,8	2,0
2	1,7	1,9
3	1,6	1,8
6	1,5	1,7

Under dynamic tests with such margins η_σ a safe number of cycles is determined according to the minimum number of cycles of loading of the sample prior to destruction $N_{без}=N_{min}$.

It is necessary, however, to consider that the carrying out of tests with such large margins with respect to the amplitude of live loads possibly only in those cases when with an increase in load the character of the distribution of stresses according to different structural parts is essentially not changed. When with an increase in loads redistribution of stresses occurs due to, let us say, the opening of a joint, the appearance of mutual movements of adjoining components operating under working loads without such movements or for other similar reasons, the application of such a method of tests is inexpedient.

8. Method of A. F. Selikhov for Calculating the Necessary Safety Margin with Respect to the Number Cycles η_N

Above, in No. 2, it was already indicated that the service life of the construction has a threshold of sensitivity with respect to the number cycles N_0, and therefore the distribution function in the region of small probabilities of destruction deviates from the normal law. In principle, it would have been possible to select such a safety margin with respect to the number of cycles η_N that the probability of destruction of the construction would be equal to zero.

But, as is shown in work [44], for a sufficiently accurate determination of the threshold of sensitivity there is required a large quantity of samples, so that it is mostly impossible to determine its value for the construction. Therefore we usually assume that logarithms of numbers of cycles prior to destruction lg N are distributed according to the normal law, and the assignment of service life of the construction is produced based on the condition that the probability of destruction P = 0 and on the condition that this probability is quite small, let us say, equal to $P = \frac{1}{10,000}$. If in reality the threshold of sensitivity takes place, then the requirement of such a small probability of destruction, calculated from the normal law of distribution, appears more rigid than the requirement P = 0, which would have been possible to impose, if the value N_0 proved to be possible to calculate. Therefore, it is possible to consider fully permissible the determination of safety margins on the basis of somewhat greater probability of destruction, let us say $P = \frac{1}{1000}$ and even $P = \frac{1}{100}$.

To determine the necessary safety margins with respect to the number cycles the method proposed by A. F. Seliikhov can be used. This method consists in the following.

If one were to assume that the distribution of logarithms of numbers of cycles prior to destruction of the construction obeys the normal law

$$\varphi(\lg N) = \frac{1}{s_{\lg N}\sqrt{2\pi}} \cdot e^{-\frac{(\lg N - m_{\lg N})^2}{2s^2_{\lg N}}}, \qquad (11.14)$$

then the distribution of minimum values of service life of a certain group of samples of this construction can be defined by formula

$$\varphi_{\min}(\lg N) = \frac{n}{2^{n-1}}\left[1 + \Phi\left(\frac{m_{\lg N} - \lg N}{s_{\lg N}\sqrt{2}}\right)\right]^{n-1}\varphi(\lg N), \qquad (11.15)$$

where n is the number of tested samples; $\Phi(x)$ – Laplace function $\left(x = \frac{m_{\lg N} - \lg N}{s_{\lg N}\sqrt{2}}\right)$.

The character of distribution $\phi_{min}(\lg N)$ for values $S_{\lg N} = 0.15$ and n = 5, 10 and 100 is shown on Fig. 1.69. Values of mathematical expectations and root-mean-square deviations of this distribution depending upon $S_{\lg N}$ and n can be found by curves shown in Fig. 1.70 and 1.71.

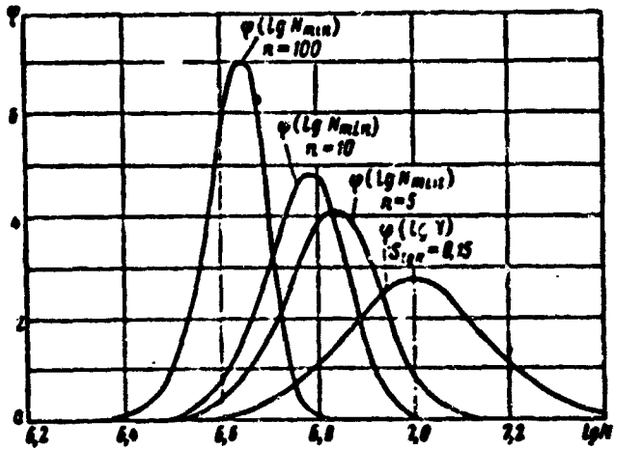

Fig. 1.69. Distribution of minimum values of service life with a different volume of the sample.

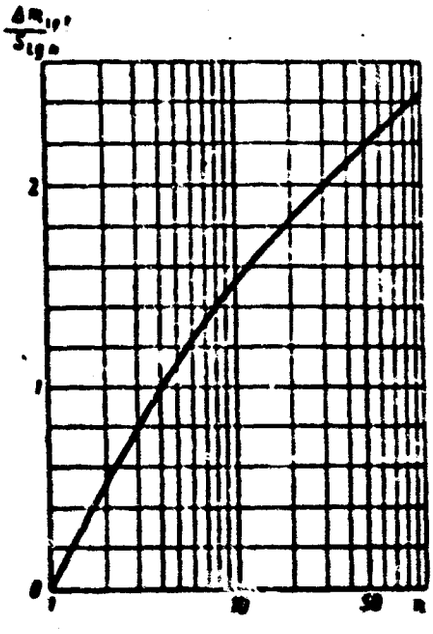

Fig. 1.70. Change in magnitude of mathematical expectation of minimum values of service life from the number of tested samples.

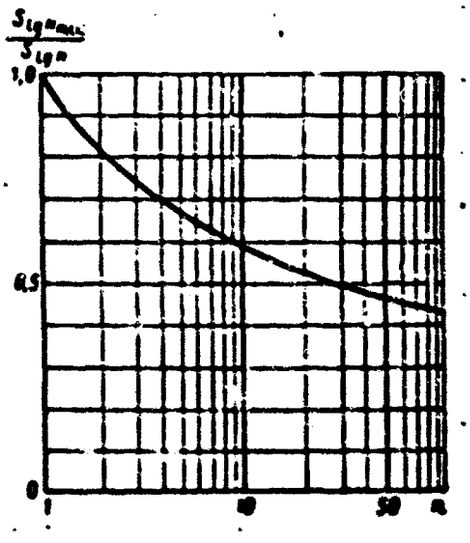

Fig. 1.71. Dependence of root-mean-square deviations of minimum values of service life on the number of tested samples.

The mathematical expectation of the minimum value of service life can be determined by the formula:

$$m_{\lg N_{min}} = m_{\lg N} - \Delta m_{\lg N}.$$

Value $\Delta m_{\lg N}$ is determined depending upon the root-mean-square deviation $S_{\lg N}$ and number of tested samples by the curve on Fig. 1.70.

The root-mean-square deviation of the minimum value of service life $S_{\lg N_{min}}$, referred to $S_{\lg N}$, is shown in Fig. 1.71.

Thus, if characteristics of the distribution of service life of the construction are known, then by formula (11.15) one can determine the distribution of minimum values of service life during tests of a small number of samples n. Knowing this distribution, one can determine the probability of destruction of the construction with the number cycles of the load

$$N_{экв} = \frac{N_{min}}{\eta_N}, \qquad (11.16)$$

where η_N is the safety factor of reliability with respect to the number cycles; N_{min} – minimum value of the number cycles prior to destruction of the construction during tests.

Having taken the logarithm of expression (11.16), we obtain

$$\lg N_{экв} = \xi - \lg \eta_N, \qquad (11.17)$$

where

$$\xi = \lg N_{min}.$$

If dynamic tests of natural samples are conducted under loads equivalent to loads acting in the examined construction in flight, then it is possible to consider that the distribution of service life during dynamic tests and under operational conditions is equal. A certain distinction in these distributions can appear only due to errors durirg dynamic tests and the scale effect in those cases when the volume of loaded material in the construction appears larger than

chat in the sample, i.e., for example, when on a sample cut from a blade, only its central part appears loaded during tests. If dynamic tests are conducted under loads different from those effective in flight, then characteristics of the distribution of service life in the operation prove to be essentially different from those obtained during tests and can be determined only approximately by means of conversion founded on definite assumptions with respect to the Wöhler curve.

If the distribution of service life under conditions of operation $\varphi_{эксс}$ is determined, then the conditional probability of destruction of one arbitrarily taken copy of the construction, in operation with the given outcome of dynamic tests ξ_2, can be determined by the expression

$$P_{усл} = \int_{-\infty}^{t_0 - \lg \eta_N} \varphi_{эксс}(t_1)\, dt_1. \qquad (11.18)$$

The total probability of destruction of this copy of the construction in operation will be equal to the sum of conditional probabilities multiplied by the absolute probability of each result $\varphi_{min}(\xi_2)\, d\xi_2$:

$$P = \int_{-\infty}^{\infty} \varphi_{min}(t_2) \left[\int_{-\infty}^{t_0 - \lg \eta_N} \varphi_{эксс}(t_1)\, dt_1 \right] dt_2. \qquad (11.19)$$

Having calculated the magnitude of this integral, it is possible to plot the dependence of probability of destruction of the construction P on the accepted value of safety margin with respect to the number cycles n_N.

In the case when the distribution of service life in operation and during tests is equal

$$m_{\lg N_{эксп}} = m_{\lg N_{исп}};\ S_{\lg N_{эксп}} = S_{\lg N_{исп}}$$

the probability P appears dependent only on two quantities: on the number of tested samples n and on the relation of the logarithm of safety margin $\lg n_N$ the root-mean-square deviation of logarithms of

logarithms of numbers of cycles prior to destruction of samples $S_{\lg N}$ (Fig. 1.72).

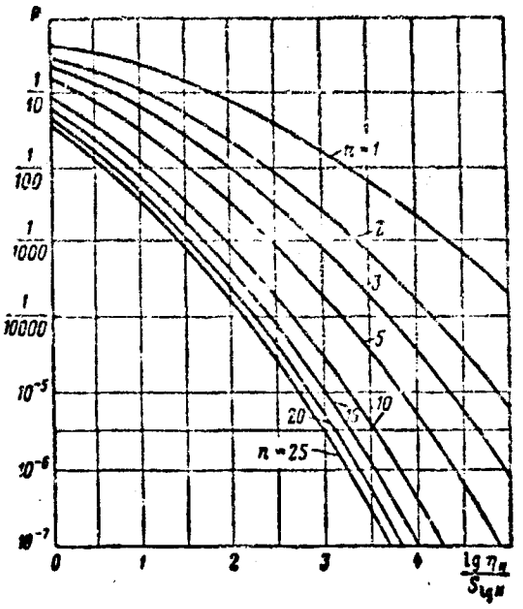

Fig. 1.72. Diagram for the selection of the magnitude of safety margin with respect to the number cycles of the load.

Thus to determine the necessary safety margin with respect to the number cycles it is necessary to conduct dynamic tests of n samples of construction, determine the root-mean-square deviation $S_{\lg N}$ and N_{min} and, having assigned a certain probability $P_{зад}$, determine η_N by curves of Fig. 1.72. After that the safe number of cycles prior to destruction can be determined by formula (11.12).

Such an approach is possible also when tests are conducted on a small number of samples. The value $S_{\lg N}$ can be taken according to results of other tests of similar constructions.[4]

If we assume beforehand that $S_{\lg N} = 0.2$ (this value is close to the minimum root-mean-square deviations observed for the majority of units of a helicopter and to assign probabilities of destruction shown in Table 1.18, then values of margins close to those which are given in Table 1.16 can be obtained. Usually the quantity $S_{\lg N}$ appears higher. Therefore margins obtained by this method are higher than those which are given in Table 1.16.

Table 1.18.

Group of units with different importance for safety.	Probability of destruction of the construction
I group	$\frac{1}{10000}$
II group	$\frac{1}{1000}$
III group	$\frac{1}{100}$
IV group	$\frac{1}{10}$.

The basic question which arises with the use of the method given here is the question of what probability of destruction of the construction should one assign during the calculation of service life. Frequently values of probabilities recommended by different sources can differ by 3-4 orders (see, for example, [43]). The values of this probability proposed here (in Table 1.18) are selected from the consideration that they to a great or lesser degree of reliability should correspond to numbers of cycles smaller than the threshold of sensitivity N_0. Therefore, these probabilities should be examined as certain conditional values referring to the normal law of distribution. Real values are considerably less or even simply equal to zero.

9. Determination of $S_{\lg N}$ with the Assigned Confidence Probability

As follows from the preceding point, the logarithm of safety margin with respect to the number cycles $\lg n_N$ necessary to provide the assigned probability of destruction appears directly proportional to the root-mean-square deviation in the distribution of logarithms of numbers of cycles prior to destruction of the construction $S_{\lg N}$. The larger $S_{\lg N}$, the greater should be taken the margin n_N. Therefore, the reliability of determining the service life of construction, depending on admissibility of the many accepted assumptions, to a considerable degree is connected with the accuracy of determination of $S_{\lg N}$.

Usually to determine the service life of a construction tests of three-five samples of the construction are conducted. In many cases it is considered sufficient to carry out tests with even one sample. There are no doubts in the fact that with such a small number of tested constructions there is no possibility for a sufficiently accurate determination of $S_{\lg N}$. Therefore, in the method which is proposed by A. F. Selikhov (see No. 8) it is assumed that $S_{\lg N}$ cannot be determined in all cases. With a small number of tested samples it is possible to take $S_{\lg N}$ according to the results of tests of analogous samples of another earlier tested construction. Such an approach very greatly simplifies the process of establishing the service life and appears extradordinarily useful in practice.

Determination of $S_{\lg N}$ with sufficient reliability is possible with tests of not less than ten samples of the construction. To evaluate this reliability we frequently use the concept of confidence probability of the determination of $S_{\lg N}$.

The confidence probability β is usually selected so that it would be possible to consider practically reliable that the value $S_{\lg N}$ lies in the interval:

$$\frac{1}{q}\tilde{S}_{\lg N} < S_{\lg N} < q\tilde{S}_{\lg N},$$

where $\tilde{S}_{\lg N}$ is the estimate of $S_{\lg N}$ obtained according to a limited number of results of tests; q – coefficient in magnitude, larger than unity.

From what has been said it follows that the sought value $S_{\lg N}$ can lie in the cofidence interval with probability β. Consequently, it can appear equal to $q\tilde{S}_{\lg N}$. In this case the logarithm of the safety margin with respect to the number cycles $\lg n_N$ in accordance with that expounded in No. 8 by the method will be increased proportional to quantity q, and this is why the computed value of service life decreases.

The value of coefficient q, depending on the number of tested samples, appears to be the accepted value of the confidence probability β.

In Table 1.19 there are given values of coefficients q and values of the confidence probability β corresponding to them taken by us from the book of Ye. S. Ventsel' Probability Theory.

Table 1.19.

Number of tested samples	Values of confidence probability β in % at different q					
	1,06	1,1	1,15	1,20	1,25	1,3
$n=5$	14,6	24,1	35,5	46,1	55,6	63,7
$n=10$	20,8	34	49	62	72,2	79,7
$n=25$	32,7	51,8	70,6	83,2	90,5	94,4
$n=50$	45,2	68,2	86	94	97,4	98,8

As follows from Table 1.19, during tests, for example, twenty-five samples and a confidence probability of not less than 70%, the value $\tilde{S}_{\lg N}$ obtained according to the experiment appears necessary with the calculation of service life still to be increased 1.15 times.

With the assignment of the confidence probability one should consider, however, that reliability of the determination of $S_{\lg N}$ should not exceed the reliability of the determination of all other parameters entering into the calculation of service life. This pertains, first of all, to parameters determining the law of distribution of service life in the region of small probabilities of the distruction, such as, the threshold q of sensitivity N_0, and to the character of the very law of distribution, which only approximately can be accepted as logarithmically normal.

Therefore, the confidence probability β characterizing the reliability of determination of $S_{\lg N}$ can be considerably lowered to values at which coefficient q will not be considerably larger than unity.

On the basis of these considerations, with the determination of margins n_N we frequently assume $q = 1$ and use the value $\tilde{S}_{1g\,N}$ and not that value which corresponds to the upper limit of the confidence interval at sufficiently high β.

10. Scattering in Levels of Loading of Different Copies of the Construction and the Safety Margin with Respect to the Amplitude of Varying Stresses n_σ

Values of amplitudes of varying stresses, effective in flight in separate copies of units of the helicopter identical in construction prove to be different.

Measurements show that in identical conditions of flight amplitudes of varying stresses are distinguished both for blades of one rotor and between blades of different rotors. This is explained by the scattering of parameters of blades, manufactured serially due to the distinction in their geometric dimensions, and, consequently, in their weight. There are usually always deviations from the contour of the profile and distinctions in the geometric twist of the blade. Furthermore, with the installation of blades on the helicopter and adjustment of coconicity of the rotor distinctions in angles of setting of the blades appear. All of this eventually leads to a certain distinction under conditions of operation of separate blades and, as a result, to the scattering in values of amplitudes of variable stresses acting in identical conditions of flight.

There is also a distinction in parameters of flight conditions connected with the manner of piloting by individual pilots.

A no smaller or even considerably greater distinction is observed in values of amplitudes of stresses and in all other units of the helicopter. The scattering in amplitudes of stresses is especially great in those components where live loads from separate blades with summation should be equal to zero (if the blades are ideally identical) for all harmonics with the exception of harmonics multiple of the number of blades. If, however, parameters of the blades are

different, and thus practically this always occurs, then in these units besides small live loads with frequencies of harmonics multiple of the number of blades there appear considerable (in magnitude) loads with other harmonics, and their magnitude appears proportional to the magnitude of distinction in parameters of the blades. The scattering in values of varying stresses in such units can appear very great. Usually these are the following units: the pitch control, components of the rotor control system and fuselage, and primarily its reduction gear frame, which is especially greatly loaded by live loads.

For an account of all enumerated factors during calculation service life the safety factor with respect to the amplitude of varying stresses η_σ is introduced. This factor should provide reliability of operation of any copy of the construction in a fleet of helicopters taking into account the available scattering in values of varying stresses.

Usually to measure the varying stresses in the construction there is arbitrarily selected a certain copy of the helicopter. Varying stresses $\sigma_{изм}$ obtained during its tests are used for carrying out dynamic tests. With this tests are conducted with stresses $\sigma_{исп} = \eta_\sigma \cdot \sigma_{изм}$. Therefore, above-stated (see No. 8) method of determination of safety margin η_N and safe period of service gives results which can be used only for that copy of construction in which stresses equal to $\sigma_{исп}$ act. For all other copies of this construction the service life will appear greater, if stresses acting in them $\sigma_{действ} < \sigma_{исп}$, and less, if $\sigma_{действ} > \sigma_{исп}$.

Let us determine the value of the safety factor η_σ from the condition of the fact that the probability of destruction of the examined unit of the helicopter P_Σ, taking into account the available scattering in values of amplitudes of varying stresses, is equal to the assigned probability $P_{зад}$. Usually this value is taken to be the same as the probability of destruction P_0 of that unit in which varying stresses $\sigma_{исп}$, accepted during dynamic tests, act.

Thus if value η_N is selected from the condition that the probability of destruction of the copy of the construction with stresses $\sigma_{исп}$ is equal to $P_0 = P_{зад}$, then the probability of destruction of other copies of this construction can be determined by formula:

$$P_\sigma = \int_{-\infty}^{\infty} \varphi_{\text{нагр}}(\xi_2) \left[\int_{-\infty}^{\xi_2 - \lg \eta_N} \varphi_{\text{экс}}(\xi_1)\, d\xi_1 \right] d\xi_2. \qquad (11.20)$$

Here P_σ is the probability of destruction of that unit of the helicopter in which stresses equal to σ act. The distribution of service life $\phi_{экс}$, entering into formula (11.20), which is determined on the basis of dynamic tests for a certain selected level of equivalent stresses should be recalculated taking into account the fact that in different copies of the construction different equivalent stresses act.

If one were to assume that the service life is changed in accordance with the law

$$\sigma^m N = \text{const}, \qquad (11.21)$$

then characteristics of the distribution $\phi_{экс}(\xi)$ can be assumed equal to:

$$(S_{\lg N})_\sigma = S_{\lg N_{исп}}; \qquad (11.22)$$

$$(m_{\lg N})_\sigma = m_{\lg N_{исп}} + m\,[\lg \sigma_{исп} - \lg \sigma_{действ}]. \qquad (11.23)$$

where $(S_{\lg N})_\sigma$ is the root-mean-square deviation of distribution of logarithms of numbers of cycles with stresses $\sigma_{действ}$, different from those at which dynamic tests are produced; $(m_{\lg N})_\sigma$ – mathematical expectation of this distribution; $\sigma_{исп}$ – stresses during tests; $\sigma_{действ}$ – stresses acting in some copy of the helicopter.

Let us assume that the distribution of amplitudes of acting varying stresses with respect to different copies of the construction can be accepted as logarithmically normal. Then the probability of destruction of the examined units of the helicopter will be equal to:

$$P_{изм} = \frac{\int_{-\infty}^{\infty} P_\sigma \varphi_{\lg \sigma_{действ}} d \lg \sigma,}{\int_{-\infty}^{\infty} P_\sigma \varphi_{\lg \sigma_{действ}} d \lg \sigma,} \qquad (11.24)$$

where $\phi_{\lg \sigma_{действ}}$ is the law of distribution of effective amplitudes of varying stresses (Fig. 1.73)

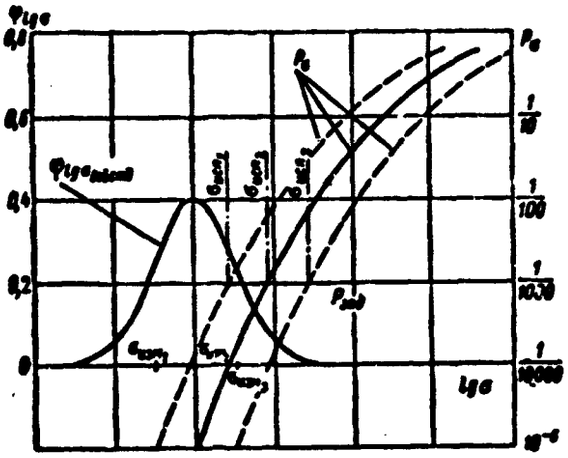

Fig. 1.73. Character of distribution $\phi_{\lg \sigma}$ and P_σ at various $\sigma_{исп} = \eta_\sigma \sigma_{изм}$.

Here one should consider that value $\sigma_{исп}$, accepted for dynamic tests, is selected accidentally according to the results of measurement of stresses on one arbitrarily taken helicopter or on several helicopters. Therefore, the probability distribution of the destruction P_σ with respect to units with different acting stresses will be displaced alcng the axis lg σ (see Fig. 1.73) depending on the accepted value $\sigma_{исп}$, thus, in order that at $\sigma_{действ} = \sigma_{исп}$ the probability of destruction P_σ is equal to $P_{зад}$, since from this condition the value η_N was selected. Hence it is clear that value $P_{изм}$ will depend on value $\sigma_{исп}$.

Consequently, the probability $P_{изм}$ is the conditional probability with the definite, accidentally selected, value $\sigma_{исп}$. The total probability of destruction, arbitrarily taken from a fleet of helicopters of unit P_Σ, can be obtained as the sum of conditional probabilities $P_{изм}$, multiplied by the probability of appearance in this unit of stresses taken as the basis with dynamic tests $\varphi_{\lg \sigma_{исп}} d \lg \sigma$:

$$P_{\Sigma} = \int_{-\infty}^{\infty} P_{изм} \varphi_{\lg \sigma_{изм}} d \lg \sigma =$$

$$= \int_{-\infty}^{\infty} \left[\int_{-\infty}^{\infty} P_{\sigma} \varphi_{\lg \sigma_{действ}} d \lg \sigma \right] \varphi_{\lg \sigma_{изм}} d \lg \sigma. \qquad (11.25)$$

If measurement of stresses is taken on one helicopter, then one may assume that

$$\varphi_{\lg \sigma_{изм}} = \varphi_{\lg \sigma_{действ}}.$$

If measurement is produced on several copies of the construction, and with dynamic tests there are assigned stresses

$$\sigma_{исп} = \eta_{\sigma} \sigma_{изм_{ср}},$$

where $\sigma_{изм_{ср}}$ is the average amplitude of varying stresses measured on several copies of the construction, then parameters of distribution $\varphi_{\lg \sigma_{изм}}$ should be determined as parameters of the distribution of mean values of varying stresses

$$\varphi_{\lg \sigma_{изм}} = \varphi_{\lg \sigma_{ср}}.$$

From expression (11.25) it follows that the total probability of destruction P_{Σ} appears dependent on quantity η_{σ}. Therefore, by assigning $P_{\Sigma} = P_{зад}$, one can determine the necessary value η_{σ}. It is obvious that the necessary value η_{σ} proves to be dependent on the law of distribution of varying stresses with respect to different copies of similar units of the helicopter $\phi_{\lg \sigma_{действ}}$. To determine characteristics of this law of distribution there can be used data of different measurements of stresses carried out frequently on the same units of the helicopter in tests conducted for different purposes.

It is natural that the scattering of values of average equivalent varying stresses can be different for different units.

The root-mean-square deviation in the distribution of varying stresses with respect to different blades of the rotor usually lies

in the range:

$$S_{\lg \sigma} = 0{,}02 \div 0{,}035.$$

If one were to take, as is frequently done, the normal law of distribution of amplitudes of varying stresses, then to these values of $S_{\lg \sigma}$ will correspond the values:

$$\gamma_\sigma = \frac{S_\sigma}{m_\sigma} = 0{,}05 \div 0{,}08, \qquad (11.26)$$

where S_σ is the root-mean-square deviation in the distribution of amplitudes of varying stresses with respect to different blades; m_σ is the mathematical expectation of this distribution, i.e., average stress in these blades.

At small γ_σ it is possible to assume $S_{\lg \sigma} \approx \gamma_\sigma \lg e$.

For units whose load depends on the quality of control of the rotor, such as the cyclic pitch control, reduction gear frame and others, the coefficient γ_σ appears somewhat larger.

From the structure of formula (11.25) it follows that the total probability of destruction P_Σ depends basically on two parameters:

$$a = \frac{m S_{\lg \sigma}}{S_{\lg N}};$$

$$b = \frac{\lg n}{S_{\lg \sigma}},$$

where m is the exponent of the Wöhler curve.

The total probability of destruction P_Σ also depends on the probability of destruction P_0 accepted in calculation of that copy of construction in which stresses $\sigma_{\text{исп}}$.

Figure 1.74 gives calculations of the total probability P_Σ for different values a, b and P_0 according to formula (11.25) in the case when measurement of stresses only in one copy of construction of the helicopter is carried out. Calculations were also conducted for

different values of the number of tested samples, but it appeared that the total probability of destruction does not greatly depend on their number. Figure 1.74 shows by dashed lines the curves for $n_{обр} = 5$ and by solid lines, for $n_{обр} = 20$.

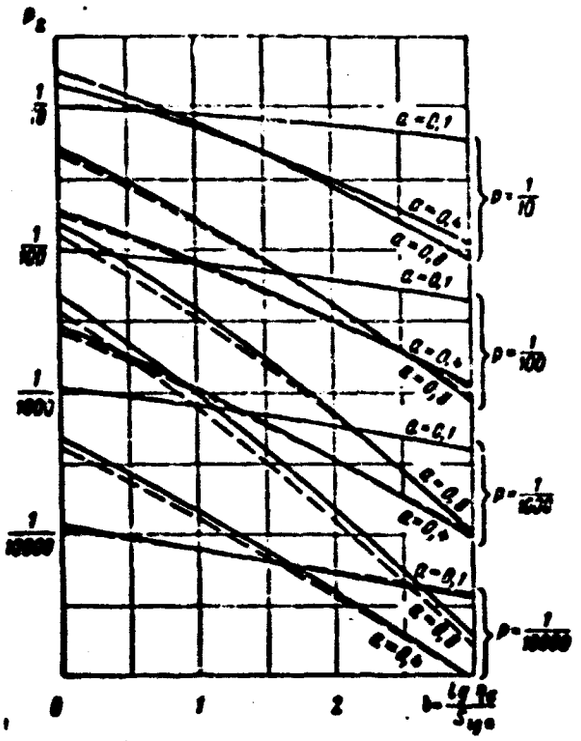

Fig. 1.74. Results of calculation of the probability of destruction taking into account scattering in values of stresses acting in different copies of the construction.

If one were to require that $P_\Sigma = P_0 = P_{зад}$, then final graphs can be obtained, by which it is easy to determine the necessary margin n_σ, if values $S_{\lg \sigma}$, $S_{\lg N}$ and $P_{зад}$ are known. These graphs are shown in Fig. 1.75. Just as in Fig. 1.74, the dashed lines pertain to the case $n_{обр} = 5$ and solid lines to the case $n_{обр} = 20$.

As an example let us find the necessary margin n_σ for the blade of the helicopter if it is known that $\gamma_* = 0{,}06$ ($S_{\lg *} = 0{,}035$), and $S_{\lg N} = 0{,}4$.

Let us determine the value of coefficient a:

$$a = \frac{mS_{\lg *}}{S_{\lg N}} = \frac{6 \cdot 0{,}035}{0{,}4} = 0{,}525.$$

Then, by assigning value $P_{\Sigma} = \frac{1}{1000}$, by curves of Fig. 1.75 we obtain:

$$b = 1{,}28 \text{ (at } n_{обр} = 5\text{)};$$

whence

$$\lg \eta_b = 1{,}28 \cdot 0{,}035 = 0{,}0448,$$

and

$$\eta_b = 1{,}11.$$

In those cases when the law of distribution ϕ_{σ} is unknown, we usually take $\eta_{\sigma} = 1.2$. This value η_{σ}, as was already noted in No. 7, is frequently used in practical calculations.

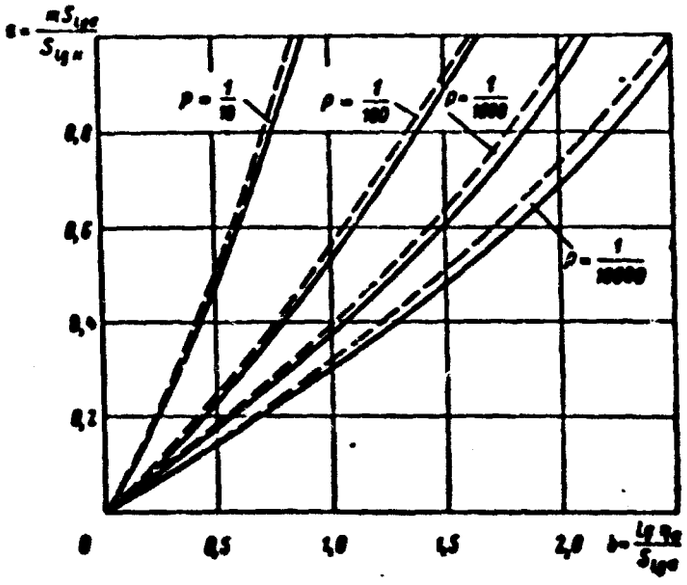

Fig. 1.75. Diagram for selection of the safety margin η_{σ}

11. Method of Determination of Safety Margin η_{σ} Proposed by A. F. Selikhov

In our account certain procedures and reasonings somewhat differ here from those which were proposed by A. F. Selikhov, but the basic principle of approach to resolving the problem is borrowed from the author.

In this method for determining the margin η_{σ} the same method is used which was described in No. 8, but in characteristics of the

distribution of service life the scattering in valves of amplitudes of stresses acting in flight is considered.

If, as earlier, we consider that with a change in the amplitude of stresses the service life under conditions of operation is changed in accordance with law (11.21), i.e., that

$$\lg N_{экс} = \lg N_{исп} + m(\lg \sigma_{исп} - \lg \sigma_{действ}), \qquad (11.27)$$

then one can determine the characteristics of distribution of service life in the operation taking into account scattering in values of amplitudes of acting stresses.

The mathematical expectation of this distribution will be equal to:

$$m_1 = m_{\lg N_{исп}} + m(\lg \sigma_{исп} - m_{\lg \sigma_{действ}}), \qquad (11.28)$$

where $m_{\lg \sigma_{действ}}$ is the mathematical expectation of the distribution of amplitudes of stresses in different copies of the investigated construction (mean value of amplitudes of varying stresses in different copies of the construction).

If tests are conducted with stresses

$$\sigma_{исп} = \eta_0 m_{\sigma_{ср}},$$

then assuming

$$m_{\lg \sigma_{действ}} \approx \lg m_{\sigma_{ср}},$$

we obtain

$$m_1 = m_{\lg N_{исп}} + m \lg \eta_0.$$

The root-mean-square deviation in values of logarithms of numbers of cycles prior to destruction under operating conditions can be determined by the formula

$$S_1 = \sqrt{S^2_{\lg N} + m^2 S^2_{\lg \sigma}}. \qquad (11.29)$$

If dynamic tests are conducted with the amplitude of stresses $\sigma_{исп} = \eta_\sigma \sigma_{ср}$ (where $\sigma_{ср}$ is the average amplitude measured in flight on different copies of the construction), then the scattering of characteristics of service life with tests will appear dependent on the scattering in acting stresses on different copies of helicopters. The amplitude established during tests proves to be the value of the accidental measurement of stresses dependent on the results. As earlier (see No. 8), we are interested in characteristics of the distribution of logarithms of minimum numbers of cycles prior to destruction.

Let us assume that values of minimum numbers of cycles up to destruction obey the law

$$\lg N_2 = \lg N_{min} + m[\lg \sigma_{исп} - \lg(\eta_\sigma \sigma_{ср})], \qquad (11.30)$$

where N_2 is the minimum number of cycles prior to destruction of the construction taking into account the fact that the amplitude of tests can be established different depending upon results of the measurement of the average amplitude of stresses $\sigma_{ср}$; N_{min} is the minimum number of cycles prior to destruction of the construction at a definite fixed value of the amplitude of stresses during tests of $\sigma_{исп}$.

Then

$$m_2 = m_{\lg N_{min}} + m(\lg \sigma_{исп} - \lg \eta_\sigma - m \lg \sigma_{ср}). \qquad (11.31)$$

If

$$\sigma_{исп} = \eta_\sigma m_{\sigma_{ср}},$$

then

$$\lg \sigma_{исп} = \lg \eta_\sigma + \lg m_{\sigma_{ср}}.$$

Let us assume that

$$\lg m_{\sigma_{ср}} \approx m_{\lg \sigma_{ср}}.$$

Then $m_2 = m_{\lg N_{min}}$, and the value of the root-mean-square deviation of logarithms of numbers of cycles during tests is

$$S_2 = \sqrt{S^2_{\lg N_{\min}} + m^2 (S_{\lg \sigma})^2_{cp}} \qquad (11.32)$$

where $(S_{\lg \sigma})_{cp}$ is the root-mean-square deviation in values of the mean logarithm of amplitude of stresses, measured in different copies of the construction.

This value depends on the number of measurement $n_{изм}$:

$$(S_{\lg \sigma})_{cp} = \frac{S_{\lg \sigma}}{\sqrt{n_{изм}}}. \qquad (11.33)$$

With one measurement ($n_{изм} = 1$)

$$(S_{\lg \sigma})_{cp} = S_{\lg \sigma}. \qquad (11.34)$$

Taking into account the relation (11.33), the root-mean-square deviation in the distribution of service life during tests can be determined by formula

$$S_2 = \sqrt{S^2_{\lg N_{\min}} + \frac{(mS_{\lg \sigma})^2}{n_{изм}}}. \qquad (11.35)$$

Using the same reasoning as above (see No. 8), we will attribute to the fact that the probability of destruction in this case can be determined by the expression analogous to (11.19):

$$P_2 = \int_{-\infty}^{\infty} \varphi_{\min}(\xi_2) \left[\int_{-\infty}^{t_0 - \lg \eta_N^0} \varphi_{экс}(\xi_1)\, d\xi_1 \right] d\xi_2. \qquad (11.36)$$

If the distribution of logarithms of the minimum number of cycles prior to destruction during tests can be approximately represented by the normal law of distribution, then expression (11.36) can be copied in the form:

$$P_2 = \frac{1}{2\pi} \int_{-\infty}^{\infty} \frac{1}{S_2} e^{-\frac{(\xi_2 - m_2)^2}{2S_2^2}} \left[\int_{-\infty}^{t_0 - \lg \eta_N^0} \frac{1}{S_1} e^{-\frac{(\xi_1 - m_1)^2}{2S_1^2}} d\xi_1 \right] d\xi_2. \qquad (11.37)$$

If one were to introduce new variables

$$\bar{\xi}_1 = \frac{\xi_1 - m_1}{S_1} \text{ and } \bar{\xi}_2 = \frac{\xi_2 - m_2}{S_2}, \qquad (11.38)$$

then expression (11.37) will be converted to the form:

$$P_3 = \frac{1}{2\pi} \int_{-\infty}^{\infty} e^{-\frac{\bar{\xi}_2^2}{2}} \left[\int_{-\infty}^{f(\bar{\xi}_2)} e^{-\frac{\bar{\xi}_1^2}{2}} d\bar{\xi}_1 \right] d\bar{\xi}_2. \qquad (11.39)$$

where the upper limit $f(\bar{\xi}_2)$ is determined by expression

$$f(\bar{\xi}_2) = \frac{S_2}{S_1} \bar{\xi}_2 + \frac{\lg \eta_N + (m_1 - m_2)}{S_1}. \qquad (11.40)$$

Substituting here values m_1 and m_2, we will obtain:

$$f(\xi_2) = \frac{S_2}{S_1} \xi_2 + \frac{m \lg n_0 + \lg \eta_N + m \lg N_{\text{исп}} - m \lg N_{\text{min}}}{S_1}. \qquad (11.41)$$

From this expression it follows that the probability of destruction P_Σ can be determined for each η_σ, if there is known these values

$$S_1,\ S_2,\ \eta_N \text{ and } \Delta m_{\lg N} = m_{\lg N_{\text{исп}}} - m_{\lg N_{\text{min}}}.$$

It is possible to propose the following method of determination of the necessary margin η_σ. Let us construct the dependences S_2/S_1 on $\frac{m \lg \eta_0 + \lg \eta_N + \Delta m_{\lg N}}{S_1}$ for assigned values of P_Σ (see Fig. 1.76). Then, by determining S_1 and S_2 by formulas (11.29) and (11.35), it is possible according to Fig. 1.76 for assigned value $P_{\text{зад}}$ to determine

$$\frac{m \lg \eta_0 + \lg \eta_N + \Delta m_{\lg N}}{S_1}, \qquad (11.42)$$

whence, knowing η_N, $\Delta m_{\lg N}$ (see Fig. 1.70) and S_1, it is easy to determine η_σ.

The method expounded here is rather simple, although it requires in the determination of service life several more complex calculations as compared to the method expounded in No. 10 where margins η_σ

are calculated from values taken directly from the graph.

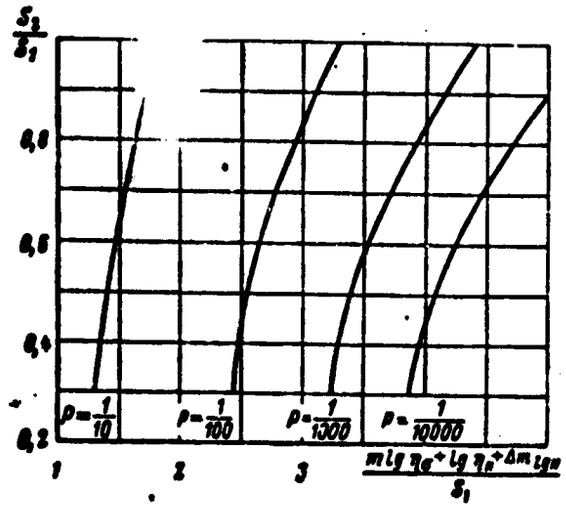

Fig. 1.76. Graph for determination $\frac{m\lg\eta_\sigma+\lg\eta_N+\Delta m_{\lg N}}{S_1}$ in the function S_1/S_2 at different assigned probabilities of destruction.

From the formulas given it follows that with the assumptions accepted here safety margins η_N and η_σ can be united into one criterion $\eta=\eta_N\eta_\sigma^m$ or we can replace one safety margin by another. This appears convenient in the fulfillment of calculations and carrying out of dynamic tests, which has already been discussed in No. 7 but does not give any alleviations in the selection of margins η_N and η_σ, since their values are determined from various conditions.

12. Example of the Calculation of Service Life

As an example let us give calculation of service life for the blade of a heavy helicopter with a spar in the form of a steel tube.

In determining service life of a blade the calculation should be carried out for sections located on different relative radii, after which service life of the whole blade obtained for the weakest section is established.

Let us assume that the weakest proved to be the section on the relative radius $\bar{r}=0{,}74$.

We will assume that results of dynamic tests of five spar samples with the amplitude of varying stresses of ± 15 kG/mm^2 consist in the following (Table 1.20).

Table 1.20.

No. of sample	Number of cycles of loading	Results of tests
№ 1	$9{,}8 \cdot 10^6$	Sample was destroyed
№ 2	$20 \cdot 10^6$	Samples were not destroyed
№ 3	$20 \cdot 10^6$	
№ 4	$20 \cdot 10^6$	
№ 5	$20 \cdot 10^6$	

From results of tests let us draw the conclusion that fatigue limits σ_w of samples Nos. 2, 3, 4 and 5 appeared above $\sigma_w = 15$ kG/mm^2. Consequently, probability P of the fact that the fatigue limit σ_w is lower than 15 kG/mm^2 can be accepted equal to 0.2.

Assuming $S_{\lg \sigma_w}$ is equal to 0.07 (see No. 13), we will obtain that the probability of 5% corresponds to fatigue limit $\sigma_{w_{5\%}} = 13$ kG/mm^2. This fatigue limit will be considered minimum.

The margin according to the number cycles can be accepted either on the basis of the practical experience of assignment of service life in accordance with Table 1.16 or by the method of A. F. Selikhov (see No. 8). On the basis of Table 1.16 for group II of units (the blade has a device indicating spar damage) and n = 5, the safety margin η_N can be accepted equal approximately to 2.7.

In the second case it is necessary to know $S_{\lg N}$. It is obvious that according to the results of the given tests it is impossible to determine the value $S_{\lg N}$. However, it is possible to assign the definite value $S_{\lg N}$ on the basis of results of tests of analogous samples.

Let us assume that $S_{\lg N} = 0.4$. Then, by assigning the value $P_{экв} = \frac{1}{1000}$ (group II of the units), from Fig. 1.72 we will obtain $\lg \eta_N = 2.3 \times S_{\lg N}$, i.e., $\eta_N = 8.3$. Thus, the required safety margin with respect to the number of cycles η_N by the method of A. F. Selikhov appear considerably larger than that which could be taken on the

basis of experience of the service life assignment. This distinction in many cases is compensated partially by introduction into the calculation of the concept of fatigue limits and by refinement of the necessary safety margins η_σ.

As was already said above in the assignment of service life with the use of safety factors selected on the basis of practical experience, value η_σ was taken always equal to 1.2. However, this coefficient can be refined in accordance with the method expounded in Nos. 10 and 11. But for this it is necessary to have more complete data on scattering of amplitudes of varying stresses with respect to different copies of the construction.

Let us assume that measurement of stresses is taken only in one copy of the construction. However, on the basis of the experience of measurements in similar units of other helicopters it is possible to consider that $\gamma_\sigma = 0.08$, and consequently $S_{lg\,\sigma} = 0.035$. Then by methods expounded in Nos. 10 and 11, we will obtain that $\eta_\sigma = 1.11$. Nevertheless we will take $\eta_\sigma = 1.2$.

The minimum value N_{min} from five tested samples ($n = 5$) with the amplitude of varying stresses $\sigma = \mp 15$ kG/mm^2 consists of $N_{min} = 9.8 \times 10^6$ cycles.

The number cycles corresponding to the minimum fatigue limit will be determined by the formula

$$N_{\sigma_{min}} = N_{min}\left(\frac{\sigma_{ke}}{\sigma_{min}}\right)^m = 23 \cdot 10^6,$$

and value N_i by the formula

$$N_i = \frac{N_{\sigma_{min}}}{n_w}\left(\frac{\sigma_{min}}{n_\sigma \sigma_{s_i}}\right)^m.$$

During calculation of service life we will consider that in those conditions where effective stresses are lower than the minimum value of fatigue limit, defectibility is not introduced into the construction.

Equivalent stresses in separate conditions of flight will not be calculated, and we will take them to be equal to the maximum measured amplitudes of stresses. In this case the value ε_i will only be equal either to zero or unity.

The calculation of equivalent stresses will be reduced in Table 1.21.

Table 1.21. Example of calculation of service life of a blade by section on the relative radius $\bar{r}=0{,}74$; $\sigma_{w\,min}=13$ kG/mm^2; $\xi=0{,}5$; $m=5$; $S_{lg\,N}=0{,}4$; $\eta_b=1{,}2$; $\eta_W=0{,}3$ $\left(P_{max}=\frac{1}{1000}\right)$; $N_{w\,min}=23\cdot10^6$.

Flight Conditions	ε_i	a_i	σ_{z_i}	σ_{y_i}	$\xi=0{,}5;\ \sigma_{z_i}$	$\eta_b\cdot\sigma_{z_i}$	N_i	$\frac{a_i}{N_i}$
Hovering	0	0,1	6,0	5,8	9,7	11,64	∞	0
Low speeds								
$V=20$ km/h	1	0,03	7,2	10,5	11,6	13,92	$1{,}84\cdot10^6$	$0{,}016\cdot10^{-6}$
$V=30$ km/h	1	0,02	10,5	13,2	15,02	18,02	$0{,}39\cdot10^6$	$0{,}051\cdot10^{-6}$
$V=60$ km/h	1	0,05	12,4	12,5	15,05	18,06	$0{,}39\cdot10^6$	$0{,}128\cdot10^{-6}$
Acceleration	1	0,02	9,5	12,4	14,0	16,8	$0{,}59\cdot10^6$	$0{,}034\cdot10^{-6}$
Climb	0	0,06	6,0	5,6	6,9	8,28	∞	0
Cruising speed	0	0,55	8,0	9,0	10,5	12,60	∞	0
Maximum speed	1	0,10	8,0	10,5	11,09	13,31	$2{,}4\cdot10^6$	$0{,}042\cdot10^{-6}$
Glide	0	0,05	7,5	7,2	8,8	10,56	∞	0
Deceleration								
1st stage-σ_{max}	1	0,002	15,2	18,4	21,11	25,33	$0{,}05\cdot10^6$	$0{,}04\cdot10^{-6}$
2nd stage-0,7 σ_{max}	1	0,007	10,64	12,88	14,79	17,75	$0{,}43\cdot10^6$	$0{,}016\cdot10^{-6}$
3rd stage-hovering	0	0,011	6,0	5,8	9,72	11,66	∞	0
		$c=0{,}229$						$\Sigma 0{,}327\cdot10^{-6}$

If one were to assume that the service life obeys the law (11 21) at levels of varying stresses and the fatigue limit does not exist (in this case $a_i=1$ in all conditions), then all flight conditions are equivalent in defectibility to conditions with the amplitude of stresses $\sigma_{max}=11.5$ kG/mm^2, acting during the whole service life of the blade. In this case

$$N_{min} = N_{\sigma_{min}} \left(\frac{13}{1,2 \cdot 11,5}\right)^m = 16,2 \cdot 10^6;$$

$$N_{exp} = \frac{N_{min}}{\eta_N} = 1,95 \cdot 10^6;$$

$$R = \frac{N_{exp}}{60f} = 271 \text{ h}.$$

If we assume that the minimum fatigue limit $\sigma_{\sigma_{min}} = 13$ kG/mm^2, then one condition [see formula (11.9)] with amplitude $\sigma_{max} = 13.6$ kG/mm^2 will be equivalent to all conditions of the flight. The duration of this condition, as follows from Table 1.21, will make up about 23% of the service life of the blade ($\varepsilon = 0.229$).

Then service life can be determined in the following way:

$$N_{min} = N_{\sigma_{min}} \left(\frac{13}{\eta_\sigma \sigma_{max}}\right)^m = 3,86 \cdot 10^6;$$

$$N_{exp} = \frac{N_{min}}{\eta_N} = 0,707 \cdot 10^6;$$

$$R = \frac{N_{exp}}{60f_1} = 429 \text{ h}.$$

The same result can be obtained with respect to total defectibility without the use of the concept of equivalent stresses [see formula (11.5)]:

$$N_{exp} = \frac{1}{\sum_i \frac{a_i}{N_i}} = 3,09 \cdot 10^6;$$

$$R = \frac{N_{exp}}{60f} = 429 \text{ h}.$$

The results given show that with the introduction of the concept of fatigue limit the service life of the blade by calculation appears greater.

It is necessary, however, to consider that margins with respect to the cycles given in Table 1.16 were introduced into the calculation not assuming existences of the fatigue limit. Therefore, in calculations with fatigue limit they should not be used.

13. Possible Means of Determining the Minimum Fatigue Limit of the Construction

From the above-mentioned example it is clear that during calculation with the use of the concept of minimum fatigue limit considerably large values of service life of the construction can be obtained. Therefore, the determination of its values in many cases appears extremely necessary.

The detecting of values $\sigma_{\min}$ according to results of tests with quite good accuracy proves to be a practically unrealizable problem. It is only possible to calculate a very tentative determination of this value. But even for this a considerable increase in the number of test samples is required. Nonetheless, the use in calculating service life of even tentative values of fatigue limits substantially approaches results of calculations to reality and opens up the possibility for the acceptance of more competent technical solutions. Therefore, it is recommended in all cases to arrive at the determination of fatigue limits by using for this both the tentative and even simple formal methods of calculation.

First of all one should try to determine parameters of the law of distribution of fatigue limits. For this it is necessary to conduct fatigue tests of samples on several levels of varying stresses lying in the region of the distribution of fatigue limits. Tests should be conducted on a quite large base with respect to the number cycles. With the selection of the base of tests we usually consider that for steel samples the base can be set somewhat greater than 10^7 cycles (for example 2×10^7 cycles) and for Duralumin samples, somewhat larger than 2×10^7 cycles (frequently a base of 5×10^7 cycles is taken).

The probability of the fact that the fatigue limit is higher than the assigned level of varying stresses is determined as a ratio of numbers of samples which underwent tests in the assigned base without destruction of n_{exp} to the total number of n samples tested in this level and one smaller in stresses.

$$P = \frac{n_{exp}}{n}.$$

The thus obtained distribution of fatigue limits can coincide with the normal law only on the small section corresponding to mean values of probability (Fig. 1.77). At small probabilities the distribution of fatigue limits deviates from the normal law and has a certain threshold of sensitivity $\sigma_{\min}$. At large probabilities, starting from some stresses $\sigma_{разр}$, all samples are destroyed and do not undergo the assigned base of tests.

Fig. 1.77.

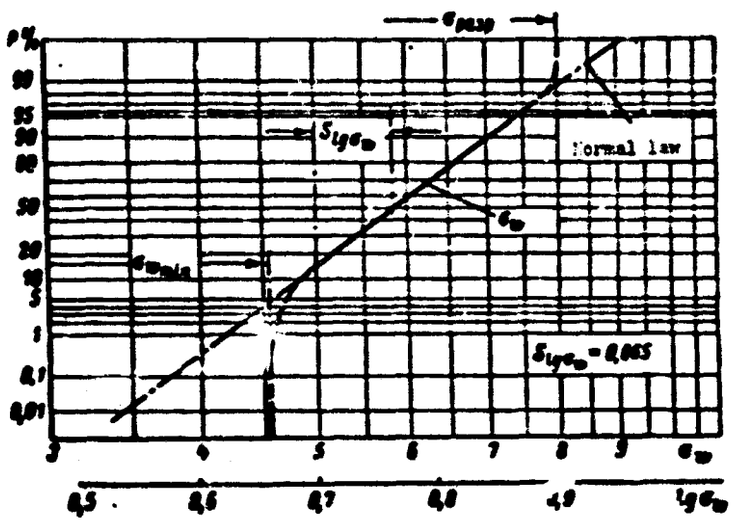

Fig. 1.77. Distribution of fatigue limits.

The distribution of fatigue limits with mean values of the probability of destruction is best represented with the help of the logarithmically normal law of distribution. It can be used for the determination of minimum values of fatigue limits.

Available results of tests of samples of the blade show that for this law there can be accepted values $S_{\lg\sigma}$, equal approximately to

$$S_{\lg\sigma} = 0{,}05 \div 0{,}07,$$

where $S_{\lg\sigma}$ is the root-mean-square deviation in the distribution of logarithms of fatigue limits.

It is impossible to propose a sufficiently reliable method for determination of σ_{min}. Therefore, only an especially formal method can be recommended, which, however, in practice gives quite good results. One can assume that the minimum fatigue limit coincides with value σ_w, which corresponds to 5% of the probability and logarithmically normal law of distribution of fatigue limits.

If one were to take such an approach, then for a refinement of values σ_{min} there can be used the method founded on the carrying out of fatigue tests for two levels of varying stresses close in amplitude. The test samples, which should not be less than 15-20, are divided into two groups.

The first group is tested during maximum varying stresses, which supposedly do not exceed the minimum fatigue limit, and therefore it is desirable that not one of them be destroyed at the number cycles corresponding to the selected base of tests. Results of tests of this group serve as confirmation of the fact that the minimum fatigue limit can indeed correspond to their level of tests.

The second group of samples is tested at greater varying stresses in such a way that some part of them is destroyed, not operating through an established number of cycles. Determining the probability of the fact that the fatigue limit is lower than the amplitude of the second level of tests and assigning some value of $S_{lg\sigma_w}$ we calculate the value σ_w corresponding to the probability of 5%. If data of tests of the first group do not contradict this result, then the thus obtained value $\sigma_{w5\%}$ can be accepted for the minimum fatigue limit.

Sometimes for greater reliability we consider that the minimum fatigue limit corresponds to smaller values of probability, let us say, the probability $\frac{1}{100}$. It is apparently inexpedient to take even lower values of this probability.

It is necessary to note that in many cases for the characteristic of fatigue limit there is used the conditional concept which would have been possible to call the given fatigue limit.

The given fatigue limit is determined by conversion of results of tests by formula (11.3) to the conditional base taken usually equal to $N_{баз} = 10^7$ cycles for steel and $N_{баз} = 2 \times 10^7$ cycles for Duralumin:

$$\sigma_{w_{пр}} = \sigma_{исп} \sqrt[m]{\frac{N_p}{N_{баз}}},$$

where $\sigma_{исп}$ is the amplitude of varying stresses during the tests; N_p – number of cycles up to destruction corresponding to the probability of destruction equal to P; m – exponent of Wöhler curve, it is usually taken that m = 6.

If one were to take N_p, which corresponds to the probability of destruction, equal to 5%, then value $\sigma_{w_{пр}}$ gives the tentative concept of the value of minimum fatigue limit. Frequently for the characteristic of fatigue strength, instead of N_p there is taken the minimum value of the number cycles up to destruction of the construction N_{min}. It must be stressed that the given fatigue limit, no matter how it is determined, does not correspond to the concept of fatigue limit in the sense in which it was used above in this paragraph.

Important also is the fact that the distribution of the given fatigue limits has a root-mean-square deviation equal to

$$(S_{lg\,\sigma_w})_{пр} = \frac{S_{lg\,N}}{m},$$

which is almost always larger than value $S_{lg\,\sigma_w}$.

14. Advantages and Deficiencies of Different Approaches in the Determination of Necessary Safety Margins and the Approximate Evaluation of Their Accuracy

The simplest approach, as was already shown above (see No. 7), should be considered the calculation of service life with the use of coefficients n_N and n_σ accepted on the basis of practical experience of the assignment of service life. These coefficients were checked on a large number of helicopters, and many hundreds of units successfully produced the service life thus established. It is necessary, however, to consider the fact that the application of

coefficients n_N and n_σ thus taken is confirmed by practice only in combination with a definite method of calculating service life, which differs, in particular, by the following assumptions:

1. The fatigue limit does not exist and the Wöhler curve is described by formula (11.21). Coefficients ε and ε_1 are respectively taken equal to unity.

2. In each condition of flight the amplitude of stresses is considered equal to the maximum measured value of it in this condition.

However, such an approach to the calculation of service life has considerable deficiencies:

1. In the determination of service life there is not considered a distinction in the scattering of characteristics of service life, which can appear unequal for units of various construction distinguished furthermore, by the application of different materials and different technology of manufacture. Not considered also is the value of scattering of stresses acting in different copies of the construction.

2. The rejection of the concept of fatigue limit and the use in calculation of only maximum amplitudes of stresses acting in each flight condition lead to incorrect concepts on the portion of defectibility introduced by different conditions of flight.

Therefore, the tendency to use more improved methods with the attracting of basic positions of the theory of probability is quite regular. One of the possible variants of such an approach is given in Nos. 8, 10 and 11.

It should be noted that in the form in which this method is expounded here, it gives quite satisfactory values of service lives rather close to those which are obtained by the preceding method. It is true that in values of safety factors a certain redistribution occurs. The margin n_N appears considerably large but then the

reserve n_σ is decreased. Furthermore, in the calculation there should be used the concept of minimum fatigue limit; otherwise service lives appear understated.

In the use of such a method there is frequently doubt in the application of so great probabilities of destruction equal to $\frac{1}{1000}$ and even greater. Actually, this means that one unit in a thousand certainly should be destroyed during service life. Therefore, here one should once again stress that the shown values of probabilities are purely conditional values which correspond to the normal law of distribution of service life. In reality, in the region of small values of the probability of destruction, this law deviates from the normal, and in characteristics of service life the threshold of sensitivity is observed. Its values lie in the region of probabilities equal approximately to $\frac{1}{100}$ or somewhat differing from this value. Consequently, assignment of the conditional probability $\frac{1}{1000}$ in reality is equivalent to the requirement of a very small or even zero probability. Therefore, it is impossible to agree with those authors who consider it possible to present a requirement on providing a probability of the order of 10^{-6} or even 10^{-7} with the use of the normal law of distribution of service life. Such requirements do not have sufficient bases.

For each one who studies the above-stated method there is usually also objections in the possibility of rejecting the refinement of values of root-mean-square deviations $\tilde{S}_{lgN}$ obtained by experiment with respect to the usually quite high values of confidence probability accepted in practice of the application of methods of the probability theory. If one were to accomplish this refinement, then in the calculation it would be necessary to use value S_{lgN}, increased in q times (see No. 9), which would lead to an increase in the required margin n_N and, accordingly, to the lowering of service life.

Besides those considerations which were already given previously (see No. 9), here one should note that in the proposed method of calculation there exists another inaccuracy. Instead of equivalent stresses acting in different conditions of flight, usually their

maximum values are taken, which leads to an understating of the service life. These two inaccuracies mutually compensate one another, and a rejection of one of them should certainly be accompanied by a rejection of the other. In this case values of service lives obtained by calculation essentially will not be changed.

There are no doubts that in the course of time with the appearance of new experimental data in the method of calculation of service life it will appear necessary to introduce more substantial refinements. Operational experience of helicopters and the ever larger number of results of dynamic tests will also probably reveal such a necessity.

15. Requirements for Strength of the Blade in the Selection of Its Design

The helicopter blade operates in conditions very difficult for its strength. During the service life it undergoes very great constant and live loads. This peculiarity of conditions of blade operation has extraordinarily stringent requirements on its design and, first of all, fatigue strength of its basic supporting member to the longeron. Therefore, the blade spar should be made only from materials possessing very high characteristics of fatigue strength.

The most widespread at present are constructions of the blade with spars in the form of a steel tube and pressed Duralumin spar.

Very good results can be expected with the manufacture of spars from different synthetic materials. Constructions of blades with a fiberglass spar are known. However, sufficiently serious operational experience of such blades is still not available. Therefore, we will not stop and dwell on their strength.

The most important requirement for blades with steel and Duralumin spars appears to be the requirement of maximum elimination of some concentrators of stresses lowering their fatigue strength. In the construction of blades application of bolt and rivet fittings is impermissible. The frame of blade is fitted to the spar only with the help of adhesive connections.

The application of fittings with large concentrators of stresses is allowed only on sections with small varying stresses, for example, the shanks of the blade near hinges of the hub. Here, in spite of the small varying stresses, the section of the longeron in the region of the shank joint must be increased 3-4 times. Only a very great lowering of varying stresses permits using fittings with concentrators.

Small technological defects, which are also concentrators of stresses sharply lower the fatigue strength. Therefore, in the manufacture of spars of blades there is used only such technology which leads to total elemination of all visible defects of the spar.

To exclude the possibilities of the passing of some defects the spars should pass careful control with the application of all contemporary means of such control.

Let us consider more specifically the strength properties of blades with steel and Duralumin spars.

16. Strength of the Blade with a Steel Tubular Spar

For the spar of the blade there is usually used a cold-rolled tube of high-alloy steel of the type 30KhGSA or 40KhNMA, hardened and tempered to a strength σ_b = 110-130 kG/mm^2.

After hot and cold rolling, embossing and hardening the external and internal surfaces of the tube are polished. Recently an obligatory operation after polishing was also work hardening of the spars.

A thus made spar without cold hardening can have a minimum fatigue-strength of the order of $\sigma_{w_{min}}$ = 12-13 kG/mm^2 with an average component of cycle σ_m = 20-25 kG/mm^2. However, its strength can decrease considerably, if in the manufacture of the spar there will be allowed different technological defects and miscalculations.

The most dangerous of them can be the following.

Tears and laps. In the process of hot rolling plastic deformations can be accompanied by a partial break in the material. This occurs usually with a decrease in the temperature of rolled blank, and also as a result of the contamination of the steel by nonmetallic and gas pockets, formation of seams, high porosity, liquation and other metallurgic defects. The breaks forming are directed into the body of the blank at an acute angle, and therefore the trace of tear emerging to the surface is often poorly seen.

With further cold rolling the degree of deformation is increased and the tear is rolled into the wall of the tube at an ever smaller angle to its surface. Usually there is observed a series of such tears. Their dimensions are small: depth, 0.1-1.0 mm, and width 4-10 mm.

Laps appear with cold rolling on the external surface. They occur due to the great unevenness of the external surface after hot rolling. Subsequent plastic cold deformation leads to a nonuniform motion of the material at which there can be formed defects called laps. Laps can also be formed as a result of the flow of metal into the clearance between gauges of rollers and the appearance of burr and lap of it with subsequent deformation.

Both defects can be revealed with magnetic control on the polished surface. Figure 1.78 shows the characteristic tears on the internal surface of a spar. The photograph was made with magnetic control. The fatigue limit of the tube with tears and laps drops down to $\sigma_{w_{min}} = 5\text{-}7\ kG/mm^2$.

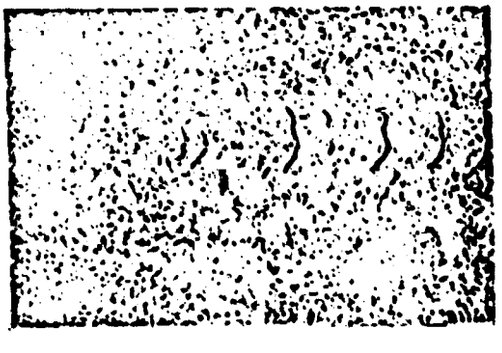

Fig. 1.78. Tears on the internal surface of a steel spar.

"Fine" on the internal surface. After hot rolling on the surface of the tube there remains a layer of scale which has greater hardness than that of metal. After each transition with cold rolling annealing is produced. Although annealing is produced in an inert atmosphere, nonetheless on the surface thin films of scale appear owing to the oxygen of the metal. If the scale is not completely eliminated, then with rolling it is crushed and enters into the metal, forming a so-called "fine." On the open external surface of the spar tube the "fine" is easily removed by machining. On the internal surface of the tube, the treatment of which is more complex and possible only by means of ribbon grinding or hydropolishing, the "fine" cannot be completely eliminated. Therefore, the small but sharp notches, with dimensions not exceeding 0.1-0.05 mm, and difficult to distinguish with inspection, can remain even after grinding. Fatigue strength of the surface descends to $\sigma_{w_{min}}$ = 10-12 kG/mm^2.

A "fine" can be removed by boring and grinding of the surface of blank up to complete removal of the scale after hot rolling and by sand chipping after annealing before each transition of cold rolling.

For complete removal of tears, laps, "fines" and other surface defects, longitudinal grinding of the external and internal surface of the tube is very effective after the final cold rolling prior to its profiling (embossing).

Lowering of fatigue strength from tube dressing. After hardening and tempering the spar tubes appear somewhat distorted. Therefore, before assembly of the tube blade it is frequently necessary to straighten it. In the material of the tube residual stresses appear. Usually with correction there are introduced limiters, which do not allow increasing the residual stresses of extension in the tube of more 10-20 kG/mm^2. These stresses increase the average component of the cycle and lead to a decrease in fatigue limit of 20-25%. Even greater losses in strength can occur with incorrect dressing. In order to exclude the necessity of correction there should be tempering

of the hardened tubes in special attachments, which remove deformations appearing in the process of hardening.

In evaluating fatigue strength of spars special attention should be payed to the possibility of the appearance of frictional corrosion. Frictional corrosion appears an almost obligatory process of cyclical load of blades and leads to considerable lowering of fatigue strength. It appears usually in places of contact with the spar parts attached to it, if among these parts and the spar there are relative microshifts. Usual place of the appearance of frictional corrosion on a steel spar are places of setting of collars for attachment of the frame of the blade.

Figure 1.79 gives a photography of a destroyed spar. The beginning of the fatigue crack coincides with the spot of frictional corrosion.

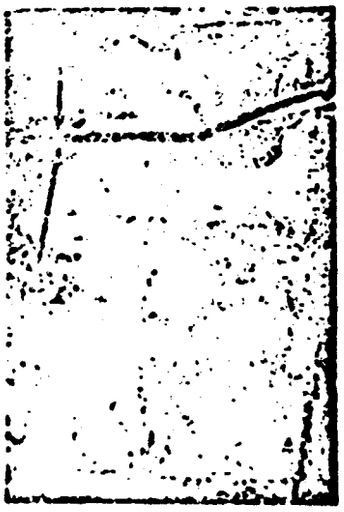

Fig. 1.79. Place of the beginning of fatigue failure from frictional corrosion.

A sharp increase in dynamic strength of steel spars occurs in the use of mechanical hardening of their surface usually called cold hardening.

At present cold hardening of spars have become almost an obligatory operation in the manufacture of blades. In helicopter construction the most widespread are three methods of mechanical hardening: the dynamic method of M. I. Kuz'min, vibration shock method of S. V. Ochagov and the shot-blasting method. The selection of some method usually depends on peculiarities of the hardenable

structural part and industrial possibilities. In those cases when for hardening of the external surface of a spar there is used the dynamic method, its internal surface is strengthened by the shot-blasting method. With the creation of complex installations for the vibration shock method one should usually consider that it is expedient to treat by this method simultaneously both the external and internal surface of the spar.

An increase in fatigue strength is observed in the application of all methods of cold hardening. The best method giving the stablest results with treatment of the external surface of the steel spar should be considered the dynamic method of M. I. Kuz'min.

The increase in fatigue strength from cold hardening is explained basically by two causes. The external surface of a hardenable component most sensitive in the beginning of fatigue failure becomes, first, smoother (Fig. 1.80), and secondly, in it are created residual stresses of compression, which in accordance with the Hay diagram (see Fig. 1.63) leads to an increase in fatigue strength of surface layer of the component.

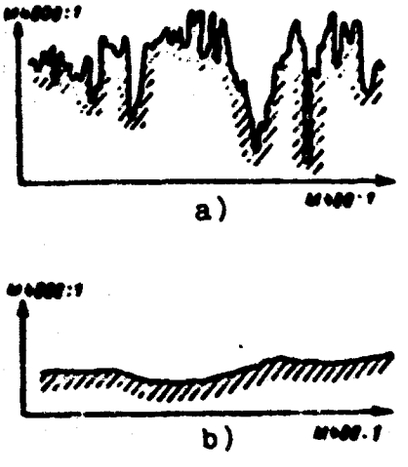

Fig. 1.80. Profilegram of the surface of a spar pressed from aluminum alloy after machining (a) and after cold hardening (b).

Figure 1.81 shows the distribution of internal stresses in the material of a steel spar obtained as a result of dynamic cold hardening and blowoff by metallic sand. Blowoff by metallic sand gives almost the same residual stresses as that of the shot-blasting method of cold hardening.

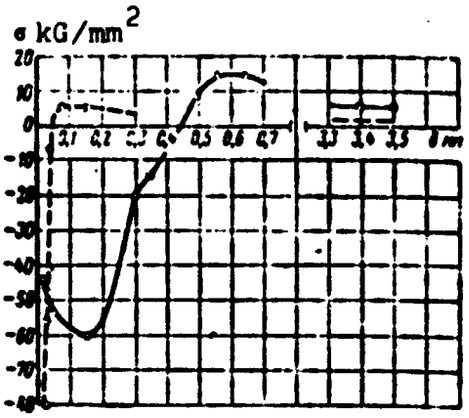

Fig. 1.81. Distribution of internal stresses from cold hardening with respect to the thickness of the wall of a steel tubular spar: ——— cold hardening according to the method of M. I. Kuz'min; ----- triple blow-off by metallic sand.

Especially great is the increase in fatigue strength from cold hardening in the presence of frictional corrosion. Apparently, compression stresses prevent propagation of corrosion in depth of the material. Figure 1.82 gives results of tests of steel spars with riveted and unriveted surfaces, operating under conditions of the appearance of frictional corrosion.

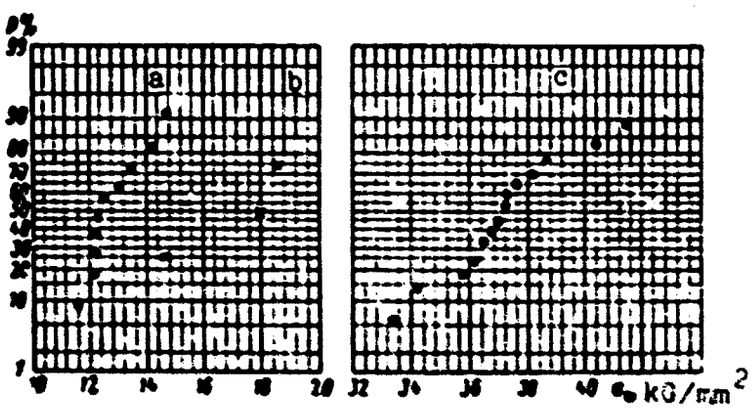

Fig. 1.82. Distribution of given fatigue limits of steel tubular spars under the influence of frictional corrosion:
a) surface is polished and sand chipped;
b) surface is polished and sand chipped; three times by metallic sand; c) surface is riveted according to the method of M. I. Kuz'min.

The fatigue strength of steel spar with the application of mechanical hardening can be increased 1.5-2 times and in the presence of frictional corrosion, 2.5-3 times.

With the application of cold hardening the fatigue limit of a steel spar can be increased up to values of the order of $\sigma_{w_{min}}$ = = 28-30 kG/mm^2 with σ_m = 20-25 kG/mm^2. Therefore, cold hardening appeared the most active means of increasing the reliability and service life of blades.

17. Strength of a Blade with a Duralumin Spar

The most important problem in the creation of blades of such construction is the providing of sufficiently high fatigue strength of the spar. Attachment of frame to the spar is accomplished, as a rule, by glue and does not create in the spar any substantial concentrators of stresses. Concentrations of stresses in the spar appear basically from small defects allowed in its manufacture.

The basic role in decreasing fatigue strength of the spar is played by the state of its surface. The milled and sand chipped spar from alloy AVT-1, without treatment of the internal surface, can have a fatigue limit of the order of $\sigma_{w_{min}}$ = 3.8-4.2 kG/mm^2 with the average component of the cycle σ_m = 6 kG/mm^2.

The fatigue strength of the spar can descend as a result of defects appearing in the process of pressing of the spar and during its machining.

Frequently the internal channel of the spar is not treated after pressing. Therefore, on the internal surface defects of the process of pressing can remain: longitudinal scratches, gas holes (Fig. 1.8[illegible]) and, finally, a macrocrystalline ferrule. These defects can lower the fatigue strength down to values $\sigma_{w_{min}}$ = 2.5-3.0 kG/mm^2 (σ_m = = 6 kG/mm^2). Therefore, the internal surface of spars of blades with relatively high stresses should be certainly subjected to machining after pressing.

GRAPHIC NOT REPRODUCIBLE

Fig. 1.83. Microsection of the section of spar web through the gas hole formed in the process of pressing.

Considerable lowering of fatigue strength occurs also from nonmetallic and gas inclusions. To eliminate the inclusions there should be used special technology of smelting (sediment of metal, overflow of it from definite levels, filtration through screen filters, etc.). The most qualitative metal is obtained with melt in electrical induction furnaces with the holding of smelted metal in electrical heatable settling tanks (mixers).

To eliminate the possibility of the passing of nonmetallic and gas inclusions each spar should obligatory pass the checking with the help of ultrasonics.

Of no less importance is the exclusion of the possibility of corrosional damage of pressed spar in the process of production (just as under conditions of operation). Experience shows that external and intercrystalline corrosion with a depth to 0.1-0.15 mm can sharply lower the fatigue limit. Therefore, for spars of blades there should be selected a metal with high corrosion resistance, but in production special measures with respect to the protection of spars from corrosion are accepted with the application of galvanic platings after intermediate operations of its treatment (for example, anodizing).

A sharp increase in fatigue strength of spars from aluminum alloys can be attained by the application of mechanical hardening of the spars. Figure 1.84 gives results of fatigue tests of strengthened spars in comparison unstrengthened ones. Here the distribution of internal stresses from cold hardening is shown. Fatigue strength of strengthened spars can be reduced to values $\sigma_{w_{min}} = 5.5\text{-}6.0$ kG/mm^2 ($\sigma_m = 6.0$ kG/mm^2).

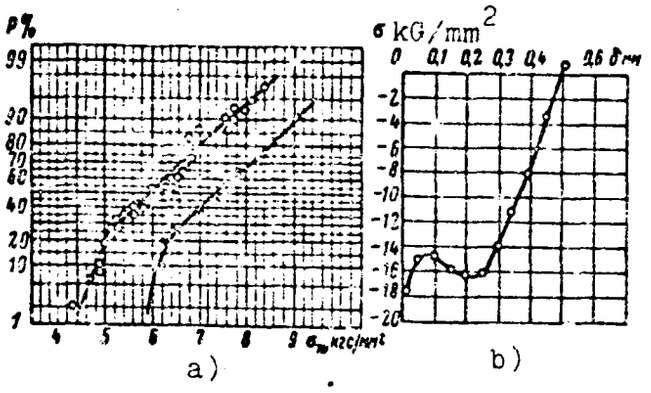

Fig. 1.84. Distribution of given fatigue strengths (to the base of 10^7 cycles) of pressed spars from alloy AVT-1 with polished (circles) and riveted (small crosses) surfaces (a), and the distribution of compression stresses with respect to thickness of the spar web from cold hardening by the vibration shock method of S. V. Ochagov (b).

It is necessary to pay attention to the fact that the strength of riveted Duralumin spars can be sharply decreased, if with gluing of the frame the spar will be heated to a temperature of about 200°C and more. Therefore, the temperature with gluing should be thoroughly checked.

18. Influence of Conditions of Operation on Fatigue Strength of Spars

The above-mentioned method of determination of fatigue strength and service life can be used only in the case when in the process of operation the construction does not undergo any mechanical and corrosional damages. Otherwise the approach to determination of service life should be completely modified and reduced to the study of the influence of these damages. From these positions the designs of

all blades should be divided into two types: blades with shielded and open spar.

In the construction of a blade based on a steel tube the spar usually is completely shielded by the frame and cannot be mechanically damaged in operation. The greatest danger for such a construction is corrosion, and therefore the period of service of such blades is determined by the quality of anticorrosive coverings of the spar.

In constructions of blades for which the spar forms the contour of the nose part of the profile, special attention must be given to its protection from mechanical damages. If this protection is weak, then the service life sharply drops and appears dependent on the magnitude of damages inflicted to the spar. Usually in these cases there is established a permissible magnitude of damages controlled with preflight inspection of blades.

To estimate the influence of damages of the spar in the operation there are usually conducted dynamic tests of samples cut from blades, which spent a definite number of hours in different conditions of operation, and there is estimated the possibility of preservation of service life set by it with respect to conditions of strength of samples unimpaired in operation. With substantial lowering of fatigue strength measures for improvement of shielding of the spar are started.

Footnotes

[1]Here and further in values of kinetic and potential energy of oscillations, for simplicity the constant coefficient 1/2 is omitted.

[2]This is correct with an accuracy to the constant factor equal to 1/2, which in expressions (3.3), (3.4) and (3.7) is omitted.

[3]Such a method for calculation of the blade of the helicopter was first used by R. M. Zanozina.

[4]An analogous approach in reference to the calculation of aircraft constructions was proposed by V. L. Raykher.

C H A P T E R II

VIBRATIONS OF THE HELICOPTER

§ 1. Forces Creating Vibrations of the Helicopter

1. Frequencies of Excitation

Since with the forward flight of a helicopter blades of the rotor, found under the action of aerodynamic forces variable in time accomplish vibrations and both in the plane of thrust of the rotor and in the plane of rotation, then forces of reaction acting on the blade in hinges of the hub are also variable with time. Accordingly, on the hub of the rotor there act variable force equal in magnitude to these forces of reaction.

Variable force, acting on the hub of the rotor on the side of the vibrating blades, can be assigned in the form of three forces $X(t)$, $Y(t)$, $Z(t)$ and three moments with respect to coordinate axes $M_x(t)$, $M_y(t)$, $M_z(t)$ (Fig. 2.1). If for a helicopter there is a

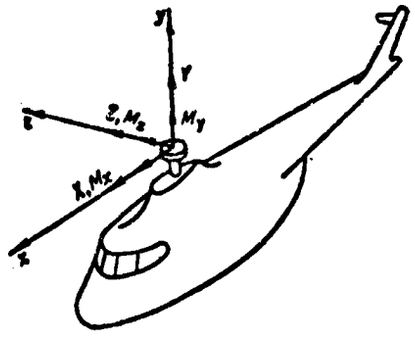

Fig. 2.1. Forces and moments acting on the helicopter from the rotor.

tail (antitorque) rotor, then on the side of blades of this rotor acting on the helicopter are also forces variable in time of the same

origin, which are also convenient to assign in the form of three variable forces and three moments.

Variable forces acting on the helicopter on the side of vibrating blades of the rotors are the main source of vibrations of the fuselage.

Vibrations of fuselage can also be caused directly by aerodynamic forces acting on the fuselage on the side of the pulsating flow of air repulsed by the rotor. Thus, the flow rate repulsed by the rotor in the region of the fuselage is increased when any of the blades of the rotor passes above the fuselage. However, numerous calculations and measurements of pulsations of pressure on the fuselage show that these variable aerodynamic forces considerably less than the variable forces acting on the hub of the rotor on the side of the vibrating blades. For example, for the Mi-4 helicopter the variable force acting on the fuselage from pulsations of flow repulsed by the rotor in the most unfavorable conditions of flight (deceleration before landing) consists of a value of the order of ±10-15 kG, while variable forces acting on the rotor hub in different conditions of flight have the order of ±(200-600) kG. Therefore, during the analysis of vibrations of the helicopter it follows, first of all, to be interested in the variable forces applied to the rotor hub.

These forces can, in general, be determined as dynamic reactions with forced oscillations of blades in flight the methods of calculation of which are discussed in Chapter I. Here one should stipulate that variable forces with such calculation are determined very inaccurately. The reason for this is that during the calculation of vibrations of the blade satisfactorily only the lowest harmonics of loads are determined, and errors of calculation increase with a growth in the number of harmonics. Meanwhile, as will be shown below, for the calculation of vibrations a decisive importance is the high harmonics of excitation. In this consists the cause of the fact that all methods of analysis of vibrations expounded in this chapter bear, mainly, a qualitative character.

An accurate calculation of vibrations with help of methods expounded in this chapter is possible only in certain special cases.

The most important of these cases is the designing of a new fuselage of the helicopter or even a helicopter of another configuration (for example, transverse or longitudinal instead of single-rotor), on which there will be installed earlier used rotors for which variable forces were determined by experimental means (for example, measurement of stresses in the rotor shaft or in a subreduction frame).

It is necessary to note that qualitative methods of evaluating vibrations permit making many highly useful conclusions in the designing of helicopters and with their finishing during flight tests. Thus, for example, it is possible to judge the influence on vibration of the form of a resonance diagram of the blade and resonance diagram of the fuselage and to determine the thus directed changes of design parameters for decreasing vibrations and sometimes estimate the degree of decrease in vibrations.

In order to make certain general conclusions about the character of the change (with time) of forces $X(t)$, $Y(t)$ and $Z(t)$ and moments $M_x(t)$, $M_y(t)$ and $M_z(t)$, let us turn to Fig. 2.2, on which there is depicted a five-blade rotor rotating evenly at angular velocity ω in

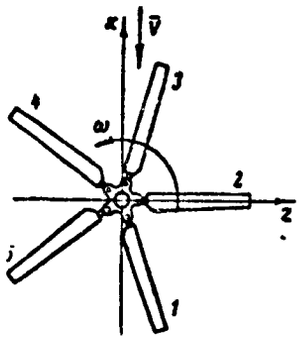

Fig. 2.2. Rotor rotating in an incident air flow.

a flow of air incident on it at constant speed V. Let us assume that at certain instant t the blades of the rotor occupy a position shown on the figure, and let us assume that at this instant force X has a certain value X(t). In a time interval equal to 1/5 of the time of a complete rotor revolution the rotor will turn 1/5 of a full revolution. Blade 1 will occupy the position of blade 2, blade 2 – position of blade 3, etc. It is clear that in this new position,

provided all blades of the rotor are absolutely identical, the entire streamline flow, and also, consequently, all forces acting on the blade, will be precisely the same as at the first instant t. In particular, the value of force X will be the same. It is obvious that with a subsequent turn of the rotor 1/5 of the revolution the situation will again be repeated. Consequently, function X(t) is a periodic function of time with the period equal to 1/5 of the time of a full revolution of the rotor. Figure 2.3 shows one of the possible forms of the graph of dependence X = X(t).

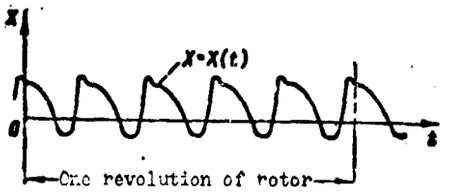

Fig. 2.3. Possible form of the dependence of longitudinal force with time.

Thus force X will change with time at an angular frequency of 5ω, while variable forces, acting on the blade of the rotor, change with the frequency ω (once per revolution of the rotor).

Function X(t), as any periodic function, can be expanded in Fourier series. With this the lowest harmonic in expansion will be the harmonic 5ω, so that the expansion will have the form

$$X(t)=X_0+X_{a_1}\cos 5\omega t+X_{b_1}\sin 5\omega t+X_{a_2}\cos 10\omega t+X_{b_2}\sin 10\omega t+ \\ +X_{a_3}\cos 15\omega t+X_{b_3}\sin 15\omega t+\ldots,$$

that is, the main frequency p = 5ω, multiple frequencies 2p = 10ω, 3p = 15ω, 4p = 20ω, etc.

Obviously, precisely the same conclusion can be made with respect to functions Y(t), Z(t), $M_x(t)$, $M_y(t)$ and $M_z(t)$.

In general, for a rotor with the number of blades equal to z, all forces and moments acting on the helicopter periodically change in time with a frequency of the so-called basic harmonic of the rotor p = zω. The expansion of these forces and moments in Fourier series has the form

$$\left.\begin{aligned} X(t) &= X_0 + X_{a_1}\cos pt + X_{b_1}\sin pt + X_{a_2}\cos 2pt + \\ &+ X_{b_2}\sin 2pt + X_{a_3}\cos 3pt + X_{b_3}\sin 3pt + \ldots; \\ M_x(t) &= M_{x_0} + M^x_{a_1}\cos pt + M^x_{b_1}\sin pt + M^x_{a_2}\cos 2pt + \\ &+ M^x_{b_2}\sin 2pt + M^x_{a_3}\cos 3pt + M^x_{b_3}\sin 3pt + \ldots, \end{aligned}\right\} \quad (1.1)$$

where

$$p = z\omega. \quad (1.2)$$

Thus on a helicopter with the number of blades z the excitation of vibrations is possible only with frequencies zω, 2zω, 3zω, etc. Let us note that this conclusion is maintained in the case when examining pulsating aerodynamic forces acting directly on the fuselage on the side of flow repulsed by the rotor.

If on the helicopter there is also a tail (antitorque) rotor having $z_{p.s}$ blades and revolving at an angular velocity $\omega_{p.s}$, then on the fuselage there will also act exciting forces containing harmonics $p_{p.s} = z_{p.s}\omega_{p.s}$, $2p_{p.s}$, $3p_{p.s}$, etc.

All these conclusions are correct only under the condition that the blades of the rotor are ideally identical. If this condition is not carried out, then low frequencies of excitation ω, 2ω, 3ω, etc., can appear. However, numerous experimental data – results of the measurement of vibrations and stresses in elements of construction of fuselages of different helicopters – show that the content of the lowest harmonics is always so insignificant that they should be disregarded both during the analysis of vibrations of the helicopter and in evaluating the strength of elements of construction of the fuselage. This indicates the fact that the existing level of production and requirements presented to the construction of blades provide quite small deviations in individual qualities of separate blades.

Let us note that all the above-mentioned reasoning could have also been repeated by examining variable force acting on the disk of the cyclic pitch control on the side of blades of the rotor. In spite of the fact that the moment of forces acting on the blade relative to the axial hinge (hinged moment) changes with time at the

basic frequency zω. Therefore, variable forces, acting in control circuits by collective and cyclical propeller pitch, change with the basic frequency p = zω, and also contain harmonics 2p, 3p, 4p, etc. The lowest harmonics of excitation can appear also only in the case of deviations in individual properties of separable blades.

2. Dependence of the Spectrum Exciting Forces on the Harmonic Composition of Oscillations of the Blade

Thus we clarified on the basis of the most general considerations that variable forces and moments X, Y, Z, M_x, M_y, and M_z, which act on the rotor hub on the side of the vibrating blades, change in time with the frequency of the basic harmonic zω of the rotor and contain also harmonics 2zω, 3zω, etc., multiple of it, while blades of the rotor and, consequently, forces acting on the hub on the side of each blade, accomplish oscillations with a main frequency ω and contain multiple harmonic 2ω, 3ω, 4ω, etc., among which there are harmonics zω, 2zω, etc. This suggests the idea that certain harmonic components of variable forces, applied to the rotor on the side of each blade, are balanced on the housing of the hub, and some are summed up. Let us show that this is indeed true. Let us turn to Fig. 2.4, on which schematically depicted is the housing of the hub with hinged blades attached to it.

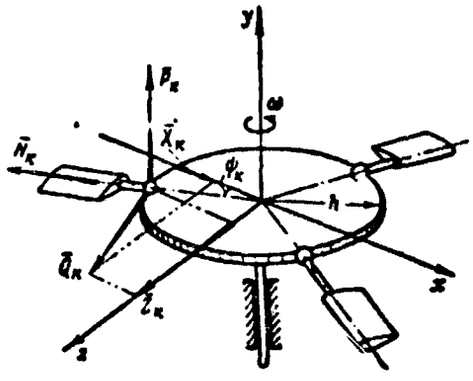

Fig. 2.4. Diagram of forces applied to rotor hub from the blade.

The force applied to the housing of the hub on the side of the k-th blade can be separated into three components: N_k, directed over the radius of the blade, P_k, parallel to the axis of the shaft of the rotor, and Q_k, perpendicular to the first two.

Each of these components is a periodic function of time with basic frequency ω. It is obvious that in a steady state of flight functions $N_k(t)$, $P_k(t)$ and $Q_k(t)$ are identical for all blades but shift in phase for each blade relative to the adjacent one by a certain value corresponding to the time of turn of the rotor at angle $2\pi/z$. This gives the basis to write expansions of these functions in Fourier series in the form

$$\begin{aligned} P_k = P_0 &+ P_{a_1}\cos(\omega t+\varphi_k)+P_{b_1}\sin(\omega t+\varphi_k)+ \\ &+P_{a_2}\cos 2(\omega t+\varphi_k)+P_{b_2}\sin 2(\omega t+\varphi_k)+\ldots+ \\ &+P_{a_n}\cos n(\omega t+\varphi_k)+P_{b_n}\sin n(\omega t+\varphi_k)+\ldots, \end{aligned} \tag{1.3}$$

where

$$\varphi_k=\frac{2\pi}{z}k \quad (k=1, 2, 3\ldots z),$$

or shorter

$$P_k=P_0+\sum_{n=1}^{\infty}[P_{a_n}\cos n(\omega t+\varphi_k)+P_{b_n}\sin n(\omega t+\varphi_k)]. \tag{1.4}$$

Analogously we have

$$Q_k=Q_0+\sum_{n=1}^{\infty}[Q_{a_n}\cos n(\omega t+\varphi_k)+Q_{b_n}\sin n(\omega t+\varphi_k)]; \tag{1.5}$$

$$N_k=N_0+\sum_{n=1}^{\infty}[N_{a_n}\cos n(\omega t+\varphi_k)+N_{b_n}\sin n(\omega t+\varphi_k)]. \tag{1.6}$$

Let us now state the following problem: knowing values of coefficients of Fourier series expansion of functions $P_k(t)$, $Q_k(t)$ and $N_k(t)$, or, in other words, knowing the harmonic components of forces P_k, Q_k, and N_k, to find variable forces X, Y, and Z and moments M_x, M_y and M_z (more accurately harmonic components) in order to trace the dependence of forces creating vibrations on different harmonic component forces acting on the hub on the side of a separate blade.

Summing the forces acting on the hub on the side of each blade, we obtain the following formulas:

$$Y=\sum_{k=1}^{z} P_k; \tag{1.7}$$

$$\left.\begin{aligned} X&=\sum_{k=1}^{z}[Q_k\sin\psi_k-N_k\cos\psi_k];\\ Z&=\sum_{k=1}^{z}[Q_k\cos\psi_k+N_k\sin\psi_k];\end{aligned}\right\} \tag{1.8}$$

$$M_y=\sum_{k=1}^{z} Q_k h; \tag{1.9}$$

$$\left.\begin{aligned} M_x&=-\sum_{k=1}^{z} P_k h\sin\psi_k;\\ M_z&=-\sum_{k=1}^{z} P_k h\cos\psi_k.\end{aligned}\right\} \tag{1.10}$$

where ψ_k is the azimuthal angle of the k-th blade:

$$\psi_k=\omega t+\varphi_k=\omega t+\frac{2\pi}{z}k; \tag{1.11}$$

h – distance from the axis of rotation to the combined horizontal flapping and vertical hinges.

If the hub has nonintegrated hinges, then in formula (1.9) it is necessary to take $h=l_{s.m.}$ and in formulas (1.10), $h=l_{r.m.}$

Let us examine in detail expression (1.7) for determination of variable force Y. Substituting into it expression (1.3) for force P_k, we arrive at the necessity of calculation of sums of the form

$$\sum_{k=1}^{z}\cos n(\omega t+\varphi_k) \quad \text{and} \quad \sum_{k=1}^{z}\sin n(\omega t+\varphi_k),$$

where n consists of integers (n = 1, 2, 3, ...).

Let us show that trigonometric sums of such a form possess the following remarkable property: at any n not multiple to the number of blades z both these sums are equal to zero at any t; at n multiple to z, i.e., if n = sz (s = 1, 2, 3, ...), then

$$\left.\begin{aligned}\sum_{k=1}^{z}\cos sz\left(\omega t+\varphi_k\right)&=z\cos\left(sz\omega t\right);\\ \sum_{k=1}^{z}\sin sz\left(\omega t+\varphi_k\right)&=z\sin\left(sz\omega t\right).\end{aligned}\right\}. \qquad (1.12)$$

Thus, for example, for a rotor with five blades (z = 5)

$$\sum_{k=1}^{5}\cos\left(\omega t+\varphi_k\right)=\sum_{k=1}^{5}\cos 2\left(\omega t+\varphi_k\right)=$$
$$=\sum_{k=1}^{5}\cos 3\left(\omega t+\varphi_k\right)=\sum_{k=1}^{5}\cos 4\left(\omega t+\varphi_k\right)=0$$

at any value t, but

$$\sum_{k=1}^{5}\cos 5\left(\omega t+\varphi_k\right)=5\cos\left(5\omega t\right).$$

Further

$$\sum_{k=1}^{5}\cos 6\left(\omega t+\varphi_k\right)=\sum_{k=1}^{5}\cos 7\left(\omega t+\varphi_k\right)=$$
$$=\sum_{k=1}^{5}\cos 8\left(\omega t+\varphi_k\right)=\sum_{k=1}^{5}\cos 9\left(\omega t+\varphi_k\right)=0,$$

but

$$\sum_{k=1}^{5}\cos 10\left(\omega t+\varphi_k\right)=5\cos\left(10\omega t\right),\ \text{etc.}$$

It is possible to prove correctness of formulas (1.12) by different methods. Let us use for this the very convenient method proposed by R. A. Mikheyev and founded on the application of the well-known Euler formula, which expresses the connection between trigonometric functions and exponential functions with the imaginary argument. Let us prove the correctness of only the first of formulas (1.12). We have

$$\cos n\gamma_k=\frac{1}{2}\left(e^{in\varphi_k}+e^{-in\varphi_k}\right);\quad\left(\gamma_k=\omega t+\frac{2\pi}{z}k\right).$$

Therefore

$$\sum_{k=1}^{z} \cos n\varphi_k = \frac{1}{2}\sum_{k=1}^{z}\left[e^{in\varphi_k} + e^{-in\varphi_k}\right] =$$

$$= \frac{1}{2}\left[e^{in\varphi_1}\sum_{k=1}^{z} e^{in\frac{2\pi}{z}k} + e^{-in\varphi_1}\sum_{k=1}^{z} e^{-in\frac{2\pi}{z}k}\right].$$

Let us examine separately the sum

$$\sum_{k=1}^{z} e^{in\frac{2\pi}{z}k} = \left(e^{in\frac{2\pi}{z}}\right) + \left(e^{in\frac{2\pi}{z}}\right)^2 + \left(e^{in\frac{2\pi}{z}}\right)^3 + \ldots + \left(e^{in\frac{2\pi}{z}}\right)^z.$$

This geometric progression with denominator $e^{in\frac{2\pi}{z}}$.

Using the well-known formula for the sum of the geometric progression, we obtain

$$\sum_{k=1}^{z} e^{in\frac{2\pi}{z}k} = \frac{e^{i2\pi\frac{n}{z}}\left(1 - e^{i2\pi n}\right)}{1 - e^{i2\pi\frac{n}{z}}}.$$

Since n is an integer, then the numerator of this expression is always equal to zero, because $e^{i2\pi n} = 1$ ($n = 1, 2, 3, \ldots$).

The denominator of this expression can turn into zero only if (n/z) is an integer, i.e., if n is a multiple of the number of blades z. Thus, the examined sum is equal to zero at any n, with the exception of n multiples to the number z. In this last case the value of the sum becomes indefinite (0/0). This uncertainty can be revealed with the help of the well-known l'Hôpital rule. Let us assume that n changes continuously, approaching to a certain value sz (s – any integer; $s = 1, 2, 3, \ldots$). Differentiating the numerator and denominator with respect to n and passing to the limit $n \to sz$, we have

$$\sum_{k=1}^{z} e^{in\frac{2\pi}{z}k} = \lim_{n\to sz} e^{i2\pi\frac{n}{z}} \lim_{n\to sz} \frac{-i2\pi e^{i2\pi n}}{\left(\frac{-i2\pi}{z}\right)e^{i2\pi\frac{n}{z}}} = z.$$

It is also possible to show accurately that

$$\sum_{k=1}^{z} e^{-in\frac{2\pi}{z}k} = \begin{cases} 0, & \text{if n is not a multiple of z;} \\ z, & \text{if } n = sz, \text{ where } s = 1, 2, 3, \ldots \end{cases}$$

As a result we arrive at the conclusion that if n is not a multiple of z, then

$$\sum_{k=1}^{z} \cos n\psi_k = 0.$$

If, however, n is a multiple of z (n = sz; s = 1, 2, 3, ...), then

$$\sum_{k=1}^{z} \cos n\psi_k = \frac{z}{2}\left(e^{inst} + e^{-inst}\right) = z\cos nst = z\cos(sz\omega t).$$

Analogously, it is possible to show the correctness of the second of formulas (1.12).

The indicated property of trigonometric sums is conveniently recorded in the form

$$\left.\begin{aligned} \sum_{k=1}^{z} \cos n\psi_k &= \begin{cases} 0, \text{ if n is not a multiple of z;} \\ z\cos n\omega t, \text{ if } n = sz;\ s = 1, 2, 3, \ldots; \end{cases} \\ \sum_{k=1}^{z} \sin n\psi_k &= \begin{cases} 0, \text{ if n is not a multiple of z;} \\ z\sin n\omega t, \text{ if } n = sz;\ s = 1, 2, 3, \ldots \end{cases} \end{aligned}\right\} \qquad (1.13)$$

Let us return now to the expression for force Y from formula (1.7), into which the value of force P_k from formula (1.4) is substituted

$$Y = \sum_{k=1}^{z} [P_0 + P_{a_1}\cos\psi_k + P_{b_1}\sin\psi_k + P_{a_2}\cos 2\psi_k + P_{b_2}\sin 2\psi_k + \ldots + P_{a_n}\cos n\psi_k + P_{b_n}\sin n\psi_k + \ldots]$$

On the basis of the established property of trigonometric sums (1.13) it is possible to affirm that with the summation of different harmonics, in this expression all harmonics not multiple to the number of blades z will vanish. Harmonics multiple of z are

summed in accordance with formulas (1.13), so that finally we will obtain

$$Y = zP_0 + zP_{a_z}\cos z\omega t + zP_{b_z}\sin z\omega t + zP_{a_{(2z)}}\cos 2z\omega t + zP_{b_{(2z)}}\sin 2z\omega t + \ldots \qquad (1.14)$$

Thus all harmonic component forces $P_k(t)$ not multiple to the number of blades are balanced on the rotor hub and do not create vibrations of the fuselage of the helicopter. As a result the variable force Y changes with time with the basic harmonic $p = z\omega$ of the rotor and also contains multiple harmonics 2p, 3p, etc. This completely confirms the basic conclusion of the preceding point of this paragraph and also gives additional information in this part, indicating exactly what harmonic component forces P_k are dangerous from the point of view of vibrations.

For an illustration let us examine an example. Let us assume that for a certain rotor there is resonance of the second tone of oscillations of the blade in the flapping plane with the 5th harmonic of the rotor (5ω). In the resolution of forces P_k for such a rotor the harmonic component corresponding to the 5th harmonic (P_{a_5} and P_{b_5}) will be great.

If the rotor has five blades the indicated resonance will lead to great vibrations of the helicopter.

If, however, the rotor has four blades, this resonance will in no way manifest itself in vibrations of the helicopter, since harmonic component forces P_k corresponding to this resonance will be balanced on the hub. As one will see subsequently, considerable variable moments M_x and M_z on the hub can appear; however, practically vibrations of the helicopter are determined mainly by variable forces X, Y, and Z. Sometimes we erroneously consider that vibrations of the helicopter are less, the more the blades of the rotor. However in this example it is clear that in reality such is not so simple, and in this case, conversely, a decrease in the number of blades leads to a decrease of vibrations.

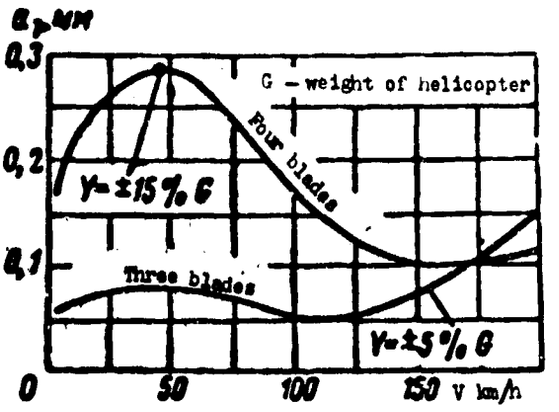

Fig. 2.5. Dependence of the amplitude of vibrations in the cockpit of a single-rotor helicopter on the speed of flight.

Let us consider one more example. Figure 2.5 shows results of experimental measurements of vibration in the cockpit of a single-rotor helicopter, which was tested with two rotors using three and four blades. The rotors had absolutely identical blades and differed only in hubs. Depicted on the graphs are dependences of amplitude a_y of vertical vibrations in the cockpit on speed of flight V for both rotors.

As calculations conducted for these rotors showed, the blade of the rotor had resonance of the second tone of oscillations in the flapping plane with the 4th harmonic of the rotor in operating revolutions. As a result vibrations of a helicopter with a four-blade rotor in the greater part of the speed range appeared considerably higher (at V = 40-50 km/h more than three times) than vibrations of a helicopter with a three-blade rotor. However, at great speed of flight vibrations of a helicopter with a four-blade rotor appeared less than that of a helicopter with a three-blade rotor. This is explained by the fact that at a low speed of flight there is a large harmonic component of aerodynamic forces, which corresponds to the 4th harmonic and is conditioned by the great irregularity of the field of induced speeds of the rotor at a low speed of flight. With an increase in speed of flight there occurs a levelling off of the field of flow rates (see Chapter I, § 8) through the rotor, and the excitation of oscillations of the blade with respect to the 4th harmonic decreases accordingly, while the 3rd harmonic decreases with an increase in speed not so rapidly or even does not decrease at all. The relatively large value of the 4th harmonic in the field of

[illegible] phenomenon for any rotor.

Let us return now to the determination of other forces and moments having an effect on the helicopter. Formula (1.9) for moment M_y is absolutely analogous to formula (1.7).

Repeating all reasonings, as in the derivation of formula (1.14) for force Y, we will obtain the following expression:

$$M_y = zh\,[Q_0 + Q_{a_z}\cos z\omega t + Q_{b_z}\sin z\omega t + \\ + Q_{a_{(2z)}}\cos 2z\omega t + Q_{b_{(2z)}}\sin 2z\omega t + \ldots]. \qquad (1.15)$$

The variable moment M_y is dangerous not only from the point of view of vibrations of the helicopter (in § 3, No. 1 it will be shown that this moment creates only lateral vibrations of the fuselage). This moment is one of the sources of torsional vibrations in the transmission system of the helicopter.

As can be seen from formula (1.15), the variable part of this moment is determined solely by harmonic components of force Q(t), which are multiples to the number of blades.

Let us turn further to the first of formulas (1.8). Substituting into it expressions for $Q_k(t)$ and $N_k(t)$ [formulas (1.5) and (1.6)], we will obtain

$$X = \sum_{k=1}^{z}(Q_0\sin\psi_k - N_0\cos\psi_k) + \sum_{k=1}^{z}[Q_{a_1}\cos\psi_k + Q_{b_1}\sin\psi_k]\sin\psi_k - \\ - \sum_{k=1}^{z}[N_{a_1}\cos\psi_k + N_{b_1}\sin\psi_k]\cos\psi_k + \ldots + \sum_{k=1}^{z}[Q_{a_n}\cos n\psi_k + \\ + Q_{b_n}\sin n\psi_k]\sin\psi_k - \sum_{k=1}^{z}[N_{a_n}\cos n\psi_k + N_{b_n}\sin n\psi_k]\cos\psi_k + \ldots$$

The first term of this sum is equal to zero in accordance with formulas (1.13), since

$$\sum_{k=1}^{z}[Q_0\sin\psi_k - N_0\cos\psi_k] = Q_0\sum_{k=1}^{z}\sin\psi_k - N_0\sum_{k=1}^{z}\cos\psi_k = 0.$$

For counting the remaining components let us examine the expression

$$X_{Q_n} = \sum_{k=1}^{z}[Q_{a_n}\cos n\psi_k + Q_{b_n}\sin n\psi_k]\sin\psi_k,$$

which constitutes a part of force X conditioned by the n-th harmonic of force Q.

Here we are encountered with sums of the form $\sum_{k=1}^{z}\cos n\psi_k\sin\psi_k$ and $\sum_{k=1}^{z}\sin n\psi_k\sin\psi_k$. These sums are also easily calculated with the help of formulas (1.13). Really

$$\sum_{k=1}^{z}\cos n\psi_k\sin\psi_k = \frac{1}{2}\sum_{k=1}^{z}\sin(n+1)\psi_k - \frac{1}{2}\sum_{k=1}^{z}\sin(n-1)\psi_k;$$

$$\sum_{k=1}^{z}\sin n\psi_k\sin\psi_k = -\frac{1}{2}\sum_{k=1}^{z}\cos(n+1)\psi_k + \frac{1}{2}\sum_{k=1}^{z}\cos(n-1)\psi_k.$$

On the basis of formulas (1.13) it is possible to affirm that these sums will be different from zero only if one of the numbers (n + 1) or (n - 1) is multiple to the number of blades. Let us assume that (n + 1) = sz (s = 1, 2, 3, ...), and, consequently, n = sz - 1. Then

$$\sum_{k=1}^{z}\cos n\psi_k\sin\psi_k = \frac{z}{2}\sin(sz\omega t);$$

$$\sum_{k=1}^{z}\sin n\psi_k\sin\psi_k = -\frac{z}{2}\cos(sz\omega t).$$

Further, if (n - 1) = sz; n = sz + 1, then

$$\sum_{k=1}^{z}\cos n\psi_k\sin\psi_k = -\frac{z}{2}\sin(sz\omega t);$$

$$\sum_{k=1}^{z}\sin n\psi_k\sin\psi_k = \frac{z}{2}\cos(sz\omega t).$$

As a result the following expression is obtained for the part of force X which is obtained from all harmonic components of force Q:

$$X_Q = z\left\{\frac{Q_{a(z-1)} - Q_{a(z+1)}}{2}\sin z\omega t - \frac{-Q_{b(z-1)} + Q_{b(z+1)}}{2}\cos z\omega t + \right.$$
$$\left. + \frac{Q_{a(2z-1)} - Q_{a(2z+1)}}{2}\sin 2z\omega t + \frac{-Q_{b(2z-1)} + Q_{b(2z+1)}}{2}\cos 2z\omega t + \ldots\right\}. \qquad (1.16)$$

For the part of force X conditioned by harmonic components of force N(t), there is analogously obtained expression of the form

$$X_N = z\left\{-\frac{N_{a(z-1)} + N_{a(z+1)}}{2}\cos z\omega t + \frac{N_{b(z-1)} - N_{b(z+1)}}{2}\sin z\omega t - \right.$$
$$\left. - \frac{N_{a(2z-1)} + N_{a(2z+1)}}{2}\cos 2z\omega t - \frac{N_{b(2z-1)} + N_{b(2z+1)}}{2}\sin 2z\omega t + \ldots\right\}. \qquad (1.17)$$

Force X can be determined by formula

$$X = X_Q + X_N.$$

If the expression for force X(t) is written in the form (1.1), then there are obtained the following formulas for its harmonic components:

$$\left.\begin{aligned} X_{a_z} &= \frac{z}{2}[Q_{b(z+1)} - Q_{b(z-1)} - N_{a(z+1)} - N_{a(z-1)}]; \\ X_{b_z} &= \frac{z}{2}[Q_{a(z-1)} - Q_{a(z+1)} - N_{b(z+1)} - N_{b(z-1)}]. \end{aligned}\right\} \qquad (1.18)$$

Components corresponding to harmonics multiple of the basic, X_{a_2}, X_{b_2}, and so on, are obtained from these formulas, if instead of index z we take, respectively, index 2z, 3z, etc.

Thus the variable part of force X(t) is determined by the harmonic components of forces Q(t) and N(t) combinational with respect to the basic harmonic of the rotor (z - 1; z + 1) or to its multiple harmonics (2z - 1; 2z + 1), etc.

Thus, for example, for a rotor with three blades (z = 3) the basic harmonic of force X (frequency 3ωt) will be determined by the

2nd and 4th harmonics of forces Q(t) and N(t), the 2nd harmonic of force (frequency ωt) will be determined by the 5th and 7th harmonics of forces Q(t) and N(t) and so on.

Absolutely analogous formulas are obtained for harmonic components of forces Z(t):

$$\left.\begin{aligned} Z_{a_z} &= \frac{s}{2}\left[Q_{a_{(z+1)}} + Q_{a_{(z-1)}} + N_{b_{(z+1)}} - N_{b_{(z-1)}}\right]; \\ Z_{b_z} &= \frac{s}{2}\left[Q_{b_{(z+1)}} + Q_{b_{(z-1)}} + N_{a_{(z-1)}} - N_{a_{(z+1)}}\right]; \end{aligned}\right\} \qquad (1.19)$$

Just as in formulas (1.18), to obtain multiples of harmonics Z_{a_2}, Z_{b_2}, Z_{a_3} and Z_{b_3} in these formulas instead of index z, it is necessary to put indices 2z, 3z, etc., respectively.

Analogously expressions for harmonic components of moments M_x and M_z are obtained from formulas (1.10):

$$\left.\begin{aligned} M^z_{a_z} &= \frac{sh}{2}\left[P_{b_{(z-1)}} - P_{b_{(z+1)}}\right]; \\ M^z_{b_z} &= \frac{sh}{2}\left[P_{a_{(z+1)}} - P_{a_{(z-1)}}\right]; \end{aligned}\right\} \qquad (1.20)$$

$$\left.\begin{aligned} M^c_{a_z} &= \frac{sh}{2}\left[-P_{a_{(z+1)}} - P_{a_{(z-1)}}\right]; \\ M^c_{b_z} &= \frac{sh}{2}\left[-P_{b_{(z+1)}} - P_{b_{(z-1)}}\right]. \end{aligned}\right\} \qquad (1.21)$$

Let us note still the following circumstance, which sometimes can facilitate the qualitative analysis of vibrations. If the variable force in the rotor plane (X or Z) or the moment (M_x, M_z) is determined by any one harmonic component of force acting from the side of the blade, then as a result there is obtained a vector of constant length, which evenly revolves in the rotor plane at angular velocity $z\omega$ (or $sz\omega$). The direction of rotation is obtained opposite the rotation of the rotor, if this vector is obtained from the harmonic component z + 1 (or sz + 1) and in the direction of the rotor rotation, if this vector is obtained from the harmonic component z - 1 (or sz - 1).

Let us assume that, for example, the rotor has five blades ($z = 5$), and there is examined the vector of the moment on the hub with components M_x and M_z, which are obtained from the harmonic component $(z - 1)$:

$$P = P_{a_4} \cos 4\omega t + P_{b_4} \sin 4\omega t.$$

Then (see 1.20 and 1.21)

$$M_x = \frac{zh}{2} [P_{b_4} \cos 5\omega t - P_{a_4} \sin 5\omega t];$$

$$M_z = \frac{zh}{2} [-P_{b_4} \sin 5\omega t - P_{a_4} \cos 5\omega t].$$

Here, as one can see from these formulas, the vector

$$\overline{M} = \overline{M}_x + \overline{M}_z$$

constitutes a vector of constant length

$$M = \frac{zh}{2} \sqrt{P_{a_4}^2 + P_{b_4}^2},$$

which evenly revolves in the rotor plane at angular velocity 5ω in a direction coinciding with the direction of the rotor rotation.

Thus, the analysis conducted above shows that the rotor is a kind of filter, which of all the harmonic components of forces on vibrating blades passes to the fuselage only certain ones corresponding to the basic harmonic of the rotor, its combinational harmonics $(z - 1)\omega$ and $z + 1)\omega$, and also harmonics multiple of the basic $2z\omega$, $3z\omega$, etc., and combinational harmonics $(2z - 1)\omega$, $(2z + 1)\omega$, $(3z - 1)\omega$, $(3z + 1)\omega$, etc.

The greatest danger, both from the point of view of the level of vibrations and from the point of view of dynamic strength of elements of the fuselage, is represented, as a rule, by the lowest harmonics $z\omega$, $(z + 1)\omega$ and $(z - 1)\omega$.

From harmonics which are the result of oscillations of the blade in the flapping plane (force $\overline{P}_k$, see Fig. 2.4), harmonic $z\omega$

(and multiples of it) leads to the appearance of a vertical variable force on the rotor, and harmonics (z - 1) and (z + 1) (and also 2z - 1, 2z + 1, etc.) lead to the appearance of variable moments on the hub with respect to axes 0x and 0z.

From harmonics which are the result of oscillations of blade in the plane of rotation (forces $\bar{Q}_k$ and $\bar{N}_k$, see Fig. 2.4), the harmonic zω (and multiples of it) leads to the appearance of variable torque on the rotor shaft and, harmonics (z - 1)ω and (z + 1)ω (and also 2z - 1, 2z + 1, etc.) – to the appearance of variable forces (longitudinal and transverse) in the plane of rotation of the rotor.

Let us note in conclusion that with summation of forces acting from the side of the blades on the disk of the cyclic pitch control there are obtained precisely the same formulas for the calculation of harmonic components of vertical force Y and moments M_x and M_z applied to the disk. Here it is possible to use directly formulas (1.14), (1.20) and (1.21), understanding by force

$$P_k(t)=P_0+\sum_{n=1}^{\infty}(P_{a_n}\cos n\psi_k+P_{b_n}\sin n\psi_k),$$

the force acting in the link controlling the k-th blade (hinged moment divided by the corresponding arm) and by quantity h – radius of the disk of the cyclic pitch control.

Thus, by knowing the harmonic composition of the hinged moment, it is not difficult to calculate the variable force acting in the circuits controlling the collective and cyclical rotor pitch.

§ 2. Flexural Vibrations of the Fuselage as an Elastic Beam

If variable forces applied to the fuselage from rotors are known, then the calculation of vibrations at different points of the fuselage can be carried out by the standard methods used during calculation of forced oscillations of an elastic beam of variable cross section. Of course, the fuselage of a real helicopter only in first approximation can be examined as a thin elastic flexural beam.

In reality transverse dimensions of the fuselage usually cannot be considered small as compared to the longitudinal. Furthermore, the fuselage of a helicopter of single-rotor configuration can have "fractures" in the region of the tail beam, sharp drops in rigidity along the length and other peculiarities. These peculiarities and their account with the calculation of oscillations are examined in § 3. Here we will examine methods of calculation of oscillations of the elastic beam, since they are fundamental. Furthermore, in this paragraph oscillations of a system consisting of two elastic beams forming a "cross" will be examined. Such a system is a fuselage with a wing.

1. Calculation of Forced Oscillations of an Elastic Beam by the Method of Expansion by Own Forms

Let us assume that to an elastic flexural ideal beam (Fig. 2.6) deprived of damping, found in a free state under the action of a

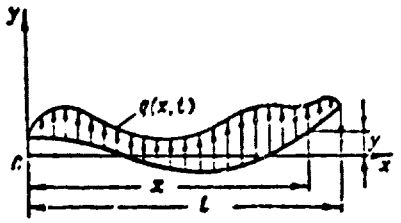

Fig. 2.6. Diagrams of a free elastic beam with a distributed load applied to it.

balanced system of time-independent forces (tractive force of the rotor balances the gravity), there is applied load q distributed along the length of the beam variable in time, which is variable by the harmonic law

$$q(x, t)=q(x)\cos pt. \tag{2.1}$$

The equation of lateral bending oscillations of such a beam has the form

$$(EIy'')''+m\ddot{y}=q(x, t) \tag{2.2}$$

This partial differential equation is derived in No. 10, § 1, Chapter I for an elastic beam in the field of centrifugal forces.

In the case of their absence (N = 0) the equation takes the form of (2.2).

To find the motion of the beam means to find function y = y(x, t) satisfying equation (2.2) and also boundary conditions, which in the case of a beam with free ends have the form

$$\left.\begin{array}{l}\text{when } x=0;\ M=EIy''=0;\ Q=(EIy'')'=0;\\ \text{when } x=l;\ M=EIy''=0;\ Q=(EIy'')'=0.\end{array}\right\} \qquad (2.3)$$

Function y(x, t), which satisfies the homogeneous equation (without the right-hand side)

$$(EIy'')''+m\ddot{y}=0 \qquad (2.4)$$

and boundary conditions (2.3), correspond to natural oscillations of the beam. The solution of equation (2.4) is sought in the form

$$y(x, t)=\bar{y}(x)\cos pt. \qquad (2.5)$$

After substitution into equation (2.4) this expression leads to the ordinary differential equation with parameter p for determination of function $\bar{y}(x)$:

$$(EI\bar{y}'')''-p^2m\bar{y}=0. \qquad (2.6)$$

The last equation has solutions different from zero only with defined values of parameter p: $p = p_0$; $p = p_1$; $p = p_2$; $p = p_3$, etc. To each value $p = p_k$ (k = 0, 1, 2, 3, ...) corresponds the defined function $\bar{y}_k(x)$, which satisfies equation (2.6) at $p = p_k$ so that

$$(EI\bar{y}_k'')''-p_k^2m\bar{y}_k=0;\ (k=1, 2, 3,\ldots). \qquad (2.7)$$

Numbers p_k (k = 0, 1, 2, 3, ...) are called frequencies of natural oscillations of the beam and functions $\bar{y}_k(x)$ – corresponding forms of natural oscillations.

Motion of the beam according to the law

$$y(x, t) = a_k \bar{y}_k(x) \cos p_k t, \qquad (2.8)$$

where a_k is constant, is called natural oscillations of the beam with respect to the k-th tone.

The general solution of the homogeneous equation (2.4) has the form

$$y(x, t) = \sum_k a_k \bar{y}_k(x) \cos(p_k t + \varphi_k), \qquad (2.9)$$

where a_k and φ_k are arbitrary constants.

Thus natural oscillation of the beam constitute motion obtained as a result of the superposition of oscillations of different tones.

Methods of finding frequencies of natural oscillations p_k and corresponding forms $\bar{y}_k(x)$ for the beam with the assigned law of the change in rigidity $EI(x)$ and linear mass $m(x)$ are discussed in § 2 of Chapter I.

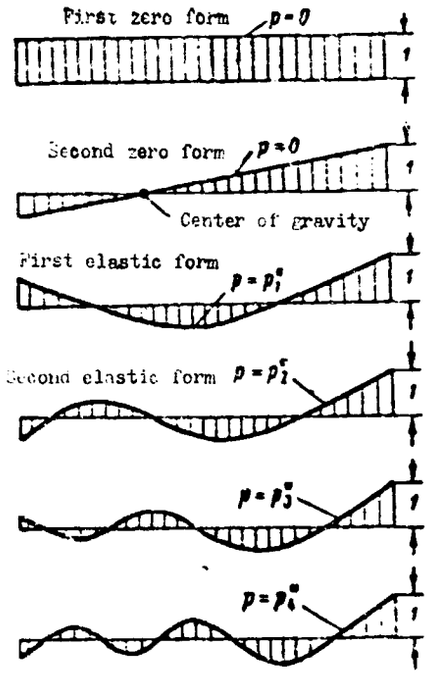

Fig. 2.7. Characteristic forms of natural oscillations of the fuselage as a free beam (p_1^*, p_2^*, etc., are frequencies of oscillations of the first, second, etc., elastic tones; in general, one should consider that $p_0 = 0$; $p_1 = 0$; $p_2 = p_1^*$; $p_3 = p_2^*$, etc.).

Figure 2.7 shows characteristic forms of natural oscillations of a free beam. Two forms correspond to oscillations of the beam as

a solid and have frequencies of natural oscillations equal to zero. The first of these forms corresponds to forward movements of the beam and the second to the angular displacement of the beam relative to its center of gravity.

All formulas which are derived in this paragraph are equally useful for the calculation of oscillations of an elastic beam with any conditions of fastening of the ends. However, in the case of application of these formulas to oscillations of the free beam and, in particular, the fuselage, it is necessary to remember that to the number of frequencies p_k and forms $\bar{y}_k(x)$ natural oscillations should be certainly included the two lowest forms which correspond to zero frequencies. So we must assume in all formulas $p_0 = 0$ and $p_1 = 0$ and consider that the corresponding standardized forms have the form

$$\bar{y}_0(x) = 1;$$
$$\bar{y}_1(x) = \frac{x - x_c}{l - x_c},$$

where x_c is the coordinate of the center of gravity of the beam.

In case the mentioned forms will not be considered during calculation of vibrations of the fuselage, the calculation of vibrations will be carried out neglecting oscillations of the fuselage as solid, and this will lead to considerable errors in magnitude of the vibrations.

Let us consider the problem of forced oscillations of the beam under the action of a "purely" harmonic load [see formula (2.1)]. In this case equation (2.2) takes the form

$$(EJy'')'' + m\ddot{y} = q(x)\cos pt. \qquad (2.10)$$

We will look for the particular solution of this equation corresponding to the stabilized forced oscillations of the beam with frequency p in the form

$$y = \bar{y}(x)\cos pt. \qquad (2.11)$$

Substituting this expression into equation (2.10), we will arrive at the ordinary differential equation for determining function $\bar{y}(x)$, which is natural to call the form of forced oscillations:

$$(EI\bar{y}')' - p^2 m\bar{y} = q(x). \tag{2.12}$$

We will look for the solution of this equation in the form of expansion with respect to natural forms:

$$\bar{y} = \sum_k c_k \bar{y}_k(x). \tag{2.13}$$

If in this sum we take a limited number of terms, then it is possible, in determining values of coefficients c_k, to obtain only approximate solutions of equation (2.12). However, it is possible to prove that with the method shown below of the determination of coefficients c_k the approximate solution with a quite large number of terms in series (2.13) will be as accurate as possible.

For finding coefficients c_k let us substitute expression (2.13) into equation (2.12) and, multiplying both sides of equation (2.12) by $\bar{y}_n(x)$, we will integrate them from 0 to ℓ. Then we will obtain the equation

$$\sum_k c_k \int_0^l (EI\bar{y}_k')'\bar{y}_n dx - p^2 \sum_k c_k \int_0^l m\bar{y}_k\bar{y}_n dx = \int_0^l q\bar{y}_n dx. \tag{2.14}$$

Integrals, standing in the first component of the left-hand side of this equation can be simplified using integration by parts:

$$\int_0^l (EI\bar{y}_k')'\bar{y}_n dx = \int_0^l \bar{y}_n d(EI\bar{y}_k') = [\bar{y}_n(EI\bar{y}_k')']\Big|_0^l - \int_0^l \bar{y}_n'(EI\bar{y}_k')' dx,$$

but

$$[\bar{y}_n(EI\bar{y}_k')']\Big|_0^l = 0,$$

since functions $\bar{y}_k(x)$ satisfy conditions (2.3).

Further:

$$\int_0^l \bar{y}_n''(EI\bar{y}_k')'\,dx = \int_0^l \bar{y}_n\,d(EI\bar{y}_k') = [\bar{y}_n'(EI\bar{y}_k')]\Big|_0^l - \int_0^l EI\bar{y}_n'\bar{y}_k'\,dx.$$

In virtue of conditions (2.3)

$$[\bar{y}_n'(EI\bar{y}_k')]\Big|_0^l = 0,$$

so that as a result there is obtained

$$\int_0^l (EI\bar{y}_k')''\bar{y}_n\,dx = \int_0^l EI\bar{y}_n'\bar{y}_k'\,dx. \tag{2.15}$$

Since all functions $\bar{y}_k(x)$ (k = 1, 2, 3, ...) satisfy equation (2.7), it is possible to write

$$(EI\bar{y}_k')' - p_k^2 m\bar{y}_k = 0;$$
$$(EI\bar{y}_n')' - p_n^2 m\bar{y}_n = 0.$$

Multiplying the first of these equations by $\bar{y}_n$ and the second by $\bar{y}_k$, we will then subtract one from the other and integrate the obtained expression from 0 to ℓ. We obtain

$$\int_0^l (EI\bar{y}_k')''\bar{y}_n\,dx - \int_0^l (EI\bar{y}_n')''\bar{y}_k\,dx = (p_k^2 - p_n^2)\int_0^l m\bar{y}_n\bar{y}_k\,dx.$$

But the left part of this equation is equal to zero in virtue of condition (2.15). Therefore, provided $p_k \neq p_n$, then

$$\int_0^l m\bar{y}_n\bar{y}_k\,dx = 0; \quad (n \neq k). \tag{2.16}$$

This is the so-called condition of orthogonality of forms of natural oscillations (see also Chapter I, § 2, No. 3).

Further, multiplying both sides of equation (2.7) by $\bar{y}_n$ and integrating from 0 to ℓ, we obtain:

$$\int_0^l (EI\bar{y}_k')''\bar{y}_n\,dx = p_k^2\int_0^l m\bar{y}_k\bar{y}_n\,dx.$$

Hence it may be concluded that if $n \neq k$, then

$$\int_0^l (EI\bar{y}_k')''\bar{y}_n\,dx = \int_0^l EI\bar{y}_n'\bar{y}_k'\,dx = 0. \tag{2.17}$$

If, however, n = k, then we obtain the expression for frequency p_n of the n-th tone of oscillations in terms of its form $\bar{y}_n(x)$:

$$p_n^2 = \frac{\int_0^l EI\bar{y}_n''^2 dx}{\int_0^l m\bar{y}_n^2 dx}. \qquad (2.18)$$

This is the well-known Rayleigh formula.

On the basis of conditions (2.16) and (2.17), it is possible to affirm that in expression (2.14) all components for which $k \neq n$ will turn into zero. Considering this, and also using formula (2.15), let us copy equation (2.14) in the form

$$c_n \int_0^l EI\bar{y}_n''^2 dx - c_n p^2 \int_0^l m\bar{y}_n^2 dx = \int_0^l q\bar{y}_n dx.$$

Dividing both sides of the last equation by $\int_0^l m\bar{y}_n^2\, dx$, solving it relative to c_n and using the Rayleigh formula (2.18), we will find

$$c_n = \frac{1}{p_n^2 - p^2} \cdot \frac{\int_0^l q\bar{y}_n dx}{\int_0^l m\bar{y}_n^2 dx}. \qquad (2.19)$$

Let us introduce notations

$$A_n = \int_0^l q\bar{y}_n dx; \qquad (2.20)$$

$$K_n = \int_0^l m\bar{y}_n^2 dx. \qquad (2.21)$$

Quantity A_n constitutes work of the exciting load q(x) on the form of the n-th tone of oscillations and quantity K_n – the largest (for the period) value of kinetic energy of the given tone of oscillations referred to quantity p_n^2. Thus

$$c_n = \frac{1}{p_n^2 - p^2} \frac{A_n}{K_n}. \qquad (2.22)$$

Considering expressions (2.13) and (2.11), we obtain the following solution of equation (2.10):

$$y(x, t)=\left[\sum_k \frac{1}{p_k^2-p^2} \frac{A_k}{K_k} \bar{y}_k(x)\right] \cos pt. \qquad (2.23)$$

From this expression certain very important conclusions can be made.

First of all it is clear that if the frequency of the change in exciting load p approaches one of frequencies p_k of natural oscillations, then the amplitude of oscillations of any point of the beam increases without limit. This is the phenomenon of resonance of the exciting load with the k-th tone of natural oscillations of the beam. Since here we did not consider the influence of damping forces (this will be done later), then the amplitude of oscillations with resonances is unlimited.

Further, if quantity p is close to the frequency p_n of the n-th tone of oscillations, then the term with number n in the sum (2.23) becomes considerably larger than the remaining terms. Therefore, it is approximately possible to consider near resonance ($p = p_n$) that

$$y(x, t)=\frac{1}{p_n^2-p^2} \frac{A_n}{K_n} \bar{y}_n(x) \cos pt=c_n \bar{y}_n(x) \cos pt,$$

i.e., near resonance with some tone of natural oscillations the form of forced oscillations differs little from the form of oscillations of the given tone.

Finally, with transition of the value of p from a quantity somewhat smaller than p_n to a quantity somewhat larger than p_n, the quantity in brackets of formula (2.23) changes sign. Therefore, if one were to construct a graph of the dependence of amplitude $\bar{y}_0$ of some point of the beam on the frequency of excitation p [at constant q(x)], then this graph will have the form depicted in Fig. 2.8. The curve of the graph has infinite discontinuities at points $p = p_1$, $p = p_2$, $p = p_3$, etc.

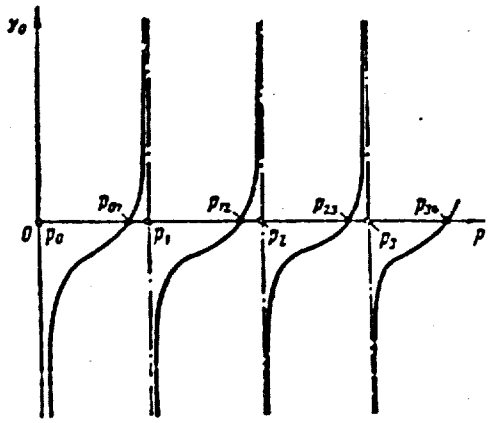

Fig. 2.8. Dependence of the amplitude of oscillations of any point of the fuselage on the frequency of excitation.

2. Dynamic Rigidity of the Beam. Resonance and Antiresonance

The case examined in the preceding point of forced oscillations of the beam under the action of an exciting load distributed along its length, which is variable with time with respect to the harmonic law (2.1), and the derived formulas remain in force under any law of the change in load along the length of the beam, i.e., at any form of function q(x). Therefore, from these formulas it is easy to obtain formulas for determining forced oscillations of the beam createable by the concentrated exciting force

$$F = F_0 \cos pt, \tag{2.24}$$

applied at certain point $x = x_0$ (Fig. 2.9).

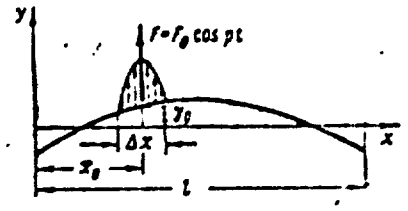

Fig. 2.9. Analysis of forced oscillations of the free beam from concentrated force.

Really, let us assume that load q(x) is applied to the beam only on some small section along length Δx in environment of point $x = x_0$. Here formulas (2.22), (2.20) and (2.21) will remain in force, but in formula (2.20) the corresponding integral must be taken not along the entire length of the beam ℓ but only on section Δx, i.e.,

$$A_k = \int_0^l q\bar{y}_k dx = \int_{\Delta x} q\bar{y}_k dx.$$

At small value of Δx this integral can be approximately replaced by the quantity

$$\int_{\Delta x} q\bar{y}_k dx = F_0 \bar{y}_k(x_0). \tag{2.25}$$

where

$$F_0 = \int_{\Delta x} q dx. \tag{2.26}$$

Formula (2.25) becomes accurate at infinitesimal Δx, i.e., in the case of the concentrated exciting force.

Thus we arrive at the following conclusion: if oscillations of the beam are caused by the concentrated force (2.24) applied at point $x = x_0$, motion of the beam is described as before by expression (2.23) in which quantity A_k is determined by the formula

$$A_k = F_0 \bar{y}_k(x_0). \tag{2.27}$$

i.e., quantity A_k constitutes work of the exciting load "on the form of the k-th tone of oscillations."

Let us note that such a method of finding forced oscillations remains in force in the case when oscillations are caused by the concentrated bending moment (variable with respect to the harmonic law)

$$M = M_0 \cos pt, \tag{2.28}$$

applied at point $x = x_0$. In this case quantity A_k should be determined by formula

$$A_k = M_0 \bar{\varphi}_k(x_0). \tag{2.29}$$

where $\bar{y}'_k(x_0)$ is the angle of rotation of the elastic line at point $x = x_0$, which corresponds to the form of the k-th tone.

In the case when oscillations of the beam are caused by the longitudinal force

$$X = X_0 \cos pt, \tag{2.30}$$

applied on a certain arm h (Fig. 2.10), all the given formulas also remain in force, since in this case force X_0 can be transferred from point A to the corresponding point B of the beam, adding then the couple with the moment equal to $M_0 = X_0 h$.

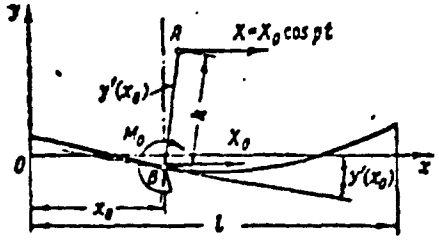

Fig. 2.10. Diagram of action of longitudinal force from the rotor on an elastic fuselage.

The longitudinal variable force applied at point B can cause only longitudinal (axial) oscillations of the beam, and lateral oscillations of the beam from the harmonic moment M_0 are determined as was indicated above.

In examining transverse forced oscillations of the beam from the concentrated force $F = F_0 \cos pt$, it is convenient to introduce the concept of dynamic rigidity of the beam at point $x = x_0$ of the application of force.

Let us call the dynamic rigidity D(p) of the beam at point $x = x_0$ the ratio of the largest value (amplitude) of exciting force F_0 to the amplitude $\bar{y}_0 = \bar{y}(x_0)$ of forced oscillations of the beam at the point of application of force, so that

$$D(p) = \frac{F_0}{\bar{y}_0}. \tag{2.31}$$

It is considered that with a change in force with respect to the harmonic law $F = F_0 \cos pt$, the point of its application accomplishes stabilized forced oscillations according to the law $y = \bar{y}_0 \cos pt$.

Thus dynamic rigidity of the beam is a function of frequency p oscillations, and it is considered positive if the force and movement change with time "in one phase" and negative if the force and movement change in "opposite phase."

The amplitude of oscillations of point $x = x_0$ of the application of force can be determined with help of formula (2.23):

$$\bar{y}_0 = \sum_k \frac{1}{p_k^2 - p^2} \frac{A_k}{K_k} \bar{y}_k(x_0). \qquad (2.32)$$

If one were to construct a graph of the change in quantity $\bar{y}_0$ with respect to frequency p at constant value F_0, then there will be obtained a curve analogous to the one depicted in Fig. 2.8. Therefore, if one were to construct a graph of the dependence of dynamic rigidity D(p) at a given point of the beam on frequency of oscillations, then this graph will have the form depicted in Fig. 2.11.

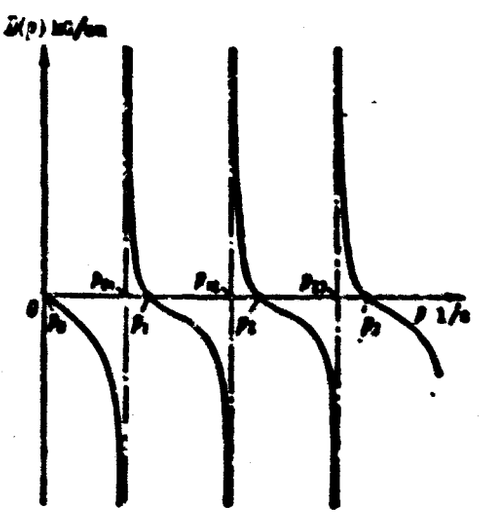

Fig. 2.11. Graph of dynamic rigidity.

Dynamic rigidity D(p) becomes zero at resonances $p = p_1$, $p = p_2$, etc., and becomes infinite at those values of frequency p ($p = p_{12}$,

$p = p_{23}$, $p = p_{34}$, etc.) at which the amplitude of oscillations of the point of application of force becomes zero. These values of frequency p are called frequencies of antiresonances and are equal to frequencies of corresponding tones of natural oscillations of the beam with hinge support at the point of application of force F.

Really, we will imagine that at the point of application of force F the beam has a support with the hinge (the beam at this point is not intersected), so that this point of the beam remains fixed during the oscillations. Such a beam has its frequencies and forms of natural oscillations. With natural oscillations of a certain tone of such a beam in the support ($x = x_0$) there will appear the dynamic reaction, variable in time with respect to the harmonic law with the frequency of this tone. The amplitude (the greatest value) of this force of reaction will depend on the amplitude (of any point, for example, the end) of natural oscillations of the beam, which can have any value (depending upon initial conditions). Therefore, it is always possible thus to select an amplitude of oscillations of the beam so that the amplitude of force of reaction has the given value F_0. If now mentally we remove the support, continuing to apply to the beam at this point force F, which changes according to the harmonic law with the same frequency, then the free beam will continue oscillations with respect to the same form with the same amplitude. However, these oscillations can be examined as forced oscillations of the free beam under the action of perturbing force F. With such forced oscillations the point of application of the perturbing force is stationary, and therefore the dynamic rigidity of the beam, which corresponds to such conditions, is infinite. This is called antiresonance.

On the graph of dynamic rigidity (Fig. 2.11) points of resonance $D(p) = 0$ and antiresonance $D(p) = \infty$ alternate. It can be shown that for an elastic beam this is always the case.

Thus at a certain frequency of excitation the point of application of the exciting force stops, and at this point a node of the form of forced oscillations is obtained. This phenomenon is called

antiresonance. The frequency of every antiresonance always is located between two neighboring frequencies of natural oscillations of the free beam.

The phenomenon of antiresonance in "pure form" can take place only in ideal oscillatory systems deprived of damping. In the presence of damping, the amplitude of oscillations of the point of application of force with antiresonance does not turn into zero. This amplitude will be less, the less the damping (see, for example, [19] – Dynamic Absorber of Vibrations).

3. Application of the Method of Dynamic Rigidity to the Calculation of Oscillations of a Helicopter of Transverse Configuration

The concept of dynamic rigidity appears very convenient in the calculation of such oscillatory systems, which can be divided into two or more parts such that for each of them separately the oscillations are easily found.

Let us consider an oscillatory system consisting of two cross elastic beams 1 and 2 depicted on Fig. 2.12. Such a system entails a fuselage with an elastic wing characteristic for helicopters of transverse configuration.

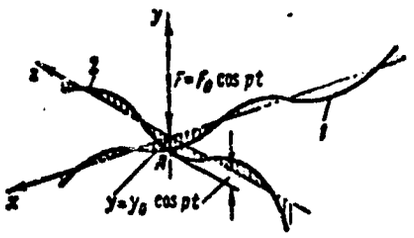

Fig. 2.12. Diagram of an oscillatory system from two cross beams.

Let us assume that it is required to calculate forced oscillations of such a system induced by variable force F, changing with respect to the law and applied at point A of the coupling of beams 1 and 2 (later the method of calculation for the case when exciting forces are applied at any points will be shown). With the help of the method expounded in Nos. 1 and 2, it is possible to calculate forced oscillations of each of the beams separately from

certain forces F_1 and F_2 applied to each of them at point A. The dynamic rigidity of each of the beams at point A can be found. Let us assume that these dynamic rigidities will be $D_1(p)$ and $D_2(p)$.

It is not difficult to show that the dynamic rigidity D(p) of the whole system is equal to the sum of dynamic rigidities of both beams:

$$D(p)=D_1(p)+D_2(p). \tag{2.33}$$

Indeed, force $F = F_0 \cos pt$, acting on the system on the whole, will be equal to the sum of forces $F_1 = F_{01} \cos pt$ and $F_2 = F_{02} \cos pt$ acting on each of the beams. But

$$F_{01}=D_1(p)\bar{y}_0;$$
$$F_{02}=D_2(p)\bar{y}_0,$$

where $\bar{y}_0$ is the amplitude of oscillations of point A identical for both beams.

Consequently,

$$F_0=F_{01}+F_{02}=[D_1(p)+D_2(p)]\bar{y}_0=D(p)\bar{y}_0.$$

Thus the dynamic rigidity of the system is easily found by formula (2.33) if the dynamic rigidities of beams 1 and 2 are known. The graph of dynamic rigidity D(p) can be obtained by simple addition of ordinates of graphs $D_1(p)$ and $D_2(p)$. Values of frequency p, at which D(p) = 0, will give values of frequencies of natural oscillations of the system from two beams. There results from this the following convenient method of determining frequencies of natural oscillations of the system. Since these frequencies are roots of the equation

$$D(p)=D_1(p)+D_2(p)=0,$$

then they can be found from the condition

$$D_1(p)=-D_2(p). \tag{2.34}$$

It is convenient to solve the last equation graphically by superposition of graphs $D_1(p)$ and $-D_2(p)$, as is shown on Fig. 2.13.

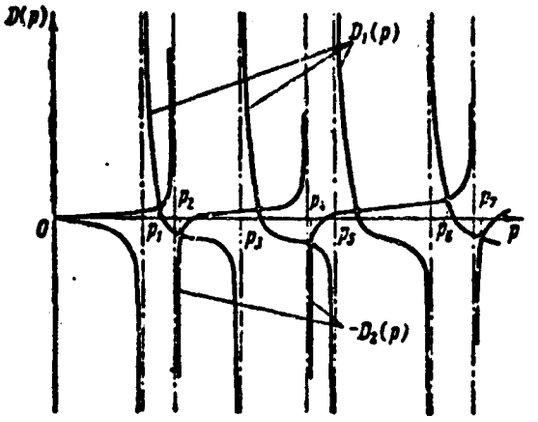

Fig. 2.13. Determination of frequencies of natural oscillations of the system by the method of dynamic rigidity.

Abscissas p_1, p_2, etc., of points of crossing of graphs $D_1(p)$ and $-D_2(p)$ will give values of frequencies of natural oscillations of the system.

With such a method of calculation forms of natural oscillations of the system are simultaneously determined. The form of natural oscillations of the system corresponding to a certain frequency p_k ($k = 1, 2, \ldots$) will consist of forms of forced oscillations of each of the beams with this frequency from forces F_{01} and F_{02}. Since with natural oscillations

$$F_0 = F_{01} + F_{02} = 0,$$

then

$$F_{01} = -F_{02},$$

i.e., force F_{01}, applied to beam 1, is equal in value and opposite in sign to force F_{02} applied to beam 2.

Forms of natural oscillations of such a system can be standardized by selecting the appropriate scale. For example, it is possible to select the scale in such a manner that form of oscillations of beam 1

would have an amplitude equal to unity on its end (x = ℓ). The scale of the form of oscillations of beam 2 connected with it should be selected from a condition of amplitude of oscillations identical with beam 1 at the point of conjugation.

Disposing by standardized forms of natural oscillations of the system, it is possible to calculate its forced oscillations from harmonic forces applied in any points by the method of expansion with respect to natural forms analogous to that as was done in the case of one isolated beam. Here oscillations of both beams are sought in the form

$$y(x, t)=\sum_k c_k \bar{y}_k(x), \qquad (2.35)$$

where $\bar{y}_k(x)$ is the form of oscillations of the given beam corresponding to the standardized form of the k-th tone of oscillations of the system (joint oscillations of both beams).

Coefficients c_k as before are determined by formula (2.22):

$$c_k=\frac{1}{p_k^2-p^2}\frac{A_k}{K_k}, \qquad (2.36)$$

where p_k is the frequency of joint oscillations of the k-th tone of the system.

Coefficients A_k and K_k are determined by the following formulas:

$$A_k=F_0\bar{y}_k(x_0). \qquad (k=1, 2, 3,\ldots) \qquad (2.37)$$

This coefficient constitutes the work of an exciting load on the form of the k-th tone of natural oscillations of the system. Quantity $\bar{y}_k(x_0)$ is the amplitude of the standardized form of oscillations of the k-th tone of the system at the point of application of the force, irrespective of that to which one of the beams is applied excitation [$\bar{y}_k(x_0)$ – it is taken with the "plus" sign if the direction of the force and deflections coincide and with the "minus" sign, if the direction of the force and deflections do not coincide].

$$K_k = \int_{\text{On 1st beam}} m\bar{y}_k^2 dx + \int_{\text{On 2nd beam}} m\bar{y}_k^2 dx. \qquad (2.38)$$

If oscillations of the system are excited not by one but several harmonic forces applied at different points, then the forced oscillations are found as a result of the addition of oscillations induced by each of the forces separately.

Here one should discuss one peculiarity of the excitation from rotors of helicopters of multirotor configurations. Depending upon how kinematic rotors (by a system of transmission) are connected with each other it can appear that variable exciting forces from different rotors change with time in one phase or in opposite phases. Thus, for example, if for a helicopter of transverse configuration the rotors are connected so that the blades of both rotors simultaneously occupy similar positions (for example, extreme front, as is shown on diagram A Fig. 2.14), then forces on both rotors simultaneously attain the largest and least value – they change in one phase. If, however, the rotors are connected as is shown on diagram B, then,

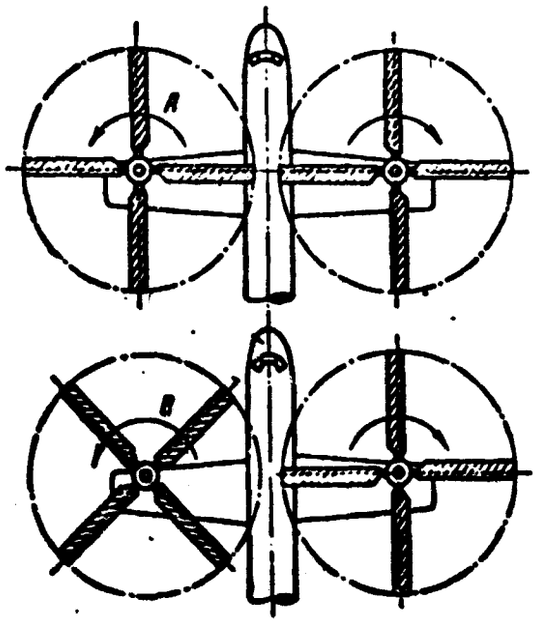

Fig. 2.14. Analysis of vibrations of a helicopter of transverse configuration.

conversely, the exciting loads from both rotors change in opposite phases. This leads to the fact that in case A exciting loads from both rotors can create only symmetric forms of joint oscillations of

the fuselage – wing system and in case B – only skew-symmetric (Fig. 2.15). Since during oscillations of skew-symmetric forms vertical vibrations of points of the fuselage are absent, then for helicopters of a transverse configuration it is desirable to connect the rotors as is shown on diagram B (Fig. 2.14). Similar considerations can be expressed with respect to tandem-rotor helicopters.

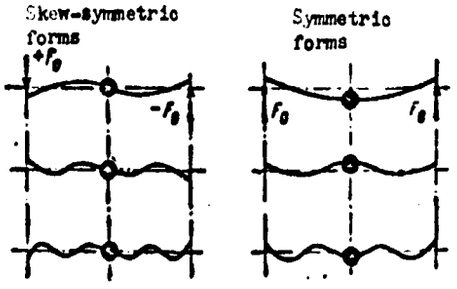

Fig. 2.15. Forms of natural oscillations of the wing with the fuselage of a helicopter of transverse configuration.

Of course, in solving the question of the most profitable mutual location of rotors, it is necessary also to consider concrete values of frequencies of natural oscillations of different tones of the fuselage and also to examine along with oscillations of the fuselage in the plane of symmetry lateral oscillation, which will be discussed in § 3.

4. Method of Additional Mass

To determine the dynamic rigidity according to the method expounded in No. 2, it is necessary to have results of the calculation of natural oscillations of the fuselage. In this case the amplitude of forced oscillations of the point of application of the force, necessary for the determination of dynamic rigidity, is determined by formula (2.32) in the form of expansion with respect to natural forms. However, in the case when there is a program of calculation of natural frequencies on an electronic computer and the calculation of natural oscillations occupies little time, it is possible to recommend for determination of dynamic rigidity of the fuselage at a given point the so-called method of additional mass. With such a method calculation is produced of natural oscillations of the fuselage with additional mass Δm, strengthened in that point at which it is necessary to calculate the dynamic rigidity.

Calculation is produced at different values Δm, and from its results a graph $\Delta m(p)$ of the dependence Δm on frequency of natural oscillations of different tones is constructed.

Figure 2.16 shows an example of such a graph for a single-rotor helicopter. Plotted on this graph along the axis of the ordinates are values of the weight of additional load $\Delta G = g\Delta m$.

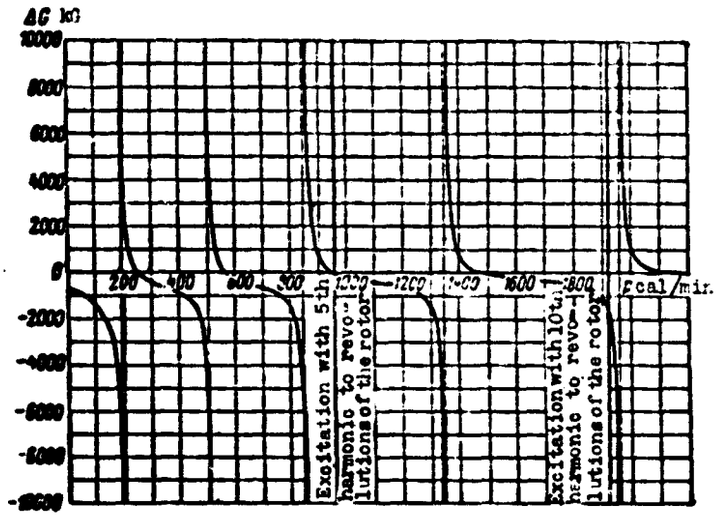

Fig. 2.16. Typical dependence of additional mass of an elastic fuselage (or dynamic rigidity) at the point of rotor attachment on the frequency of excitation.

It is not difficult to show that such a graph can in a certain sense completely replace the graph D(p) shown on Fig. 2.11. Really, with natural oscillations of the beam with additional mass Δm with frequency p this beam is loaded by the corresponding additional force of inertia whose amplitude is

$$F_0 = \Delta m p^2 y_0, \qquad (2.39)$$

where y_0 is the amplitude of oscillations at the attaching point of the additional mass.

The force of inertia F_0 at the time of the greatest deviation from the position of equilibrium is directed in that same side as that of deviation y_0. Negative values of Δm physically correspond to the spring fastened to beam with rigidity $|c| = |\Delta m p^2|$, giving a force proportional to deviation y_0 and directed opposite to the deviation.

It is natural that it is possible to obtain precisely the same oscillations of the beam without the additional mass but forced from the action of harmonic force with the same amplitude $\overline{F}_0$ changing with the same frequency p.

Dynamic rigidity of the beam is determined by the formula

$$D(p) = \frac{\overline{F}_0}{y_0}.$$

Comparing this expression with expression (2.39), we find

$$D(p) = p^2 \Delta m(p). \tag{2.40}$$

Using this formula, it is easy to construct a graph of the dependence D(p), disposing by dependence $\Delta m(p)$. However, this cannot be done, but we can use directly graph $\Delta m(p)$ or $\Delta G(p)$. Thus, for example, for detecting frequencies of natural oscillations of the fuselage of transverse configuration it is possible instead of points of intersection on graphs $D_1(p)$ and $-D_2(p)$ (see Fig. 2.13) to detect the point of intersection of graphs $\Delta G_1(p)$ and $-\Delta G_2(p)$.

5. Effect of Damping Forces. Oscillations with Resonance

The above-stated theory and methods of calculation resulting from it are based on the assumption that the beam is ideally elastic and damping forces are absent. As for any other oscillatory system, in examining oscillations of the beam far from resonances, damping forces can be disregarded, and this does not lead to great errors.

However, in examining oscillations of the beam near resonance or directly in resonance, it is necessary to take into account forces of damping, since the amplitude of oscillations with resonance is determined exclusively by the presence of damping and assuming that damping is absent, the amplitude with resonance is obtained unlimited.

Damping forces with oscillations of the elastic beam appear mainly due to the friction between elements of construction of the beam during its deformations and also due to the so-called internal friction in the material of the beam, which for a beam of compound construction, as a rule, is negligible as compared to the friction between elements of construction [16].

The equation of oscillations of bending of the beam in the presence of damping can be derived, assuming that the bending moment M in the section of the beam is proportional to its curvature $\frac{\partial^2 y}{\partial x^2}$ (in accordance with the Hooke law) and also the speed of change of curvature with time, so that it is possible to write

$$M=EI\frac{\partial^2 y}{\partial x^2}+\eta\frac{\partial}{\partial t}\left(EI\frac{\partial^2 y}{\partial x^2}\right). \qquad (2.41)$$

where η is a certain coefficient characterizing damping properties of the beam in a given cross section, which is assumed the assigned function of coordinate x.

Using further the well-known relations

$$\frac{\partial^2 M}{\partial x^2}=q^*(x,t),$$

where $q^*(x, t)$ is the intensity of the transverse load applied to the beam, and considering that this load is added with oscillations from the external perturbing load $q(x, t)$ and load from forces of inertia, so that

$$q^*(x,t)=q(x,t)-m\frac{\partial^2 y}{\partial t^2}.$$

using equation (2.41), we obtain the following partial differential equation, which describes lateral oscillation of the beam with damping:

$$\frac{\partial^2}{\partial x^2}\left(EI\frac{\partial^2 y}{\partial x^2}\right)+\eta\frac{\partial^3}{\partial t\,\partial x^2}\left(EI\frac{\partial^2 y}{\partial x^2}\right)+m\frac{\partial^2 y}{\partial t^2}=q(x,\ t). \tag{2.42}$$

This equation differs from equation (2.2) only by the presence of the term with factor η and at $\eta = 0$ coincides with (2.2).

In the case if $q(x, t) = 0$ there is obtained an equation describing natural oscillations of the beam with damping:

$$\frac{\partial^2}{\partial x^2}\left(EI\frac{\partial^2 y}{\partial x^2}\right)+\eta\frac{\partial^3}{\partial t\,\partial x^2}\left(EI\frac{\partial^2 y}{\partial x^2}\right)+m\frac{\partial^2 y}{\partial t^2}=0. \tag{2.43}$$

An accurate solution of this equation is rather complicated. However, with relatively small damping it is possible to use a simple approximate solution. The approximate solution of this equation corresponding to natural oscillations of the beam with respect to the k-th tone can be detected, assuming

$$y=\bar{y}_k(x)e^{\lambda_k t}, \tag{2.44}$$

where $\bar{y}_k(x)$ is form of natural oscillations of the k-th tone of the beam in the absence of damping.

Substituting this solution into equation (2.43) and reducing the factor $e^{\lambda_k t}$, multiplying by $\bar{y}_k(x)$ and integrating the equation within limits from 0 to ℓ, and also considering formulas (2.17) and (2.18), we will obtain the following equation for determining λ_k:

$$\lambda_k^2+2n_k\lambda_k+p_k^2=0, \tag{2.45}$$

where

$$2n_k=\frac{1}{K_k}\int_0^l \eta EI\bar{y}_k''^2\,dx. \tag{2.46}$$

Roots of this equation will be

$$\lambda_k = -n_k \pm i p_k^*, \qquad (2.47)$$

where

$$p_k^* = \sqrt{p_k^2 - n_k^2}. \qquad (2.48)$$

Accordingly, expression (2.44) can be written in the form

$$y = \bar{y}_k(x) e^{-n_k t} \cos(p_k^* t + \gamma), \qquad (2.49)$$

i.e., quantity n_k constitutes the attenuation factor of oscillations of the k-th tone, and p_k^* is the frequency of natural oscillations of the k-th tone in the presence of damping.

It is possible to show that the less such an approximate solution of equation (2.43) differs from exact, the less as compared to unity is the dimensionless attenuation factor of the k-th tone, determined by formula

$$\bar{n}_k = \frac{n_k}{p_k}. \qquad (2.50)$$

This coefficient is the most important characteristic of oscillations of the given tone and can be determined experimentally, either by analysis of the oscillogram of attenuated oscillations of the given tone or according to the results of measuring the amplitude of forced oscillations of the beam under the action of the vibrator (this will be discussed later).

For a fuselage of the conventional type (riveted fuselage with Duralumin sheathing) attenuation factors $\bar{n}_k$ of different tones lie within limits of 0.02 to 0.05. These are minute values of attenuation factor, at which the frequency of oscillations of the k-th tone can be considered equal to the frequency calculated neglecting damping, since $p_k^* = p_k \sqrt{1 - \bar{n}_k^2}$. With the shown values of $\bar{n}_k$ this correction is insignificant.

With the calculation of forced oscillations of the beam with damping described by equation (2.42), inasmuch as the damping is small it is also expedient to use the method of approximation founded on the fact that far from the resonances the damping, in general, is not considered, and near the resonances there is the approximate solution obtained on the assumption that the form of forced oscillations near resonance of the k-th tone, just as in the case of the absence of damping, is close to the form of natural oscillations of given tone.

In the presence of damping the equation of forced oscillations of the beam under the action of the harmonic load

$$q(x, t) = q(x)\cos pt \tag{2.51}$$

is conveniently written in the complex form

$$\frac{\partial^2}{\partial x^2}\left(EI\frac{\partial^2 y}{\partial x^2}\right)+\eta\frac{\partial^3}{\partial x^2\partial t}\left(EI\frac{\partial^2 y}{\partial x^2}\right)+m\frac{\partial^2 y}{\partial t^2}=q(x)e^{ipt}. \tag{2.52}$$

Since the real part of the right-hand side of this equation coincides with expression (2.51), then the real motion of the beam will be described in virtue of the linearity of the equation of the real part of the complex solution of equation (2.52). Near resonance with the k-th tone of natural oscillations it is expedient to seek the solution of this equation in accordance with the expounded considerations in the form

$$y(x, t) = c_k\bar{y}_k(x)e^{ipt}, \tag{2.53}$$

where $\bar{y}_K(x)$ as before is the form of the k-th tone of oscillations in the absence of damping.

Let us substitute this expression into equation (2.52). Then we will multiply both parts of equation (2.52) by $\bar{y}_K(x)$ and integrate from 0 to ℓ. Transforming the obtained integrals and considering relations (2.17) and (2.18), and also (2.46), we will obtain the following equation for determining coefficient c_K:

$$c_k(p_k^2+i2n_kp-p^2)=\frac{A_k}{K_k},$$

where A_k and K_k are determined as before by formulas (2.20) and (2.21). Hence

$$c_k=\frac{1}{p_k^2-p^2+i2n_kp}\cdot\frac{A_k}{K_k}. \tag{2.54}$$

The modulus of the complex quantity c_k determines the amplitude of oscillations

$$|c_k|=\frac{1}{\sqrt{(p_k^2-p^2)^2+4n_k^2p^2}}\cdot\frac{A_k}{K_k}, \tag{2.55}$$

and the argument c_k:

$$\arg c_k=\operatorname{arc\,tg}\left(\frac{2n_k}{p^2-p_k^2}\right) \tag{2.56}$$

– the phase of forced oscillations with respect to the exciting load (2.51). With resonance the value c_k [see expression (2.54)] becomes purely imaginary:

$$c_k=-i\frac{A_k}{2n_kpK_k} \quad \text{(when } p=p_k\text{)}.$$

This means that with resonance the phase angle between the exciting load and oscillations of the beam is equal to $\pi/2$. As this is easy to check by direct substitution into the equation, oscillations will occur according to the law

$$y(x,t)=\bar{c}_k\bar{y}_k(x)\sin pt, \tag{2.57}$$

where

$$\bar{c}_k=\frac{A_k}{2\bar{n}_kp_k^2K_k}. \tag{2.58}$$

Thus the amplitude of oscillations with resonance is completely determined by the value $\bar{n}_k$ of the dimensionless attenuation factor of the k-th tone. This can be used for experimental determination of $\bar{n}_k$. If one were to excite oscillations of the beam with the help of the vibrator, i.e., the assigned concentrated force $F=F_0\cos pt$,

applied at the fixed point $x = x_0$, and with resonance ($p = p_k$) to measure the amplitude $\bar{y}_0$ of oscillations at the point of application of the force, then it is easily possible to find quantity $\bar{n}_k$. With this A_k will be determined by formula (2.27) and quantity y_0 by formula

$$y_0 = \bar{c}_k \bar{y}_k(x_0).$$

Therefore, considering expression (2.58), we find

$$\bar{n}_k = \frac{1}{2} \frac{F_0 [\bar{y}_k(x_0)]^2}{y_0 p_k^2 K_k}$$

or

$$\bar{n}_k = \frac{1}{2} \frac{F_0}{m_k p_k^2 y_0}, \tag{2.59}$$

where quantity m_k, which can be called the mass of the k-th tone, reduced to point $x = x_0$, is determined by formula

$$m_k = \int_0^l m \tilde{y}_k^2 dx. \tag{2.60}$$

Here

$$\tilde{y}_k = \frac{\bar{y}_k(x)}{\bar{y}_k(x_0)}. \tag{2.61}$$

The value of the reduced mass m_k with sufficient accuracy is determined by calculation, but it can also be determined experimentally by means of measurement of the form of forced oscillations of the beam during resonance with the k-th tone.

In those cases when it is necessary to estimate beforehand the amplitude during resonance of the fuselage, which is in the designing stage and still not made, it is possible to use formula (2.58), taking values of $\bar{n}_k$ known for another fuselage of similar design, since values of $\bar{n}_k$ for similar designs are distinguished little.

§ 3. Calculation of Vibrations Taking into Account Peculiarities of the Fuselage

1. Peculiarities of the Fuselage. Transverse and Vertical Vibrations

In the preceding paragraph methods were discussed of the calculation of vibrations of a fuselage as an elastic beam (or system of two cross beams for a helicopter of transverse configuration), for which dimensions of cross sections are small as compared to the length. In many cases such a method of calculation gives fully satisfactory results. However, in certain cases when the fuselage of the helicopter possesses peculiarities greatly distinguishing it from the model of an elastic beam, it is necessary to examine more complex calculation diagrams. Constructive configurations of fuselages of helicopters of different types (single-rotor, transverse configuration, longitudinal (tandem-rotor) configuration) are very diverse. Therefore, it would be difficult to indicate some general method of calculation which in all cases would allow quite accurately calculating vibrations of the fuselage from assigned forces.

Every new constructive configuration of a fuselage can require considerable changes in the method of calculation of vibrations. This problem can sometimes appear quite complex. However, in all cases the method of calculation should be based on the general principles of the theory of oscillations of elastic systems. The engineer-designer who must analyze vibrations of a future helicopter of new design should possess these general methods so as to be able to modify the calculation diagram in reference to each new problem. Therefore, the account of the material of this chapter is put together in such a way to show the essence of the most important procedures used in the calculation of vibrations. Thus the method of expansion with respect to natural forms, the method of dynamic rigidity and the concept of resonance and antiresonance can be applied not only to an elastic beam or system of two cross beams, but also to any other more complex oscillatory system. These methods were discussed in reference to the beam, since, on the one hand, in this example they can be most easily shown, and, on the other hand, by itself the

method of calculation of oscillations of the beam can in many cases be used for the calculation of vibrations of the fuselage without any changes.

For an illustration of certain peculiarities of the real fuselage let us turn to Fig. 2.17, on which there is schematically

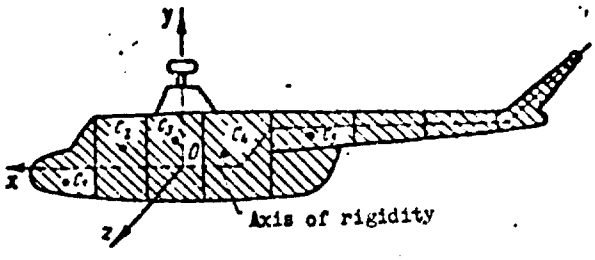

Fig. 2.17. Reduction of the problem of vibrations of an elastic fuselage to the problem of vibrations of an elastic beam.

depicted the fuselage of a single-rotor helicopter. The peculiarity of such a fuselage consists in the fact that its axis of rigidity constitutes a broken line, the centers of gravity of sections of the fuselage do not lie on the axis of rigidity, and each section of the fuselage is a body for which all measurements are of one order, and with calculation of oscillations it is necessary to take into account not only the mass of the seciton but also the moments of inertia of it relative to all three axes. Calculations show that with determination of the lowest tone of oscillations of bending of such a fuselage, both in plane xOy (vertical oscillations) and in plane xOz (lateral oscillation) there can be obtained quite satisfactory results, calculating the fuselage as elastic thin beam with a rectilinear axis.

If during the calculation of the vibrations it is possible to be limited by consideration of vibrations of the fuselage as a solid and to consider only lowest elastic tone (first three forms on Fig. 2.7), then the calculation of vibrations of the fuselage as a thin beam with a rectilinear axis will lead to satisfactory results. However, if the second elastic tone of oscillations has a frequency close to the frequency of the basic harmonic of the rotor zω (and this frequently happens), then such a calculation can lead to certain errors. With the calculation of vibrations in the cockpit (in the

nose part of the fuselage) the error can be insignificant, but amplitudes of vibrations in the region of tail beam can very greatly differ from the real. To increase the accuracy of the calculation it is required to determine vibrations taking into account a large number of elastic tones (second and third tone). But already the determination of the second elastic tone with sufficient accuracy will require complication of the calculation model.

Considerable refinement in the results of the calculation can be obtained with the use of the calculation model depicted in Fig. 2.18. The fuselage here is replaced by an elastic beam with a rectilinear axis to which are fastened separate loads 1, 2, 3, etc.

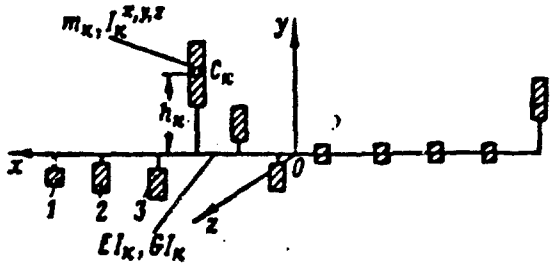

Fig. 2.18. Calculation model for the calculation of vibrations of an elastic fuselage.

The center of gravity of each load will be from axis of the beam at a certain distance h_k. For each load there is assigned its mass m_k and moments of inertia I_x and I_z with respect to axes parallel, respectively, to axes Ox and Oz and passing through the center of gravity of the load. For each section of the elastic beam located between loads k and k + 1 there are assigned bending rigidities EI_k^z and EI_k^y in both planes xOz and xOy and torsional rigidity GI_k.

For such a calculation model the lateral oscillations (in plane xOz) are joint flexural-torsional vibrations. Frequencies and forms of natural flexural-torsional vibrations of such a system can be calculated with the help of the method expounded in § 6 of Chapter I (see Fig. 1.19), in reference to the blade of the rotor. Here we must assume that the centrifugal force N = 0, rigidity of the control link $c_{y+\psi}=0$, $EIy''(0)=0$ and $(EIy'')'\big|_{-0}^{-0}$. This corresponds to the fact that the left end of the beam is not secured. Instead of value $x_{\mu,\tau}$ in the calculation of the blade one should substitute values of staggers h_k.

With the calculation of forced lateral oscillations of such a system it is possible to use the method of expansion with respect to natural forms (flexural-torsional). Here it is possible to use all formulas of § 2 of this chapter, in which by quantity A_k we mean the work of the exciting load on the standardized form of the given tone and by quantity K_k, the kinetic energy of the given tone referred to the square of its frequency p_k^2. Figure 2.19 shows the characteristic forms of natural lateral flexural-torsional vibrations of a single-rotor helicopter.

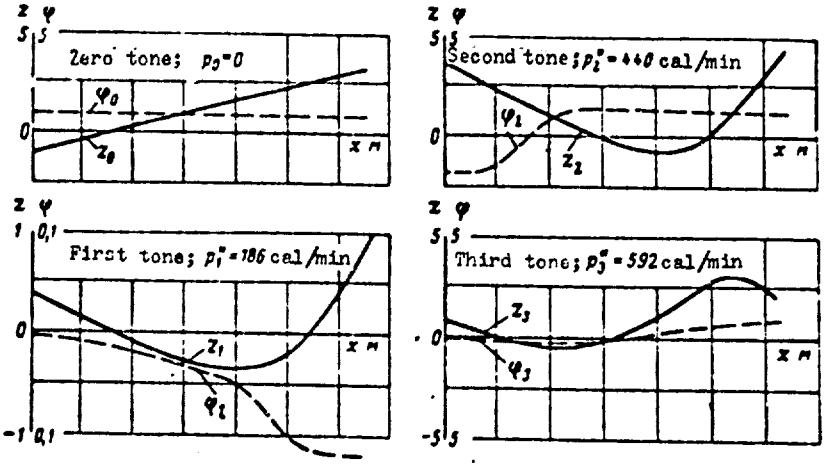

Fig. 2.19. Forms of natural oscillations of an elastic fuselage of a single-rotor helicopter in the plane of symmetry.

Absolutely the same method of calculation and model shown on Fig. 2.18 can be used for the calculation of vertical flexural-torsional vibrations of the wing of a helicopter of transverse configuration with pods on the tips (Fig. 2.20). If the centers of gravity of pods have large extensions h, then with the calculation of vibrations of such a wing it is impossible to examine the isolated oscillations of bending in a vertical plane, but it is necessary to examine the joint flexural-torsional vibrations. To calculate the joint vibrations of the fuselage-wing system in this case it is necessary to use the method of dynamic rigidity.

The greatest calculation model simulating a real fuselage of a helicopter should, apparently, be considered the model depicted on

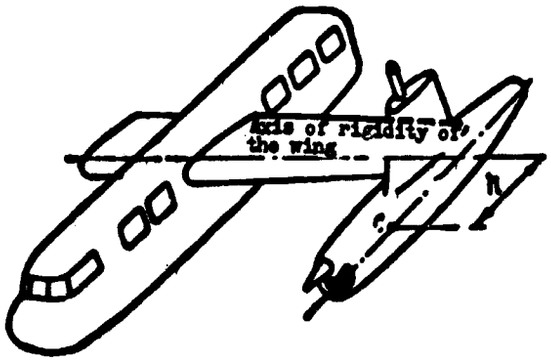

Fig. 2.20. Diagram of pod with great stagger.

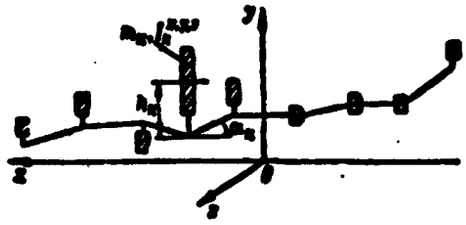

Fig. 2.21. Calculation model for the calculation of vibrations of an elastic fuselage with a broken axis of rigidity.

Fig. 2.21. Here the axis of rigidity of the beam is given as a certain broken line. The angle of inclination of the k-th section of the broken line is given by angle α_k. Such a calculation model reflects well the properties of any fuselage which has the plane of symmetry xOy. For a fuselage which has the plane of symmetry xOy, it is possible to calculate separately vertical oscillations of bending (or oscillations in the plane of symmetry) and transverse flexural-torsional vibrations.

In the calculation of vertical oscillations for every load it is necessary to consider three degrees of freedom:

- displacement of the center of gravity of the load along axis Ox;

- displacement of the center of gravity of load along axis Oy;

- turn of load with respect to axis Oz.

In the calculation of transverse flexural-torsional vibrations for every load it also is necessary to consider these three degrees

of freedom:

– displacement of the center of gravity of the load along axis Oz;

– turn around axis Ox;

– turn around axis Oy.

The calculation of vertical oscillations of such a system is examined in the following point of this paragraph. Here there is illustrated the application of the so-called method of remainder for the calculation of oscillations, which often appears very convenient.

The calculation of lateral oscillations of such a system in general is not examined here, since for the calculation of transverse flexural-torsional vibrations quite good results are given by using the calculation model depicted on Fig. 2.18. Let us only note that for the system depicted on Fig. 2.21 the calculation of transverse flexural-torsional vibrations could have also been conducted by the remainder method.

2. Calculation of Oscillations of the Fuselage in the Plane of Symmetry by the Remainder Method

Let us assume that the plane elastic system depicted on Fig. 2.21 accomplishes stabilized forced oscillations in its plane xoy under the action of a harmonic exciting load consisting of forces and moments

$$\left.\begin{aligned} P_{kx} &= P^0_{kx}\cos pt;\\ P_{ky} &= P^0_{ky}\cos pt;\\ M_k &= M^0_k\cos pt, \end{aligned}\right\} \qquad (3.1)$$

applied to each load (Fig. 2.22).

With steady-state oscillations all points of the system will accomplish harmonic oscillations with a frequency of excitation p so that if one were to designate by $\bar{x}$, $\bar{y}$ and φ, respectively, the

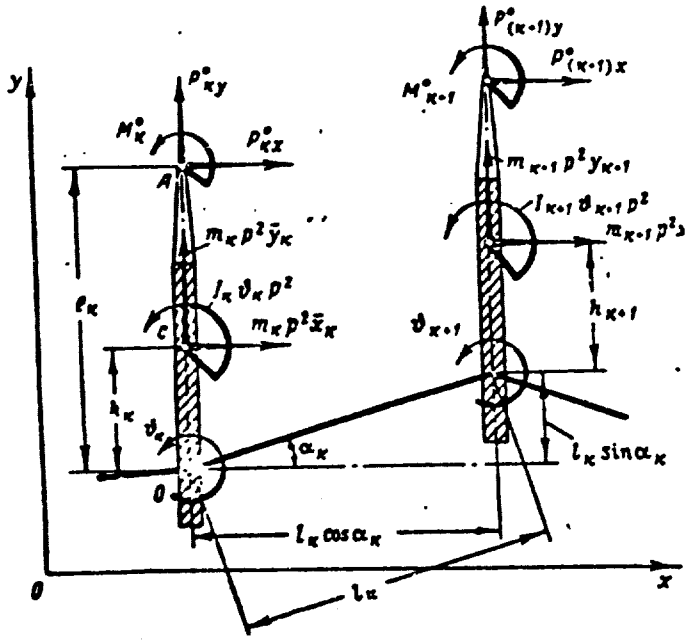

Fig. 2.22. Diagram of forces acting on a section of elastic model of the fuselage.

displacements of the center of gravity c load along axes Ox and Oy and angle of rotation of the load relative to its center of gravity, then for the k-th load it is possible to write

$$\left.\begin{aligned} \bar{x} &= \bar{x}_k \cos pt; \\ \bar{y} &= \bar{y}_k \cos pt; \\ \vartheta &= \vartheta_k \cos pt. \end{aligned}\right\} \quad (k = 1, 2, 3, \ldots \qquad (3.2)$$

Let us establish dependences connecting forces applied to loads with deformations of sections of the beam. We will examine forces and deformation only for the position of the system corresponding to the greatest deflection from the position of equilibrium (i.e., we will examine only the amplitude of forces and deformations). Let us formulate the equation of equilibrium for the k-th load (Fig. 2.23). To the load there are applied the following:

– external forces P^0_{kx}, P^0_{ky}, M^0_k (applied at point A);

– forces of inertia of the load $m_k p^2 \bar{x}_k$; $m_k p^2 \bar{y}_k$; $J_k p^2 \vartheta_k$ (applied at point C);

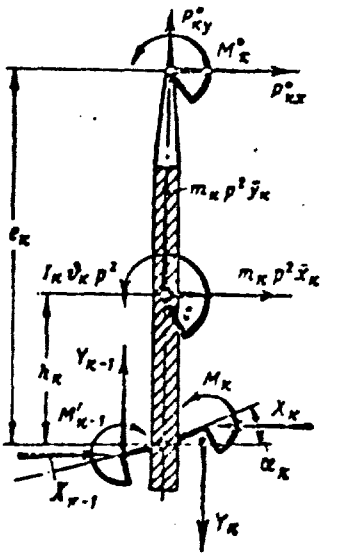

Fig. 2.23. Diagram of forces applied to the k-th element of the elastic model of the fuselage.

– forces acting on the load from the side of the left section of the beam adjoining to it: X_{k-1}, Y_{k-1}, M'_{k-1};

– forces acting on the load from the side of the right section of the beam adjoining to it: X_k, Y_k, M_k.

Equations of equilibrium of the load will be written in the form

$$X_k = X_{k-1} + m_k p^2 \bar{x}_k + P^0_{kx}; \tag{3.3}$$

$$Y_k = Y_{k-1} + m_k p^2 \bar{y}_k + P^0_{ky}; \tag{3.4}$$

$$M_k = M'_{k-1} + m_k \bar{x}_k h_k p^2 - \vartheta_k I_k p^2 + P^0_{kx} e_k - M^0_k. \tag{3.5}$$

Positive directions of forces and displacements are shown on Figs. 2.22; 2.23; 2.24. Quantity I_k constitutes the distance from the point of application of external exciting forces P^0_{kx} to the point of attachment of the load to the elastic beam.

From conditions of equilibrium of a section of the beam (Fig. 2.24) we have

$$M'_k = M_k + Y_k l_k \cos\alpha_k - X_k l_k \sin\alpha_k. \tag{3.6}$$

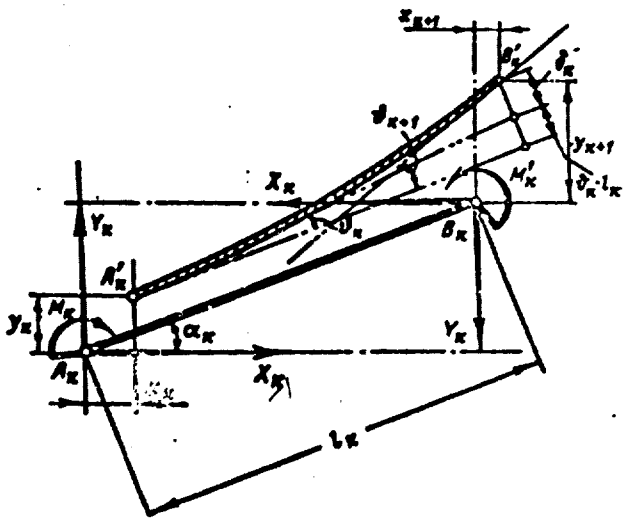

Fig. 2.24. Diagram of forces applied to the section of the elastic model of the fuselage.

For an examination of the deformations let us turn to Fig. 2.24, on which there is depicted the k-th section of the elastic beam A_kB_k in the position of equilibrium and the same section in the displaced position $A_k'B_k'$. Let us assume that quantities x_k, y_k, x_{k+1} and y_{k+1} are displacements of points A_k and B_k – ends of the section, and $\$_k$ and $\$_{k+1}$ are angles of rotation of the tangent to the elastic axis on the left and right ends. Let us assume that further δ_k is the sag of the beam on the k-th section, i.e., the displacement of the right end of the beam – point B_k in a direction perpendicualr to A_kB_k relative to the tangent to the elastic axis on the left and – at point A_k. Then it is possible to write

$$\left.\begin{aligned} x_{k+1} &= x_k - (l_k + \delta_k/2)\sin\alpha_k; \\ y_{k+1} &= y_k + (l_k + \delta_k/2)\cos\alpha_k. \end{aligned}\right\} \qquad (3.7)$$

where l_k and α_k are the length and angle of inclination, respectively, of the k-th section of the beam (Fig. 2.24).

Using the usual procedures of the strength of materials, let us find the following equations connecting forces and deformations:

$$l_k = \frac{l_k^2}{EI_k}\left[\frac{1}{3}M_k + \frac{1}{6}M_k'\right]; \qquad (3.8)$$

$$\$_{k+1} = \$_k + \Delta\$_k; \qquad (3.9)$$

$$\Delta\$_k = \frac{l_k}{2EI_k}[M_k + M_k']. \qquad (3.10)$$

Displacements of points of the beam x_k and y_k are connected with displacements of centers of gravity of loads by evident formulas:

$$\left.\begin{aligned}\bar{y}_k &= y_k;\\ \bar{x}_k &= x_k - \delta_k h_k.\end{aligned}\right\} \qquad (3.11)$$

Recurrence formulas (3.3), (3.4), (3.5) and (3.7) together with expressions (3.8), (3.9), (3.10) and (3.11) allow, by knowing forces and displacements of the k-th load, to determine forces and displacements of the (k + 1)-th load. Using these formulas, it is possible to solve the problem by the "chain method," namely: assigning amplitudes $x_0 y_0$ and $\$_0$ on the left end of the beam, it is possible, consecutively, passing from section to section, to determine amplitudes and forces on the extreme right end of the beam, expressing them by quantities x_0, y_0 and $\$_0$. If the beam has n loads, then it is thus possible to determine quantities X_n, Y_n and M_n on the right end or "remainder." But since the right end of the beam is free, then the "remainder" should be equal to zero, i.e., on the right end of the beam there should be fulfilled these conditions:

$$X_n = Y_n = M_n = 0.$$

These conditions constitute a system of three equations for the determination of unknowns x_0, y_0, and $\$_0$, in terms of which amplitudes of oscillations and forces on all loads of the beam are already expressed.

Such a method of calculation of forced oscillations of the system (Fig. 2.21) is absolutely analogous to the well-known "remainder" method – the Tolle method, used for the calculation of torsional vibrations of a multiple-disk system [20]. An analogous method is used for the calculation of oscillations of bending of elastic balls. In American and English works such a method is called the McIlstead method [33], [34]. It permits finding the curve of dynamic rigidity (Fig. 2.11) of the system at any point and in any direction by means of calculation of oscillations at different values of p, and also of the frequency and form of natural oscillations of the system from an examination of forced oscillations of the system

near resonances when amplitudes of forced oscillations increase without limit.

This method is especially convenient when using electronic computers, without which at present the carrying out in necessary quantity of all dynamic calculations is impossible.

For a practical application of this method it is convenient to express magnitudes of forces and displacements on the k-th section in terms of values x_0, y_0 and $\$_0$ in the form

$$\left.\begin{aligned} x_k &= A_k^x + B_k^x x_0 + C_k^x y_0 + D_k^x \vartheta_0; \\ y_k &= A_k^y + B_k^y x_0 + C_k^y y_0 + D_k^y \vartheta_0; \\ \vartheta_k &= A_k^\vartheta + B_k^\vartheta x_0 + C_k^\vartheta y_0 + D_k^\vartheta \vartheta_0; \\ X_k &= A_k^X + B_k^X x_0 + C_k^X y_0 + D_k^X \vartheta_0; \\ Y_k &= A_k^Y + B_k^Y x_0 + C_k^Y y_0 + D_k^Y \cdot \vartheta_0; \\ M_k &= A_k^M + B_k^M x_0 + C_k^M y_0 + D_k^M \vartheta_0. \end{aligned}\right\} \qquad (3.12)$$

where A_k^X, B_k^X, etc., are certain coefficients.

With calculation by the "chain" method according to values of these coefficients for the k-th section it follows to determine their values for the (k + 1)-th section. Using recurrence formulas for forces and movements, it is easy to formulate recurrence formulas for appropriate coefficients. With this the following formulas are obtained.

For coefficients $A_k^\$$, $B_k^\$$, $C_k^\$$ and $D_k^\$$:

$$A_k^\vartheta = A_{k-1}^\vartheta + \frac{l_{k-1}}{EI_{k-1}} A_{k-1}^M + \frac{l_{k-1}^2 \cos\alpha_{k-1}}{2EI_{k-1}} A_{k-1}^Y - \frac{l_{k-1}^2 \sin\alpha_{k-1}}{2EI_{k-1}} A_{k-1}^X. \qquad (3.13)$$

For quantities $B_k^\$$, $C_k^\$$ and $D_k^\$$ analogous formulas are obtained by replacement of quantity A respectively by B, C and D. The same pertains to subsequent formulas (3.14) and (3.15).

For coefficients A_k^X, B_k^X, C_k^X and D_k^X:

$$A^x_{k+1} = A^x_k - \frac{l_k^2 \sin\alpha_k}{2EI_k} A^M_k - \frac{l_k^3 \sin\alpha_k \cos\alpha_k}{6EI_k} A^Y_k + \\ + \frac{l_k^3 \sin^2\alpha_k}{6EI_k} A^X_k - l_k \sin\alpha_k A^\phi_k. \qquad (3.14)$$

For coefficients A^y_k, B^y_k, C^y_k and D^y_k:

$$A^y_{k+1} = A^y_k + \frac{l_k^2 \cos\alpha_k}{2EI_k} A^M_k + \frac{l_k^3 \cos^2\alpha_k}{6EI_k} A^Y_k - \\ - \frac{l_k^3 \cos\alpha_k \sin\alpha_k}{6EI_k} A^X_k + l_k \cos\alpha_k A^\phi_k. \qquad (3.15)$$

For coefficients A^X_k, B^X_k, C^X_k and D^X_k:

$$A^X_k = A^X_{k-1} + m_k p^2 A^X_k - m_k p^2 h_k A^\phi_k + P^0_{kx}; \qquad (3.16)$$

$$\left.\begin{aligned} B^X_k &= B^X_{k-1} + m_k p^2 A^x_k - m_k p^2 h_k B^\phi_k; \\ C^X_k &= C^X_{k-1} + m_k p^2 C^x_k - m_k p^2 h_k C^\phi_k; \\ D^X_k &= D^X_{k-1} + m_k p^2 D^x_k - m_k p^2 h_k D^\phi_k. \end{aligned}\right\} \qquad (3.17)$$

For coefficients A^Y_k, B^Y_k, C^Y_k and D^Y_k:

$$A^Y_k = A^Y_{k-1} + m_k p^2 A^Y_k + P^0_{ky}; \qquad (3.18)$$

$$\left.\begin{aligned} B^Y_k &= B^Y_{k-1} + m_k p^2 B^y_k; \\ C^Y_k &= C^Y_{k-1} + m_k p^2 C^y_k; \\ D^Y_k &= D^Y_{k-1} + m_k p^2 D^y_k. \end{aligned}\right\} \qquad (3.19)$$

And, finally, for coefficients A^M_k, B^M_k, C^M_k and D^M_k:

$$A^M_k = A^M_{k-1} + A^Y_{k-1} l_{k-1} \cos\alpha_{k-1} - A^X_{k-1} l_{k-1} \sin\alpha_{k-1} + m_k h_k p^2 A^x_k - \\ - p^2 (m_k h_k^2 + I_k) A^\phi_k - M^0_k + P^0_{kx} e_k; \qquad (3.20)$$

$$B^M_k = B^M_{k-1} + B^Y_{k-1} l_{k-1} \cos\alpha_{k-1} - B^X_{k-1} l_{k-1} \sin\alpha_{k-1} + \\ + m_k h_k p^2 B^X_k - p^2 (m_k h_k^2 + I_k) B^\phi_k. \qquad (3.21)$$

Formulas for C^M_k and D^M_k are obtained from the last replacement of quantities B respectively by quantities C and D.

The formulas given permit determining the values of coefficients on the following section according to their known values on the preceding section. Thus, moving from section to section from left to right, we will determine values of coefficients on the right end of the beam. On right free end (k = n) there should be fulfilled these conditions:

$$\left.\begin{aligned} X_n &= A_n^X + B_n^X x_0 + C_n^X y_0 + D_n^X \vartheta_0 = 0; \\ Y_n &= A_n^Y + B_n^Y x_0 + C_n^Y y_0 + D_n^Y \vartheta_0 = 0; \\ M_n &= A_n^M + B_n^M x_0 + C_n^M y_0 + D_n^M \vartheta_0 = 0. \end{aligned}\right\} \qquad (3.22)$$

Solving this system, let us find the values interesting us x_0, y_0 and $\$_0$:

$$\left.\begin{aligned} x_0 &= \frac{\Delta_{x_0}}{\Delta}; \\ y_0 &= \frac{\Delta_{y_0}}{\Delta}; \\ \vartheta_0 &= \frac{\Delta_\vartheta}{\Delta}. \end{aligned}\right\} \qquad (3.23)$$

where Δ is the determinant of the system (3.22); Δ_{x_0}, Δ_{y_0}, Δ_ϑ are determinants obtained from the determinant Δ by means of replacement of the corresponding column by free terms of the equations.

Knowledge of quantities x_0, y_0 and $\$_0$ permits by formulas (3.12) finding the movement and forces acting in every section of the beam.

Figure 2.25 shows the form of forced oscillations of a single-rotor helicopter determined by the indicated method. The form of oscillations in this case should be represented by the three graphs: $x_k(x)$, $y_k(x)$ and $\vartheta_k(x)$.

Table 2.1 gives initial data for the calculation conducted.

Forced oscillations were calculated from the following forces applied to the rotor hub (load No. 3)

$$P_{3x}^0 = 0{,}05G; \quad P_{3y}^0 = 0{,}03G; \quad M_3^0 = 0,$$

where G is the weight of the helicopter.

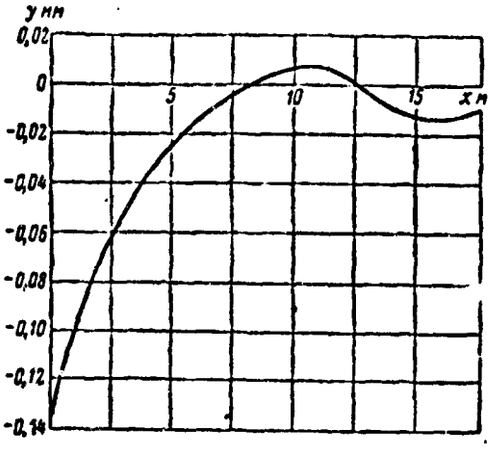

Fig. 2.25. Form of forced oscillations of an elastic fuselage of a single-rotor helicopter obtained by the remainder method.

Table 2.1.

Numbers of sections	0	1	2	3	4	5	6	7	8	9	10
x_k (м)	0	1,7	3,45	5,1	7,2	9,1	12,4	13,7	15,1	16,7	18,2
G_k (кГ)	30	1471	1692	3564	3599	259	24	24	22	92	153
I_k (кг/м·с^2)	0,10	37,65	63,0	260,5	286,7	4,62	0,19	0,10	0,05	0,077	0,165
h_k (м)	−0,15	−0,024	−0,025	0,778	0,316	−0,15	0	0	0	0	0
I_k (м^4)	0,00155	0,0066	0,0068	0,207	0,0015	0,00042	0,00028	0,00017	0,00013	1,0	—
a_k^0	0	0	0	0	21	0	0	0	0	43	—

One of the merits of such a method of calculation consists in the fact that for the calculation of forced oscillations it is not required to conduct a preliminary calculation of frequencies and forms of natural oscillations of the system. Furthermore, in conducting such a calculation for different values of frequencies p, it is possible to construct a graph of the dynamic rigidity of system D(p) at any point and also to find all frequencies and forms of natural oscillations. Figure 2.26 gives results of the calculation of the graph of dynamic rigidity for the same system assigned by Table 2.1 for force P^0_{ky}. Values of p_k at which D(p) = 0 give frequencies of natural oscillations of the system, and the form of forced oscillations at value p, close to any of frequencies

p_k (k = 1, 2, 3, ...) of natural oscillations, gives with any degree of accuracy the form of natural oscillations of this tone. Forms of the first three tones for the examined system, obtained in such a way, are shown on Fig. 2.27.

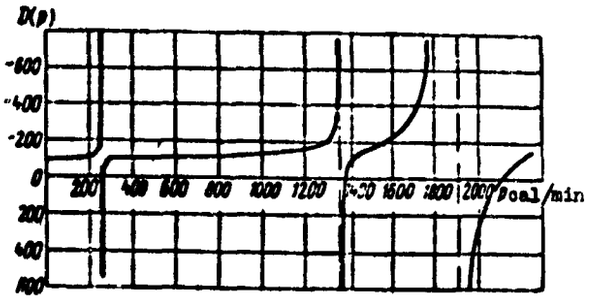

Fig. 2.26. Curve of dynamic rigidity of the fuselage obtained by the remainder method.

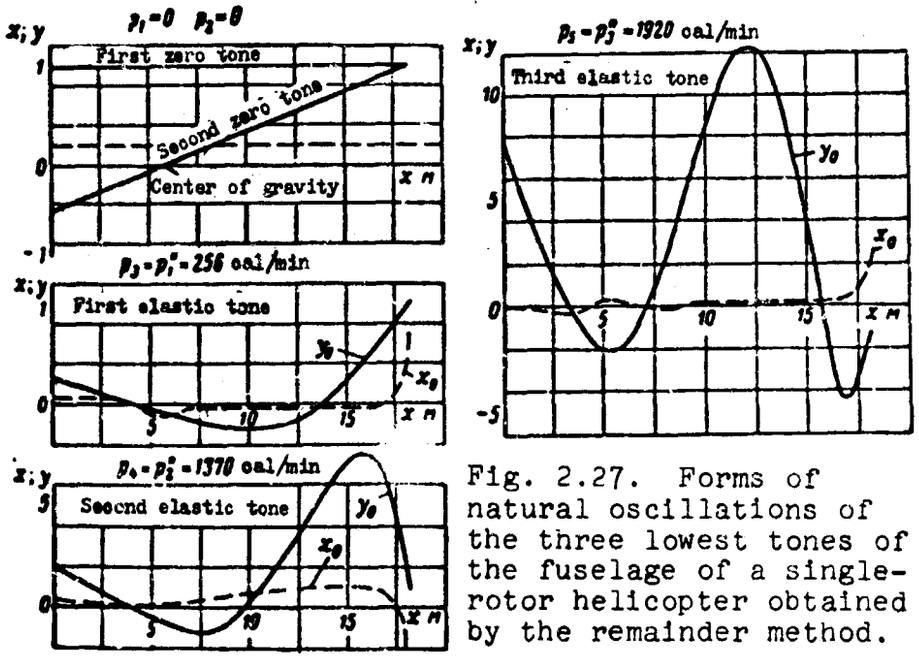

Fig. 2.27. Forms of natural oscillations of the three lowest tones of the fuselage of a single-rotor helicopter obtained by the remainder method.

Let us note in conclusion that the "remainder" method given here requires fulfillment of the calculation with very great accuracy (not less than four-five significant digits). This makes the indicated method practically unfit for manual calculation. However, as was already indicated, calculations of oscillations in the necessary volume, in general, can be conducted only with the application of high-speed computing machines, for which the indicated accuracy is usual.

3. Calculation of Influence of Shearing Strains

All the examined methods of the calculation of oscillations of the fuselage were based on the use of the usual relationships of strength of materials for bending of a thin beam. These relationships are considered only tensile strains and compressions of fibers of material of the beam and do not consider shearing strains. Meanwhile the calculation of these deformations introduces certain corrections into results of the calculation, and these corrections are obtained very insignificant for the first tone of oscillations (lowering of the frequency by 5-7%), for the second tone of correction they are obtained somewhat more (lowering of the frequency by 10-15%), for the third tone even more (20-30%), etc. Therefore, if with the calculation of vibrations it is necessary to consider high tones of the oscillations, the oscillations should be calculated taking into account shearing strains caused by tangential stresses in the sheathing of the fuselage. This can be fulfilled in the following way. If calculation is produced for the model depicted on Fig. 2.21, then it is possible to use all formulas of the "remainder" method, with the exception of formula (3.8), which in this case should be written in the form

$$\delta_k = \frac{l_k^2}{EI_k}\left(\frac{1}{3}M_k + \frac{1}{6}M_k'\right) + \delta_k', \tag{3.24}$$

where δ_k' is the additional sag of the k-th section from shear force Q_k.

$$Q_k = X_k \sin\alpha_k - Y_k \cos\alpha_k. \tag{3.25}$$

The additional sag δ_k' can be determined by the formula (see, for example [21])

$$\delta_k' = \frac{Q_k l_k}{GF_k}\varkappa, \tag{3.26}$$

where F_k is the area of the cross section of the fuselage on the k-th section, and $\varkappa$ is a certain dimensionless coefficient determined by formula

$$\varkappa = \frac{F_k}{I_k^2}\int \frac{S_k^2(z)\,dz}{2\delta(z)}, \qquad (3.27)$$

where I_k is the moment of inertia of the cross section with respect to the neutral line; $S_k(z)$ is the static moment with respect to the neutral line of the part of the cross section located higher than the straight line parallel to the neutral line and remote from it at distance z; $\delta(z)$ – thickness of the sheathing of the fuselage at distance z from the neutral line.

The integral in formula (3.27) is taken over the whole cross section F of the fuselage.

In conformity with the correction in formula (3.8) it is necessary to introduce corrections into recurrence formulas for coefficients A_k^X, A_k^Y, A_k^δ, etc.

§ 4. Joint Oscillations of the Fuselage-Rotor System

1. Oscillations of the Fuselage-Rotor System

Methods of calculation of oscillations of elastic blades, which were discussed in Chapter I, assume that the blade is hinged fastened to the hub, which is attached to a fixed support. In fact the hub is attached to the elastic fuselage and with oscillations of the blades there are forces causing its movement so that in reality during oscillations of the blade a sag in the hinge of the hub is equal not to zero but to a corresponding sag in the fuselage.

Results of flight tests in many cases showed that calculations of frequencies of natural oscillations of blades, carried out neglecting the elasticity of the fuselage, can lead to considerable errors. In connection with this M. L. Mil' formulated and stated the problem of the calculation of joint vibrations of the fuselage-rotor system as a single vibrational system. Basic results of investigations which were conducted in this direction are given below.

Frequencies and forms of natural joint oscillations of the fuselage-rotor system can be found with the help of the method of dynamic rigidity, the essence of which is discussed in Nos. 2, 3, and 4 of § 2.

However, the carrying out of such calculations is connected with a great quantity of calculating work. This especially pertains to the determination of frequencies of transverse natural oscillations of the fuselage-rotor system when it is necessary to determine dynamic rigidity of the rotor in the plane of rotation. Furthermore, the calculations conducted show that the connection of vibrations of the fuselage and blades is, as a rule, weak, and frequencies of natural oscillations of the fuselage-rotor system can always be divided into two such groups which frequencies of the first group are very close to frequencies of natural oscillations of the isolated fuselage, during the calculation of which the mass of the blades is considered concentrated in the center of the rotor, and frequencies of the second group are quite close to frequencies of natural oscillations of blades calculated on the assumption that the blades are mounted on an absolutely rigid and infinitely heavy fuselage.

In those cases when attachment of the hub to the fuselage is not rigid enough (elastic shaft of the rotor, elastic sub-reduction gear frame, crankcase of reduction gear), it can appear that some of the frequencies of oscillations of the second group noticeably change as compared to frequencies of blades calculated by the usual method.

Therefore, as a rule, frequencies of natural oscillations of the first group can be determined with the help of methods discussed in this chapter as frequencies of the fuselage, not taking into account elasticity of the blades. The exception can be special cases when, for example, rotors are attached to light and elastic wings on a helicopter of transverse configuration. In these cases it is necessary to calculate frequencies of joint oscillations of the fuselage-rotor system by the mentioned method of dynamic rigidity.

Regarding, however, frequencies of natural oscillations of blades, it is apparently necessary always to estimate the possible change of some of these frequencies conditioned by local elasticity of attachment of the rotor to the fuselage.

Thus, to account for the connection between vibrations of the fuselage and blades it is practically enough to estimate only the change in frequencies of natural oscillations of blades, which is conditioned by the local elasticity of the blade attachment.

In the following point of this paragraph there is discussed the method of such calculation for determining frequencies of natural oscillations of blades in the plane of rotation taking into account bending elasticity of the rotor shaft. This case is practically the most important.

The elasticity of other elements of rotor fastening (reduction gear frame, housings of the reduction gear frame, etc.) can always be joined to the elasticity of the rotor shaft. Let us indicate here certain important fundamental considerations from which it becomes clear that only certain of the frequencies of natural oscillations of the blades can be changed as a result of the effect of the rotor's fastening elasticity.

In § 1 of this chapter it was shown that not all harmonic components of forces from vibrating blades "pass" to the fuselage, since many of their components are balanced on the body of the rotor hub.

Thus, for example, with vibrations of the blades of a five-blade rotor in the flapping plane, the first four harmonic components of forces applied to the hub from the blades (ω, 2ω, 3ω, 4ω) are balanced on the hub, and only the fifth harmonic component is transferred to the fuselage.

Hence it is clear when calculating forced oscillations of blades from forces corresponding to harmonics ω, 2ω, 3ω, and 4ω, it is

necessary to examine forms and frequencies of natural oscillations of the blades (with the method of expansion with respect to natural forms) calculated for the usual boundary conditions when the blade is assumed to be hinged supported on the fixed hub.

As regards the forced oscillations with respect to the fifth harmonic, it is necessary here to take into consideration the presence of joint vibrations of the blade and fuselage.

The physical essence of this phenomenon is that the forms of natural oscillations of the rotor with elastic blades can be divided into two groups:

1) forms of oscillations of the rotor at which forces from separate blades are balanced on the housing of the hub;

2) forms of oscillations of the rotor at which forces from separate blades are summed on the housing of the hub and are transmitted to the fuselage.

Figure 2.28, for example, shows two such forms of oscillations for a rotor with four blades, since for such a rotor the clearest picture is obtained. Both forms of oscillations A and B correspond to the frequency p_1 of oscillations of a mononodal tone of an isolated blade in the flapping plane and differ from one another only in the distribution of the phase of oscillations with respect to separate blades. The form of oscillations A corresponds to a situation when pairs of opposite blades vibrate in opposite phases. Here forces P_1, P_2, P_3 and P_4, acting on the rotor hub, are mutually balanced at every instant and are not transmitted to the fuselage. The form of oscillations B corresponds to a situation when all four blades vibrate in one phase. Here forces P_1, P_2, P_3 and P_4 are summed on the hub and give a certain force acting on the fuselage and changing in time with frequency p_1.

If the rotor hub is mounted on an absolutely rigid support, the frequencies of both forms of oscillations A and B of the rotor are

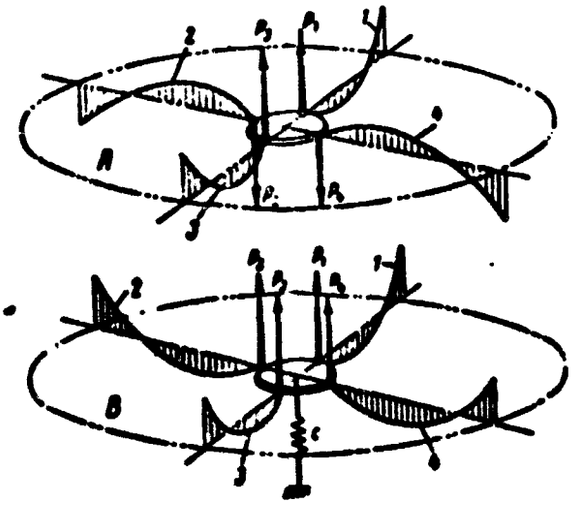

Fig. 2.28. Forms of oscillations of a rotor with elastic blades.

identical and equal to frequency p_1 of natural oscillations of the first tone of one isolated blade with a hinged attached shank end. If, however, the hub is mounted on a certain elastic support with vertical rigidity c, the frequency of the form of oscillations A will not be changed and will remain equal to p_1, and the frequency of form B will drop more, the less the rigidity c.

It is possible to show that forms of the two indicated types exist for a rotor with any number of blades z. These forms of oscillations can be characterized by a certain formula. Thus, for example, all forms of oscillations of a z-blade rotor, which correspond to the k-th tone of oscillations of the isolated blade, are characterized by the following law of oscillations of the blades:

$$y_n(x, t) = y_k(x) \cos s\psi_n \cos p_k t \qquad (4.1)$$

where $y_n(x, t)$ is the deflection of the point with coordinate x belong to the n-th blade; cos s ψ_n – characterizes the law of distribution of phases of oscillations with respect to separate blades, i.e., characterizes the form of oscillations of the rotor as a whole; s – any integer which can be called the order of the given form of oscillations of the rotor (s = 1, 2, 3, ..., z).

Quantities ψ_n are determined by the formula

$$\psi_n = \frac{2\pi}{z} n.$$

It can be easily shown by using formulas (1.13) of § 1 that forms of oscillations of the order s = 1, 2, 3, ..., z - 1 correspond to the situation at which forces from separate blades are balanced on the hub, and only the form of the order s = z corresponds to the situation when forces from separate blades are summed and transmitted to the fuselage.

Forms A and B, shown in Fig. 2.28, are forms of the second and fourth orders for a four-blade rotor. From what has been said it is clear that frequencies of natural oscillations of the rotor, which correspond to forms of oscillations of all orders with the exception of s = z, do not depend on the elasticity of attachment of the hub, and only frequencies corresponding to the form of oscillations of the rotor of the order of s = z depend on the elasticity of attachment of the hub.

It is possible to show further that all harmonics of forces exciting oscillations of blades in the flapping plane with the exception of "passage" harmonics $z\omega$, $2z\omega$, $3z\omega$, etc., excite only those forms of oscillations of the rotor at which forces from blades are balanced on the hub, and only harmonic components of exciting forces corresponding to "passage" harmonics excite forms of oscillations of the rotor with which forces from the blades are summed and transmitted to the hub.

Hence a useful practical conclusion can be made. If there is constructed the standard resonance diagram of the blade (see Fig. 1.6, Chapter I) in the flapping plane calculated neglecting the elasticity of attaching the rotor to the fuselage, then resonances with all harmonics except for resonances with harmonics $z\omega$, $2z\omega$, etc., correspond to actuality. Resonances with harmonics $z\omega$, $2z\omega$, etc., must be additionally examined by taking into account the elasticity of attaching the rotor hub and refining values of corresponding natural frequencies.

It is necessary, however, to note that in examining vibrations of blades in the flapping plane usually for these harmonics it is possible not to consider the elasticity of the hub attachment, since the rigidity of the hub attachment in a vertical direction, as a rule, is great and has little effect on frequencies of natural oscillations of the blades (an exception is the case of rotor attachment of a helicopter of transverse configuration having light and flexible wings).

In examining the resonance diagram of the blade in the flapping plane, it is certainly necessary to take into account the influence of elasticity of attachment of the rotor hub to the fuselage.

With respect to oscillations of blades in the flapping plane all the above-stated considerations are also correct with the only difference being that in this case the "passage" harmonics are $(z - 1)\omega$, $(z + 1)\omega$, $(2z - 1)\omega$, $(2z + 1)\omega$, etc. Furthermore, at resonance with harmonics $z\omega$, $2z\omega$, etc., in the plane of rotation one should consider joint vibrations of the rotor with torsional vibrations in the system of transmission (appropriate calculations can be also carried out on the basis of the method of dynamic rigidity).

2. Calculation of Frequencies of Natural Oscillations of Blades of the Rotor in the Flapping Plane Taking into Account Elasticity of the Shaft of the Rotor and Its Attachment to the Fuselage

Let us consider the problem of natural oscillations of blades of the rotor attached to the elastic flexural shaft (Fig. 2.29).

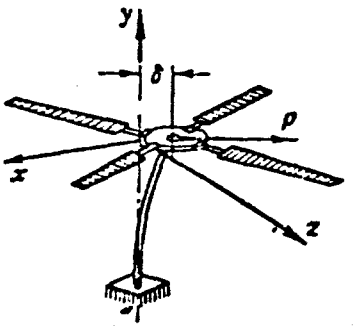

Fig. 2.29. Diagram of a rotor on an elastic shaft.

Let us assume that the rigidity of the shaft with respect to force P, applied to the shaft in the center of the hub and lying in the plane of the rotor rotation, is equal to c_0. Consequently, force P and displacement δ of the end of the shaft which it causes, are connected by the relation

$$P = c_0 \delta. \tag{4.2}$$

It does not matter whether displacement δ occurs from bending of the shaft itself or is due to the elasticity of its attachment to the fuselage.

Let us consider only the case when the indicated rigidity is identical in all directions in plane xOz, i.e., when the elastic base to which the rotor is fastened is isotropic. In reality this is not so, but usually rigidities of attachment in directions of axes Ox and Oz are little distinguished, and it is possible to consider the base to be isotropic, understanding by quantity c_0 to be the arithmetic mean of rigidities c_x and c_z:

$$c_0 = \frac{c_x + c_z}{2}. \tag{4.3}$$

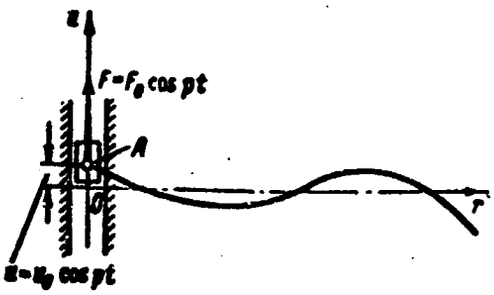

Fig. 2.30. Diagram of the calculation of forced oscillations of the blade for the determination of dynamic rigidity of the rotor.

The calculation of natural oscillations of the rotor on the elastic base can be conducted on the basis of the method of dynamic rigidity.

First of all let us introduce the concept of dynamic rigidity of the blade in the plane of rotation. Let us assume that elastic bending blade, which is found in the central field of centrifugal forces, is fastened in the shank part by a hinge in such a way that the hinge is able to move freely in a direction perpendicular to the axis of undeformed blade (see Fig. 2.30).

Let us assume further that the blade accomplishes steady-state forced oscillations under the action of a transverse exciting harmonic force

$$F=F_0\cos pt,$$

applied in hinge A. Here point A of the application of force will also accomplish oscillations according to the law

$$u=u_0\cos pt.$$

We will call dynamic rigidity of blade the quantity

$$D_л(p)=\frac{F_0}{u_0}. \qquad (4.4)$$

It is possible to determine dynamic rigidity of the blade either with the help of the method expounded in No. 2 of § 2 or by the method of additional mass (§ 2, No. 4). It is necessary to consider that the blade is in the field of centrifugal forces and to solve not the equation of the (2.2) type, as was done during calculation of the fuselage, but the equation of oscillations of the blade in

the plane of rotation (see Chapter I, § 1, No. 11), which has the form:

$$(EIu'')'' - (Nu')' + m\ddot{u} - \omega^2 u = q(r,t). \qquad (4.5)$$

Here N is the centrifugal force in the section of the blade on radius r.

With application of the method of additional mass one should calculate the frequencies and forms of natural oscillations of the blade in the plane of rotation with fastening with respect to the scheme depicted in Fig. 2.30 with a different value of the additional mass Δm_A at point A with the help of the method expounded in Chapter I, § 2, No. 5.

According to the results of such a calculation it is possible to construct a graph $\Delta m_A = f(p)$. An example of such a graph is shown in Fig. 2.32. Points of infinite discontinuities of function f(p) give values of frequencies of natural oscillations of the blade with a fixed hinge at point A, i.e., frequencies of natural oscillations of the blade for the case when the rigidity of the rotor shaft is infinitely great. Points at which $\Delta m_A = 0$ give frequencies of natural oscillations of the blade, freely fastened according to the scheme depicted on Fig. 2.30.

The value of dynamic rigidity of the blade corresponding to the given value p can be determined by formula

$$D_A(p) = (p^2 + \omega^2)\Delta m_A(p). \qquad (4.5)$$

The additional term $\omega^2 \Delta m_A(p)$ appears in this formula from the component centrifugal force of mass Δm_A directed along the normal to the blade.

Let us show further that the dynamic rigidity of the rotor on the whole can be found if the dynamic rigidity of the blade is known. Let us turn to Fig. 2.31 on which the form in the plan of the hub of the rotor with vertical hinges and the k-th elastic blade

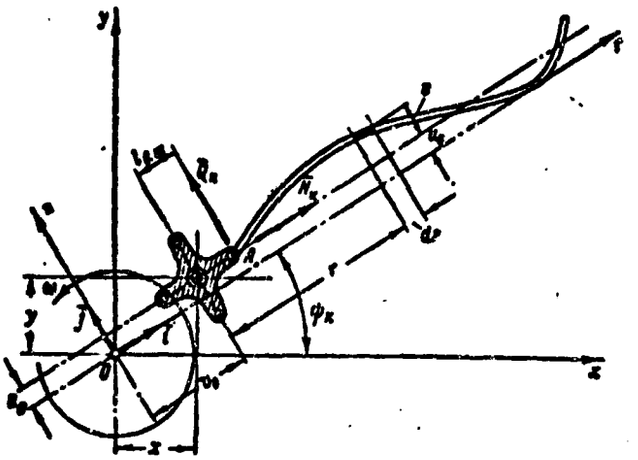

Fig. 2.31. Calculation of dynamic rigidity of a rotor with elastic blades.

is depicted. Let us assume that xOy is the system of coordinates rotating together with the rotor with angular velocity ω. Let us assume that further the center of the rotor hub accomplishes the prescribed harmonic oscillations in the plane of rotation according to the law

$$\left.\begin{aligned} x &= x_0 \cos pt; \\ y &= y_0 \sin pt. \end{aligned}\right\} \qquad (4.6)$$

Such oscillations of the hub create oscillations of elastic blades in the plane of rotation, and the problem is to find the forces by which the vibrating blades load the hub with its movement.

Let us select an additional rectangular system of coordinates nOr, rotating together with the rotor, for which the axis Or is parallel to a straight line passing through the center of the hub and vertical hinge A of the k-th blade. Axis Or forms with axis Ox a certain angle ψ_k. Let us designate by u_0 and v_0 the coordinates of the center of the hub in the system nOr. Then, obviously:

$$\begin{aligned} u_0 &= -x \sin \psi_k + y \cos \psi_k; \\ v_0 &= x \cos \psi_k + y \sin \psi_k. \end{aligned}$$

With oscillations of the hub, according to the law (4.6) coordinates u_0 and v_0 will change with time according to the law:

$$\left.\begin{aligned} u_0 &= (-x_0 \sin\varphi_h)\cos pt + (y_0\cos\varphi_h)\sin pt; \\ v_0 &= (x_0\cos\varphi_h)\cos pt + (y_0\sin\varphi_h)\sin pt. \end{aligned}\right\} \qquad (4.7)$$

Let us designate further by u the deviation of the point of elastic axis of the blade on radius r from a straight line passing through the vertical hinge A of the blade and parallel to axis Or. With oscillations of the blade quantity u is a function of radius r and time t so that u = u(r, t).

Let us assume that $\bar{w}$ is the vector of full acceleration of the point with radius r of elastic axis of the blade. Then

$$\bar{w} = \bar{w}_{отн} + \bar{w}_{пер} + \bar{w}_{кор},$$

where $\bar{w}_{отн}$ is the vector with respect to acceleration of the point from motion in the moving coordinate system nOr; $\bar{w}_{пер}$ — vector of translational acceleration from motion of the point together with the system of coordinates nOr; $\bar{w}_{кор}$ — vector of Coriolis acceleration.

Let us introduce unit vectors $\bar{i}$ and $\bar{j}$ directed along axes r and n respectively. Then it is possible to write:

$$\begin{aligned} \bar{w}_{отн} &= \bar{i}(\ddot{v}_0) + \bar{j}(\ddot{u}_0 + \ddot{u}); \\ \bar{w}_{пер} &= \bar{i}[-\omega^2(r + v_0)] + \bar{j}[-\omega^2(u_0 + u)]; \\ \bar{w}_{кор} &= \bar{i}[-2\omega(\dot{u}_0 + \dot{u})] + \bar{j}[(2\omega\dot{v}_0]. \end{aligned}$$

If we designate projections of the vector of full acceleration on axes On and Or by w_n and w_r, then for them these expressions are obtained:

$$\left.\begin{aligned} w_n &= (\ddot{u}_0 - \omega^2 u_0) + (\ddot{u} - \omega^2 u) + 2\omega\dot{v}_0; \\ w_r &= (\ddot{v}_0 - \omega^2 v_0) - \omega^2 r - 2\omega\dot{u}_0 - 2\omega\dot{u}. \end{aligned}\right\} \qquad (4.8)$$

The equation of equilibrium of the beam in the field of centrifugal forces has the form:

$$(EIu'')'' - (Nu')' = q, \qquad (4.9)$$

where q is the intensity of the transverse load applied to the beam.

With oscillations of the blade the transverse load from forces of inertia can be written in the form:

$$q(r, t) = -mw_a = -m[(\ddot{u}_0 - \omega^2 u_0) + (\ddot{u} - \omega^2 u) + 2\omega\dot{v}_0],$$

where m is the linear mass of the blade [m = m(r)].

Substituting this expression into equation (4.9), we will obtain the following partial differential equation for determination of function u(r, t):

$$(EIu'')'' - (Nu')' + m\ddot{u} - \omega^2 u = q^*(r, t), \tag{4.10}$$

where

$$q^*(r, t) = -m[\ddot{u}_0 - \omega^2 u_0 + 2\omega\dot{v}_0]. \tag{4.11}$$

If the motion of the hub center is assigned by expressions (4.7), then load q*(r, t) is the well-known time function.

Unknown function u(r, t) should satisfy equation (4.10) and also boundary conditions:

$$\left.\begin{aligned} u(0, t) = u''(0, t) = 0; \\ u''(R, t) = (EIu'')'|_{r=R} = 0. \end{aligned}\right\} \tag{4.12}$$

Differentiating the expressions (4.7) and substituting them into (4.11), we will find

$$q^*(r, t) = mA_k \cos pt + mB_k \sin pt, \tag{4.13}$$

where constants A_k and B_k are determined by the formulas:

$$\left.\begin{aligned} A_k = -[(p^2 + \omega^2)x_0 + 2\omega p y_0] \sin\gamma_k; \\ B_k = [(p^2 + \omega^2)y_0 + 2\omega p x_0] \cos\gamma_k. \end{aligned}\right\} \tag{4.14}$$

The solution to equation (4.10), which corresponds to steady-state forced oscillations from the load [see expression (4.13)], is sought in the form:

$$u(r, t) = \bar{u}(r)[A_k \cos pt + B_k \sin pt]. \tag{4.15}$$

Substituting this expression into (4.10) with the right side for q^* from (4.13) we will find that function $\bar{u}(r)$ should satisfy the ordinary differential equation

$$(E\bar{I}\bar{u}'')'' - (N\bar{u}')' - (p^2+\omega^2)m\bar{u} = m, \tag{4.16}$$

and also boundary conditions

$$\left.\begin{aligned} \bar{u}(0) = \bar{u}'(0) = 0; \\ \bar{u}''(R) = (E\bar{I}\bar{u}'')'|_{r=R} = 0. \end{aligned}\right\} \tag{4.17}$$

Let us note further that in the calculation of oscillations of the blade, which are excited by the oscillation of hinge A according to the scheme depicted in Fig. 2.30, it is necessary to solve the equation of the form:

$$(EIu'')'' - (Nu')' - m\ddot{u} - \omega^2 u = 0,$$

where u is the total displacement of the point of elastic axis of the blade with radius r. Here function u(r, t) should satisfy conditions:

$$\left.\begin{aligned} u(0, t) = u_0 \cos pt; \\ u''(0, t) = 0. \end{aligned}\right\}$$

$$\left.\begin{aligned} u''(R, t) = 0; \\ (EIu'')'|_{r=R} = 0. \end{aligned}\right\}$$

Searching for the solution of this equation in the form:

$$u = [u_0 + \bar{u}(r)] \cos pt,$$

we arrive at the conclusion that function $\bar{u}(r)$ should satisfy equation

$$(E\bar{I}\bar{u}'')'' - (N\bar{u}')' - (p^2+\omega^2)\, m\bar{u} = (p^2+\omega^2)\, mu_0,$$

which differs from equation (4.16) only by the constant factor $u_0(p^2+\omega^2)$. Boundary conditions for function $\bar{u}(r)$ in this case completely coincide with expressions (4.17).

Thus during oscillations of the blade according to the scheme shown in Fig. 2.30, function $\bar{u}(r)$ is obtained in the same way as

in the problem interesting us [see expressions (4.16) and (4.17)], if the amplitude u_0 is selected in such a manner that there is fulfilled the condition

$$u_0(p^2+\omega^2)=1. \tag{4.18}$$

Physically this means that the form of forced oscillations of the blade in the problem interesting us coincides with the form of oscillations of the blade excited according to scheme shown in Fig. 2.30. Using this result, we will obtain one important formula. For this let us note that during oscillations of the blade fastened according to the scheme shown in Fig. 2.30, which are excited by force $F = F_0 \cos pt$, the sum of projections of all transverse inertial forces applied to the blade should be balanced by force F. Hence we will find:

$$F_0=\Delta m_{\text{в}}(p)(p^2+\omega^2)u_0=-(p^2+\omega^2)\int_{l_{\text{в.ш}}}^{R} m(u_0+\bar{u})\,dr=$$

$$=-(p^2+\omega^2)u_0 m_{\text{в}}-(p^2+\omega^2)\int_{l_{\text{в.ш}}}^{R} m\bar{u}\,dr,$$

where $m_{\text{в}}$ — the mass of the blade up to the vertical hinge

$$\left(m_{\text{в}}=\int_{l_{\text{в.ш}}}^{R} m\,dr\right).$$

With fulfillment of condition (4.18) we hence obtain formula:

$$\int_{l_{\text{в.ш}}}^{R} m\bar{u}\,dr=-\frac{\Delta m_{\text{в}}+m_{\text{в}}}{p^2+\omega^2}, \tag{4.19}$$

i.e., the integral with respect to the blade from function $m\bar{u}$ [where $\bar{u}$ is the solution of equation (4.16)] is expressed in terms of dynamic rigidity of the blade or which is the same, in terms of additional mass $\Delta m_{\text{в}}(p)$.

It is now easy to obtain expressions for forces acting on the hub from the side of vibrating blades. Let us designate by Q_K and M_K

respectively, projections on axes On and Or of the force applied from the side of the k-th blade to the vertical hinge of the hub. Then:

$$\left.\begin{aligned} Q_k &= -\int_{l_{0.m}}^{R} mw_\tau\,dr = -\int_{l_{0.m}}^{R} m(\ddot{u}-\omega^2 u)\,dr - \\ &\quad -(\ddot{u}_0-\omega^2 u_0+2\omega\dot{v}_0)\,m_s; \\ N_k &= -\int_{l_{0.m}}^{R} mw_r\,dr = -m_s(\ddot{v}_0-\omega^2 v_0-2\dot{u}_0\omega)+ \\ &\quad +\omega^2\int_{l_{0.m}}^{R} mr\,dr+2\omega\int_{l_{0.m}}^{R} mu\,dr. \end{aligned}\right\} \qquad (4.20)$$

Substituting here expressions (4.15), (4.7), (4.14), and considering formula (4.19), we will find:

$$\begin{aligned} Q_k &= \Delta m_s\{[(p^2+\omega^2)x_0+2\omega p y_0]\sin\psi_k\cos pt - \\ &\quad -[(p^2+\omega^2)y_0+2\omega p x_0]\cos\psi_k\sin pt\}; \end{aligned} \qquad (4.21)$$

$$\begin{aligned} N_k &= N_0+\left[m_s(p^2+\omega^2)x_0-\Delta m_s 2p\omega y_0-\frac{\Delta m_s+m_s}{(p^2+\omega^2)}4p^2\omega^2 x_0\right]\cos\psi_k\cos pt+ \\ &\quad +\left[m_s(p^2+\omega^2)y_0-\Delta m_s 2p\omega x_0-\frac{\Delta m_s+m_s}{p^2+\omega^2}4p^2\omega^2 y_0\right]\sin\psi_k\sin pt, \end{aligned} \qquad (4.22)$$

where $N_0=\omega^2\int_{l_{0.m}}^{R} mr\,dr$ is the centrifugal force of the blade on the vertical hinge of the hub.

Designating by X and Y forces applied to the hub from the side of the vibrating blades, we obtain formulas:

$$X=\sum_{k=1}^{z}(-Q_k\sin\psi_k+N_k\cos\psi_k);$$

$$Y=\sum_{k=1}^{z}(Q_k\cos\psi_k+N_k\sin\psi_k).$$

Substituting here expressions (4.21) and (4.22) and considering properties of the trigonometric sums, which were described in No. 2 of § 1 of this chapter [formula (1.13)], we arrive at the following expressions:

$$X=\left\{-\frac{z}{2}\Delta m_0\left[(p^2+\omega^2)x_0+2\omega p y_0\right]+\frac{n}{2}\left[m_0(p^2+\omega^2)x_0-\right.\right.$$
$$\left.\left.-\Delta m_0 2p\omega y_0-\frac{\Delta m_0+m_0}{p^2+\omega^2}\cdot 4p^2\omega^2 x_0\right]\right\}\cos pt; \qquad (4.23)$$
$$Y=\left\{-\frac{z}{2}\Delta m_0\left[(p^2+\omega^2)y_0+2\omega p x_0\right]+\right.$$
$$\left.+\frac{z}{2}\left[m_0(p^2+\omega^2)y_0-\Delta m 2p\omega x_0-\frac{\Delta m_0+m_0}{p^2+\omega^2}\cdot 4p^2\omega^2 y_0\right]\right\}\sin pt. \qquad (4.24)$$

On the other hand, it is possible to formulate equations of motion of the rotor hub on an elastic shaft which have the form:

$$m_{кр}(\ddot{x}-\omega^2 x-2\omega\dot{y})+c_0 x=X;$$
$$m_{кр}(\ddot{y}-\omega^2 y+2\omega\dot{x})+c_0 y=Y,$$

where $m_{кр}$ is the mass of the housing of the hub; c_0 – rigidity of the shaft.

If motion of the hub occurs according to the law (4.6), then the last equations will yield:

$$X=\left[m_{кр}\left[-(p^2+\omega^2)x_0-2\omega p y_0\right]+c_0 x_0\right]\cos pt;$$
$$Y=\left[m_{кр}\left[-(p^2+\omega^2)y_0-2\omega p x_0\right]+c_0 y_0\right]\sin pt.$$

If one were to equate these expressions to (4.23) and (4.24), then we will obtain the system of two linear homogeneous equations for the determination of amplitudes x_0 and y_0:

$$\left.\begin{aligned}Ax_0+By_0=0;\\ Bx_0+Ay_0=0,\end{aligned}\right\} \qquad (4.25)$$

where

$$A=(p^2+\omega^2)\left[\frac{z}{2}(m_0-\Delta m_0)+m_{кр}\right]-2z\frac{\Delta m_0+m_0}{(p^2+\omega^2)}p^2\omega^2-c_0; \qquad (4.26)$$

$$B=2\omega p\left[m_{кр}-z\Delta m_0\right]. \qquad (4.27)$$

Equating the determinant of this system to zero, we will obtain the characteristic equation for the determination of natural frequencies p:

$$\begin{vmatrix} A & B \\ B & A \end{vmatrix} = A^2 - B^2 = 0, \qquad (4.28)$$

whence

$$A = \pm B.$$

In the case A = -B [as can be seen from (4.25)] $x_0 = y_0$. This corresponds to the rotation of the center of the hub in the direction of rotation of the rotor [see formula (4.6)].

In the case A = B there is obtained $x_0 = -y_0$, which corresponds to the rotation of the center of the rotor opposite the rotation of the rotor.

It is possible to solve characteristic equation (4.28) with respect to value $\Delta m_л(p)$. Thus is obtained the following equation:

$$\Delta m_л(p) = \frac{(p^2+\omega^2)\left(\frac{z}{2}m_л + m_{вт}\right) - c_0 - \frac{2zp^2\omega^2}{p^2+\omega^2}\cdot m_л \mp 2\omega p m_{вт}}{\frac{z}{2}\cdot(p^2+\omega^2) + \frac{2zp^2\omega^2}{p^2+\omega^2} \pm 2n\omega p}. \qquad (4.29)$$

This equation can be solved graphically by superimposing on the curve of additional mass of the blade $\Delta m_л = \Delta m_л(p)$ two curves, which correspond to the right side of this expression, in which there are taken either the upper signs (minus sign in the numerator and plus sign in the denominator) or lower signs. Let us designate the first of these quantities $\Delta m_1(p)$ and the second, $\Delta m_2(p)$.

Abscissas of points of intersection of curve $\Delta m_1(p)$ with the graph of additional mass $\Delta m_л(p)$ of the blade will give frequencies of natural oscillations of the rotor on an elastic shaft, which correspond to such forms of oscillations at which the center of the hub rotates in the direction of rotation of the rotor with angular velocity p with respect to the system of coordinates xOy connected with the rotor, and, consequently, with angular velocity p + ω relative to the fixed system of coordinates (housing of the helicopter). Such forms obviously can be excited only by harmonics (z - 1)ω, (2z - 1)ω, etc. Abscissas of points of intersection of curves $\Delta m_2(p)$ and $\Delta m_л(p)$ will give frequencies of natural oscillations of the rotor on the elastic shaft at which the center of the hub

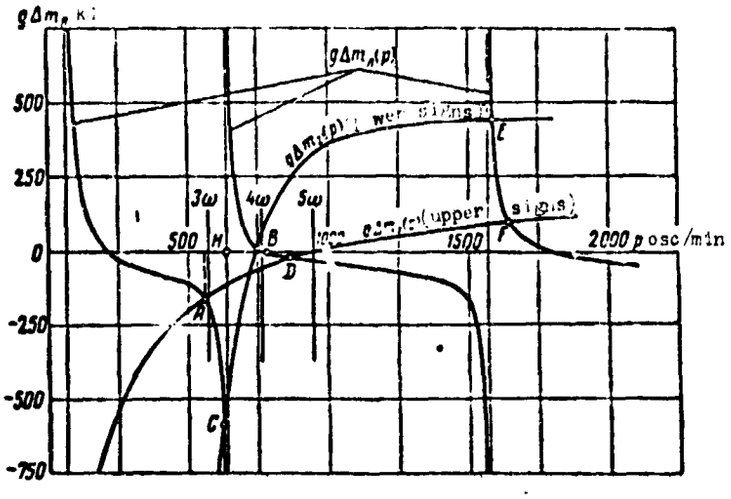

Fig. 2.32. Determination of frequencies of oscillations of the rotor on the elastic shaft by the method of dynamic rigidity.

rotates in a direction opposite the direction of rotation of the rotor. Such forms of oscillations can be excited only by harmonics $(z + 1)\omega$, $(2z + 1)\omega$, etc.

Figure 2.32 gives graphs of curves $\Delta m_2(p)$, $\Delta m_1(p)$ and $\Delta m_2(p)$, plotted for the following initial data: $c_0 = 500$ kG/mm; $m_{вт} = 38$ kG·s^2/m; $m_л = 15$ kG·s^2/m; $\omega_0 = 190$ r/min; $z = 5$. The given graphs show considerable distinctions in frequencies of natural oscillations of the rotor on the elastic shaft from frequencies of natural oscillations of the isolated blade. Thus, for example, the frequency of mononodal tone of natural oscillations of the isolated blade of this rotor (with a fixed bushing) corresponds to point H of infinite discontinuity of curve $\Delta m_2(p)$. With this $p = p_1 = 640$ osc/m. Figure 2.33 gives the form of oscillations of this tone.

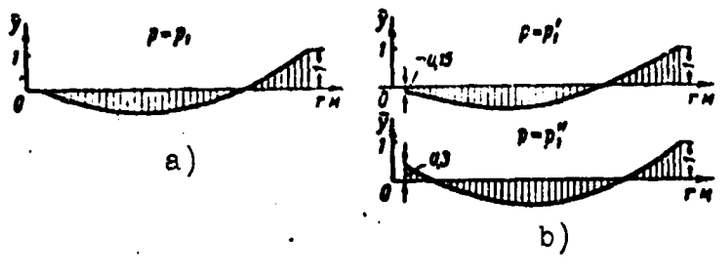

Fig. 2.33. Forms of oscillations of the blade: a) form of oscillations of the blade neglecting elasticity of the shaft; b) form of oscillations of blade taking into account elasticity of the shaft.

For the rotor on an elastic shaft, besides this frequency of natural oscillations, there are also frequencies of oscillations corresponding to points A, B, C, and D of the crossing of curves $\Delta m_1(p)$ and $\Delta m_2(p)$ with curve $\Delta m_{II}(p)$. Oscillations with forms corresponding to points A and D can be excited only by harmonics $(z - 1)\omega$, $(2z - 1)\omega$, etc., (in this case 4ω and 9ω, etc.). Oscillations corresponding to points C and B can be excited only by harmonics $(z + 1)\omega$, $(2z + 1)\omega$, etc., (in this case 6ω, 11ω, etc.).

These resonance curves are plotted for a helicopter which in the beginning had a four-blade rotor, but then because of great resonance of the blade with the harmonic 3ω in the flapping plane (point A) the hub had to be altered and the rotor made five-bladed.

Figure 2.33 gives forms of natural oscillations of the blade in the plane of rotation taking into account elasticity of the shaft, which correspond to points A ($p_1' = 560$ osc/min) and B ($p_1'' = 761$ osc/min).

In conclusion let us indicate that the method given here for finding frequencies of natural oscillations of the rotor in the plane of rotation, taking into account elasticity of the shaft, is one of the most complex examples of the application of the method of dynamic rigidity, and therefore it was considered expedient to discuss it here. Regarding, however, the finding of frequencies of characteristic blades in the flapping plane taking into account elasticity of the hub fastening and frequencies of oscillations of blades in the plane of rotation taking into account torsional elasticity of the system of transmission (which are excited by harmonics $z\omega$, $2z\omega$, $3z\omega$, etc.), then these calculations are considerably simpler and can be completely carried out on the basis of principles expounded in § 2.

C H A P T E R III

GROUND RESONANCE

It is accepted to call ground resonance spontaneously generated oscillations (swaying) of the helicopter on land with growing amplitude. This phenomenon began to appear after the construction of the hub of the rotors of helicopters had a vertical hinge introduced, allowing the blades to sway in the plane of rotation of the rotor.

In the history of helicopter construction there has been a great deal of cases when the helicopter was destroyed from the formations of such type of oscillations. Attempts to eliminate ground resonance on a fabricated helicopter sometimes led to the necessity of great alterations in the construction of the helicopter. These circumstances forced engineers to work on the creation of a theory of ground resonance and reliable methods of its calculation, which would allow competently to select characteristics of elements of construction determining the center of gravity margin of the helicopter on land.

At present there is theory of ground resonance which explains all the most important features of this phenomenon and permits calculating characteristics of construction on which ground resonance depends. This theory appeared as a result of numerous theoretical and experimental investigations of ground resonance, which were conducted both by us in the Soviet Union and abroad. According to the theory of ground resonance from Soviet works one should note in the first place the works of B. Ya. Zherebtsov and A. I. Pozhalostin.

Investigations of ground resonance showed that the physical

essence of this phenomenon consists in the following. With natural oscillations of blades of the rotor in the plane of rotation (with reference to vertical (drag) hinges), which can appear from any shock (gust of wind, rough landing and so forth), inertial forces in the plane of rotation of the rotor appear. Being transmitted to the fuselage of the helicopter, they create its oscillations on the elastic chassis. Forces swaying helicopter change with a definite frequency dependent on the frequency of natural oscillations of the blade in the plane of rotation and angular velocity of the rotor's rotation. A helicopter sways most easily when the frequency of the change in exciting forces is close to the frequency of natural oscillations of the helicopter on an elastic chassis. Simultaneously with oscillations of the helicopter body forces appear which sway the blade in the plane of rotation. The presence of such two-way connection between oscillations of the helicopter and blades leads to the fact that at a certain angular velocity of the rotor's roatation the helicopter can become unstable, i.e., the oscillations of the helicopter which once started (due to some shock) can appear not attenuated but growing.

The following are the main ways of combatting ground resonance:

1. Installation of special dampers on vertical hinges of the blades of the rotor which damp oscillations of blades in the plane of rotation.

2. Introduction of special damping elements into the construction of shock absorbers of the chassis or the correct selection of characteristics of hydraulic drag of shock absorbers on the forward and recovery stroke, and also characteristics of rigidity of shock absorbers and tires.

The main purpose of calculation of the helicopter for ground resonance is a correct selection of characteristics of dampers of blades and characteristics of rigidity and damping of the chassis.

The theory of ground resonance, which will be discussed later is only for rotors with the number of blades $n \geq 3$.

The theory of ground resonance of a two-blade rotor possesses a number of peculiarities and is considerably more complicated [36].

§ 1. Stability of the Rotor on an Elastic Base

1. Formulation of the Problem and Equations of Motion

All the most important features of ground resonance of a helicopter can be obtained from consideration of the motion of a certain idealized mechanical system, which we will call the "rotor on an elastic base." Such a system is depicted schematically on Fig. 3.1. The shaft of the rotor with heavy and absolutely rigid blades 3, joined with the rotor hub by means of vertical hinges 4, rotates in supports rigidly joined with a certain heavy housing (body) 1, which is elastically fastened to the fixed base 2 and has only one degree of freedom – forward displacement along axis Ox parallel to the plane of rotation of the rotor. With displacement of body 1 along axis Ox there appears an elastic restoring force from spring c and damping force from damper к. We will consider the elastic and damping characteristics of the base linear, i.e., we will assume that force X, acting on body 1 with its displacement x(t), is expressed by the formula:

$$X = -cx - \kappa \frac{dx}{dt}, \tag{1.1}$$

where c is the stiffness coefficient of the spring; к – damping factor.

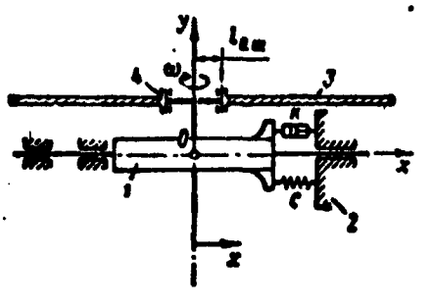

Fig. 3.1. Diagram of a rotor on an elastic support: 1 – body; 2 – base; 3 – blade; 4 – hinge.

We will call quantities c and к coefficients of rigidity and damping of the elastic support. If m_0 is the mass of body 1, and P_x is the projection on axis Ox of a force acting on the body from the rotor, then the equation of motion of the body can be recorded in the form:

$$m_0\ddot{x} + \kappa\dot{x} + cx = P_x. \qquad (1.2)$$

Here and subsequently the dots denote differentiation with respect to time.

We will consider further that the rotor revolves evenly at angular velocity ω in a vacuum, i.e., we will not take into account aerodynamic forces. The theory of ground resonance, not considering aerodynamic forces, will quite well agree with the experiment. Thus only inertial forces appearing during vibrations of blades in the plane of rotation are taken into account.

To formulate equations of motion of the blade let us turn to Figs. 3.1 and 3.2.

Let us select a fixed rectangular system of coordinates Oxyz. We will direct axis Oy along the axis of the rotor shaft with the position of the body 1 corresponding to the static equilibrium. The direction of axis Ox will be selected so that the uniquely virtual displacement of the body is directed along axis Ox.

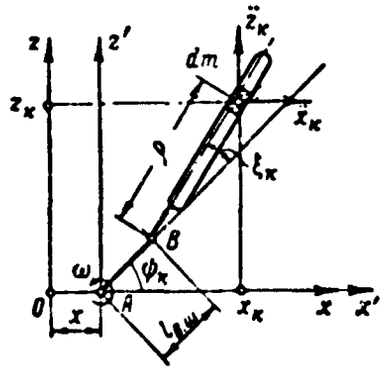

Fig. 3.2. Derivation of equations of motion.

Let us assume that as before x is the displacement of the axis of the rotor shaft together with the body along axis Ox (Fig. 3.2). Let us assume that further ψ_k is the azimuthal angle of the k-th blade of the rotor reckoned from the positive direction of axis Ox.

Angles ψ_k of different blades of the rotor are determined by the formula:

$$\psi_k = \omega t + \frac{2\pi}{n} k,$$

where n is the number of blades of the rotor; k = 1, 2, ..., n.

Let us designate by $l_{B,III}$ the distance AB (Fig. 3.2) from the axis of rotation A up to the axis of the drag hinge B and by ξ_k, the angle of deviation of the k-th blade with a turn of it relative to the drag hinge, considering ξ_k positive with deflection of the blade in direction of rotation of the rotor.

Then coordinates x_k and z_k of the element of the k-th blade with mass dm, which is at distance ρ from the axis of the drag hinge, will be expressed by the following formulas:

$$\left.\begin{aligned} x_k &= x + l_{B,III}\cos\psi_k + \rho\cos(\psi_k + \xi_k); \\ z_k &= l_{B,III}\sin\psi_k + \rho\sin(\psi_k + \xi_k). \end{aligned}\right\} \qquad (1.4)$$

Differentiating these expressions twice with respect to time, we will obtain formula for determining components of acceleration of the element of the blade:

$$\begin{aligned} \ddot{x}_k &= \ddot{x} - \omega^2 l_{B,III}\cos\psi_k - \rho(\omega + \dot{\xi}_k)^2\cos(\psi_k + \xi_k) + \ddot{\xi}_k\rho\sin(\psi_k + \xi_k); \\ \ddot{z}_k &= -\omega^2 l_{B,III}\sin\psi_k - \rho(\omega + \dot{\xi}_k)^2\sin(\psi_k + \xi_k) + \ddot{\xi}_k\rho\cos(\psi_k + \xi_k). \end{aligned}$$

With the formulation of equations of small oscillations of the blade relative to the drag hinge it follows, as usual, to be limited by smalls of the first order. Therefore, it is possible to consider

$$(\omega + \dot{\xi}_k)^2 \approx \omega^2 + 2\omega\dot{\xi}_k.$$

Thus with an accuracy of smalls of the second order, formulas for accelerations $\ddot{x}_k$ and $\ddot{y}_k$ can be written in the form:

$$\left.\begin{aligned} \ddot{x}_k &= \ddot{x} - \omega^2 l_{B,III}\cos\psi_k - \rho(\omega^2 + 2\omega\dot{\xi}_k)\cos(\psi_k + \xi_k) + \ddot{\xi}_k\rho\sin(\psi_k + \xi_k); \\ \ddot{z}_k &= -\omega^2 l_{B,III}\sin\psi_k - \rho(\omega^2 + 2\omega\dot{\xi}_k)\sin(\psi_k + \xi_k) + \ddot{\xi}_k\rho\cos(\psi_k + \xi_k). \end{aligned}\right\} \qquad (1.5)$$

With motion of the system in a vacuum the rotor blades at each instant t are loaded only by inertial forces. Elementary inertial forces, which act on the element of the blade, are expressed by formulas:

$$\left.\begin{aligned} dX_k &= -dm_k\ddot{x}_k; \\ dZ_k &= -dm_k\ddot{z}_k. \end{aligned}\right\} \qquad (1.6)$$

Let us assume that in drag hinges of the rotor hub there are linear elastic and damping devices, which with rotation of the blade relative to the drag hinge load by its moment

$$M = -c_л\xi_k - \kappa_л\dot{\xi}_k, \qquad (1.7)$$

directed to the side opposite the positive direction ξ_K. We will call $c_л$ and $\kappa_л$, respectively, coefficients of elasticity and damping of the blade.

At every instant the moment from forces of inertia applied to the blade relative to the drag hinge should be balanced by moment M. Therefore, it is possible to write:

$$\int [\ddot{x}_k\varrho \sin(\varphi_k + \xi_k) - \ddot{z}_k\varrho\cos(\varphi_k + \xi_k)]\, dm = c_л\xi_k + \kappa_л\dot{\xi}_k,$$

where integration is conducted along the length of the blade ℓ.

From the last expression and formulas (1.5), after simple transformations, the equation of motion of the k-th blade is obtained. Since we are interested in equations of small oscillations of the blade, we can be limited to only terms of the first order of smallness with respect to quantities x, $\dot{x}$, ξ_K and $\dot{\xi}_K$, rejecting terms containing squares and products of these quantities. Then it is possible to assume:

$$\cos\xi_k \approx 1;$$
$$\sin\xi_k \approx \xi_k;$$
$$\sin(\varphi_k + \xi_k) \approx \sin\varphi_k + \xi_k\cos\varphi_k;$$
$$\cos(\varphi_k + \xi_k) \approx \cos\varphi_k - \xi_k\sin\varphi_k.$$

After such simplifications the equation of small oscillations of the k-th blade will take the following form:

$$\ddot{\zeta}_k + 2n_\zeta \dot{\zeta}_k + (p^2_{\zeta_0} + \nu_0^2\omega^2)\zeta_k = \frac{\nu_0^2}{I_{k,m}} \ddot{x} \sin\psi_k. \qquad (1.8)$$

Here the following designations are used: $n_\zeta = \frac{c_\zeta}{2I_{k,m}}$ – relative damping factor of the blade; $p^2_{\zeta_0} = \frac{c_\zeta}{I_{k,m}}$ – frequency of natural oscillations of irrotational blade (at $\omega = 0$) relative to the drag hinge; ν_0 – dimensionless parameter of the blade determined by formula

$$\nu_0 = \sqrt{\frac{I_{k,m} S_{k,m}}{I_{k,m}}}, \qquad (1.9)$$

where $S_{k,m} = \int \varrho\, dm$ is the static moment of the blade relative to the drag hinge; $I_{k,m} = \int \varrho^2\, dm$ is the moment of inertia of the blade relative to the drag hinge.

The right-hand side of equation (1.8) constitutes the moment from inertial forces acting on the blade from displacement of the rotor shaft ($\ddot{x}$). With a fixed shaft, when $\ddot{x} = 0$, equation (1.8) describes the natural oscillations of the blade of an evenly rotating rotor in the plane of rotation.

The general solution of equation (1.8) without the right side has the form:

$$\zeta_k = \zeta_{k_0} e^{-n_\zeta t} \cos(p_\zeta t + \varphi_k).$$

where ζ_{k_0} and ϕ_k are arbitrary constants, and quantity p_ζ is determined by formula

$$p_\zeta = \sqrt{p^2_{\zeta_0} + \nu_0^2\omega^2 - n_\zeta^2}$$

and constitutes the angular frequency of natural oscillations of the blade in the plane of rotation.

Further it is necessary to determine force P_x acting on the body from the side of the rotor. Force P_x constitutes resultant forces of inertia of vibrating blades of the rotor, on the basis of the well-known theorem of the motion of the center of mass (center of gravity) of a mechanical system can be determined as the product of the mass of the system of blades by the component of acceleration of the common center of gravity of the system of the blades along axis ox.

Let us formulate formulas for the determination of coordinates of the common center of gravity of the system of blades.

Let us assume that x_{k_c} and z_{k_c} are coordinates of the center of gravity of the k-th blade. Then coordinates x_c and z_c of the center of gravity of the system of blades can be calculated with the help of expressions:

$$\left.\begin{aligned} x_c &= \frac{1}{n}\sum_{k=1}^{n} x_{k_c}; \\ z_c &= \frac{1}{n}\sum_{k=1}^{n} z_{k_c}. \end{aligned}\right\} \qquad (1.10)$$

Let us assume that further ρ_c is the distance of the center of gravity of the blade from the axis of the drag hinge. Then, in accordance with formulas (1.4), coordinates x_c and z_c can be thus determined:

$$\begin{aligned} x_{k_c} &= x + l_{k.m}\cos\psi_k + \rho_c\cos(\psi_k+\xi_k); \\ z_{k_c} &= l_{k.m}\sin\psi_k + \rho_c\sin(\psi_k+\xi_k). \end{aligned}$$

Substituting these expressions (1.10) and considering that at $n \geq 3$ [see Chapter II, § 1, No. 2, formulas (1.13)]

$$\left.\begin{aligned} \sum_{k=1}^{n}\cos\psi_k &= 0; \\ \sum_{k=1}^{n}\sin\psi_k &= 0. \end{aligned}\right\} \qquad (1.11)$$

we will obtain the following simple expressions for coordinates of the common center of gravity of the system of blades:

$$\left.\begin{aligned} x_c &= -\frac{e_c}{n}\sum_{k=1}^{n}\xi_k \sin\psi_k + x; \\ z_c &= \frac{e_c}{n}\sum_{k=1}^{n}\xi_k \cos\psi_k. \end{aligned}\right\} \qquad (1.12)$$

Force P_x, acting on the elastic support, can be determined by formula

$$P_x = -nm_x\ddot{\bar{x}}_c.$$

Differentiating the first of expressions (1.12) twice, we will obtain:

$$P_x = -nm_x\ddot{x} + S_{s.m}\sum_{k=1}^{n}[(\ddot{\xi}_k - \omega^2\xi_k)\sin\psi_k + 2\omega\dot{\xi}_k\cos\psi_k].$$

Substituting this expression into equation (1.2), we will finally obtain the following equation of motion of the body:

$$(m_0 + nm_x)\ddot{x} + \kappa\dot{x} + cx = S_{s.m}\sum_{k=1}^{n}[(\ddot{\xi}_k - \omega^2\xi_k)\sin\psi_k + 2\omega\dot{\xi}_k\cos\psi_k].$$

It is convenient to write this equation in the form:

$$\ddot{x} + 2n_0\dot{x} + p_0^2 x = \frac{S_{s.m}}{M}\sum_{k=1}^{n}[(\ddot{\xi}_k - \omega^2\xi_k)\sin\psi_k + 2\omega\dot{\xi}_k\cos\psi_k],$$

where quantity

$$M = m_0 + nm_x \qquad (1.13)$$

constitutes the general mass of the system, n_0 is the relative damping factor of the elastic support determined by formula

$$n_0 = \frac{\kappa}{2M}, \qquad (1.14)$$

and quantity p_0 constitutes the angular frequency of natural oscillations of a rigid rotor (without drag hinges) on the elastic support and is determined by the formula

$$p_0^2 = \frac{c}{M}. \tag{1.15}$$

Let us copy now together equations of motion of the rotor on an elastic support, which consist of equations of motion of blades (1.8) and equations of motion of the housing of the base:

$$\left.\begin{aligned} &\ddot{\xi}_k + 2n_\lambda \dot{\xi} + (p_{\lambda_0}^2 + \nu_0^2\omega^2)\xi_k = \frac{\nu_0^2}{I_{0.m}}\ddot{x}\sin\psi_k; \\ &\ddot{x} + 2n_0\dot{x} + p_0^2 x = \frac{S_{0.m}}{M}\sum_{k=1}^{n}[(\ddot{\xi}_k - \omega^2\xi_k)\sin\psi_k + 2\omega\dot{\xi}_k\cos\psi_k], \end{aligned}\right\} \tag{1.16}$$

where k = 1, 2, ..., n.

Thus equations of small oscillations of the rotor on an elastic support constitute a uniform system (n + 1) linear differential equations with periodic coefficients for determination (n + 1) of unknown functions x(t), $\xi_k(t)$ (where k = 1, 2, ... n).

2. Analysis of Stability and Basic Results

Investigations conducted Coleman [35] and B. Ya. Zherebtsov showed that for a rotor with the number of blades n ≥ 3 this system of equations can be reduced to a system of linear equations with constant coefficients, if instead of $\xi_k(t)$ there are introduced new variables $x_c(t)$ and $z_c(t)$, which are coordinates of the center of gravity of the system of blades. In the case of a two-blade rotor equations (1.16) cannot be reduced to equations with constant coefficients. The analysis of the stability of motion of a two-blade rotor on an elastic support is very complicated. An account of it can be found in work [36]. B. Ya. Zherebtsov also investigated the case of a two-blade rotor on an isotropic elastic support when the housing of base has two degrees of freedom – in the direction of axes Ox and Oz (see Fig. 3.2), – and rigidity of the base in both these directions is identical. In this exceptional case the problem is also easily reduced to a system of equations with constant coefficients.

Here there will be examined the analysis of the stability of the rotor with the number of blades $n \geq 3$ having the greatest practical importance.

In order to obtain equations of motion with constant coefficients, let us transform equations (1.16) to new variables $x(t)$, $\eta(t)$, $\zeta(t)$ connected with the former formulas:

$$\left.\begin{aligned} \eta &= \sum_{k=1}^{n} \xi_k \sin\psi_k; \\ \zeta &= \sum_{k=1}^{n} \xi_k \cos\psi_k. \end{aligned}\right\} \tag{1.17}$$

New quantities η and ζ, as one can see from formulas (1.12), with an accuracy of the constant factor ρ_c/n are equal to coordinates of the center of gravity of the system of blades in the moving coordinate system $x'Az'$, the axes of which are parallel to axes Ox and Oz of the fixed system, and the origin of the coordinates A coincides with the center of the rotor (see Fig. 3.2).

To formulate equations of motion in new variables we will multiply all equations of motion of blades (the first of equations (1.16) first by $\cos\psi_k$ and add their left and right sides from $k = 1$ to $k = n$ and then by $\sin\psi_k$ and also add. With this let us note that for a rotor with the number of blades $n \geq 3$ in virture of formulas (1.13) of Chapter II:

$$\left.\begin{aligned} \sum_{k=1}^{n} \sin\psi_k \cos\psi_k &= 0; \\ \sum_{k=1}^{n} \sin^2\psi_k &= \frac{n}{2}. \end{aligned}\right\} \tag{1.18}$$

Furthermore,

$$\left.\begin{aligned} \sum_{k=1}^{n} \dot{\xi}_k \sin\psi_k &= \dot{\eta} - \omega\zeta; \\ \sum_{k=1}^{n} \dot{\xi}_k \cos\psi_k &= \dot{\zeta} + \omega\eta; \\ \sum_{k=1}^{n} \ddot{\xi}_k \sin\psi_k &= \ddot{\eta} - 2\omega\dot{\zeta} - \omega^2\eta; \\ \sum_{k=1}^{n} \ddot{\xi}_k \cos\psi_k &= \ddot{\zeta} + 2\omega\dot{\eta} - \omega^2\zeta. \end{aligned}\right\} \tag{1.19}$$

The last formulas are obtained by means of consecutive differential expressions (1.17).

As a result we will obtain the following system of equations:

$$\left.\begin{aligned}
&\ddot{x}+2n_0\dot{x}+p_0^2x-\frac{S_{0.m}}{M}\ddot{\eta}=0;\\
&\ddot{\eta}+2n_x\dot{\eta}-[\omega^2(1-\nu_0^2)-p_{x_0}^2]\eta-2\omega\dot{\zeta}-2n_x\omega\zeta-\\
&\quad-\frac{n}{2}\cdot\frac{S_{0.m}}{I_{0.m}}\ddot{x}=0;\\
&\ddot{\zeta}+2n_x\dot{\zeta}-[\omega^2(1-\nu_0^2)-p_{x_0}^2]\zeta+2\omega\dot{\eta}+2n_x\omega\eta=0.
\end{aligned}\right\}\qquad(1.20)$$

Thus there is obtained a uniform system of three linear differential second order equations with constant coefficients relative to the three unknown functions $x(t)$, $\eta(t)$ and $\zeta(t)$.

Now the analysis of stability of the system can be conducted by the usual means.

Let us assume that:

$$x=x_0e^{\lambda t};$$
$$\eta=\eta_0e^{\lambda t};$$
$$\zeta=\zeta_0e^{\lambda t},$$

where x_0, η_0 and ζ_0 are certain constants.

Substituting these expressions into equations (1.20), we will obtain a system of three algebraic linear homogeneous equations for the determination of quantities x_0, η_0 and ζ_0. Equating to zero the determinant of this system, we will obtain the characteristic equation for determination of λ. Developing this equation in powers of λ, we will obtain:

$$\bar{\lambda}^6+a\bar{\lambda}^5+b\bar{\lambda}^4+c\lambda^3+e\lambda+f=0,\qquad(1.21)$$

Here and further the following designations are introduced:

$$\left.\begin{aligned}\bar{\lambda}&=\frac{\lambda}{p_0};\\ \bar{\omega}&=\frac{\omega}{p_0};\\ \bar{p}_{s_0}&=\frac{p_{s_0}}{p_0}.\end{aligned}\right\} \qquad (1.22)$$

$$\left.\begin{aligned}a&=A_0;\\ b&=B_0+B_1\bar{\omega}^2;\\ c&=C_0+C_1\bar{\omega}^2;\\ d&=D_0+D_1\bar{\omega}^2+D_2\bar{\omega}^4;\\ e&=E_0+E_1\bar{\omega}^2+E_2\bar{\omega}^4;\\ f&=F_0+F_1\bar{\omega}^2+F_2\bar{\omega}^4.\end{aligned}\right\} \qquad (1.23)$$

$$\left.\begin{aligned}A_0&=\frac{2}{1-\varepsilon}\left[\bar{n}_0+\bar{n}_s(2-\varepsilon)\right];\\ B_0&=\frac{1}{1-\varepsilon}\left[1+8\bar{n}_0\bar{n}_s+4\bar{n}_s^2+\bar{p}_{s_0}^2(2-\varepsilon)\right];\\ B_1&=\frac{1}{1-\varepsilon}\left[4-(2-\varepsilon)(1-\nu_0^2)\right];\\ C_0&=\frac{4}{1-\varepsilon}\left[\bar{n}_s+2\bar{n}_0\bar{n}_s^2+(\bar{n}_0+\bar{n}_s)\bar{p}_{s_0}^2\right];\\ C_1&=\frac{4}{1-\varepsilon}\left[\bar{n}_0+\bar{n}_s\right](1+\nu_0^2);\\ D_0&=\frac{1}{1-\varepsilon}\left[4\bar{n}_s^2+\bar{p}_{s_0}^4+2(1+4\bar{n}_0\bar{n}_s)\bar{p}_{s_0}^2\right];\\ D_1&=\frac{2}{1-\varepsilon}\left[2\bar{n}_s^2+(1+\nu_0^2)(1+4\bar{n}_0\bar{n}_s)-\bar{p}_{s_0}^2(1-\nu_0^2)\right];\\ D_2&=\frac{(1-\nu_0^2)^2}{1-\varepsilon};\\ E_0&=\frac{2}{1-\varepsilon}\left(2\bar{n}_s\bar{p}_{s_0}^2+\bar{n}_0\bar{p}_{s_0}^4\right);\\ E_1&=\frac{2}{1-\varepsilon}\left[4\bar{n}_0\bar{n}_s^2+2\bar{n}_s(1+\nu_0^2)-2\bar{p}_{s_0}^2\bar{n}_0(1-\nu_0^2)\right];\\ E_2&=\frac{2\bar{n}_0(1-\nu_0^2)^2}{1-\varepsilon};\\ F_0&=\frac{\bar{p}_{s_0}^4}{1-\varepsilon};\\ F_1&=\frac{1}{1-\varepsilon}\left[4\bar{n}_s^2-2\bar{p}_{s_0}^2(1-\nu_0^2)\right];\\ F_2&=\frac{(1-\nu_0^2)^2}{1-\varepsilon}.\end{aligned}\right\} \qquad (1.24)$$

Dimensionless damping factors $\bar{n}_0$ (elastic support) and $\bar{n}_л$ (blade) are determined by formulas:

$$\left.\begin{aligned}\bar{n}_0 &= \frac{n_0}{p_0};\\ \bar{n}_a &= \frac{n_a}{p_0}.\end{aligned}\right\} \qquad (1.25)$$

Dimensionless coefficient ε is determined by formula:

$$\varepsilon = \frac{n}{2}\frac{S^2_{\text{в.ш}}}{I_{\text{в.ш}}M}. \qquad (1.26)$$

It is easy to clarify the mechanical meaning of this important coefficient. Quantities $S_{\text{в.ш}}$ and $I_{\text{в.ш}}$ can be written in the form:

$$S_{\text{в.ш}} = m_a\rho_c;$$
$$I_{\text{в.ш}} = m_a\rho_i^2.$$

whence $\rho_i = \sqrt{\frac{I_{\text{в.ш}}}{m_a}}$ is the radius of gyration of the blade relative to the drag hinge. Therefore, expression (1.26) can be copied in the form:

$$\varepsilon = \frac{1}{2}\frac{nm_a}{m_0 + nm_a}\left(\frac{\rho_c}{\rho_i}\right)^2. \qquad (1.27)$$

Quantity ρ_c/ρ_i depends on the law of distribution of mass along the length of the blade and lies for different blades in the narrow limits: $\rho_c/\rho_i \approx 0.8\text{-}0.9$.

Therefore, it is possible to consider approximately that quantity ε is proportional to the ratio of general mass of the blades to the mass of the whole system (mass of the body of the elastic support + mass of the blades) and can be called the relative mass of the rotor.

A detailed analysis of the characteristic equation shows that in the system only oscillatory instability is possible, and aperiodic instability is impossible [35]. Borders of zones of oscillatory instability (corresponding values of $\bar{\omega}$) can be found by the following method: on the border of the zone of instability there takes place purely harmonic (not attenuating and not growing) oscillations which corresponds purely to an imaginary value of one of the roots of the

characteristic equation (1.21). Assuming in this equation $\bar{\lambda} = i\bar{p}$ (where $\bar{p}$ is the real value) and equating to zero the real and imaginary parts, we obtain the following equations:

$$\left.\begin{aligned} a\bar{p}^4 - c\bar{p}^2 + e = 0; \\ \bar{p}^6 - b\bar{p}^4 + d\bar{p}^2 - f = 0. \end{aligned}\right\} \qquad (1.28)$$

Since coefficients a, b, c, d, e, and f are well-known functions of $\bar{\omega}$ [see formulas (1.23) and (1.24)], then equation (1.28) can be examined as a system of two equations with two unknowns $\bar{p}$ and $\bar{\omega}$. Values $\bar{\omega}$ and $\bar{p}$, being the solution of system (1.28), constitute the dimensionless angular velocity $\bar{\omega}$ of rotation of the rotor, with which harmonic oscillations of the system are possible, and a corresponding dimensionless angular frequency $\bar{p}$ of the oscillations.

It is possible to solve system (1.28) using the fact that the first of equations (1.28) is biquadratic with respect to $\bar{p}$. Prescribing different values of $\bar{\omega}$, it is possible from this equation to determine $\bar{p}$, after which we can compute the value of certain quantity $D(\bar{\omega})$ equal to the left part of the second of equations (1.28) with this value of $\bar{p}$:

$$D(\bar{\omega}) = \bar{p}^6 - b\bar{p}^4 + d\bar{p}^2 - f. \qquad (1.29)$$

According to the results of such a calculation it is possible to construct a curve of the dependence of D on $\bar{\omega}$. Values $\bar{\omega}$ at which D turns into zero will be borders of the zone of instability. It is possible to show that values $\bar{\omega}$ at which $D > 0$ correspond to the stable motion of the system and values $\bar{\omega}$ at which $D < 0$ to unstable motion.

Calculation of zones of instability is very laborious, and it can be practically carried out only on digital computers. Figures 3.3-3.12 shows certain results of such calculations carried out on the digital computer "Strela" by engineer V. G. Pashkin. The graphs on these figures permit determining the stability limits and damping margins.

Stability of the system is determined in general by the following five parameters: ν_0, ε, $\bar{p}_{Л_0}$, $\bar{n}_0$, $\bar{n}_Л$. The graphs are plotted for the two most frequently encountered values $\nu_0 = 0.25$ and $\nu_0 = 0.3$. The value $\bar{p}_{Л_0} = 0$, i.e., there is examined a rotor on whose drag hinges are only dampers. The elastic elements are absent, and the influence of elastic elements will be clarified below. For each of values ν_0 there yields a series of graphs corresponding to different values ε. Plotted along the axis of the abscissas on each graph are values of the dimensionless angular velocity $\bar{\omega}$, which corresponds to limits of the zone of instability, and plotted along the axis of the ordinates is the dimensionless coefficient $\bar{n}_Л$ of damping of the blade with which the given zone of instability is obtained. The graphs are plotted for different values $\bar{n}_0$ of the dimensionless damping factor of the elastic support.

As can be seen from these graphs, the zone width of instability essentially depends on damping factors $\bar{n}_Л$ and $\bar{n}_0$. With an increase in damping $\bar{n}_Л$ (at fixed $\bar{n}_0$) the zone of instability narrows, and at a certain critical value $\bar{n}^*_Л$ the zone contracts into a point. At value $\bar{n}_Л > \bar{n}^*_Л$ the zone of instability is absent at all values $\bar{\omega}$. Thus, for example, at $\varepsilon = 0.02$, and $\nu_0 = 0.25$ (see Fig. 3.3), if $\bar{n}_0 = 0.06$ the zone of instability contracts into a point at $\bar{n}_Л = 0.128$, and at $\bar{n}_Л > 0.128$ the systems is stable at any $\bar{\omega}$ (in this case $\bar{n}^*_Л = 0.128$).

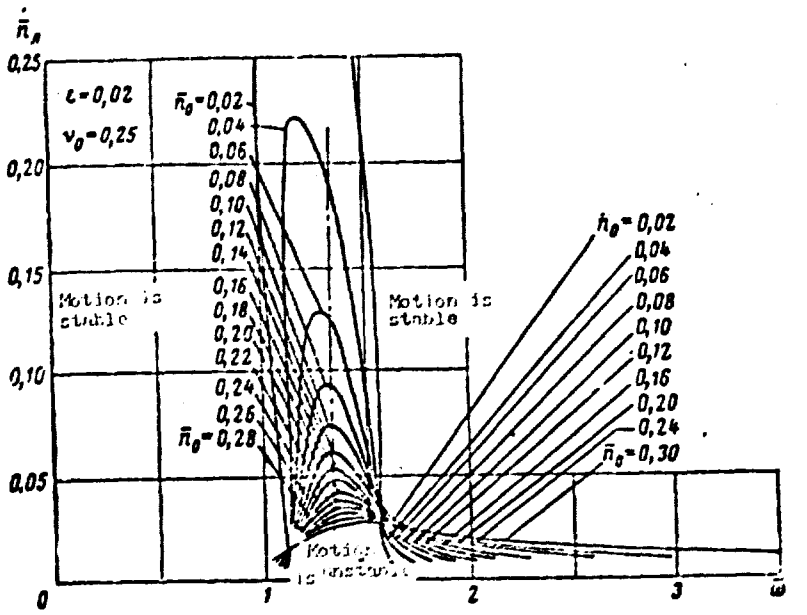

Fig. 3.3. Graphs for determining limits of instability ($\varepsilon = 0.02$; $\nu_0 = 0.25$).

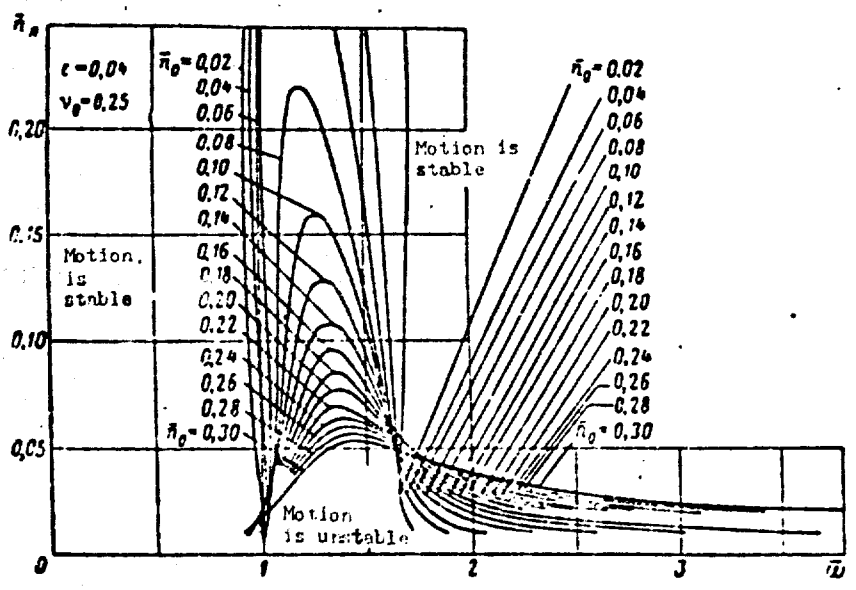

Fig. 3.4. Graphs for determining limits of instability ($\varepsilon = 0.04$; $\nu_0 = 0.25$).

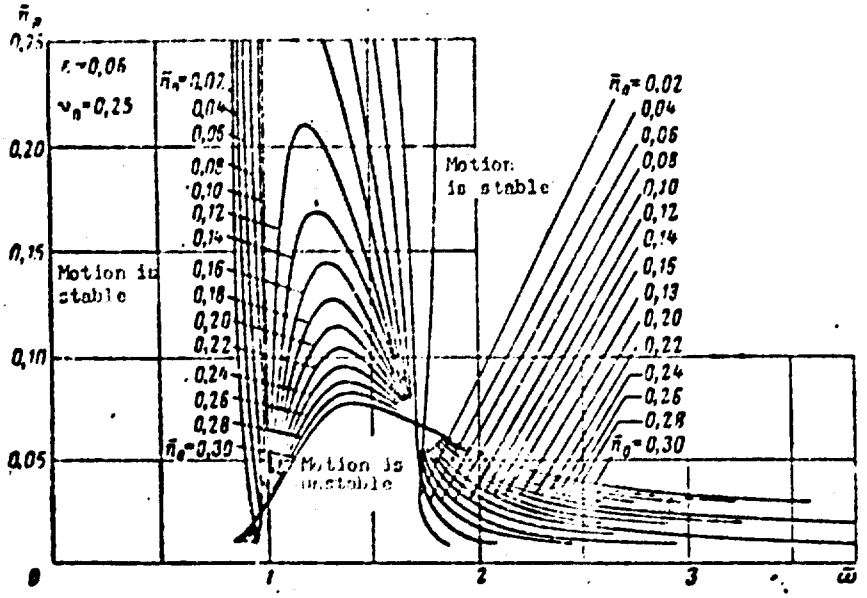

Fig. 3.5. Graphs for determining limits of instability ($\varepsilon = 0.06$; $\nu_0 = 0.25$).

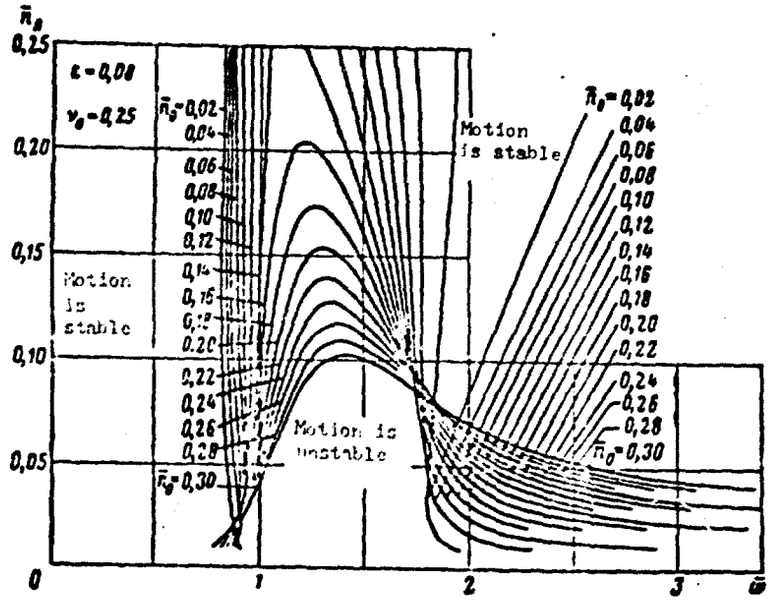

Fig. 3.6. Graphs for determining limits of instability ($\varepsilon = 0.08$; $\nu_0 = 0.25$).

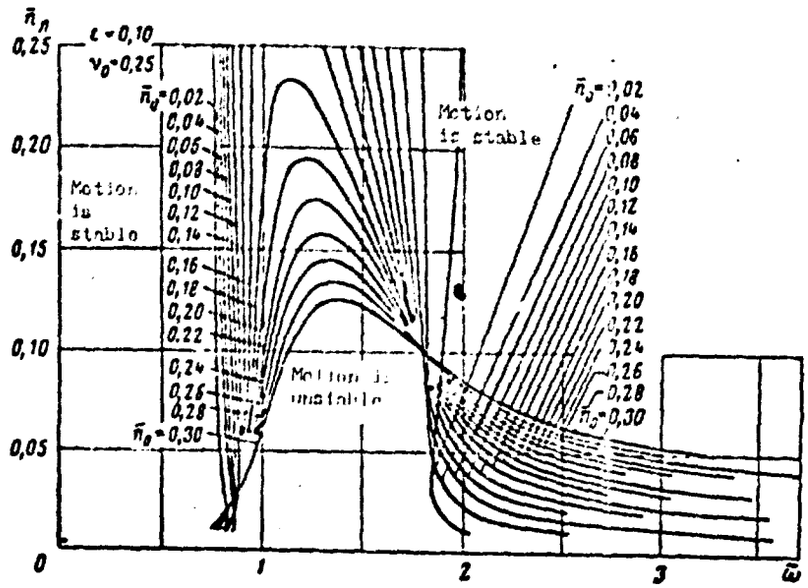

Fig. 3.7. Graphs for determining limits of instability ($\varepsilon = 0.10$; $\nu_0 = 0.25$).

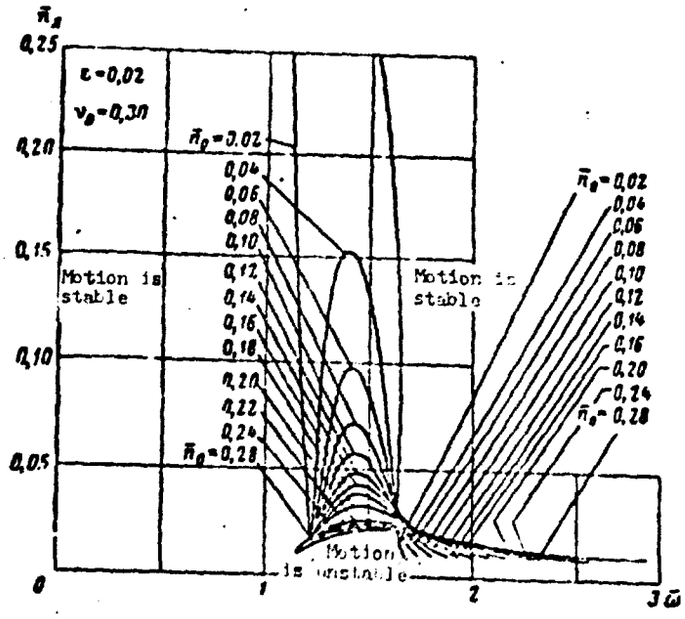

Fig. 3.8. Graphs for determining limits of instability ($\varepsilon = 0.02$; $\nu_0 = 0.30$).

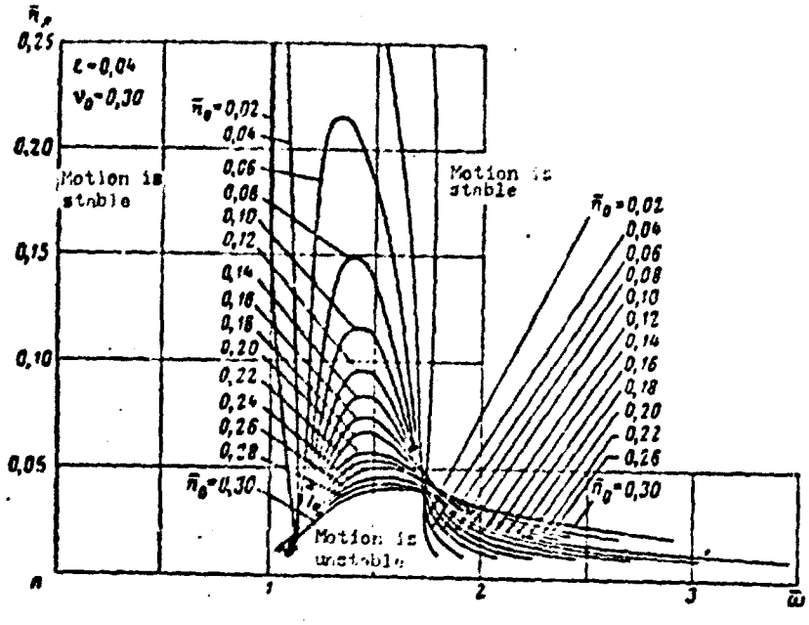

Fig. 3.9. Graphs for determining limits of instability ($\varepsilon = 0.04$; $\nu_0 = 0.30$).

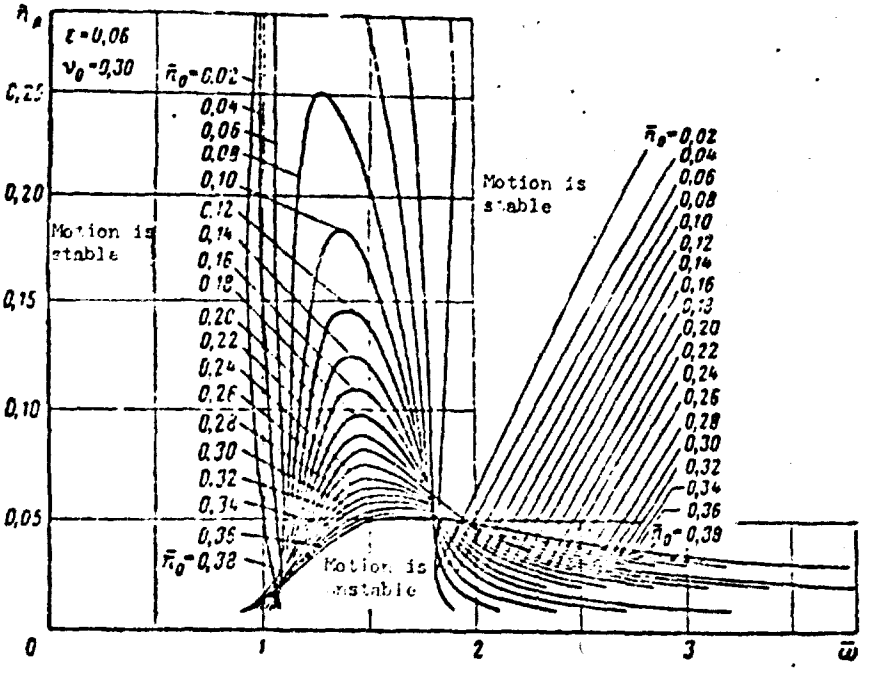

Fig. 3.10. Graphs for determining limits of instability ($\varepsilon = 0.06$; $\nu_0 = 0.30$).

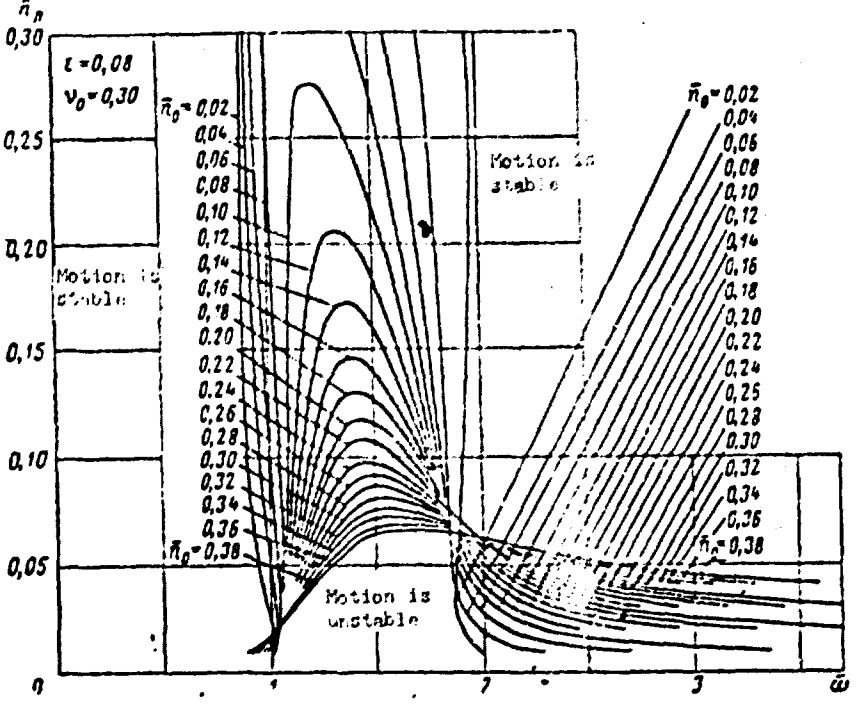

Fig. 3.11. Graphs for determining limits of instability ($\varepsilon = 0.08$; $\nu_0 = 0.30$).

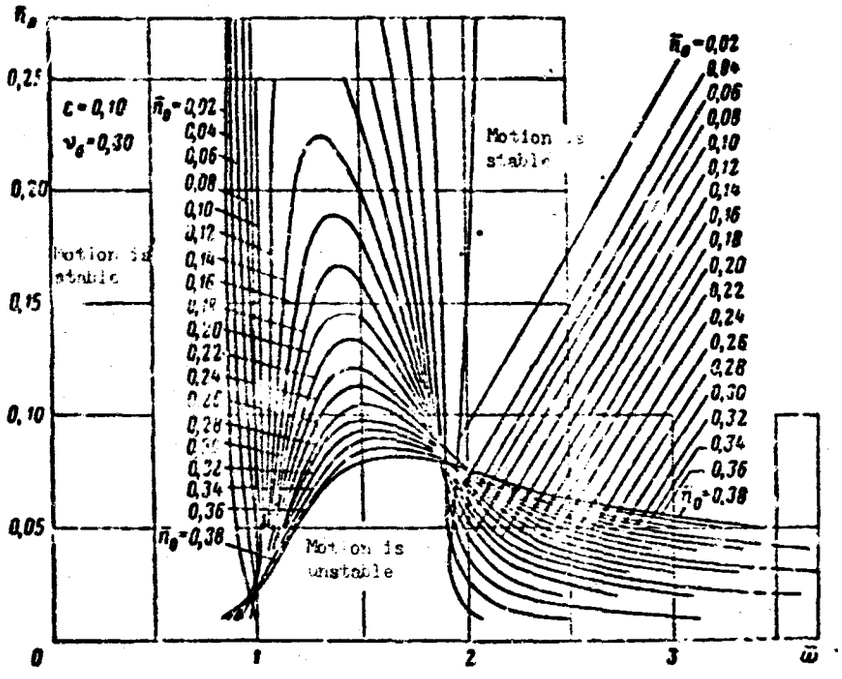

Fig. 3.12. Graphs for determining limits of instability ($\varepsilon = 0.10$; $\nu_0 = 0.30$).

It is convenient to call the ratio $\delta = \frac{\bar{n}_0}{\bar{n}_д}$ the damping margin in the case when it is larger than unity.

The value $\bar{\omega}$ at which the zone of instability is contracted into a point is called critical and can be calculated by the approximate formula:

$$\bar{\omega}_{кр} = \frac{1}{1 - \nu_0}.$$

Below we will give a physically graphic explanation of this formula.

It is necessary to note that an increase in value $\bar{n}_д$ does not always lead to an improvement in stability. At small values $\bar{n}_0$ (this can be traced on the graphs) an increase in $\bar{n}_д$ can lead even to a small movement in the lower limit of the zone of instability in the direction of smaller values of $\bar{\omega}$. This can lead to the appearance of instability at values $\bar{\omega}$ for which at smaller $\bar{n}_д$ the motion was stable.

An increase in damping $\bar{n}_0$ of the elastic support at mean values of $\bar{n}_д$ also leads to an improvement in stability; however, at minute

values of $\bar{n}_{Л}$ an increase in $\bar{n}_0$ can lead to a displacement of the upper limit of the zone of instability to the right and, thereby, to an expansion of the zone of instability.

An analysis of graphs permits making the following important conclusion: in those cases when quantities $\bar{n}_{Л}$ and $\bar{n}_0$ are of one order and are distinguished to a certain side by not more than 2-3 times, any increase in damping $\bar{n}_{Л}$ or $\bar{n}_0$ leads only to an increase in stability. At such values of $\bar{n}_{Л}$ and $\bar{n}_0$ the greatest necessary damping is obtained approximately at

$$\bar{\omega} = \bar{\omega}_{кр} = \frac{1}{1-\nu_0}.$$

For this case very important for practice the simple approximate formula of B. Ya. Zherebtsov,[1] which shows that the damping margin is proportional to the product of quantities $\bar{n}_{Л}$ and $\bar{n}_0$ can be obtained. This formula gives the value of the product $\bar{n}_{Л}\bar{n}_0$ at which the zone of instability is contracted into the point:

$$\bar{n}_{Л}\bar{n}_0 = \frac{\varepsilon(1-\nu_0)}{8\nu_0}. \qquad (1.30)$$

This approximate formula is true only when $\bar{p}_{Л_0} = 0$; its correctness can be traced by the graphs. In the case when $\bar{p}_{Л_0} \neq 0$ it is possible to use another approximate formula:

$$\bar{n}_{Л}\bar{n}_0 = \frac{\varepsilon(1-\nu_0)}{8\cdot\nu_0}\Delta, \qquad (1.31)$$

where the dimensionless quantity Δ is determined by formula

$$\Delta = \frac{1+\nu_0}{\nu_0 + \sqrt{1+\bar{p}_{Л_0}^2\left(\frac{1-\nu_0^2}{\nu_0^2}\right)}}. \qquad (1.32)$$

Figure 3.13 shows the dependence of Δ on $\bar{p}_{Л_0}$ at $\nu_0 = 0.25$. From the graph it is clear that the required damping can be considerably decreased by the introduction of an elastic element in the drag hinge of the hub. An improvement in stability of the system with an increase

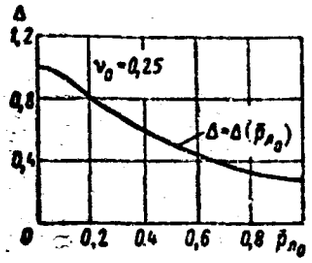

Fig. 3.13. Effect of elasticity in the drag hinge on required damping.

in $\bar{p}_{\Pi_0}$ is illustrated also by a series of graphs on Fig. 3.14.

However, with the introduction of an elastic element into the construction of the drag hinge or the introduction of so-called elastic interblade connections, it is necessary to remember that the bending moment, acting on the shank part of the blade in flight, is conditioned both by a damper and elastic element on the drag hinge. Therefore, with an increase in rigidity of the elastic element (with an increase in $\bar{p}_{\Pi_0}$) simultaneously with a decrease in the necessary damping moment there will be increased the moment acting on the blade from the side of the elastic element (or interblade connection). The optimum value $\bar{p}_{\Pi_0}$ should be considered such that with the bending moment, acting on the blades in flight, will be least at the constant damping margin with respect to ground resonance. This optimum value $\bar{p}_{\Pi_0}$ depends on

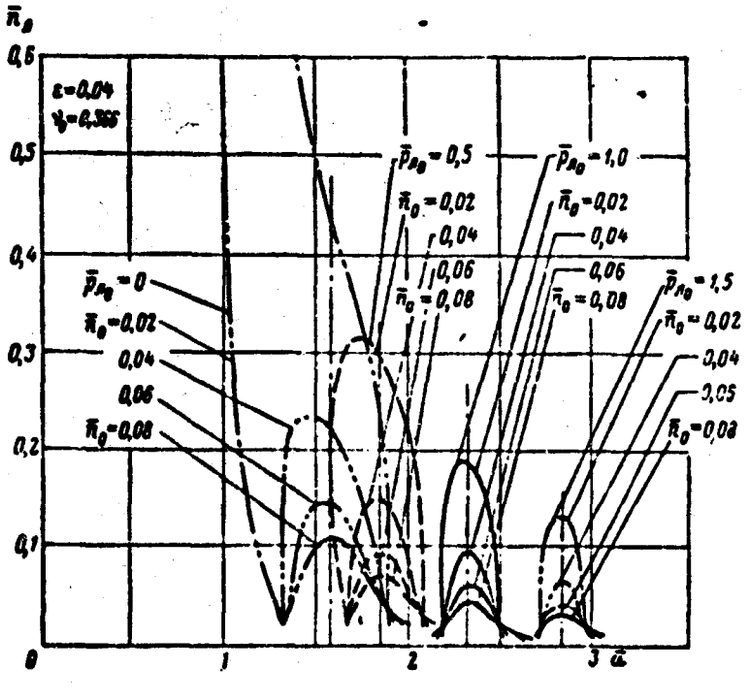

Fig. 3.14. Graphs illustrating the effect of elasticity in a drag hinge (ε = 0.04; ν_0 = 0.366).

$\bar{n}_0$ and should be specially selected for each helicopter. For a more detailed description of this see § 6.

3. Physical Pattern of Behavior of the Rotor with Ground Resonance

For a clarification of the physical pattern of the behavior of the rotor with ground resonance let us examine the following problem.

Let us assume that the body of the elastic support (Fig. 3.1) accomplishes harmonic oscillations with respect to the assigned law:

$$x = x_0 \sin pt, \tag{1.33}$$

where x_0 and p are the amplitude and frequency of oscillations of the body.

We will examine forced oscillations of blades with such motion of the body. Equation (1.8) of the motion of the k-th rotor blade here will take the following form:

$$\ddot{\xi}_k + 2n_{\text{э}}\dot{\xi}_k + (p^2_{\text{э}} + \nu_0^2\omega^2)\xi_k = \\ = -\frac{\nu_0^2}{I_{\text{э.пр}}} p^2 x_0 \sin pt \sin \psi_k. \tag{1.34}$$

Considering that $\psi_k = \omega t + \frac{2\pi}{n}k$ $(k = 1,2, \ldots, n)$ and presenting the right-hand side of this equation in the form of two harmonics, it is possible to write the equation in the form:

$$\ddot{\xi}_k + 2n_{\text{э}}\dot{\xi}_k + (p^2_{\text{э}} + \nu_0^2\omega^2)\xi_k = \\ = -\frac{\nu_0^2}{2I_{\text{э.пр}}} p^2 x_0 \left\{\cos\left[(\omega - p)t + \frac{2\pi}{n}k\right] - \cos\left[(\omega + p)t + \frac{2\pi}{n}k\right]\right\}. \tag{1.35}$$

This is the conventional equation of forced oscillations of the system with one degree of freedom.

The right-hand side of equation (1.35) constitutes an exciting force which, in this case, consists of two parts. Each part constitutes a load changing with respect to the simple harmonic law with a frequency

respectively equal to $(\omega - p)$ or $(\omega + p)$. In virture of the linearity of equation (1.35) oscillations of the blade from each of these loads can be examined independently. Forced (stabilized) oscillations of the blade will occur according to the law:

$$\xi_2(t) = \xi_1 \cos[(\omega + p)t + \varphi_1] + \xi_2 \cos[(\omega + p)t + \varphi_2], \tag{1.36}$$

where ξ_1, ξ_2, φ_1, φ_2 are certain constants which can easily be determined from equation (1.35).

Thus with oscillations of the body of the elastic support according to the simple harmonic law with frequency p of the rotor blade, forced oscillations with two combination frequencies $(\omega + p)$ and $(\omega - p)$ dependent on the angular velocity ω of rotation of the rotor will be accomplished.

The most intense oscillations of the blades will be obtained with resonance when one of the frequencies of excitation $(p + \omega)$ or $(p - \omega)$ will be close to the frequency of natural oscillations of the blade $p_z = \sqrt{p_{z_0}^2 + v_0^2\omega^2}$.

Let us examine first the case of resonance when

$$\sqrt{p_{z_0}^2 + v_0^2\omega^2} = |p - \omega|. \tag{1.37}$$

In this case the quantity ξ_1 in expression (1.36) will be considerably larger than quantity ξ_2, and therefore the second term in formula (1.36) can be disregarded. With such simplification and under condition (1.37), the law of motion of the blade will have the form:

$$\xi_2 = \xi_0 \sin\left[(p - \omega)t - \frac{2\pi}{n}k\right]. \tag{1.38}$$

where

$$\xi_0 = \frac{v_0^2 p^2}{4l_{z_0}\omega_z(\omega - p)} x_0. \tag{1.39}$$

Let us calculate further the force P_x acting on the body of the elastic support from the inertia of thus vibrating rotor blades. For this we will find the motion of the center of gravity of the system of blades by the formulas (1.12). Substituting into these formulas the expression (1.38) for ξ_k and considering that

$$\sum_{k=1}^{n} \cos\left[(2\omega - p)t + \frac{4\pi}{n}k\right] = 0$$

and

$$\sum_{k=1}^{n} \sin\left[(2\omega - p)t + \frac{4\pi}{n}k\right] = 0,$$

after simple transformations we will obtain the following law of motion of the center of gravity of the system of blades:

$$\left.\begin{aligned} x_c &= x + \frac{\varrho_c}{2}\xi_0 \cos pt; \\ z_c &= \frac{\varrho_c}{2}\xi_0 \sin pt. \end{aligned}\right\} \qquad (1.40)$$

If one were to consider that coordinates of the center of gravity in the coordinate system x'Az' connected with the body are expressed by formulas $x'_c = x_c - x$ and $z'_c = z_c$, then the center of gravity of the system of blades in this system of coordinates moves according to the law:

$$\left.\begin{aligned} x'_c &= \frac{1}{2}\varrho_c\xi_0 \cos pt; \\ z'_c &= \frac{1}{2}\varrho_c\xi_0 \sin pt. \end{aligned}\right\} \qquad (1.41)$$

Thus, with resonance, when equality (1.37) is fulfilled, the center of gravity of the system of blades describes in the system of coordinates connected with the body a circle with a radius $\frac{1}{2}\varrho_c\xi_0$. Here the angular velocity of its rotation about this is equal to frequency p of the assigned oscillations of the body.

We will determine now force P_x, acting on the body, from the formula $P_x = -mx_c''$. Then the following expression will be obtained:

$$P_x = +nm_0p^2\left[x_0+\frac{\varrho_c}{2}\xi_0\right]\cos pt.$$

Substituting here the expression for ξ_0 from (1.39), we will obtain:

$$P_x = nm_0p^2\left[1+\frac{\varrho_c}{8}\frac{v_0^2p^2}{l_{0.m}n_0(\omega-p)}\right]x_0\cos pt. \qquad (1.42)$$

Thus with oscillations of the body according to the harmonic law (1.33) and under the condition of resonance of the blade (1.37), the force acting on the body from the side of vibrating blades is changed with time also according to the harmonic law with the same frequency p, with the phase of oscillations $\pi/2$ (with respect to oscillations of the body), and is proportional to the amplitude x_0 of oscillations of the body.

Expression (1.42) can also be presented in the form:

$$P_x = -nm_0\ddot{x}+nm_0p^2\frac{\varrho_c}{8}\cdot\frac{v_0^2p^2}{l_{0.m}\cdot n_0(\omega-p)}x_0\cos pt.$$

If one were to formulate the equation of oscillations of the body (1.2) under the action of force P_x assigned by such an expression, then the following will be obtained:

$$m_0\ddot{x}+2n\dot{x}+c\dot{x} = -nm_0\ddot{x}+nm_0p^2\frac{\varrho_c}{8}\frac{v_0^2p^2}{l_{0.m}n_0(\omega-p)}x_0\cos pt.$$

Using the designations already accepted by us earlier, this equation can be written in the form:

$$\ddot{x}+2n_0\dot{x}+p_0^2x = \frac{nm_0p^2}{m_0+nm_0}\frac{\varrho_c}{8}\cdot\frac{v_0^2p^2}{l_{0.m}n_0(\omega-p)}x_0\cos pt. \qquad (1.43)$$

If there can be found parameters of system at which the law of motion of the body (1.33) satisfies this equation, then this means that with such parameters of the system a purely harmonic motion (sustained oscillations) with frequency p is possible. Substituting

expression (1.33) into equation (1.43), it is easy to see that this is obtained with the fulfillment of the following two conditions:

$$\left.\begin{aligned} p &= p_0; \\ \bar{n}_0\bar{n}_{II} &= \frac{\varepsilon p_0}{8(\omega - p_0)}. \end{aligned}\right\} \qquad (1.44)$$

Furthermore, it is necessary to remember that equation (1.43) was obtained under the condition of resonance of the blade, i.e., under condition (1.37), which, considering that $p_0 = p$, can be written in the form:

$$\sqrt{p_{\text{л}}^2 + \nu^2} = |p_0 - \omega|. \qquad (1.45)$$

From this equation one can determine the value of the critical angular velocity $\omega_{\text{кр}}$ of rotation of the rotor at which sustained oscillations in the system are possible.

Formula (1.44) gives the value of the product $\bar{n}_0\bar{n}_{II}$, at which sustained oscillations are possible, and, as we will now see, from this formula and condition (1.45) there is obtained approximate formula (1.31).

Thus sustained oscillations are possible only at such value of ω when two resonances simultaneously take place: resonance of the blade [condition (1.45)] and resonance of the elastic support $p = p_0$. At such value of ω and with fulfillment of condition (1.44), natural oscillation of the rotor on the elastic support can be sustained by a variable exciting force appearing from vibrating blades, which here are in a state of resonance.

In examining equation (1.35), we saw that resonance of blade is possible in two cases, namely: when one of the combination frequencies $(p + \omega)$ or $(p - \omega)$ coincides with the natural frequency of oscillations of the blade, i.e.,

$$p_0 = p - \omega$$

and

$$p_0 = p + \omega.$$

Of these two cases we examined only the first. In the second case all the derived formulas will be obtained by the same means, but in all expressions instead of quantity ω there will be quantity $-\omega$, including in formulas (1.44). From this formula it is clear that at $p_{Л} = |p + \omega|$ sustained oscillations are possible only under the condition $\bar{n}_0 \bar{n}_{Л} < 0$, i.e., in this case one of the quantities $\bar{n}_0$ or $\bar{n}_{Л}$ should be negative. This means that ground resonance is possible only when $p_{Л} = |p - \omega|$ and is impossible when $p_{Л} = |p + \omega|$.

Let us consider further the resonance diagram (Fig. 3.15). On this figure there is depicted the curve of the dependence of frequency of natural oscillations of the blade $p_{Л}$ on angular velocity ω, and straight lines $p = p_0 + \omega$ and $p = |p_0 - \omega|$ are plotted. The diagram is depicted for the case when $p_{Л_0} < p_0$.

As can be seen from the diagram, there are two values of ω at which the condition $p_{Л} = |p_0 - \omega|$ corresponding to points A and B is fulfilled. For point A conditon $p_{Л} = p_0 - \omega$ takes place and for point B, condition $p_{Л} = \omega - p_0$.

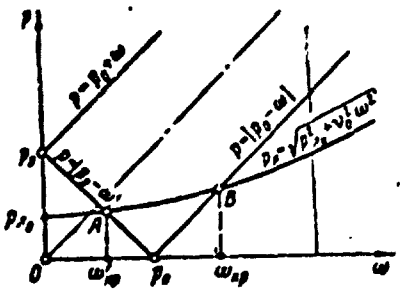

Fig. 3.5. Resonance diagram.

Thus in the first case $\omega < p_0$, and in the second $\omega > p_0$. Turning to the second of conditions (1.44), we see that it can be satisfied (with positive values of $\bar{n}_0$ and $\bar{n}_{Л}$) only if $\omega > p_0$. Consequently, from the two possible values of ω at which there can be resonance of the blade only one ($\omega > p_0$) can correspond to sustained oscillations of the system.

We will define this value ω and call it ($\omega_{кр}$) critical. Solving equation (1.45) with respect to ω and rejecting one of the obtained

values ($\omega < p_0$), we find

$$\omega_{кр} = p_0 \frac{1 + \sqrt{\nu_0^2 + \bar{p}_{z_0}^2 (1 - \nu_0^2)}}{1 - \nu_0^2}. \qquad (1.46)$$

When $\bar{p}_{z_0} = 0$ there is obtained the formula

$$\omega_{кр} = \frac{p_0}{1 - \nu_0}. \qquad (1.47)$$

Substituting value $\omega_{кр}$ from expression (1.46) into the second condition (1.44), we will find:

$$\bar{n}_0 \bar{n}_z = \frac{\varepsilon (1 - \nu_0)}{8 \nu_0} \Delta,$$

where

$$\Delta = \frac{1 + \nu_0}{\nu_0 + \sqrt{1 + \bar{p}_{z_0}^2 \left(\frac{1 - \nu_0^2}{\nu_0^2} \right)}}.$$

These formulas accurately coincide with the approximate formulas (1.31) and (1.32).

The arguments, given here, together with the analysis of stability given in § 2, permit making the following conclusion: condition $\bar{n}_0 \bar{n}_z > \frac{\varepsilon (1 - \nu_0)}{8 \nu_0} \Delta$ always provides stability with critical angular velocity of rotor rotation determined by formula (1.46). However, as was indicated during the analysis of graphs on Figs. 3.3-3.12, this condition is true only when quantities $\bar{n}_п$ and $\bar{n}_0$ are of one order. This means that the provision of stability at $\omega = \omega_{кр}$ still does not certainly provide stability at any ω.

4. Rotor on an Isotropic Elastic Base

The theory of stability of the rotor on an elastic base discussed in this paragraph is correct only for the case when the number of blades of the rotor is $n \geq 3$ and when the elastic support has only one degree of freedom -- movement along the axis Ox (Fig. 3.2).

However, an analogous theory of stability can be constructed for a more general case when the elastic support has two degrees of freedom: displacement along axes Ox and Oz. Calculations of stability for more complex system are very bulky. On the other hand, in practice almost in all cases it is possible to use formulas for the case of an elastic support with one degree of freedom. Thus this can always be done when frequencies of natural longitudinal and lateral oscillations of the helicopter on an elastic chassis (see § 5) are far from each other.

It is of interest to indicate certain simple results which are obtained in the theory of stability of the rotor on an elastic support with two degrees of freedom in the special case of the so-called isotropic elastic support when rigidity and damping of elastic bracing of the body of the base are identical in both directions (Ox and Oz). In this case the elastic and damping properties of the base are identical in all directions parallel to the plane xOz. Therefore such a base is called isotropic.

Let us assume that the rigidity and damping of the isotropic base, identical in directions of axes Ox and Oz, are characterized respectively by coefficients c and κ so that forces P_x, and P_z, applied to the base, are connected with corresponding movements x and z by formulas:

$$\left.\begin{aligned} P_x &= -cx - \kappa \frac{dx}{dt}; \\ P_z &= -cz - \kappa \frac{dz}{dt}. \end{aligned}\right\} \qquad (1.48)$$

It appears that in this case instability of the rotor on the elastic support can also take place. Here the zone of instability is obtained near the same value of $\omega = \omega_{кр}$, as earlier:

$$\omega_{кр} = p_0 \frac{1 + \sqrt{\nu_0^2 + \bar{p}_{x_0}^2 (1 - \nu_0^2)}}{1 - \nu_0^2}. \qquad (1.49)$$

In the case $\bar{p}_{x_0} = 0$, just as earlier, there is obtained a simpler

formula:

$$\omega_{кр} = \frac{p_0}{1 - \nu_0}. \tag{1.50}$$

Here quantities p_0, $\bar{p}_{л}$, and ν_0 are determined as before by formulas:

$$\left.\begin{aligned} p_0 &= \sqrt{\frac{c}{M}}; \\ p_{л} &= \sqrt{\frac{c_л}{I_{л.т}}}; \\ \nu_0 &= \sqrt{\frac{I_{л.т} S_{л.т}}{I_{л.т}}}. \end{aligned}\right\} \tag{1.51}$$

Analogous formulas for the determination of required damping also are obtained, but required damping in this case is twice greater.

The formula for required damping, at which the zone of instability is contracted into a point, has the form:

$$\beta_{n_0 \bar{n}_{л}} = \frac{\varepsilon (1 - \nu_0)}{4\nu_0} \Delta. \tag{1.52}$$

Quantities ε and Δ are determined as before by formulas (1.26) and (1.32).

§ 2. Transverse Vibrations of a Single-Rotor Helecopter

1. Preliminary Remarks

In the calculation of oscillations of a helicopter on an elastic undercarriage it is possible to examine the fuselage as a rigid body fastened to a fixed base (ground) with the help of a system of elastic elements.

The calculation of ground resonance of a helicopter, as will be shown below, can be reduced to the calculation of a rotor on an elastic base which is examined in § 1. Initial data for such a calculation (characteristics of an elastic base) are obtained from a certain preliminary calculation of natural oscillations of a rigid

fuselage on an elastic undercarriage.

The helicopter, examined as a solid body on an elastic undercarriage, has six degrees of freedom. However, since the fuselage has, as a rule, a plane of symmetry, then longitudinal and lateral natural oscillations of the helicopter can be examined independently of each other.

For a single-rotor helicopter having an extended fuselage, calculations from the point of view of ground resonance are, as a rule, lateral oscillations. With longitudinal oscillations the damping margin for eliminating ground resonance is obtained considerably larger. Therefore, to calculate ground resonance of a single-rotor helicopter it is sufficient to examine only lateral oscillations (see also § 5).

In examining transverse vibrations it follows to consider three degrees of freedom:

1) lateral displacement of the center of gravity of the helicopter;

2) turn of the helicopter around the longitudinal axis (rolling);

3) turn of the helicopter around the vertical axis (yawing).

Oscillations of a helicopter corresponding to these three degrees of freedom, in general, cannot be examined as independent oscillations. Thus, for example, with lateral displacement of the center of gravity of the helicopter there appear forces causing rolling, etc.

However, for a single-rotor helicopter, for which the longitudinal dimension of the fuselage is relatively great as compared to its lateral dimensions (this is not possible, for example, for helicopters of tandem and transverse configuration), oscillations of yawing appear weakly connected with transverse oscillations of the helicopter and its rotation around the longitudinal axis. Therefore, in the first

approximation oscillations of yawing for a single-rotor helicopter can be examined as independent. Furthermore, with oscillations of yawing of the helicopter movements of the center of the rotor in the plane of rotation are relatively small (as compared to lateral oscillations), and therefore oscillations of yawing for a single-rotor helicopter, as a rule, present no danger in the part of ground resonance. As we will further see (§ 5), such oscillations are dangerous for helicopters of longitudinal and transverse configuration.

Thus in examining lateral oscillations of a single-rotor helicopter it is sufficient in the first approximation to examine the fuselage as a body having two degrees of freedom:

1) lateral displacement of the center of gravity of the helicopter;

2) turn of the helicopter around the longitudinal axis (rolling).

With such simplifications the problem of natural lateral oscillations of the helicopter can be reduced to the problem of natural oscillations of a flat solid body elastically fastened in its plane (Fig. 3.16).

2. Lateral and Angular Rigidity of the Undercarrage. Center of Rigidity

Let us assume that a rigid body A, simulating the fuselage of helicopter, is fastened to a fixed base with the help of a system of springs (Fig. 3.16). Let us select the fixed system of coordinates yc_0z, directing axis c_0y along the axis of symmetry of the body and axis c_0z – along the axis of the horizontal springs c'_z.

If to body A there is applied force P_z, parallel to axis c_0z at distance y from point c_0, then owing to the deformation of the springs the body A will move in its plane so that its axis of symmetry will occupy a certain position c'_0y'. Let us designate by ϕ the angle of rotation of the axis of symmetry of the body (angle of bank) and by z the displacement of point c_0 (segment $c_0c'_0$).

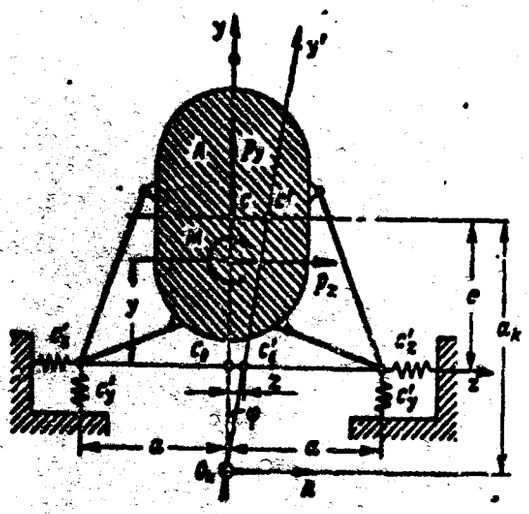

Fig. 3.16. Diagram of elastic bracing of a helicopter.

Let us assume that the springs have linear characteristics. Then, as is known, there is always found such a point of the application of force on axis c_0y (or such value y) for which the angular displacement ϕ of the body will be equal to zero, i.e., with the application of force P_z at this point the body will obtain a purely forward displacement ($\phi = 0$). Let us call such a point the center of rigidity of the shock absorption system.

If to body A there is applied a pair of forces with moment M, then the body will obtain only an angular displacement – turn around the center of rigidity.

It is not difficult to see that for the simplest system of shock absorption, depicted in Fig. 3.16, the center of rigidity will be at point c_0. It is convenient to characterize the position of the center of rigidity of the shock absorption system by the magnitude of distance e from the center of gravity c body to the center of rigidity c_0.

If to the body there is applied force P_y, directed along the axis of symmetry c_0y, the body will obtain only forward displacement y along axis c_0y. Since characteristics of all elastic elements of the shock absorption system are linear, then forces P_z and P_y and pair moment M are linearly connected with corresponding displacements y, z, and ϕ of body A.

Let us assume that this dependence is expressed by formulas:

$$P_y = c_y y; \tag{2.1}$$
$$P_z = c_z z; \tag{2.2}$$
$$M = c_\varphi \varphi. \tag{2.3}$$

We will call quantities c_y, c_z and c_ϕ respectively coefficients of vertical, lateral and angular rigidity of the shock absorption system.

Elastic properties of the shock absorption system are completely determined by these parameters: the position of the center of rigidity (e) and coefficients of rigidity c_y, c_z and c_ϕ.

For the simplest system of shock absorption depicted on Fig. 3.16, stiffness coefficients of shock absorption can be determined by formulas:

$$\left.\begin{aligned} c_y &= 2c'_y; \\ c_z &= 2c'_z; \\ c_\varphi &= 2c'_y a^2, \end{aligned}\right\} \tag{2.4}$$

where c'_y and c'_z are stiffness coefficients of vertical and horizontal springs;

2a is the distance between axes of the vertical springs (wheel track).

Undercarriage designs of helicopters are basically two types:

1) pyramidal undercarriages;

2) undercarriage with vertical struts.

Diagrams of elastic shock absorption corresponding to these two types of landing gear are depicted in Fig. 3.17a and b.

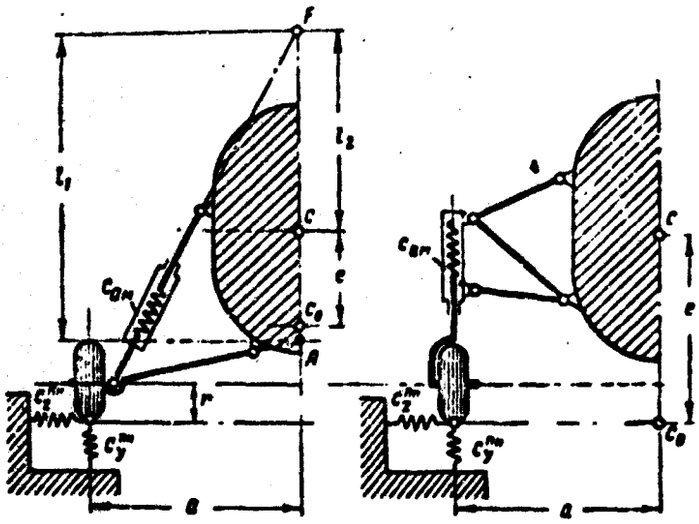

a) b)

Fig. 3.17. Different undercarriage configurations: a) pyramidal; b) with vertical struts.

The tires in such a diagram can be considered absolutely rigid, and their elasticity can be simulated by special springs with rigidity $c_y^{пн}$ and $c_z^{пн}$, which are respectively equal to the vertical and lateral rigidity of the pneumatic tire.

The coefficient of vertical rigidity of the tire can be determined by diagram of static tire pressing, which is always in the wheel catalog and constitutes the ratio of the magnitude of force pressing the tire to the support surface to the magnitude of the corresponding tire pressing. Lateral rigidity of the tire, if there are no values of it, can be determined experimentally. The value of lateral rigidity of the tire must also be known for carrying out shimmy calculation. Therefore, if for a given wheel calculation of shimmy was conducted, the value of lateral rigidity is known. For a tentative determination of lateral rigidity of a tire it is possible to use Table 3.1 also.

The shock-absorber strut in Fig. 3.17a and b is also replaced by a certain spring with rigidity c_{aM}. In reality the shock-absorber strut is a nonlinear elastic element, and its characteristic is determined by the diagram of static pressing of the strut, which gives

Table 3.1.

Type of pneumatic tire	$c_z^{пн}/c_y^{пн}$
Arch	0.7-0.9
Medium-pressure	0.4-0.64
High-pressure	0.3-0.4

the dependence of force P acting on the strut on movement s of the strut.

With the calculation of small oscillations the strut can be replaced by an equivalent linear elastic element (spring) whose rigidity is determined by the formula:

$$c_{ам} = \frac{dP}{ds}\Big|_{s=s_{ст}}, \tag{2.5}$$

where $s_{ст}$ is the strut pressing of the shock absorber.

In a landing gear system with vertical struts (Fig. 3.17b) the center of rigidity of the shock absorption is always at point c_0 lying on the ground surface. Stiffness coefficients of such a landing gear are determined by formulas (2.4), in which c_z' and c_y' are respectively equal to

$$\left.\begin{aligned} c_z' &= c_z^{пн}; \\ c_y' &= \frac{c_{ам} \cdot c_y^{пн}}{c_{ам} + c_y^{пн}}. \end{aligned}\right\} \tag{2.6}$$

For a pyramidal undercarriage (Fig. 3.41a) the center of rigidity is always higher than the ground surface, and its position must be calculated by special formulas, which we will give below.

A pyramidal undercarriage is a special case of a certain more complex undercarriage system developed by the English firm Bristol [39] and depicted (schematically) in Fig. 3.18. This undercarriage

system differs from the pyramidal landing gear by the presence of a rocker AB and special horizontal spring with rigidity $c_{пр}$. In such a system there is the possibility of changing the height of the position of the center of rigidity c_0 (i.e., quantity e) by means of selection of definite rigidity of the spring $c_{пр}$. In particular, by selecting a certain value $c_{пр}$ it is possible to achieve a position at which the center of rigidity of the shock absorption system coincides with the center of gravity of the helicopter. As it will subsequently be seen, the connection between oscillations of rolling and transverse oscillations of the helicopter is absent, which permits obtaining good characteristics of the helicopter with respect to ground resonance (see § 4, No. 3).

For a landing gear system depicted on Fig. 3.18, it is possible to write the following formulas, which can easily be derived by the usual methods of structural mechanics:

$$c_\varphi = \frac{1}{\left(\frac{1}{2c_y^{пн}a^2}\right)+\left(\frac{1}{2c_{ам}l^2}\right)+\left(\frac{1}{c_{пр}l_1^2}\right)}; \tag{2.7}$$

$$c_z = \frac{1}{\frac{1}{c_{пр}}\left(\frac{l_2^*}{l_1}\right)^2+\frac{1}{2c_{ам}}\left(\frac{l_1-l_2^*}{l}\right)^2+\frac{1}{2c_y^{пн}}\left(\frac{h_0-l_2^*}{a}\right)^2+\frac{1}{2c_z^{пр}}}; \tag{2.8}$$

$$e = \frac{c_\varphi}{2}\left(\frac{l_1}{c_{ам}l_2^2}+\frac{h_0}{c_y^{пн}a^2}\right)-l_2; \tag{2.9}$$

$$l_2^* = e+l_2 = \frac{c_\varphi}{2}\left(\frac{l_1}{c_{ам}l^2}+\frac{h_0}{c_y^{пн}a^2}\right). \tag{2.10}$$

where h_0 is the distance from the ground surface to point F of the crossing of axes of the shock-absorbing struts (see Fig. 3.18); ℓ – distance from the axis of the shock absorber to point A; ℓ_1 – distance between points F and A; ℓ_2 – distance from point F to the center of gravity of the helicopter.

The given formulas contain as a special case formulas for calculating the pyramidal landing gear (see Fig. 3.17a). To obtain formulas of a pyramidal landing gear it follows in formulas (2.7) and (2.8) to take $c_{пр} = \infty$.

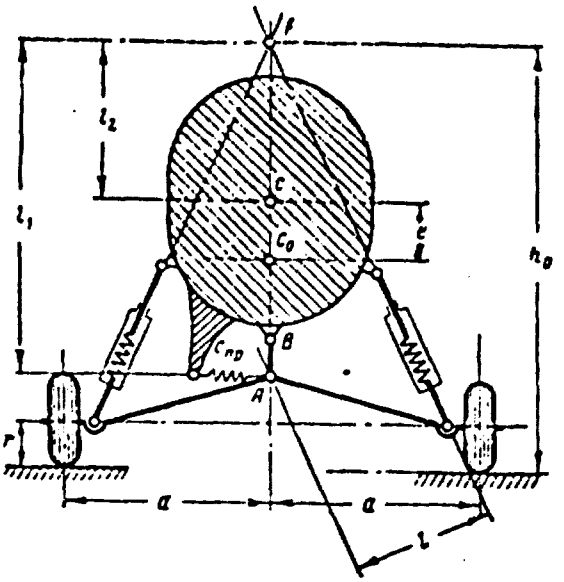

Fig. 3.18. Undercarriage diagram of the "Bristol 192" helicopter.

3. Natural Transverse Oscillations of the Helicopter

Let us turn to Fig. 3.16. During the study of lateral oscillations we will examine for body A two degrees of freedom corresponding to coordinates ϕ and z. Let us put an additional limitation on the motion of body A, namely, let us require that point O_k, belonging to body A and at distance a_k from the center of gravity of the body, would remain fixed. Then body A will have one degree of freedom - turn around point O_k. The equation of natural oscillations of body A, thus fastened will have the form:

$$I_{O_k}\ddot{\gamma}+c_{O_k}\gamma=0, \tag{2.11}$$

where I_{O_k} is the moment of inertia of the body with respect to point O_k:

$$I_{O_k}=I_c+ma_k^2; \tag{2.12}$$

I_c is the moment of inertia of the body with respect to the center of gravity; m is the mass of the body.

Coefficient c_{O_k} is the angular rigidity of the system of shock absorption with the turn of body A with respect to a point O_k.

Quantity c_{O_k} is easily determined if the position of the center of rigidity c_O of the shock absorption system and also its angular c_ϕ and lateral c_z rigidities are known.

With turn of the body at angle ϕ with respect to point O_k the center of rigidity will be displaced by the magnitude

$$z=\varphi(a_k-e). \tag{2.13}$$

Then to the body in the center of rigidity there will be applied force $P_z = c_z z$, directed to the left, and a pair of forces with moment $M = c_\phi \phi$, directed counterclockwise. The moment of these forces with respect to point O_k is

$$M=P_z(a_k-e)+c_\varphi\varphi=[c_\varphi+c_z(a_k-e)^2]\varphi.$$

Whence there is obtained following formula for angular rigidity c_{O_k}:

$$c_{O_k}=c_\varphi+c_z(a_k-e)^2. \tag{2.14}$$

The frequency of natural oscillations of the body with the secured point O_k is

$$p_k=\frac{c_{O_k}}{I_{O_k}},$$

or

$$p_k=\frac{c_\varphi+c_z(a_k-e)^2}{I_c+ma_k^2}. \tag{2.15}$$

During oscillations of the system at point O_k there will appear a reaction R, depending on the position of point O_k. If it were possible for us to select such a point of fastening O_k (such value a_k) for which R = 0, then this would mean that such a point O_k is the node of natural oscillations of a free system with unfastened point O_k, and the corresponding frequency p_k would be the frequency of natural oscillations of the free system.

The reaction R can be easily determined. With oscillations body A is loaded by the force of inertia $F_и$, applied in the center of gravity and parrallel to the O_z,

$$F_u = -m\ddot{z}_c = -m\ddot{\varphi}a_k,$$

and also by the pair of forces of inertia. Forces from shock absorption, applied to body, also lead to the horizontal force

$$P_z = c_z z = c_z \varphi (a_k - e)$$

and pair of forces. Therefore, by projecting all forces applied to the body on axis $c_c z$, we obtain

$$R = P_z + F_u.$$

If

$$\varphi = \varphi_0 \cos p_k t,$$

then

$$R = [c_z (a_k - e) - m p_k^2 a_k] \varphi_0 \cos p_k t.$$

Equating this expression to zero, we get

$$c_z (a_k - e) - m p_k^2 a_k = 0.$$

Hence there is obtained the following formula, which connects the frequency of natural oscillations of the system with position a_k of the node of oscillations:

$$a_k = \frac{e}{1 - \left(\frac{p_k}{p_z}\right)^2}, \qquad (2.16)$$

where

$$p_k^2 = \frac{c_z}{m}. \qquad (2.17)$$

Excluding value p_k from equations (2.15) and (2.16), we will obtain the quadratic equation for determining quantity a_k. This quadratic equation always has two real roots a_1 and a_2, which correspond to two tones of natural oscillations of the system. For each tone there is obtained a definite frequency p_k of natural oscillations, which at the known a_k can be determined from formula

(2.16) or (2.15).

To determine frequencies p_k of natural oscillations and corresponding values a_k it is convenient to reduce all formulas to a dimensionless form, introducing the notations

$$\bar{a}_k = \frac{a_k}{e}; \tag{2.18}$$

$$\bar{p}_k = \frac{p_k}{p_z}; \tag{2.19}$$

$$\varkappa = \frac{J_c}{me^2}; \tag{2.20}$$

$$\beta = \frac{c_\varphi}{c_z e^2}. \tag{2.21}$$

In such designations the final formulas for determination of a_k ($k = 1, 2$) and $\bar{p}_k$ ($k = 1, 2$) can be written in the form

$$\bar{a}_{1,2} = \gamma^2 \pm \sqrt{\gamma^2 + \varkappa}, \tag{2.22}$$

where

$$\gamma = \frac{1 + \beta - \varkappa}{2}; \tag{2.23}$$

$$\bar{p}_k = \sqrt{1 - \frac{1}{\bar{a}_k}}; \text{ (at } k = 1, 2). \tag{2.24}$$

For the convenience of calculation of positions of nodes of natural oscillations of the first and second tone and corresponding frequencies of oscillations, Figs. 3.19 and 3.20 give graphs computed by the formulas (2.22), (2.23) and (2.24).

The smaller of the frequencies p_1 and p_2 will be called the frequency of the first tone of oscillations and the larger – the frequency of the second tone. The node of oscillations of the first tone is always lower than the center of gravity of the helicopter ($\bar{a}_1 > 0$) and the node of oscillations of the second tone – higher than the center of gravity ($a_2 < 0$).

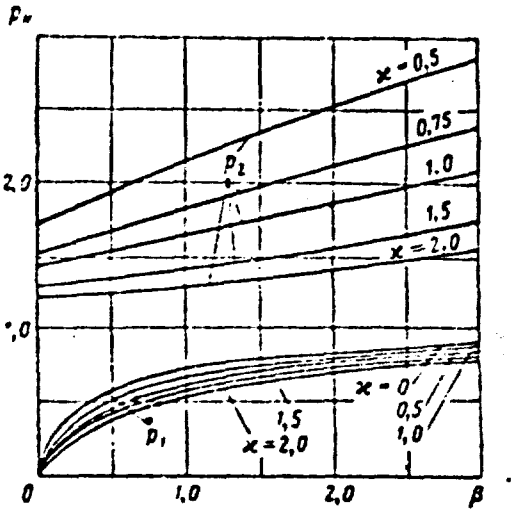

Fig. 3.19.

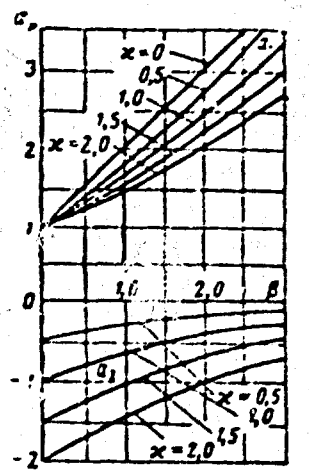

Fig. 3.20.

Fig. 3.19. Graphs for determining frequencies of natural oscillations of the helicopter.

Fig. 3.20. Graphs for determining the position of nodes of oscillations.

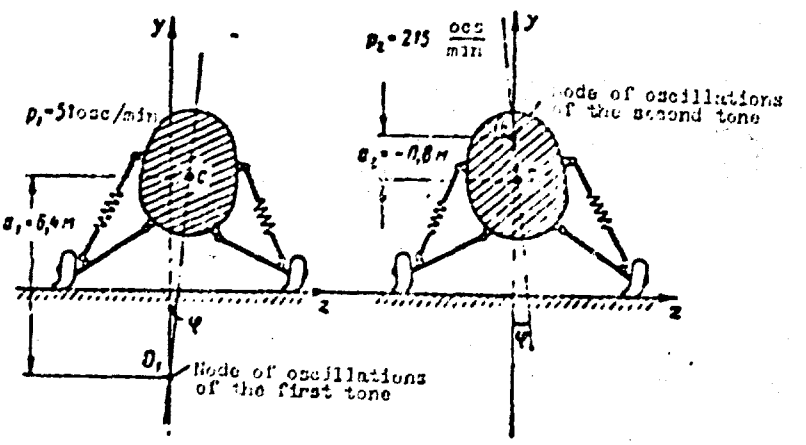

Fig. 3.21. Characteristic forms of oscillations of the first and second tone.

Figure 3.21 shows characteristic forms of oscillations of the first and second tones for a single-rotor helicopter with a pyramidal landing gear.

4. Determining Damping Factors

Oscillation damping (i.e., the absorption of energy during oscillations) is, as a rule, small and for determination of frequencies of natural oscillations and positions of nodes it can be disregarded (as this is done in No. 3).

Oscillation damping occurs, mainly, in shock-absorber struts of the landing gear. Damping in tires in the first approximation cannot be taken into account.

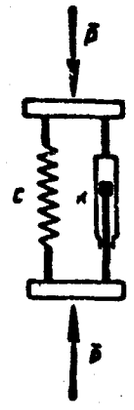

Fig. 3.22. Diagram of the linear elastic element with damping.

Let us examine the system depicted in Fig. 3.16. Let us assume that instead of springs certain linear elastic elements with damping are furnished. Such an element is schematically depicted in Fig. 3.22. Let us assume that force P, acting on this element, and its displacement s (movement of the element) are connected by the relation

$$P=cs+k\frac{ds}{dt}. \qquad (2.25)$$

We will call quantities c and k coefficients of rigidity and damping, respectively, of the elastic element.

We will designate the stiffness coefficient and damping factors of elastic elements in the system depicted in Fig. 3.16, respectively, c'_z, c'_y, k'_z, k'_y.[2] The equation of oscillations of body A with respect to the node can be written analogous to expression (2.11) in the form:

$$I_{O_k}\ddot{\varphi}+k_{O_k}\dot{\varphi}+c_{O_k}\varphi=0, \tag{2.26}$$

where quantities I_{O_k} and c_{O_k} are determined by formulas (2.12) and (2.14) and quantity k_{O_k}, by formula

$$k_{O_k}=2k'_y a^2+2k'_z(a_k-e)^2. \tag{2.27}$$

We will call this quantity the angular damping factor of the system of shock absorption with rotation of the body with respect to the node of oscillations O_k.

Equation (2.26) can be written in the form:

$$\ddot{\varphi}+2n_k\dot{\varphi}+p_k^2\varphi=0, \tag{2.28}$$

where p_k (k = 1, 2) is the frequency of the k-th tone of oscillations, and the damping factor n_k is determined by the formula

$$n_k=\frac{k_{O_k}}{2I_{O_k}}. \tag{2.29}$$

Natural oscillation of the k-th tone of the helicopter can be approximately described by the law:

$$\varphi=\varphi_0 e^{-n_k t}\cos(p_k t+\psi), \tag{2.30}$$

where ϕ_0 is the initial angle of deflection; ψ – phase angle.

The frequency of natural oscillations p_k can be taken approximately to equal the frequency of natural oscillations of the k-th tone, which is calculated neglecting damping.

In order to calculate quantities k'_y and k'_z for a concrete system of the landing gear (see Fig. 2.17a and b), it is necessary preliminarily to examine the action of the so-called shock-absorbing strut-tire system.

5. Joint Action of the Shock-Absorbing Strut-Tire System

Let us examine the landing gear system with vertical struts (see Fig. 3.17b). The shock absorber-tire system constitutes two springs with rigidities c_{aM} and $c^{y}_{пн}$ united in series.

Let us consider the work of such a system in the case when the shock absorber has damping. Such a system is depicted in Fig. 3.23. Let us assume that the shock absorber has a linear characteristic analogous to expression (2.25):

$$P_{ам}=c_{ам}s_{ам}+k_{ам}\frac{ds_{ам}}{dt}. \tag{2.31}$$

Having formulated the equation of motion of the shock absorber-tire system, it is easy to show that with the assigned harmonic law of the change in its general movement s with frequency p of the force P, acting on the shock absorber, is expressed by formula

$$P=c_{экв}s+k_{экв}\frac{ds}{dt}, \tag{2.32}$$

where $c_{экв}$ and $k_{экв}$ are characteristic of a certain equivalent linear shock absorber of the standard type (Fig. 3.22) and can be defined by formulas:

$$c_{экв}=c^{y}_{ам}\frac{(c^{y}_{ам}+c_{ам})c_{ам}+k^{2}_{ам}p^{2}}{(c^{y}_{ам}+c_{ам})^{2}+k^{2}_{ам}p^{2}}; \tag{2.33}$$

$$k_{экв}=k_{ам}\frac{(c^{y}_{ам})^{2}}{(c^{y}_{ам}+c_{ам})^{2}+k^{2}_{ам}p^{2}}. \tag{2.34}$$

Thus, with the calculation of oscillations the undercarriage configuration with vertical struts (see Fig. 3.17b) can be replaced by the configuration, depicted in Fig. 3.16, in which characteristics of elasticity and damping of vertical springs are selected by the formulas (2.33) and (2.34). At $k_{aM} = 0$ formula (2.33) gives the value of $c_{экв}$ equal to the value of c'_{y} obtained by the second of formulas (2.6). Thus in the presence of damping, formula (2.6), generally speaking, is not true. However, for an approximate

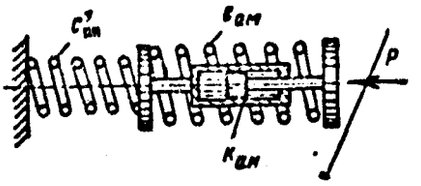

Fig. 3.23. Schematic representation of the shock-absorbing strut-tire system.

calculation of frequencies of natural oscillations it is possible to use formula (2.6) for the determination of c'_y, since value $c_{экв}$, determined by formula (2.33), is obtained close to the value c'_y, found by formula (2.6). After frequency of natural oscillations p is found, it is possible to refine value c'_y with help of formula (2.33) and then refine the calculation of frequency p.

For an accurate calculation of frequencies of natural oscillations it is possible to use the method of successive approximations (in practice the above-mentioned correction equivalent to the first approximation is sufficient) or to use the following procedure: assigning values of c'_y in the interval

$$\frac{c_{ам}c^{y}_{ш}}{c_{ам}+c^{y}_{ш}}<c'_y<c^{ш}_{y},$$

find frequencies of natural oscillations, and then from formula (2.33) according to the assigned $c_{экв} = c'_y$ find the corresponding value of $k_{ам}$. As a result of such calculation it is possible to construct a graph of the dependence of frequencies of natural oscillations of the system on $k_{ам}$. The calculations show that frequencies and forms of natural oscillations depend slightly on quantity $k_{ам}$. Therefore, it is practically sufficient to make the above-described approximate calculation with subsequent single refinement of the frequencies.

For calculation of the damping factor n_x (2.29) it is possible, by disregarding damping of the tire, to assume in formula (2.27) that:

$$k'_x=0 \quad k'_y=k_{экв}.$$

In case of a pyramidal landing gear it is possible approximately to calculate oscillation damping by the same method, but with calculation of $k_{экв}$ into formulas (2.34) instead of quantities $c_{ам}$ and $k_{ам}$ there are substituted values of the so-called rigidities reduced to

the tire and dampings of the shock absorber $c_{aM}^{пр}$ and $k_{aM}^{пр}$ determined by formulas:

$$\left.\begin{aligned} c_{aM}^{пр} &= c_{aM}\left(\frac{l}{a}\right)^2; \\ k_{aM}^{пр} &= k_{aM}\left(\frac{l}{a}\right)^2. \end{aligned}\right\} \qquad (2.35)$$

where l is the distance from the axis of the shock absorber to point A (see Figs. 3.18 and 3.17a) of the crossing of axes of the lower struts.

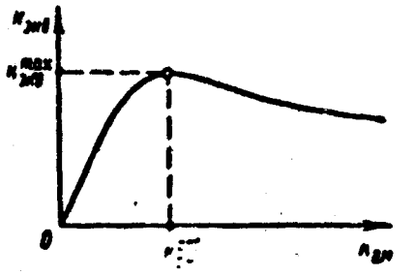

Fig. 3.24. Dependence of equivalent damping on damping of the shock absorber.

Let us examine in greater detail the dependence of the equivalent damping factor $k_{эКВ}$ of the shock absorber-tire system on value k_{aM}. Figure 3.24 shows the graph of this dependence. As can be seen from this graph, quantity $k_{эКВ}$ is increased with an increase in k_{aM} only up to a certain definite value $k_{aM} = k_{aM}^{опт}$, at which the greatest damping $k_{эКВ}^{max}$ is attained. With a further increase in k_{aM} damping of the shock absorber-tire system decreases.

From formula (2.34) it is easy to obtain the expression for the optimum value $k_{aM}^{опт}$:

$$k_{aM}^{опт} = \frac{c_{aM}^{п} + c_{aM}}{p}. \qquad (2.36)$$

Here values of k_{aM} of formula (2.33) and (2.34) give corresponding values of $c_{эКВ}^{0}$ and $k_{эКВ}^{max}$:

$$c_{эКВ}^{0} = \frac{1}{2} c_{aM}^{п}\left(1 + \frac{c_{aM}}{c_{aM} + c_{aM}^{п}}\right); \qquad (2.37)$$

$$k_{\text{ОКВ}}^{\max} = \frac{1}{2} \cdot \frac{c_{\text{ШН}}^{\gamma}}{p} \cdot \frac{1}{\left(1 + \frac{c_{\text{ОН}}}{c_{\text{ШН}}^{\gamma}}\right)}. \qquad (2,38)$$

From the last formula it is clear that the more the greatest value of $k_{\text{ОКВ}}^{\max}$ which can be obtained the less the ratio $\frac{c_{\text{ОН}}}{c_{\text{ШН}}^{\gamma}}$ and the more $c_{\text{ШН}}^{\gamma}$. Therefore, from the point of view of damping of lateral oscillations of the helicopter it follows to have as rigid a tire as possible and less rigid a shock absorber as possible. With an incorrect selection of characteristics of the landing gear greater relative rigidity of the shock absorber $\frac{c_{\text{ОН}}}{c_{\text{ШН}}^{\gamma}}$ it can occur that by no increase in damping in the shock absorber it is possible to eliminate ground resonance.

6. Reduction of the Problem to the Calculation of a Rotor on an Elastic Base

After calculation is carried out of natural oscillations of the helicopter on the ground: (there are determined frequencies, positions of nodes of oscillations and attenuation factors for both tones of natural oscillations), it is possible to produce an approximate calculation of ground resonance, reducing the problem to the calculation of the rotor on an elastic support.

It would have been possible to produce an accurate calculation of ground resonance by formulating the equation of motion of blades of the rotor and body of the helicopter similar to that as was done in § 1 for the rotor on an elastic support. In this case the order of the characteristic equation would be higher, the greater the degrees of freedom of the helicopter on the elastic landing gear are taken into account. For each case it would have been necessary to produce a very cumbersome calculation.

The approximate calculation, founded on the reduction of the problem to the rotor on an elastic support, permits using prepared results obtained for the rotor on an elastic support. The accuracy of such a calculation is quite sufficient for practical use.

The essence of the approximate calculation consists in the

following: a separate calculation of ground resonance for each tone of natural oscillations of the helicopter on the ground is produced; then the body of the helicopter is examined as a body having one degree of freedom – turn around the corresponding node of oscillations.

The equation of motion of the helicopter with an attached node of oscillations has the form:

$$I_{\theta_k}\ddot{\varphi}+h_{\theta_k}\dot{\varphi}+c_{\theta_k}\varphi=P(h+a_k). \tag{2.39}$$

The right-hand side of this equation constitutes the moment of force P from vibrating blades of the rotor with respect to the node of oscillations of the examined tone. Quantity h is the distance from the rotor plane to the center of gravity of the helicopter.

Let us introduce the new variable $x = \phi(h + a_k)$, which is the magnitude of displacement of the center of the rotor. Then equation (2.39) can be rewritten in the form similar to equation (1.2) of motion of the elastic support:

$$m^k_{экв}\ddot{x}+h^k_{экв}\dot{x}+c^k_{экв}x=P, \tag{2.40}$$

where quantities $m^k_{экв}$, $h^k_{экв}$, $c^k_{экв}$ are the mass, damping and rigidity of the equivalent elastic support and are calculated by formulas:

$$m^k_{экв}=\frac{I_{\theta_k}}{(a_k+h)^2}=\frac{I_c+ma_k^2}{(a_k+h)^2}; \tag{2.41}$$

$$h^k_{экв}=\frac{h_{\theta_k}}{(a_k+h)^2}; \tag{2.42}$$

$$c^k_{экв}=\frac{c_{\theta_k}}{(a_k+h)^2}. \tag{2.43}$$

Thus the problem is reduced to the calculation of the rotor on the equivalent elastic support whose characteristic is determined by formulas (2.41), (2.42) and (2.43).

It is easy to be convinced that for calculation of ground

resonance by formulas of § 1 there are required only three characteristics of the elastic support $m_0 = m_{экв}$, $n_0 = n_k$ [see (2.29)] and $p_0 = p_k$, which are obtained from the calculation of natural transverse oscillations of the helicopter.

Thus for every tone of natural oscillations of the helicopter on elastic landing gear an approximate calculation of ground resonance is produced by the formulas derived for the rotor on an elastic support (§ 1). With such a calculation there can be determined limits of zones of instability and values of damping factors of the blade and landing gear necessary for eliminating instability with respect to each tone of the oscillations.

7. Analysis of Results of the Calculation of Ground Resonance

Results of the calculation of ground resonance are conveniently represented in the form of a diagram of safe revolutions. Figure 3.25 shows such a diagram for the Mi-4 helicopter. Plotted along the axis of the abscissas on the diagram are the number of turns per minute of the rotor and along the axis of the ordinates – tractive force T of the rotor.

Frequencies of oscillations of the helicopter on the ground are calculated in two variants:

1) shock-absorbers struts operate;

2) shock-absorber struts do not operate.

This must be done because landing gear shock-absorber struts operate only when the compressing force on the strut is larger than the so-called force of preliminary tightening of the shock absorber. Therefore, at a certain (critical) value of thrust $T = T_{кр}$ of the rotor the force compressing the strut becomes less than the force of the preliminary tightening of the shock absorber, and the strut ceases to operate. For $T > T_{кр}$ the shock-absorber struts behave as rigid rods, and the helicopter can rock only due to the elasticity of the tires, which are practically deprived damping. Zones of

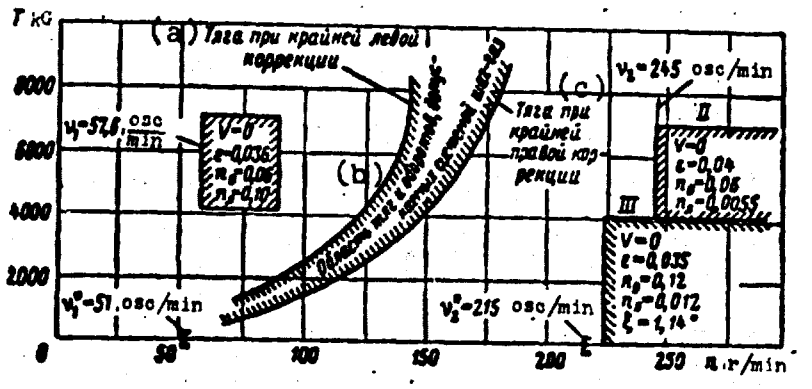

Fig. 3.25. Diagram of safe revolutions for the Mi-4 helicopter: ν_1 – frequency of the first type of oscillations with nonoperating struts; ν_2 – frequency of the second tone of oscillations with nonoperating struts; ν_1^* and ν_2^* – frequencies of the first and second tone with operating struts.
KEY: (a) Thrust with extreme left correction; (b) Region of thrusts and revolutions allowed by the pitch-throttle control system; (c) Thrust with extreme right correction.

instability of the helicopter with nonoperating struts are usually impossible to eliminate, and they are always on the diagram of safe revolutions (in Fig. 3.25 these zones are shaded).

Plotted on the diagram of safe revolution are limits of zones of instability and also the region of possible values of thrust T and revolutions n of the rotor allowed by the control system of the rotor and engine (pitch-throttle system). If not one of the possible combinations of values T and n falls beyond the limits of the zone of instability, this means that the stability of the helicopter is ensured. It is always desirable (see § 6 for more detail) to have a certain stability margin, i.e., sufficient distances on the diagram between limits of zones of instability and limits of possible values T and n.

For a single-rotor helicopter with conventional design of the undercarriage (pyramidal landing gear one with vertical struts, see Fig. 3.17a and b), the frequency of the first tone of oscillations,

as a rule, is lower than the rotor's operating revolutions (Fig. 3.25), and the frequency of the second tone is higher than the operating revolutions. Therefore, selection of the damping factors of oscillations should guarantee the absence of the zone of instability of the first tone of oscillations with operating struts. Here it is necessary to have a reliable damping margin. The stability margin with respect to the second tone of oscillations can be provided practically only "by revolutions of the rotor," and it can be characterized by a certain quantity η:

$$\eta = \frac{n_1}{n_{max}}, \qquad (2.46)$$

where n_{max} is the highest possible number of rotor revolutions; n_1 – revolutions corresponding to the lower limit of the zone of instability of the second tone.

§ 3. Characteristics of Damping of the Undercarriage and Blade. Their Effect on Ground Resonance

1. Determining the Damping Factor of the Undercarriage Shock Absorber

With the calculation of natural oscillations of the helicopter we assumed that shock absorbers of the undercarriage have linear characteristics. In reality, characteristics of the shock-absorber strut, as a rule, are nonlinear. However, for the calculation of small oscillations of the helicopter it is possible (as is usually done in the theory of nonlinear oscillations) to replace the nonlinear shock absorber by a certain equivalent linear shock absorber, for which coefficients of stiffness and damping depend on the frequency and amplitude of the oscillations. For an approximate determination of rigidity of the equivalent linear shock absorber formula (2.5) was proposed. To determine the coefficient k of damping of the equivalent linear shock absorber it is possible also to propose a simple formula. This formula can be derived in considering equivalent such a linear shock absorber which absorbs for one period of oscillations the same energy as that of a real shock absorber with identical frequency and amplitude of oscillations.

The most widespread designs of undercarriage shock-absorber struts absorb energy due to friction in the seal and flow friction with the flow of hydraulic fluid through small holes.

If one were to consider the force of flow friction in such a shock-absorber strut proportional to the square of the speed, then

dependence of the resisting force P of the strut on speed $\frac{ds}{dt}$ its pressing can be thus expressed

$$P=\begin{cases}+\left[P_0+\sigma_1\left(\frac{ds}{dt}\right)^2\right] \text{ when } \frac{ds}{dt}>0;\\ -\left[P_0+\sigma_2\left(\frac{ds}{dt}\right)^2\right] \text{ when } \frac{ds}{dt}<0.\end{cases} \tag{3.1}$$

where P_0 is the frictional force in the seals, and σ_1 and σ_2 are coefficients of flow friction of the strut on the forward and back strokes.

Let us assume that the rod of the shock absorber accomplishes oscillations according to the law $s = s_0 \sin pt$ and, consequently, $\dot{s}=\frac{ds}{dt}=ps_0\cos pt$.

Let us calculate the energy which is absorbed under these conditions by the shock absorber for one period of oscillations. This energy is determined by the formula

$$A=\int_0^T P(t)\dot{s}(t)\,dt; \quad \left(T=\frac{2\pi}{p}\right). \tag{3.2}$$

Calculating this integral for the case when function P(t) is assigned by equations (3.1), we will obtain:

$$A=4P_0s_0+\frac{8}{3}\sigma p^2s_0^3,$$

where

$$\sigma=\frac{\sigma_1+\sigma_2}{2}. \tag{3.3}$$

The damper with linear damping $\left(P=k\frac{ds}{dt}\right)$ absorbs the energy $A_1=\pi kps_0$ under those same conditions for one period of oscillations.

Comparing expression for A and A_1, we will obtain the following formula for determining the coefficient of the equivalent linear damper:

$$k_{экв}=\frac{4}{\pi}\left(\frac{P_0}{ps_0}+\frac{2}{3}\sigma ps_0\right). \tag{3.4}$$

Thus in a real undercarriage shock-absorber strut quantity $k_{экв}$ depends on the amplitude s_0 and frequency p of oscillations, and with this circumstance it is necessary to consider the calculation of oscillations of the helicopter.

Figure 3.26 gives the dependence of quantity $k_{экв}$ on the amplitude s_0 of oscillations. With an increase in amplitude of oscillations quantity $k_{экв}$ decreases, attains the least value $k_{экв}^{min}$ at certain amplitude s_0^* and increases with further increase in amplitude.

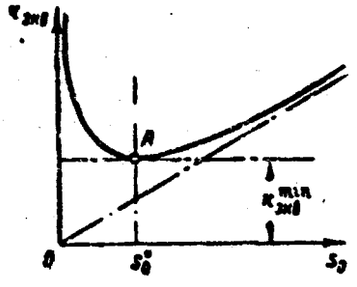

Fig. 3.26. Dependence of the equivalent damping for a shock absorber with dry friction and quadratic hydraulic drag on the amplitude of oscillations.

Analyzing expression (3.4), it is easy to obtain the following formulas for determination of the minimum value $k_{экв}^{min}$ and corresponding amplitude s_0^* of oscillations of the rod:

$$k_{экв}^{min} = \frac{8}{\pi}\sqrt{\frac{2}{3}\sigma P_0}; \qquad (3.5)$$

$$s_0^* = \frac{1}{p}\sqrt{\frac{3}{2}\frac{P_0}{\sigma}}. \qquad (3.6)$$

From formula (3.5) it is clear that the least damping of the shock absorber does not depend on the frequency and amplitude of the oscillations. Therefore, with a rough estimate of damping ability of shock absorption of the undercarriage it is very convenient to use formula (3.5) and assume with calculation of the shock absorber-tire system $k_{а.м} = k_{экв}^{min}$. It is also useful to determine quantity s_0^* by the formula (3.6).

In those cases when there is the possibility of conducting tests of prepared shock-absorber struts for damping, such tests should certainly be conducted, since the proposed formulas give only

approximate characteristics of damping.

Tests for damping can be conducted by one of two methods:

1) determination of the dependence of the force of hydraulic drag on the speed of the rod;

2) determination of the energy absorbed by the shock absorber with harmonic oscillations of the rod.

In the carrying out of tests by any of these methods, air (or nitrogen) should be purged from the shock-absorber strut, since in the tests one should determine only the damping forces.

Tests by the first method can be conducted by measuring the steady speed of the shock-absorber rod under the impact of constant load at different values of it.

With the second method of tests harmonic oscillations on a special test stand with a revolving eccentric are imported to the rod of the shock absorber. At different values of amplitude and frequency (revolutions of the eccentric) of oscillations of the rod variable axial stress in the shock absorber is measured.

For an undercarriage with vertical struts (Fig. 3.17b) one should conduct direct tests of the shock absorber-tire system. It is desirable to conduct such tests for a pyramidal landing gear (see Fig. 3.17a). It is possible to test a shock absorber series-conducted with the tire according to the same configuration as in the case of the undercarriage with vertical struts but to select for tests a special tire monotypic with that used on a helicopter whose rigidity is higher than the rigidity of the tire corresponding to the pyramidal landing gear n times. Number n is calculated by the formula:

$$n=\left(\frac{P_{\text{ш}}}{P_{\text{ш}}^{\text{в}}}\right)^2,$$

where $P_{ам}$ is the stress in the shock absorber at vertical stress $P_{ш}^{y}$ on the tire.

2. Effect of Cutoff of the Shock Absorber Due to Friction in the Seals and Natural Oscillation of the Helicopter

Frictional force P_0 in seals (collars) of the shock absorber practically does not depend on the speed of the rod (3.1). Therefore, the effect of friction in the seals is analogous to the effect of the so-called dry (or Coûlomb) friction.

This effect consists in that at small oscillations, when the variable force $P<P_0$, the shock absorber does not operate and behaves as a rigid rod. Therefore, at quite small amplitude of oscillations of the helicopter the shock absorbers do not operate, and the elastic elements in the undercarriage system appear to be only the tires practically deprived of damping.

If the angular velocity of rotor rotation lies inside the zone of instability of the helicopter with nonoperating shock absorbers, then the position of equilibrium of the helicopter, in general, is always unstable, and small oscillations of the helicopter with growing amplitude centainly appear. With an increase in amplitude of oscillations the variable force in the shock absorber increases. At a certain amplitude of oscillations a^* the force in the shock absorber P becomes equal to P_0. At large amplitudes of oscillations $a>a^*$ the force $P>P_0$, and (if $T<T_{кр}$) the shock absorbers start to operate.

If damping of the shock absorption is selected correctly, in the system natural oscillations with a certain constant small amplitude a greater than a^* are established.

Thus, for any helicopter inside the zone of instability with nonoperating struts natural oscillations, caused by the effect of dry friction in shock absorbers of the undercarriage certainly take place.

Such natural oscillations should in no way be confused with ground resonance in the usual understanding of this term. Natural oscillations are safe and occur even when the ground resonance margin (in movements) is sufficiently great.

In the most widespread designs of shock absorbers (in pneumatic hydraulic shock absorbers) friction in the seals is relatively great, and it appears that with calculation of the amplitude of such natural oscillations it is possible to consider only damping caused by this friction and not to consider the force of hydraulic drag in the shock absorber. With such approximate calculation the amplitude of natural oscillations can be only larger than the actual.

To evaluate the amplitude of natural oscillations there can be obtained certain simple formulas.

Let us consider a system consisting of two series-connected springs 1 and 2, one of which with rigidity $c''_{ш}$ simulates the tire and the other with rigidity $c_{ам}$, the shock absorber (Fig. 3.27). Connected in parallel with spring 2 is a certain element (piston 3) with dry friction, characterized by force P_0.

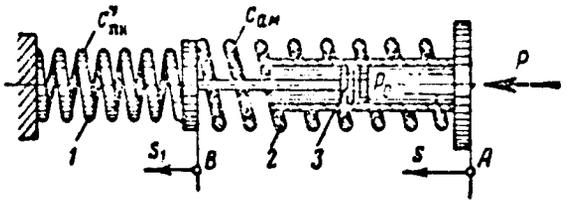

Fig. 3.27. Diagram of series connection of a tire and shock absorber with dry friction: 1 and 2 – springs; 3 – piston.

Let us assume that under the action of force $P(t)$, changing with time by a certain law, the system accomplishes oscillations so that point A, whose displacement we will designate by s, accomplishes harmonic oscillations

$$s = s_0 \cos pt. \qquad (3.7)$$

If amplitude s_0 is small, then spring 2 does not operate, and spring 1 has deformation $s_1 = s$, which changes according to the harmonic law (3.7). Here force P also changes according to the harmonic law

$$P = c_{\text{экв}}^{y} \cdot s_0 \cos pt.$$

But such operation of the system will occur only under the condition $P_{\max} < P_0$ and, consequently, under condition $s_0 < \frac{P_0}{c_{\text{экв}}^{y}}$. At $s_0 > \frac{P_0}{c_{\text{экв}}^{y}}$ spring 2 operates. There are certain time intervals when spring 2 operates (slipping in element 3), and there are time intervals when the spring does not operate.

Let us assume that $\delta = s - s_1$ is the deformation of spring 2, which we will consider positive if spring 2 is compressed. Then the dependence of the compressing force P on quantity δ can be recorded in form:

$$P = \begin{cases} c_{\text{экв}}\delta + P_0, & \text{if} \quad \dot{\delta} > 0; \\ c_{\text{экв}}\delta - P_0, & \text{if} \quad \dot{\delta} < 0. \end{cases} \tag{3.8}$$

With oscillatory motion the dependence $P = P(\delta)$ has the form of a hysteresis loop (Fig. 3.28).

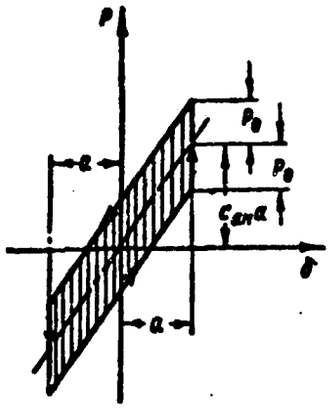

Fig. 3.28. Hysteresis loop for a shock absorber with dry friction.

When quantity δ reaches the greatest value a and remains after that constant ($\dot{\delta} = 0$), force P can take any value in the interval $c_{\text{экв}}a - P_0 \leq P \leq c_{\text{экв}}a + P_0$.

The dependence $\delta(t)$ for intervals of time corresponding to slipping ($\dot{\delta}\neq 0$), can be determined from the equation

$$c''_{\text{ш}}(s_0\cos pt-\delta)=c_{\text{ам}}\delta\pm P_0,$$

which expresses the equality of forces on both elements 1 and 2.

From this equation we find $\delta(t)$ for sections of slipping:

$$\delta(t)=\frac{c''_{\text{ш}}s_0}{c''_{\text{ш}}+c_{\text{ам}}}\cos pt\pm\frac{P_0}{c''_{\text{ш}}+c_{\text{ам}}}.$$

For sections where slipping is absent $\dot{\delta}=\pm a$.

Figure 3.29 gives graphs which show how quantities $s(t)$, $\delta(t)$ and $P(t)$ change with time for the case $c_{\text{ам}}=c''_{\text{ш}}$ and $s_0=2\frac{P_0}{c''_{\text{ш}}}$. The quantity

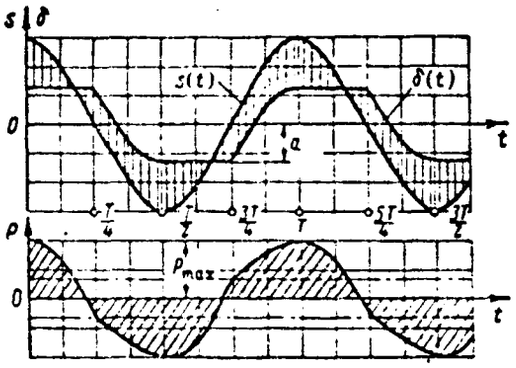

Fig. 3.29. Law of the change with time of forces and displacements in a shock absorber.

of amplitude a of oscillations of the rod of the shock absorber can be found from the expression for $\delta(t)$, if in it we assume $\cos pt=1$. Then there will be obtained

$$a=\frac{c''_{\text{ш}}s_0-P_0}{c''_{\text{ш}}+c_{\text{ам}}}. \qquad (3.9)$$

The work which is produced during oscillations by the frictional force can be determined by the formula

$$A_{P_0}=4P_0a.$$

We will compare the system depicted on Fig. 3.27 with a certain equivalent linear shock absorber, which with that same amplitude of the rod s_0 absorbs the same work and has the same value of the greatest force P_{max}.

Equating the expression of work of the linear shock absorber ($A=\pi k_{экв} p s_0^2$) to the work of frictional force A_{p_1}, we will obtain the following expression for damping factor $k_{экв}$ of the equivalent linear shock absorber:

$$k_{экв}=\frac{4}{\pi}\frac{(c_{пр}^{y})^2}{p(c_{пр}^{y}+c_{пр})}\eta, \tag{3.10}$$

where η – certain dimensionless coefficient, depending from amplitude of oscillations s_0 and determined by formula

$$\eta=\frac{1}{\bar{s}_0}-\frac{1}{\bar{s}_0^2}\ (\text{when } \bar{s}_0>1). \tag{3.11}$$

$$\bar{s}_0=s_0\frac{c_{пр}^{y}}{P_0}. \tag{3.12}$$

We will obtain the expression for rigidity $c_{экв}$ of the equivalent linear shock absorber, comparing values of the greatest force for linear ($P_{max}=c_{экв}s_0$) and nonlinear [$P_{max}=c_{пр}^{y}(s_0-a)$] of the shock absorbers:

$$c_{экв}=c_{пр}^{y}\cdot\frac{\frac{c_{пр}}{c_{пр}^{y}}+\frac{P_0}{c_{пр}^{y}\cdot s_0}}{\frac{c_{пр}}{c_{пр}^{y}}+1}. \tag{3.13}$$

Figure 3.30 shows the dependence of quantity η on the dimensionless amplitude of oscillations $\bar{s}_0$. Quantity η reaches the greatest

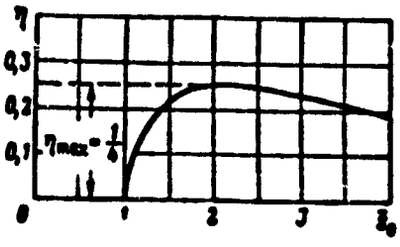

Fig. 3.30. Dependence of the dimensionless damping factor η on the relative amplitude of oscillations $\bar{s}_0$.

value $\eta_{max}=\frac{1}{4}$ when $\bar{s}_0=2$. When $\bar{s}_0>2$ the damping decreases with an increase in amplitude of the oscillations.

The greatest value of $k_{экв}=k_{экв}^{max}$ is obtained equal to

$$k_{экв}^{max}=\frac{1}{\pi}\frac{(c_{кш}^{y})^2}{p(c_{кш}^{y}+c_{ам})}. \qquad (3.14)$$

Comparing this value with value $k_{экв}^{max}$, obtained for the linear shock absorber-tire system [see formula (2.38)], we see that the shock absorber with dry friction in the system with the tire gives under those same conditions the greatest damping, $\pi/2$ times less than that of the linear shock absorber.

Thus the amplitude of natural oscillations of the helicopter, caused by friction in seals of shock absorbers can be found from condition (3.10):

$$k^{потр}=k_{экв}=\frac{4}{\pi}\frac{(c_{кш}^{y})^2}{p(c_{кш}^{y}+c_{ам})}\eta,$$

where $k^{потр}$ is the damping necessary to eliminate ground resonance.

From this equation there is determined the appropriate value η and then on Fig. 3.30, the appropriate value s_0.

3. Characteristics of Blade Dampers and Their Analysis

In the account of methods of calculation of ground resonance we assumed that dampers of drag hinges of the blades have linear characteristics, i.e., that the moment of damper M is proportional to the angular velocity $\dot{\xi}$ of rotation of the blade relative to the drag hinge: $M=k_д\dot{\xi}$.

In reality characteristics of dampers of the blade, as a rule, are nonlinear. Basically two types of dampers are used:

1) hydraulic dampers;

2) frictional dampers.

Hydraulic dampers can have different characteristics depending upon the design. In particular, the hydraulic damper can be linear

(so-called laminar damper, characteristic a on Fig. 3.31). However, linear dampers are used extremely rarely, since they have serious deficiencies.

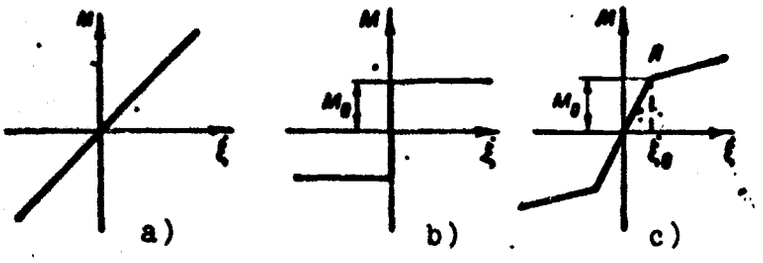

Fig. 3.31. Model characteristics of dampers of a blade: 2) linear damper; b) frictional damper; c) step damper.

One of the deficiencies is the great sensitivity of linear dampers to temperature, which is explained by the fact that damping in them is proportional to the viscosity of the hydraulic fluid, which is greatly dependent on temperature.

Another deficiency of linear dampers is the fact that the moment of such a damper is proportional to the frequency of oscillations of the blade. Really, if the blade accomplishes harmonic oscillations relative to the drag hinge $\zeta=\zeta_0\sin\nu t$, then the moment of the linear damper changes according to the law $M=k_\text{д}\dot{\zeta}=\nu k_\text{д}\zeta_0\cos\nu t$.

This circumstance leads to the fact that with forward flight of the helicopter the linear dampers load the shank part of the blade by great bending moments, since the frequency of oscillations of the blade in flight is approximately four times higher than with ground resonance.

This deficiency to a considerable degree is established for the most widely used hydraulic dampers with a step characteristic (see Fig. 3.31c) and also for frictional dampers (see Fig. 3.31b). Point A on the characteristic of the step damper corresponds to the moment of the opening of special valves.

The characteristic of the frictional damper (see Fig. 3.31b) can be examined as a special case of the step characteristic.

To calculate ground resonance of a helicopter with nonlinear dampers of blades these dampers can be replaced by certain "equivalent" linear dampers the damping factors of which depends on the amplitude and frequency of oscillations of the blade. Coefficient $k_{экв}$ of such an equivalent linear damper can be determined from the condition of absorption by this damper at the given amplitude and frequency of harmonic oscillations of the same energy for one period of oscillations which the nonlinear damper absorbs under those same conditions. For the frictional damper

$$k_{экв} = \frac{4}{\pi} \frac{M_0}{v\xi_0}, \qquad (3.15)$$

where M_0 is the moment of tie of the damper (see Fig. 3.31b); ξ_0 – amplitude of oscillations of the blade; v – frequency of oscillations of the blade.

By this formula it is possible to determine approximately the value $k_{экв}$ for hydraulic dampers with a step characteristic if the latter is close to the characteristic of the frictional damper.

In general quantity $k_{экв}$ can be determined by the known characteristic $M(\dot{\xi})$ of the nonlinear damper with help of formula

$$k_{экв}(\xi_0, v) = \frac{1}{\pi v \xi_0^2} \int_0^T M(\dot{\xi})\, d\xi; \qquad (3.16)$$

at

$$\xi = \xi_0 \sin vt \text{ and } T = \frac{2\pi}{v}.$$

For a prepared damper quantity $k_{экв}$ can also be determined experimentally by means of special laboratory tests. With such tests harmonic oscillations are imparted to the rod of the damper, and a recording is produced on an oscillogram of the magnitude of moment of the damper.

The main deficiency in dampers with a step characteristic and, in particular, frictional dampers, is the presence for a helicopter with such dampers of the so-called threshold of excitation. A helicopter being stable at small amplitudes of oscillations can become unstable at great amplitudes of oscillations exceeding the threshold of excitation.

Let us consider this phenomenon in the example of a frictional damper. Figure 3.32 shows the dependences of work A, absorbed for a period of oscillations by frictional (curve a) and linear (curve b) dampers on the amplitude of oscillations ξ_0 of the blade (at a constant frequency of oscillations). For the frictional damper graph $A(\xi_0)$ is a straight line and for the linear damper, a parabola. Let us

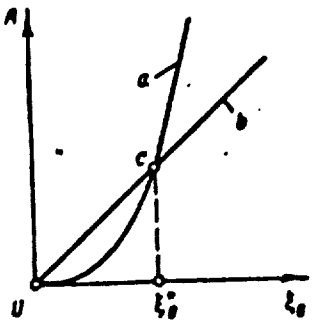

Fig. 3.32. Dependence of work absorbed for one period of oscillations on the amplitude for a damper with dry friction and damper with a linear characteristic.

assume that as a result of the calculation of ground resonance there was determined the value $k_{\Delta}^{потр}$ necessary damping of the blade in the case of the linear damper, and curve a on Fig. 3.32 corresponds to this value k_{Δ}, and curve b corresponds to the available damping of the frictional damper actually available on a helicopter.

Let us assume that these curves intersect at a certain point c, corresponding to amplitude ξ_0^*. Then with oscillations of the blade with amplitude $\xi_0<\xi_0^*$, the damping provided by the frictional damper will be greater than necessary, and with oscillations of the blade with amplitude $\xi_0>\xi_0^*$ the damping will be insufficient. The amplitude of oscillations ξ_0^* constitutes the threshold of excitation. Value ξ_0^* can be determined from formula (3.15):

$$\xi_0^* = \frac{4}{\pi} \frac{M_0}{v k_{\Delta}^{потр}}.$$

Thus if the helicopter obtained some disturbance (shock) as a result of which oscillations began (of both the helicopter and blades), then if the amplitude of oscillations of the blades is less than ζ_0^*, the motion will be stable – the oscillations attenuate. If, however, the disturbance is quite great ($\zeta_0 > \zeta_0^*$), then increasing oscillations of the helicopter will appear.

The presence of the threshold of excitation for helicopters with dampers of blades having step characteristics is a serious deficiency.

In practice there were a great deal of cases when on the helicopter, being in operation for a long time, there appeared ground resonance as a result of some strong shock, most frequently as a result of a rough landing with a blow against the ground by one of the wheels of the landing gear.

This basic deficiency of nonlinear dampers can be completely eliminated only with the application of dampers providing great damping at low frequencies of oscillations (ground resonance) of the blade and little damping at a frequency of oscillations equal to revolutions of the rotor (and above). Such a damper can be, in particular, linear. Figure 3.33 shows a diagram of such a linear damper. The damper consists of a series-connected elastic element with rigidity c and the damper itself with coefficient k.

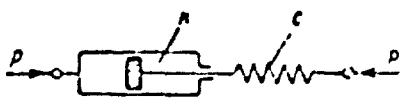

Fig. 3.33. Diagram of the element in which the elastic element and damper are united in series.

Characteristics k and c this damper can be thus selected in order, by providing sufficient damping with ground resonance, to have small bending moments on the blade during forward flight of the helicopter (see § 6). For calculation such an element can be replaced by a certain equivalent element with rigidity $c_{экв}$ and damping factor

$k_{экв}$, determined by formulas

$$\left.\begin{aligned} c_{экв} &= c\frac{1}{1+\left(\frac{c}{kp}\right)^2};\\ k_{экв} &= k\frac{1}{1+\left(\frac{kp}{c}\right)^2}. \end{aligned}\right\} \qquad (3.17)$$

These formulas are obtained analogous to formulas (2.33) and (2.34).

4. Effect of Flapping Motion of the Rotor on Ground Resonance

As was already stated, dampers of blades used usually are nonlinear. The basic peculiarity of any nonlinear damper is that if motion of the blade consists of two harmonic components, then the damping of one of these components depends on the amplitude and frequency of the other harmonic component, whereas the linear damper absorbs energy from harmonic components independently of the value of the other.

This peculiarity of the nonlinear damper is explained by the following important phenomenon, which long ago was noticed during tests of helicopters. With operation of the helicopter on the ground there is sometimes the possibility of creating ground resonance by a smooth deflection of the cyclical pitch control stick from the neutral position. If then the control stick is quite rapidly put in the neutral position, then oscillations attenuate. It is very convenient to use this phenomenon during an experimental check of the helicopter on ground resonance. This phenomenon is analogous to the effect of the influence of flapping motion on flutter. Let us consider the mechanism of this phenomenon for the case of the frictional damper (see Fig. 3.31b).

Let us first take the following abstract problem. Let us assume that about a certain plate B (see Fig. 3.34), accomplishing in a horizontal direction harmonic oscillations according to the law

$y=y_0\sin\omega t$, a certain body A evenly slips at speed V.

Body A is pressed to the vibrating plate B by a certain normal force N. We will consider that the friction between the surface of body A and plate B corresponds to the ideal law of dry friction, i.e., frictional force is constant in value and equal to $P_0=\mu N$, where μ is the coefficient of sliding friction.

The direction of the frictional force depends on the direction of speed of body A with respect to plate B.

We will consider force P (of the friction) applied to the plate positive if it is directed opposite the absolute velocity of body A, i.e., to the right. Displacement y of plate B will be considered positive if it is directed to the left. Then the law friction can be thus written:

$$P=\begin{cases}+P_0 & \text{for } V>\dot{y};\\ -P_0 & \text{for } V<\dot{y}.\end{cases}$$

For the relative speed of the plate we have the expression:

$$V_{om}=V-\dot{y}=V-\omega y_0\cos\omega t.$$

Figure 3.35 shows a graph of this dependence. The relative speed as a function of time is depicted by cosine curve shifted by magnitude V along the axis of the ordinates.

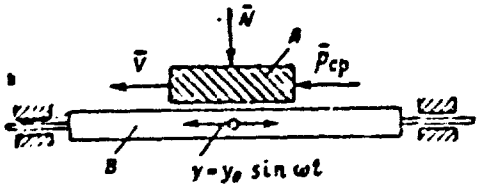

Fig. 3.34. Diagram of the motion of a body on a plate vibrating in a horizontal direction.

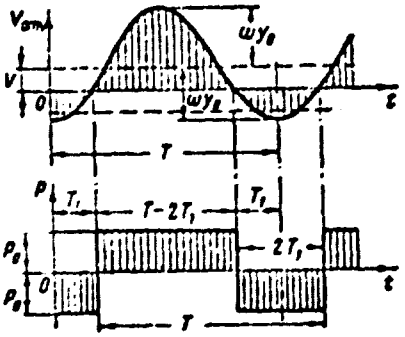

Fig. 3.35. Law of the change with time of the relative speed and frictional force with uniform motion of the body on a vibrating plate.

From the graph it is clear that at $V<\omega y_0$ during one period of T oscillations the time interval $(T-2T_1)$, during which $V_{отн}$ is positive, is greater than the time interval $2T_1$, during which $V_{отн}$ is negative. Shown under this graph is a corresponding graph of the dependence of frictional force P on time. During one period of oscillations in a certain time interval $2T_1$ the frictional force is directed to the left (negative), and in the time interval $(T-2T_1)$ the frictional force is directed to the right opposite the motion.

Thus with the motion of body A (see Fig. 3.34) on the vibrating plate B the frictional force periodically changes its direction provided $V<\omega y_0$. The frictional force is directed a great part of the time opposite the motion, and, consequently, on the average the friction renders resistance to the motion of body A.

In order to carry out uniform motion of body A to the left, to it must be applied force variable with time which at each instant would balance the frictional force. Let us calculate the average value $P_{ср}$ this force for the period, understanding by this such a constant force which for one period of oscillations produces in absolute movement of body A the same work as that of the actual frictional force. If the mass of body A would be infinitely great, and it would have been possible to disregard vibrations of body A and also consider its motion on the vibrating plate to be uniform, then force $P_{ср}$ would be the actual force necessary for a uniform motion of body A.

Work of the averaged force for one period of oscillations of the plate will be equal to:

$$A_{ср}=P_{ср}VT.$$

Work produced for one period of frictional force will be equal to:

$$A_{тр}=P_0V[T-2T_1]-P_0V[2T_1]=P_0V[T-4T_1].$$

Equating these two values of work $A_{тр}$ and $A_{ср}$, we will obtain the following expression for the averaged driving force:

$$P_{ср}=P_0\left[1-4\frac{T_1}{T}\right].$$

To determine values of $\frac{T_1}{T}$ let us note that

$$\cos\omega T_1=\frac{V}{\omega y_0}.$$

Hence, considering that $T=\frac{2\pi}{\omega}$, we obtain

$$\frac{T_1}{T}=\frac{1}{2\pi}\arccos\left(\frac{V}{\omega y_0}\right).$$

Consequently,

$$P_{ср}=P_0\left[1-\frac{2}{\pi}\arccos\left(\frac{V}{\omega y_0}\right)\right].$$

The expression obtained is correct only under the condition that $V<\omega y_0$. If, however, $V>\omega y_0$, then the frictional force changes neither the magnitude nor the sign, remaining equal to P_0. Considering what has been said and introducing the dimensionless averaged force $\bar{P}_{ср}=\frac{P_{ср}}{P_0}$, we will obtain for the latter the following expression:

$$\bar{P}_{ср}=\frac{P_{ср}}{P}=\begin{cases}1-\frac{2}{\pi}\arccos\left(\frac{V}{\omega y_0}\right), & \text{if } V<\omega y_0;\\ 1, & \text{if } V>\omega y_0.\end{cases} \qquad (3.18)$$

Figure 3.36 shows a graph of the dependence of quantity $\bar{P}_{ср}$ on the dimensionless speed of motion $\bar{V}=\frac{V}{\omega y_0}$.

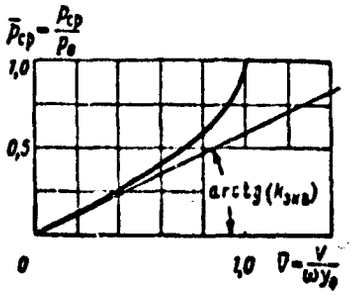

Fig. 3.36. Dependence of relative averaged frictional force on the dimensionless speed of a body on a vibrating plate.

At a low relative speed V of motion of the plate it is possible to use the simplified linear dependence $F_{ср}(V)$, which is obtained if in expansion of arc cos V in series in powers of V we are limited to the first two terms. Then

$$F_{ср} = \frac{2}{\pi} \frac{V}{\omega y_0}.$$

Thus with the slow motion of the body on a rapidly vibrating plate, the averaged frictional force can be approximately considered proportional to the first degree of speed:

$$P_{ср} = k_{экв} V, \tag{3.19}$$

where the proportionality factor

$$k_{экв} = \frac{2}{\pi} \frac{P_0}{\omega y_0}. \tag{3.20}$$

From what has been said it is clear that under the examined conditions dry friction in a certain sense is equivalent to linear viscous friction, and the equivalent damping factor is inversely proportional to the frequency and amplitude of vibrations of the plate. This important circumstance was revealed for the first time by Heinrich [41] and was checked experimentally by A. A. Krasovskiy [14].

It is obvious that with slow harmonic oscillations of body A on a rapidly vibrating plate B it is also possible approximately to calculate the damping of these oscillations by using formulas (3.19) and (3.20).

Thus if in the element with dry friction the relative motion of friction surfaces constitutes the sum of two harmonic oscillations, one low-frequency and the other high-frequency, then the damping of low-frequency oscillations can be approximately calculated by using formulas (3.19) and (3.20), understanding by ω and y_0, respectively, the frequency and amplitude of the other (high-frequency) harmonic component.

Let us return now to the consideration of oscillations of the blade of a helicopter equipped with a frictional damper with reference to the vertical hinge. With the deflection of the cyclical pitch control stick of the blades when the helicopter operates on land there appears flapping motion of blades of the rotor with reference to the flapping hinges. As is known, the flapping angle β of the blade changes with time according to the harmonic law:

$$\beta = a_0 - a_1 \cos \omega t - b_1 \sin \omega t,$$

where a_0 is the angle of conicity; a_1 and b_1 – coefficients of flapping motion.

With flapping motion of the blade there appear Coriolis forces which cause oscillations of the blade with reference to the drag hinge. The amplitude of the first harmonic ξ_1 of oscillations of the blade with reference to the drag hinge can be defined by well-known formula:[3]

$$\xi_1 = \frac{a_0 \sqrt{a_1^2 + b_1^2}}{1 - \nu_0^2}. \tag{3.21}$$

As was already clarified in §§ 1 and 3, with ground resonance (in the case $p_{s_0} = 0$) the blades accomplish oscillations with a frequency $\nu_0 \omega$ ($\nu_0 \approx 0{,}25$), i.e., with the frequency approximately four times lower than the frequency of forced oscillations of the blade induced by the flapping motion. Therefore, in accordance with the expounded damping moment acting on the blade during ground resonance, it is possible to calculate approximately by the formula:

$$M = k_{s_0} \dot{\xi}_1, \tag{3.22}$$

where

$$k_{s_0} = \frac{2}{\pi} \frac{M_0}{\omega \xi_1}. \tag{3.23}$$

Quantity M_0 constitutes the moment of tightening of the frictional damper (see Fig. 3.31b).

Thus forced oscillations in the plane of rotation of the blade with the frictional damper, caused by the flapping motion of the blade in the plane of traction, lead to the effect equivalent to the introduction of the linear damper in the drag hinge whose damping factor (3.23) is inversely proportional to the amplitude ξ_1 of forced oscillations of the blade relative to the drag hinge. Therefore, all that has been said about the threshold of excitation of the helicopter with frictional dampers (No. 3) is correct only in the case when the flapping motion of the blades is absent. This usually takes place with operation of the rotor at low revolutions. Consequently, the threshold of exitation should be estimated for ground resonance with respect to the first tone. Formula (3.23) should be used for an evaluation of ground resonance in the presence of flapping motion of the rotor (at operating revolutions of the rotor). This is especially important in the calculation of ground resonance of a helicopter on a landing run, which is the subject of discussion in § 4.

§ 4. Ground Resonance of a Helicopter on a Landing Run

In the account of methods of calculation of natural lateral oscillations of a helicopter on the ground (§ 2) it was assumed that rolling of the tire along the surface of earth is absent.

With rolling of the tire its lateral rigidity decreases, and the vertical rigidity remains constant. A decrease in lateral rigidity of the tire when rolling and also a certain additional damping with lateral displacements of the rolling tire can be determined on the basis of the existing shimmy theory of directive wheels. In this section the method of such a calculation is given.

A decrease in lateral rigidity of the tire with rolling (decrease in quantity c_z'', see Fig. 3.17) leads to a lowering of frequencies of natural oscillations of the first and second tones and, consequently, also to a lowering of limits of corresponding zones of instability. As was already noted earlier (§ 2, No. 7), usually for single-rotor helicopters the zone of instability, which corresponds to the second tone of oscillations, is higher than the

operating revolutions of the rotor, the margin with respect to revolutions of the rotor mounting sometimes to not more than 30%. The lowering of the zone of instability with rolling of the tire can be of a magnitude of the order of 20-30%. Therefore, it can appear that the helicopter, which is stable when operating at a standstill becomes unstable on a landing run. In this case is possible to indicate the critical speed of motion of the helicopter on the ground at which motion becomes unstable.

1. Rigidity and Damping of the Tire During Rolling

Let us examine the tire which evenly rolls along the ground (Fig. 3.37). Let us assume that the wheel accomplishes lateral oscillation according to the harmonic law so that the axis of rotation of the wheel remains all the time parallel to its initial position and the distance from the axis to the earth remains constant.

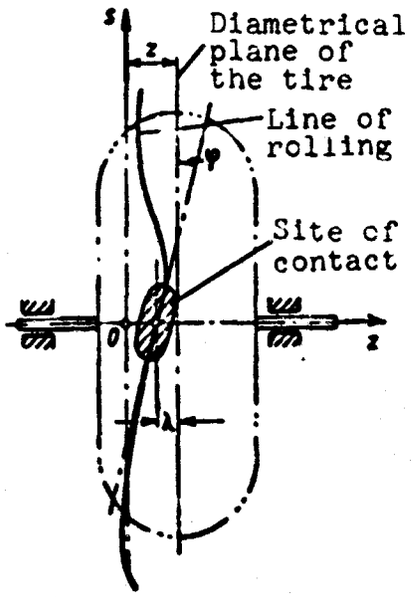

Fig. 3.37. Form in the plan on the site of contact and line of rolling of the tire: ϕ – angular deformation of the tire; λ – lateral deformation of the tire ("tilt").

Let us select the fixed rectangular system of coordinates z0s, lying on the surface of earth, and we will direct axis 0z in parallel to the axis of the wheel. Let us assume that the lateral displacement of the diametrical plane of wheel changes with time according to the harmonic law:

$$z = z_0 e^{i\omega t},$$ (3.47)

where z_0 is the amplitude of oscillations; ω – angular frequency of oscillations.

We will determine the lateral force P_z applied to the tire from the side of earth with such motion of it.

Let us assume that λ is the lateral deformation of the tire, i.e., the distance between the diametrical plane of the wheel and the point of the tire, which was the center of the area of contact before lateral deformation. Then the lateral force P_z will be equal to:

$$P_z = c_z^{ш} \lambda, \tag{4.2}$$

where $c_z^{ш}$ is the lateral rigidity of the tire in the absence of rolling.

Let us assume that further s is the path reckoned along the line of rolling, and ϕ is the angular deflection of the tire, i.e., the angle between the line of intersection of the diametrical plane of the wheel with the surface of the earth and tangent to the material line belonging to the surface of the tire and constituting a line of intersection of the diametrical plane of the wheel with the surface of an undeformed tire.

Quantities z, λ and ϕ are connected by the so-called rolling conditions, which in accordance with the hypothesis M. V. Keldysh [15], have the form:

$$\left.\begin{aligned} \frac{dz}{ds} &= -\varphi + \frac{d\lambda}{ds}; \\ \frac{d\varphi}{ds} &= \alpha\lambda - \beta\varphi. \end{aligned}\right\} \tag{4.3}$$

Here α and β are certain constant quantities for the given tire, which can be found by experimental means.

Passing to time derivatives t and considering that s = Vt (where V is the speed of the tire in the direction of axis Os), we will obtain:

$$\left.\begin{aligned}\frac{dz}{dt}&=V\varphi+\frac{d\lambda}{dt};\\ \frac{d\varphi}{dt}&=V(a\lambda-b\varphi).\end{aligned}\right\} \tag{4.4}$$

Assuming

$$\left.\begin{aligned}\lambda&=\lambda_0 e^{i\omega t}\\ \varphi&=\varphi_0 e^{i\omega t}\end{aligned}\right\} \tag{4.5}$$

and considering (4.1), we will obtain from equations (4.4) the following equations for determining constants λ_0 and φ_0 :

$$\begin{aligned}V\varphi_0+i\omega\lambda_0&=i\omega z_0;\\ (i\omega+\beta V)\varphi_0-aV\lambda_0&=0.\end{aligned}$$

Whence

$$\lambda_0=\frac{i\omega z_0}{i\omega+\dfrac{aV^2}{i\omega+\beta V}}. \tag{4.6}$$

Substituting the found value λ_0 into the first of formulas (4.5) and then into (4.2), we will obtain the following expression for force P_z, acting on the tire from the side of the earth:

$$P_z=P_0 e^{i\omega t}, \tag{4.7}$$

where

$$P_0=\frac{i\omega c_z^{\text{шн}}}{i\omega+\dfrac{aV^2}{i\omega+\beta V}}z_0$$

Let us call the complex quantity

$$D(\omega)=\frac{P_0}{z_0}=c_z^{\text{шн}}\frac{i\omega}{i\omega+\dfrac{aV^2}{i\omega+\beta V}} \tag{4.8}$$

The lateral complex dynamic rigidity of the tire during transverse harmonic oscillations of the wheel.

The modulus of the complex dynamic rigidity constitutes the ratio amplitude P_0 of lateral force to the amplitude of oscillations z_0 of the diametrical plane of the wheel. The argument of the complex quantity $D(\omega)$ constitutes the phase of oscillations of force P_z with respect to oscillations z of the wheel.

Let us consider further a certain linear elastic element with damping (see Fig. 3.22). Force P, acting on this element, and its deformation s (movement of the element) are connected by the relation (2.25):

$$P=cs+k\frac{ds}{dt}.$$

Let us introduce the concept of the complex dynamic rigidity of such an element and determine how it is connected with coefficients c and K of its rigidity and damping.

Let us assume that displacement s of the elastic element changes with time according to the harmonic law $s=s_0e^{i\omega t}$. Then the force, acting on this element, will also change according to the harmonic law:

$$P=(c+i\omega k)s_0e^{i\omega t}$$

or

$$P=P_0e^{i\omega t},$$

where

$$P_0=(c+i\omega k)s_0.$$

We will call the quantity

$$D(\omega)=c+i\omega k \qquad (4.9)$$

the complex dynamic rigidity of the elastic element with damping. As can be seen from expression (4.9), the real part of the complex quantity $D(\omega)$ is the coefficient c of rigidity of the spring, and the imaginary part is the coefficient k of damping of the element multiplied by ω.

In order to calculate natural oscillation of the helicopter on the ground in accordance with the diagram, depicted on Fig. 3.16, it is necessary to select correctly the characteristics of elasticity and damping of elements c'_z and c'_y.

It is obvious that for the calculation of oscillations of the helicopter on landing run it is sufficient to select the horizontal elastic elements ($c_z^{пш}$ on Fig. 3.17) so that their complex dynamic rigidity is equal to the complex lateral rigidity of the tire during rolling. Coefficients of stiffness and damping, which is thus selected of the "equivalent" elastic element, can be determined respectively as the real and imaginary part of the complex quantity $D(\omega)$, which is expressed by formula (4.8).

Separating in expression (4.8) the real and imaginary part, we will obtain:

$$c_{экв}=c_z^{пш}\frac{\left(1-\frac{\alpha V^2}{\omega^2}\right)+\frac{\beta^2 V^2}{\omega^2}}{\left(1-\frac{\alpha V^2}{\omega^2}\right)^2+\frac{\beta^2 V^2}{\omega^2}}; \tag{4.10}$$

$$k_{экв}=\frac{c_z^{пш}}{\omega}\frac{\left(\frac{\beta V}{\omega}\right)\left(\frac{\alpha V^2}{\omega^2}\right)}{\left(1-\frac{\alpha V^2}{\omega^2}\right)^2+\frac{\beta^2 V^2}{\omega^2}}. \tag{4.11}$$

The obtained formulas are comparatively complicated and require knowledge of constants of the tire α and β.

Formulas for determining $c_{экв}$ and $k_{экв}$ can be considerably simplified if instead of the rolling conditions of M. V. Keldysh we use the so-called hypothesis of "tilt", in accordance with which the lateral deformation of the tire λ ("tilt") is connected with the angular deformation of the tire ϕ by the simple relation

$$\lambda = \eta\beta. \tag{4.12}$$

where $\eta = \frac{l}{e}$ is the so-called coefficient of "tilt".

As was shown in the work of M. V. Keldysh [15], this coefficient is approximately equal to radius r of the undeformed tire

$$\eta = \frac{l}{e} \approx r \tag{4.13}$$

(r is the distance from the axis of the tire to the ground in the absence of pressing).

With this hypothesis the first of conditions (4.4) yields:

$$\frac{dz}{dt} = \frac{V}{\eta}\lambda + \frac{d\lambda}{dt}.$$

Assuming, as earlier, that

$$z = z_0 e^{i\omega t};$$
$$\lambda = \lambda_0 e^{i\omega t};$$
$$P = P_0 e^{i\omega t},$$

we obtain:

$$D(\omega) = \frac{P_0}{z_0} = c_z^{\text{пр}} \frac{1 + i\left(\frac{V}{\omega\eta}\right)}{1 + \left(\frac{V}{\omega\eta}\right)^2}. \tag{4.14}$$

Separating in this expression the real and imaginary part, we obtain the following expressions for coefficients of stiffness and damping of the equivalent elastic element:

$$c_{экв} = c_z^{\text{пр}} \frac{1}{1 + \left(\frac{V}{\eta\omega}\right)^2}; \tag{4.15}$$

$$h_{экв} = \frac{c_z^{\text{пр}}}{\omega} \frac{\left(\frac{V}{\eta\omega}\right)}{1 + \left(\frac{V}{\eta\omega}\right)^2}. \tag{4.16}$$

The simplified formulas (4.15) and (4.16) are more convenient for practical calculations and do not require knowledge of constants of the tire α and β. The accuracy of the approximate formulas is fully sufficient for practical purposes. This is illustrated by the comparative graphs on Fig. 3.38, which are obtained as a result of calculations carried out for the main wheels of the Mi-1 helicopter ($\omega = 18\,\frac{1}{s}$ corresponds to the frequency of the second tone of oscillations) according to the theory of Keldysh and according to the theory of "tilt".

Thus, in the carrying out of calculations of natural oscillations of the helicopter on landing run it is expedient to use formulas (4.15) and (4.16). It is necessary to substitute the frequency p of lateral oscillations of the helicopter into the formulas instead of ω. Figure 3.39 gives graphs of the dependence of the dimensionless

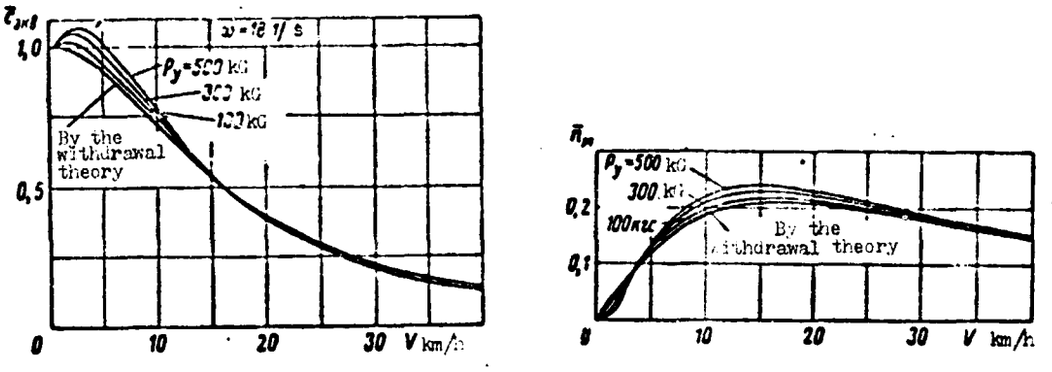

Fig. 3.38. Dependence of the relative lateral rigidity and lateral damping of the tire on the speed of the helicopter on the ground $\left(\omega = 18\,\frac{1}{s}\right)$.

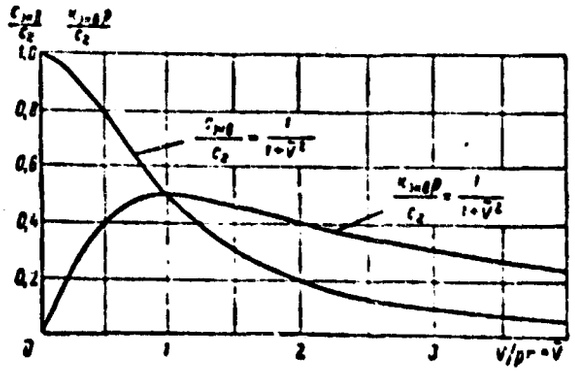

Fig. 3.39. Dependence of relative lateral rigidity and lateral damping of the tire on the dimensionless speed of the helicopter on the ground.

lateral rigidity $\left(\frac{c_{экв}}{c_z^{max}}\right)=\bar{c}_{экв}$ and damping $\left(\frac{h_{экв}\rho}{c_z^{max}}\right)$ on the dimensionless relative speed $\nu=\frac{V}{\rho r}=\frac{V}{pr}$ of motion. As can be seen from the graph, the lateral rigidity of the tire very greatly depends on the speed of the helicopter. At $\nu=3$ (which for the tire an Mi-1 helicopter at $p=18\frac{1}{s}$ amounts approximately to 50 km/h) the lateral rigidity of the tire is 10 times less than that for a rigid tire.

2. Calculation of Ground Resonance and Its Results

The calculation of ground resonance on landing run can be performed just as in the usual case (§ 2), but values of lateral rigidity c_z^{max} of the tire during calculation of natural oscillations should be replaced by values of $c_{экв}$, enumerable by the formula (4.15), and with the determination of damping factors of natural oscillations (§ 2, No. 4) an additional damping of the horizontal elastic elements (see Fig. 3.17) should be considered in accordance with formula (4.16). In formulas (4.15) and (4.16), instead of values ω one should substitute values of p of the frequency of the corresponding tone of oscillations of the helicopter. Such a procedure of calculation is fully justified, since on the limits of zones of instability purely harmonic (undamped) oscillations are observed and formulas (4.15) and (4.16) are obtained precisely for the case of harmonic lateral oscillations of the tire. The purpose of calculation of ground resonance consists exactly in finding the limits of zones of instability.

During use of formula

$$c_{экв}=c_z^{max}\frac{1}{1+\left(\frac{V}{rp}\right)^2} \qquad (4.17)$$

in the calculation of frequencies of natural oscillations of the helicopter there is the difficulty connected with the fact that for finding the frequency natural oscillations p it is necessary to know the value $c_{экв}$, which in turn depends on p. Therefore the calculation of natural oscillations (determination of p) should be produced by assigning different values of $c_{экв}$ in the interval $0<c_{экв}<c_z^{max}$, and then after determination of p the corresponding value of speed of the landing run from formula (4.17) should be found. To determine

the speed of the landing run there is obtained the formula:

$$V = rp\sqrt{\frac{c_z^{шв}}{c_{шв}} - 1}. \qquad (4.18)$$

As a result of such calculation it is possible to construct a graph of the dependence of limits of zones of instability on the speed of landing run V. Figure 3.40 gives results of such a calculation for the Mi-1 helicopter. On the graph there is depicted the dependence of the lower limit of the zone of instability corresponding to the second tone of oscillations on the speed of the landing run V.

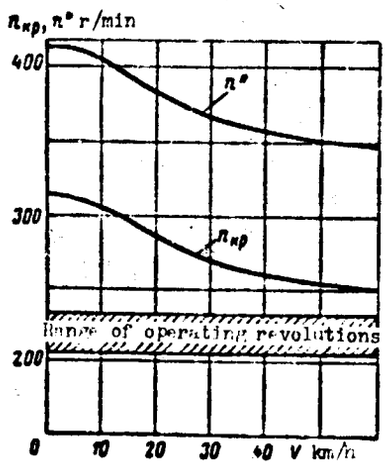

Fig. 3.40. Dependence of lower limit of the zone of instability on the speed of the landing run for the Mi-1 helicopter: $n_{кр}$ – critical revolutions corresponding to the beginning of self-excited oscillations; n° – revolutions corresponding to the center of zone of instability.

As can be seen from the graph, critical revolutions $n_{кр}$ of the rotor corresponding to the beginning of ground resonance noticeably descend with an increase in speed of the helicopter. If for a motionlessly standing helicopter the revolution margin is 36%, then at a speed of landing of run 60 km/h the margin decreases to 8%.

It is important to note that with an increase in speed V curve $n_{кр}$ approaches to a certain asymptote. This has following physical meaning.

With an increase in V the lateral rigidity of the tire, determined by quantity $c_{шв}$ [formula (4.17)], decreases without limit approaching to zero. Then the frequencies of natural oscillations of the first and second tones decrease, and the frequency of the first tone p tends to zero and the frequency of the second tone to

the value

$$p_0=\sqrt{\frac{2c'_z\rho^2}{I_x}}. \tag{4.19}$$

Quantity p_0 is the frequency of natural lateral oscillations of the helicopter in the absence of lateral rigidity of the tires.

The form of oscillations of helicopter corresponding to this frequency, constitutes the rotation of the body of the helicopter around the main longitudinal axis of inertia. The corresponding node of oscillations (see § 2, No. 3) coincides with the center of gravity of the helicopter.

Such a situation can appear for a helicopter standing motionlessly or moving about a smooth surface of ice, when one can assume that the friction between the tire and ground is absent (here also $c_z^{ш}=0$).

From this reasoning follows the possibility of a simplified (appraisal) calculation of ground resonance on a landing run, when the frequency of natural oscillations is determined by formula (4.19). For a mass of equivalent elastic support (§ 2, No. 6) there is obtained the formula

$$m_{экв}=\frac{I_x}{h^2}. \tag{4.20}$$

For the attenuation factor of the helicopter there is obtained the formula

$$\bar{n}_0=\frac{k_{экв}H^2}{I_xp_0}+\frac{k'_y c^2}{I_x p_0}, \tag{4.21}$$

where H is the distance from the surface of earth to the center of gravity of the helicopter.

Quantity $k_{экв}$ is determined by the formula

$$k_{экв}=\frac{c_z^{ш}}{p_0}\frac{\left(\frac{V}{rp_0}\right)}{1+\left(\frac{V}{rp_0}\right)^2}. \tag{4.22}$$

Quantity k'_y constitutes the damping factor of vertical elastic elements (see Fig. 3.16), which depends on damping properties of shock-absorber struts and is determined just as was shown in No. 5 of § 2.

Such an approximate calculation for a helicopter having a zone of instability located above the operating revolutions gives a small error in the "safety margin."

3. Ground Resonance with Separation of the Tires from the Surface of the Earth

All the above-stated methods of calculation of ground resonance assumed the linearity of characteristics of the tires. However, in reality, the characteristic of the tire can be (even approximately) considered linear provided one were to examine such situations at which the tire in the process of deformation remains pressed to the surface of the earth. In general, the characteristic of the tire has the form depicted on Fig. 3.41.

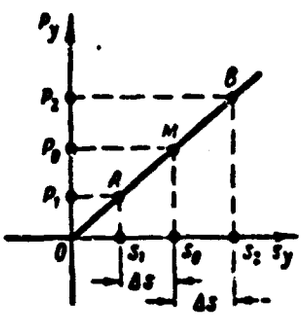

Fig. 3.41. Nonlinear dependence of force acting on the tire from the side of the earth on the vertical displacement of the axis of the wheel.

If P_y is the force acting on the tire from the side of the earth, and s_y is the corresponding displacement, then the characteristic of the tire has the form:

$$P_y = \begin{cases} c_y s_y & \text{for } s_y > 0; \\ 0 & \text{for } s_y < 0. \end{cases}$$

If there are examined small oscillations of the helicopter near the position of equilibrium corresponding to the given traction T of the rotor at which $P_y = P_0$ and $s_y = s_0$ such that the point

depicting on the diagram the state of the tire is found during oscillations on a certain segment AB wholly lying in the linear part of the characteristic, then all methods of the calculation founded on the linearity of the characteristic of the tire remain in force (for such small oscillations).

However, at large amplitudes of oscillations it can appear that the point depicting the state of the tire on the diagram exceeds the bounds of linearity of the characteristic. Thus, obviously, it will be in the case when the amplitude of displacement Δs is larger than the value of static pressing s_0. The value of static pressing s_0, just as force P_0, depends on thrust of the rotor of the helicopter and decreases when thrust T of the rotor increases, approaching to a value of the weight of the helicopter G. If $T < G$, then the tire is pressed to the ground; however, the less the amplitude of oscillations of the helicopter at which the tire will start to be detached from the surface of earth, the nearer quantity T is to the value $T = G$. Therefore, the tires are detached most easily from earth during takeoff and landing of the helicopter at moments when thrust of the rotor is less than the weight of the helicopter but is quite great.

Calculation of oscillations of the helicopter with separation of tires is very complicated, but it is possible in not producing such calculation to make certain very important qualitative conclusions. Really, during oscillations with separation of the tires the helicopter constitutes a nonlinear oscillatory system with a clearance. It is known that the frequencies of natural oscillations of the system with a clearance depend on the amplitude of oscillations and on the magnitude of the clearance, and the larger the clearance (at the assigned amplitude), the lower the frequency of natural oscillations. This is physically clear, since the presence of the clearance is equivalent to the lowering of the average (for the period of oscillations) of rigidity of the elastic element.

Consequently, during oscillations of the helicopter with separation of the tires the frequencies of natural oscillations

decrease, and together with them limits of zones of instability also decrease. Therefore, if the zone of instability corresponding to the second tone of oscillations is higher than the working revolutions of the rotor, then the margin with respect to revolutions up to the lower limit of the zone of instability decreases during oscillations with separation of the tires; and it can appear that at a quite large amplitude of oscillations the lower limit of the zone of instability will be "released" prior to the working revolutions.

Thus the helicopter having with small oscillations a zone of instability located higher than the working revolutions is stable only at small amplitudes of oscillations not exceeding a certain critical amplitude $a^{кр}$, which can be called the threshold of excitation during oscillations with breakaway of the tires.

From what has been said above it is clear that the less the value of the threshold of excitation, the smaller the forces pressing the tires to earth, i.e., and the nearer value of thrust of the rotor to the weight of the helicopter. Consequently, the most dangerous is the situation at the time of separation of the helicopter from earth and directly after landing. Therefore, when oscillations form during takeoff or landing it is necessary to decrease immediately the thrust of the rotor. Shock-absorber struts are included into the operation, and oscillations with separation of the tires are hampered.

It is important to note that oscillations with separation of the tires present a danger only in the case when there is a zone of instability located higher than the working revolutions of the rotor. From this point of view the undercarriage configuration proposed by the Bristol firm is of interest (see Fig. 3.18). As was noted already above (§ 2, No. 2), in this undercarriage configuration it is possible by selection of the value of rigidity of the special spring $c_{пр}$ to obtain coincidence of the center of rigidity of the system of shock absorption with the center of gravity of the helicopter with satisfactory landing characteristics of the landing

gear. With this lateral forward oscillations of the helicopter and angular oscillations around the main longitudinal axis of inertia of the fuselage, become independent.

Calculations show that in this case the frequency of lateral forward oscillations is approximately the same (somewhat lower) as the frequency of the first tone of oscillations of the helicopter with an undercarriage of standard design, and the frequency of angular oscillations can be considerably decreased as compared to the frequency of the second tone with the standard undercarriage design (it can be made in this case even equal to the frequency of the first tone).

Thus the application of the undercarriage of the "Bristol" system permits obtaining a very low frequency of the second tone of oscillations such that the corresponding zone of instability is obtained below the operating revolutions of the rotor. For such a helicopter ground resonance with separation of the tires from the surface of earth is not possible.

§ 5. Ground Resonance of Helicopters of Other Configurations

1. General Remarks

As was already noted above (§ 2, No. 1), for the calculation of natural oscillations of the helicopter on the ground it is necessary to examine the problem of oscillations of a solid body (if one were not to consider the elasticity of the fuselage) on an elastic support. A solid body on an elastic support has six degrees of freedom. Accordingly, there are six tones of natural oscillations of such a system to each of which corresponds a definite frequency and form of oscillations. For a single-rotor helicopter having an elongated fuselage, it appeared possible approximately to examine only the lateral oscillations and not to consider oscillations of yawing (§ 2, No. 1).

For a helicopter for which moments of inertia of the fuselage with reference to the three principal axes of inertia are magnitudes of one order, such a simplification is inadmissible. However, if there is a plane of symmetry of the fuselage, then it is possible to examine the longitudinal and lateral oscillations as being independent. In the calculation of lateral oscillations it is necessary to examine three degrees of freedom:

1) transverse displacement;

2) angle of bank;

3) angle of yaw.

During the calculation of oscillations in the plane of symmetry (longitudinal oscillations) it is necessary also to examine these three degrees of freedom:

1) longitudinal displacement;

2) vertical displacement;

3) pitch angle.

From the point of view of ground resonance both lateral and longitudinal oscillations can be dangerous.

Given in this paragraph are methods of the calculation of natural oscillations of the helicopter which considering all the mentioned degrees of freedom.

It should be noted that these methods are applied to the single-rotor helicopter and permit obtaining results more accurately than results of the approximate calculation according to the method expounded in § 2.

In this paragraph the method of calculation of ground resonance in air, caused by the elasticity of the fuselage, is also discussed.

2. Calculation of Lateral Natural Oscillations Taking into Account Three Degrees of Freedom

Figure 3.42 depicts a helicopter on an elastic undercarriage. Let us select the rectangular fixed system of coordinates cxyz with the beginning in the center of gravity of the helicopter c. We will direct forward axis cx (in the plane of symmetry of the fuselage) in parallel to the surface of earth, axis cy upwards and axis cz to the right, if one looks in the direction of axis cx. Let us assume that z is the displacement of the center of gravity of the helicopter in the direction of axis cz, and ϕ_x and ϕ_y are angles of rotation of the fuselage, respectively, with respect to axes cx and cy (ϕ_x – angle of bank, ϕ_y – angle of yaw).

Equations of lateral oscillations of the helicopter can be written in the form:

$$\left.\begin{aligned} I_x\ddot{\varphi}_x - I_{xy}\ddot{\varphi}_y &= M_x;\\ I_y\ddot{\varphi}_y - I_{xy}\ddot{\varphi}_x &= M_y;\\ m\ddot{z} &= Z, \end{aligned}\right\} \qquad (5.1)$$

where m is the mass of the helicopter; I_x and I_y – moments of inertia of the fuselage with respect to axes cx and cy; I_{xy} – corresponding product of inertia; M_x and M_y – moments of external forces acting on the fuselage with respect to axes cx and cy; Z – projection of external forces acting on the fuselage on axis cz.

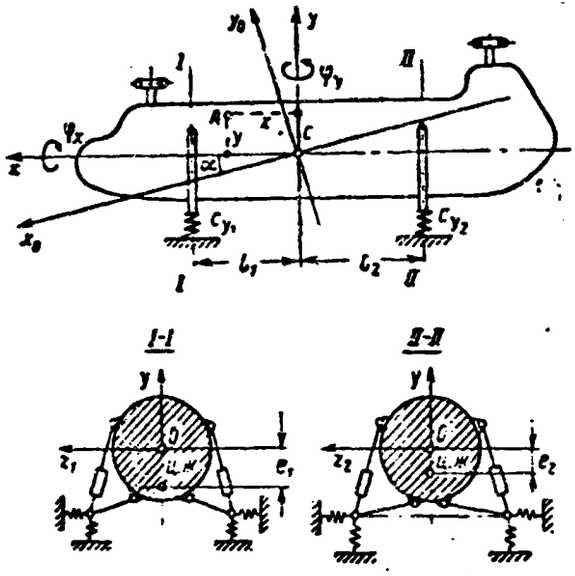

Fig. 3.42. Diagram of bracing of the helicopter on an elastic undercarriage.

Let us consider first the oscillations in the absence of damping. In this case quantities M_x, M_y, and z during small natural oscillations of the helicopter with respect to the position of equilibrium can be linearly expressed by displacements z, ϕ_x and ϕ_y. Let us write expressions for the displacement of centers of rigidity of shock absorbtions (Ц.Ж) in sections I-I and II-II of the fuselage (Fig. 3.42), which correspond to the front and rear undercarriages by quantities z, ϕ_x, and ϕ_y:

1) front undercarriage:

$$z_1 = z - \varphi_y l_1 - \varphi_x e_1;$$

2) rear chassis:

$$z_2 = z + \varphi_y l_2 - \varphi_x e_2,$$

where l_1 and l_2 are distances of planes of the front and rear undercarriages from the center of gravity c; e_1 and e_2 – distances from axis cx to centers of rigidity of the front and rear undercarriages.

By knowing the displacement of the center of rigidity of the section of the fuselage z in the plane of the given undercarriage and also the turn of this section with respect to the center of rigidity (which for both sections will be equal to ϕ_x), one can determine elastic forces and moments acting on the fuselage in this section similar to that which was done earlier (§ 2, No. 2) for a flat body on an elastic support. Determining then quantities M_x, M_y, and Z, we will obtain for them the following expressions:

$$\left.\begin{aligned} M_x &= -c_{\varphi_x}\varphi_x - c_{\varphi\beta}\varphi_y + c_\varphi z + Gz;\\ M_y &= -c_{\varphi_y}\varphi_y - c_{\varphi\beta}\varphi_x + c_\beta z;\\ Z &= -c_z z + c_\varphi\varphi_x + c_\beta\varphi_y. \end{aligned}\right\} \qquad (5.2)$$

where the appropriate stiffness coefficients are determined by formulas:

$$\left.\begin{aligned} c_z &= c_{z_1} + c_{z_2};\\ c_{\varphi_x} &= c_{\varphi_1} + c_{\varphi_2} + c_{z_1}e_1^2 + c_{z_2}e_2^2;\\ c_{\varphi_y} &= c_{z_1}l_1^2 + c_{z_2}l_2^2;\\ c_\varphi &= c_{z_1}e_1 + c_{z_2}e_2;\\ c_\beta &= c_{z_1}l_1 - c_{z_2}l_2;\\ c_{\varphi\beta} &= c_{z_1}e_1l_1 - c_{z_2}e_2l_2. \end{aligned}\right\} \qquad (5.3)$$

Quantities c_{z_1}, c_{z_2}, c_{ϕ_1}, and c_{ϕ_2} constitute coefficients of lateral and angular rigidity of the front and rear undercarriages.

In the first of formulas (5.2) there is also the term Gz, which is the moment of force of weight of the helicopter G with respect to axis cx appearing with lateral displacement z.

Substituting expressions (5.2) into equations (5.1), we will obtain finally the following equations of small lateral oscillations of the helicopter:

$$\left.\begin{aligned} I_x\ddot{\varphi}_x - I_{xy}\ddot{\varphi}_y &= (G + c_\varphi)z - c_{\varphi_x}\varphi_x - c_{\varphi\beta}\varphi_y;\\ I_y\ddot{\varphi}_y - I_{xy}\ddot{\varphi}_x &= c_\beta z - c_{\varphi\beta}\varphi_x - c_{\varphi_y}\varphi_y;\\ m\ddot{z} &= -c_z z + c_\varphi\varphi_x + c_\beta\varphi_y. \end{aligned}\right\} \qquad (5.4)$$

Searching for the solution of this system in the form of:

$$z = z_0 \cos pt;$$
$$\varphi_x = \varphi_x^\circ \cos pt;$$
$$\varphi_y = \varphi_y^\circ \cos pt,$$

where z_0, φ_x°, φ_y° and p are constants, we arrive at the following system of linear algebraic equations for determining these constants:

$$\left.\begin{aligned} &(c_z - mp^2) z_0 - c_\varepsilon \varphi_x^\circ - c_l \varphi_y^\circ = 0; \\ &-(G + c_\varepsilon) z_0 + (c_{\varphi_x} - I_x p^2) \varphi_x^\circ + (c_{el} + I_{xy} p^2) \varphi_y^\circ = 0; \\ &-c_l z_0 + (c_{el} + I_{xy} p^2) \varphi_x^\circ + (c_{\varphi_y} - I_y p^2) \varphi_y^\circ = 0. \end{aligned}\right| \qquad (5.5)$$

Equating to zero the determinant of this system

$$\begin{vmatrix} (c_z - mp^2); & -c_\varepsilon; & -c_l \\ -(G + c_\varepsilon); & (c_{\varphi_x} - I_x p^2); & (c_{el} + I_{xy} p^2) \\ -c_l; & (c_{el} + I_{xy} p^2); & (c_{\varphi_y} - I_y p^2) \end{vmatrix} = 0$$

and producing simple transformations, we arrive at the following characteristic equation for determining frequencies of natural lateral oscillations p of the helicopter:

$$Ap^6 + Bp^4 + Cp^2 + D = 0, \qquad (5.6)$$

where

$$\left.\begin{aligned} &A = h_x h_y - 1; \\ &B = p_z^2 + p_{\varphi_x}^2 + p_{\varphi_y}^2 - h_x h_y p_z^2 + 2h_y p_{xy}^2; \\ &C = p_{xy}^2 p_{yx}^2 - p_{\varphi_y}^2 p_{\varphi_x}^2 + p_{xy}^2 p_{yz}^2 - p_z^2 (p_{\varphi_y}^2 + p_{\varphi_x}^2) + \\ &\quad + p_{zx}^2 (p_{xz}^2 + p_0^2) + (2p_{zy}^2 p_{xz}^2 - 2p_z^2 p_{xy}^2 + p_{zy}^2 p_0^2) h_y; \\ &D = p_z^2 p_{\varphi_x}^2 p_{\varphi_y}^2 + 2p_{zx}^2 p_{yz}^2 p_{xy}^2 + p_{zy}^2 p_{yz}^2 p_0^2 - \\ &\quad - p_{xy}^2 p_{yz}^2 p_{\varphi_x}^2 - p_z^2 p_{xy}^2 p_{yx}^2 - p_{zx}^2 p_{\varphi_y}^2 p_0^2 - p_{xz}^2 p_{zx}^2 p_{\varphi_y}^2; \end{aligned}\right| \qquad (5.7)$$

$h_x = \frac{I_{xy}}{I_x}$; $h_y = \frac{I_{xy}}{I_y}$ are dimensionless coefficients.

Partial frequencies p_z, p_{φ_x}, p_{φ_y} and quantities p_{xy}^2, p_{yz}^2 etc., are given by formulas:

$$\left.\begin{aligned}
&p_z^2=\frac{c_z}{m};\quad p_{\varphi_x}^2=\frac{c_{\varphi_x}}{I_x};\quad p_{\varphi_y}^2=\frac{c_{\varphi_y}}{I_y};\\
&p_{xy}^2=\frac{c_{xl}}{I_x};\quad p_{yx}^2=\frac{c_{xl}}{I_y};\\
&p_{xy}^2=\frac{c_1}{m};\quad p_{yz}^2=\frac{c_1}{I_x};\\
&p_{zx}^2=\frac{c_z}{m};\quad p_{xz}^2=\frac{c_z}{I_x};\\
&p_0^2=\frac{G}{I_x}.
\end{aligned}\right\} \qquad (5.8)$$

Equation (5.6) is a cubic equation with respect to quantity p^2. It is possible to show that its roots p_k^2 ($k = 1, 2, 3$) are always real and positive. Therefore, one of the possible methods of finding frequencies of natural oscillations p_k is the graphic method where there is constructed a graph of the left-hand side of this equation, which is examined as a function of quantity p. Points of intersection of this graph with the axis of the abscissas will give values of frequencies of natural oscillations (Fig. 3.43).

Let us number the frequencies of natural oscillations of the system in ascending order: $p_1 < p_2 < p_3$. We will call quantities p_1, p_2, and p_3, respectively, frequencies of the first, second and third tones of natural lateral oscillations of the helicopter. Each frequency of natural oscillations corresponds to a definite form of oscillations characterized by a definite relationship of amplitudes $z_0, \varphi_x^\circ, \bar{\varphi}_y^\circ$, which can be found for given p_k ($k = 1, 2, 3$) from equations (5.5) if into them instead of quantity p we substitute p_k. Then we obtain expressions

$$\left.\begin{aligned}
(\bar{\varphi}_x^\circ)_k&=\left(\frac{\varphi_x^\circ}{z_0}\right)_k=\frac{(c_z-mp_k^2)(c_{\varphi_y}-I_yp_k^2)-c_1^2}{(c_{\varphi_y}-I_yp_k^2)c_e-(c_{xl}+I_{xy}p_k^2)c_1};\\
(\bar{\varphi}_y^\circ)_k&=\left(\frac{\varphi_y^\circ}{z_0}\right)_k=\frac{(c_z-mp_k^2)(c_{xl}+I_{xy}p_k^2)-c_1c_e}{(c_{xl}+I_{xy}p_k^2)c_1-(c_{\varphi_y}-I_yp_k^2)c_e}.
\end{aligned}\right\} \qquad (5.9)$$

where k = 1, 2, 3.

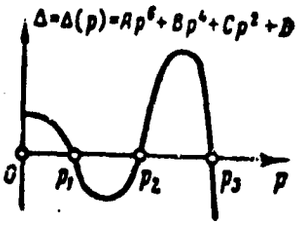

Fig. 3.43. Character of the graph $\Delta = \Delta(p)$ for determining frequencies of natural oscillations of the helicopter on an elastic undercarriage.

It is easy to show that the form of oscillations of the given tone is characterized by a defined straight line, which lies in the plane of symmetry of fuselage xcy and is a locus of points (belonging to the fuselage) remaining fixed during oscillations of this tone.

Really, displacement z_A of a certain point A of the fuselage lying in plane xcy and having coordinates x and y (see Fig. 3.42), obviously, can be determined by formula

$$z_A = z + \varphi_x y - \varphi_y x.$$

With oscillations of the k-th tone:

$$z = z_0 \cos p_k t;$$
$$\varphi_x = \varphi_x^\circ \cos p_k t;$$
$$\varphi_y = \varphi_y^\circ \cos p_k t.$$

Consequently,

$$z_A = (z_0 + \varphi_x^\circ y - \varphi_y^\circ x)\cos p_k t =$$
$$= z_0 [1 + (\bar{\varphi}_x^\circ)_k y - (\bar{\varphi}_y^\circ)_k x] \cos p_k t.$$

Therefore, condition

$$1 + (\bar{\varphi}_x^\circ)_k y - (\bar{\varphi}_y^\circ)_k x = 0 \qquad (5.10)$$

constitutes an equation of the locus of points in plane xcy the amplitudes of oscillations of which are equal to zero during oscillations of the k-th tone. But this is an equation of a certain straight line.

Thus the form of oscillations of the k-th tone can be characterized by the position of a certain straight line in plane xcy. This straight

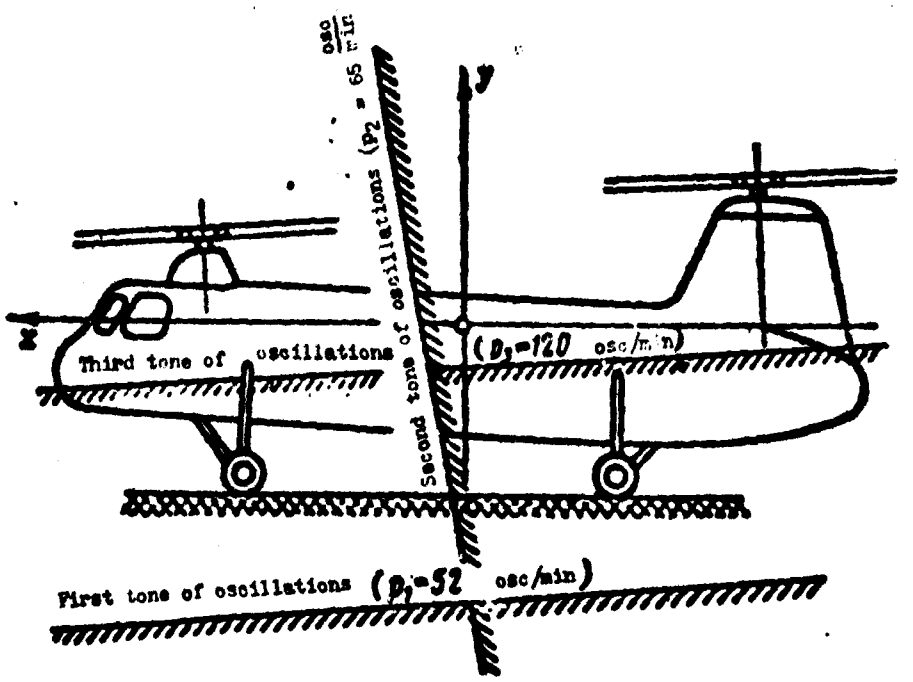

Fig. 3.44. Characteristic location of nodal lines of oscillations of the first, second and third tones.

line will be called the nodal line of the k-th tone of lateral oscillations. The equation of the nodal line (5.10) is easily found with the help of expressions (5.9) for the given value p_k.

It is convenient to present the results of the calculation of natural lateral oscillations of the helicopter in the form of a figure on which there is depicted the form with a side view of the helicopter and applied nodal lines of all three tones of oscillations with an indication of corresponding frequencies (Fig. 3.44).

The method of approximation of the calculation of natural lateral oscillations, discussed in § 2 and founded on the assumption of the independence of oscillations of yawing, can be obtained as a special case of the equations derived here.

If axis cx and cy are the principal axes of inertia ($I_{xy} = 0$), and there are also carried out conditions

$$c_l = c_{\varphi_x} l_1 - c_{z_2} l_2 = 0;$$
$$c_{el} = c_{z_1} e_1 l_1 - c_{z_2} e_2 l_2 = 0,$$

then equations (5.4) break up into two independent systems of equations:

$$\left.\begin{aligned} I_x \ddot{\varphi}_x &= (G - c_l) z - c_{\varphi_x} \varphi_x; \\ m\ddot{z} &= -c_z z + c_l \varphi_x; \end{aligned}\right\} \qquad (5.10')$$

$$I_y \ddot{\varphi}_y = -c_{\varphi_y} \varphi_y. \qquad (5.10'')$$

Equation (5.10") determines the independent oscillations of yaw, and the system of equations (5.10') determines lateral oscillations corresponding to physical pattern expounded in § 2 (two of the nodal lines are parallel to axis cx, and the third coincides with axis cy).

For a real helicopter conditons $c_l = c_{el} = 0$ and $I_{xy} = 0$ are never fulfilled accurately. However, for helicopters with an extended fuselage when angle α between the principal axis of inertia cx_0 and axis cx is small (see Fig. 3.42), and the moment of inertia I_x is small as compared to the two others (I_y and I_z), results of "accurate" and approximate calculations can coincide with the degree of accuracy sufficient for practice.

To determine the camping factors of natural oscillations it is possible to use the approximation method analogous to that expounded in § 2 (No. 4) for the system with two degrees of freedom. For each tone of natural oscillations there is determined the damping factor on the assumption that in the presence of damping, oscillations of this tone also constitute angular oscillations around the nodal line of this tone. Just as earlier (§ 2, No. 4), the equation of natural angular oscillations of the helicopter around the nodal line can be written in the form:

$$I_k \ddot{\varphi} + k_{\varphi_k} \dot{\varphi} + c_{\varphi_k} \varphi = 0, \qquad (5.11)$$

where I_k is the moment of inertia of the helicopter with respect to the nodal line of the k-th tone; $c_{\varphi_k} = \rho_k^2 / l_k$ – angular rigidity of the shock absorption during a turn with respect to the nodal line of the

k-th tone; λ_{φ_k} — corresponding damping factor.

The moment of inertia of the helicopter with respect to the nodal line can be determined by the formula:

$$I_k = mh_k^2 + I_x \cos^2 \gamma_k + I_y \sin^2 \gamma_k + I_{xy} \sin 2\gamma_k, \qquad (5.12)$$

where h_k is the distance from the center of gravity of the helicopter to the nodal line; γ_k is the angle which is formed by the nodal line with axis cx (Fig. 3.44).

Quantities h_k and γ_k are determined by the formulas:

$$\operatorname{tg} \gamma_k = -\frac{(\dot{\varphi}_y)_k}{(\dot{\varphi}_x)_k}; \qquad (5.13)$$

$$h_k = \frac{1}{\sqrt{(\dot{\varphi}_x)_k^2 + (\dot{\varphi}_y)_k^2}}. \qquad (5.14)$$

The coefficient of angular damping k_{φ_k} is determined by the expression:

$$k_{\varphi_k} = 2k'_{z_1} d_{1k}^2 + 2k_{z_2} d_{2k}^2 + 2(k'_{y_1} a_1^2 + k'_{y_2} a_2^2) \cos^2 \gamma_k, \qquad (5.15)$$

where d_{1k} and d_{2k} are distances from the nodal line (Fig. 3.45) to lines connecting points of contact with earth of the tires of the front and rear undercarriages, respectively; a_1 and a_2 – tracks of the front and rear wheels (Fig. 3.16); k'_{z_1}, k'_{z_2}, k'_{y_1}, k'_{y_2} – damping factors of lateral and vertical springs (see Fig. 3.16), respectively, of the front and rear undercarriages having the same meaning as that in § 2 (No. 4).

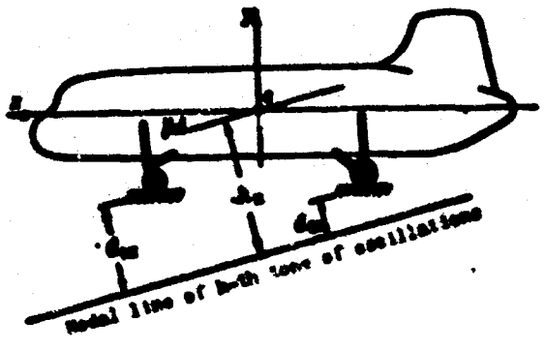

Fig. 3.45. Conclusion of basic relationships with oscillations of the helicopter with respect to the nodal line of the k-th tone of oscillations.

After determining quantity k_{ϕ_k} the dimensionless damping factor of the k-th tone is determined:

$$\bar{n}_k = \frac{n_k}{2l_{\phi_k}}. \qquad (5.16)$$

3. Calculation of Natural Oscillations of the Helicopter in the Plane of Symmetry (Longitudinal Oscillations)

Let us turn to Fig. 3.46. The problem of oscillations of the helicopter in the plane of symmetry is reduced to the investigation of oscillations of a flat elastic secured solid body in its plane (xOy). Vertical springs with coefficients of rigidity c_{y_1} and c_{y_2}, simulate the vertical rigidity of the front and rear undercarriages and horizontal c_{x_1} and c_{x_2}, the rigidity of the front and rear undercarriages in the direction of axis Ox. If the tires of the undercarriage are not braked, then $c_{x_1} = c_{x_2} = 0$. In the case of braked tires the elasticity of the undercarriage in the direction of axis Ox is comprised of the elasticity of the tire and elasticity of the suspension system of the tire (for example, bending elasticity of landing gear struts, etc.). The longitudinal rigidity of one tire $c_x^{ш}$ can be for tentative calculations accepted equal to $c_x^{ш} = 1{,}5c_y^{ш}$.

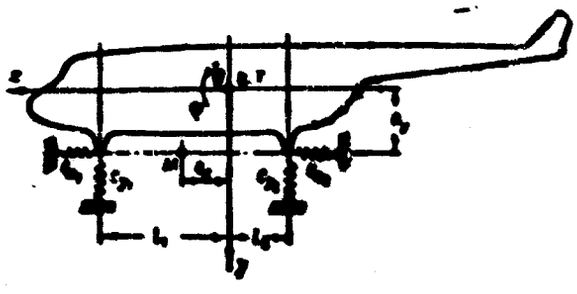

Fig. 3.46. Diagram of bracing of the helicopter on an elastic undercarriage for the calculation of oscillations in the plane of symmetry. [Ц.т. = center of gravity].

Let us assume that point X (Fig. 3.46) with coordinates e_x and e_y is the center of rigidity of the system of shock absorption during longitudinal oscillations. Quantity e_y constitutes the distance of the center of gravity of the helicopter from the surface of earth, and quantity e_x is determined from the expression

$$e_x = \frac{c_{y_1} l_1 - c_{y_2} l_2}{c_{y_1} + c_{y_2}}. \qquad (5.17)$$

Let us assume that x and y are displacements of the center of gravity of the helicopter in the direction of axes Ox and Oy, and ϕ_z is the angle of rotation of the fuselage with respect to axis Oz. Then equations of small oscillations of the helicopter in plane xOy in the absence of damping have the form:

$$\left.\begin{aligned} m\ddot{x} &= -c_x x + c_x l_1 \varphi_z; \\ m\ddot{y} &= -c_y y - c_y l_2 \varphi_z; \\ I_z \ddot{\varphi}_z &= -(c_\varphi + c_x l_1^2 + c_y l_2^2)\varphi_z + c_x l_1 x - c_y l_2 y + Gx_0. \end{aligned}\right\} \qquad (5.18)$$

where

$$\left.\begin{aligned} c_x &= c_{x_1} + c_{x_2}; \\ c_y &= c_{y_1} + c_{y_2}; \\ c_\varphi &= c_{y_1}(l_1 - e_z)^2 + c_{y_2}(l_2 + e_z)^2. \end{aligned}\right\} \qquad (5.19)$$

Let us introduce the following designations:

$$\left.\begin{aligned} c_0 &= c_x e_y^2 + c_y e_x^2 + c_\varphi; \\ p_x^2 &= \frac{c_x}{m}; \quad p_y^2 = \frac{c_y}{m}; \quad p_\varphi^2 = \frac{c_\varphi}{I_z}; \\ \varrho &= \frac{I_z}{m}; \quad \bar{e}_x = \frac{e_x}{\varrho}; \quad \bar{e}_y = \frac{e_y}{\varrho}; \quad \bar{c}_0 = \bar{c}_\varphi\left(1 + \frac{a}{c_\varphi e_y}\right). \end{aligned}\right\} \qquad (5.20)$$

Let us also introduce instead of ϕ_z the new variable

$$s = \varphi_z. \qquad (5.21)$$

Then equation (5.18) can be written in the form:

$$\left.\begin{aligned} \ddot{x} &= -p_x^2 x + p_x^2 \bar{e}_x s; \\ \ddot{y} &= -p_y^2 y - p_y^2 \bar{e}_x s; \\ \ddot{s} &= -p_\varphi^2 s + p_x^2 \bar{e}_y x - p_y^2 \bar{e}_x y. \end{aligned}\right\} \qquad (5.22)$$

Searching for the solution of this system of equations in the form of

$$x = x_0 \cos pt; \quad y = y_0 \cos pt; \quad s = s_0 \cos pt, \qquad (5.23)$$

we will come to the following system of linear uniform algebraic equations for determining quantities x_0, y_0, and s_0:

$$\left.\begin{aligned}(p_x^2-p^2)x_0-p_x^2\bar{e}_y s_0=0;\\(p_y^2-p^2)y_0+p_y^2\bar{e}_x s_0=0;\\-p_x^2\bar{e}_y^* x_0+p_y^2\bar{e}_x y_0+(p_\gamma^2-p^2)s_0=0.\end{aligned}\right\} \qquad (5.24)$$

Equating to zero the determinant of this system

$$\Delta=\begin{vmatrix} p_x^2-p^2; & 0; & -p_x^2\bar{e}_y\\ 0; & p_y^2-p^2; & p_y^2\bar{e}_x\\ -p_x^2\bar{e}_y^*; & p_y^2\bar{e}; & p_\gamma^2-p^2\end{vmatrix}=0,$$

we will obtain the following characteristic equation for the determination of frequencies p of natural oscillations:

$$p^6+ap^4+bp^2+c=0, \qquad (5.25)$$

where

$$\left.\begin{aligned}a=p_x^2+p_y^2+p_\gamma^2;\\b=p_x^4\bar{e}_y\bar{e}_y^*+p_y^4\bar{e}_x^2-p_x^2p_y^2-p_y^2p_\gamma^2-p_\gamma^2p_x^2;\\c=-p_y^2p_x^2(p_x^2\bar{e}_y\bar{e}_y^*+p_y^2\bar{e}_x^2).\end{aligned}\right\} \qquad (5.26)$$

This equation has three real roots of p^2, which can be found graphically by constructing a graph of function $\Delta = \Delta(p) = p^6 + ap^4 + bp^2 + c$, similar to that which was indicated in § 5 (No. 2) for equation (5.6) (see Fig. 3.43). Let us arrange roots of equation (5.25) in ascending order $p_1 < p_2 < p_3$, and we will call quantities p_1, p_2, and p_3, respectively, frequencies of the first, second and third tones of natural oscillations of the helicopter in the plane of symmetry or longitudinal oscillations. Each tone of longitudinal oscillations corresponds to its form of oscillations of the helicopter which is conveniently characterized by the position on plane xOy the corresponding node of oscillations O_k (here $k = 1, 2, 3$), i.e., the point of the fuselage which remains fixed during oscillations of this tone. Coordinates of the node of oscillations x_k and y_k can be found in the following manner: amplitudes a_x and a_y of oscillations of any point of the fuselage with coordinates x_k and y_k in directions of axes Ox and Oy are determined by the evident formulas:

$$a_x = x_0 - \varphi_0 y_k;$$
$$a_y = y_0 + \varphi_0 x_k.$$

where $\varphi_0 = s_{0Q}$ is the amplitude of angular oscillations of the helicopter.

Coordinates x_k and y_k are determined from conditions $a_x = 0$ and $a_y = 0$, and therefore

$$x_k = -\frac{y_0}{\varphi_0} = -\frac{y_0}{s_0} Q;$$
$$y_k = \frac{x_0}{\varphi_0} = \frac{x_0}{s_0} Q.$$

Quantities of ratios $\frac{y_0}{s_0}$ and $\frac{x_0}{s_0}$ can be found from the first two equations of system (5.24), if is known the frequency of oscillations p. With oscillations of the k-th tone we obtain

$$\left(\frac{x_0}{s_0}\right)_k = \frac{p_x^2 a_y}{p_x^2 - p_k^2};$$
$$\left(\frac{y_0}{s_0}\right)_k = -\frac{p_y^2 a_x}{p_y^2 - p_k^2}.$$

Hence there are obtained the following formulas for determining coordinates of the node of oscillations:

$$\left.\begin{aligned} x_k &= \frac{a_x}{1 - \left(\frac{p_k}{p_y}\right)^2}; \\ y_k &= \frac{a_y}{1 - \left(\frac{p_k}{p_x}\right)^2}. \end{aligned}\right\} \qquad (5.27)$$

Let us indicate two possibilities of the simplified calculation of natural oscillations of the helicopter in the plane of symmetry.

In the case when the center of rigidity of shock absorption M (see Fig. 3.46) lies on axis Oy ($e_x = 0$), the equations of motion (5.18) are simplified and take the form:

$$m\ddot{y} = -c_y y; \tag{5.28}$$

$$\left.\begin{aligned} m\ddot{x} &= -c_x x + c_x e_y \varphi_z; \\ I_z \ddot{\varphi}_z &= -c_\varphi \varphi_z + (c_x e_y + G) x. \end{aligned}\right\} \tag{5.29}$$

Equation (5.28) describes the vertical forward oscillations of the helicopter, which are not of interest from the point of view of ground resonance.

Equations (5.29) describe longitudinal oscillations of the helicopter, which in this case can be examined as a system with two degrees of freedom x and ϕ_z. Such a system is mechanically equivalent to the system which was examined in § 2 (No. 3) and is depicted on Fig. 3.16. Therefore, with the calculation of frequencies of natural oscillations of the helicopter in this case (if we disregard the moment of force of weight G) it is possible to use the graphs in Figs. 3.19 and 3.20 and also formulas (2.22), (2.23) and (2.24), assuming in them

$$\varkappa = \frac{I_z}{m e_y^2}; \tag{5.30}$$

$$\beta = \frac{c_{\varphi_z}}{c_x e_y^2} = \frac{c_{y_1} l_1^2 + c_{y_2} l_2^2}{c_x e_y^2}. \tag{5.31}$$

Quantity $\bar{a}_k = \frac{y_k}{e_y}$ will be the relative distance from the node of oscillations of the k-th tone, which in this case will be located on axis Oy up to the center of gravity of the helicopter.

For the real helicopter quantity e_x, as a rule, is not equal to zero. However, it is usually small as compared to quantity $l_1 + l_2$. The approximate calculation, in which we assume $e_x = 0$, in most cases gives values of frequencies of natural oscillations close to values obtained by means of an exact calculation and can be used with success as a preliminary calculation when it is necessary to obtain results rapidly, and there is no need in greater accuracy.

In the case when longitudinal oscillations with nonbraked tires ($c_{x_0} = 0$), are calculated, the equations of motion (5.18) again break up into two independent systems:

$$m\ddot{x}=0;$$
$$m\ddot{y}=-c_{y}y-c_{y}e_{x}\varphi_{z};$$
$$I_{z}\ddot{\varphi}_{z}=-c_{\varphi}\varphi_{z}+Gx-c_{y}e_{x}y.$$

In this case with the oscillations it is possible to consider $x = 0$, since the projection of external forces on axis Ox is absent. One of the frequencies of natural oscillations of the system is equal to zero and corresponds to the uniform motion of the center of gravity of the helicopter along axis Ox. Two other frequencies of natural oscillations, as in the preceding case, can be found by graphs in Figs. 3.19 and 3.20 or by formulas (2.22), (2.23), and (2.24), in which one should take:

$$\varkappa=\frac{I_{z}}{me_{x}^{2}}; \tag{5.32}$$

$$\beta=\frac{c_{y_1}(l_1-e_x)^2+c_{y_2}(l_2+e_x)^2}{c_{y}e_{x}^{2}}. \tag{5.33}$$

Quantity $a_k=\frac{x_k}{e_x}$ will constitute the relative distances from the center of gravity of the helicopter to nodes of oscillations, which in this case will lie on axis Ox.

Finally, in the case when the tires are not braked, and quantity $e_x = 0$, the simplest formulas for frequencies of natural oscillations in the plane of symmetry are obtained:

$$p_1=0;$$
$$p_2=p_3=\sqrt{\frac{c_y}{m}};$$
$$p_4=p_5=\sqrt{\frac{c_{y_1}l_1^2+c_{y_2}l_2^2}{I_z}}.$$

To determine the attenuation damping factors of natural longitudinal oscillations it is again possible to use the method of approximation, founded on assumption that in the presence of damping

forces oscillations of the given tone are angular oscillations with respect to the nodal line of the given tone, which in this case is a straight line parallel to axis Oz and intersecting plane xOy at the point with coordinates x_k and y_k [see formula (5.27)]. The equation of oscillations of the given stream can again be written in the form (5.11), and only quantity I_k is found by the formula:

$$I_k = I_z + m(x_k^2 + y_k^2). \tag{5.34}$$

With the determination of the damping factor k_{φ_k} it is possible not to consider the damping of longitudinal elastic elements c_{x_1} and c_{x_2} (see Fig. 3.46) and to consider only the damping of vertical elastic elements with rigidities c'_{y_1} and c'_{y_2} of the front and rear undercarriages (see Fig. 3.16).

Corresponding damping factors k'_{y_1} and k'_{y_2} are determined as is shown in § 2 (Nos. 4 and 5).

In calculating the moment from damping forces with respect to the nodal line, we will obtain the expression for determining quantity k_{φ_k}:

$$k_{\varphi_k} = 2[k'_{y_1}(l_1 - x_k)^2 + k'_{y_2}(l_2 + x_k)^2] \tag{5.35}$$

The dimensionless damping factor $\bar{n}_k$ of the given tone of oscillations is determined by the formula

$$\bar{n}_k = \frac{k_{\varphi_k}}{2I_k p_k^2}. \tag{5.36}$$

4. Reduction of the Problem to the Calculation of the Rotor on an Elastic Base

After frequencies and forms of natural oscillations of the helicopter on an elastic undercarriage are found, the calculation of ground resonance can be reduced to the calculation of the rotor on the elastic support discussed in § 1.

The method of calculation founded on the reduction of the problem to the rotor on an elastic base, is approximate and similar to the method expounded in § 2 (No. 6) for a single-rotor helicopter.

The essence of the method of approximation consists in the following: a separate calculation of ground resonance for each tone of natural oscillations is made; then the body of the helicopter is examined as a solid body having one degree of freedom – a turn around the nodal line of the given tone. Of course, such a method of approximation is justified only in the case when the frequencies of natural oscillations of different tones are quite "far" from each other.

In the case when there are two "close" frequencies of natural oscillations, certain corrections must be introduced into the calculation. A method of refinement of the calculation in this case will be discussed later.

Thus to calculate ground resonance there are examined oscillations of the helicopter with respect to each tone separately as angular oscillations of the fuselage around a certain fixed straight line – nodal line of the given tone.

It is possible to show that with such a simplification the equations of motion of the system are reduced to a system of equations similar to the system (1.16) (§ 1). All formulas of § 1 remain in force, and it is possible to use graphs for determining limits of zones of instability (see Figs. 3.3-3.12); however, by the quantity $\bar{n}_0$ it is necessary in this case to imply the dimensionless damping factor $\bar{n}_k$ of the given tone of oscillations, determined by the formulas (5.16) or (5.36) (§ 5, Nos. 2 and 3), and by quantity ε_k enumerable for the given tone by the formula:

$$\varepsilon_k = \varepsilon_{k1} + \varepsilon_{k2} + \ldots + \varepsilon_{kn} = \sum_{i=1}^{n} \varepsilon_{ki}. \qquad (5.37)$$

where i = 1, 2, ..., s; s is the number of rotors, and each of the quantities ε_{ik} is determined by the formula:

$$\varepsilon_{ik}=\left(\frac{n}{2}\frac{S^2_{\text{л.м}}\,l^2_{ik}}{I_{\text{л.м}}\,I_k}\right)_i. \qquad (5.37)$$

Here I_k is the moment inertia of the fuselage (with masses of rotors concentrated in their centers) with respect to the nodal line of the k-th tone [see formulas (5.12) and (5.34)]; l_k – distance from the center of the given i-th rotor to the nodal line of the k-th tone, if lateral oscillations are examined, or the distance from the nodal line k-th tone to the plane of rotation of the given rotor, if longitudinal oscillations of the helicopter are examined; n – number of blades of the given rotor; $S_{\text{в.м}}$ and $I_{\text{в.м}}$ – static moment and moment, respectively, of the inertia of the blade of the rotor relative to the drag hinge.

The rotors can be different, but the indicated procedure is correct only when all rotors have identical angular velocities of rotation and identical values of parameters ν_0 [see formula (1.9)].

As was already noted above, the method of approximation of calculation expounded here is justified only when frequencies of oscillations of different tones are quite "far" from each other. It is possible to show that if there are two close frequencies of natural lateral (or longitudinal) oscillations, for example, p_n and p_m, then the calculation of limits of zones of instability can be conducted for one tone, for example, p_m, but it is refined by introduction into the calculation of a certain quantity $\bar{n}_{\text{экв}}$ instead of $\bar{n}_m$ (for the given tone, and $\bar{n}_{\text{экв}}<\bar{n}_m$), which is determined by the formula:

$$\bar{n}_{\text{экв}}=\bar{n}_m\frac{1}{1+\frac{\bar{n}_n}{\bar{n}_m}\frac{I_n}{I_m}}. \qquad (5.39)$$

This formula is derived for the case when $p_n = p_m$, i.e., when the frequencies of natural oscillations of two examined tones accurately coincide. If, however, $p_n \neq p_m$, then formula (5.39) gives the decreased value $\bar{n}_{\text{экв}}$.

In the case when there are two close frequencies of natural oscillations p_n and p_m, where one of them, for example, p_n, is the frequency of the n-th tone of lateral oscillations and the other p_m, the frequency of the m-th tone of longitudinal oscillations, then, in general, it is necessary to examine the rotor on an elastic support with two degrees of freedom (see § 1, No. 4). In this case it is possible approximately (in a safety margin) to estimate the necessary damping by the formula (1.52) for a rotor on an isotropic elastic support, substituting into it quantities $\bar{n}_0$ and ε for one of the two examined tones for which the quantity of the ratio $\frac{\bar{n}_0}{\varepsilon_0}$ is less.

It should be noted that the necessity of such a calculation appears only in the practically very rare case when for both examined tones not only values of frequencies p_n and p_m are close but also values $\frac{\bar{n}_0}{\varepsilon_0}$ and $\frac{\bar{n}_0}{\varepsilon_0}$. If, however, quantity $\frac{\bar{n}_0}{\varepsilon_0}$ for one of the tones is more than 2.5-3 times larger than for the other, for example $\frac{\bar{n}_0}{\varepsilon_0} = 3 \cdot \frac{\bar{n}_0}{\varepsilon_0}$, then it is possible to disregard oscillations of n-th tone and to examine only oscillations of the m-th tone (as independent).

5. Self-Excited Oscillations in the Flight of a Helicopter with an Elastic Fuselage

During the flight of a helicopter in air self-excited oscillations of the ground resonance type are also possible. The fuselage of a real helicopter constitutes and elastic system which has natural frequencies and forms of natural oscillations. If the form of oscillations of any tone of the elastic fuselage is such that the center of the rotor (or centers of rotors) during oscillations of this tone is displaced in the plane of rotation of the rotor, then ground resonance is possible at which the fuselage will accomplish oscillations with a form of this tone.

Frequencies of natural oscillations of the elastic fuselage are usually high in comparison with frequencies of oscillations of the helicopter on shock absorption of the undercarriage, and only the low one or two tones of natural oscillations can be dangerous from the point of view of the possibility of self-excited oscillations.

The lowest frequencies of natural oscillations of the fuselage usually correspond to flexural oscillations of the fuselage.

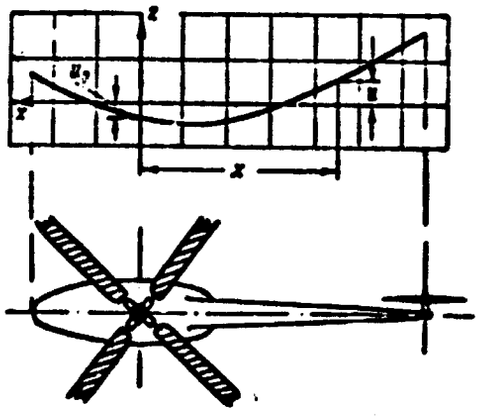

Fig. 3.47. Form of the first tone of oscillations of the elastic fuselage of the helicopter.

Figure 3.47 shows the form of oscillations of the first tone of bending of the fuselage of the Mi-4 helicopter in a horizontal plane. The form of oscillations is depicted in the form of a graph of an elastic line $u = u(x)$ (u – amplitude of oscillations of the point with coordinate x).

Frequencies and forms of natural oscillations of bending of the fuselage can be found by the usual methods developed for elastic beams of variable cross section (see, for example, Chapter II of this book) or are determined experimentally (in case of an available ready helicopter).

If the frequency p_0 and form $u(x)$ of any tone of oscillations of the bend of the fuselage is known, then the calculation of self-excited oscillations with the form of this tone can be reduced to the calculation of the rotor on an elastic support by formulas of § 1 or by graphs on Figs. 3.3-3.12. With this quantity ε should be determined by the formula:

$$\varepsilon = \varepsilon_1 + \varepsilon_2 + \ldots \varepsilon_s = \sum_{k=1}^{s} \varepsilon_k \qquad (5.40)$$

where s is the number of rotors.

Quantities ε_i ($i = 1, 2, \ldots, s$) are determined by the formulas:

$$\varepsilon_i = \frac{z}{2} \frac{S^2_{i.\text{ш}}}{I_{\text{ш}} m^{(i)}_{\text{экв}}}; \tag{5.41}$$

$$m^{(i)}_{\text{экв}} = \int \rho [\bar{u}_i(x)]^2 dx, \tag{5.42}$$

where

$$\bar{u}_i(x) = \frac{u(x)}{u(x_i)};$$

x_i is the coordinate of the center of the i-th rotor; ρ is the linear mass of the fuselage (the integral is taken along the whole length of the fuselage).

Quantity $\bar{u}_i(x)$ is the amplitude of oscillations at the point with coordinate x referred to the amplitude of oscillations of the center of the i-th rotor. Quantity $m_{\text{экв}}$ is the largest value of kinetic energy of the fuselage during oscillations with respect to the form of the given tone with the amplitude of oscillations in the center of the i-th rotor equal to unity referred to quantity p_i^2.

Quantity $\bar{n}_0$ should be equal in this case to the dimensionless damping factor of the given tone of oscillations of the fuselage. It is determined solely by losses to hysteresis in the construction of the fuselage and usually amounts to 0.02-0.05.

Such a comparatively small value $\bar{n}_0$ does not permit eliminating ground resonance in flight with the help of the blade damper, and the reliability of the helicopter can be provided only with a sufficient revolution margin of the rotor up to the lower limit of the zone of instability. Therefore, self-excited oscillations in air present a danger only for helicopters having comparatively low frequencies of natural oscillations of the elastic fuselage. For example, for the Mi-4 helicopter the revolution margin up to the lower limit of the zone of instability, which corresponds to the first tone of oscillations of the fuselage (see Fig. 3.47), amounts to 28%.

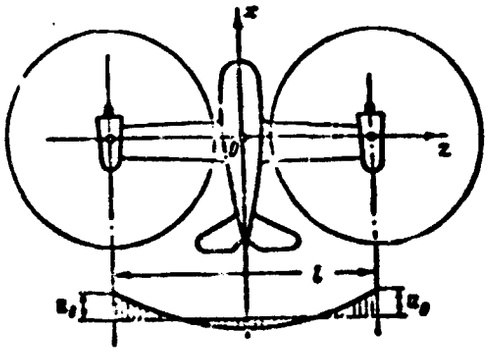

Fig. 3.48. Form of lowest tone of oscillations of a helicopter of transverse configuration most dangerous from the point of view of ground resonance.

The greatest danger of ground resonance in air is for helicopters of transverse configuration having a long elastic wing (Fig. 3.48). The danger of self-excited oscillations for such helicopters is aggravated by the fact that centers of the rotors are located in antinodes of the corresponding tone of oscillations, which gives comparatively small values $m_{\text{ЭКВ}}$ [formula (5.42)] and, consequently, relatively wide zones of instability.

§ 6. Selection of Basic Undercarriage Parameters and Dampers of Blades. Recommendations on Designing

As one can see from the general theory of stability of the rotor on an elastic support, the stability margin, in general, can be increased both by means of increasing the degree of oscillation damping of blade and by increasing the oscillation damping of the fuselage, i.e., increasing the damping ability of the undercarriage.

However, the possibilities of increasing both of these forms of damping are practically very limited, since the damper of the blade and undercarriage fulfill a number of other functions not connected with ground resonance.

The damper of the blade operates during forward flight of the helicopter, and the greater it loads the shank part of the blade by a variable bending moment the greater the degree of its damping. The strength of the shank part of the blade and hub and, consequently, their weight are determined exactly by the presence of the damper.

An excessive increase in the degree of damping of the undercarriage without the application of special devices leads to an increase in rigidity of shock absorption and, consequently, to an increase in dynamic loads during landing of the helicopter.

It is necessary to consider these peculiarities of operation of the dampers of the blade and undercarriage in the designing of the helicopter. Often it is not possible to provide sufficient margin with respect to ground resonance without the application of certain special constructive devices, sometimes in the damper of the blade and sometimes in the system of the undercarriage.

For single-rotor helicopters and those of longitudinal configuration the most dangerous usually appears to be the case of ground resonance on a landing run. Therefore, it is convenient to consider the given case calculated for the selection of

characteristics of damping of the blade and undercarriage. Here, for simplicity, one may assume that the helicopter rocks around the horizontal axis passing through its center of gravity, which is quite true at a high speed of the landing run (see § 4, No. 2). In this case, as we have seen, there are obtained especially simple calculation formulas (4.18)-(4.21), and it is possible by the simplest method to determine the required characteristics of the undercarriage and damper of the blade. However, after characteristics of the undercarriage and dampers of the blade are selected, it is necessary to conduct a full calculation of ground resonance for all possible cases, including ground resonance on a landing run, and to construct a diagram of safe revolutions (see Fig. 3.25). After that, when indispensable, it is necessary to correct the selected characteristics of the undercarriage and hub.

1. Selection of Characteristics of the Blade Damper

The main characteristic of operation of blade damper is the circumstance that the frequency of natural oscillations of the blade (characteristic for ground resonance) is always approximately 3-4 times lower than the frequency of forced oscillations of the blade during forward flight.

Really, in flight the blade accomplishes forced oscillations relative to the flapping and drag hinges with a frequency ω equal to the revolutions of the rotor, whereas the frequency of natural oscillations of the blade $p_л = \nu_0\omega$. Usually $\nu_0 = 0.25\text{-}0.3$, and the angular velocity ω of rotation of the rotor during ground resonance, in any case, cannot be larger than the angular velocity of rotor rotation in flight.

This peculiarity is explained, in particular, by the inexpediency of the application of dampers with a linear characteristic (§ 3, No. 3), conditioned by the fact that the linear damper with a constant amplitude of oscillations develops a moment proportional to the frequency of oscillations.

The simplest dampers giving a moment not dependent on the

frequency of oscillations are frictional dampers and also hydraulic dampers with a step characteristic, and this characteristic should as far as possible approximate the characteristic of the frictional damper (see Fig. 3.51b). A hydraulic damper with such a characteristic is an advantage to use on heavy helicopters, since such a damper is lighter than the corresponding frictional damper, and the gain in weight of the damper increases with an increase in its power.

With the application of conventional dampers moment M_0 of the damper is selected from considerations of strength of the blade, and its damping factor is determined by formula (3.23). The damping margin with respect to ground resonance can be provided in this case only by an appropriate selection of characteristics of the undercarriage. In those cases when this is not possible, it is necessary to think about the application of special designs of dampers of the blade, which would give great damping of the blade at low frequencies of oscillations (characteristic for ground resonance) and small damping at the frequency of oscillations corresponding to the flight of the helicopter. One of the simplest types of such a damper is a damper connected in series with an elastic element (see Fig. 3.33). Figure 3.49 shows one of the possible variants of design of such a damper. We will call such a damper a spring damper.[5]

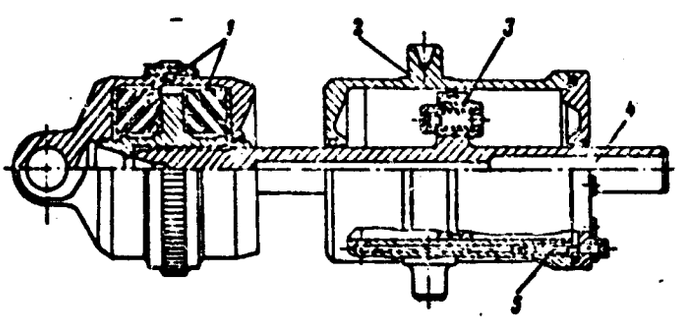

Fig. 3.49. Damper with series-connected elastic element: 1 — elastic elements (rubber); 2 — housing; 3 — safety valve; 4 — rod; 5 — regulating needle.

In order to estimate the advantages of the spring damper, let us compare it with the standard frictional damper. Let us assume that the helicopter has ground resonance on the landing run such that the center of the zone of instability coincides with the

operating rotor revolutions. Let us assume that further the greatest moment in flight permissible with respect to considerations of strength of the blade is equal to M_0. Then the equivalent damping factor in the case of the application of the frictional damper is determined by formula (3.23):

$$k_{экв}^{фрикц} = \frac{2}{\pi} \cdot \frac{M_0}{\omega \xi_1},$$

where ξ_1 is the amplitude of the first harmonic of oscillations of the blade in the plane of rotation.

In the case of application of a spring damper the corresponding equivalent damping factor is determined by formula (3.17):

$$k_{экв}^{пруж} = k \frac{1}{1 + \left(\frac{k p_л}{c}\right)^2},$$

where $p_л$ is the frequency of oscillations of the blade during ground resonance, which can be considered equal to the product $\nu_0 \omega$.

$$p_л = \nu_0 \omega.$$

The moment which will be given in flight by a spring damper can be determined by the formula

$$M = c_{экв} \xi + k_{экв} \frac{d\xi}{dt},$$

which with harmonic oscillations of the blade with frequency ω gives the following value of the amplitude of moment M [see formula (3.17)]:

$$M = \frac{k \omega \xi_1}{\sqrt{1 + \left(\frac{k\omega}{c}\right)^2}}. \qquad (6.1)$$

Let us state now the following question: if one were to select values c and k for a spring damper in such a manner that it gives in flight the same moment M_0 as the frictional, then what is the largest value of $k_{экв}^{пруж}$ that can be obtained by varying quantities c and k? We will consider that the amplitude of oscillations of the blade with respect to the first harmonic ξ_1 in flight and with a landing run of the helicopter on the ground is the same.

It is convenient to characterize relative increase in damping with the application of spring damper by the quantity

$$\psi = \frac{h_{\text{дем}}^{\text{пруж}}}{h_{\text{дем}}^{\text{пруж отсут}}} = \frac{\pi}{2} \frac{\omega \xi_1}{M_0} \frac{k}{1 + \left(\frac{k p_a}{c}\right)^2}. \qquad (6.2)$$

Substituting $p_a = v_0 \omega$ in this formula and considering the condition $M = M_0$, we will obtain

$$\psi = \frac{\pi}{2} \cdot \frac{\sqrt{1 + \bar{k}^2}}{1 + v_0^2 \bar{k}^2}, \qquad (6.3)$$

where the dimensionless quantity

$$\bar{k} = \frac{k\omega}{c}. \qquad (6.4)$$

Thus the relative advantage of the application of the spring damper depends especially on the selection of value $\bar{k}$. Figure 3.50

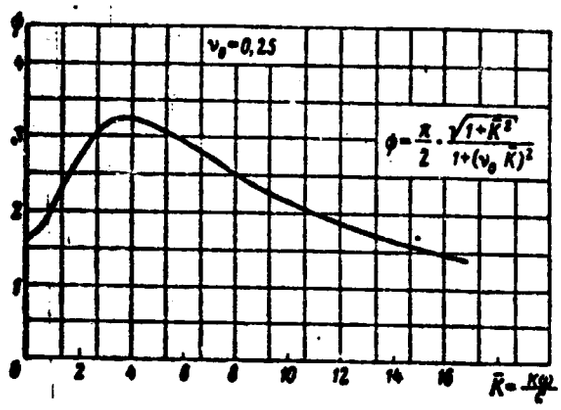

Fig. 3.50. Dependence of $\psi = f(\bar{k})$ at $\nu_0 = 0.25$.

gives a graph of the dependence $\psi(\bar{k})$ for the case $\nu_0 = 0.25$. As can be seen from this graph, with an increase in $\bar{k}$ quantity ψ first increases and then decreases, attaining the greatest value $\psi = \psi_{max}$ at a certain value $\bar{k} = \bar{k}_{opt}$, which we call optimum.

Equating the derivative $\frac{d\psi}{dk}$ to zero, we will find:

$$\bar{k}_{opt} = \frac{\sqrt{1 - 2\nu_0^2}}{\nu_0}; \qquad (6.5)$$

$$\psi_{max}=\frac{\pi}{2}\frac{1}{\nu_0\sqrt{1-\nu_0^2}}. \qquad (6.6)$$

At $\nu_0 = 0.25$, there is obtained $\bar{K}_{opt} = 3.74$ and $\psi_{max} = 3.24$.

Thus the application of a spring damper permits by more than three times increasing the damping during ground resonance, preserving the constant moment which loads the blade in flight.

This, however, does not exhaust the advantage of the spring damper as compared to the conventional. The fact is that the spring damper gives "elasticity" in the drag hinge ($c_{экв}$), and the presence of such elasticity, as was shown in No. 2 of § 1, lowers value of the required damping [see formula (1.31) and graph on Fig. 3.13].

Calculations show that by taking into account everything discussed previously the damping margin with ground resonance can be increased 5-6 times with preservation of the constant moment acting on the blade in flight.

2. Rotor with Interblade Elastic Elements and Dampers

Thus far we examined only the case when the elastic element and damper in the drag hinge are included between the blade and housing of the hub, so that the moment acting on the blade depends only on motion of the given blade and does not depend on motion of the remaining blades. Sometimes hub designs with so-called interblade connections are used. A diagram of such a hub is depicted on Fig. 3.51. We will consider that each such interblade element possesses a certain rigidity c and damping, characterized by the coefficient k, so that force P acting on such an element is connected with a change in its length s by the relation:

$$P=cs+k\frac{ds}{dt}.$$

In this case the moment acting on the given (k-th) blade from the side of the interblade elements will depend not only on the motion of this blade, characterized by angle $\zeta_k(t)$, but also on motions of the two adjacent blades $\zeta_{k-1}(t)$ and $\zeta_{k+1}(t)$.

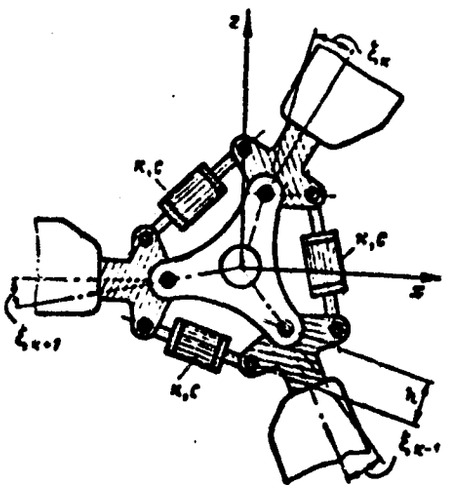

Fig. 3.51. Diagram of hub of a rotor with interblade connections.

With small oscillations of blades relative to drag hinges, the moment acting on the k-th blade will be expressed by the formula:

$$M = c_0(\xi_k - \xi_{k-1}) + c_0(\xi_k - \xi_{k+1}) + k_0(\dot{\xi}_k - \dot{\xi}_{k-1}) + k_0(\dot{\xi}_k - \dot{\xi}_{k+1}),$$

where

$$\left.\begin{aligned} c_0 &= ch^2; \\ k_0 &= kh^2, \end{aligned}\right\} \qquad (6.7)$$

where h is the arm of the interblade element (see Fig. 3.51).

Therefore, equations of motion of blades in this case have the following form [compare with (1.8)]:

$$\begin{aligned} &I_{0.m}\ddot{\xi}_k + k_0(\dot{\xi}_k - \dot{\xi}_{k-1}) + k_0(\dot{\xi}_k - \dot{\xi}_{k+1}) + \\ &+ c_0(\xi_k - \xi_{k-1}) + c_0(\xi_k - \xi_{k+1}) + \\ &+ I_{0.m}S_{0.m}\cdot\omega^2\xi_k = \frac{\omega_0^2 I_{0.m}}{e}\ddot{x}\sin\varphi_k, \end{aligned} \qquad (6.8)$$

where

$$k = 1, 2, 3, \ldots n.$$

If the shaft of the rotor accomplishes oscillations with respect to the harmonic law

$$x = x_0 \cos pt,$$

then forced oscillations of the blades can be found. The right-hand side of equations (6.8) in this case has the form:

$$x_0 \frac{v_0^2 p^2}{2 I_{n.m}} I_{n.m} \left\{ \sin\left[(p-\omega)t + \frac{2\pi}{n} k\right] + \sin\left[(p+\omega)t + \frac{2\pi}{n} k\right] \right\}.$$

Equations (6.8) allow in this case the solution of the form

$$\xi_k(t) = \xi_{01} \sin\left[(p-\omega)t - \frac{2\pi}{n} \cdot k\right] + \xi_{02} \sin\left[(p+\omega)t + \frac{2\pi}{n} \cdot k\right].$$

Let us calculate the elastic moment acting on the k-th blade from the side of the interblade elastic elements during oscillations of the blade with respect to any one of these harmonics, for example, harmonic $(p-\omega) = p_n$. We have:

$$M_{y.p} = c_0(\xi_k - \xi_{k-1}) + c_0(\xi_k - \xi_{k+1}) = c_0(2\xi_k - \xi_{k-1} - \xi_{k+1}).$$

Further

$$\xi_k = \xi_{01} \sin\left(p_n t - \frac{2\pi}{n} k\right) = \xi_{01} \sin \varphi_k;$$

$$\xi_{k-1} = \xi_{01} \sin\left[p_n t - \frac{2\pi}{n}(k-1)\right] = \xi_{01} \sin\left(\varphi_k + \frac{2\pi}{n}\right);$$

$$\xi_{k+1} = \xi_{01} \sin\left[p_n t - \frac{2\pi}{n}(k+1)\right] = \xi_{01} \sin\left(\varphi_k - \frac{2\pi}{n}\right),$$

where

$$\varphi_k = p_n t - \frac{2\pi}{n} k.$$

Using these expressions, we obtain

$$M_{y.p} = c_0 \xi_0 \left\{ 2 \sin \varphi_k - \sin\left(\varphi_k - \frac{2\pi}{n}\right) - \sin\left(\varphi_k + \frac{2\pi}{n}\right) \right\}.$$

Considering that

$$\sin\left(\varphi_k + \frac{2\pi}{n}\right) = \sin \varphi_k \cos \frac{2\pi}{n} + \cos \varphi_k \sin \frac{2\pi}{n};$$

$$\sin\left(\varphi_k - \frac{2\pi}{n}\right) = \sin \varphi_k \cos \frac{2\pi}{n} - \cos \varphi_k \sin \frac{2\pi}{n},$$

we finally obtain the following expression:

$$M_{упр} = 2c_0\left[1-\cos\frac{2\pi}{n}\right]\xi_0\sin\varphi_k =$$
$$= 2c_0\left[1-\cos\frac{2\pi}{n}\right]\xi_0\sin\left[p_\beta t - \frac{2\pi}{n}\cdot k\right].$$

In the case of the usual elastic elements with angular rigidity $c_{экв}$ included between the blade and housing of the hub, we had:

$$M_{упр} = c_{экв}\xi_0\sin\left[p_\beta t - \frac{2\pi}{n}\cdot k\right].$$

Thus the interblade elastic elements for the given blade are equivalent to one standard elastic element with rigidity

$$c_{экв} = 2c_0\left[1-\cos\frac{2\pi}{n}\right]. \qquad (6.9)$$

It is possible to establish accurately that interblade dampers for the given blade are equivalent to one conventional damper, included between the blade and housing of the hub and having a damping factor

$$k_{экв} = 2k_0\left[1-\cos\frac{2\pi}{n}\right]. \qquad (6.10)$$

Consequently, the calculation of ground resonance of the helicopter with interblade elastic couplings and dampers can be made by the standard formulas, taking the coefficient of the damper equal to $k_{экв}$, and the stiffness coefficient in the drag hinge equal to $c_{экв}$.

Number of blades	2	3	4	5	6
$\frac{c_{экв}}{c_0} = \frac{k_{экв}}{k_0}$	4	3,73	2	1,382	1

Table 3.2 gives values of the quantity:

$$\frac{c_{экв}}{c_0} = \frac{k_{экв}}{k_0} = 2\left(1-\cos\frac{2\pi}{n}\right) \qquad (6.11)$$

for rotors with different number of blades.

One of the deficiencies of a rotor with interblade dampers is the fact that with simultaneous deflections of blades relative to the drag hinges (all to one side and at one angle), which can happen in transition operating conditions of the flight, and also with the starting of the rotor, such dampers do not work.

On existing designs of hubs this deficiency is sometimes eliminated by using combined designs in which elastic elements are made in the form of interblade connections, and dampers are made individually for each blade, i.e., they are included between the blade and housing of the hub.

3. Selection of Characteristics of Rigidity and Damping of the Undercarriage[e]

After characteristics of dampers of the blade are selected, it is possible to proceed to the selection of basic parameters of the undercarriage. For helicopters of conventional single-rotor and longitudinal configurations the wheel track 2a (see Fig. 3.17) should be selected in such a way that the frequency p_{m} of natural oscillations of the helicopter on a landing run (rotation around the longitudinal axis passing through the center of gravity) with nonoperating struts (only the tires operate) is approximately 20% higher than the operating revolutions of the rotor. This gives condition (4.19):

$$p_{m} = 1{,}2\omega_{p.o} = \sqrt{\frac{2c_{ш}^{y}a^{2}}{I_{x}}}.$$

If the undercarriage is four-wheeled, then in this formula, instead of quantity $2c_{y}^{ш}a^{2}$ it is necessary to take quantity $c_{y_{x}} = c_{y_{1}} + c_{y_{2}}$ [see formula (5.3)].

Since the tires are selected according to strut load, then quantity $c_{ш}^{y}$ in the given formula can be considered known; and therefore the appropriate value of a can be found from it.

The rigidity of the shock absorbers and their damping can be selected, assuming that the center of the zone of instability on a landing run (during oscillations with operating struts) coincides with operating revolutions of the rotor. Such an approach results from the following considerations: if one were to select the rigidity of the shock absorbers in such a manner that the zone of instability on the landing run is higher than the operating revolutions, then there appears the danger of the formation of ground resonance with separation of the tires from surface of the ground (see § 4, No. 3), since during oscillations of the helicopter with separation of the tires the zone of instability can "descend" on the operating revolutions. To make the zone of instability lower than the operating revolutions is usually not possible (the exception is the undercarriage of the Bristol system, the construction of which, however is quite complicated), since for this an unrealizably low rigidity of shock absorbers is required. On the other hand, if the zone of instability is directly on the operating revolutions and the margin of damping is sufficient, then the ground resonance with separation of the tires cannot appear, since with separation of the tires the zone of instability will appear lower than the operating revolutions. This circumstance was checked by numerous calculations and modeling on an electronic computer of ground resonance with separation of the tires, which was carried out by engineer Yu. A. Myagkov.

We will consider for simplicity that the undercarriage has vertical damping struts (see Fig. 3.17b). As was shown in § 2, No. 5, the greatest damping of the shock absorber-tire system, which can be obtained with the selection of optimum damping of the shock absorber, depends on the ratio $\frac{c_{ш}}{c_{ш}^{*}}$. If one were to use formulas (2.37) and (2.38) and to consider that on the landing run

$$\bar{a}_0 = \frac{k_{ш} c^{*}_{ш}}{l_0 p_0}; \quad p_0 = \sqrt{\frac{2 k_{ш} c^{*}_{ш}}{l_0}},$$

then there can be obtained the following formula, which determines the greatest possible coefficient of available damping of the helicopter on a landing run:

$$[\bar{n}_0]_{max}^{расч} = \frac{0{,}25}{\sqrt{\varkappa(1+\varkappa)}}, \qquad (6.12)$$

where

$$\varkappa = \frac{c_{ам}}{c_{ам}^{y}}. \qquad (6.13)$$

This means that the greatest possible damping factor which can be obtained on a landing run, varying by quantity $k_{ам}$, depends especially on the ratio $\frac{c_{ам}}{c_{ам}^{y}}$. Therefore, by knowing damping required for eliminating ground resonance, it is easy to determine the necessary rigidity of the shock absorber $c_{ам}$. If damping of the blade is known, the required damping $\bar{n}_0$ can be determined by formula (1.31):

$$[\bar{n}_0]_{потр} = \frac{\varepsilon(1-\nu_0)}{8\nu_0 \bar{n}_s^{вв}} \bar{p}^{*}\Delta, \qquad (6.14)$$

where $\bar{n}_s^{вв}$ is the damping factor of the blade $\bar{n}_s$, referred to the frequency $p_{вв}$ of natural oscillations of the helicopter on a landing run with nonoperating (on only some tires):

$$\left.\begin{aligned} \bar{n}_s^{вв} &= \frac{n_s}{p_{вв}}; \\ p_{вв} &= \sqrt{\frac{2c_y^{вв}a^2}{I_x}}; \end{aligned}\right\} \qquad (6.15)$$

$\bar{p}^{*}$ is the frequency of natural oscillations of the helicopter with operating struts with optimum damping referred to quantity $p_{вв}$:

$$\bar{p}^{*} = \frac{p^{*}}{p_{вв}} = \sqrt{\frac{2\varkappa}{1+2\varkappa}}. \qquad (6.16)$$

Let us assume that it is required to provide a damping margin

$$\eta = \frac{[\bar{n}_0]_{max}^{расч}}{[\bar{n}_n]_{потр}}. \qquad (6.17)$$

Using formulas (6.12), (6.14), and (6.16), we will obtain:

$$\eta = \frac{0{,}25}{\sqrt{\varkappa(1+\varkappa)}} \frac{8\nu_0 \bar{n}_s^{вв}}{\varepsilon(1-\nu_0)} \sqrt{\frac{1+2\varkappa}{2\varkappa}} \cdot \frac{1}{\Delta}.$$

This relation can be rewritten in the following way:

$$\frac{s(1-\eta_0)}{\eta_0}\frac{g}{p_{ст}^2}\Delta = \alpha, \qquad (6.18)$$

where

$$s = \sqrt{\frac{2(1+2\varkappa)}{\varkappa^2(1+\varkappa)}}. \qquad (6.19)$$

After the selection of characteristics of the blade and tire and assignment of the necessary damping margin η, the left part of equation (6.18) is a known quantity. By knowing quantity α, it is easy to find quantity $\varkappa$ from equation (6.19) and then the necessary rigidity $c_{ам}$ of the shock absorber. For convenience of the determination of $\varkappa$ Fig. 3.52 gives a graph of the dependence $\alpha(\varkappa)$.

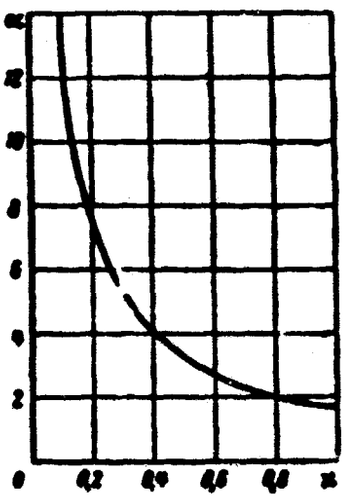

Fig. 3.52. Graph of the dependence of coefficient α on $\varkappa$.

To select the rigidity $c_{ам}$ by the method indicated it is possible to take $\eta_0 = 1$, since in the formulas given "kinematic" damping of the tire on a landing run is not considered [see formula 4.21)]. The real damping margin η_0, taking into account this additional damping, should be obtained not less than 1.5-2.

After the rigidity of the shock absorber is found, its optimum damping factor can be determined by formula (2.36), namely:

$$h_{ам}^{опт} = \frac{c_{ам}^0 + c_{ам}}{\rho^2}. \qquad (6.20)$$

where

$$p^{\circ}=p_{\text{ст}}\bar{p}^{\circ}=p_{\text{ст}}\sqrt{\frac{2\varkappa}{1+2\varkappa}}. \qquad (6.21)$$

Since in reality the characteristic of damping of the shock absorber, as a rule, is nonlinear (§ 3, No. 1), then by quantity $k_{\text{ст}}^{\circ}$ one should imply the damping factor of the equivalent linear shock absorber.

4. Some Recommendations on the Designing of an Undercarriage

One of the basic difficulties appearing in the designing of the undercarriage is the complexity of providing the necessary damping of the shock-absorber strut. If dimensions of the holes through which hydraulic fluid flows when the shock absorber is operating are selected from conditions of ground resonance, then, as a rule, operation of the shock absorber during landing will be unsatisfactory (there will be too great forces with a shock against the ground). If, however, we select them from conditions of landing there will be obtained too little damping with lateral oscillations of the helicopter, which is absolutely insufficient for eliminating ground resonance.

This difficulty can be surmounded by two methods [18]:

1) increase in damping on the recoil stroke of the shock absorber;

2) installation of special valves in the construction of shock absorber.

The former of these methods is the simplest and consists in the fact that dimensions of holes through which hydraulic fluid flows on the forward stroke of the shock absorber (compression) are selected from conditions of landing, and dimensions of holes through which hydraulic fluid flows on the recoil of the shock absorber (extension) are selected from conditions of ground resonance. This

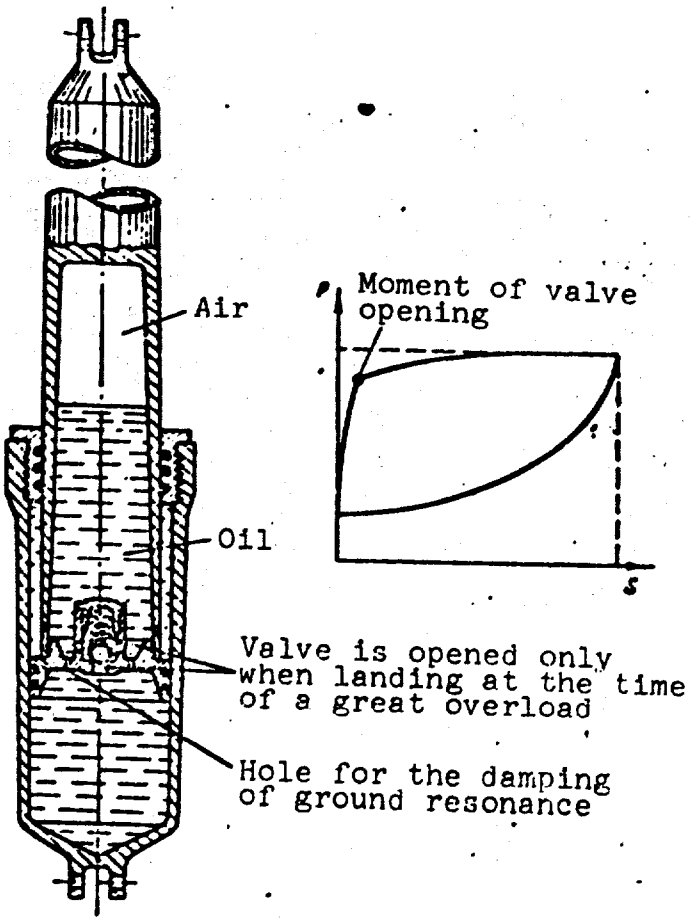

Fig. 3.53. Shock-absorber strut with valve.

appears possible because with oscillations of the helicopter at every instant one of the shock-absorber struts (right or left) operates on the recoil. Therefore, in general, the needed damping factor of the helicopter during ground resonance can be provided by only one damping on the recoil of the shock absorbers.

However, to increase damping on recoil is possible only in known limits. Excessive increase in damping on recoil (very small holes) leads to a very slow "yield" of shock-absorber struts from the pressed state after a landing shock. Therefore, if the helicopter in conditions of operation should accomplish a running landing on uneven ground, when after the first shock against the ground further shocks can follow, such a method of the increase in damping can appear unacceptable.

The second method does not have the mentioned deficiency and consists in the fact that in the shock absorber there is a special spring valve, which is opened only if the force of compression in the shock absorber exceeds (with a shock against the ground) a certain critical value $P_{ам}^{пр}$. At $P_{ам}<P_{ам}^{пр}$ the holes whose dimensions are selected from conditions of ground resonance operate, and at $P_{ам}>P_{ам}^{пр}$ additional holes of larger diameter operate, the dimensions of which are selected from conditions of limitation of overload with landing. Figure 3.53 gives a diagram of the design and a diagram of dynamic pressing of such a shock absorber.

Another important factor which one should consider in the designing of an undercarriage is the inevitable presence for any shock absorber of the force of preliminary tightening (§ 2, No. 7), i.e., the force with which the shock absorber starts to operate. For a helicopter undercarriage it is desirable to have as few forces of preliminary tightening P_0 as possible, since at great thrust of the rotor forces P on the undercarriage decrease and at $P<P_0$ the shock absorbers do not operate. Ground resonance can develope with nonoperating shock absorbers on elastic tires practically deprived of shock absorption. For helicopter undercarriages it is necessary to select characteristics of the strut so that the force of preliminary tightening is not more than 10% of the strut load on the shock absorber with zero thrust of the rotor.

Footnotes

[1]This formula will be derived in § 3 as well as formula (1.31).

[2]It will be shown in No. 5 of this paragraph and also in Nos. 1 and 2 of § 3 how to determine coefficients k'_z and k'_y.

[3]See, for example, A. Gessow and G. Myers, Aerodynamics of the Helicopter, Oborongiz, 1964.

[4]It is considered that the actual displacement is a real part of the indicated complex expression. The application of complex expressions in the derivation of basic formulas permits considerably simplifying the calculations.

[5]The diagram of a spring damper of the blade for eliminating ground resonance was proposed by engineers O. P. Bakhov, L. N. Grodko, I. V. Kurova, and M. A. Leykand. (Author's certificate No. 184142).

[6]The method of selection of undercarriage parameters expounded here was developed by engineer Yu. A. Myagkov.

[7]It should be remembered that the case when kinematic damping is absent is realized with oscillations of a helicopter on ice, when friction between the tire and ground is absent (see § 4, No. 2).

CHAPTER IV

THEORETICAL BASES OF THE CALCULATION OF BEARINGS OF BASIC UNITS OF A HELICOPTER

The service life of basic units of a helicopter in many respects depends on the efficiency of their bearing subassemblies, and therefore questions of the theory of the calculation of antifriction bearings in helicopter design are given much attention.

It is known that the service life of general-purpose antifriction bearings, because of different factors of a metallurgical and technological character, can vary over a wide range. In connection with this the necessary reliability of bearing subassemblies in general machine building is attained owing to the introduction of corresponding safety factors, i.e., definite oversized calculation loads. It is understandable that requirements for the accuracy of calculation of bearings can be considerably lowered. For articles of aviation materiel, where the increase in reliability should be attained owing to the perfection of the construction without an increase in dimensions and weight of the bearing subassemblies, such a means, naturally, is unacceptable. This is even more so because aviation bearings are made from improved materials, have a high accuracy and are subjected in production to specially thorough control, as a result of which the dispersion of service life for them noticeably decreases. Aviation bearings, including bearings used in helicopters should be calculated as accurate as possible, taking into account peculiarities of their load and operation.

In recent years, owing to works of Soviet and foreign researchers, practical methods of the calculation of antifriction bearings have

obtained considerable development, but nonetheless they by far do not always possess the necessary accuracy. This especially pertains to cases of operation of bearings with complex combinations of external loads and during oscillatory motion with small amplitudes, and these cases represent the greatest interest for helicopter construction. The absence of reliable methods of calculation of antifriction bearings operating in the indicated conditions hampers the designing of reduction gears, cyclic pitch controls, and hubs of main and antitorque rotors of helicopters. It is possible to cite many examples when these vitally important units were put out of operation before the end of the service life because of the destruction of unsuccessfully selected bearings.

In this chapter there is made an attempt to generalize the results of theoretical and experimental investigations carried out for the purpose of refinement of methods of calculation of bearings of units of the helicopter. As practical experience showed, the methods of calculation expounded below permit more fully using the carrying capacity of the bearings. The application of these methods in the designing of bearing subassemblies in many cases made it possible to create sufficiently compact and light constructions, which were able to work reliably for a long time under very high loads.

§ 1. Equations of Static Equilibrium of Radial and Radial Thrust Ball Bearings Under a Combined Load

The dependences utilized during calculations of bearings are based on results of investigation of the distribution of the external load between rolling solids.

Let us formulate equations with the help of which pressures on balls in general of loading of radial and radial thrust ball bearings can be found.

Let us assume that a single-row ball bearing has a radial clearance of 2Δ after fitting on the shaft and in the housing with a stabilized temperature regime of operation of the subassembly.

Let us take a rectangular system of coordinates xyz with the origin at the center O of the outer ring. We will direct axis x along the axis of rotation of this ring (Fig. 4.1).

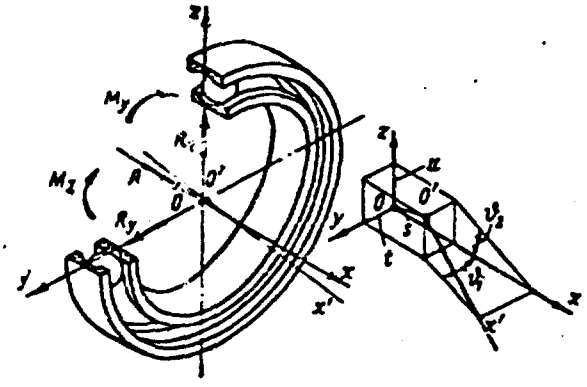

Fig. 4.1. Diagram of movements of inner ring of the bearing under the action of an arbitrary external load applied to it.

With the application to the bearing of an arbitrary external load the center of the inner ring moves to point O' with coordinates s, t, and u, and its axis of rotation x' is deflected with respect to axis x at a certain angle $, the projections of which on plane xOy and xOz are respectively equal to $_1$ and $_2$ (Fig. 4.1).

We will consider that on the ball, the center of which O_{III} lies in plane Π, which forms with plane xOz the angle ψ, there act normal forces P_ψ identical in magnitude and directed along a common line passing through centers O_H and O_B of sections of grooves of the inner and outer rings and point O_{III} (Fig. 4.2). Displacement of the center of the site of contact of the ball with the inner ring from plane Π and tangential forces appearing at points of contact of the ball with the rings, as is usually accepted in the theory of antifriction bearings, will be disregarded.

According to the well-known formulas of Hertz

$$P_\psi = B\delta_\psi^{3/2}. \qquad (1.1)$$

Here δ_ψ is the approach of grooves of rings in the direction O_HO_B owing to the elastic deformations in the zones of contact.

For ball bearings with the usual internal geometry it is possible

to assume

$$B=\nu B_0\frac{d_m^2}{i^{3/2}}, \qquad (1.2)$$

where ν is a factor dependent on the relationship between radii r_n and r_n of grooves of the outer and inner rings and the diameter of the ball d_m; $g=r_n+r_n-d_m$ – distance between points O_n and O_n at the time of contact of the ball with the rings (at $\delta_\psi=0$).

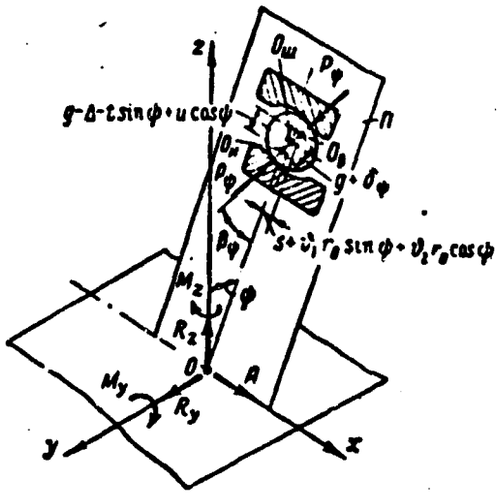

Fig. 4.2. Diagram of forces acting on the ball.

If diameter d_m is expressed in millimeters and forces in kilograms, then with the elastic modulus of material of the rings and balls $E=2{,}08\times10^6$ kG/cm^2 the coefficient B_0 is equal to 62.

Factor ν has the values shown in Table 4.1.

Table 4.1.

$r_{n(n)}/d_m$	0,510	0,515	0,520
ν	0,63	1,00	1,39

From conditions of static equilibrium of elements of the bearing it follows that external forces and moments applied to the inner ring can be thus written (see Fig. 4.2):

$$\left.\begin{aligned} A &= \sum P_\psi \sin \beta_\psi; \\ R_y &= -\sum P_\psi \cos \beta_\psi \sin \psi; \\ R_z &= \sum P_\psi \cos \beta_\psi \cos \psi; \\ M_y &= r_0 \sum P_\psi \sin \beta_\psi \cos \psi; \\ M_z &= r_0 \sum P_\psi \sin \beta_\psi \sin \psi. \end{aligned}\right\} \qquad (1.3)$$

Here β_ψ is the angle of contact of the ball with the rings; r_0 – radius on which centers of the balls are located. Sign Σ extend over all the loaded balls.

Let us assume that the rings have an absolutely correct geometric form not variable with application of loading. In this case to determine the approach of grooves δ_ψ and angle of contact β_ψ there can be used formulas,

$$\delta_\psi = [(s + \theta_1 r_0 \sin \psi + \theta_2 r_0 \cos \psi)^2 + (g - \Delta - t \sin \psi + u \cos \psi)^2]^{1/2} - g; \qquad (1.4)$$

$$\beta_\psi = \operatorname{arc\,tg} \frac{s + \theta_1 r_0 \sin \psi + \theta_2 r_0 \cos \psi}{g - \Delta - t \sin \psi + u \cos \psi}. \qquad (1.5)$$

Expressing in formulas (1.4) and (1.5) all linear quantities in fractions of distance g, we will copy them in the form:

$$\bar{\delta}_\psi = [(\bar{s} + \bar{\varepsilon}_1 \sin \psi + \bar{\varepsilon}_2 \cos \psi)^2 + (\cos \beta_0 - \bar{t} \sin \psi + \bar{u} \cos \psi)^2]^{1/2} - 1; \qquad (1.6)$$

$$\beta_\psi = \operatorname{arc\,tg} \frac{\bar{s} + \bar{\varepsilon}_1 \sin \psi + \bar{\varepsilon}_2 \cos \psi}{\cos \beta_0 - \bar{t} \sin \psi + \bar{u} \cos \psi}, \qquad (1.7)$$

where $\beta_0 = \arccos \frac{g - \Delta}{g}$ is the so-called initial angle of contact (angle of contact with purely axial displacement of the rings owing to the working radial clearance 2Δ).

In expressions (1.6) and (1.7) $\bar{\varepsilon}_1$ and $\bar{\varepsilon}_2$ denote quantities $\theta_1 \frac{r_0}{g}$ and $\theta_2 \frac{r_0}{g}$.

It is necessary to consider that the working axial clearance of the bearing s_0 is connected with angle β_0 by the following relation:

$$2s_0 = 2g \sin \beta_0$$

or, by passing to relative values,

$$2\bar{s}_0 = 2 \sin \beta_0. \qquad (1.8)$$

Relative quantities everywhere are designated by the same letters as the absolute with dashes above them.

The equations given describe conditions of static equilibrium of radial and radial thrust ball bearings with any combinations of external loads. From them there can be found all parameters characterizing the distribution of forces between the separate balls. It is necessary, however, to consider that because of the complexity of dependences connecting quantities δ_4 and β_4 with relative displacements of the rings, the practical application of these equations is conjugate with the large volume of calculations. In connection with this, with engineering calculations they are usually replaced by some approximate relations. One of the variants of such relations most convenient for practice, which possesses quite high accuracy, is described below.

An analysis of operating conditions of the bearing subassemblies of different types shows that in most cases the resultant radial force $R=(R_y^2+R_z^2)^{1/2}$ and resultant moment $M=(M_y^2+M_z^2)^{1/2}$ absorbed by the bearing act in one plane. In accordance with this, disposing the plane of coordinates xOz in such a way that it coincides with the plane of action of external loads applied to bearing, it is possible to write

$$\left.\begin{aligned} R_y&=0;\\ R_z&=R;\\ M_y&=M;\\ M_z&=0. \end{aligned}\right\} \qquad (1.9)$$

As the calculations indicate, the distribution of the load depends on the angular location of the set of balls. Taking into account this circumstance, we will consider that the balls are located symmetrically with respect to plane xOz. Under this condition

$$\left.\begin{aligned} \bar{i}&=0;\\ \bar{\varepsilon}_1&=0;\\ \bar{\varepsilon}_2&=\bar{\varepsilon}=\theta\frac{r_0}{\varepsilon}. \end{aligned}\right\} \qquad (1.10)$$

Considering equalities (1.10), let us expand expression (1.6) in Maclaurin in the environment $\bar{n}=0$ and $\bar{\varepsilon}_2=\bar{\varepsilon}=0$. Being limited to linear

terms, after simple transformations we obtain

$$\bar{\delta}_\psi = \bar{\delta} + (\bar{u}\cos\beta + \bar{\varepsilon}\sin\beta)\cos\psi. \tag{1.11}$$

In equality (1.11)

$$\bar{\delta} = (\bar{s}^2 + \cos^2\beta_0)^{1/2} - 1 \tag{1.12}$$

and

$$\beta = \operatorname{arctg}\left(\frac{\bar{s}}{\cos\beta_0}\right). \tag{1.13}$$

Quantities $\bar{\delta}$ and β are nothing but the relative approach of grooves, and the angle of contact in section $\psi = 90°$.

As follows from expression (1.7),

$$\left.\begin{aligned}\sin\beta_\psi &= \frac{\bar{s} + \bar{\varepsilon}_1\sin\psi + \bar{\varepsilon}_2\cos\psi}{[(\bar{s} + \bar{\varepsilon}_1\sin\psi + \bar{\varepsilon}_2\cos\psi)^2 + (\cos\beta_0 - \bar{\varepsilon}\sin\psi + \bar{u}\cos\psi)^2]^{1/2}};\\ \cos\beta_\psi &= \frac{\cos\beta_0 - \bar{\varepsilon}\sin\psi + \bar{u}\cos\psi}{[(\bar{s} + \bar{\varepsilon}_1\sin\psi + \bar{\varepsilon}_2\cos\psi)^2 + (\cos\beta_0 - \bar{\varepsilon}\sin\psi + \bar{u}\cos\psi)^2]^{1/2}}.\end{aligned}\right\} \tag{1.14}$$

Proceeding with equalities (1.14) in the same way as and with expression (1.6), after rejecting the nonlinear terms and corresponding formations we have

$$\left.\begin{aligned}\sin\beta_\psi &= \sin\beta\left[1 - \frac{\cos^2\beta}{\cos\beta_0}(\bar{u} - \bar{\varepsilon}\operatorname{ctg}\beta)\cos\psi\right];\\ \cos\beta_\psi &= \cos\beta\left[1 + \frac{\sin^2\beta}{\cos\beta_0}(\bar{u} - \bar{\varepsilon}\operatorname{ctg}\beta)\cos\psi\right].\end{aligned}\right\} \tag{1.15}$$

Assuming

$$\frac{\bar{u}\cos\beta + \bar{\varepsilon}\sin\beta}{\bar{\delta}} = \lambda, \tag{1.16}$$

let us present dependences (1.11) and (1.15) in the form

$$\bar{\delta}_\psi = \bar{\delta}(1 + \lambda\cos\psi); \tag{1.17}$$

$$\left.\begin{aligned}\sin\beta_\psi &= \sin\beta\left[1 - \frac{\cos\beta}{\cos\beta_0}\left(\lambda\bar{\delta} - \frac{\bar{\varepsilon}}{\sin\beta}\right)\cos\psi\right];\\ \cos\beta_\psi &= \cos\beta\left[1 + \frac{\cos\beta}{\cos\beta_0}\operatorname{tg}^2\beta\left(\lambda\bar{\delta} - \frac{\bar{\varepsilon}}{\sin\beta}\right)\cos\psi\right].\end{aligned}\right\} \tag{1.18}$$

Quantity $\bar{\delta}$ determining the pressure on the ball, the center of which is plane x0y, can be expressed in terms of angles β and β_ψ:

$$\bar{\delta} = \frac{\cos\beta_0}{\cos\beta} - 1. \qquad (1.19)$$

The zone of loading of the bearing, as is known, is found from the condition that on its limits $\bar{\delta}_\psi = 0$.

Assuming in equality (1.17) $\bar{\delta}_\psi = 0$, we obtain the following expression which establishes limits of the zone of loading:

$$\psi_n^{\circ} = \arccos\left(-\frac{1}{\lambda}\right). \qquad (1.20)$$

The relative approach of grooves of the rings $\bar{\delta}_\psi$ reaches a maximum value $\bar{\delta}_0$ in the center of zone of loading, which is located in the section $\psi = \psi_0 = 0$ if $\bar{a}\cos\beta + \bar{e}\sin\beta = \bar{\delta}\lambda > 0$ and in section $\psi = \psi_0 = 180°$ if $\bar{a}\cos\beta + \bar{e}\sin\beta = \bar{\delta}\lambda < 0$ (Fig. 4.3).

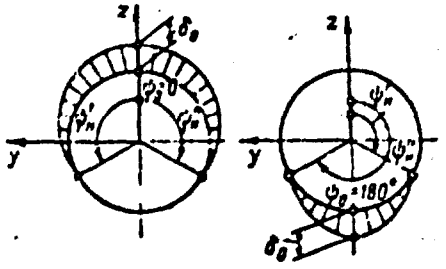

Fig. 4.3. Zone of loading of the bearing.

In the case $\psi_0 = 0$, $0 < \psi_n' \leq 180°$ and $\psi_n'' = -\psi_n'$, and when $\psi_0 = 180°$, $180° < \psi_n' \leq 360°$ and $\psi_n'' = 360° - \psi_n'$.

It is clear that expression (1.20) is correct only if parameter λ exceeds unity in absolute value. If $|\lambda| < 1$, then the zone of loading forms $360°$, i.e., in the bearing all balls carry the load, and quantity $\bar{\delta}$ in this case is always positive, and the sign λ coincides with the sign $\cos\psi_0$. The latter means that for bearings for which all balls are loaded, when $\psi_0 = 0$, $0 < \lambda < 1$ and at $\psi_0 = 180°$, $-1 < \lambda < 0$.

Taking in equality (1.17) $\psi = \psi_0$, we find

$$\bar{\delta}_0 = \bar{\delta}(1 + \lambda\cos\psi_0). \qquad (1.21)$$

With the help of expressions (1.2), (1.17), and (1.21), remembering that $\bar{\delta}_\psi = \frac{\delta_\psi}{\varepsilon}$, let us give formula (1.1) in the form

$$P_\psi = B_0 z d_w^2 \bar{\delta}_0^{3/2}\left(\frac{1 + \lambda\cos\psi}{1 + \lambda\cos\psi_0}\right)^{3/2}. \qquad (1.22)$$

Dependences (1.19) and (1.21) show that in the case $\lambda=\infty$, i.e., with a loading zone of 180°, $\bar{\delta}=0$ and, consequently, $\beta = \beta_0$ independently of the level of the load.

Let us introduce into the consideration of the sums

$$J_k=\frac{1}{z(1+\lambda\cos\psi_0)^{3/2}}\sum(1+\lambda\cos\psi)^{3/2}\cos^{k-1}\psi, \qquad (1.23)$$

where

$$k=1, 2, 3.$$

Here, as in all preceding equalities, angle ψ can take only those discrete values which determine the angular position of the loaded balls.

Let us convert now with the help of the obtained expressions, equations (1.3).

Replacing in these equations P_ψ, $\sin\beta_\psi$, and $\cos\beta_\psi$ by their values according to the formulas (1.22) and (1.18), in accordance with equalitites (1.9) and (1.23), considering the dependence (1.21), we will obtain

$$\begin{aligned}
&\frac{\lambda}{zvd_w^2}=B_0\bar{\gamma}_0^{3/2}\sin\beta J_1\times\\
&\quad\times\left[1-\frac{\cot\beta}{\cos\beta_0}\left(\frac{\lambda\bar{\delta}_0}{1+\lambda\cos\psi_0}-\frac{\bar{\varepsilon}}{\sin\beta}\right)\frac{J_2}{J_1}\right];\\
&\frac{R}{zvd_w^2}=B_0\bar{\gamma}_0^{3/2}\cos\beta J_2\times\\
&\quad\times\left[1+\frac{\cos\beta}{\cos\beta_0}\operatorname{tg}^2\beta\left(\frac{\lambda\bar{\delta}_0}{1+\lambda\cos\psi_0}-\frac{\bar{\varepsilon}}{\sin\beta}\right)\frac{J_3}{J_2}\right];\\
&\frac{M}{r_0zvd_w^2}=B_0\bar{\gamma}_0^{1/2}\sin\beta J_2\times\\
&\quad\times\left[1-\frac{\cos\beta}{\cos\beta_0}\left(\frac{\lambda\bar{\delta}_0}{1+\lambda\cos\psi_0}-\frac{\bar{\varepsilon}}{\sin\beta}\right)\frac{J_3}{J_2}\right].
\end{aligned} \qquad (1.24)$$

From dependences (1.19) and (1.21) there results the following expression for angle β:

$$\cos\beta=\frac{\cos\beta_0}{1+\frac{\bar{\delta}_0}{1+\lambda}}. \qquad (1.25)$$

Equalities (1.24) and (1.25) are those relationships which can be replaced with engineering calculations, "exact" equations of static equilibrium of radial and radial thrust ball bearings. As corresponding investigations show, an error in final results, caused by such a replacement, usually does not exceed several percent.

With a change in the number of balls sums (1.23) are changed insignificantly. This permits expressing them in terms of integrals

$$j_k=\frac{1}{2\pi(1+\lambda\cos\psi_0)^{3/2}}\int_{-\psi_n}^{\psi_n}(1+\lambda\cos\psi_0\cos\psi)^{3/2}\cos^{k-1}\psi\,d\psi, \qquad (1.26)$$

which are functions of the product $\lambda\cos\psi_0$. Here k = 1, 2, 3.

It is easy to be convinced that with the usual quantities of the balls

$$J_k\approx\cos^{k-1}\psi_0 j_k. \qquad (1.27)$$

Value of integrals j_k are given in Table 4.2.

Table 4.2.

$\lambda\cos\psi_0$	j_1	j_2	j_3	w	$\lambda\cos\psi_0$	j_1	j_2	j_3	w
0	1,000	0,000	0,500	1,000	3,33	0,323	0,247	0,210	0,612
0,1	0,868	0,065	0,435	0,879	5	0,309	0,242	0,207	0,605
0,2	0,766	0,114	0,385	0,804	10	0,294	0,236	0,203	0,596
0,3	0,686	0,151	0,346	0,757	20	0,286	0,233	0,201	0,59
0,4	0,622	0,180	0,316	0,726	$\pm\infty$	0,279	0,229	0,199	0,587
0,5	0,570	0,202	0,292	0,705	−20	0,271	0,225	0,197	0,583
0,6	0,528	0,220	0,273	0,690	−10	0,262	0,221	0,194	0,578
0,7	0,494	0,233	0,258	0,676	−5	0,247	0,212	0,188	0,567
0,8	0,466	0,243	0,246	0,670	−3,33	0,229	0,201	0,181	0,556
0,9	0,443	0,250	0,237	0,663	−2,5	0,211	0,189	0,172	0,543
1	0,425	0,255	0,231	0,657	−2	0,192	0,175	0,162	0,528
1,111	0,409	0,257	0,226	0,651	−1,667	0,171	0,159	0,149	0,512
1,25	0,395	0,258	0,223	0,645	−1,429	0,147	0,140	0,133	0,488
1,429	0,380	0,258	0,220	0,639	−1,25	0,120	0,116	0,112	0,459
1,667	0,366	0,256	0,218	0,633	−1,111	0,084	0,083	0,060	0,414
2	0,352	0,254	0,215	0,626	−1	0,000	0,000	0,000	0,000
2,5	0,338	0,251	0,212	0,619					

§ 2. Calculation of Radial and Radial Thrust Ball Bearings Under Combined Loads in the Case of the Absence of Mutual Misalignment of Rings

1. Pressures on the Balls

If the distance between the bearings is great as compared to the diametrical dimensions of the bearings and all the parts of bearing subassembly possess high rigidity, then with the calculation of pressures on rolling solids it is possible to disregard mutual misalignment of the rings under a load and consider only their displacements in radial and axial directions.

Entering into formula (1.22), which determines pressures on the balls in radial and radial thrust ball bearings, are quantities $\bar{\delta}_0$ and λ.

Relations (1.24) and (1.25), which connect these quantities with external loads applied to the bearing, in the absence of mutual misalignment of the rings, i.e., in the case $\psi = 0$, can be represented in the form

$$\left.\begin{aligned} \frac{A}{zvd_w^2} &= B_0\bar{\delta}_0^{3/2}\sin\beta J_1\left(1-\frac{\cos\beta}{\cos\beta_0}\frac{\lambda\bar{\delta}_0}{1+\lambda}\frac{J_2}{J_1}\right); \\ \frac{R}{zvd_w^2} &= B_0\bar{\delta}_0^{3/2}\cos\beta J_2\left(1+\frac{\cos\beta}{\cos\beta_0}\operatorname{tg}^2\beta\,\frac{\lambda\bar{\delta}_0}{1+\lambda}\frac{J_2}{J_2}\right); \end{aligned}\right\} \tag{2.1}$$

$$\cos\beta = \frac{\cos\beta_0}{1+\frac{\bar{\delta}_0}{1+\lambda}}. \tag{2.2}$$

We do not write out the expression for the moment, since at $\psi = 0$ it does not play an independent role and is not used in the calculations.

For convenience let us assume that the direction of axis z coincides with the direction of the radial loading R. Under this condition the radial displacement u is positive, and, consequently, angle ψ_0 is equal to zero. This circumstance is considered both in equations (2.1) and (2.2) and in all subsequent dependences.

It is necessary to note that case $ = 0 is basic in the theory of antifriction bearings. Usually when we make no special reservations on the design and peculiarities of loading of the bearing subassembly we consider precisely this case. In reference to it there are carried out basic investigations [22], [23], [29], [42] directed towards the refinement of methods of calculation of antifriction bearings, operating under combined loads.

Static loading of the bearing is characterized by the magnitude of maximum pressure on the rolling solid.

According to the formulas (1.22) the maximum pressure on the ball

$$P_0 = B_0 w d_w^2 \overline{\delta}_0^{3/2}. \qquad (2.3)$$

With prolonged static loading of an irrotational bearing the greatest stress of crumpling σ_{max} on the rolling path of the inner ring caused by this pressure should not exceed 40,000 kG/cm^2. If static loads acting on an irrotational bearing create greater contact stresses then on the rolling paths there appear noticeable traces of permanent deformations in the form of dents from the balls.

The indicated allowed value of σ_{max} is selected from the condition that the magnitude of permanent deformation of the rolling path amounts to not more than one micrometer for every centimeter of diameter of the ball. In this case the smoothness of rotation of the bearing is not disturbed, and its carrying capacity does not decrease.

In calculation dependences, which are used for calculation of service life of the bearings, there appears the quantity

$$P_e = \left(\frac{1}{2\pi} \int_{\psi_n}^{\psi_n^*} P_\psi^m \, d\psi \right)^{1/m}, \qquad (2.4)$$

where m is the exponent under load in formulas of service life.

With the help of equalities (1.22) and (2.3) we will give expression (2.4) in the form

$$P_э = wP_0. \tag{2.5}$$

Coefficient w here is equal to

$$w = \left[\frac{1}{2\pi(1+\lambda\cos\psi_0)^{3/2m}} \int_{\psi_н'}^{\psi_н''} (1+\lambda\cos\psi_0\cos\psi)^{3/2m}\, d\psi \right]^{1/m}. \tag{2.6}$$

Let us note that value $P_э$ is the constant pressure P_ψ = const at which the probability of fatigue breakdown of the ball race in the given operational conditions is the same as that with real distribution of forces between rolling solids. This gives the basis to call it the equivalent pressure on a rolling solid for a ball race.

It should be borne in mind that quantity $P_э$ sometimes refers not to the whole length of the rolling path, as is done in expression (2.4), but only to the loaded zone $\psi_н''-\psi_н'$.

At m = 3.33, as is accepted in Soviet practice,

$$w = \left\{ \frac{1}{\pi(1+\lambda\cos\psi_0)^5} \left[\frac{\psi_н'' - \psi_н'}{2} \left(1+5\lambda^2+\frac{15}{8}\lambda^4\right) - \right.\right.$$
$$\left.\left. - \operatorname{tg}\frac{\psi_н''}{2} \left(\frac{137}{60}+\frac{607}{120}\lambda^2+\frac{8}{15}\lambda^4\right)\right]\right\}^{0,3}. \tag{2.7}$$

With the practical use of formulas (2.6) and (2.7) it is necessary to remember that for the selected direction of axis z angle ψ_0 is equal to zero. Angles $\psi_н'$ and $\psi_н''$ in formula (2.7) are taken in radians. Values of the coefficient w, found by this formula, are given in Table 4.2 together with values of integrals j_k.

Pressures P_0 and $P_э$ under the assigned external loads R and A can be calculated in two ways.

The first of them consists in the calculation of these quantities by the formulas (2.3) and (2.5) with the use of values $\bar{\delta}_0$ and λ, obtained as a result of the direct solution of equations (2.1) and (2.2).

Since equations (2.1) and (2.2) have a complex structure, then this way, naturally, is associated with great difficulties. They are sufficiently great even when the problem is solved approximately.

The second means, which is more acceptable for practical applications, for determing pressures P_0 and $P_э$ is based on the following considerations.

If the angle of contact of all the balls is identical $\beta_\psi = \beta = \text{const}$, then

$$\left.\begin{aligned} \frac{A}{z v d_w^2} &= B_0 \bar{\delta}_0^{3/2} \sin\beta j_1; \\ \frac{R}{z v d_w^2} &= B_0 \bar{\delta}_0^{3/2} \cos\beta j_2. \end{aligned}\right\} \qquad (2.8)$$

Relations (2.8) differ from equations (2.1) in that in them terms are absent which consider the change in the angle of contact depending upon the position of the ball with respect to plane x0z.

With a zone of loading of 180°, when in the bearing half of the balls operates, $\lambda = \pm\infty$ and, consequently, $\beta = \beta_0$, $j_1 = 0.279$, $j_2 = 0.229$ and $w = 0.587$.

From relations (2.8) for the given case we find

$$\frac{A}{R} = \frac{j_1}{j_2} \operatorname{tg}\beta = 1{,}217 \operatorname{tg}\beta_0. \qquad (2.9)$$

besides

$$\left.\begin{aligned} P_0 &= \frac{R}{z\cos\beta j_2} = 4{,}37 \frac{R}{z\cos\beta_0}; \\ P_э &= wP_0 = 2{,}57 \frac{R}{z\cos\beta_0}. \end{aligned}\right\} \qquad (2.10)$$

Formulas (2.10) are known in the theory of antifriction bearings by the name of Schtribeck formulas.

For the case $\frac{A}{R} \neq 1{,}217 \operatorname{tg}\beta_0$ pressures P_0 and $P_э$ can be represented in the form

$$\left.\begin{aligned} P_0 &= 4{,}37\,\frac{K_0 F}{z\cos\beta_0}; \\ P_э &= 2{,}57\,\frac{KF}{z\cos\beta_0}. \end{aligned}\right\} \qquad (2.11)$$

where $F=(R^2+A^2)^{1/2}$ is the resultant load on the bearing (Fig. 4.4).

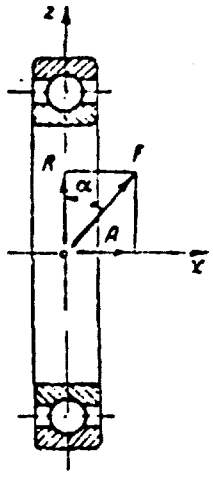

Fig. 4.4. Resultant force applied to the bearing.

This form of recording can be preserved taking into account the variability of angle β_ψ.

Substituting into expression (2.11) values P_0 and $P_э$ from equalities (2.3) and (2.5), we have

$$\left.\begin{aligned} K_0 &= \frac{B_0\bar{\delta}_0^{3/2}\cos\beta_0}{4{,}37\,\dfrac{F}{z\nu d_w^2}}; \\ K &= \frac{w}{0{,}587}K_0. \end{aligned}\right\} \qquad (2.12)$$

Coefficients K_0 and K are unique coefficients of reduction referred to the resultant load F. It is important that they can be found from equations (2.1) and (2.2) by different indirect methods excluding the necessity of a direct solution of these equations.

Values of coefficients K_0 and K for bearings with initial angles of contact $\beta_0 = 0^\circ$, 12°, 18°, and 36°, obtained from equations (2.1) and (2.2) by the graphoanalytical method [30], are given in Table 4.3.

Table 4.3.

$\frac{F}{\pi d_m^2}$ \ α	0°	10°	20°	30°	40°	50°	60°	70°	80°	90°
Values of coefficient K_0										
					$\beta_0 = 0$					
0,02	1,000	0,889	1,070	1,210	1,308	1,380	1,422	1,428	1,398	1,308
0,04	1,000	0,890	0,966	1,091	1,146	1,196	1,212	1,192	1,152	1,080
0,07	1,000	0,880	0,924	1,014	1,078	1,116	1,116	1,094	1,050	0,976
0,11	1,000	0,920	0,880	0,958	1,010	1,034	1,030	1,000	0,950	0,874
0,14	1,000	0,926	0,873	0,933	0,974	0,994	0,984	0,952	0,906	0,826
0,21	1,000	0,936	0,858	0,898	0,930	0,938	0,916	0,880	0,830	0,750
0,35	1,000	0,948	0,858	0,858	0,876	0,872	0,850	0,804	0,746	0,667
0,53	1,000	0,956	0,874	0,836	0,842	0,828	0,798	0,750	0,686	0,602
0,70	1,000	0,961	0,882	0,824	0,822	0,802	0,748	0,718	0,648	0,566
1,00	1,000	0,967	0,893	0,818	0,800	0,774	0,734	0,678	0,602	0,526
					$\beta_0 = 12°$					
0,02	1,399	1,171	0,839	0,897	0,963	0,999	1,005	0,992	0,937	0,877
0,04	1,249	1,109	0,842	0,875	0,933	0,959	0,956	0,938	0,883	0,808
0,07	1,184	1,077	0,847	0,858	0,902	0,918	0,914	0,879	0,824	0,752
0,11	1,136	1,046	0,853	0,841	0,871	0,881	0,870	0,831	0,777	0,705
0,14	1,114	1,034	0,860	0,831	0,859	0,862	0,847	0,809	0,754	0,681
0,21	1,086	1,018	0,870	0,816	0,833	0,833	0,809	0,771	0,713	0,636
0,35	1,056	1,008	0,889	0,803	0,806	0,799	0,781	0,721	0,655	0,579
0,53	1,038	1,002	0,899	0,802	0,789	0,772	0,734	0,688	0,623	0,538
0,70	1,028	0,995	0,908	0,810	0,778	0,754	0,715	0,665	0,601	0,514
1,00	1,020	0,983	0,912	0,813	0,761	0,734	0,694	0,636	0,567	0,479
					$\beta_0 = 18°$					
0,02	1,628	1,476	1,001	0,785	0,804	0,813	0,804	0,770	0,718	0,647
0,04	1,453	1,328	0,961	0,818	0,797	0,799	0,789	0,759	0,697	0,625
0,07	1,327	1,238	0,961	0,786	0,780	0,782	0,766	0,727	0,672	0,597
0,11	1,252	1,172	0,951	0,781	0,777	0,770	0,749	0,707	0,649	0,572
0,14	1,217	1,140	0,948	0,782	0,771	0,761	0,741	0,696	0,637	0,560
0,21	1,169	1,108	0,941	0,784	0,763	0,749	0,719	0,675	0,612	0,534
0,35	1,108	1,058	0,932	0,789	0,748	0,730	0,694	0,646	0,582	0,496
0,53	1,073	1,027	0,924	0,789	0,739	0,717	0,671	0,618	0,554	0,466
0,70	1,056	1,018	0,926	0,797	0,736	0,707	0,661	0,604	0,536	0,455
1,00	1,035	1,008	0,915	0,806	0,732	0,682	0,647	0,590	0,518	0,429

$\frac{F}{2\pi d_{in}^2}$ \ α	0°	10°	20°	30°	40°	50°	60°	70°	80°	90°
					$\beta_0 = 26°$					
0,02	1,914	1,815	1,478	0,872	0,692	0,667	0,641	0,594	0,530	0,454
0,04	1,609	1,528	1,321	0,865	0,692	0,665	0,635	0,587	0,523	0,447
0,07	1,483	1,415	1,218	0,858	0,692	0,661	0,629	0,577	0,514	0,440
0,11	1,389	1,326	1,150	0,850	0,692	0,656	0,621	0,566	0,504	0,431
0,14	1,336	1,279	1,119	0,847	0,692	0,655	0,618	0,560	0,500	0,424
0,21	1,249	1,204	1,069	0,845	0,692	0,650	0,611	0,551	0,492	0,413
0,35	1,175	1,125	1,011	0,837	0,693	0,647	0,600	0,544	0,480	0,398
0,53	1,121	1,078	0,975	0,828	0,696	0,642	0,593	0,535	0,466	0,383
0,70	1,087	1,051	0,955	0,826	0,698	0,639	0,589	0,527	0,455	0,373
1,00	1,051	1,016	0,932	0,819	0,701	0,632	0,580	0,515	0,440	0,358
					$\beta_0 = 36°$					
0,02	2,171	2,051	1,823	1,426	0,795	0,580	0,507	0,455	0,388	0,310
0,04	1,815	1,756	1,574	1,242	0,777	0,575	0,507	0,453	0,388	0,307
0,07	1,629	1,567	1,403	1,132	0,757	0,574	0,514	0,453	0,385	0,304
0,11	1,496	1,425	1,272	1,052	0,746	0,576	0,514	0,451	0,380	0,299
0,14	1,445	1,359	1,205	1,011	0,742	0,578	0,514	0,449	0,379	0,299
0,21	1,343	1,262	1,144	0,970	0,736	0,578	0,510	0,449	0,375	0,299
0,35	1,207	1,156	1,060	0,913	0,724	0,578	0,510	0,445	0,370	0,291
0,53	1,129	1,086	0,999	0,870	0,714	0,578	0,509	0,444	0,364	0,285
0,70	1,098	1,053	0,967	0,848	0,707	0,578	0,506	0,440	0,364	0,283
1,00	1,053	1,006	0,925	0,821	0,696	0,578	0,502	0,434	0,356	0,275
					Values of coefficient K					
					$\beta_0 = 0°$					
0,02	1,000	0,995	1,297	1,520	1,710	1,882	2,030	2,150	2,230	2,270
0,04	1,000	0,902	1,150	1,350	1,502	1,655	1,758	1,825	1,870	1,900
0,07	1,000	0,950	1,055	1,212	1,355	1,475	1,540	1,608	1,650	1,710
0,11	1,000	0,968	1,005	1,130	1,232	1,325	1 400	1,452	1,477	1,490
0,14	1,000	0,966	0,985	1,093	1,190	1,275	1,330	1,375	1,395	1,408
0,21	1,000	0,963	0,952	1,045	1,120	1,175	1,225	1,260	1,275	1,283
0,35	1,000	0,970	0,937	0,979	1,041	1,082	1,107	1,122	1,133	1,140
0,53	1,000	0,972	0,934	0,944	0,986	1,015	1,025	1,032	1,030	1,029
0,70	1,000	0,977	0,934	0,928	0,952	0,973	0,976	0,972	0,968	0,966
1,00	1,000	0,982	0,935	0,907	0,919	0,926	0,922	0,905	0,896	0,890
					$\beta_0 = 12°$					
0,02	1,237	1,090	0,929	1,039	1,190	1,301	1,384	1,438	1,460	1,489
0,04	1,125	1,051	0,919	0,991	1,142	1,235	1,299	1,333	1,360	1,377
0,07	1,093	1,034	0,913	0,979	1,082	1,159	1,213	1,257	1,270	1,290
0,11	1,065	1,014	0,913	0,963	1,040	1,10	1,146	1,181	1,186	1,197

Table 4.3. Continued

$\frac{F}{\rho v_0^2}$ \ α	0°	10°	20°	30°	40°	50°	60°	70°	80°	90°
0,14	1,053	1,006	0,914	0,951	1,017	1,071	1,111	1,136	1,149	1,152
0,21	1,037	0,999	0,916	0,921	0,981	1,022	1,051	1,057	1,062	1,077
0,35	1,017	0,994	0,923	0,897	0,937	0,969	0,983	0,986	0,991	0,969
0,53	1,010	0,988	0,929	0,885	0,911	0,927	0,931	0,925	0,918	0,917
0,70	1,006	0,982	0,931	0,883	0,891	0,897	0,892	0,885	0,877	0,869
1,00	1,001	0,976	0,933	0,873	0,870	0,864	0,851	0,834	0,826	0,812
					$\beta_0 = 18°$					
0,02	1,336	1,260	0,972	0,879	0,944	1,003	1,048	1,070	1,091	1,102
0,04	1,231	1,175	0,962	0,873	0,931	0,979	1,008	1,036	1,056	1,062
0,07	1,170	1,115	0,952	0,866	0,915	0,957	0,981	0,999	1,017	1,013
0,11	1,125	1,077	0,941	0,860	0,899	0,933	0,957	0,965	0,973	0,965
0,14	1,104	1,057	0,937	0,856	0,889	0,920	0,942	0,944	0,951	0,942
0,21	1,067	1,033	0,932	0,856	0,872	0,894	0,906	0,906	0,913	0,906
0,35	1,041	1,011	0,935	0,856	0,856	0,865	0,865	0,865	0,858	0,856
0,53	1,024	0,996	0,934	0,856	0,837	0,846	0,836	0,825	0,810	0,808
0,70	1,013	0,988	0,932	0,856	0,830	0,830	0,818	0,799	0,780	0,780
1,00	0,999	0,974	0,929	0,856	0,819	0,806	0,789	0,770	0,751	0,737
					$\beta_0 = 26°$					
0,02	1,451	1,411	1,227	0,863	0,775	0,778	0,782	0,778	0,775	0,767
0,04	1,285	1,249	1,132	0,863	0,773	0,776	0,773	0,772	0,767	0,759
0,07	1,215	1,195	1,078	0,859	0,772	0,769	0,764	0,761	0,754	0,747
0,11	1,182	1,159	1,034	0,856	0,769	0,762	0,754	0,749	0,741	0,732
0,14	1,150	1,120	1,011	0,854	0,768	0,758	0,749	0,741	0,732	0,722
0,21	1,096	1,071	0,980	0,850	0,766	0,755	0,741	0,729	0,719	0,705
0,35	1,043	1,021	0,959	0,847	0,764	0,746	0,728	0,707	0,692	0,678
0,53	1,016	0,992	0,936	0,841	0,764	0,737	0,714	0,690	0,668	0,652
0,70	1,015	0,971	0,923	0,836	0,764	0,732	0,705	0,678	0,652	0,634
1,00	0,989	0,953	0,905	0,836	0,764	0,726	0,701	0,658	0,634	0,615
					$\beta_0 = 30°$					
0,02	1,535	1,480	1,363	1,149	0,778	0,643	0,603	0,566	0,549	0,526
0,04	1,367	1,333	1,124	1,080	0,769	0,639	0,603	0,566	0,538	0,525
0,07	1,288	1,233	1,141	0,900	0,736	0,636	0,600	0,564	0,534	0,521
0,11	1,195	1,157	1,076	0,942	0,748	0,637	0,599	0,558	0,531	0,518
0,14	1,157	1,120	1,045	0,922	0,746	0,636	0,599	0,557	0,527	0,514
0,21	1,098	1,066	0,986	0,888	0,744	0,639	0,597	0,554	0,520	0,506
0,35	1,035	1,012	0,948	0,858	0,738	0,639	0,592	0,550	0,511	0,498
0,53	0,993	0,970	0,910	0,832	0,720	0,639	0,589	0,544	0,502	0,491
0,70	0,970	0,948	0,889	0,815	0,723	0,639	0,585	0,540	0,500	0,488
1,00	0,945	0,914	0,868	0,798	0,718	0,639	0,582	0,534	0,493	0,473

The introduction of tabulated coefficients of reduction K_0 and K considerably facilitates the detecting of pressures P_0 and $P_э$, which allow using for this purpose very simple and convenient formulas (2.11).

Coefficients K_0 and K are given in Table 4.3 in the function of quantity $\frac{F}{zvd_w^2}$, which characterizes the level of the load absorbed by the bearing, and angle $\alpha=\operatorname{arctg}\frac{A}{R}$, which determines the direction of resultant force F.[1]

2. Reduced Loads

Let us designate by Q the radial force creating in combination with the longitudinal force $A=1{,}217\ \operatorname{tg}\beta_0 Q$ at a constant angle of contact of the balls with the rings $\beta_\psi = \beta_0 = \text{const}$ the same equivalent pressure $P_э$ as that of the real combination of external loads applied to the bearing.

Force Q can be called the given dynamic load.

Along with the concept of reduced dynamic load in the theory of antifriction bearings there is widely used the concept of reduced static load. By the latter it is understood radial force Q_0, which creates in the indicated conditions the maximum pressure on the ball P_0 equal to the real.

Replacement of real loads by reduced loads, determined by the above-mentioned way, permits using in the calculation of bearings working under combined loads data of catalogs and reference books referring to radial loaded bearings.

Comparing equalities (2.10) and (2.11), we see that

$$\left.\begin{aligned} Q&=\kappa F;\\ Q_0&=\kappa_0 F. \end{aligned}\right\} \qquad (2.13)$$

In foreign and recently in Soviet practice, to determine reduced loads there is frequently used a formula of the form

$$Q=xR+yA.$$

Various sources give different values of coefficients of reduction x and y, and therefore the reduced loads calculated for the same calculation cases can differ considerably form each other.

Since all methods used of the calculation of radial and radial thrust ball bearings under combined loads are based on the same initial equations (1.1)-(1.7) and in fact differ from each other only by assumptions accepted for the simplification of their solution, then one of the main criteria of perfection of a certain calculation method can be the proximity of reduced loads calculated on its basis to "exact" values of these loads resulting from the indicated equations.

On Fig. 4.5 there are compared reduced loads, determined with help of coefficients of Table 4.3, with reduced loads found as a result of the "exact" solution of equations (1.1)-(1.7). On the same table there are shown reduced loads calculated by the method of the International Organization on Standardization (ISO[2]), accepted abroad recently, and also by the method of M. P. Belyanchikov [24], which is recommended now for the calculation of general-purpose bearings.

As can be seen from Fig. 4.5, reduced loads, obtained with the use of data of Table 4.3, are the closest to their "exact" values.

The application of the ISO method gives under certain conditions an overestimate of reduced loads of 20-30%, which for bearing subassemblies of aviation units, naturally, is impermissible.

With the calculation of radial thrust ball bearings with angles of contact $\beta_0 > 26°$, according to the method of M. P. Belyanchikov quite accurate values of reduced loads are obtained. However, at smaller angles of contact the accuracy of the method decreases considerably. This in the case of angles of contact $\beta_0 = 12-18°$ the error in a reduced load can reach 40%. For angles of contact less than 12° this method, in general, is inapplicable.

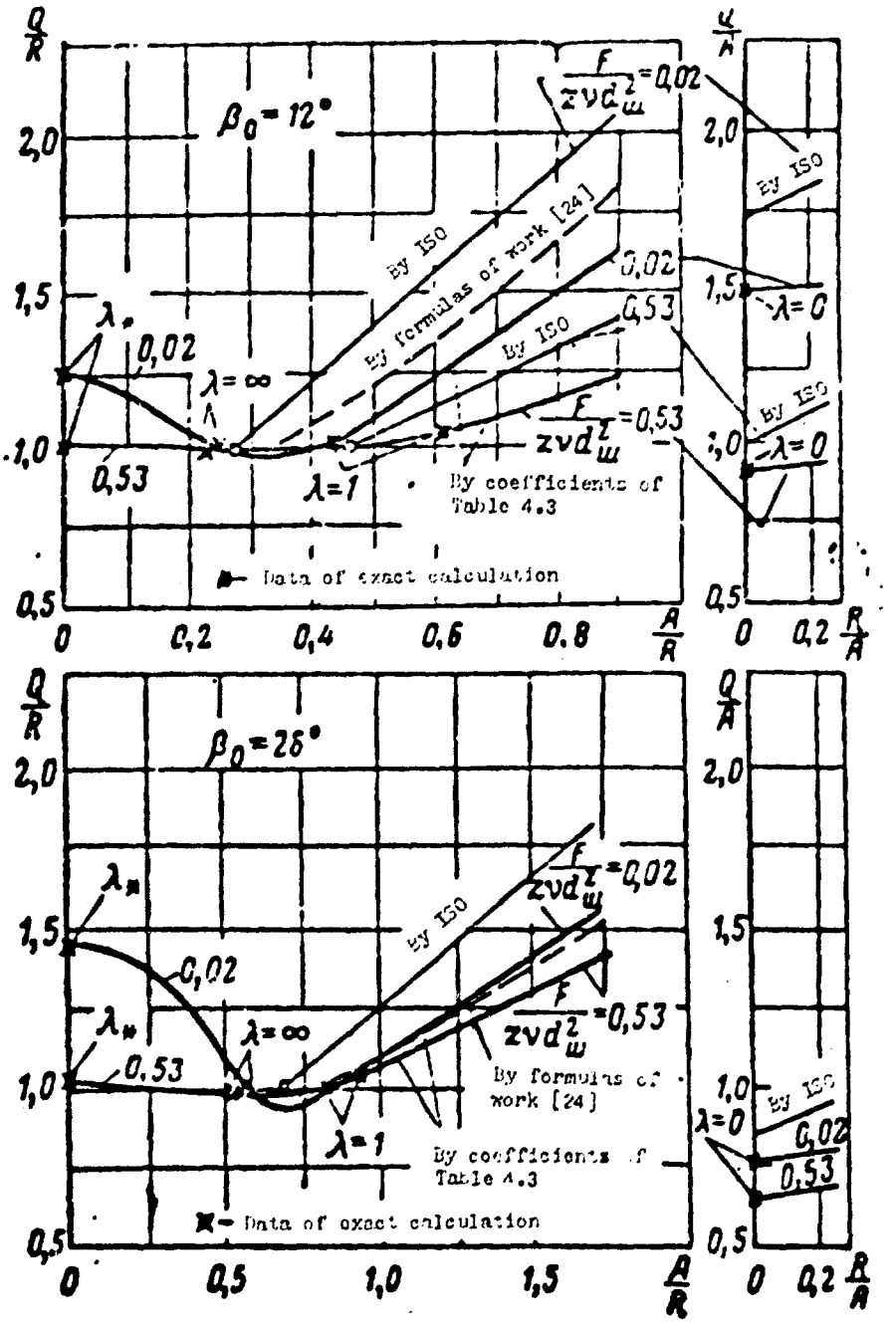

Fig. 4.5. Comparison of different methods of calculation of reduced loads on a bearing.

3. Static Theory of Dynamic Load Capacity

In calculations for service life there are usually used general regularities of the static theory of fatigue of metals, which assume that the destruction of the material under the action of live loads is a random process of the accumulation of fatigue damages possessing some probabilistic characteristics. Such an approach to the problem

of service life is valid for all machine parts operating under varying stresses, including antifriction bearings, which are put out of service due to fatigue crumbling of tracks or rolling solids.

Statistical representations, lying as the basis of contemporary methods of the determination of service lives of antifriction bearings, were developed mainly by Weibull [43], Lundberg, and Palmgren [44]. The development of these representations for small probabilities of destruction are the subject of the investigation of Harris [45] and others.

The basic positions of the statistical theory of the dynamic load capacity of antifriction bearings can be thus formulated.

Let us assume that $q_{\text{п}}$ is the probability of the fact that the bearing, rotating with the number of n revolutions per minute, will operate h hours without signs of fatigue.

On the basis of the theorem of mathematical statistics on the production of independent events, disregarding the probability of destruction of rolling solids in view of its smallness as compared to the probability of destruction rolling tracks, it is possible to write

$$q_{\text{п}} = q_{\text{вр}} q_{\text{вн}}, \tag{2.14}$$

where $q_{\text{вр}}$ and $q_{\text{вн}}$ are corresponding probabilities characterizing the reliability of revolving and fixed rings.

Considering the peculiarities of the stress condition under the action of contact loads and also the character of primary fatigue microscopic cracks, which form in antifriction bearings, Lundberg and Palmgren introduced the following distribution, which determines the probability F_{Δ} of the appearance of traces of fatigue on the section of the rolling track with a length ΔL after rolling about it of N rolling solids loaded by force P:

$$F_{\Delta} = 1 - \exp\left(-H_1 \frac{\tau_0^{m_1} N^l}{z_0^{m_1}} \Delta V\right). \tag{2.15}$$

Here H_1 is the coefficient dependent on properties of material,

cleanness of treatment and accuracy of manufacture; τ_0 – the greatest tangential stress acting in areas parallel to the surface of the area of contact deformation; z_0 – depth at which this stress appears; ΔV – stressed volume.

At $m_2 = 0$, which would take place in the case when the probability of destruction, introduced by each elementary volume, does not depend on its location with respect to the surface, and distribution (2.15) becomes the standard Weibull distribution.

Stress τ_0 and depth z_0 can be respectively expressed in terms of the greatest stress of crumpling σ_0 in the center of the area of contact deformation and the semiminor axis b of this area:

$$\left.\begin{aligned} \tau_0 &= \alpha_1 \sigma_0; \\ z_0 &= \alpha_2 b. \end{aligned}\right\} \tag{2.16}$$

Stressed volume ΔV in the first approximation can be taken equal to

$$\Delta V = 2az_0\Delta L, \tag{2.17}$$

where a is the semimajor axis of the area of contact deformation.

As follows from the theory of contact stresses and deformations, for radial and radial thrust ball bearings

$$\left.\begin{aligned} \sigma_0 &= \frac{4100}{\mu\nu}\left(4 \pm \frac{2}{\frac{1}{\eta} \mp 1} - \frac{1}{\theta}\right)^{\frac{2}{3}} P^{\frac{1}{3}} d_w^{-\frac{2}{3}}; \\ a &= 0{,}0108\mu\left(4 \pm \frac{2}{\frac{1}{\eta} \mp 1} - \frac{1}{\theta}\right)^{-\frac{1}{3}} P^{\frac{1}{3}} d_w^{\frac{1}{3}}; \\ b &= 0{,}0108\nu\left(4 \pm \frac{2}{\frac{1}{\eta} \mp 1} - \frac{1}{\theta}\right)^{-\frac{1}{3}} P^{\frac{1}{3}} d_w^{\frac{1}{3}}. \end{aligned}\right\} \tag{2.18}$$

In equalities (2.18) the following notations are accepted:

$$\eta = \frac{d_w \cos\beta_0}{2r_0} \quad \text{and} \quad \theta = \frac{r_{s(w)}}{d_w}.$$

Coefficients H_1, α_τ, and α_z, strictly speaking, are not constants; however, in practice this cannot be taken into account, since limits in which their values change (depending upon ratio b/a) are very insignificant.

It is not difficult to be convinced that

$$\Delta L=\frac{1}{2}d_w\cos\beta_0\left(\frac{1}{\eta}\mp 1\right)\Delta\psi, \tag{2.19}$$

where $\Delta\psi$ is the central angle corresponding to the examined section of the rolling tracks.

With help of equalities (2.16)-(2.19) let us give expression (2.15) in the form

$$F_\Delta=1-\exp\left(-H_2\cos^{\frac{9}{2}}\beta_0\frac{P^{ml}N^l}{d_w^{mlc}}\frac{\Delta\psi}{2\pi}\right). \tag{2.20}$$

The quantity of balls contacting with every section of the rolling track for h hours of bearing operation will be

$$N=30znh(1\pm\eta). \tag{2.21}$$

Substituting this value into formula (2.20), we finally obtain

$$F_\Delta=1-\exp\left[-H_3z^l\cos^{\frac{9}{2}}\beta_0(nh)^l\frac{P^{ml}}{d_w^{mlc}}\frac{\Delta\psi}{2\pi}\right]. \tag{2.22}$$

Indices m and c are expressed in terms of indices m_1, m_2, and l in the following way:

$$\left.\begin{aligned} m&=\frac{m_1+2-m_2}{3l};\\ c&=\frac{2m_1+m_2-5}{m_1+2-m_2}l. \end{aligned}\right\} \tag{2.23}$$

According to data of foreign bearing firms, generalized in recommendations of the ISO, m = 3 and c = 1.8 (at $d_w<25$ мм).

The section of rolling track of the fixed ring, located on azimuth ψ, with rolling about it of the balls is loaded each time by the same force P_ψ. Assuming in accordance with this in equality (2.22) $P = P_\psi$, for such a section we have

$$F_\Delta=1-\exp\left[-H_3z^l\cos^{\frac{9}{2}}\beta_0(nh)^l\frac{P_\psi^{ml}}{d_w^{mlc}}\frac{\Delta\psi}{2\pi}\right]. \tag{2.24}$$

From expression (2.24) it follows that probability $q_{кш}$, which characterizes the reliability of the fixed ring as a whole, is equal to

$$q_{кш}=\Pi(1-F_{\Delta j})=\exp\left[-H_3 z^l \cos\beta_0 (nh)^l \frac{P_{эк}^{ml}}{d_m^{mlc}}\right], \qquad (2.25)$$

where

$$P_{эш}=\left(\frac{1}{2\pi}\int_{\psi_н'}^{\psi_н''} P_\psi^{ml}\, d\psi\right)^{\frac{1}{ml}}.$$

During a quite long time interval each element of the rolling track of the ball race contacts with balls practically on all azimuths.

Taking this circumstance into account considering the hypothesis of linear summation of damage nature, for any section of the rolling track of the ball race from expression (2.22) we find

$$F_\Delta=1-\exp\left[-H_3 z^l \cos\beta_0 (nh)^l \frac{P_э^{ml}}{d_m^{mlc}}\frac{\Delta\psi}{2\pi}\right]. \qquad (2.26)$$

Here $P_э=\left(\frac{1}{2\pi}\int_{\psi_н'}^{\psi_н''} P^m\, d\psi\right)^{\frac{1}{m}}$ is the same equivalent pressure which was examined in No. 1.

The probability $q_{вр}$, which characterizes the reliability of the whole ball race in accordance with expression (2.26), will be

$$q_{вр}=\Pi(1-F_{\Delta j})=\exp\left[-H_3 z^l \cos\beta_0 (nh)^l \frac{P_э^{ml}}{d_m^{mlc}}\right]. \qquad (2.27)$$

Coefficient H_3, appearing in the above-mentioned equalities, can be represented in the form of the product of a certain constant H_4 and quantity

$$H_0=\frac{(1\pm\eta)^l\left(\frac{1}{\eta}\mp 1\right)}{(\mu\nu)^{m_1-1}\nu^{m_2}}\left(4\pm\frac{2}{\frac{1}{\eta}\mp 1}-\frac{1}{\theta}\right)^{\frac{2m_1+m_2-2}{3}}, \qquad (2.28)$$

which are functions η and θ, i.e., parameters characterizing the internal geometry of the bearing.

Let us assume that internal ring revolves. For this case from formulas (2.14), (2.25), and (2.27) we have

$$\ln\frac{1}{q_n}=\ln\frac{1}{q_{np}}+\ln\frac{1}{q_{nn}}=$$
$$=H_4\left[H_3+\left(\frac{P_{nn}}{P_n}\right)^{\omega_1}H_n\right]z^l\cos^{\gamma}\alpha_0(nh)^l\frac{P_n^{\omega l}}{d_n^{\omega lc}}. \qquad (2.29)$$

Subscripts "в" and "н" and also the upper and lower signs in formulas (2.18), (2.19), (2.21), and (2.28) respectively pertain to the inner and outer rings of the bearing.

Let us assume that at $\eta = 0.2$, $\theta = 0.52$, and $\lambda = \infty$

$$H_3+\left(\frac{P_{nn}}{P_n}\right)^{\omega l}H_n=H_5.$$

Let us introduce further quantities C_0 and f_q according to formulas:

$$C_0=f'f''d_n^c z^{\left(1-\frac{1}{\omega}\right)}, \qquad (2.30)$$

where

$$f'=\frac{1}{2{,}57}\left[\frac{1}{H_4H_5}\ln\frac{1}{0{,}9}\right]^{\frac{1}{\omega l}}$$

and

$$f''=\left[\frac{H_5}{H_3+\left(\frac{P_{nn}}{P_n}\right)^{\omega l}H_n}\right]^{\frac{1}{\omega l}};$$
$$f_q=\left[\frac{\lg\frac{1}{q_n}}{\ln\frac{1}{0{,}9}}\right]^{\frac{1}{\gamma}}. \qquad (2.31)$$

Using formulas (2.30) and (2.31), let us transform expression (2.29) thus:

$$0{,}39z\cos^{\gamma}\alpha_0P_n(nh)^{\frac{1}{\omega}}=C_0(\cos\alpha_0)^{\left(1-\frac{1}{\omega l}\right)}f_q^{\frac{1}{\omega l}}. \qquad (2.32)$$

Expressing here $P_э$ in terms of the equivalent dynamic load $Q_э$

we obtain:

$$Q(nh)^{\frac{1}{m}} = Cf_q^{\frac{1}{m}}, \tag{2.33}$$

where

$$C = C_0(\cos\beta_0)^{\left(1-\frac{1}{mi}\right)}.$$

Analogously there can be examined the case when the outer ring is revolving.

Uniting formulas of service life for cases of rotation of inner and outer rings, after the introduction into them of coefficients $K_б$ and $K_т$, considering the influence on carrying capacity of the character of load and temperature regime of the bearing, we finally have

$$K_б K_т K_к Q(nh)^{\frac{1}{m}} = Cf_q^{\frac{1}{m}}. \tag{2.34}$$

Here $K_к = 1$, if the inner ring rotates and

$$K_к = \left[\frac{H_в + \left(\frac{P_{вн}}{P_в}\right)^{mi} H_н}{H_н + \left(\frac{P_{вн}}{P_в}\right)^{mi} H_в}\right]^{\frac{1}{mi}}, \tag{2.35}$$

if the outer ring rotates.

With concrete numerical calculations of radial and radial thrust ball bearings, on the basis of tables of coefficients K_0 and K, values of kinematic coefficient K_K can be approximately determined depending upon quantity $w = 0.587 \frac{K}{K_0}$ according to the graph of Fig. 4.6.

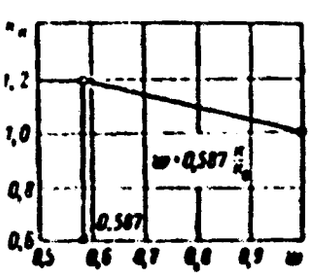

Fig. 4.6. Kinematic coefficient K_K.

In foreign practice in the calculation of coefficients of efficiency C_0 and C, coefficient f' is usually considered equal to 150-200.

Calculations show that at the given θ coefficient f" depends mainly upon η. At m = 3, C = 1.8 and l = 1.11, which corresponds to recommendations of ISO, it has the values shown in Table 4.4.

Table 4.4.

η	0,05	0,10	0,20	0,30	0,40
f''	0,77	0,92	1	0,93	0,81

For general-purpose bearings service life h_{10} is considered the calculated, at which the probability of destruction is equal to 10%.

Since at q = 0.9, f_q = 1, then

$$\kappa_\theta \kappa_t \kappa_\alpha Q (n h_{10})^{\frac{1}{m}} = C. \tag{2.36}$$

Comparing equalities (2.34) and (2.36), we find

$$\frac{h}{h_{10}} = f_q. \tag{2.37}$$

From formulas (2.37) and (2.31) it follows that the average service life of antifriction bearings is determined by the expression:

$$\frac{h_{cp}}{h_{10}} = \frac{\Gamma\left(1+\frac{1}{l}\right)}{\left(\ln \frac{1}{0,9}\right)^{\frac{1}{l}}}, \tag{2.38}$$

where Γ is the gamma function of the argument $\left(1+\frac{1}{l}\right)$.

The ratio of the median value of service life $h_{0,5}$, which corresponds to the reliability q = 0.5, to the calculation of service life h_{10} will be:

$$\frac{h_{0,5}}{h_{10}} = \left(\frac{\ln \frac{1}{0,5}}{\ln \frac{1}{0,9}}\right)^{\frac{1}{l}}. \tag{2.39}$$

Relations (2.38) and (2.39) show that the basic parameter characterizing the dispersion of service life of antifriction bearings is exponent l.

In most cases the ratio $\frac{h_{50}}{h_{10}}$ varies within limits of 4.08 to 5. At $\frac{h_{50}}{h_{10}}=4{,}08$, l = 1.34, and $\frac{h_{cp}}{h_{10}}=4{,}95$. If $\frac{h_{50}}{h_{10}}=5$, then l = 1.17 and $\frac{h_{cp}}{h_{10}}=6{,}5$.

As experimental investigations indicate, the given dependences satisfactorily describe the dispersion of service life at $q_n<0{,}9$. In the region of small probabilities of destruction noticeable deviations are observed from them. These deviations can be considered if for this region expression (2.37) is replaced by the following:

$$\frac{h-h_0}{h_{10}-h_0}=f_q. \tag{2.40}$$

Here h_0 is a certain threshold of service life up to which the probability of destruction is equal to zero.

Since at $q_n<0{,}9$ $f_q\approx[10(1-q_n)]^{\frac{1}{l}}$, then formula (2.40) can finally be written in the form

$$\frac{h}{h_{10}}=\left(1-\frac{h_0}{h_{10}}\right)[10(1-q_n)]^{\frac{1}{l}}+\frac{h_0}{h_{10}}. \tag{2.41}$$

According to data of Harris [45], for ball bearings $\frac{h_0}{h_{10}}\approx 0{,}045$. This denotes that to ensure 100 percent reliability it is necessary to have a reserve of calculation of service life of the order of 22, which corresponds to a reserve with respect to loads of 2.8.

Above the basic positions of the statistical theory of dynamic load capacity of radial and radial thrust ball bearings were discussed. Likewise corresponding statistical theories of dynamic load capacity for bearings of other types were constructed.

Main results emanating from statistical concepts about the service life of antifriction bearings were reflected both in foreign and in Soviet practice. With this, however, it is necessary to note

that certain dependences, used in the composition of Soviet catalogs and reference books, have a different form than that which is accepted abroad. Thus, for example, our coefficients of efficiency C_0 and C are calculated not by formulas (2.30) and (2.33), but are taken equal to

$$\left.\begin{aligned} C_0 &= f\frac{d_w^2}{1+0{,}02d_w}z^{\left(1-\frac{1}{m}\right)}; \\ C &= C_0\cos\beta_0. \end{aligned}\right\} \qquad (2.42)$$

For general-purpose bearings f = 65. Let us remember that in Soviet practice the exponent m is considered equal to 3.33.

The service life of two-row bearings, and also of rolling bearings, consisting of several identical bearings, which can be examined as one multiple bearing, is determined by the expression:

$$0{,}39\kappa_\phi\kappa_\tau z\cos\beta_0 P_{эк}(nh_{10})^{\frac{1}{m}} = C. \qquad (2.43)$$

The equivalent pressure entering here

$$P_{эк} = \left[\sum_{j=1}^{i}(\kappa_{\kappa j}P_э)^m\right]^{\frac{1}{m}}, \qquad (2.44)$$

where $P_{эj}$ and $\kappa_{\kappa j}$ are the equivalent load and kinematic coefficient for the j-th bearing.

Formulas (2.43) and (2.44) directly follow from the above-mentioned dependences for separate bearings.

If all bearings are loaded equally, then

$$P_{эк} = i^{\frac{1}{m}}\kappa_\kappa P_э. \qquad (2.45)$$

As the analysis of values of coefficients f" given in Table 4.4 shows, the efficiency of antifriction bearings noticeably depends on quantity η. In expressions (2.42) this important circumstance was not reflected, which is their considerable deficiency.

As is known, for aviation bearings possessing high accuracy and made from a specially qualitative metal, the coefficients of efficiency

have much greater values than do those which are obtained from formula (2.-3) at $f = 65$.

Therefore, using in calculation aviation constructions data of machine construction catalogs and reference books, it is possible to expect that in reality calculation service life h_{10} will correspond not to the 10 percent probability of destruction but to one considerably smaller. With such an approach to the determination of service life of bearing subassemblies of aviation units, this service life is frequently identified with the required service life. In practice this is achieved by the fact that in formulas (2.36) and (2.43) h_{10} is replaced by h, and by h is understood service life at which the level of reliability of bearings necessary for articles of aviation materiel is provided.

4. Effect of Axial Load on the Efficiency of Bearings

Let us trace how the axial load influences the efficiency of radial and radial thrust ball bearings.

Figures 4.7 and 4.8 show model graphs of the dependence $\frac{Q}{R} = f\left(\frac{A}{R}\right)$ at $\frac{R}{zvd_w^2} = \text{const}$, constructed according to data of calculation carried out in the composition of tables of coefficients K_0 and K.

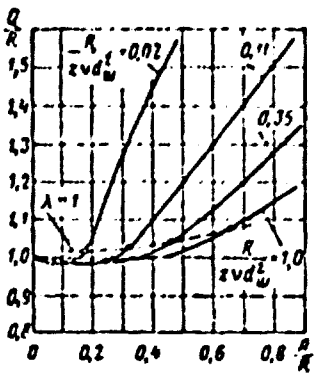

Fig. 4.7. Graphs of the dependence Q/R = f(A/R) at certain constant values $\frac{R}{zvd_w^2}$ and $\beta_0 = 0$.

As can be seen from these graphs, for each level of load there exists a range of values $\frac{A}{R}$ in which $\frac{Q}{R} < 1$. Its limits are given in Table 4.5.

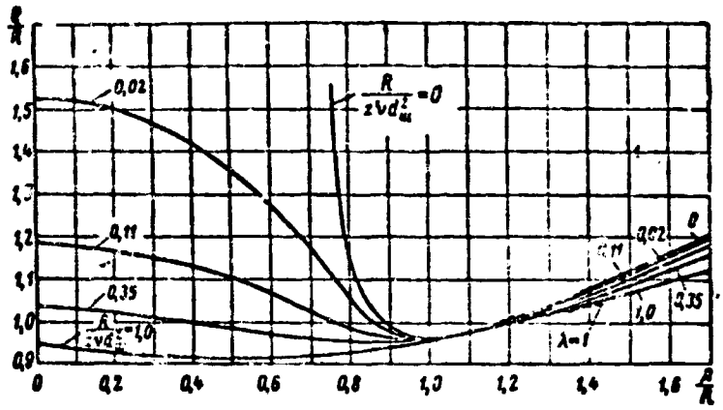

Fig. 4.5. Graphs of the dependence $Q/R = f(A/R)$ at certain constant values $\frac{R}{zvd_w^2}$ and $\beta_0 = 36°$.

Table 4.5.

$\frac{R}{zvd_w^2}$	Value A/R at initial angles of contact β_0 deg				
	0	12	18	26	36
0,02	0—0,15	0,26—0,38	0,39—0,56	0,56—0,82	0,34—1,20
0,11	0—0,28	0,25—0,45	0,37—0,60	0,55—0,84	0,76—1,21
0,35	0—0,37	0,22—0,47	0,35—0,63	0,47—0,85	0,38—1,21
1,00	0—0,43	0,04—0,49	0,00—0,65	0,00—0,86	0,00—1,22

At values $\frac{A}{R}$, shown in Table 4.5, the axial load not only does not lower the carrying capacity of the bearing but even increases it somewhat. It is true that this increase is insignificant, since a possible decrease in the given dynamic load amounts to several percent.

In radial thrust ball bearings acting on the balls are Coriolis forces, which try to force them to revolve around axes perpendicular to the surfaces of contact. Such "spinning" of the balls are prevented by frictional forces appearing at points of tangency with the rings. If in bearing there is an unloaded zone, then in this zone frictional forces preventing "spinning" of the balls are absent, and the balls start to slip with respect to grooves of the rings, which at high speeds of rotation leads to overheating and rapid wear of the bearings. It is natural that with the designing of high-speed bearing subassemblies with radial thrust ball bearings, it is necessary always to try to have the load carried by all the balls. In practice this is

attained either by means of the installation of bearings with appropriate angles of contact or by their certain additional axial load owing to preliminary interference.

The magnitude of the zone of loading depends on relationship of axial and radial loads applied to the bearing. The larger the ratio A/R, the bigger this zone. As was already indicated earlier, when $\psi_0 = 0$ the zone of load amounts to 360° if $0 \leq \lambda \leq 1$. The value $\lambda = 0$ corresponds to the case of axial loading of the bearing at which pressures on the balls are identical. The value $\lambda = 1$ determines the minimum value of the ratio A/R at which all the balls are loaded. This, in particular, follows from formula (1.22), which shows that in the case $\psi_0 = 0$ and $\lambda = 1$ the force absorbed by the ball located at the azimuth $\psi_0 = 180°$ turns into zero.

Considering that $\lambda = 1$, $j_1 = 0.425$, $j_2 = 0.225$, and $j_3 = 0.231$, from equations (2.1) and (2.2) we find

$$\frac{A}{R_{(\lambda=1)}} = 1{,}666 \frac{\left(\sin^2\beta_0 + \bar{\delta}_0 + \frac{\bar{\delta}_0^2}{4}\right)^{1/2}}{\cos\beta_0} \cdot \frac{1 - 0{,}6\frac{\bar{\delta}_0}{2+\bar{\delta}_0}}{1 + 0{,}905\frac{\sin^2\beta_0 + \bar{\delta}_0 + \frac{\bar{\delta}_0^2}{4}}{\cos^2\beta_0}\frac{\bar{\delta}_0}{2+\bar{\delta}_0}}, \tag{2.46}$$

and here the radial loading R is determined by the expression

$$\frac{R}{z v d_w^2} = 0{,}51 B_0 \cos^{\frac{3}{2}}\beta_0 \frac{\bar{\delta}_0^{3/2}}{2+\bar{\delta}_0}\left(1 + 0{,}905\frac{\sin^2\beta_0 + \bar{\delta}_0 + \frac{\bar{\delta}_0^2}{4}}{\cos^2\beta_0}\frac{\bar{\delta}_0}{2+\bar{\delta}_0}\right), \tag{2.47}$$

and relation

$$\left(\frac{Q}{R}\right)_{\lambda=1} = 0{,}5025 \cdot \frac{2+\bar{\delta}_0}{1 + 0{,}905\frac{\bar{\delta}_0}{2+\bar{\delta}_0}\frac{\sin^2\beta_0 + \bar{\delta}_0 + \frac{\bar{\delta}_0^2}{4}}{\cos^2\beta_0}}. \tag{2.48}$$

As can be seen from equalities (2.46), (2.47), and (2.48), quantities $\left(\frac{A}{R}\right)_{\lambda=1}$ and $\left(\frac{Q}{R}\right)_{\lambda=1}$ depend both on the initial angle of contact and also on the level of the load absorbed by the bearing.

For the most frequently encountered initial angles of contact

$\beta_0 = 0°$, 12°, 18°, 26°, and 36° with the help of equalities (2.46), (2.47), and (2.48) on Figures 4.9 and 4.10 there are plotted curves which determine values $\left(\frac{A}{R}\right)_{\lambda=1}$ and $\left(\frac{Q}{R}\right)_{\lambda=1}$ in function $\frac{R}{z\nu d_w^2}$.

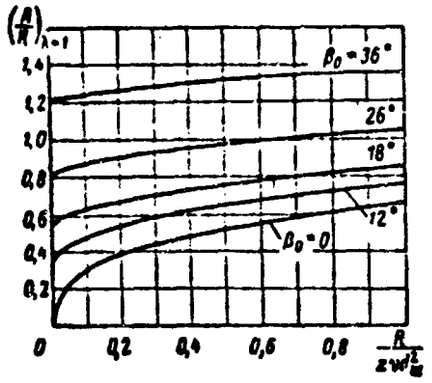

Fig. 4.9. Dependence of the ratio $\left(\frac{A}{R}\right)_{\lambda=1}$ on the level of the load.

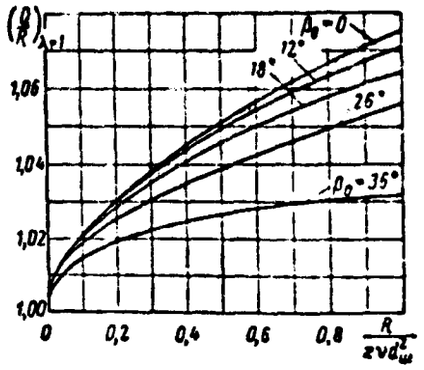

Fig. 4.10. Dependence of the ratio $\left(\frac{Q}{R}\right)_{\lambda=1}$ on the level of the load.

At small loads

$$\left(\frac{A}{R}\right)_{\lambda=1} \approx 1{,}67 \operatorname{tg} \beta_0 \text{ and } \left(\frac{Q}{R}\right)_{\lambda=1} \approx 1.$$

With an increase in load quantities $\left(\frac{A}{R}\right)_{\lambda=1}$ and $\left(\frac{Q}{R}\right)_{\lambda=1}$ increase. Thus, for example, for angle $\beta_0 = 18°$ when $\frac{R}{z\nu d_w^2} = 1$

$$\left(\frac{A}{R}\right)_{\lambda=1} = 2{,}6 \operatorname{tg} \beta_0 \text{ and } \left(\frac{Q}{R}\right)_{\lambda=1} = 1{,}064.$$

As was shown above, in the case of a constant angle of contact of the balls with rings with the zone of loading of 180°, when parameter $\lambda = \pm\infty$, the ratio $\frac{A}{R} = 1{,}217 \operatorname{tg} \beta_0$.

Values of ratio $\left(\frac{A}{R}\right)_{\lambda=\infty}$, taking into account the change in the angle of contact depending upon the position of the ball with respect to plane x0z, can be found by the curves shown on Fig. 4.11. Figure 4.12 depicts curves by which there can be determined appropriate values of the ratio $\left(\frac{Q}{R}\right)_{\lambda=\infty}$.

Graphs on Figs. 4.11 and 4.12 are plotted with the help of formulas

$$\left.\begin{aligned}
\left(\frac{A}{R}\right)_{\lambda=\infty} &= 1{,}217 \operatorname{tg}\beta_0 \cdot \frac{1-0{,}822\bar{\delta}_0}{1+0{,}868\operatorname{tg}^2\beta_0\bar{\delta}_0};\\
\left(\frac{R}{zvd_w^2}\right)_{\lambda=\infty} &= 0{,}229 B_0 \bar{\delta}_0^{3/2}\cos\beta_0(1+0{,}868\operatorname{tg}^2\beta_0\bar{\delta}_0);\\
\left(\frac{Q}{R}\right)_{\lambda=\infty} &= \frac{1}{1+0{,}868\operatorname{tg}^2\beta_0\bar{\delta}_0}.
\end{aligned}\right\} \qquad (2.49)$$

which results from equations (2.1) and equalities (2.12) and (2.13).

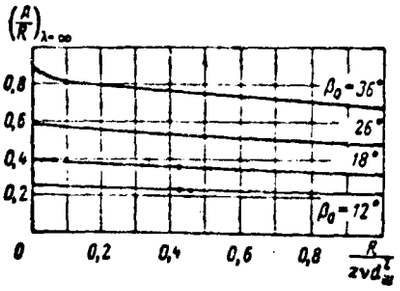

Fig. 4.11. Dependence of ratio $\left(\frac{A}{R}\right)_{\lambda=\infty}$ on the level of the load.

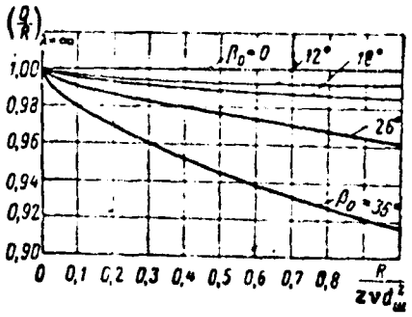

Fig. 4.12. Dependence of ratio $\left(\frac{Q}{R}\right)_{\lambda=\infty}$ on the level of the load.

The given data permit estimating the influence of the axial load on the carrying capacity of radial and radial thrust ball bearings. With their help there can be set the optimum axial preliminary interference with which bearings should be assembled in the subassembly, and the most rational values of the initial angle of contact β_0 for different combinations of the radial and axial loads are selected.

5. Approximate Solutions of Equations (2.1) and (2.2)

It is necessary to remember that the angle β_0 is determined by the working radial clearance 2Δ, which is in the bearing after its fitting on the shaft and into the housing at a stabilized temperature regime of operation of the unit and also at the actual distance g between centers O_H and O_B of sections of grooves of the rings [see Fig. 4.2 and formula (1.7)].

Because of the effect of landing interferences, the irregularity in the heating of separate elements of the subassembly and also the possible difference in values of coefficients of linear expansion of the shaft and housing, the clearance 2Δ can considerably differ from the initial radial clearance in the free bearing. The magnitude of distance g can noticeably be affected by deviations in radii of grooves of the rings and diameter of the ball. In connection with this, in the calculation of high-loaded radial and radial thrust ball bearings the angle β_0 cannot always be replaced by the nominal initial angle of contact shown in the catalog. It is impossible to forget this circumstance in the designing of specially critical bearing subassemblies of units of helicopters and other aircraft.

Values of coefficients K_0 and K for radial and radial thrust ball bearings with initial angles of contact β_0 different from the standard can be obtained by the interpolation of data given in Table 4.3. At the same time there are many cases when it is more convenient to resort to this method but to solve problems connected with the calculation of such bearings by means of direct determination of quantities $\bar{\delta}_0$ and λ from equations (2.1) and (2.2), using with this purpose the methods of approximation.

If $\frac{A}{R} > \left(\frac{A}{R}\right)_{\lambda=1}$, i.e., the load is carried by all the balls, then integrals can be found from expressions:

$$\left.\begin{aligned} J_1(1+\lambda)^{3/2} &= 1+\frac{3}{16}\lambda^2; \\ J_2(1+\lambda)^{3/2} &= \frac{3}{4}\lambda\left(1-\frac{1}{32}\lambda^2\right); \\ J_3(1+\lambda)^{3/2} &= \frac{1}{2}\left(1+\frac{9}{32}\lambda^2\right). \end{aligned}\right\} \qquad (2.50)$$

The right-hand side of equalities (2.50) constitute first terms of a power series, in which products $j_\lambda(1+\lambda)^{5/3}$ at $\psi_0=0$ and $0<\lambda<1$ are expanded. Considering the rapid convergence of this series in the shown region, terms containing parameter λ in a power higher than the third are rejected here.

Solving equations (2.1) and (2.2) taking into account equalities (2.50), as a result of successive approximations we obtain the working formulas:

$$\bar{\delta}_0=\left(\frac{\bar{\lambda}}{D_3}\right)^{2/3}\frac{\left[1+\left(\frac{\bar{\lambda}}{1{,}41\,D_3}\right)^{1/2}\right]^{2/3}}{\left[\sin^2\beta_0+2\left(\frac{\bar{\lambda}}{1{,}41\,D_3}\right)^{1/2}\right]^{1/3}}\left(1+D_2\,\frac{1+\frac{3}{16}D_2^2}{1-\frac{1}{32}D_2^2}\right); \tag{2.51}$$

$$\lambda=D_2\,\frac{1+\frac{3}{16}D_2^2}{1-\frac{1}{32}D_2^2}, \tag{2.52}$$

where

$$\bar{\lambda}=\frac{\lambda}{B_0 z w d_m^2}.$$

Coefficients D_1, D_2, and D_3 are respectively equal to:

$$\left.\begin{aligned}
D_1&=\bar{\lambda}^{2/3}\frac{\left[1+\left(\frac{\bar{\lambda}}{1{,}41}\right)^{1/2}\right]^{2/3}}{\left[\sin^2\beta_0+2\left(\frac{\bar{\lambda}}{1{,}41}\right)^{1/2}\right]^{1/3}};\\
D_2&=\frac{4}{3}\cdot\frac{R}{A}\,\frac{(\sin^2\beta_0+2D_1)^{1/2}}{\cos\beta_0\left(1+\frac{2}{3}\,\frac{\sin^2\beta_0+2D_1}{\cos^2\beta_0}\,\frac{D_1}{1+D_1}\right)};\\
D_3&=\left(1+\frac{3}{16}D_2^2\right)\left(1-\frac{3}{4}D_2^2\cdot\frac{1-\frac{1}{32}D_2^2}{1+\frac{3}{16}D_2^2}\cdot\frac{D_1}{1+D_1}\right).
\end{aligned}\right\} \tag{2.53}$$

At $\frac{A}{R}\geq\left(\frac{A}{R}\right)_{\lambda=1}$ the formula for maximum pressure on the ball can be represented in the form

$$P_0=\bar{\alpha}_0^{(A)}\frac{A}{\pi}. \tag{2.54}$$

From expressions (2.3) and (2.51) it follows that coefficient

$\bar{\kappa}_0^{(A)}$ in formula (2.54) can be assumed equal to

$$\bar{\kappa}_0^{(A)} = \frac{\left(1 + D_2 \dfrac{1 + \frac{3}{16} D_2^2}{1 - \frac{1}{32} D_2^2}\right)^{3/2} \left[1 + \left(\dfrac{\bar{\lambda}}{1{,}41 D_3}\right)^{1/2}\right]}{D_3 \left[\sin^2 \beta_0 + 2\left(\dfrac{\bar{\lambda}}{1{,}41 D_3}\right)^{1/2}\right]^{3/2}}. \tag{2.55}$$

It is easy to note that in the examined case the reduced loads Q_0 and Q can be expressed in the following way:

$$\left.\begin{aligned} Q_0 &= 0{,}229 \bar{\kappa}_0^{(A)} \cos \beta_0 A; \\ Q &= 0{,}390 w \bar{\kappa}_0^{(A)} \cos \beta_0 A. \end{aligned}\right\} \tag{2.56}$$

Comparing equalities (2.56) and (2.13), for the given case we find:

$$\left.\begin{aligned} \kappa_0 &= 0{,}229 \bar{\kappa}_0^{(A)} \cos \beta_0 \sin \alpha; \\ \kappa &= 0{,}390 w \bar{\kappa}_0^{(A)} \cos \beta_0 \sin \alpha. \end{aligned}\right\} \tag{2.57}$$

If radial loading R = 0, then in accordance with equalities (2.53) $D_2 = 0$, and $D_3 = 1$. Substituting these values into expression (2.55), for the case of a purely axial load we have

$$\bar{\kappa}_0^{(A)} = \bar{\kappa}_{00}^{(A)} = \frac{1 + \left(\dfrac{\bar{\lambda}}{1{,}41}\right)^{1/2}}{\left[\sin^2 \beta_0 + 2\left(\dfrac{\bar{\lambda}}{1{,}41}\right)^{1/2}\right]^{3/2}}. \tag{2.58}$$

Figure 4.13 gives curves of the dependence $\bar{\kappa}_{00}^{(A)} = \bar{\kappa}_{00}^{(A)}(\bar{\lambda})$, obtained from initial equations of static equilibrium of radial and radial

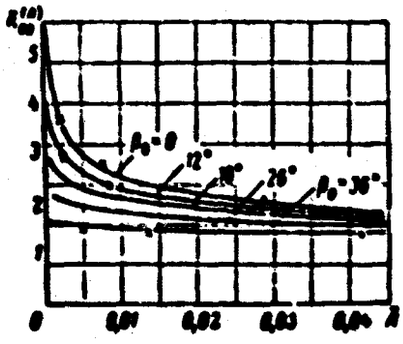

Fig. 4.13. Curves of the dependence $\bar{\kappa}_{00}^{(A)} = \bar{\kappa}_{00}^{(A)}(\bar{\lambda})$.

thrust ball bearings without any simplifying assumptions. On the same figure sign "×" denotes value of the coefficient $\bar{K}_{\omega}^{(A)}$, calculated by formula (2.58), which makes it possible visually to be convinced of its quite satisfactory accuracy.

The described method of the determination of quantities $\bar{\delta}_0$ and λ can be used only in the case when in the bearing there are no unloaded balls.

Let us assume that now the zone of loading amounts to less than 360°. With a zone of loading smaller than 360° quantity λ can vary from ∞ to 1 and from $-\infty$ to a certain negative value λ_*, which corresponds to the case when the bearing absorbs a purely radial loading. In the absence of an axial load the center of the area of contact "creeps" to the middle of the groove, and angle β turns into zero. Assuming in formula (1.19) angle β is equal to zero, we see that with radial loading of the bearing

$$\bar{\delta} = \cos\beta_0 - 1. \tag{2.59}$$

Let us introduce the notations

$$\left.\begin{aligned} E_1 &= \frac{1}{(1+\lambda)f_2^{2/3}}; & E_2 &= \frac{\lambda}{1+\lambda}\cdot\frac{f_1}{f_2^{2/3}}; \\ E_3 &= \frac{f_1}{f_2}; & E_4 &= \lambda\cdot\frac{f_1}{f_2}. \end{aligned}\right\} \tag{2.60}$$

Values of quantities E in function λ are given in Table 4.6.

Table 4.6.

$\frac{1}{\lambda}$	E_1	E_2	E_3	E_4	$\frac{1}{\lambda}$	E_1	E_2	E_3	E_4
1	1,244	1,125	1,666	0,800	−0,1	−0,304	2,670	1,185	−8,441
0,9	1,173	1,149	1,594	0,697	−0,2	−0,704	3,126	1,164	−4,296
0,8	1,097	1,187	1,532	0,816	−0,3	−1,245	3,146	1,139	−2,927
0,7	1,017	1,242	1,476	0,968	−0,4	−2,021	4,597	1,115	−2,243
0,6	0,930	1,317	1,430	1,166	−0,5	−3,191	5,899	1,093	−1,829
0,5	0,831	1,409	1,386	1,443	−0,6	−5,111	7,988	1,075	−1,550
0,4	0,717	1,522	1,346	1,857	−0,7	−8,663	11,74	1,061	−1,360
0,3	0,586	1,662	1,309	2,546	−0,8	−16,93	20,23	1,032	−1,210
0,2	0,429	1,836	1,277	3,915	−0,9	−47,4	52,48	1,015	−1,054
0,1	0,238	2,055	1,247	8,021	−1	−∞	∞	1	−1
0	0	2,321	1,217	∞					

At $\bar{\delta} = \cos \beta_0 - 1$ and $\beta = 0$ the second equation (2.1) can be thus represented:

$$\bar{R}^{2\alpha} = \frac{\cos \beta_0 - 1}{E_1}, \tag{2.61}$$

where

$$\bar{R} = \frac{R}{B_0 r w_m^2}.$$

Let us remember that in accordance with the accepted direction of axis z angle $\psi_0 = 0$ and, consequently, $\lambda \cos \psi_0 = \lambda$ and $\bar{\delta}_0 = \bar{\delta}(1+\lambda)$.

From equality (2.62) [sic] it follows that λ_* should satisfy the condition

$$E_1(\lambda_*) = \frac{\cos \beta_0 - 1}{\bar{R}^{2\alpha}}. \tag{2.62}$$

To solve equations (2.1) and (2.2) in the case $\frac{A}{R} < \left(\frac{A}{R}\right)_{\lambda=1}$ we will proceed in the following way. Considering parameter λ to be known, with the help of the method of iterations we will find from the second equation (2.1) quantity $\bar{\delta} = \frac{\bar{\delta}_0}{1+\lambda}$. Replacing trigonometric functions of angle β by corresponding values emanating from equation (2.2), as the approximate value $\bar{\delta}$ we will take

$$\bar{\delta} = G_1^{2\alpha} E_1 \left(\frac{\bar{R}}{\cos \beta_0}\right)^{2\alpha}. \tag{2.63}$$

where

$$G_1 = \frac{1 + E_1 \left(\frac{\bar{R}}{\cos \beta_0}\right)^{2\alpha}}{1 + E_1 \left(\frac{\bar{R}}{\cos \beta_0}\right)^{2\alpha}} \cdot \frac{\sin^2 \beta_0 + 2E_1 \left(\frac{\bar{R}}{\cos \beta_0}\right)^{2\alpha} + E_1^2 \left(\frac{\bar{R}}{\cos \beta_0}\right)^{4\alpha}}{\cos^2 \beta_0 \left[1 + E_1 \left(\frac{\bar{R}}{\cos \beta_0}\right)^{2\alpha}\right]}. \tag{2.64}$$

It should be kept in mind that inasmuch as expression (2.63) is approximate, value $\bar{\delta}$, determined from this expression when $\lambda = \lambda_*$, somewhat differs from the value corresponding to formula (2.59).

From equations (2.1) we have further

$$\frac{A}{R}=\frac{E_3}{\cos\beta_0}\frac{(\sin^2\beta_0+2\bar{\delta}+\bar{\delta}^2)^{1/2}}{1+\frac{\sin^2\beta_0+2\bar{\delta}+\bar{\delta}^2}{\cos^2\beta_0}\cdot\frac{E_2}{E_1}\cdot\frac{\bar{\delta}}{1+\bar{\delta}}}\left(1-E_4\frac{\bar{\delta}}{1+\bar{\delta}}\right). \qquad (2.65)$$

Assigning λ, we construct with the help of formulas (2.63) and (2.65) a graph of the dependence $\frac{A}{R}=F(\lambda)$ (Fig. 4.14). According

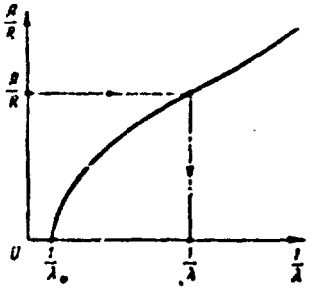

Fig. 4.14. Auxiliary graph for the approximate solution of equations (2.1) with the zone of loading smaller than 360°.

to this graph, knowing ratio A/R, we find value λ, which is the approximate solution to equations (2.1) and (2.2). Using the obtained value of λ, we calculate by formula (2.63) the real value $\bar{\delta}$ and find by it $\bar{\delta}_0$.

As numerical calculations show, the accuracy of formulas (2.63) and (2.65), just as that of formulas (2.51) and (2.52), is quite sufficient for engineering applications. Deviations of quantities $\bar{\delta}_0$ and λ, calculated with the help of the indicated formulas, from corresponding "exact" values, determined by equations (2.1) and (2.2), at initial angles of contact $\beta_0 \leq 45^\circ$ amount to, as a rule, not more than 3-4%.

Following by expression (2.63), we can write

$$P_0=B_0\nu d_w^2(1+\lambda)^{3/2}G_1E_1^{1/2}\frac{\bar{\delta}^{3/2}}{\cos\beta_0}. \qquad (2.66)$$

Remembering that $E_1=\frac{1}{(1+\lambda)\beta_2^{3/2}}$ and $\bar{\delta}=\frac{R}{B_0\nu d_w^2}$, for the case $\frac{A}{R}<\left(\frac{A}{R}\right)_{\lambda=1}$ we find

$$P_0=K_0^{(R)}\frac{R}{z\cos\beta_0}. \qquad (2.67)$$

Here

$$\kappa_0^{(n)}=\frac{\sigma_1}{h}. \tag{2.68}$$

Comparing equalities (2.11) and (2.67), it is easy to be convinced that coefficient κ_0 in this case can be thus expressed:

$$\kappa_0=0{,}229\kappa_0^{(n)}\cos\alpha.$$

Accordingly,

$$\kappa=0{,}390\omega\kappa_0^{(n)}\cos\alpha.$$

6. Relative Displacements of Rings

For certain high-precision high-speed bearing subassemblies the correct determination of relative displacements of rings of bearings under a load is important. With the absorption by radial and radial thrust ball bearings of combined loads this problem is solved in this way.

As can be seen from relations (1.13) and (1.16), in the absence of mutual misalignment of rings $\left(\bar{\varepsilon}=\theta\frac{2}{g}=0\right)$

$$\left.\begin{aligned}\bar{s}&=\operatorname{tg}\beta\cos\beta_0;\\ \bar{u}&=\frac{\bar{\Delta}}{\cos\beta}.\end{aligned}\right\} \tag{2.69}$$

Using the dependence (1.19), we find

$$\left.\begin{aligned}\bar{s}&=(\sin^2\beta_0+2\bar{\delta}+\bar{\delta}^2)^{1/2};\\ \bar{u}&=\frac{\bar{\Delta}(1+\bar{\delta})}{\cos\beta_0}.\end{aligned}\right\} \tag{2.70}$$

Let us assume that $\frac{\Delta}{R}>\left(\frac{\Delta}{R}\right)_{-1}$. Under this condition, disregarding in equalities (2.49) quantity $\bar{\delta}^2$ in view of its smallness, with the help of formulas (2.51) and (2.52) we obtain for relative displacements $\bar{s}$ and $\bar{u}$ the following expressions:

$$\bar{s}=\left\{\sin^2\beta_0+2\left(\frac{\bar{\lambda}}{D_3}\right)^{2/3}\frac{\left[1+\left(\frac{\bar{\lambda}}{1{,}41D_3}\right)^{1/2}\right]^{2/3}}{\left[\sin^2\beta_0+2\left(\frac{\bar{\lambda}}{1{,}41D_3}\right)^{1/2}\right]^{1/3}}\right\}^{1/2};$$

$$\bar{u}=\frac{D_2}{\cos\beta_0}\cdot\frac{1+\frac{3}{16}D_2^2}{1-\frac{1}{32}D_2^2}\left(\frac{\bar{\lambda}}{D_3}\right)^{2/3}\frac{\left[1+\left(\frac{\bar{\lambda}}{1{,}41D_3}\right)^{1/2}\right]^{2/3}}{\left[\sin^2\beta_0+2\left(\frac{\bar{\lambda}}{1{,}41D_3}\right)^{1/2}\right]^{1/3}}. \qquad (2.71)$$

As displacements $\bar{s}$ and $\bar{u}$ are changed with a change in relationships of radial and axial loads, this can be traced in the example of bearing 36207, for which on Fig. 4.15 by formulas (2.71) there

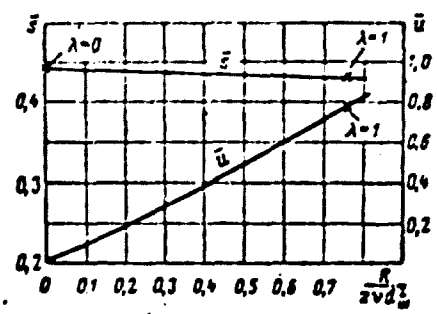

Fig. 4.15. Curves $\bar{u}=\bar{u}\left(\frac{R}{zvd_w^2}\right)$ and $\bar{s}=\bar{s}\left(\frac{R}{zvd_w^2}\right)$ at a constant value of the axial load.

are plotted curves $\bar{u}=\bar{u}\left(\frac{R}{zvd_w^2}\right)$ and $\bar{s}=\bar{s}\left(\frac{R}{zvd_w^2}\right)$ at a constant value of the axial load $\left(\frac{\lambda}{zvd_w^2}=0{,}53\right)$. For a comparison on the same figure the sign "x" denotes accurate values of displacements $\bar{s}$ and $\bar{u}$ calculated with the help of equations (1.3), (1.6), and (1.7) for cases $\lambda = 0$ and $\lambda = 1$, which determine the limits of applicability of formulas (2.71).

As follows from the cited data, the equation of moments does not enter into the system of equations with the help of which there is investigated the distribution of the load in radial and radial thrust ball bearings operating without misalignment of the rings. Therefore, the assumption of the action of radial force and moment in one plane, used in the formulation of relations (1.24), does not introduce any additional limitations narrowing the field of application of the above-stated method of calculation of such bearings.

Thus far radial and axial loads acting on bearing were considered assigned.

Radial loadings on bearings are found from equations of equilibrium of the shaft on which they are mounted.

At great distances between bearings determination of these loads is not especially difficult, since in this case they depend little on moments absorbed by bearings, for which with their calculation the latter need not be considered.

Regarding the axial load, then with its calculation frequently considerable difficulties are encountered. Strictly speaking, the axial load can be considered known only in the case when the examined bearing absorbs all the axial force applied to the shaft, as this takes place in bearing subassemblies with one bearing fixed in the axial direction.

If equations of equilibrium of the shaft are not enough for finding loads acting on its bearings, then, naturally, it is impossible to calculate separately bearings mounted in separate bearings. In similar cases for determining pressures on balls, it is necessary jointly to solve equations of equilibrium of the shaft with equations of static equilibrium of all the bearings installed in it.

§ 3. Certain Problems of the Calculation of Radial Thrust Ball Bearings Taking into Account Misalignment of Their Races Under a Load

1. Fundamental Relationships

In a number of units of the helicopter radial thrust ball bearings, located at a short distance from each other, absorb combined loads, in which, the moment plays if not the main, in any case, a considerable role. It is clear that during the determination of parameters characterizing the efficiency of such bearings, it is impossible to disregard mutual misalignment of the rings, as was done in the preceding paragraph in connection with which their calculation is greatly complicated.

The absence of reliable methods of calculation of radial thrust ball bearings absorbing considerable moments at small distances between the bearings hampers the designing of many bearing subassemblies, in particular, the subassembly of the disk of the cyclic pitch control, which is one of the most loaded and important elements of the helicopter.

Let us consider certain problems of the calculation of radial thrust ball bearings, taking into account misalignment of their rings under a load. Results obtained in the solution of these problems permit answering main questions appearing in the designing of bearing subassemblies of units of a helicopter intended for absorbing great moments.

Let us assume that the bearing subassembly, which consists of two radial thrust ball bearings, absorbs a combined load in the form of radial force R, applied in the middle between the bearings, axial force A and moment M (Fig. 4.16). It is assumed that force R and moment M act in one plane.

Let us confer subscript 1 to the bearing of the subassembly for which the pressures on the balls, caused by the action of force R and moment M, are added. All quantities referring to this bearing

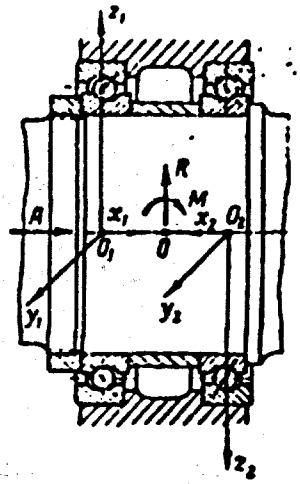

Fig. 4.16. Diagram of the loading of two ball bearings by radial and axial forces and moment.

will be recorded with this subscript. The second bearing making up the subassembly and all quantities pertaining to it will have the subscript 2.

Let us direct axes of coordinates for bearings 1 and 2 as is shown on Fig. 4.16. It is easy to note that in the system of coordinates $x_1y_1z_1$, force R and moment M always have positive values, but axial force A can be both positive and negative.

Conditions of equilibrium of the shaft, on which the bearings are mounted, are reduced to the system of equations:

$$\left.\begin{aligned} A &= A_1 - A_2; \\ R &= R_1 - R_2; \\ M &= M_1 + M_2 + R_1\frac{L}{2} + R_2\frac{L}{2}, \end{aligned}\right\} \qquad (3.1)$$

where L is the distance between the bearings.

Since moments M_1 and M_2 at short distances between the bearings are not only commensurable with moments $R_1\frac{L}{2}$ and $R_2\frac{L}{2}$ but also can considerably exceed them, then equation (3.1) should be solved jointly with equations of static equilibrium of bearings 1 and 2.

Let us assume that in the loaded subassembly the center of the pack of inner rings is displaced in the direction of action of

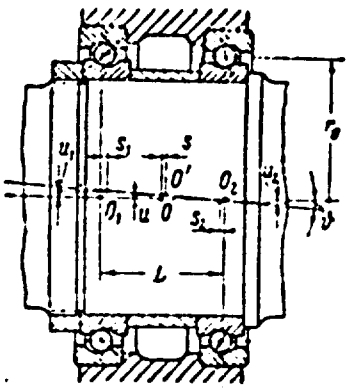

Fig. 4.17. Diagram of movements of internal rings of bearings under the action of an arbitrary external load applied to them.

forces A and R at distances s and u, and the common axis of rotation of these rings is turned in the direction of action of moment M at angle ϑ. Angle ϑ is the angularity both for bearing 1 and for bearing 2.

Relative displacements[3] determining the position of centers of the inner rings of bearings 1 and 2 in systems of coordinates $x_1y_1z_1$ and $x_2y_2z_2$, according to Fig. 4.17, are equal to

$$\left.\begin{aligned} \bar{s}_1 &= \sin\vartheta_0 + \bar{\Delta}_n + \bar{s};\\ \bar{u}_1 &= \bar{u} + \zeta\bar{\varepsilon};\\ \bar{s}_2 &= \sin\vartheta_0 + \bar{\Delta}_n - \bar{s};\\ \bar{u}_2 &= -\bar{u} + \zeta\bar{\varepsilon}. \end{aligned}\right\} \qquad (3.2)$$

Here Δ_n is half of the axial preliminary interference at which the bearings are set; $\zeta = \frac{L}{2r_0}$ ratio of the distance between the bearings to the diameter on which the balls are located; $\bar{\varepsilon} = \vartheta\frac{r_0}{\varepsilon}$.

Having written for both bearings equalities (1.16) and substituting in them expressions (3.2), after simple transformations we will obtain

$$\left.\begin{aligned} \bar{u} &= \frac{1}{2\left(\frac{\operatorname{tg}\beta_1 + \operatorname{tg}\beta_2}{2} + \zeta\right)}\cdot\left[\frac{(\operatorname{tg}\beta_2 + \zeta)\lambda_1\bar{\varepsilon}_1}{\cos\beta_1} - \frac{(\operatorname{tg}\beta_1 + \zeta)\lambda_2\bar{\varepsilon}_2}{\cos\beta_2}\right];\\ \bar{s} &= \frac{1}{2\left(\frac{\operatorname{tg}\beta_1 + \operatorname{tg}\beta_2}{2} + \zeta\right)}\cdot\left[\frac{\lambda_1\bar{\varepsilon}_1}{\cos\beta_1} + \frac{\lambda_2\bar{\varepsilon}_2}{\cos\beta_2}\right]. \end{aligned}\right\} \qquad (3.3)$$

In the bearing subassemblies of the type examined there are usually used radial thrust ball bearings with large initial angles of contact, for which relative displacements $\bar{\delta}_1$ and $\bar{\delta}_2$ rarely exceed $0.25 \sin^2\beta_0$. With the indicated values of quantities $\bar{\delta}_1$ and $\bar{\delta}_2$ equalities (3,3) can be replaced by the following approximate relations:

$$\left.\begin{aligned} \bar{\alpha} &= \frac{1}{2\cos\beta_0}(\lambda_1\bar{\delta}_1 - \lambda_2\bar{\delta}_2); \\ \bar{\zeta} &= \frac{1}{2\cos\beta_0(\operatorname{tg}\beta_0 + \zeta)}(\lambda_1\bar{\delta}_1 + \lambda_2\bar{\delta}_2). \end{aligned}\right\} \qquad (3.4)$$

With the selected direction of axes of coordinates, angle ψ_0 which determines the position of the most loaded ball in bearing 1, is always equal to zero. Angle ψ_{02}, which characterizes the position of the most loaded ball in bearing 2, depending upon the relationship between radial force R and moment M, can have both a zero value (with the predominant moment) and be equal to 180° (with the predominant radial loading).

Considering the last circumstance, with the help of equalities (1,24), (1,25), (1.21), (1.27), and (3.4), considering the remarks made on the order of quantities $\bar{\delta}_1$ and $\bar{\delta}_2$, we will represent the forces and moments absorbed by bearings 1 and 2 thus:

$$\left.\begin{aligned} \frac{A_1}{z\omega d_m^2} &= B_0\bar{\delta}_{01}^{3/2}\sin\beta_0 J_{11}\left(1 + b_{11}\cdot\frac{\bar{\delta}_{01}}{1+\lambda_1} + c_{11}\cdot\frac{\bar{\delta}_{02}}{1+\lambda_2\cos\psi_{02}}\right); \\ \frac{R_1}{z\omega d_m^2} &= B_0\bar{\delta}_{01}^{3/2}\cos\beta_0 J_{21}\left(1 - b_{21}\operatorname{tg}^2\beta_0\cdot\frac{\bar{\delta}_{01}}{1+\lambda_1} - c_{21}\operatorname{tg}^2\beta_0\cdot\frac{\bar{\delta}_{02}}{1+\lambda_2\cos\psi_{02}}\right); \\ \frac{M_1}{r_0 z\omega d_m^2} &= B_0\bar{\delta}_{01}^{3/2}\sin\beta_0 J_{21}\left(1 + b_{21}\cdot\frac{\bar{\delta}_{01}}{1+\lambda_1} + c_{21}\frac{\bar{\delta}_{02}}{1+\lambda_2\cos\psi_{02}}\right); \\ \frac{A_2}{z\omega d_m^2} &= B_0\bar{\delta}_{02}^{3/2}\sin\beta_0 J_{12}\left(1 + b_{12}\cdot\frac{\bar{\delta}_{02}}{1+\lambda_2\cos\psi_{02}} + c_{12}\cdot\frac{\bar{\delta}_{01}}{1+\lambda_1}\right); \\ \frac{R_2}{z\omega d_m^2} &= B_0\bar{\delta}_{02}^{3/2}\cos\beta_0 J_{22}\left(1 - b_{22}\operatorname{tg}^2\beta_0\cdot\frac{\bar{\delta}_{02}}{1+\lambda_2\cos\psi_{02}} - \right. \\ &\qquad \left. - c_{22}\operatorname{tg}^2\beta_0\cdot\frac{\bar{\delta}_{01}}{1+\lambda_1}\right)\cos\psi_{02}; \\ \frac{M_2}{r_0 z\omega d_m^2} &= B_0\bar{\delta}_{02}^{3/2}\sin\beta_0 J_{22}\left(1 + b_{22}\cdot\frac{\bar{\delta}_{02}}{1+\lambda_2\cos\psi_{02}} + c_{22}\frac{\bar{\delta}_{01}}{1+\lambda_1}\right)\cos\psi_{02}. \end{aligned}\right\} \qquad (3.5)$$

In expressions (3.5) the following notations are accepted:

$$\left.\begin{aligned}
b_{11} &= \operatorname{ctg}^2\beta_0 + \frac{f_{21}}{f_{11}}\left[\frac{1}{\sin 2\beta_0(\operatorname{tg}\beta_0+\zeta)} - 1\right]\lambda_1;\\
c_{11} &= \frac{f_{21}}{f_{11}}\cdot\frac{\lambda_2}{\sin 2\beta_0(\operatorname{tg}\beta_0+\zeta)};\\
b_{21} &= \operatorname{ctg}^2\beta_0 + \frac{f_{31}}{f_{21}}\left[\frac{1}{\sin 2\beta_0(\operatorname{tg}\beta_0+\zeta)} - 1\right]\lambda_1;\\
c_{21} &= \frac{f_{31}}{f_{21}}\cdot\frac{\lambda_2}{\sin 2\beta_0(\operatorname{tg}\beta_0+\zeta)};\\
b_{12} &= \operatorname{ctg}^2\beta_0 + \frac{f_{22}}{f_{12}}\left[\frac{1}{\sin 2\beta_0(\operatorname{tg}\beta_0+\zeta)} - 1\right]\lambda_2\cos\psi_{02};\\
c_{12} &= \frac{f_{22}}{f_{12}}\cdot\frac{\lambda_1}{\sin 2\beta_0(\operatorname{tg}\beta_0+\zeta)}\cdot\cos\psi_{02};\\
b_{22} &= \operatorname{ctg}^2\beta_0 + \frac{f_{32}}{f_{22}}\left[\frac{1}{\sin 2\beta_0(\operatorname{tg}\beta_0+\zeta)} - 1\right]\lambda_2\cos\psi_{02};\\
c_{22} &= \frac{f_{32}}{f_{22}}\left[\frac{\lambda_1}{\sin 2\beta_0(\operatorname{tg}\beta_0+\zeta)}\cdot\cos\psi_{02}\right].
\end{aligned}\right\} \qquad (3.6)$$

As follows from formulas (3.2) and (1.13),

$$\operatorname{tg}\beta_1 + \operatorname{tg}\beta_2 = \frac{\bar{\delta}_1+\bar{\delta}_2}{\cos\beta_0} = 2\operatorname{tg}\beta_0 + \frac{2\bar{\Delta}_n}{\cos\beta_0}.$$

Since at $\bar{\delta} < 0{,}25\sin^2\beta_0$ it is possible approximately to assume $\operatorname{tg}\beta = \operatorname{tg}\beta_0 + \frac{\bar{\delta}}{\sin\beta_0\cos\beta_0}$, then from the last expression we find

$$\bar{\delta}_1 + \bar{\delta}_2 = 2\bar{\Delta}_n\sin\beta_0.$$

Using equality (1.21), we finally have

$$\frac{\bar{\delta}_{01}}{1+\lambda_1} + \frac{\bar{\delta}_{02}}{1+\lambda_2\cos\psi_{02}} = 2\bar{\Delta}_n\sin\beta_0. \qquad (3.7)$$

Dependences (3.5), (3.6), and (3.7) jointly with equations (3.1) permit determining all parameters characterizing the efficiency of radial thrust ball bearings at short distances between the bearings, when mutual misalignment of the rings under the load cannot be disregarded. As numerical calculations show, the accuracy of these dependences, obtained on the assumption that quantities $\bar{\delta}_1$ and $\bar{\delta}_2$ do not exceed $0.25\sin^2\beta_0$, at initial angles of contact $\beta_0 \geq 26^\circ$ with which it is usually necessary to encounter in bearing subassemblies, intended for absorption of large moments, is sufficient.

Let us analyze the main calculation cases encountered in the designing of bearing subassemblies of this type for units of the helicopter.

2. Case of "Pure" Moment

If the bearing subassembly, which consists of two identical radial thrust ball bearings, absorbes the "pure" moment (Fig. 4.18),

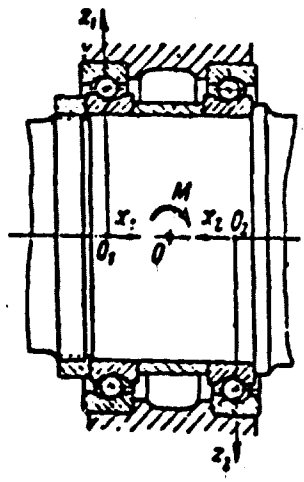

Fig. 4.18. Diagram of loading of two ball bearings by "pure" moment.

then in view of the identity of loading of both bearings $R_1 = R_2$, $A_1 = A_2$ and $M_1 = M_2$. It is natural that in this case $\psi_{02} = \psi_{01} = 0$, $\lambda_1 = \lambda_2$, and $\bar{\delta}_{01} = \bar{\delta}_{02}$.

As can be seen from formula (3.7), at $\psi_{02} = 0$, $\lambda_1 = \lambda_2$ and $\bar{\delta}_{01} = \bar{\delta}_{02}$

$$\frac{\bar{\delta}_{01}}{1+\lambda_1} = \sin\beta_0 \bar{\Delta}_a. \qquad (3.8)$$

Consequently, with the action of "pure" moment

$$\lambda_1 = \frac{\bar{\delta}_{01}}{\sin\beta_0 \bar{\Delta}_a} - 1. \qquad (3.9)$$

It is clear that relation $\frac{\bar{\delta}_{01}}{\sin\beta_0 \bar{\Delta}_a}$ should be always greater than unity. This becomes evident if one were to consider that the product $\sin\beta_0\bar{\Delta}_a$ constitutes a relative approach of grooves of the rings caused by preliminary interference, i.e., the relative approach of grooves of the rings which there is prior to application to the subassembly of the external load.

Relation (3.9) determines the zone of loading depending upon the level of the load and preliminary interference. From it, in particular, it is clear that so that all the balls bear the load, the bearings should be mounted with relative preliminary interference $2\bar{\Delta}_{a} \geq \frac{\bar{\delta}_{01}}{\sin\beta_0}$.

The influence of preliminary interference on the zone of the loading is shown on Fig. 4.19.

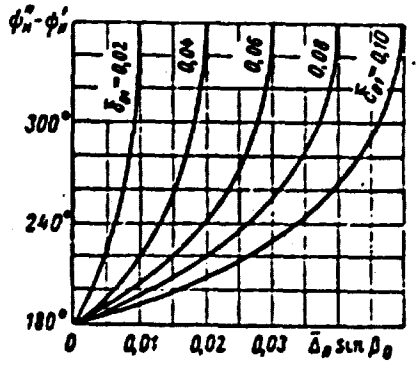

Fig. 4.19. Influence of preliminary interference on the zone of loading.

Preliminary interference is frequently assigned not in the form of the relative axial displacement $2\bar{\Delta}_{a}$ but in the form of the corresponding axial load A_a, determined by expression

$$A_a = zB_0 vd_w^2 \bar{\Delta}_a^{3/2} \sin^{5/2}\beta_0 \left(1 + \frac{\cos^2\beta_0}{\sin\beta_0} \cdot \bar{\Delta}_a\right). \qquad (3.10)$$

Since with the action of the "pure" moment $R_1 = R_2$ and $A_1 = A_2$, then the first two equations of system (3.1) are satisfied identically. The third equation of this system for the case of the "pure" moment can be converted with the help of dependences (3.5), (3.6), and (3.7) in the following way:

$$\frac{M}{r_0 zvd_w^2} = 2B_0 \bar{\delta}_{01}^{3/2} \sin^2\beta_0 (1 + \zeta \operatorname{ctg}\beta_0) J_{21} \times$$
$$\times \left[1 + \operatorname{ctg}^2\beta_0 \cdot \frac{1 - \zeta\operatorname{tg}\beta_0}{1 + \zeta\operatorname{ctg}\beta_0} \left(1 + \frac{J_{31}}{J_{21}} \frac{1 - \zeta\operatorname{tg}\beta_0}{1 + \zeta\operatorname{ctg}\beta_0} \cdot \lambda_1\right) \frac{\bar{\delta}_{01}}{1 + \lambda_1}\right]. \qquad (3.11)$$

Using equalities (2.3), (2.5), (3.9), and (3.11), it is easy to construct graphs of dependences $\frac{P_{01}}{vd_w^2} = F_6\left(\frac{M}{r_0 zvd_w^2}\right)$ and $\frac{P_{a1}}{vd_w^2} = F_7\left(\frac{M}{r_0 zvd_w^2}\right)$.

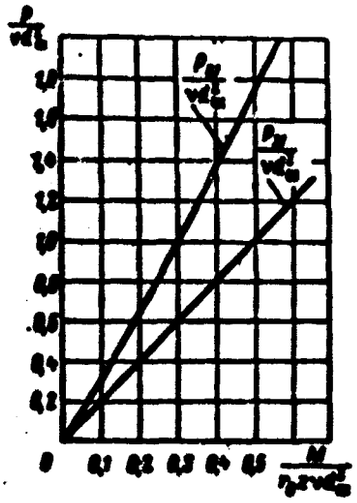

Fig. 4.20. Values $\frac{P_{01}}{\omega_1^2}$ and $\frac{P_{02}}{\omega_1^2}$ depending upon $\frac{M}{r_0^3 \omega_1^2}$ when $\beta_0 = 36^\circ$.

on which the maximum and equivalent pressure on the balls can be found. An example of such graphs can be the curves depicted on Fig. 4.20. They are obtained on the assumption that $\beta_0 = 36^\circ$, $\zeta = 0$, and $\bar{A}_1 \sin\beta_0 = 0.01$.

Let us present the maximum pressure on the ball P_{01} in the form:

$$P_{01} = \frac{\alpha_0^{(M)} M}{2 f_{n_1 - n}\, r_0 \sin\beta_0 (1 + \zeta \operatorname{ctg}\beta_0)} = \frac{4{,}37 \alpha_0^{(M)} M}{2 r_0 \sin\beta_0 (1 + \zeta \operatorname{ctg}\beta_0)}. \qquad (3.12)$$

Accordingly, we will assume

$$P_{01} = \max P_{01} = \frac{2{,}57 \alpha^{(M)} M}{2 r_0 \sin\beta_0 (1 + \zeta \operatorname{ctg}\beta_0)}, \qquad (3.13)$$

where $\alpha^{(M)} = \frac{\omega}{0{,}367} \cdot \alpha_0^{(M)}$.

It should be noted that with the action of the "pure" moment $P_{02} = P_{01}$ and $P_{02} = P_{01}$.

It is easy to be convinced that coefficient

$$\alpha_0^{(M)} = \frac{f_{n_1 - n}}{f_{n_1} \left[1 + \operatorname{ctg}^2 \beta_0 \frac{1 - \zeta \operatorname{ctg}\beta_0}{1 + \zeta \operatorname{ctg}\beta_0} \left(1 + \frac{f_{n_1}}{f_{n_1}} \frac{1 - \zeta \operatorname{ctg}\beta_0}{1 + \zeta \operatorname{ctg}\beta_0} \cdot \lambda_1 \right) \frac{\lambda_{n_1}}{1 + \lambda_1} \right]}. \qquad (3.14)$$

With zero preliminary interference, when according to the formula (3.9) $\lambda_1 = \alpha$, from the relation (3.14) we have

$$\kappa_0^{(M)} = \frac{1}{1 + 0{,}868\left(\frac{1-\zeta \operatorname{tg}\beta_0}{\operatorname{tg}\beta_0 + \zeta}\right)^2 \bar{\delta}_{u1}}. \qquad (3.15)$$

Values of coefficient $\kappa_0^{(M)}$ corresponding to expression (3.15) can be determined on the graph on Fig. 4.21. Plotted here along the axis of the abscissas is the quantity $\overline{M} = \frac{1}{z v d_m^2 \sin\beta_0 (1 + \zeta \operatorname{ctg}\beta_0)} \frac{M}{r_0}$. Quantity $\rho = \left|\frac{1-\zeta \operatorname{tg}\beta_0}{\operatorname{tg}\beta_0 + \zeta}\right|$ is accepted as a parameter.

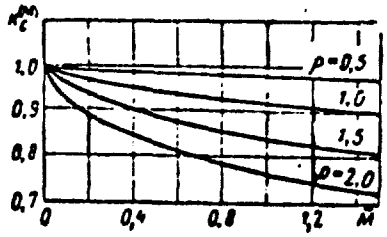

Fig. 4.21. Values of coefficient $\kappa_0^{(M)}$ depending upon parameters ρ and $\overline{M}$.

The graphs on Figs. 4.22 and 4.23 show how coefficients $\kappa_0^{(M)}$ and $\kappa^{(M)}$ are changed depending upon the preliminary interference at

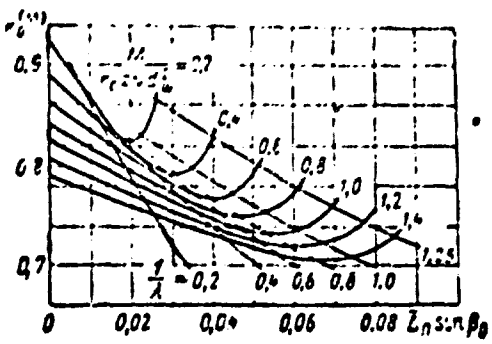

Fig. 4.22.

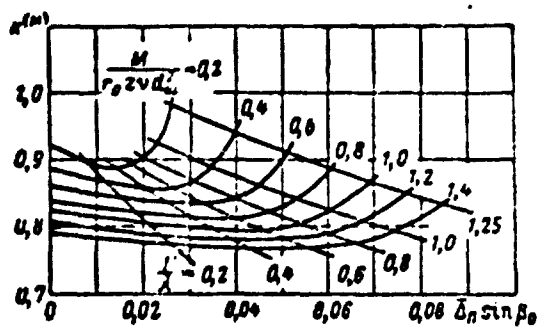

Fig. 4.23.

Fig. 4.22. Values of coefficient $\kappa_0^{(M)}$ depending upon the preliminary interference at certain constant values $\frac{M}{r_0 z v d_m^2}$.

Fig. 4.23. Values of coefficient $\kappa^{(M)}$ depending upon the preliminary interference at certain constant values $\frac{M}{r_0 z v d_m^2}$.

$\beta_0 = 36^\circ$ and $\zeta = 0$. From the given curves it is clear that it is expedient to select the preliminary interference in such a way that parameter λ_1 lies within limits of 1 to 1.25. With such a selection

of preliminary interference coefficient $\kappa_0^{(M)}$, and, consequently, the maximum pressure on the ball descend by 10-12%. Coefficient $A^{(M)}$, and, together with it, the equivalent pressure on ball, maintain approximately the same value as in case when the preliminary interference is absent. Similar conclusions can be drawn in the examining of other combinations of quantities β_0 and ζ.

It is extremely important to estimate the influence of the preliminary interference on the angular rigidity of the bearing subassembly. This is easy to do with the help of the second of relations (3.4), which for the case of "pure" moment can be represented in the form:

$$\bar{\varepsilon} = \frac{\bar{\delta}_{01}}{\cos\beta_0 (\operatorname{tg}\beta_0 + \zeta)} \frac{\lambda_1}{1+\lambda_1}. \qquad (3.16)$$

Formula (3.16) shows that the transition from $\lambda_1 = \infty$ to $\lambda_1 = 1\text{-}1.25$ leads to a decrease in misalignment of rings of the bearings 2.2-2 times.

From what has been said it is clear that with the installation of radial thrust ball bearings with optimum preliminary interference, which correspond to values of parameter λ_1 from 1 to 1.25, conditions of operation of bearing subassemblies loaded by the moment are noticeably improved.

The preliminary interference at which the parameter $\lambda_1 = 1\text{-}1.25$ with practical calculations can be calculated by the approximate formula:

$$\bar{\delta}_0 = \frac{1}{(2+2{,}25)\sin\beta_0} \left\{ \frac{(1{,}96+1{,}94)\bar{M}}{1+H\left[(1{,}96+1{,}94)\bar{M}\right]^{2/3}} \right\}^{2/3}. \qquad (3.17)$$

where

$$H = \frac{1}{2+2{,}25} \operatorname{ctg}^2\beta_0 \frac{1-\zeta\operatorname{tg}\beta_0}{1+\zeta\operatorname{ctg}\beta_0} \left[1 + (0{,}905 \div 1{,}08) \frac{1-\zeta\operatorname{tg}\beta_0}{1+\zeta\operatorname{ctg}\beta_0} \right].$$

Here quantities P_{01} and P_{a1} are respectively equal to:

$$\left.\begin{aligned} P_{01} &= \frac{(3{,}92+3{,}88)M}{2r_0 z \sin\beta_0 (1+\zeta\operatorname{ctg}\beta_0)\left[1+H\left[(1{,}96+1{,}94)\bar{M}\right]^{2/3}\right]}; \\ P_{a1} &= (0{,}657 \div 0{,}645) P_{01}. \end{aligned}\right\} \qquad (3.18)$$

3. Joint Action of the Moment and Axial Force

With the joint action of the moment and axial force (Fig. 4.24) conditions of loading of bearings 1 and 2 are unequal, which

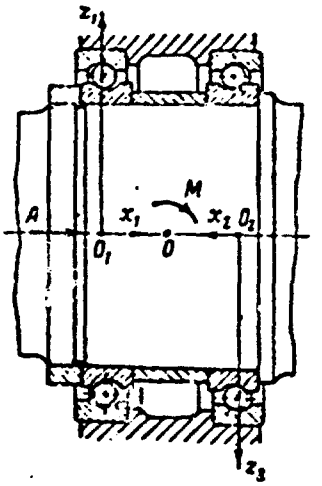

Fig. 4.24. Diagram of loading of two ball bearings by moment and axial force.

considerably complicates calculations connected with the determination of pressures on the balls. In order to find quantities P_{01}, $P_{\vartheta 1}$, P_{02} and $P_{\vartheta 2}$, in this case it is necessary to construct a number of auxiliary graphs. The order of construction of these graphs is easy to comprehend by the following example.

Let us assume that the initial angle of contact $\beta_0 = 36^\circ$. For simplicity we will consider that the relative preliminary interference $\bar{\Delta}_a = 0$ and relative base $\zeta = 0$, i.e., we will examine the case having a direct relation to the calculation of bearings of the disk of the cyclic pitch control for which to a sufficient degree these assumptions are correct.

According to equations (3.5) with radial loading $R = R_1 = R_2 = 0$ quantities $\bar{\delta}_{01}$, $\bar{\delta}_{02}$, λ_1 and λ_2 are connected with each other by the following relation:

$$J_{21} - \left(\frac{\bar{\delta}_{02}}{\bar{\delta}_{01}}\right)^{3/2} J_{22} = \operatorname{tg}^2 \beta_0 \left[J_{21} b_{21} - \left(\frac{\bar{\delta}_{02}}{\bar{\delta}_{01}}\right)^{3/2} J_{22} c_{22} \right] \frac{\bar{\delta}_{01}}{1+\lambda_1} +$$
$$+ \operatorname{tg}^2 \beta_0 \left[J_{21} c_{21} - \left(\frac{\bar{\delta}_{02}}{\bar{\delta}_{01}}\right)^{3/2} J_{22} b_{22} \right] \frac{\bar{\delta}_{02}}{1+\lambda_2}. \qquad (3.39)$$

In equality (3.19), as in all subsequent dependences, it is considered that with the joint action of the moment and axial force, as in the case of the action of "pure" moment, $\psi_{02}=\psi_{01}=0$.

From formula (3.7) with zero preliminary interference we have:

$$\frac{\bar{\delta}_{01}}{1+\lambda_1}+\frac{\bar{\delta}_{02}}{1+\lambda_2}=0. \tag{3.20}$$

Whence

$$\lambda_2=-\left[\frac{\bar{\delta}_{02}}{\bar{\delta}_{01}}(1+\lambda_1)+1\right]. \tag{3.21}$$

Subsequently, relation $\frac{\bar{\delta}_{02}}{\bar{\delta}_{01}}$ will everywhere by designated by n.

Using equalities (3.6), (3.19), (3.20), and (3.21), let us construct curves $\bar{\delta}_{01}=\bar{\delta}_{01}(x, \lambda_1)$ satisfying the condition $R = R_1 - R_2 = 0$ (Fig. 4.25). Intersecting the obtained curves by lines $\bar{\delta}_{01}$=const,

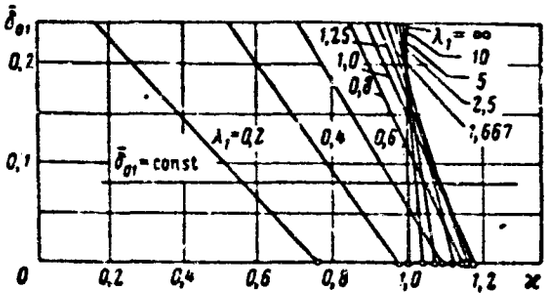

Fig. 4.25. Model graph $\bar{\delta}_{01}=\bar{\delta}_{01}(x, \lambda)$ when $R = R_1 - R_2 = 0$.

we find values of x corresponding at given values of λ_1 (from ∞ to 0) to selected values of $\bar{\delta}_{01}$. Taking further λ_1 as a parameter, with the help of equations (3.1), (3.5), and the above-mentioned equalities, we calculate quantities $\frac{A}{\varepsilon v d_m^2}$, $\frac{Al}{r_0 \varepsilon v d_m^2}$, and also relation $\frac{P_{02}}{P_{01}}=x^{3/2}$ and $\frac{P_{02}}{P_{01}}=x^{3/2}\frac{w_2}{w_1}$.

Results of the calculation are given graphically, as was done on Figs. 4.26-4.28. Figure 4.26 permits by the assigned values $\frac{A}{\varepsilon v d_m^2}$ and $\frac{Al}{r_0 \varepsilon v d_m^2}$ determining quantities $\bar{\delta}_{01}$ and λ_1, knowing which it is easily possible to calculate the maximum and equivalent pressures

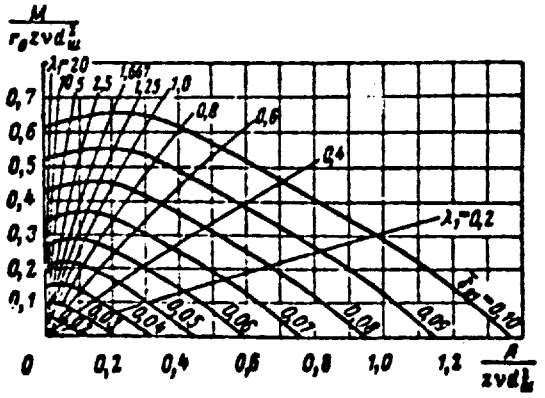

Fig. 4.26. Dependence of $\frac{M}{r_0 z v d_w^2}$ on $\frac{A}{z v d_w^2}$ at certain constant values $\bar{\delta}_{01}$ and λ_1.

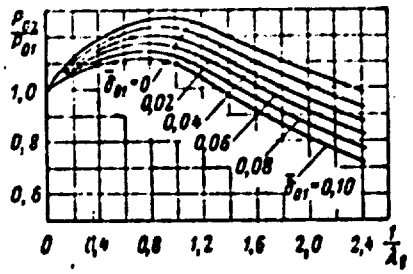

Fig. 4.27.

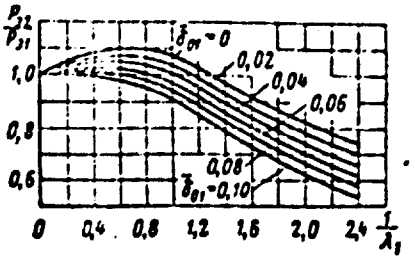

Fig. 4.28.

Fig. 4.27. Dependence of ratio $\frac{P_{02}}{P_{01}}$ on $\frac{1}{\lambda_1}$ at certain constant values of $\bar{\delta}_{01}$.

Fig. 4.28. Dependence of ratio $\frac{P_{e2}}{P_{e1}}$ on $\frac{1}{\lambda_1}$ at certain constant values of $\bar{\delta}_{01}$.

P_{01} and P_{e1}. From Figs. 4.27 and 4.28 we find ratios $\frac{P_{02}}{P_{01}}$ and $\frac{P_{e2}}{P_{e1}}$ and then calculate the maximum and equivalent pressures P_{02} and P_{e2}.

Analyzed above was the case $\bar{\Delta}_a = 0$ and $\zeta = 0$. At arbitrary quantities of these values, and also at other initial angles of contact β_0 the determination of pressures P_{e1}, P_{e1}, P_{e2} and P_{e2} is produced in the same way as in the examined example. It is necessary only to remember that in the presence of preliminary interference quantity $\bar{\delta}_{01}$ cannot be less $\sin\beta_0\bar{\Delta}_a$.

It should be noted that the case $\bar{\Delta}_a = 0$ and $\zeta = 0$ is characteristic not only for bearings of the disk of the cyclic pitch control mut

also for many roller bearings of large diameters, which are used in turning devices of contemporary machines and mechanisms.

From the given data it is clear that at the prevailing moment, when $\lambda_1 > 1$, most frequently bearing 2 appears the most loaded, although at first glance conditions of operation of bearing 1, in the direction of which axial load A is directed, are more difficult.

The expounded method of the calculation of radial thrust ball bearings with the joint action of the moment and axial force requires fulfillment of a large number of calculations and constructions. Therefore, its application is justified only in special investigations which have the purpose of revealing peculiarities of the distribution of the load in the bearing subassemblies with short distances between the bearings and also for development of auxiliary graphs with the help of which separate model constructions can be calculated. If such graphs are not constructed beforehand, then in engineering calculations one should use the simplified method founded on maximum dependences obtained for the case of small loads, when forces are distributed between the balls by the most unfavorable manner.

4. Maximum Dependences on Small Loads

At small loads one can assume that the angles of contact of all balls are approximately identical and equal to β_0.

Rejecting in equations (3.5) terms considering the change in angles of contact, and introducing into them instead of quantities $\bar{\delta}_{01}$ and $\bar{\delta}_{02}$ the maximum pressures on balls P_{01} and P_{02}, which is more convenient for small loads, we have

$$\left.\begin{aligned} R_1 &= zP_{01}\cos\beta_0 j_{21};\\ A_1 &= zP_{01}\sin\beta_0 j_{11};\\ M_1 &= r_0 zP_{01}\sin\beta_0 j_{21};\\ R_2 &= zP_{02}\cos\beta_0 j_{22};\\ A_2 &= zP_{02}\sin\beta_0 j_{12};\\ M_2 &= r_0 zP_{02}\sin\beta_0 j_{22}. \end{aligned}\right\} \qquad (3.22)$$

Substituting dependences (3.22) into equations (3.1), we will obtain

$$\left.\begin{aligned} R &= zP_{01}\cos\beta_0\,(j_{21}-\varkappa^{3/2}j_{22}\cos\psi_{02});\\ A &= zP_{01}\sin\beta_0\,(j_{11}-\varkappa^{3/2}j_{12});\\ M &= r_0zP_{01}\sin\beta_0\,(1+\zeta\operatorname{ctg}\beta_0)\,(j_{21}+\varkappa^{3/2}j_{22}\cos\psi_{02}), \end{aligned}\right\} \qquad (3.23)$$

where, as before, $\varkappa=\frac{\bar{\delta}_{02}}{\bar{\delta}_{01}}=\left(\frac{P_{02}}{P_{01}}\right)^{2/3}$.

Since in this case angle ψ_{02} cannot be equal to zero, then taking into account this circumstance from equality (3.7) we find

$$\lambda_2\cos\psi_{02}=-\left[1+\frac{\varkappa(1+\lambda_1)}{1-(1+\lambda_1)\dfrac{2\bar{\Delta}_n\sin\beta_0}{\bar{\delta}_{01}}}\right]. \qquad (3.24)$$

Let us examine the system of equations:

$$\left.\begin{aligned} &\frac{j_{21}+\varkappa^{3/2}j_{22}}{j_{11}-\varkappa^{3/2}j_{12}}=\tau;\\ &\frac{j_{21}-\varkappa^{3/2}j_{22}}{j_{21}+\varkappa^{3/2}j_{22}}=\upsilon;\\ &\lambda_2\cos\psi_{02}=-[\varkappa(1+\lambda_1)+1. \end{aligned}\right\} \qquad (3.25)$$

It is easy to be convinced that values λ_1 λ_2 and ν at zero preliminary interference, which satisfy equations (3.25), also satisfy equations (3.23) and (3.24) if one were to assume that

– at $\frac{r_0R(1+\zeta\operatorname{ctg}\beta_0)\operatorname{tg}\beta_0}{M}\leqslant 1$:

$$\left.\begin{aligned} \tau &= -\frac{M}{r_0A(1+\zeta\operatorname{ctg}\beta_0)};\\ \upsilon &= \frac{r_0R(1+\zeta\operatorname{ctg}\beta_0)\operatorname{tg}\beta_0}{M}; \end{aligned}\right\} \qquad (3.26)$$

– at $\frac{r_0R(1+\zeta\operatorname{ctg}\beta_0)\operatorname{tg}\beta_0}{M}\geqslant 1$:

$$\left.\begin{aligned} \tau &= \frac{R}{A}\operatorname{tg}\beta_0;\\ \upsilon &= \frac{M}{r_0R(1+\zeta\operatorname{ctg}\beta_0)\operatorname{tg}\beta_0}. \end{aligned}\right\} \qquad (3.27)$$

It is necessary to consider that in the first case angle ψ_{02} is equal to zero and in the second, 180^0.

If in the external load the main role is the axial force, then pressures on the balls are usually written in the form

$$\left.\begin{aligned} P_{01} &= \frac{\kappa_{01}^{(A)} A}{z \sin \beta_0}; \\ P_{11} &= \frac{\kappa_{1}^{(A)} A}{z \sin \beta_0}; \\ P_{02} &= \frac{\kappa_{02}^{(A)} A}{z \sin \beta_0}; \\ P_{12} &= \frac{\kappa_{2}^{(A)} A}{z \sin \beta_0}. \end{aligned}\right\} \qquad (3.28)$$

If the moment prevails, then, as a rule, there is used the form of recording which was already used earlier:

$$\left.\begin{aligned} P_{01} &= \frac{4{,}37\kappa_{01}^{(M)} M}{2r_0 z \sin \beta_0 (1 + \zeta \operatorname{ctg} \beta_0)}; \\ P_{11} &= \frac{2{,}57\kappa_{1}^{(M)} M}{2r_0 z \sin \beta_0 (1 + \zeta \operatorname{ctg} \beta_0)}; \\ P_{02} &= \frac{4{,}37\kappa_{02}^{(M)} M}{2r_0 z \sin \beta_0 (1 + \zeta \operatorname{ctg} \beta_0)}; \\ P_{12} &= \frac{2{,}57\kappa_{2}^{(M)} M}{2r_0 z \sin \beta_0 (1 + \zeta \operatorname{ctg} \beta_0)}. \end{aligned}\right\} \qquad (3.29)$$

According to equations (3.23)

$$\left.\begin{aligned} \kappa_{01}^{(M)} &= \frac{2}{4{,}37 (j_{21} + \varkappa^{3,2} j_{22} \cos \gamma_{12})}; \\ \kappa_{02}^{(M)} &= \varkappa^{3,2} \kappa_{01}^{(M)}; \\ \kappa_{01}^{(A)} &= \frac{1}{j_{11} - \varkappa^{3/2} j_{12}}; \\ \kappa_{02}^{(A)} &= \varkappa^{3/2} \kappa_{01}^{(A)}. \end{aligned}\right\} \qquad (3.30)$$

Regarding coefficients $\kappa_1^{(M)}$, $\kappa_1^{(A)}$, $\kappa_2^{(M)}$ and $\kappa_2^{(A)}$, they are equal to $\kappa_1^{(M)} = \frac{\omega_1}{0{,}587} \kappa_{01}^{(M)}$; $\kappa_1^{(A)} = \omega_1 \kappa_{01}^{(A)}$; $\kappa_2^{(M)} = \frac{\omega_2}{0{,}587} \kappa_{02}^{(M)}$; $\kappa_{02}^{(A)} = \omega_2 \kappa_{02}^{(A)}$.

Let us note that between coefficients $\kappa_0^{(A)}$ and $\kappa_0^{(M)}$ there exists the following connection:

$$\kappa_0^{(A)} = \frac{4{,}37}{2} \kappa_0^{(M)} \frac{M}{r_0 A (1 + \zeta \operatorname{ctg} \beta_0)}. \qquad (3.31)$$

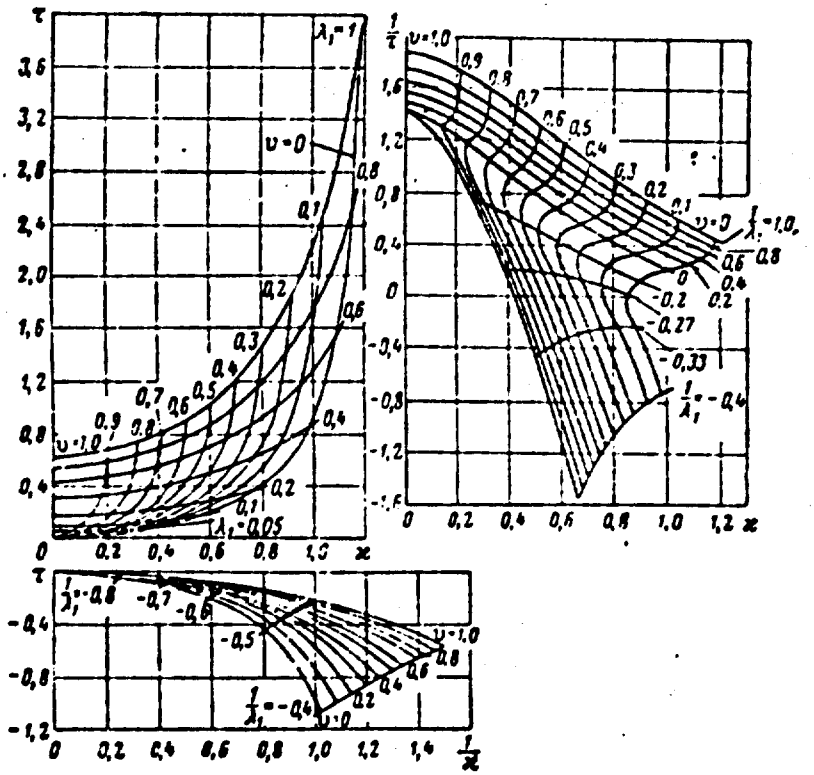

Fig. 4.29. Nomographs for the approximate calculation of bearings loaded by the axial and radial forces and moment.

The solution of system (3.25) can be represented in the form of the graphs depicted on Fig. 4.29. From these graphs, knowing τ and v, it is easy to find values $\varkappa$ and λ_1, by which the product $\lambda_2 \cos\psi_{02}$ is calculated and then coefficients $\kappa_{01}^{(I)}, \kappa_1^{(I)}, \kappa_{02}^{(I)}, \kappa_2^{(I)}$ or $\kappa_{01}^{(II)}, \kappa_1^{(II)}, \kappa_{02}^{(II)}, \kappa_2^{(II)}$ are calculated. After that the determination of pressures on the balls does not pose any special difficulty.

Graphs on Fig. 4.29 are interesting in the fact that in them neither angle β nor ζ appear. Thus we arrived at the very convenient practical approximate method of calculation of radial thrust ball bearings with large initial angles of contact in the most general case of their loading. Preliminary interference, as we were already convinced in examining bearing subassemblies loaded by the "pure" moment, has an effect, mainly, on the rigidity of the system, changing little the computer values of maximum and equivalent

pressures on the balls. Therefore, the expounded method of approximation of determining these values, founded on the assumption that the preliminary interference is equal to zero, can be used for solving a sufficiently wide range of problems connected with the calculation of radial thrust ball bearings with large initial angles of contact which are set in bearing subassemblies having a short distance between the bearings and absorbing the arbitrary combined load. In simpler cases of loading in the examining of maximum distribution of forces between the balls corresponding to small loads, preliminary interference when necessary can be comparatively easily considered.

Let us assume that the subassembly is loaded only by the moment and axial force. In the absence of radial loading, as follows from equations (3.23), $j_{21}-x^{3/2} j_{22}\cos\psi_{02}=0$. Using this relationship, we will give expressions for coefficients $\kappa^{(M)}$ and $\kappa^{(A)}$ to the form:

$$\left.\begin{aligned}
&\kappa_{01}^{(M)}=\frac{1}{4{,}37j_{21}};\quad \kappa_{01}^{(A)}=\frac{\tau}{2j_{21}};\\
&\kappa_{02}^{(M)}=\frac{1}{4{,}37j_{22}};\quad \kappa_{02}^{(A)}=\frac{\tau}{2j_{22}};\\
&\kappa_{1}^{(M)}=\frac{w_1}{2{,}57j_{21}};\quad \kappa_{1}^{(A)}=\frac{\tau w_1}{2j_{21}};\\
&\kappa_{2}^{(M)}=\frac{w_2}{2{,}57j_{22}};\quad \kappa_{2}^{(A)}=\frac{\tau w_2}{2j_{22}}.
\end{aligned}\right\} \qquad (3.32)$$

Relations (3.32) are real in the presence of preliminary interference.

Coefficients $\kappa_{01}^{(M)}, \kappa_{02}^{(M)}, \kappa_{1}^{(M)}$ and $\kappa_{2}^{(M)}$, determined by formulas (3.32), at zero preliminary interference can be found from graphs on Figs. 4.30 and 4.31. Since at small values of the ratio $\frac{1}{\tau}$ coefficients $\kappa_{0}^{(M)}$ and $\kappa^{(M)}$ for bearing 2 are considerably larger than those for bearing 1, then naturally there appears the question whether it is impossible to vary their values owing to the corresponding selection of preliminary interference. Not discussing the transformations connected with the solution of this problem, inasmuch as they are quite evident from that stated above, we will give immediately the final solution. Figure 4.32 gives curves showing at what values

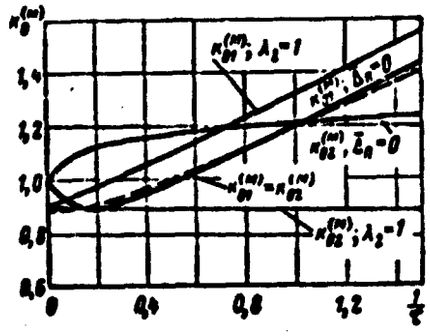

Fig. 4.30.

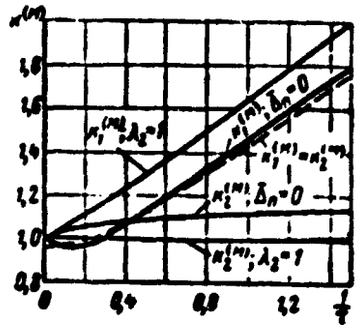

Fig. 4.31.

Fig. 4.30. Values of the coefficient $\kappa_0^{(M)} = \kappa_0^{(M)}\left(\frac{1}{\tau}\right)$ for the case of the combined action of the moment and axial force.

Fig. 4.31. Values of the coefficient $\kappa^{(M)} = \kappa^{(M)}\left(\frac{1}{\tau}\right)$ for the case of the combined action of the moment and axial force.

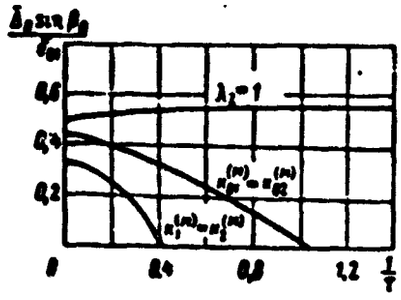

Fig. 4.32. Values of preliminary interference to ensure conditions $\kappa_1^{(M)} = \kappa_2^{(M)}$, $\kappa_{01}^{(M)} = \kappa_{02}^{(M)}$ and $\lambda_2 = 1$.

of the ratio $\frac{\bar{\delta}_0 \sin \beta_0}{\bar{\delta}_{00}}$ the identity of the static and dynamic load of bearings 1 and 2 can be theoretically provided, i.e., the equality of coefficients $\kappa_{01}^{(M)}$ and $\kappa_{02}^{(M)}$ or $\kappa_1^{(M)}$ and $\kappa_2^{(M)}$. Values of these equalized coefficients are plotted on Figs. 4.30 and 4.31 by dashed lines.

For subassemblies which should have increased rigidity, it is desirable that in both bearings all the balls be loaded. This problem is also easily solved by means of the selection of preliminary interference. Since with joint action of the moment and axial force the zone of loading in bearing 1 is always greater than that in

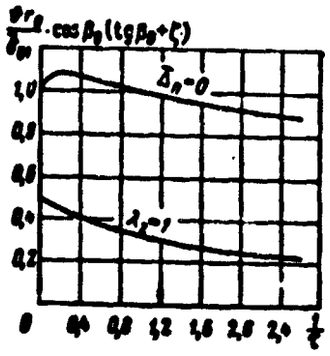

Fig. 4.33. Influence of preliminary interference (condition $\lambda_2 = 1$) on the angular rigidity of the subassembly.

bearing 2, then the condition of full loading of the balls of both bearings is the inequality $\lambda_2 \geq 1$. Values of coefficients $\kappa_{01}^{(M)}, \kappa_{02}^{(M)}, \kappa_1^{(M)}$ and $\kappa_2^{(M)}$ and the ratio $\frac{\bar{\Delta}_a \sin\beta_0}{\delta_{01}}$, which correspond to case $\lambda_2 = 1$, are also given on Fig. 4.31 and Fig. 4.32. Figure 4.33 shows that in the presence of preliminary interference, which provides loading of all balls on both bearings, the angular rigidity of the subassembly increases more two times, and the maximum and equivalent pressures on the balls are increased by approximately 10-15%.

Maximum dependences obtained for the case of small loads are very convenient for practical calculations, since they considerably decrease the laboriousness of the determination of pressures on the balls. It is necessary only to consider that the use of these maximum dependences leads to a definite overestimate of design pressures on the balls. At contact stress of the order of 20,000 kG/cm^2 it amounts to 15-25% for the angle $\beta_0 = 26^\circ$ and 2-17% for the angle $\beta_0 = 60^\circ$. Considering the last circumstance, with calculation of calculation loads on a bearing subassembly in the case of application of the indicated maximum dependences, it is possible to take the smaller values of the safety factor.

On the basis of the above-mentioned dependences the pressure on the balls of the eccentrically loaded two-row thrust ball bearings can be determined. Here one should remember that for the initial angle of contact $\beta_0 = 90^\circ$ at $\bar{\Delta}_a = 0$ formulas (3.32) give "accurate" values of coefficients entering into formulas (3.28) and (3.29). Let us note that in this case quantity τ constitutes the relative eccentricity $\frac{e}{r_0}$ (Fig. 4.34).

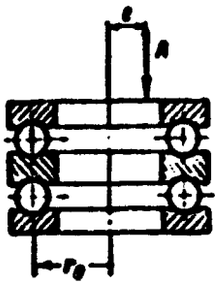

Fig. 4.34.

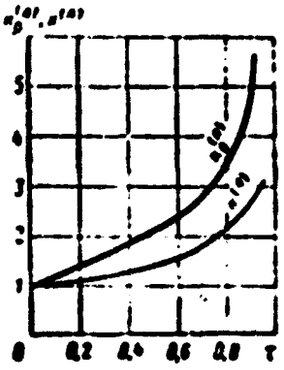

Fig. 4.35.

Fig. 4.34. Thrust two-row ball bearing loaded by the axial force and moment (eccentrically applied axial force).

Fig. 4.35. Values of coefficients $\kappa_0^{(A)}$ and $\kappa^{(A)}$ depending upon τ.

If the eccentrically applied axial force is absorbed by the single-row thrust ball bearing, then

$$\left.\begin{aligned} P_0 &= \kappa_0^{(A)} \cdot \frac{A}{z}; \\ P_1 &= \kappa^{(A)} \frac{A}{z}, \\ \kappa_0^{(A)} &= \frac{1}{h}, \ \kappa^{(A)} = \frac{w}{h}. \end{aligned}\right\} \qquad (3.33)$$

Values of coefficients $\kappa_0^{(A)}$ and $\kappa^{(A)}$ are found from the curve represented on Fig. 4.35. These curves are obtained from values λ corresponding to the equation $\frac{h}{h} = \tau$, directly resulting from conditions of static equilibrium.

5. Distribution of the Load Between Rows of Balls of Two-Row Radial Thrust Ball Bearings

To absorb jointly effective radial and axial loads in units of a helicopter there are widely used radial thrust ball bearings with initial angles of contact of 26° and 36°, which have small preliminary interference (Fig. 4.36).

Let us try to establish now the load is distributed between

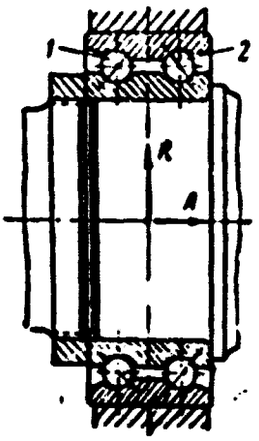

Fig. 4.36. Two-row radial thrust ball bearing loaded by radial and axial forces.

rows of balls of such bearings operating under conditions excluding the possibility of noticeable mutual misalignment of their rings.

Considering that the small preliminary interference has little effect on the magnitude of pressures on the balls, let us use for the approximate solution of the problem the maximum dependences given in the preceding point.

Assuming in equalities (3.4) and (3.7) $\bar{\varepsilon}=0$ and $\bar{\Delta}_a=0$ and remembering that $\bar{\delta}_1=\frac{\bar{\delta}_{01}}{1+\lambda_1}$ and $\bar{\delta}_2=\frac{\bar{\delta}_{02}}{1+\lambda_2\cos\psi_{02}}$, we find $\lambda_2=\lambda_1$. Subscript "1" is given to the row of balls in the direction of which the axial force is directed. Since with loading of the bearing by radial and axial forces angle $\psi_{02}=180^\circ$ and, consequently, $\cos\psi_{02}=-1$, then for the examined case from equations (3.23) we have

$$\varepsilon=\frac{\lambda_1-1}{\lambda_1+1}; \tag{3.34}$$

$$\left.\begin{aligned} A&=zP_{01}\sin\beta_0\left[J_{12}-\left(\frac{\lambda_1-1}{\lambda_1+1}\right)^{3/2}J_{12}\right];\\ R&=zP_{01}\cos\beta_0\left[J_{12}+\left(\frac{\lambda_1-1}{\lambda_1+1}\right)^{3/2}J_{12}\right]. \end{aligned}\right\} \tag{3.35}$$

Dependences determining pressures P_{01} and P_{02} for two-row radial thrust ball bearings can be written in the following way

$$\left.\begin{aligned} P_{01}&=\frac{4,37}{z\cos\beta_0}\frac{c_0^{(0)}R}{2};\\ P_{02}&=\left(\frac{\lambda_1-1}{\lambda_1+1}\right)^{3/2}P_{01}. \end{aligned}\right\} \tag{3.36}$$

$$\kappa_{01}^{(R)} = \frac{2}{4{,}37\left[f_{21} + \left(\frac{\lambda_1 - 1}{\lambda_1 + 1}\right)^{3/2} f_{22}\right]}.$$

Equivalent pressures for both rows of balls are respectively equal to

$$\left.\begin{aligned} P_{01} &= w_1 P_{01}, \\ P_{02} &= w_2 P_{02}. \end{aligned}\right\} \qquad (3.37)$$

Values of parameter λ_1 and coefficient $\kappa_{01}^{(R)}$ depending upon quantity $\frac{1}{\tau} = \frac{A}{R}\operatorname{ctg}\beta_0$ can be found from graphs on Fig. 4.37.

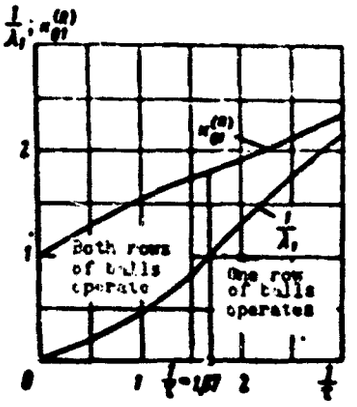

Fig. 4.37. Values of λ_1 and of coefficients $\kappa_{01}^{(R)}$ depending upon $\frac{1}{\tau}$.

As calculations show, the first row is always more loaded. At $\frac{1}{\tau} \geqslant 1{,}67$, when $\lambda_1 < 1$, it bears the entire load applied to the bearing. Let us note that at $\tau = 0{,}6$ the ratio $\frac{A}{R} = 1{,}67 \operatorname{tg}\beta_0$.

With the predominant axial loads, when one row of the balls operates, for the purpose of obtaining more accurate results the calculation of two-row radial thrust ball bearings of all types, including those examined in the given section, should be produced with the help of dependences of § 2.

6. Examples of the Calculation

Example 1. To determine the calculation of the service life of bearings of the disk of the cyclic pitch control (Fig. 4.38),

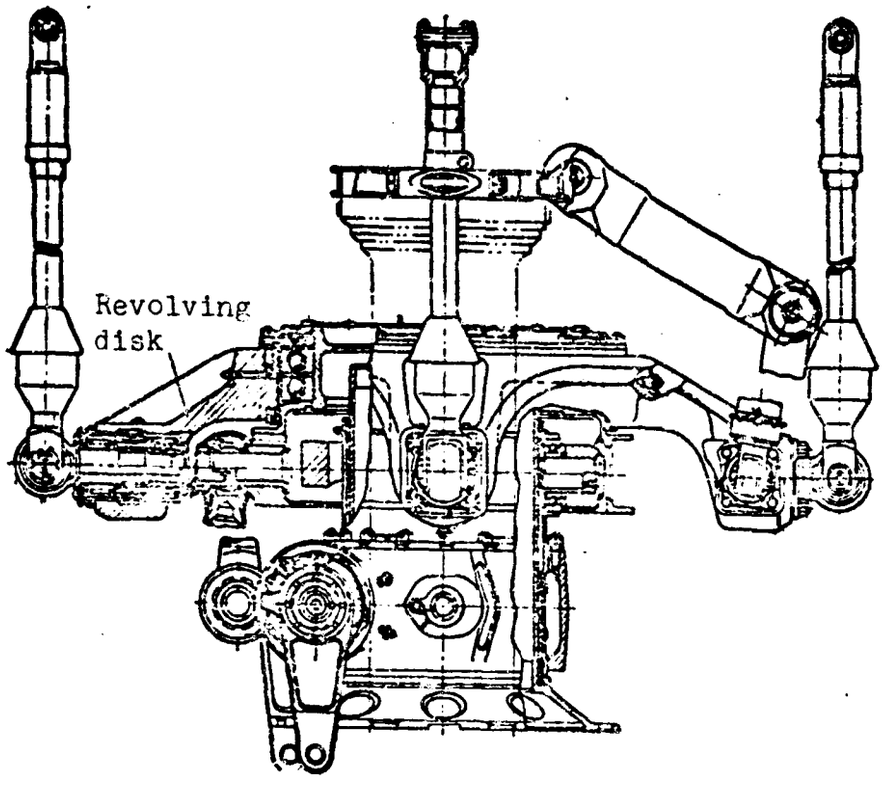

Fig. 4.38. Cyclic pitch control of the rotor of a helicopter.

loaded of moments M = 150 kG·m and revolving at 240 revolutions per minute. The bearings have the following parameters: $\beta_0 = 36^\circ$, $d_ш = 9.525$ mm, $z = 42$, $r_0 = 7^\circ$ m.

The relative base $\zeta = 0.1$, and the preliminary interference $\Delta_n = 0$.

Since the bearing has zero preliminary interference, the coefficients $\kappa_0^{(M)}$ and $\kappa^{(M)}$, necessary for calculating loads on balls, are determined with the help of Fig. 4.21.

These quantities are calculated

$$Q = \left| \frac{1 - \zeta \operatorname{tg} \beta_0}{\operatorname{tg} \beta_0 + \zeta} \right| = \left| \frac{1 - 0{,}1 \cdot 0{,}726}{0{,}726 + 0{,}1} \right| = 1{,}12;$$

$$\overline{M} = \frac{1}{z v d_ш^2 \sin \beta_0 (1 + \zeta \operatorname{ctg} \beta_0)} \cdot \frac{M}{r_0} =$$

$$= \frac{1}{42 \cdot 1 \cdot 9{,}525^2 \cdot 0{,}588 (1 + 0{,}1 \cdot 1{,}376)} \cdot \frac{150}{0{,}079} = 0{,}744.$$

Since $\frac{r_{0(\kappa)}}{d_ш}$ = 0.515, then coefficient ν is accepted equal to unity.

According to Fig. 4.21, the obtained values of ρ and $\bar{M}$ correspond to the value $\kappa_0^{(M)}$ = 0.912.

Thus maximum pressures on the balls in both bearings will be

$$P_{01}=P_{02}=\frac{4{,}37\kappa_0^{(M)}M}{2r_0z\sin\beta_0(1+\zeta\operatorname{ctg}\beta_0)}=$$

$$=\frac{4{,}37\cdot0{,}912\cdot150}{2\cdot0{,}079\cdot42\cdot0{,}588\,(1+0{,}1\cdot1{,}376)}=134{,}7\text{ kG}.$$

In the examined case $\lambda_1=\lambda_2=\infty$. Consequently,

$$P_{s1}=P_{s2}=\omega_{\lambda=\infty}P_{01}=0{,}587\cdot134{,}7=79{,}1\text{ kG}.$$

The equivalent pressure $P_{эу}$, which determines the longevity of the subassembly, can be found by the formula (2.44). Considering that at $\lambda_1=\lambda_2=\infty$ and $\kappa_{s1}=\kappa_{s2}$ = 1.2 (see Fig. 4.5), from this formula we find

$$P_{э.у}=2^{\frac{1}{3{,}33l}}\kappa_{s1}P_{s1}=1{,}21\cdot1{,}2\cdot79{,}1=114{,}8\text{ kG}.$$

Here it is accepted that $l=\frac{10}{9}$.

For bearings with the indicated dimensions, according to the formula (2.42), the coefficient of efficiency

$$C=65\cdot z^{0{,}7}\cdot\frac{d_ш^2}{1+0{,}02d_ш}=65\cdot42^{0{,}7}\cdot\frac{9{,}525^2}{1+0{,}02\cdot9{,}525}=67\,794.$$

As results of bench tests show, for bearings of the disk of the cyclic pitch control the product of coefficients $\kappa_б\kappa_т\kappa_м$ = 1.1.

In accordance with this from expression (2.43), considering that $h=h_{10}$, we obtain

$$(nh)^{0{,}3}=\frac{C}{0{,}39\cdot\kappa_б\kappa_т\kappa_м zP_{э.у}\cos\beta_0}=\frac{67\,794}{0{,}39\cdot1{,}1\cdot42\cdot114{,}8\cdot0{,}809}=40{,}5.$$

Whence

$$nh = 228\,370 \text{ and } h = \frac{228\,370}{240} \approx 950 \text{ hours.}$$

Example 2. To calculate the maximum and equivalent pressures on the balls in the bearings examined in Example 1 at the moment absorbed by them M = 60 kG·m and axial force A = 500 kG.

Since the relative base ζ is small, then for the determination of the indicated pressures we will use Figs. 4.26-4.28.

According to quantities

$$\frac{M}{r_0 z v d_m^2} = \frac{60}{0{,}079 \cdot 42 \cdot 1 \cdot 9{,}525^2} \approx 0{,}1993 \text{ kG/mm}^2$$

and

$$\frac{A}{z v d_m^2} = \frac{500}{42 \cdot 1 \cdot 9{,}525^2} = 0{,}1312 \text{ kG/mm}^2$$

with the help of Fig. 4.26 we find: $\bar{\delta}_{01} = 0.055$ and $\lambda_1 = 0.7$.

Let us calculate further P_{01} and P_{a1}. Since $\lambda_1 = 0.7$ corresponds to the value w = 0.678, then according to the formulas (2.2) and (2.6) we have:

$$P_{01} = B_0 v d_m^2 \delta_0^{3/2} = 62 \cdot 1 \cdot 9{,}525^2 \cdot 0{,}055^{3/2} = 72{,}5 \text{ kG};$$
$$P_{a1} = w P_{01} = 49{,}2 \text{ kG}.$$

From the graphs on Figs. 4.27 and 4.28 let us find the values P_{a2}/P_{a1} and P_{02}/P_{01}. Using these values, we obtain

$$P_{02} = 1{,}085 P_{01} = 78{,}7 \text{ kG}; \quad P_{a2} = 0{,}875 P_{a1} = 43 \text{ kG}.$$

§ 4. Calculation of Tapered Roller Bearings Under Combined Loads

1. Calculation of Single-Row Tapered Roller Bearings

Discussed above were methods of calculation of radial and radial thrust ball bearings absorbing combined loads. Let us consider

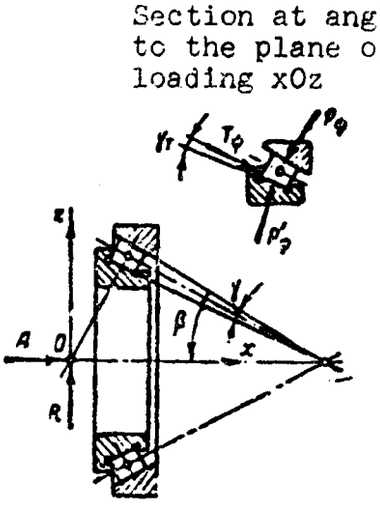

Fig. 4.39. Diagram of the loading of a tapered roller bearing by radial and axial forces.

now the peculiarities of the calculation of tapered roller bearings operating under conditions of a complex load.

First of all, let us resolve the problem of the determination of forces acting on the rollers of a single-row tapered roller bearing, with assigned values of radial and axial loads applied to it (Fig. 4.39).

Normal forces P_ψ and P'_ψ, acting on the roller from the side of the inner and outer rings, are connected with each other by the relation

$$P'_\psi = \frac{\cos(\gamma - \gamma_T)}{\cos \gamma_T} P_\psi. \qquad (4.1)$$

At usual values of angles γ and γ_T we can practically assume that

$$P'_\psi = P_\psi. \qquad (4.2)$$

In conformity with the Hertz theory, for the case of linear contact it can be assumed quite accurately that

$$P_\psi = B\delta_\psi, \qquad (4.3)$$

where δ_ψ is the approach of rings in the section located at angle ψ to the plane of loading.

In the absence of mutual misalignment of rings under a load

the approach δ_ψ is determined by the expression

$$\delta_\psi = s \sin\beta + u \cos\beta \cos\psi. \tag{4.4}$$

Here u and s are the radial and axial displacements of the inner ring relative to the outer ring reckoned from a position at which in the bearing the clearances are selected; β — angle of cone of the outer ring.

Assuming that

$$\frac{u}{s} \operatorname{ctg}\beta = \lambda, \tag{4.5}$$

from expressions (4.3) and (4.4) we obtain

$$P_\psi = B s \sin\beta (1 + \lambda \cos\psi). \tag{4.6}$$

If the direction of radial loading coincides with a positive direction of axis z ($R > 0$), then displacement $u > 0$. In this case the center of the zone of loading is in section $\psi = \psi_0 = 0$. If the radial loading acts in an opposite direction ($R < 0$), then displacement $u < 0$, and then the center of the zone of loading is disposed in section $\psi = \psi_0 = 180^\circ$.

According to formula (4.6) the maximum value of force P_ψ is equal to

$$P_0 = B s \sin\beta (1 + \lambda \cos\psi_0). \tag{4.7}$$

Using equality (4.7), we finally have

$$P_\psi = \frac{P_0}{1 + \lambda \cos\psi_0} (1 + \lambda \cos\psi). \tag{4.8}$$

As follows from conditions of static equilibrium

$$\left.\begin{aligned} R &= \frac{P_0}{1 + \lambda \cos\psi_0} \cos\beta \sum (1 + \lambda \cos\psi) \cos\psi; \\ A &= \frac{P_0}{1 + \lambda \cos\psi_0} \sin\beta \sum (1 + \lambda \cos\psi). \end{aligned}\right\} \tag{4.9}$$

With the usual quantities of rollers equations (4.9) can be replaced by relations:

$$\left.\begin{aligned} R &= P_0 z \cos\beta / 2 \cos\psi_0; \\ A &= P_0 z \sin\beta / 2. \end{aligned}\right\} \tag{4.10}$$

Here

$$\left.\begin{aligned} j_1 &= \frac{1}{2\pi(1+\lambda\cos\psi_0)}\int_{\psi_a'}^{\psi_a'}(1+\lambda\cos\psi_0\cos\psi)\,d\psi = \\ &= \frac{1}{2\pi(1+\lambda\cos\psi_0)}\left[(\psi_a'-\psi_a')+2\lambda\cos\psi_0\sin\psi_a'\right]; \\ j_2 &= \frac{1}{2\pi(1+\lambda\cos\psi_0)}\int_{\psi_a'}^{\psi_a'}(1+\lambda\cos\psi_0\cos\psi)\cos\psi\,d\psi = \\ &= \frac{1}{2\pi(1+\lambda\cos\psi_0)}\left\{2\sin\psi_a'+\frac{\lambda\cos\psi_0}{2}\left[(\psi_a'-\psi_a')+\sin 2\psi_a'\right]\right\}. \end{aligned}\right\} \qquad (4.11)$$

Limits of the zone of loading ψ_a' and ψ_a' are determined just as for radial and radial thrust ball bearings [see formula (1.20) and explanations to it].

From relations (4.10), assuming for simplicity R > 0 and, consequently, $\psi_0 = 0$, we find

$$P_0 = \frac{1}{j_2}\frac{R}{z\cos\beta}. \qquad (4.12)$$

The equivalent pressure P_e for a tapered roller bearing can be represented in the form:

$$P_e = wP_0, \qquad (4.13)$$

where

$$w = \frac{1}{1+\lambda\cos\psi_0}\left[\frac{1}{2\pi}\int_{\psi_a'}^{\psi_a'}(1+\lambda\cos\psi_0\cos\psi)^{3,33}d\psi\right]^{0,3}.$$

The value of quantities j_1, j_2, and w in function $\lambda\cos\psi_0$ is given in Table 4.7.

The calculation of tapered roller bearings, just as that of radial thrust ball bearings is usually conducted with the help of reduced static and dynamic loads. These loads are found from

Table 4.7.

$\lambda\cos\varphi_0$	J_1	J_2	w	$\lambda\cos\varphi_0$	J_1	J_2	w
0	1	0,5	1	2,000	0,405	0,268	0,698
0,1	0,909	0,454	0,913	2,500	0,389	0,267	0,692
0,2	0,833	0,417	0,853	3,333	0,371	0,264	0,686
0,3	0,769	0,385	0,806	5,000	0,354	0,261	0,679
0,4	0,714	0,357	0,773	10,000	0,336	0,256	0,670
0,5	0,667	0,333	0,751	$\pm\infty$	0,318	0,250	0,660
0,6	0,625	0,312	0,738	−10,000	0,300	0,242	0,648
0,7	0,588	0,294	0,729	−5,000	0,281	0,234	0,634
0,8	0,555	0,278	0,725	−3,333	0,261	0,222	0,617
0,9	0,526	0,263	0,722	−2,500	0,240	0,210	0,598
1,0	0,500	0,250	0,720	−2,000	0,218	0,196	0,575
1,111	0,479	0,258	0,718	−1,667	0,194	0,178	0,548
1,250	0,460	0,264	0,714	−1,428	0,167	0,156	0,518
1,428	0,440	0,266	0,708	−1,250	0,136	0,130	0,484
1,667	0,424	0,268	0,704	−1,000	0,000	0,000	0,000

from the condition that

$$\left.\begin{aligned} P_0 &= \frac{1}{J_{2\lambda=\infty}}\frac{Q_0}{z\cos\beta} = 4\frac{Q_0}{z\cos\beta};\\ P_0 &= \frac{w_{\lambda=\infty}}{J_{2\lambda=\infty}}\frac{Q}{z\cos\beta} = 2{,}64\frac{Q}{z\cos\beta}. \end{aligned}\right\} \qquad (4.14)$$

In comparing equalities (4.14) with equalities (4.12) and (4.13), we obtain

$$\left.\begin{aligned} Q_0 &= \kappa_0^{(R)} R;\\ R &= \kappa^{(R)} R_0 \end{aligned}\right\} \qquad (4.15)$$

where

$$\left.\begin{aligned} \kappa_0^{(R)} &= \frac{J_{2\lambda=\infty}}{J_2} = \frac{0{,}25}{J_2};\\ \kappa^{(R)} &= \frac{w}{w_{\lambda=\infty}}\kappa_0^{(R)} = \frac{0{,}38\,w}{J_2}. \end{aligned}\right\} \qquad (4.16)$$

In accordance with relations (4.10), the values of parameter λ necessary for the determination of coefficients $\kappa_0^{(R)}$ and $\kappa^{(R)}$ should satisfy the condition

$$\frac{J_2}{J_1} = \frac{R}{\lambda}\operatorname{tg}\beta = \ldots \qquad (4.17)$$

Since at $\lambda=1$ $\frac{j_1}{j_2}=0.5$, then so that in the single-row tapered roller bearing all rollers are loaded quantity τ should not exceed 0.5.

At $\tau\geqslant 0,5$ values of coefficients $\kappa_0^{(R)}$ and $\kappa^{(R)}$ can be determined by the graphs shown in Fig. 4.40. These graphs are plotted on the basis of equalities (4.16) and (4.17).

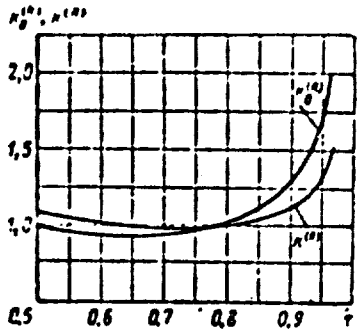

Fig. 4.40. Values of coefficients $\kappa_0^{(R)}$ and $\kappa^{(R)}$ depending upon τ.

If $\tau<0,5$ and, consequently $\lambda<1$, then expressions for integrals j_1 and j_2 take the form

$$\left.\begin{aligned} j_1&=\frac{1}{1+\lambda};\\ j_2&=\frac{1}{2}\frac{\lambda}{1+\lambda}.\end{aligned}\right\} \qquad (4.18)$$

From expressions (4.17) and (4.18) we find

$$\left.\begin{aligned} \lambda&=2\tau;\\ \frac{1}{j_2}&=2+\frac{1}{\tau}.\end{aligned}\right\} \qquad (4.19)$$

Thus, at $\tau<0,5$, when the load is carried by all rollers,

$$\left.\begin{aligned} \kappa_0^{(R)}&=\frac{0,25}{j_2}=0,5+\frac{0,25}{\tau};\\ \kappa^{(R)}&=\frac{\omega}{\omega_{\lambda=\infty}}\kappa_0^{(R)}=0,76\omega+0,38\frac{\omega}{\tau}.\end{aligned}\right\} \qquad (4.20)$$

As follows from equalities (4.20), with all loaded rollers

$$Q_0=0,5R+0,25A\operatorname{ctg}\beta; \qquad (4.21)$$

$$Q=0,76\omega R+0,38\omega A\operatorname{ctg}\beta. \qquad (4.22)$$

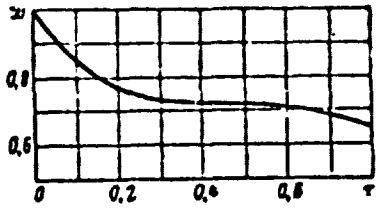

Fig. 4.41. Values w depending upon τ.

It is convenient to determine values w in function τ by the curve shown on Fig. 4.41.

The dependences cited give an answer to all basic questions appearing in the calculation of tapered roller bearings absorbing combined loads, under the condition that mutual misalignment of their rings can be disregarded.

As can be seen from Fig. 4.40, in the region τ = 0.6-0.8 curves $K_0^{(P)} \div K_0^{(P)}(\tau)$ and $A^{(2)} \div K^{(R)}(\tau)$ have a quite clearly expressed minimum. This indicates that the appropriate selection of the angle of contact β can be achieved in order that with the assigned combination of radial and axial loads the maximum and equivalent pressure on

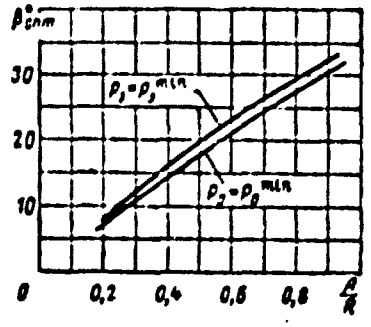

Fig. 4.42. Values of the optimum angle of contact depending upon the ratio $\frac{A}{R}$.

rollers have least value. The optimum angles of contact at which conditions $P_0 = P_0^{min}$ and $P_e = P_e^{min}$ are fulfilled are determined by the graphs shown on Fig. 4.42. These graphs are obtained as a result of the investigation of dependences $\frac{zP_0}{R} = F_0\left(\frac{A}{R}\right)$ and $\frac{zP_e}{R} = F\left(\frac{A}{R}\right)$, plotted for a number of angles of contact lying in the range of 0^o to 30^o.

2. Some Remarks on the Calculation of Bearing Subassemblies Consisting of Two Tapered Roller Bearings

If the bearing subassembly, consisting of two tapered roller bearings, is loaded by the moment acting in combination with radial

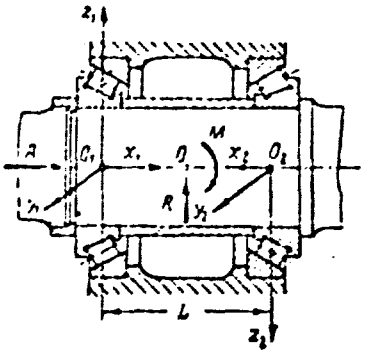

Fig. 4.43. Diagram of loading of two tapered roller bearings by radial and axial forces and the moment.

and axial forces (Fig. 4.43), then to calculate it there can be used the system of equations

$$\left.\begin{aligned} R &= zP_{01}\cos\beta\,(J_{21} - \varkappa j'_{22}\cos\gamma_{02});\\ A &= zP_{01}\sin\beta\,(J_{11} - \varkappa j_{12});\\ M &= r_0 zP_{01}\sin\beta\,(1 + \zeta\operatorname{ctg}\beta)(J_{21} + \varkappa J_{22}\cos\gamma_{02});\\ \lambda_2\cos\gamma_{02} &= -\left[1 + \frac{\varkappa(1+\lambda_1)}{1-(1+\lambda_1)\dfrac{2\delta_n\sin\beta}{t_{0i}}}\right]. \end{aligned}\right\} \qquad (4.23)$$

analogous to the system of equations (3.23) and (3.24) describing conditions of static equilibrium of bearing subassemblies with two radial thrust ball bearings on the assumption that angles of contact of all balls are identical and equal to the initial.

It is necessary to note that equations (4.23) are "exact," inasmuch as in tapered roller bearings the angles of contact are indeed constant and do not change under load, and these equations are real both in the presence, and in the absence of mutual misalignment of the rings.

In equations (4.23) instead of quantity $\varkappa^{3/2}$ quantity $\varkappa$ appears.

This is explained by the fact that for tapered roller bearings

$$\frac{P_{02}}{P_{01}} = \frac{b_{02}}{b_{01}} = \varkappa.$$

In the case of zero preliminary interference values λ_1 and $\varkappa$, which satisfy equations (4.23), are found by the graphs shown on Fig. 4.44. Quantities τ and v here have the same meaning as they do for radial thrust ball bearings [see formulas (3.26) and (3.27)].

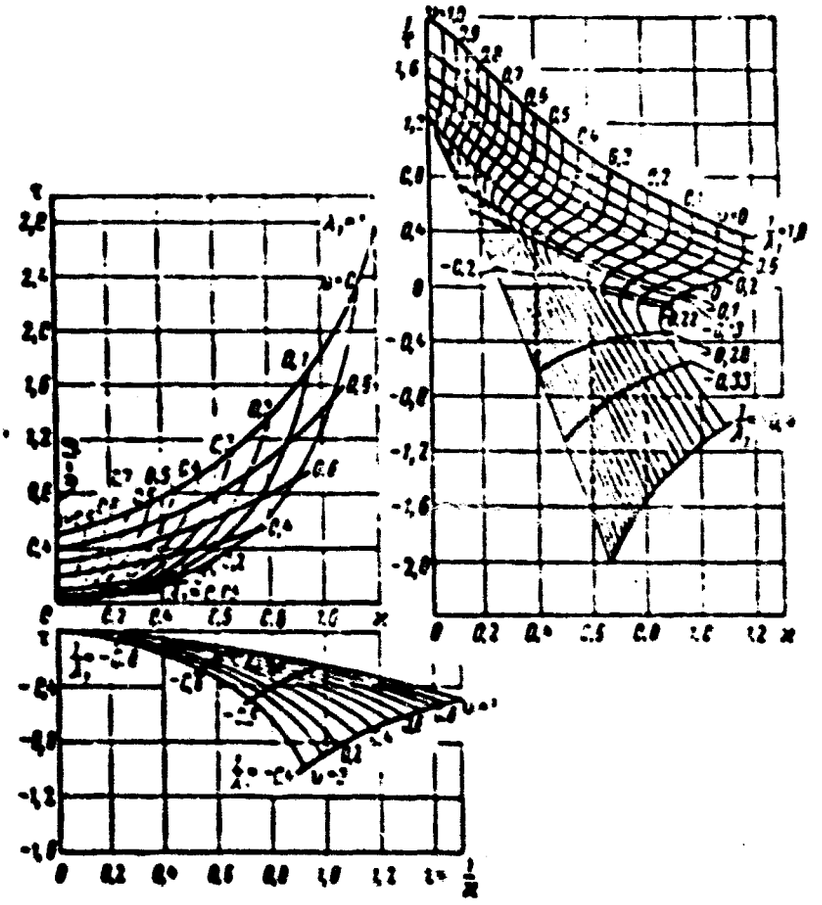

Fig. 4.44. Nomographs for the calculation of bearings loaded by radial and axial forces and the moment.

With respect to the found values λ_1 and $\varkappa$ the quantity $\lambda_1 \cos\alpha_{01}$ is calculated.

Maximum and equivalent pressures on rollers in bearings 1 and 2 are determined from the expressions:

$$\left.\begin{aligned} P_{01} &= \frac{2\kappa_{01}^{(M)} M}{r_0 z \sin\beta (1+\zeta \operatorname{ctg}\beta)} = \frac{\kappa_{01}^{(A)} A}{z \sin\beta}; \\ P_{02} &= \frac{2\kappa_{02}^{(M)} M}{r_0 z \sin\beta (1+\zeta \operatorname{ctg}\beta)} = \frac{\kappa_{02}^{(A)} A}{z \sin\beta}; \\ P_{s1} &= \frac{1{,}32\kappa_1^{(M)} M}{r_0 z \sin\beta (1+\zeta \operatorname{ctg}\beta)} = \frac{\kappa_1^{(A)} A}{z \sin\beta}; \\ P_{s2} &= \frac{1{,}32\kappa_2^{(M)} M}{r_0 z \sin\beta (1+\zeta \operatorname{ctg}\beta)} = \frac{\kappa_2^{(A)} A}{z \sin\beta}. \end{aligned}\right\} \qquad (4.24)$$

Here

$$\left.\begin{aligned} \kappa_{01}^{(M)} &= \frac{1}{2(j_{21} + \varkappa j_{22}\cos\psi_{02})}; \quad \kappa_{02}^{(M)} = \varkappa \kappa_{01}^{(M)}; \\ \kappa_{01}^{(A)} &= \frac{1}{j_{11} - \varkappa j_{12}}; \quad \kappa_{02}^{(A)} = \varkappa \kappa_{01}^{(A)}; \\ \kappa_1^{(M)} &= \frac{\omega_1}{0{,}66}\kappa_{01}^{(M)}; \quad \kappa_2^{(M)} = \frac{\omega_2}{0{,}66}\kappa_{02}^{(M)}; \\ \kappa_1^{(A)} &= \omega_1 \kappa_{01}^{(A)}; \quad \kappa_2^{(A)} = \omega_2 \kappa_{02}^{(A)}. \end{aligned}\right\} \qquad (4.25)$$

Assuming in system (4.23) $\beta = 90^\circ$, we arrive at the following equations, which describe conditions of static equilibrium of two-row thrust roller bearings:

$$\left.\begin{aligned} A &= zP_{01}(j_{11} - \varkappa j_{12}); \\ M &= r_0 z P_{01}(j_{21} + \varkappa j_{22}). \end{aligned}\right\} \qquad (4.26)$$

Methods of solving equations (4.26) are clear from the foregoing, and therefore discussing them has no special meaning.

If in equations (4.26) we assume that $\varkappa = 0$, then they will obtain the form:

$$\left.\begin{aligned} A &= zP_0 j_1; \\ M &= r_0 z P_0 j_2. \end{aligned}\right\} \qquad (4.27)$$

Relations (4.27) characterize the distribution of load in single-row thrust roller bearings.

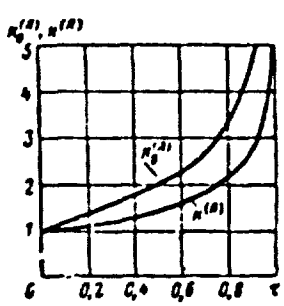

Fig. 4.45. Values of coefficients $\kappa_0^{(A)}$ and $\kappa^{(A)}$ depending upon τ.

Value of maximum $P_0=\kappa_0^{(A)}\frac{A}{z}$ and equivalent $P_0=\kappa^{(A)}\frac{A}{z}$ of pressures on the roller, which satisfy relations (4.27), are conveniently found with the help of curves $\kappa_0^{(A)}=\kappa_0^{(A)}(\tau)$ and $\kappa^{(A)}=\kappa^{(A)}(\tau)$, shown on Fig. 4.45.

For $\lambda<1$, when in the bearing all rollers are loaded, integrals j_1 and j_2 are determined by expressions (4.18).

It is easy to be convinced that in this case, taking place when $\tau=\frac{M}{r_0\lambda}\leqslant 0.5$,

$$\left.\begin{aligned}&\lambda=2\tau;\\ &\kappa_0^{(A)}=\frac{1}{j_1}=1+\lambda=1+2\tau.\end{aligned}\right\} \qquad (4.28)$$

§ 5. Calculation of Bearings Operating with a Vibrating Motion

In the designing of helicopters there are considerable difficulties in the correct selection of bearings of hubs of the main and antitorque rotors. These bearings, as is known, operate in specific conditions of a vibrating motion. They are put out of service not because of contact fatigue but due to the local weak rolling tracks, which received the name of "false ball test." It is understandable that the usual methods of calculation for such bearings are inapplicable.

Properties of lubrication have a great influence on the efficiency of vibrating bearings. Practice has showed that the reliable operation of many critical bearing subassemblies of a helicopter is possible only with the application of special oils and lubricants. Therefore, in helicopter design it is necessary to pay serious attention to questions of the selection of lubricating materials for antifriction bearings. This, first of all, pertains to bearings of hub axial hinges of main and antitorque rotors, which absorb considerable axial loads from centrifugal forces of the blades.

The complexity of calculation of bearings of hubs of main and

antitorque rotors consists in the fact that the relatively low rigidity of their basic parts, especially on heavy helicopters, can lead to noticeable deformations of the rings, which is difficult to consider in determining forces acting on rolling solids. The development of general methods of calculation which consider the influence of all factors determining the carrying capacity of bearings of hubs of main and antitorque rotors thus far has been unsuccessful. However, experimental data accumulated up to the present time permit giving definite recommendations on the selection of allowed loads and determination of longevity of the most widespread forms of bearings used in these complex and critical units. Analogously there is the case with the calculation of bearings of hinges of cyclic pitch controls and control mechanisms of helicopters, which just as bearings of hubs, operate with an oscillatory motion. Only here it should be additionally considered that loads absorbed by the majority of these bearings have a dynamic character.

1. Peculiarities of the Mechanism of Wear of Antifriction Bearings Under Conditions of Vibrating Motion

Let us examine the peculiarities of the mechanism of wear of antifriction bearings in vibrating motion.

At small amplitudes of oscillations, when the contact of rolling solids with rings occurs only on separate sections of rolling tracks in the bearings, dents will be formed in the form of holes from the balls or grooves from the rollers, which with the crumbing of their surface are turned into deep pits (Fig. 4.46). The failure of rolling solids in the majority of the cases starts only after considerable damage to the rings.

An analysis of results of tests shows that with vibrating motion the wear of bearings to a considerable degree is determined by oxidizing processes and special conditions of lubrication in zones of contact of rolling solids with the rings.

In zones of contact there occurs intense frictional corrosion.

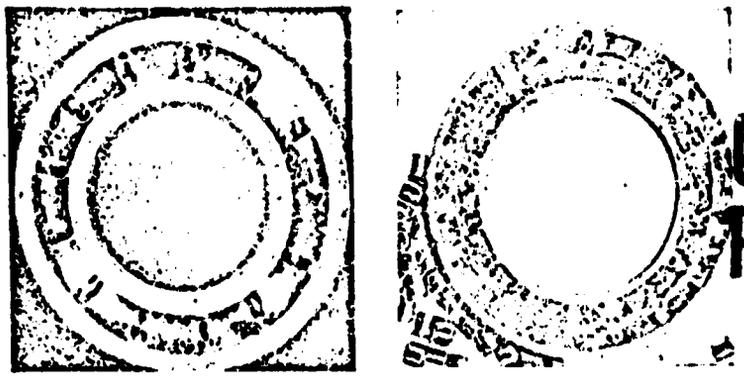

Fig. 4.46. Rings of thrust ball and roller bearings after prolonged operation under vibrating motion with small amplitudes.

The obtained products of iron oxidation, being mixed with the lubrication, will form a unique polishing mixture which causes rapid wear of rolling tracks. With the rolling of a rolling solid in front of the contact area there will be formed a "threshold" of lubrication but after it, streams of lubrication trying to fill the space behind the moving rolling solid (Fig. 4.47). If the

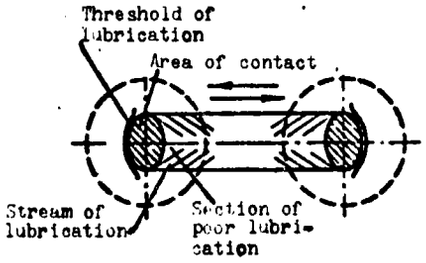

Fig. 4.47. Lubrication chart during vibrating motions.

lubrication is insufficiently mobile and does not succeed immediately in filling this space, then the section of the rolling track directly adjacent to the area of contact will appear covered only by a thin film of lubrication. It is natural that at the time of the change in direction of motion the rolling solid will pass this poorly lubricated section earlier than lubrication will proceed to it again. Due to this on limits of sections of the contact of rolling solids with the rings, where a change in the direction of the motion occurs, pressure peaks appear leading to the acceleration of wear. At very small amplitudes of oscillations, when the areas of contact in extreme positions of the rolling solid are covered, the

disturbance in the lubrication layer can appear constant. In this case peaks of pressures increase even more, and the life of the bearings noticeably decreases. The increase in mobility of lubrication improves conditions of operation of vibrating bearings. Nonetheless, even with the application of oils possessing high mobility the conditions of their operation differ considerably from conditions of operation of bearings revolving in one direction.

From what has been said it is clear that in bearing subassemblies operating with a vibrating motion, in all cases when it is possible by constructive considerations one should use an oil and hot grease lubricants. When using grease lubrications the carrying capacity of vibrating bearings noticeably decreases.

2. Lubrication of High-Loaded Vibrating Bearings at Small Amplitudes of Oscillations

Inasmuch as properties of lubrication have a great effect on the life of vibrating bearings, then to discuss allowed loads for such bearings in the separation from lubricating materials used in them has no meaning.

Bearings of helicopters, which operate with a vibrating motion, can be divided into two basic groups:

1. Bearings of hubs of main and antitorque rotors, cyclic pitch controls and certain elements of control operating at amplitudes of oscillations up to 10°. For these bearings the total number of oscillations between two overhauls, during which they are replaced, usually amounts to not less than 10 million.

2. Bearings of control mechanisms accomplishing a limited number of oscillations (up to 100,000) with amplitudes of more than 20°. It is kept in mind that the covering of neighboring areas of contact does not occur.

Practice has showed that bearings of the second group can satisfactorily operate on good grease lubricants. This is explained

by the fact that on rolling tracks of such bearings considerable dents from rolling solids can be allowed, inasmuch as their efficiency is usually limited only by the magnitude of the permissible moment of friction.

In bearings of the cyclic pitch control and elements of control belonging to the first group, the application of grease lubrications involves a noticeable lowering of the carrying capacity; however, according to constructive considerations with this it is necessary to accept and compensate the insufficiently high lubricating properties of lubricants by a certain decrease in allowed loads. Regarding bearings of hubs of main and antitorque rotors, then considering that for them permissible wears of rolling tracks are comparatively small, they can operate a long time at high contact stresses only in the case of the application of oils possessing a definite complex of physical and chemical properties.

The life of vibrating bearings essentially depends on the quality of packing of bearing subassemblies. With poor packings, which allow atmospheric oxygen to penetrate inside the subassemblies, and also with small volumes of lubrication and large volumes of air the life of vibrating bearings noticeably decreases. A very effective means for increasing the service life of bearings operating in a vibrating motion is a supply of lubrication under pressure and especially the transition to circulation lubrication, which provides continuous entering of fresh nonoxidized oil to zones of contact and the removal from them of wear products.

Let us discuss questions of the selection of oils for hubs of main and antitorque rotors more specifically, since these questions are very urgent for helicopter construction.

Oils for axial hinges of hubs of main and antitorque rotors. As experiments show, bearings of axial hinges, absorbing considerable axial loads from centrifugal forces of the blades, are especially sensitive to physical and chemical properties of lubrication. Oils for these subassemblies, the service life of which usually determines

the total service life of hubs of main and antitorque rotors, should satisfy the following basic requirements:

– first, these oils should not create amplifications of oxidizing processes in the zones of contact;

– secondly, they should preserve high mobility in the whole range of operating temperatures and provide sufficient strength of the oil film over the whole extent of sections of contact.

The permissible level of viscosity of the oil is limited also by the permissible magnitude of the moment of friction of the axial hinge. If one proceeds from the operational experience of Mi-1 and Mi-4 helicopters, then one can assume that at minimum operating temperature the kinematic viscosity should not exceed 90,000 cSt. Tests show that in this case there is observed neither a noticeable increase in moments of friction nor the reduction in life of the bearings because of a decrease in mobility of the oil. It is necessary to note that oil MS-14, successfully operating in axial hinges of hubs of rotors of helicopters Mi-1 and Mi-4 at temperatures down to -25°C, has the indicated kinematic viscosity at a temperature of -20°C.

In virtue of specific conditions of operation of vibrating bearings oils and lubricants for them should be selected only according to results of tests with vibrating motion. The standard method of tests of oils and lubricants on a four-ball instrument for these purposes is absolutely unfit. Lubricating properties of oils and lubricants for axial hinges of hubs of main and antitorque rotors can be expediently checked in thrust ball bearings, since they operate at higher contact stresses. Experiments show that lubricating materials possessing the highest efficiency in such bearings are best for vibrating bearings of other types, including thrust bearings with "turned" rollers, which at present are successfully used in hubs of rotors of all Soviet commerical helicopters and also for multiple radial thrust ball bearings installed in hubs of main and antitorque rotors of a number of foreign helicopters. Inasmuch as

in thrust ball bearings the load is distributed evenly between the balls, then with an oscillatory motion each contacting section of the rolling track can be examined as an independent object of tests.

Of importance in tests of oils and lubricants for bearings of axial hinges of hubs of main and antitorque rotors is the correct evaluation of the state of rolling tracks. Even with the most moderate contact stresses after a short operation on rolling tracks holes from the balls appear. If we consider the appearance of such holes, independently of their depth, as the beginning of the bearing being put out of commission, then it will be necessary to reject the bearings, which could still reliably operate for a long time.

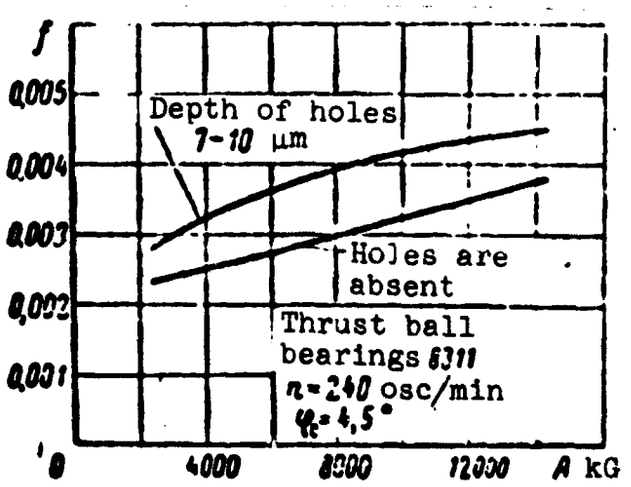

Fig. 4.48. Dependence of coefficient of friction of a thrust ball bearing on the depth of holes on rings.

Curves on Fig. 4.48 show how the depth of the holes affects the coefficient of friction of a thrust ball bearing. With the depth of the holes at 7-10 μm the coefficient of friction increases by 30-40%. The increase in the coefficient of friction in such limits is usually not felt in an operation. Therefore the state of thrust ball bearings at a depth of the holes down to 10 μm should be considered as satisfactory. The same depth of the holes can be allowed in radial thrust ball bearings.

Tests have established that MS-20 oil is one of the best for vibrating bearings. In accordance with this it can be accepted

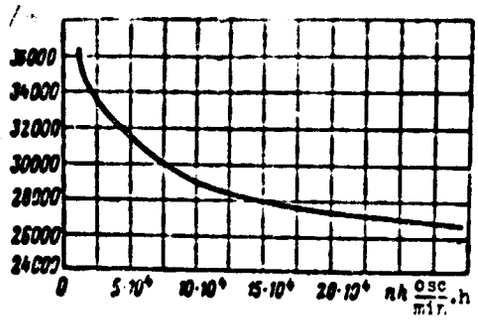

Fig. 4.49. Life curve $\sigma = \sigma(nh)$ for thrust ball bearings.

as the standard for the evaluation of lubricating properties intended for operation in axial hinges of hubs of main and antitorque rotors. Results of tests of thrust ball bearings on MS-20 oil are represented on Fig. 4.49 in the form of a life curve $\sigma = \sigma(nh)$, which establishes the connection between contact stress σ and the product nh of the number of oscillations per minute for a duration of operation in hours. Tests were conducted with the amplitude of oscillations of the mobile ring $\varphi_0 = 4.5^\circ$, frequency, n = 240 oscillations per minute and temperature of oil bath, 20-40°C.

With values of contact tensions determined by the life curve, depicted on Fig. 4.49, 98% of the holes on rolling tracks have a depth not exceeding 10 μm.

It should be noted that between maximum Δ_n^{max} and average Δ_n^{cp} depth of holes there is a definite statistical connection. This connection is set by the experimental distribution curve $F\left(\frac{\Delta_n^{max}}{\Delta_n^{cp}}\right)$ of ratio $\frac{\Delta_n^{max}}{\Delta_n^{cp}}$, which, as one can see on Fig. 4.50, is close to the Maxwellian distribution often encountered in technology.

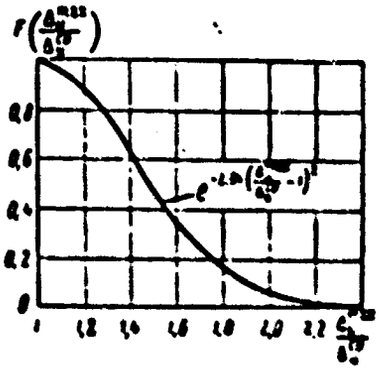

Fig. 4.50. Distribution curve of ratio $\frac{\Delta_n^{max}}{\Delta_n^{cp}}$.

An analysis of the life curve on Fig. 4.49 permits proposing the following conditions of accelerated elimination tests of oils and lubricants for axial hinges of hubs of rotors: duration, 100 h, number of oscillations, 240 per minute, amplitude of oscillations 4.5°, contact stresses 34,000 kG/cm^2. Such conditions permits comparing lubricating properties of the test oil with lubricating properties of MS-20 oil.

It should be kept in mind that with an increase in duration of the tests, the role of the oxidizing processes occurring in zones of contact increases. Nevertheless, preliminary elimination tests of oils and lubricants for bearings of axial hinges can be conducted by given reduced program, since accelerated tests in many cases permit immediately rejecting a considerable number of samples.

MS-20 oil under conditions of oscillatory motion possesses very high lubricating properties. However, it can be used only in the summertime. In winter MS-20 oil is usually replaced by MS-14 oil whose lubricating properties are also quite satisfactory. Since at a temperature of $-30^{\circ}C$ MS-14 oil congeals, then at lower temperatures its application appears impossible, which greatly hampers winter operation of helicopters. The replacement of MS-14 oil by low-congealing general-purpose oils does not give positive results. Tests showed that when operating on standard low-congealing oils axial hinges of hubs of rotors, as when operating on grease lubricants, are rapidly put out of service. This question must be specially discussed, inasmuch as the regularity of such a result was disputed for a long time by certain specialists in the field of lubricating materials, which prolonged the delay of the solution of the problem of lubrication of axial hinges of rotor hubs at low temperatures.

Experiments have established that oil for axial hinges of hubs of main and antitorque rotors should have at a temperature of $100^{\circ}C$ a kinematic viscosity of not less than 9-10 cSt. When operating on low-viscosity oils increased wear of rolling tracks and the crumbling and destruction of rolling solids are observed.

Low-congealing oils with a high level of viscosity in the region of positive temperatures usually consist of a low-viscosity mineral or synthetic base and high polymer thickener. In most cases the thickeners, as the base itself, possess low lubricating properties. Therefore, added to such oils are special antiwear additives containing sulfur, chlorine, phosphorus or definite combinations of these chemically active elements. In zones of high contact temperatures of the additives interact with the surface of the metal, forming respectively films of sulfides, chlorides and phosphides of iron, which prevent direct contact of friction bodies and decrease wear.

According to data of the standard four-ball instrument, lubricating properties of low-congealing thickened oils with antiwear additives considerably exceed lubricating properties of MS-20 and MK-1A oils. Nevertheless, for operating under conditions of vibrating motion they are absolutely unfit. This is explained by the fact that under the influence of antiwear additives oxidizing processes are intensified in the zones of contact and play a decisive role in the mechanism of wear of vibrating bearings. It should also be kept in mind that a majority of the high polymer compounds, used in low-congealing oils, is easily destroyed during mechanical action with the formation of polymers of lesser molecular weight. Destruction of the thickener leads to a decrease in viscosity of the oil. In bearing subassemblies operating with vibrating motion the average destruction of the oil is usually small. However, inasmuch as there is mechanical influence on only small volumes of oil directly adjoining the rolling solids, local destruction and, consequently, the drop in viscosity in zones of contact can reach a considerable magnitude and leads to a noticeable reduction of the strength of the oil film.

During tests of oils with antiwear additives it is often necessary to encounter contradictory results. This shows that tests of such oils should be conducted on a sufficiently large number of samples and that their lubricating properties cannot be judged by single positive results.

From what has been said it follows that oils for axial hinges of hubs of main and antitorque rotors should have neither antiwear additives nor destructive thickeners. This clarifies the unsatisfactory operation of these subassemblies on all standard low-congealing oils, with the creation of which the indicated circumstances were not considered.

Following the given materials according to the efficiency of lubricating materials under conditions of vibrating motion, VNII NP [Editor's Note: All-Union Scientific Research Institute of the Petroleum Industry] proposed for axial hinges of hubs of main and antitorque rotors the low-congealing oil VNII NP-25 [28].

VNII NP-25 oil contains low-viscosity petroleum fraction with a solidification point of -67°C and thickening high-viscous component, which is distinguished by extremely high mechanical and thermal stability. Under the action of high temperatures of friction the petroleum fraction in zones of contact can evaporate; however, the contact of rolling solids with rings will not occur because of the presence of a thickener film, which possesses great adhesion properties. The high thermal and mechanical stability of the thickening component and antioxidant additive provide insignificant changes in properties of VNII NP-25 oil in the operational process.

Basic properties of VNII NP-25 oil are given in Table 4.8.

As results of tests indicate, VNII NP-25 oil in lubricating properties with oscillatory motion is similar to oil MS-20.

Bearings of all types, which operate on VNII NP-25 oil at both positive and negative temperatures, have little wear.

Improvement of lubricating properties of oils can be a most important factor, which is able to increase sharply the service life of hubs of main and antitorque rotors of helicopters. Therefore, works in this direction will take on an even greater character. With the carrying out of these works there should be considered the

Table 4.3.

Solidification point °C	Kinematic viscosity cSt		Lubricating ability on a four-ball instrument (d_w=19 мм)		Corrosiveness in the Pinkevich instrument (at a temperature of +70°C for 50 h)		
	at +100° C	at −35° C	ultimate load P_k kG	width of wear spot мм	steel 30ХГСА	alloy Бр.АЖМц 10-3-1,5	brass ЛС-59
−56	10,2	23 660	64	0,85	+0,11	÷0,26	+0,24

above-described peculiarities of the mechanism of wear and conditions of lubrication of high-loaded vibrating bearings.

Oils for needle bearings of flapping and drag hinges. These bearings, as a rule, are less loaded than bearings of axial hinges, and therefore they are not so sensitive to properties of lubrication. The selection of lubricating materials for needle bearings of flapping and drag hinges of hubs of rotors is facilitated by the fact that thickening in them of the lubricant with a nonoperating rotor does not involve unpleasant consequences. In flapping and drag hinges of antitorque rotors thickening of the lubricant cannot be allowed, since increased moments of friction in these subassemblies can cause shaking of the helicopter.

At present in flapping and drag hinges of hubs of main and antitorque rotors of Soviet helicopters hypoid oil is used. Operational experience of helicopters shows that hypoid oil, in spite of presence in it of free sulfur under standard specific pressures provides a sufficiently high service life of vibrating needle bearings. For axial hinges hypoid oil, just as other oils with antiwear additives is unfit.

Hypoid oil possesses very high adhesiveness, and in connection with this it provides the necessary lubrication of contacting elements

even with incomplete airtightness of the hubs. The replacement of hypoid oil by grease lubricants (this must sometimes be done in antitorque rotors of helicopters operating at especially low temperatures) considerably lowers the service life of needle bearings of flapping and drag hinges.

3. Calculation of Bearings of Hubs of Main and Antitorque Rotors

Bearings of axial hinges. Figure 4.51 gives a model construction of axial hinges of hubs of rotors of Soviet helicopters.

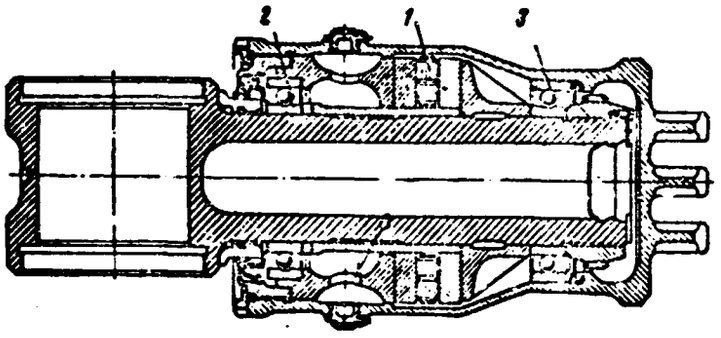

Fig. 4.51. Axial hinge of rotor hub.

In the calculation of bearings of axial hinges of hubs of rotors it is accepted to consider the centrifugal force of the blade N and the moment in the plane of rotation $M_з$, created by the damper.

In axial hinges made according to the diagram shown on Fig. 4.51, the centrifugal force of blade is absorbed by the thrust bearing 1. The damper moment is partially absorbed by this bearing and partially by radial bearings 2 and 3.

Loads in flight on radial bearings 2 and 3 are comparatively small, and therefore they are usually selected from static considerations according to the weight moment of the blade transmitted to them when the helicopter is standing, when the main rotor does not rotate and the blade lies on the overhand limiters. As practice shows, the loads on radial bearings of axial hinges from the weight

moment of the blade can reach 100-110 percent of their static load capacity indicated in the manuals.

The service life of thrust bearings of axial hinges is calculated on the basis of experimental dependences $\sigma = \sigma(nh)$ obtained as a result of tests of corresponding types of bearings under conditions of vibrating motion under a purely axial load. For thrust ball bearings the curve of service life $\sigma = \sigma(nh)$ was shown in Fig. 4.49.

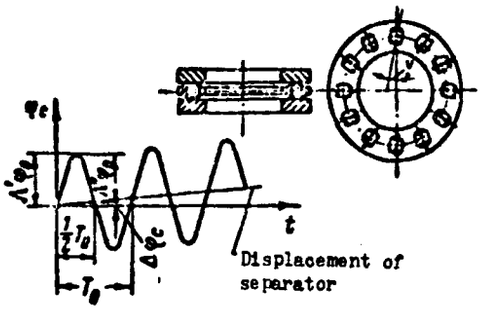

Fig. 4.52. Thrust bearing with turned rollers; recording of motion of bearing separator with vibrating motion.

As was already stated, at present in axial hinges of hubs of rotors of all commerical Soviet helicopters bearings with turned rollers are used. A schematic diagram of such bearings is depicted on Fig. 4.52. Owing to the location of recesses of the separator at an angle to the radial direction in bearings of this type the separator not only vibrates together with the mobile ring but also continuously, although very slowly, is displaced in one direction. The continuous displacement of the separator prevents a "ball test" of the rolling tracks and leads to a considerable increase in the carrying capacity of the bearing.

As a result of the tests it is established that the service life of thrust bearings with turned rollers to a considerable degree depends on the speed of displacement of the separator. This speed can be characterized by time T_c, during which the separator turns at an angle of 360°. Optimum values of time T_c for amplitudes and frequencies of oscillations, with which thrust bearings of axial hinges of hubs of rotors operate, amount to 40-80 min. At $T_c > 80$ min

the probability of putting the bearing out of commission increases because of the crumbling of metal on the rollers. In spite of the continuous displacement of the separator in contact with the rings there are the same sections of the surface of the rollers. Therefore, destruction of thrust bearings with turned rollers in most cases begins with damage of the rollers. It is necessary to note that at T_c = 2.5-6 h, the stability of rollers decreases approximately twice. At T_c < 40 min losses to friction and wear of rolling tracks are noticeably increased.

The curve of service life $\sigma = \sigma(nh)$ for thrust bearings with turned rollers, which have an optimum speed of displacement of the separator T_c = 40-80 min, is shown on Fig. 4.53. This curve is

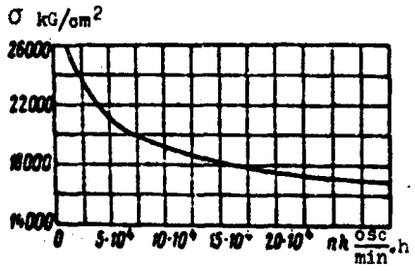

Fig. 4.53. Curve of service life $\sigma = \sigma(nh)$ for thrust ball bearings with turned rollers.

plotted according to results of tests of several groups of such bearings with MS-20 oil at the amplitude of the mobile ring $\varphi_0 = 4.5^\circ$ and frequency n = 240 osc/min, i.e., under conditions similar to conditions of tests whose results were used in the construction of the dependence $\sigma = \sigma(nh)$ on Fig. 4.49.

Bench tests and operational experience indicate that curves of service life, depicted on Figs. 4.49 and 4.53, can be used for the determination of the calculation service life of thrust bearings of hubs of rotors under all operating conditions of these units encountered in real conditions.

As can be seen from Figs. 4.49 and 4.53, equations of curves of service life $\sigma = \sigma(nh)$ for vibrating bearings have the same form as for bearings revolving in one direction:

$$\sigma^{m_e}(nh) = \text{const}, \qquad (5.1)$$

where in case of the point contact m* = 10 and in the case of linear contact m* = 6.66.

Let us take for the base product nh = 120,000, which approximately corresponds to a 500 hour service life of operation of helicopters of the Mi-1 type. At nh = 120,000 the allowed contact stresses amount to 29,000 kG/cm^2 for thrust ball bearings and 18,800 kG/cm^2 for thrust bearings with turned rollers. Let us designate by A_0 the axial force, which creates in the bearing at equal distribution of forces between rolling solids, contact stresses equal to those allowed at nh = 120,000. Then, in accordance with formula (3.1) the allowed force on the ball will be:

$$P_0 = \frac{A_0}{z}\left(\frac{120\,000}{nh}\right)^{0.3}. \qquad (5.2)$$

Here it is considered that for ball bearings contact stresses are proportional to the cube root and for roller bearings, to the square root of the load.

Special experiments have established that the moment which must be taken into account in calculating the service life of a thrust bearing of the axial hinge, depending upon peculiarities of design of the subassembly and clearances in radial bearings, consists of 25 to 50 percent of the moment of the damper. With this calculation is conducted with respect to the instantaneous maximum pressure on the rolling solid, i.e., the moment acting on the thrust bearing of the axial hinge is conditionally considered constant in magnitude and direction.

The maximum pressure on the rolling solid of the thrust bearing loaded by axial force and moment can be represented in the form

$$P_0 = \kappa_0^{(A)} \frac{A}{z}.$$

Comparing this equality with equality (5.2), we obtain the following expression, which determines the calculation service life of thrust bearings of axial hinges of hubs of rotors:

$$\left(\frac{nh}{120\,000}\right)^{0.3} = \frac{A_0}{\kappa_0^{(A)} N}. \qquad (5.3)$$

As follows from §§ 3 and 4, coefficient $\kappa_0^{(A)}$ depends on the relative eccentricity of the application of the axial force, which in this case is equal to

$$\tau = (0{,}25 \div 0{,}5)\frac{M_a}{r_0 N}. \qquad (5.4)$$

With the usual relationships between the moment of the damper and centrifugal force, τ does not exceed 0.1, and therefore in thrust bearings of axial hinges all rolling solids[4] are always loaded.

For thrust roller bearings in which the load is carried by all the rollers,

$$\kappa_0^{(A)} = 1 + 2\tau. \qquad (5.5)$$

At small values of τ coefficients $\kappa_0^{(A)}$ for thrust ball and roller bearings practically coincide. This permits using formula (5.5) in the calculation of thrust ball bearings.

From equalities (5.4) and (5.5) we finally find

$$\kappa_0^{(A)} = 1 + (0{,}5 \div 1)\frac{M_a}{r_0 N}. \qquad (5.6)$$

It is necessary to note that the calculation of radial thrust bearings of different types, intended for operation in axial hinges of hubs of main and antitorque rotors, can also be produced with the help of formulas (5.3) and (5.5), provided first for these bearings there are determined the permissible axial loads A_0 corresponding to the value nh = 120,000. It is assumed that moments acting on bearings are known from calculations or experiments.

It should be kept in mind that values of A_0, obtained not by a complete curve of service life $\sigma = \sigma(nh)$ corresponding to a definite probability of the breakdown of the bearings and by means of conversion, according to the results of experiments conducted with any one value of nh, at an insufficiently large number of test samples can appear incorrect, which, apparently, is connected with the considerable

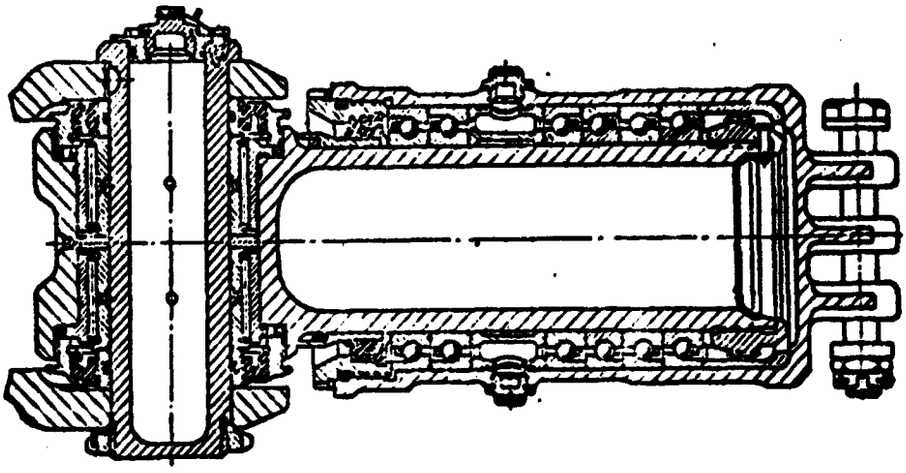

Fig. 4.54. Axial hinge of rotor hub implemented on multiple radial thrust bearings.

dispersion of service life, which is difficult to reveal with one level of the load.

In axial hinges of hubs of main and antitorque rotors of certain helicopters, there are successfully used multiple radial thrust ball bearings with angles of contact $\beta_0 = 45^\circ$ and decreased ratio of the radius of the groove to the diameter of the ball (Fig. 4.54). Usually in antifriction bearings this ratio is equal to 0.515. In the indicated multiple bearings it is decreased to 0.510, which leads to a lowering of the contact stresses by approximately 7% and, consequently, increases the calculation service life of the bearings 2 times. It is clear that such a means of increasing the carrying capacity of radial thrust ball bearings is useful mainly for the case of vibrating motion, since a decrease in the ratio of the radius of the groove to the diameter of the ball increases the length of the area of contact deformation, because of which losses to friction increase noticeably. Results of tests indicate the fact that with qualitative fulfillment providing sufficiently equal distribution of the external load between bearings of the set, for multiple radial thrust ball bearings permissible contact stresses, proceeding from which it is necessary to calculate the axial force, amount to 24,000 kG/cm^2.

There is still no sufficiently proven data on permissible contact stresses for radial thrust roller bearings with operation of them under conditions of vibrating motion.

The above-mentioned values of permissible contact stresses pertain to cases of operation of axial hinges of hubs of main and antitorque rotors on oils not yielding in lubricating properties to oils MS-20 and MS-14. If this condition is not carried out, then they should be lowered accordingly.

Permissible contact stresses are noticeably influenced by dimensions of rolling solids, and therefore with the application of bearings of large dimensions there should be introduced a definite correction for scale factor. As results of tests indicate, the above-mentioned values of permissible stresses can be considered real for bearings with balls with a diameter up to 25 mm and rollers with a diameter up to 15 mm. In the transition from rollers 15 mm in diameter to rollers 24 mm in diameter, permissible contact stresses for thrust bearings with turned rollers decrease by approximately 10%.

Needle bearings of flapping and drag hinges. For the majority of hubs of rotors in flapping and drag hinges needle bearings are used.

The efficiency of needle bearings is usually estimated in the magnitude of specific pressure per unit area of projection of the rolling track of the internal ring.

In the calculation of needle bearings of drag hinges, as a rule, it is considered that the load is distributed evenly over the length of the needles (Fig. 4.55a). In accordance with this the specific pressure for bearings is taken equal to

$$\sigma_{пр} = \frac{N}{D l_{\Sigma}}, \qquad (5.7)$$

where D is the diameter of the rolling track of the internal ring; l_{Σ} is total effective length of the needles.

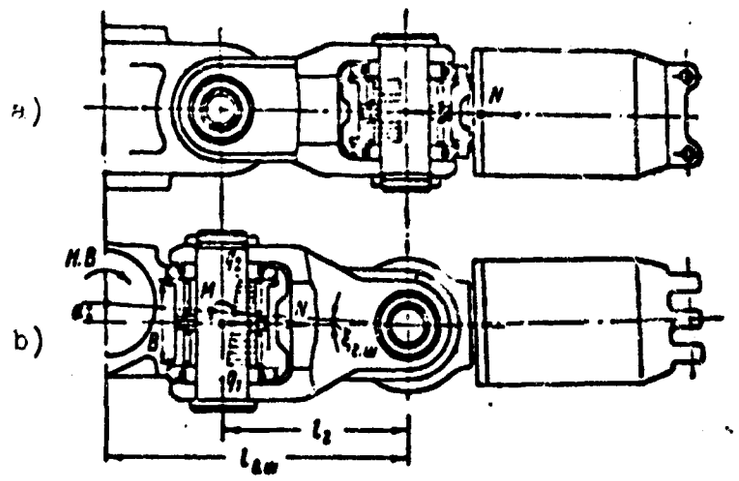

Fig. 4.55. Calculation of needle bearings of flapping and drag hinges of hubs of rotors.

Needle bearings of flapping hinges absorb besides the centrifugal force of blade N still the certain moment M (Fig. 4.55b), the constant part of which M_a with a sufficient degree of accuracy is determined by the expression

$$M_a = \left(\frac{M_{кр}}{z_{кр}} - Na\right)\frac{l_2}{l_{a.m}}. \qquad (5.8)$$

Here $M_{кр}$ is the torque of the rotor; $z_{кр}$ – number of blades of the rotor; a – "drift" of the middle of the flapping hinge from the axis of rotation; l_2 – distance between flapping and drag hinges; $l_{a.m}$ – "stagger" of the drag hinge.

The variable component M_v of moment M in the calculation of needle bearings of flapping hinges of hubs of rotors is not considered, since it has little effect on their service life. It is accepted to consider that in flapping hinges, made according to the configuration shown on Fig. 4.55b, the load is distributed along the length of the bearings according to the trapezium law. The loading of the bearings is characterized by specific pressures q_1 and q_2 on external edges of the rings, which is caused by the joint action of force N and moment M_a. These pressures are calculated by the formula

$$q_{1,2} = \frac{N}{Dl_2} \pm 6\frac{M_a}{Dl_2^2\left[1-\left(1-\frac{l_2}{B}\right)^n\right]}. \qquad (5.9)$$

where B is the effective width of the set of bearings.

Substituting into formula (5.9) value M_a, let us reduce it to the form:

$$q_{1,2}=\frac{N}{Dl_\Sigma}\left[1\pm 6\,\frac{\frac{M_{вр}}{z_л N}-a}{B}\,\frac{\frac{l_2}{l_1}\cdot\frac{l_2}{B}}{1-\left(1-\frac{l_2}{B}\right)^3}\right]. \qquad (5.10)$$

As the experiment of designing corresponding to selection of "drift" a indicates, it is possible to provide that in basic conditions of the motor flight specific pressures q_1 and q_2 would be quite close to the average specific pressure $q_0 = N/Dl_\Sigma$. It is necessary to note that the "drift" of the middle of the flapping hinge from the axis of rotation at distance a is equivalent to the turn of this hinge at angle $\varepsilon_{ш}=\operatorname{arctg}\frac{a}{l_{ш}}$ (see Fig. 4.55).

According to expression (5.10), specific pressures q_1 and q_2 depend on the centrifugal force N and torque $M_{вр}$. Therefore, they can be examined as certain functions of the number of revolutions and power of the rotor. Constructing with the help of expression (5.10) graphs of dependences $q_1=q_1(N_{вр})$ and $q_2=q_2(N_{вр})$ with the most characteristic revolutions of the rotor, as is done on Fig. 4.56, it is possible to determine easily the values of specific pressures

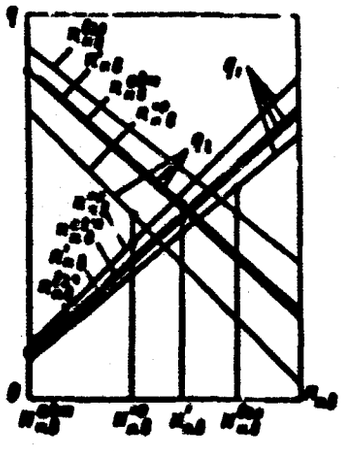

Fig. 4.56. Dependence of specific pressures q_1 and q_2 on the number of revolutions and power of the rotor: $n_{вр}^{кр}, N_{вр}^{кр}$ – revolutions and power of the rotor at cruising; $n_{вр}^{к}, N_{вр}^{к}$ – revolutions and power of rotor in conditions of cruising speed; $n_{вр}^{взл}, N_{вр}^{взл}$ – revolutions and power of rotor in takeoff conditions; $n_{вр}^{авт}, N_{вр}^{авт}$ – revolutions and power of rotor in autorotation conditions.

q_1 and q_2 in basic conditions of the helicopter flight and also to estimate the correctness of selection of "drift" a in the necessity of introducing appropriate corrective in the design of the rotor hub.

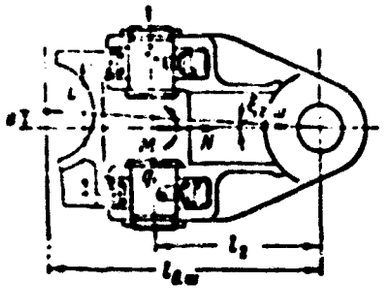

Fig. 4.57. Calculation of wide-spaced needle bearings of flapping hinges.

If the flapping hinges are made in the form of two independent supports, distance L between which considerably exceeds the diameter of the rolling tracks D (Fig. 4.57), then one can assume that within limits of each support specific pressures in the bearings are constant.

In this case the calculated specific pressures, which determine the service life of needle bearings of flapping hinges, are equal to

$$q_{1,2}=\frac{N}{Dl_\Sigma}\left[1\pm\frac{2\left(\frac{M_{a.g}}{r_{a.g}N}-e\right)}{L}\frac{l_\Sigma}{l_{a.g}}\right]. \qquad (5.11)$$

where l_Σ is the total length of the needles in both bearings.

With the application of hypoid oil permissible specific pressures in well consolidated needle bearings, which correspond to a service life of 1000 hours at 240 osc/min, amount to not less than 350 kG/cm^2 for flapping hinges and 400 kG/cm^2 for drag hinges. A relatively smaller value of permissible specific pressures in bearings of flapping hinges to a certain degree can be explained by the fact that they operate at amplitudes of oscillations from 2° to 6°, whereas the amplitude of oscillations of bearings of drag hinges usually does not exceed 1°. Although this contradicts the established opinions, practice shows that at amplitudes of oscillations up to 1° the service life of needle bearings appears higher than that at

amplitudes of 2°-6°. Possibly here a definite role is played by the fact that because of deformation of part under a load in known cases the actual specific pressures on edges of needle bearings of flapping hinges can exceed the calculated pressures.

Perennial operational experience confirms that in the selection of dimensions of needle bearings of flapping and drag hinges of hubs of rotors in light and medium helicopters, it is possible to follow reliably the above-indicated values of permissible specific pressures. For heavy helicopters whose parts, as a rule, have relatively lesser rigidity, it is possible to be oriented to these figures only in the case when special measures are accepted which provide uniformity of distribution of the load in bearings of drag hinges and the approach of the diagram of distribution of the load in horizontal hinges to the trapezoidal (see diagram on Fig. 4.55b). As a rule, distribution of the load along the length of the needle bearings of flapping and drag hinges can be obtained by means of selection of rigidities of ears and fingers and also by the corresponding increase in the pliability of ends of the rings. This, in particular, can be seen from Fig. 4.58, on which there are shown experimental diagrams

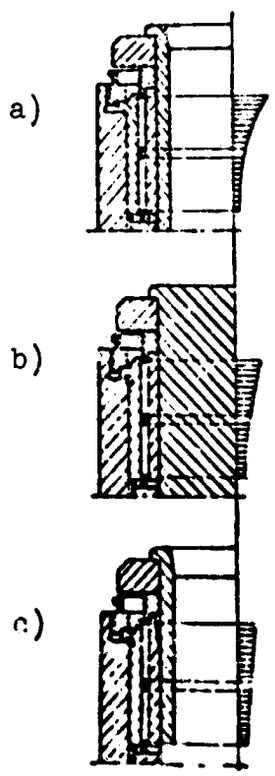

Fig. 4.58. Effect of rigidity of the pin and pliability of rings on the distribution of specific pressures along the length of needle bearings of the flapping hinge: a) initial variant; b) effect of pin of increased rigidity; c) effect of "pliable" ends of rings of the bearing.

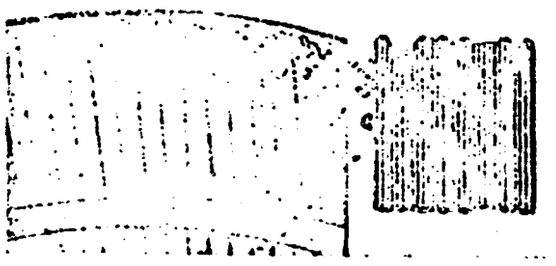

Fig. 4.59. Distribution of needle bearing because of insufficient rigidity of construction.

of the change in distance between generators of outer and inner rings with three variants of the constructive fulfillment of the flapping hinge of the rotor hub of a heavy helicopter. It should be noted that insufficient rigidity of the ears and fingers of flapping and drag hinges can lead not only a local increase in dept of the "ball test" on edges of rolling tracks but also to the crumbling of large sections of their surface and sometimes to the breakdown of the needles (Fig. 4.59).

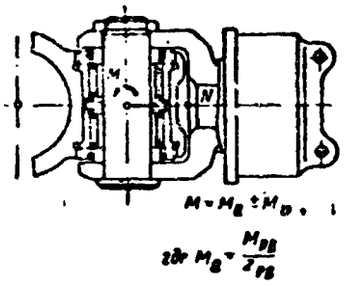

Fig. 4.60. Calculation of needle bearings of hubs of tail rotors.

The calculation of needle bearings of flapping hinges of hubs of antitorque rotors (Fig. 4.60) is a considerably more difficult problem than the calculation needle bearings of flapping hinges of hubs of main rotors, since they, as a rule, absorb a considerable variable moment, which in the evaluation of their efficiency is impossible to disregard. This moment is created by variable aerodynamic and inertial (Coriolis) forces acting on the blade of the antitorque rotor in the plane of rotation. With the estimated calculations it is accepted to characterize the loading of needle bearings of flapping hinges of antitorque rotors by the instantaneous maximum specific pressure appearing on the edge of the rolling track. On the assumption that the load is distributed along the length

of the bearings, according to the trapezium law, this pressure is equal to

$$q=\frac{N}{Dl_2}\left[1+6\frac{\frac{M_{p.s}}{z_{p.s}}+M_v}{BN}\frac{\frac{l_2}{B}}{1-\left(1-\frac{l_2}{B}\right)^2}\right], \qquad (5.12)$$

where $M_{p.s}$ is the torque of the antitorque rotor; $z_{p.s}$ – number of blades of the antitorque rotor; M_v – amplitude of variable moment loading the flapping hinge.

Values of specific pressure q, calculated by formula (5.12), for antitorque rotors of light and medium helicopters in conditions of a cruising flight should not exceed 300-350 kG/cm^2. In the case of the application of hypoid oil in flapping hinges it is possible to expect that the service life of the bearings will not be less than 1000 h.

Finally the service life of needle bearings of flapping and drag hinges of hubs of main and antitorque rotors is determined as a result of tests of these units on special test benches.

4. Calculation of Bearings of Cyclic Pitch Controls and Control Mechanisms

Allowed loads on bearings of hinges of a cyclic pitch control and, directly connected with them, control elements are usually determined experimentally. For this on special, very complex stands, which permit creating all forms of forces acting on the cyclic pitch control in flight, prolonged tests are conducted.

Loads on the cyclic pitch control have a dynamic character. This, in particular, can be seen from oscillographic recordings shown on Fig. 4.61 of the hinged moment of the blade $M_ш$ and forces $P_{прод}$ and $P_{пов}$ in rods of longitudinal and lateral control connecting corresponding rockers of the cyclic pitch control with power-assisted controls.

It is natural that with such a complex character of the load,

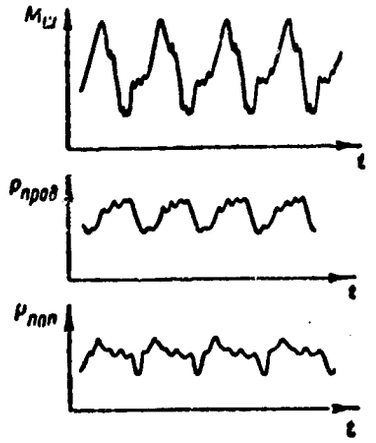

Fig. 4.61. Oscillograms of the hinged moment of the blade and forces in rods of longitudinal and lateral controls.

any recommendations according to the calculation of bearings of hinges of the cyclic pitch control will inevitably have a very conditional character. Nevertheless, some of them can help designers to be oriented in problems of the selection of bearings for these critical units, for which it follows to discuss them briefly.

If it is considered that with similar designs of rotors only the absolute value of the hinged moment of the blade is changed, and the relationship between amplitudes and phases of its separate harmonics remains constant, then in the selection of bearings for similar hinges of the cyclic pitch control, made according to the same design scheme, it is possible to proceed from the maximum value of load P_{max} absorbed by them (Fig. 4.62).

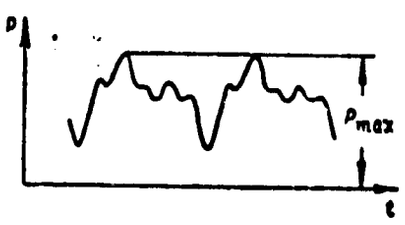

Fig. 4.62. Load on bearings of hinges of the cyclic pitch control.

For cyclic pitch controls similar in design to cyclic pitch controls of Mi-1 and Mi-4 helicopters (see Fig. 4.38), with all-metal blades of the rotor having a rectangular form in the plan, when using grease lubricants of the TsIATIM-201 type the allowed loads $P_{доп}^{max}$ can be determined with the help of Table 4.9. This table was compiled according to results of bench tests, taking into account the operational experience of cyclic pitch controls.

Table 4.9.

Place of installation	Permissible values of $P_{доп}^{max}$ (kG) for different bearings					
	ball radial, radial thrust and thrust	ball spheric	roller spheric	roller radial thrust and thrust	needle	hinged types, (BS) ball spheric
Hinges of disk, rods and levers for turning the blade	0.8 $Q_{ст}$				2 Dl	
Bearings of Cardan joint	$Q_{ст}$		0.8 $Q_{ст}$			
Bearings of rockers of longitudinal and lateral control	$Q_{ст}$	$Q_{ст}$		0.8 $Q_{ст}$	2 Dl	
Bearings of rods of longitudinal and lateral controls connecting the rockers with the external ring of the Cardan joint						Db
Bearings of the lever of general step	$Q_{ст}$	$Q_{ст}$		0.8 $Q_{ст}$	2 Dl	

$Q_{ст}$ – permissible static load on irrotational bearing indicated in catalogs and reference books; D – diameter of rolling track of inner ring of the needle bearing or sphere of hinged bearing in mm; b – width of outer ring of hinged bearing in mm; l – effective length of needles in mm.

The values given in Table 4.9 of allowed loads $P_{доп}^{max}$ at the number of revolutions of the rotor of 240 per minute correspond to a service life of 1000-1200 h. With other revolutions the service life is found from expression:

$$h \approx \frac{210000}{n}, \qquad (5.13)$$

where n represents nominal revolutions of the rotor.

If the character of the loads is different than that for cyclic pitch controls of Mi-1 and Mi-4 helicopters with all-metal blades of rotor, then permissible values $P_{доп}^{max}$ should be refined as a result of corresponding bench and performance tests.

Thus far there have been examined vibrating bearings which accomplished during the calculated service life a large number of oscillations (over 10^7).

Permissible loads on bearings of control mechanisms of aircraft, for which the total number of oscillations does not exceed 100,000, and the amplitude of oscillations is equal to 20° and more, the VNIPP [Editor's Note: VNIPP = All-Union Scientific Research, Design and Technological Institute of the Bearing Industry] recommends determining by following experimental formula:[5]

$$R_{доп} = a_{доп} z d_w^2. \qquad (5.14)$$

Value of coefficients $a_{доп}$ for certain types of bearings operating on grease lubricants, at 25,000 and 100,000 oscillations, are given in Table 4.10.

Table 4.10.

Type of bearing	Designation of bearing	Inner diameter of the bearing мм	Values of coefficient $a_{доп}$ at 25,000 oscillations	Values of coefficient $a_{доп}$ at 100,000 oscillations
Ball Radial	7000100 100 200	Up to 10	5	2
	900000	Up to 9 Above 9	5 4	2 1,6
	980000 6	Up to 9 Above 9	5 4	2 1,6
	981000	Up to 9 Above 9	2,5 2	2 1,6

Table 4.10 (Continued).

Type of bearing	Designation of bearing	Inner diameter of the bearing, mm	Values of coefficient $\alpha_{доп}$	
			at 25,000 oscillations	at 100,000 oscillations
Ball spheric	1000	Up to 10	4	2,8
	1200	Up to 50	4	2,8
	1300 971000	Up to 50	4,7	3,3

§ 6. Theory and Selection of Basic Parameters of Thrust Bearings with "Turned" Rollers

As was already indicated in the preceding paragraphs, in axial hinges of hubs of rotors of Soviet helicopters thrust bearings with cylindrical rollers located at an angle to the radial direction are used successfully. High carrying capacity of such bearings, which are called thrust bearings with "turned" rollers, is explained by the fact that in them the separator during vibrating motion not only oscillates together with mobile ring but also is continuously displaced in one direction. The time of turn of the separator T_c at angle 360° which characterizes the speed of this displacement, is determined by a number of factors. It depends on the coefficient of friction of the slip between rollers and rings, the amplitude and frequency of oscillations of the mobile ring, and also on a number of geometric parameters the main role of which is played by angles of inclination of recesses of the separator. It is understandable that these angles should be selected in such a way that the time T_c lay in optimum limits, which provide high stability of rollers with acceptable wear of the rolling tracks. Below there is expounded the theory with the help of which this problem can be solved.

1. Determination of Time T_c

In thrust bearings with turned rollers the ratio of angular velocity of the separator to the angular velocity of the mobile ring $A=\frac{\omega_c}{\omega}$ depends on the direction of the rotation. This conditions

the continuous displacement of the separator, which is observed in such bearings during vibrating motion.

Values of ratio A, corresponding to cases of rotation of the bearing counterclockwise and clockwise, are found in the following way.

Frictional force of slip, appearing at points of contact of roller with the rings, are reduced to resultant forces F_{1y}, F_{1x}, F_{2y}, and F_{2x} and moments M_{1z} and M_{2z} (Fig. 4.63). With a constant

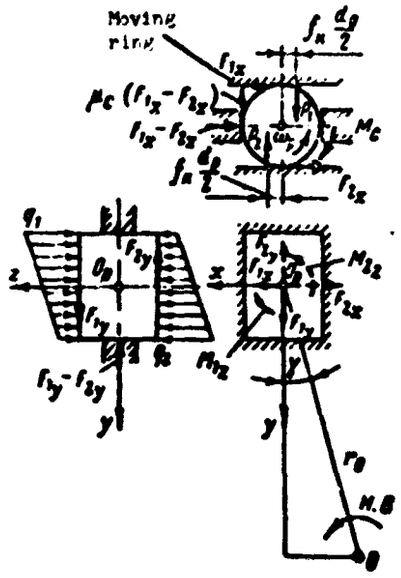

Fig. 4.63. Forces and moments affecting the "turned" roller.

coefficient of sliding friction μ between the rollers and rings, values of these forces and moments can be calculated with a sufficient degree of accuracy by the formulas:

$$\left.\begin{aligned}
F_{1y} &= \mu P\left(B_{10} + p\frac{d_p}{2}B_{11}\frac{x_1}{l}\right);\\
F_{1x} &= \mu P\left(p\frac{d_p}{2}A_{10} + A_{11}\frac{x_1}{l}\right);\\
F_{2y} &= \mu P\left(B_{20} - p\frac{d_p}{2}B_{21}\frac{x_1}{l}\right);\\
F_{2x} &= \mu P\left(-p\frac{d_p}{2}A_{20} + A_{21}\frac{x_1}{l}\right);\\
M_{1z} &= \mu Pl\left[C_{10} + p\frac{d_p}{2}C_{11}\frac{x_1}{l} + C_{12}\left(\frac{x_1}{l}\right)^2\right];\\
M_{2z} &= \mu Pl\left[C_{20} - p\frac{d_p}{2}C_{21}\frac{x_1}{l} + C_{22}\left(\frac{x_1}{l}\right)^2\right].
\end{aligned}\right\} \qquad (6.1)$$

Here P is the force absorbed by the examined roller; y_1 and y_2 – coordinates of points contact, in which slipping in a direction perpendicular to the axis of the roller is absent; d_p – diameter of the roller; l – effective length of the roller.

In deriving formulas (6.1) it was assumed that normal loads q_1 and q_2 are distributed along the length of the roller according to the law:

$$\left.\begin{aligned} q_1 &= \frac{P}{l}\left(1-K\frac{x}{l}\right); \\ q_2 &= \frac{P}{l}\left(1+K\frac{x}{l}\right). \end{aligned}\right\} \qquad (6.2)$$

where

$$K = 6\frac{F_{1x}+F_{2x}}{P}\frac{d_p}{2l}.$$

Such a distribution of normal loads is caused by the action of the moment $(F_{1y}+F_{2y})\frac{d_p}{2}$, which strives to turn the roller around axis $O_p x$. Since the usual concentration of the load on edges of the roller has little effect on time T_c, then for simplification of calculation dependences it is not considered. In view of smallness of the frictional force $\mu_c(F_{1x}-F_{2x})$ we consider that

$$\int q_1 dy = \int q_2 dy = P.$$

Coefficients entering into formulas (6.1) are determined by equalities

$$\left.\begin{aligned} A_{11} &= \frac{1}{\left(\frac{1}{4}+\frac{1}{\beta^2}\right)^{1/2}}; \\ B_{10} &= \frac{1}{\beta}\ln\frac{\frac{1}{2}+\left(\frac{1}{4}+\frac{1}{\beta^2}\right)^{1/2}}{-\frac{1}{2}+\left(\frac{1}{4}+\frac{1}{\beta^2}\right)^{1/2}}; \\ C_{10} &= \frac{1}{2}\left(\frac{B_{10}}{\beta}-\frac{1}{A_{11}}\right); \\ A_{10} &= 6B_{10}\left(\frac{1}{A_{11}}-\frac{B_{10}}{\beta}\right); \\ B_{11} &= 12B_{10}\left(\frac{A_{11}}{\beta}-B_{10}\right); \\ C_{11} &= \frac{B_{11}}{l\beta}; \\ C_{10} &= \frac{A_{10}}{6}. \end{aligned}\right\} \qquad (6.3)$$

here

$$p=\frac{l}{r_0\sin\gamma}.$$

From kinematic relationships and the equation of moments with respect to axis $O_p y$ the following expressions can be obtained.[6]

$$\left.\begin{aligned}\frac{y_1}{l}&=-\frac{\frac{f}{p}\pm\mu_c\frac{d_p}{2l}A_{10}}{A_{11}}-\\&-\left[(1\pm\mu_c)\left(\frac{r_0\cos\gamma}{l}-\frac{\frac{f}{p}\pm\mu_c\frac{d_p}{2l}A_{10}}{A_{11}}\right)\right](2A-1);\\\frac{y_2}{l}&=\frac{\frac{f}{p}\pm\mu_c\frac{d_p}{2l}A_{10}}{A_{11}}+\\&+\left[(1\mp\mu_c)\left(\frac{r_0\cos\gamma}{l}-\frac{\frac{f}{p}\pm\mu_c\frac{d_p}{2l}A_{10}}{A_{11}}\right)\right](2A-1).\end{aligned}\right\}\qquad(6.4)$$

In these expressions

$$f=f_0+\frac{M_p}{Pd_p},$$

where f_0 is the coefficient of rolling friction; M_p – moment considering the friction on ends of the roller and friction against the lubricant; μ_c – coefficient of friction between rollers and the separator.

Upper signs pertain to the case when $F_{1z}-F_{2z}>0$, and the lower, to case when $F_{1z}-F_{2z}<0$.

The angle of inclination γ is considered positive if the roller can be set in a radial position by a turn around point O_p counterclockwise. Under this condition positive values of forces, calculated by the formulas (6.1), correspond to directions shown on Fig. 4.6. Signs of angles of inclination of rollers and the direction of rotation are determined in examining the bearing from the side of the mobile ring.

The roller with the angle of inclination γ creates, with

respect to the axis of rotation of separator, the moment

$$M=(F_{1z}-F_{2z})r_0\cos\gamma+(F_{1y}-F_{2y})r_0\sin\gamma-(M_{1z}-M_{2z}).$$

As calculations show, the resistance to rolling and friction of the roller against the separator and lubricant have practically no effect on the value of this moment. Taking in accordance with this $f = \mu_c = 0$ and considering that in real constructions angle $\gamma < 6^\circ$ and, consequently, $\gamma \approx 1$, with the help of expressions (6.1), (6.3), and (6.4) let us convert the last equality thus

$$M=\mu Pr_0\overline{M}, \qquad (6.5)$$

where

$$\overline{M}=2p\frac{d_p}{2l}\cdot A_{10}-2A_{11}\frac{r_0}{l}(2\Lambda-1).$$

Table 4.11 gives values of coefficients A_{10} and A_{11} depending upon quantity 1/p.

Table 4.11.

	Values of coefficients A_{10} and A_{11} with 1/p										
	0	0.05	0.10	0.15	0.20	0.25	0.30	0.35	0.40	0.45	0.50
A_{10}	0	0.47[illegible]	1.3[illegible]	1.[illegible]	1.[illegible]	1.[illegible]	1.[illegible]	1.[illegible]	1.[illegible]	1.[illegible]	1.[illegible]
A_{11}	2	1.[illegible]	1.[illegible]	1.[illegible]	1.[illegible]	1.[illegible]	1.[illegible]	1.[illegible]	1.[illegible]	1.[illegible]	1.[illegible]

In the case of negative values of p for the determination of coefficients A_{10} and A_{11} there can be used these relations:

$$\left.\begin{aligned} &A_{10}(-p)=-A_{10}(p)\\ \text{and}\quad &A_{11}(-p)=A_{11}(p). \end{aligned}\right\} \qquad (6.6)$$

These relations directly follow from equalities (6.3).

At small amplitudes of oscillations, when inertial forces can be disregarded, the equation of motion of the separator of the bearing with "turned" rollers is reduced to the condition

$$M_c-M_0=0. \qquad (6.7)$$

Here $M_c = \sum M$ is the total moment of forces of sliding friction acting on the rollers on the side of the rings of the bearing; $M_т$ — drag torque to the motion.

Let us assume that the separator has z recesses, in each of which there is s rollers. Let us designate the angles of inclination of recesses of the separator on the average radius r_c by γ_{c_i} and angles of inclination of the rollers by γ_{i_k}. Subscript i denotes the number of the recess of the separator, and subscript k indicates the position in it of the roller. Usually in each recess two rollers are placed. The load on the roller with an effective length l_{1_k} is equal to:

$$P_{l_k} = \frac{N}{z} \cdot \frac{l_{l_k}}{l_\Sigma}, \tag{6.8}$$

where l_Σ is the total effective length of the rollers located in one recess; N is the axial force applied to the bearing.

A change in the direction of rotation of the bearing is equivalent to a change in signs of angles of slope of the rollers. Considering this circumstance, from equalities (6.5), (6.6), and (6.7), we obtain

$$M_c = 2\pi N r_c \frac{r_c}{zl_\Sigma}\left[\pm\rho\frac{d_p}{2r_c}\sum_{i=1}^{z}\sum_{l=1}^{s}\frac{r_{l_k}}{r_c}A_{10}(p_{l_k}) - (2\Lambda-1)\sum_{i=1}^{z}\sum_{k=1}^{s}\frac{r_{l_k}^2}{r_c^2}A_{11}(p_{l_k})\right]. \tag{6.9}$$

where $A_{10}(p_{l_k})$ and $A_{11}(p_{l_k})$ are values of coefficients A_{10} and A_{11} at

$$p = p_{l_k} = \frac{l_{l_k}}{r_{l_k}\sin\gamma_{l_k}}.$$

For definiteness we will consider the signs of angles of the slope of rollers are given for the case of rotation of the bearing counterclockwise. Substituting expression (6.9) into equation (6.7), we obtain:

– with rotation counterclockwise:

$$\Lambda=\Lambda'=\frac{1}{2}+\frac{1}{2}\frac{\mu\frac{d_p}{2r_c}\sum_{i=1}^{z}\sum_{k=1}^{s}\frac{r_{i_k}}{r_c}\cdot A_{10}(p_{i_k})-\frac{1}{2}\frac{zl_z}{r_c}\frac{M_T}{\mu N r_c}}{\sum_{i=1}^{z}\sum_{k=1}^{s}\frac{r_{i_k}^2}{r_c^2}A_{11}(p_{i_k})}; \qquad (6.10)$$

– with rotation clockwise:

$$\Lambda=\Lambda''=\frac{1}{2}-\frac{1}{2}\frac{\mu\frac{d_p}{2r_c}\sum_{i=1}^{z}\sum_{k=1}^{s}\frac{r_{i_k}}{r_c}A_{10}(p_{i_k})+\frac{1}{2}\frac{zl_z}{r_c}\frac{M_T}{\mu N r_c}}{\sum_{i=1}^{z}\sum_{k=1}^{s}\frac{r_{i_k}^2}{r_c^2}A_{11}(p_{i_k})}. \qquad (6.11)$$

Knowing quantities Λ' and Λ'', it is easy to calculate the time T_c. From Fig. 4.52 it follows that for each half-period of oscillations the separator is displaced by the angle $\Delta\varphi_c=(\Lambda'-\Lambda'')\varphi_0$. Consequently, the time of turn of the separator at angle 360° will be

$$T_c=\frac{360}{2|\Lambda'-\Lambda''|n\varphi_0},$$

where $n = 1/T_0$ is the number of oscillations of the moving ring per minute.

Since moment M_T of resistance to motion of the separator should not depend on the direction of rotation, then in accordance with the relations given above

$$T_c=\frac{180}{n\varphi_0\mu}\frac{2r_c}{d_p}\frac{\sum_{i=1}^{z}\sum_{k=1}^{s}\frac{r_{i_k}^2}{r_c^2}A_{11}(p_{i_k})}{\left|\sum_{i=1}^{z}\sum_{k=1}^{s}\frac{r_{i_k}}{r_c}A_{10}(p_{i_k})\right|}. \qquad (6.12)$$

Formula (6.12) is basic for the theory of a thrust bearing with "turned" rollers. From it, in particular, it follows that resistance to motion of the separator does not affect the time T_c. This

Table 4.12.

Time T_c (min) at temperature of oil (deg)		
+ (20+30)	− (30+40)	− (45+55)
63	54	58

Oil VNII NP-25 (ν = 10 cSt at t = = +100°C and ν = 50,000 cSt at t = -40°C).

conclusion important for practice is confirmed by results of experiments in determination of time T_c at low temperatures, when because of the increase in viscosity of oil moment $M_т$ can reach a noticeable value (Table 4.12).

2. Selection of Angles of Slope of Recesses of the Separator

The prescribed speed of displacement of the separator is provided by the appropriate selection of angles of slope of its recesses. Here there should be kept in mind not only nominal values of the angles but also allowances for manufacture, which have a noticeable influence on the time T_c. The remaining geometric parameters of the bearing influencing time T_c are selected by constructive considerations.

Industrial deviations of angles of the slope of recesses of the separator with greatly improved technology and strict control of the prepared articles reach 7'-10'. If, however, special measures in the manufacture of bearings are not taken, then these deviations can reach 20'-30'.

Time T_c depends also on clearances between the rollers and the separator. In the presence of clearances the position of the rollers in recesses of the separator and, consequently, the actual angles of inclination of the rollers are determined by forces of

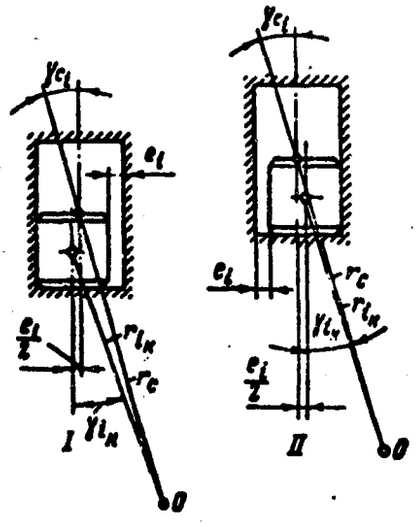

Fig. 4.64. Determination of quantities p in the presence of clearances between rollers and the separator.

sliding friction, which act on them from the side of the rings. Since in general the determination of these forces is difficult, then we will consider that rollers with equal probability can occupy any of the two positions shown on Fig. 4.64:

– in position I:

$$p_{l_k} = \frac{l_{l_k}}{r_c \sin \gamma_{c_j} + \frac{e_l}{2}} \approx \frac{l_{l_k}}{r_c \sin\left(\gamma_{c_j} + \frac{e_l}{2r_c}\right)};$$

– in position II:

$$p_{l_k} = \frac{l_{l_k}}{r_c \sin \gamma_{c_j} - \frac{e_l}{2}} \approx \frac{l_{l_k}}{r_c \sin\left(\gamma_{c_j} - \frac{e_l}{2r_c}\right)}.$$

From the given equalities it is clear that the influence of clearances for the time T_c can be considered by the increase in calculation deviations of angles of slope of recesses of the separator up to the quantity

$$\xi = \pm \xi_n + \frac{e_{max}}{2r_c},$$

where ξ_n is half of industrial allowance and e_{max} is the maximum clearance.

The most general case of the location of recesses of the separator representing practical interest is the case when in the separator there is z_1 recesses with an angle of slope $\gamma_1 \pm \xi$ ($\gamma_1 > 0$) and z_2 recesses with an angle of slope at $0 \pm \xi$.

For the simplification of further computations let us assume that $l_{1_k} = l = \text{const}$. If quantity ξ is such that the difference $\Lambda' - \Lambda''$ is positive, then under the condition $l_{1_k} = l = \text{const}$ time T_c can change from a certain

$$T_c^{(\max)} = \frac{180}{\pi_0 n v \mu'} \frac{2r_c}{d_p} \frac{A_{11}(p_1') + \chi A_{11}(p_2')}{A_{10}(p_1') + \chi A_{10}(p_2')} \tag{6.13}$$

up to a certain

$$T_c^{(\min)} = \frac{180}{\pi_0 n v \mu''} \frac{2r_c}{d_p} \frac{A_{11}(p_1'') + \chi A_{11}(p_2'')}{A_{10}(p_1'') + \chi A_{10}(p_2'')}. \tag{6.14}$$

Here

$$p_1' = \frac{l}{r_c \sin(\gamma_1 - \xi)}; \qquad p_2' = -\frac{l}{r_c \sin \xi};$$

$$p_1'' = \frac{l}{r_c \sin(\gamma_1 + \xi)}; \qquad p_2'' = \frac{l}{r_c \sin \xi};$$

$$\chi = \frac{z_2}{z_1} \quad \text{and} \quad v = \frac{\sum_{k=1}^{s} \frac{r_{1_k}}{r_c}}{\sum_{k=1}^{s} \frac{r_{1_k}^2}{r_c^2}}.$$

Coefficient v is usually close to unity (v = 0.98-1). This indicates that time T_c depends little on the number of rollers s being in one recess.

In expressions for $T_c^{(\max)}$ and $T_c^{(\min)}$, μ' and μ'' denote the minimum and maximum value of the coefficient of sliding friction μ. With good lubrication $\mu' \approx 0.05$ and $\mu'' \approx 0.08$.

Let us assume that the upper and lower limits of the range of optimum values T_c are respectively equal to T_c' and T_c''. As follows

from results of tests, for thrust bearings with turned rollers operating in axial hinges of hubs of the rotors, $T_c' = 80$ min and $T_c'' = 40$ min. It is established that to provide maximum stability of the speed of displacement of the separator quantities γ_1 and χ should be selected so that at the given value ξ $T_c^{(max)}$ they are equal to T_c'. At $T_c^{(max)} = T_c'$ quantities γ_1, χ, and ξ are connected with each other by a definite relationship. Considering in expression (6.13) $T_c^{(max)} = T_c'$, we will present this relation graphically in the form of a family of corresponding curves.[7] From Fig. 4.65, on

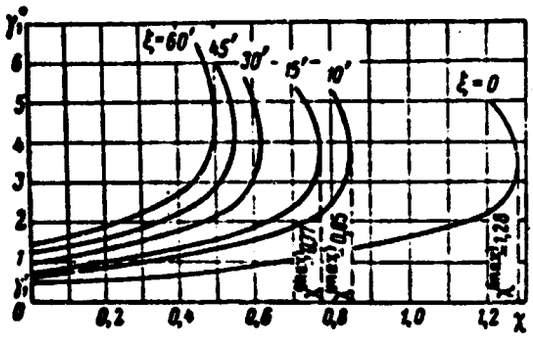

Fig. 4.65. Curves $\gamma_1 = \gamma_1(\chi)$ at different values of deviation ξ.

which there is given a family of such curves, it is clear that condition $T_c^{(max)} = T_c'$ imposes known limitations on the selection of quantities γ_1 and ξ. Thus in the case $T_c' = 80$ min the relation χ should not exceed 1.28 at $\xi = 0$ and 0.77 at $\xi = 15'$, and angle γ_1 should be not less than a certain minimum angle $\gamma_1^{(min)} = \nu_1' + \xi$ (where γ_1' is the value $\gamma_1^{(min)}$ when $\chi = 0$ and $\xi = 0$). The range of the variation in speeds of displacement of the separator is characterized by the ratio $\eta = \frac{T_c^{(min)}}{T_c^{(max)}}$.

Figure 4.66 gives curves $\eta = \eta(\xi)$ for angles $\gamma_1 = 5^\circ$ and $\gamma_1 = 30^\circ$, plotted on the assumption that $T_c^{(max)} = T_c'$. Figure 4.66 shows that the relation η depends mainly on quantity ξ. Angle γ_1 has very little effect on η. Thus from the point of view of the stability of the speed of displacement of the separator, different combinations of angles of slope of recesses are approximately equivalent provided they ensure fulfillment of the condition $T_c^{(max)} = T_c'$. According to Fig. 4.66, the deviation ξ at which

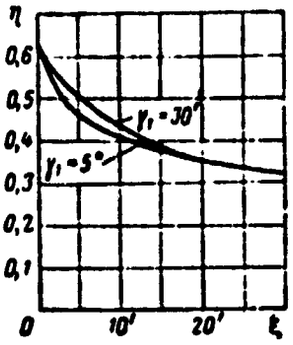

Fig. 4.66. Dependence of relation η on deviation ξ at different angles γ_1.

$T_c^{(min)} = T_c = 40$ min and, consequently, $\eta = \frac{40}{80} = 0.5$, amounts to about 5'. It follows from this that even with the most thorough manufacture of separators, there are not excluded cases when time T_c will fall outside the limits of the optimum range.

In practice two variants of the location of recesses of the separator are encountered. In the first of them all the recesses have an identical angle of inclination not exceeding 1°, in second — several recesses are located at an angle 3°-6°, and all the remaining recesses — radial. We compare these variants in the following examples.

Let us consider a bearing for which $\gamma_1 = 45'$, $\chi = 0$, $d_p = 9$ mm, $r_c = 40$ mm, $l = 8$ mm, $e_{max} = 0.2$ mm, $\xi_п = 7'$ and $s = 2$; the bearing operates at $\varphi_0 = 4.5°$ and $n = 240$ osc/min.

In the case when all rollers have an angle of inclination equal to γ,

$$T_c = \frac{180}{\gamma_0 \omega_{ср}} \frac{2r_c}{d_p} \frac{A_{11}(\rho)}{A_{10}(\rho)}, \qquad (6.15)$$

where

$$\rho = \frac{l}{r_c \sin \gamma}.$$

Figure 4.67 gives curves $T_c = T_c(\gamma)$ which show how time T_c changes depending upon angle γ at $\mu = \mu'' = 0.05$ and $\mu = \mu'' = 0.08$. Let us separate between curves $T_c = T_c(\gamma)$ the region limited by vertical straight lines $\gamma = \gamma_1 + \xi_п + \frac{e_{max}}{2r_c} = 60'$ and $\gamma = \gamma_1 - \xi_п - \frac{e_{max}}{2r_c} = 30'$. Within

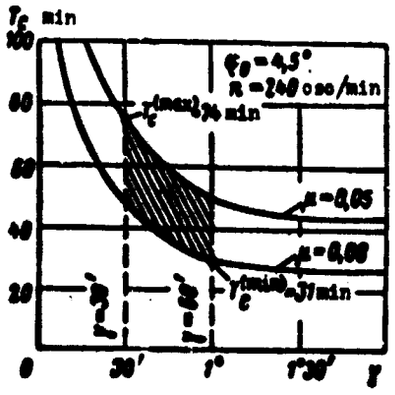

Fig. 4.67. Dependence of time T_c on the angle of inclination of recesses of the separator γ.

limits of this region the actual values of time T_c should lie. It is easy to note that for such a bearing $T_c^{(max)}$ = 74 min and $T_c^{(min)}$ = 31 min. These values are quite close to the optimum. Results of experiments in the determination of time T_c for several hundreds of bearings with the given parameters showed that the actual values of T_c practically do not fall outside the limits of the indicated range, being grouped around mean values $T_c^{(cp)}$ = 50-60 min.

Let us assume that now the bearing has the following parameters: $\gamma_1 = 5°$, $\chi = 5$, $d_p = 5$ mm, $r_c = 28$ mm, $l = 4.2$ mm, $e_{max} = 0.2$ mm, $\xi_п = 7'$, $s = 2$ and operates at $\varphi_0 = 4.5°$ and $n = 300$ osc/min.

Let us assume that the actual angles of inclination of radial recesses are equal to ξ. Then

$$T_c = \frac{180}{\pi\omega} \frac{2r_c}{d_p} \frac{A_{11}(\rho_1) + \chi A_{11}(\rho_2)}{|A_{10}(\rho_1) + \chi A_{10}(\rho_2)|}, \qquad (6.16)$$

where

$$\rho_1 = \frac{l}{r_c \sin\gamma_1} \quad \text{and} \quad \rho_2 = \frac{l}{r_c \sin\xi}.$$

From Figure 4.68, on which there are given curves $T_c = T_c(\xi)$, plotted by the formula (6.16), it is clear that at $\xi = 0$, depending upon the coefficient of friction μ, time T_c = 163-261 min. If $\xi \approx -5'$, then time T_c will tend to infinity. In other words, at small negative deviations of angles of slope of radial recesses stopping of separator is possible. Such cases were repeatedly

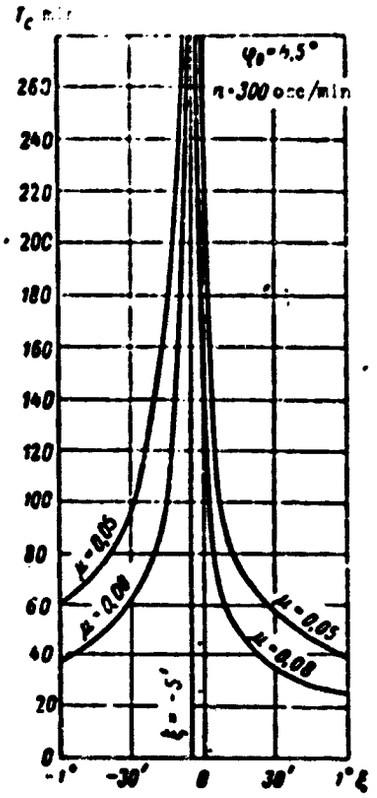

Fig. 4.68. Dependence of time T_c on deviation ξ.

observed with tests of bearings with large values of χ.

When $\mu = 0.08$ and $\xi=\xi_m+\frac{\chi\cdot\varphi_{max}}{2r_c}=15'$ the time $T_c = 47$ min. Consequently, in the examined case time T_c can change from $T_c^{(max)}=\infty$ to $T_c^{(max)} = 47$ min.

From the examined examples it is clear that only the first variant of the location of recesses of the separator provides operation of the bearings under conditions, close to the optimum.

With the location of recesses of the separator under identical angles losses to friction and the irregularity of distribution of the normal load along the lines of contact also decrease.

5. Losses to Friction

Losses to friction in thrust bearings with "turned" rollers depend both on the speed of displacement of the separator and also on how quantities γ_1 and χ, providing displacement of the separator with the given speed are selected.

The moment of friction of the bearing is usually recorded thus:

$$M_{тр} = f_{тр} N r_c, \tag{6.17}$$

where $f_{тр}$ is the given coefficient of friction.

Using dependences obtained in the preceding points, after a number of transformations we find

$$f_{тр} = f_к + f_c + \frac{M_з}{2N r_c}. \tag{6.18}$$

Here $f_к$ is the coefficient of rolling friction; f_c – coefficient characterizing losses to the sliding friction.

Coefficient f_c can be represented in the form (see work [27]):

$$f_c = \mu \frac{\sin\gamma_1 [\beta_{12}(\rho_1) - \rho_1 C_{12}(\rho_1)] + \frac{A_{11}(\rho_1)}{\cdot 8} \cdot \frac{1}{r_c}\left[\frac{T_c}{T_c^{(0)}} \cdot \frac{A_{12}(\rho_1)}{A_{11}(\rho_1)} - 1\right]}{1 + \frac{A_{11}(\rho_1)}{2}\left[\frac{T_c}{T_c^{(0)}} \cdot \frac{A_{12}(\rho_1)}{A_{11}(\rho_1)} - 1\right]}, \tag{6.19}$$

where

$$T_c^{(0)} = \frac{100}{\omega_{сеп} \omega} \cdot \frac{2r_c}{d_p}.$$

With the help of Table 4.10 it is easy to be convinced that with an increase in the angle of inclination of the rollers the ratio $\frac{|A_{12}(\rho)|}{A_{11}(\rho)}$ in the beginning increases rapidly, reaching at γ = arc sin 0.57 i/r_c values equal to unity. With a further increase in the angle the ratio $\frac{|A_{12}(\rho)|}{A_{11}(\rho)}$ does not change. This means that quantity $T_c^{(0)}$ is the minimum time which can be obtained at the given value of the coefficient of friction μ [see formula 6.15)].

From Fig. 4.69 it is clear that at the same speed of displacement of the separator with a decrease in angle γ_1, losses to friction decrease. It follows from this that minimum losses to friction indeed take place with the location of all recesses of the separator

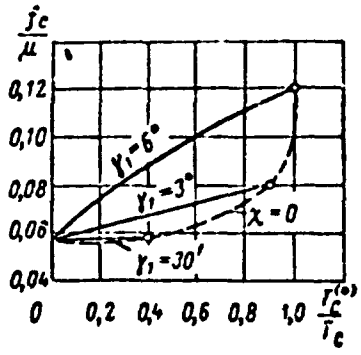

Fig. 4.69. Losses to sliding friction.

at identical angles to the radial direction. At optimum speeds of displacement of the separator $\left(\frac{T_c^{(\gamma)}}{T_c}\approx 0{,}5\right)$ rejection of such a location of the recesses can lead to an increase in losses to sliding friction of 1.5 times.

4. Additional Considerations on the Optimum Construction of Thrust Bearings with "Turned" Rollers

According to the above-mentioned formulas, coefficient K, characterizing the irregularity of distribution of the load along the length of the roller, is equal to:

$$K=6\mu\frac{d_p}{2l}\left(2B_{10}+\mu\frac{d_p}{2l}B_{11}\frac{\gamma_1-\gamma_2}{l}\right).$$

Since $|2B_{10}|\geqslant\left|\mu\frac{d_p}{2l}B_{11}\frac{\gamma_1-\gamma_2}{l}\right|$, then with sufficient accuracy it is possible to consider that $K\approx 12\mu\frac{d_p}{2l}B_{10}$. Thus coefficient K depends only on angle γ. From curve $K = K(\gamma)$, given in Fig. 4.70, it

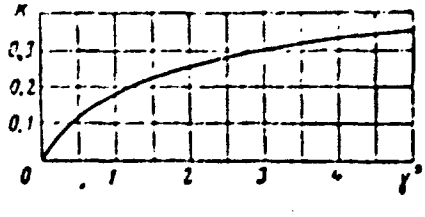

Fig. 4.70. Dependence of coefficient K on the angle of slope of the rollers.

follows that with the transition from an angle of 5° to an angle of 45', which corresponds to the location of all recesses at identical angles, coefficient K decreases from 0.35 to 0.14.

The location of all recesses of the separator at equal angles is more preferable according to the following considerations. If the angle of inclination of recesses is identical, then forces $F_{1_x} - F_{2_x}$, which press the rollers to their lateral surfaces, are very small. In the case $M_T = 0$ and $s = 1$ theoretically, in general, they are absent.

At various angles of inclination of the recesses, when "turned" rollers must surmount the resistance of radially located rollers, forces $F_{1_x} - F_{2_x}$ can reach a noticeable value (up to 0.1 μP) and cause wear of the separator (especially at large χ).

Thus far it was assumed that all the rollers have identical length. Now let us see what the alternating of long and short rollers staggered can give.

Table 4.13. Effect of the distribution of lengths of rollers on quantities T_c, f_{TP}, and K.

Variant of distribution of lengths of rollers	T_c min	f_T (at f_K = = 0.003)	K
Rollers of identical length ($l_1 = l_2 = 8$ mm)	48	0.00616	0.14
Long and short rollers alternated staggered ($l_1 = 11$ mm, $l_2 = 5$ mm)	45.7	0.00674	0.43 (for short rollers)

From Table 4.13 it is clear that in the last case time T_c and the given coefficient of friction f_T are changed insignificantly, and coefficient K for short rollers increases 3 times. This indicates that in the thrust bearings with turned rollers it is expedient to use rollers of identical length.

In the evaluation of the effect on longevity of the bearing of irregularity of distribution of the load, caused by the action of moment $(F_{1_y} + F_{2_y})(d_p/2)$, it is impossible to overlook that the load at each point of contact does not remain constant but changes with a change in the direction of rotation. In particular, on ends of rollers the normal load changes according to the law:

$$q = \frac{P}{l} \pm \frac{1}{2}|K|\frac{P}{l}.$$

Due to this the irregularity of distribution of the load, caused by the action of the indicated moment, should not greatly lower the service life of the bearing.

Of greater importance is the usual concentration of the load on ends of rollers, which we did not consider, assuming that at $\gamma = 0$, $q = \text{const}$. To decrease the harmful effect of the latter it is expedient to use rollers with a cylinder.

5. Example of the Calculation of a Thrust Bearing with "Turned" Rollers

In conclusion let us give an example of the calculation of a thrust bearing with "turned" rollers.

The axial load is N = 20,000 kG, the amplitude of oscillations of the moving ring, $\varphi_0 = 4.5^\circ$, and the frequency is n = 180 osc/min.

For the given conditions a bearing with the following parameters is selected: $d_p = 12$ mm, $r_c = 61$ mm, $l = 18.5$ mm (full length of rollers $l' = 12$ mm), $z = 20$ and $s = 2$.

It is required to determine the angles of inclination of recesses of the separator providing its displacement with optimum speed and service life of the bearing.

We calculate coefficient v:

$$v=\frac{\sum_{k=1}^{i}\frac{r_{1k}}{r_c}}{\sum_{k=1}^{i}\frac{r_{1k}^2}{r_c^2}}=\frac{1}{1+\left(\frac{l'}{2r_c}\right)^2}=\frac{1}{1+\left(\frac{12}{2\cdot 61}\right)^2}=0{,}99.$$

Let us assume that all recesses have an identical angle of inclination. Substituting into formula (6.15) $\varphi_0 = 4.5^\circ$, n = 180 osc/min, v = 0.99 and $\mu = \mu' = 0.05$, with the help of Table 4.11 we construct curve $T_c = T_c(\gamma)$. We find along the curve the value of γ' and angles γ at which $T_c = T_c' = 80$ min. In our case $\gamma' = 46'$. Taking $\xi_п = 7'$ and $e_{max} = 0.18$ mm, we determine the calculation deviation ξ:

$$\xi=7+57{,}3\cdot 60\frac{0{,}18}{2\cdot 61}=12'.$$

The nominal value of angles of slope of recesses of the separator

$$\gamma=\gamma'+\xi=46+12=58'.$$

Contact stresses in the bearing

$$\sigma=860\sqrt{\frac{N}{zs\cdot d_p l}}=860\sqrt{\frac{20\,000}{20\cdot 2\cdot 1{,}2\cdot 1{,}05}}\approx 17\,000\ \text{kG/cm}^2.$$

According to Fig. 4.53, this value of σ corresponds to $nh = 27\cdot 10^4$. Consequently, the service life of the bearing

$$h=\frac{27\cdot 10^4}{180}=1500\ \text{hours}.$$

LITERATURE

1. Riz P. M., Pozhalostin A. I., "Vibratsii i dinamicheskaya prochnost' vozdushnykh vintov" ("Vibrations and dynamic strength of propellers"), Trudy TsAGI No. 609, 1947.

2. Mil' M. L. O dinamicheskom zakruchivanii lopasti rotora avtozhira v polete (Dynamic twisting of a rotor blade of an autogiro in flight). "Tekhnika vozdushnogo flota" No. 2, 1937.

3. Baskin V. E., "Induktivnyye skorosti vozdushnogo vinta, obduvayemogo pod uglom k ego osi" ("Induced speeds of a propeller blown at an angle to its axis"), Doklad na Vsesoyuznom s"yezde po teoreticheskoy i prikladnoy mekhanike, Moskva, 1960.

4. Nekrasov A. V., "Raschet form i chastot sobstvennykh kolebaniy lopastey vozdushnykh vintov"("Calculation of forms and frequencies of natural oscillations of blades of propellers"), Trudy TsAGI No. 898, 1964.

5. Nekrasov A. V., "Raschet form i chastot sobstvennykh izgibno-krutil'nykh kolebaniy lopasti vertoleta v pustote" (Calculation of forms and frequencies of natural flexural-torsional vibrations of the blade of a helicopter in a vacuum"), Trudy TsAGI No. 898, 1964.

6. Nekrasov A. V., "Raschet Napryazheniy v lopasti nesushchego vinta vertoleta na bol'shikh skorostyakh poleta" ("Calculation of stresses in a blade of a helicopter rotor at high speeds of flight"), Trudy TsAGI No. 898, 1964.

7. Nekrasov A. V., "Raschet izgibnykh napryazheniy v lopasti vertoleta na malykh i srednikh skorostyakh poleta" ("Calculation of flexural stresses in the blade of a helicopter at low and average speeds of flight"), Trudy TsAGI No. 913, 1964.

8. Galkin M. S., "O reshenii zadachi Koshi dlya odnogo uravneniya" ("Resolution of the Cauchy problem for one equation"),

AN SSSR, "Prikladnaya matematika i mekhanika", t. XX, vyp. 2, 1956.

9. Lipskaya M. E., "Opredeleniye vysokikh sobstvennykh chastot vintovykh lopastey i turbinnykh lopatok" ("Determination of high natural frequencies of rotor blades and turbine blades"). Trudy MAP SSSR, No. 676, 1949.

10. Marchenko V. M., Sarmina L. A., Vronskiy G. V., "Raschet sobstvennykh kolebaniy lopastey s pomoshch'yu integral'nykh uravneniy na bystrodeystvuyushchikh vychislitel'nykh mashinakh" ("Calculation of natural oscillations of blades with the help of integral equations on high-speed computers"), Trudy TsAGI No. 898, 1964.

11. Ryzhik I. M. i Gradshteyn M. S., "Tablitsy integralov, summ, ryadov i proizvedeniy" ("Tables of integrals, sums, series and products"), GITTL, 1951.

12. Bogatyrev B. V., "Staticheskaya i dinamicheskaya prochnost' lopastey rotorov vintokrylykh appapatov" ("Static and dynamic strength of blades of rotors of helicopters"), AN SSSR, 1948.

13. Gureyev D. I., "Samokolebaniya lopastey gelikoptera" ("Natural vibrations of blades of a helicopter"), Izd. VVA im. Zhukovskogo, vypusk 391, 1950.

14. Krasovskiy A. A., "O vibratsionnom sposobe linearizatsii nekotorykh nelineynykh sistem" ("Vibration method of linearization of certain nonlinear systems"), "Avtomatika i telemekhanika", 1948, No. 1, t. 9.

15. Keldysh M. V., "Shimmi perednego kolesa shassi samoleta" ("Shimmy of the front wheel of the undercarriage of an aircraft"), Trudy TsAGI, vyp. 564, 1945.

16. Panovko Ya. G., "Vnutrenneye treniye pri kolebaniyakh uprugikh sistem" ("Internal friction with oscillations of an elastic system"), Fizmatgiz, 1960.

17. Grodko L. N., "Vynuzhdennyye kolebaniya izgiba sterzhnya pri nalichii lineynogo dempfera v sharnirnoy zadelke" ("Forced oscillations of bending of a rod in the presence of a linear damper in hinged sealing"), Zhurnal "Prikladnaya matematika i mekhanika", AN SSSR, tom XVII, vyp. 5, 1953.

18. Belozerov A. I., Grodko L. N., Litvakov B. M., "Sposob ustraneniya zemnogo rezonansa vertoletov" ("Method of eliminating ground resonance of helicopters"), "Byulleten' izbreteniy", No. 18, 1961, avtorskoye svidetel'stvo No. 141391.

19. Den-Gartog J. P., "Mekhanicheskiye kolebaniya" ("Mechanical oscillations"), Fizmatgiz, Moskva, 1960.

20. Babakov I. M., "Teoriya kolebaniy" ("Theory of oscillations"), Gostekhteoretizdat, 1958.

21. Belyayev I. M., "Soprotivleniye materialov" ("Resistance of materials"), Gostekhteoretizdat, 1958.

22. Kantorovich L. V., Krylov V. I., "Priblizhennyye metody vysshego analiza" ("Methods of approximation of highest analysis"), Gostekhteoretizdat, 1950.

23. Reshetov D. N., "Sovmestnoye deystviye na sharikovyye podshipniki radial'noy i osevoy nagruzki" ("Combined action on ball bearings of radial and axial load"), "Podshipnik", 1939, No. 10-11.

24. Belyanchikov M. P., "Novaya metodika rascheta gruzopod'yemnosti i dolgovechnosti radial'no-upornykh sharikopodshipnikov" ("New method of calculation of load capacity and life of radial thrust ball bearings"), "Podshipnikovaya promyshlennost'", 1960, No. 3.

25. Beyzel'man R. D., Tsypkin B. V., "Podshipniki kacheniya", Spravochnik ("Antifriction bearings", a reference book), Mashgiz, 1960.

26. Spitsyn N. A., Sprishevskiy A. I., "Podshipniki kacheniya", Spravochnoye posobiye ("Antifriction bearings", a reference book), Mashgiz, 1961.

27. Leykand M. A., Korostashevskiy R. V., "Upornyye podshipniki povyshennoy gruzopod"yemnosti dlya kachatel'nogo dvizheniya" ("Thrust bearings of increased load capacity for oscillatory motion"), Trudy VNIPP, 1961, No. 4.

28. Leykand M. A., Kurova I. V., Komissarova T. M., "Smazka podshipnikov kacheniya rabotayushchikh pri kachatel'nom dvizhenii" ("Lubrication of antifriction bearings operating with oscillatory motion"), "Podshipnikovaya promyshlennost'", 1962, No. 6.

29. Bochkov V. S., "Teoreticheskoye opredeleniye smeshcheniya tsentra tyazhesti radial'no-upornykh sharikopodshipnikov pri kombinirovannoy nagruzke" ("Theoretical determination of the displacement of the center of gravity of radial thrust ball bearings under combined load"), Trudy VNIPP, No. 4, 1962.

30. Leykand M. A., "Raschet sharikopodshipnikov, rabotayushchikh pri kombinirovannykh nagruzkakh" ("Calculation of ball bearings operating under combined loads"), Collection "Prochnost' i dinamika aviatsionnykh dvigateley", Mashgiz, 1966, No. 3.

31. Pal'mgren M., "Sharikovyye i rolikovyye podshipniki" ("Ball and roller bearings"), Mashgiz, 1949.

32. Morris T., Tye W., „The Stressing of Rotor Blades", Aircraft Engineering, Vol. X, № 112, 1938.

33. Horvay G., „Stress Analysis of Rotor Blades", Journal of the Aeronautical Sciences, Vol. 14, 1947.

34. Horvay G., „Chordwise and Beamwise Bending Frequencies of Hinged Rotor Blades", Journal of the Aeronautical Sciences, Vol. 15, 1918.

35. Coleman R. P., „Theory of Self Excited Mechanical Oscillations of Hinged Rotor Blades", NACA, ARR, July 1942; NACA, ARR, № 3009, 1943.

36. Coleman R. P. and Feingold A. M., „Theory of Ground Vibrations of a Two-Blade Helicopter Rotor on Anisotropic Flexible Supports", NACA, T. N. № 1184, 1947.
37. Horvay G., „Vibrations of a Helicopter on the Ground", Journ. Aero. Sci., November, 1946, Vol. 13, № 11, pp. 605—619.
38. Hawarth and Jones, „Ground Resonance of the Helicopters," The Journal of the Helicopter Association of G. B., April—1954, Vol. 7, № 4.
39. Sibley and Jones, „Some Design Aspects of Tandem Rotor Helicopters", The Journal of the Helicopter Association of G. B. October, 1959, Vol. 13, № 15.
40. Gilly L., Normand Y., „Stabilité au sol des hélicoptères tripales", Technique et science aéronautiques, № 6, 1952.
41. Heinrich, „Über die Kompensation der Reibung durch zusätzliche, Schwingbewegung", ZAMM, № 22, pp. 136—142, 1942.
42. Meldau E., „Druckverteilung im Radial Rollen Kugellager", „Werkstatt und Betrieb", N 87, 1954.
43. Weibull W., „A Statistical Representation of Fatigue in Solids", Transactions of Royal Institute of Technology, N 27, 1949.
44. Lundberg G. and Palmgren A., „Dynamic Capacity of Roller Bearings". Acta Polytechnica 96, 1952.
45. Harris A., „Predicting Bearing Reliability", Machine Design, N 1, 1963.
46. Lariviere J. S., „Calcul de la duree d'utilisation des pales d'helicopteres", Technical note STA/VT, N 165.
47. Selichov A. F., „On the theory of Calculation of Service Life of a Structure", Proseeding of the 4 th Congress of ICAS Spartan Press, 1965.

Footnotes

[1]In the calculation of quantities $\frac{P}{zvd_m^2}$, and also $\frac{R}{zvd_m^2}$ and $\frac{A}{zvd_m^2}$ diameter d_m is always expressed in millimeters.

[2]Draft of recommendations according to the calculation of dynamic load capacity of ball and roller bearings, ISO, No. 278, 1960.

[3]All relative quantities, as earlier, are expressed in fractions of distance $g = r_H + r_B - d_m$.

[4]The relative eccentricity at which unloaded rolling solids appear, as is known, amounts to 0.5 for thrust roller bearings and 0.6 for thrust roller bearings.

[5]It is assumed that the area of contact of adjacent rolling solids are not covered.

[6]It is assumed that quantity $\mu_c(2A-1)$ can be disregarded as compared to unity. The inertial moment of the roller is not considered.

[7]Everywhere where no special reservations are made, it is assumed that $T_c' = 80$ min. Here all concrete numerical values pertain to the case $d_p = 9$ mm, $r_c = 40$ mm, $i = 8$ mm, $v = 1$, $\varphi_0 = 4.5^\circ$, $n = 240$ osc/min, $\mu = 0.06$.

U. S. BOARD ON GEOGRAPHIC NAMES TRANSLITERATION SYSTEM

Block	Italic	Transliteration	Block	Italic	Transliteration
А а	*А а*	A, a	Р р	*Р р*	R, r
Б б	*Б б*	B, b	С с	*С с*	S, s
В в	*В в*	V, v	Т т	*Т т*	T, t
Г г	*Г г*	G, g	У у	*У у*	U, u
Д д	*Д д*	D, d	Ф ф	*Ф ф*	F, f
Е е	*Е е*	Ye, ye; E, e*	Х х	*Х х*	Kh, kh
Ж ж	*Ж ж*	Zh, zh	Ц ц	*Ц ц*	Ts, ts
З з	*З з*	Z, z	Ч ч	*Ч ч*	Ch, ch
И и	*И и*	I, i	Ш ш	*Ш ш*	Sh, sh
Й й	*Й й*	Y, y	Щ щ	*Щ щ*	Shch, shch
К к	*К к*	K, k	Ъ ъ	*Ъ ъ*	"
Л л	*Л л*	L, l	Ы ы	*Ы ы*	Y, y
М м	*М м*	M, m	Ь ь	*Ь ь*	'
Н н	*Н н*	N, n	Э э	*Э э*	E, e
О о	*О о*	O, o	Ю ю	*Ю ю*	Yu, yu
П п	*П п*	P, p	Я я	*Я я*	Ya, ya

* ye initially, after vowels, and after ъ, ь; e elsewhere. When written as ё in Russian, transliterate as yё or ё. The use of diacritical marks is preferred, but such marks may be omitted when expediency dictates.

FOLLOWING ARE THE CORRESPONDING RUSSIAN AND ENGLISH

DESIGNATIONS OF THE TRIGONOMETRIC FUNCTIONS

Russian	English
sin	sin
cos	cos
tg	tan
ctg	cot
sec	sec
cosec	csc
sh	sinh
ch	cosh
th	tanh
cth	coth
sch	sech
csch	csch
arc sin	$\sin^{-1}$
arc cos	$\cos^{-1}$
arc tg	$\tan^{-1}$
arc ctg	$\cot^{-1}$
arc sec	$\sec^{-1}$
arc cosec	$\csc^{-1}$
arc sh	$\sinh^{-1}$
arc ch	$\cosh^{-1}$
arc th	$\tanh^{-1}$
arc cth	$\coth^{-1}$
arc sch	sech^{-1}
arc csch	csch^{-1}
rot	curl
lg	log